Investigating virus-specific T-dependent antibody responses in early life and their modulation by farmyard microbes

Lucia Labeur Iurman, MSc

Inflammation, Repair and Development Section
National Heart and Lung Institute
Sir Alexander Fleming Building
Imperial College London
London, SW7 2AZ
United Kingdom

A thesis submitted to Imperial College London
for the degree of Doctor of Philosophy
2025

Statement of Originality

I hereby declare that the work described in this thesis was performed by myself, with the following exceptions. The *in vivo* dosing of the mice was mostly performed by Chloe Pyle (for the data in chapter 3) and Dr. Kunyuan Tian (for the data in chapters 4 and 5 with the exception of experiments in figures 4.32-44 which was done by me) with some punctual exceptions in which it was performed by me, Dr. James Harker, Dr. Kornelija Suveizdyte, Simone Walker or Dr. Senthil Deivasigamani. The *in vivo* experiments in figures 3.1b,c; 3.4-6 and 3.16 were performed by Chloe Pyle. Figures 3.1b,c and 3.6 were analysed by Chloe Pyle and figures 3.4-5 and 3.16 were analysed by me. The viral load in figures 4.1b, 4.15b and 4.24b was quantified by Dr. Kunyuan Tian. Urea concentration analysis for early life antibody avidity in figure 4.11 was performed by Lorena Mejias Martinez as part of an MSc project directly supervised by me. *In vitro* BMDC cultures and stimulant exposure were done by me with help from Angela Minerva Garcia Martin and Lorena Mejias Martinez, two MSc students under my direct supervision. I further declare that the intellectual content of this thesis is the product of my own work and that all sources have been appropriately referenced.

Copyright Declaration

The copyright of this thesis rests with the author. Unless otherwise indicated, its contents are licensed under a Creative Commons Attribution-NonCommercial 4.0 International Licence (CC BY-NC). Under this licence, you may copy and redistribute the material in any medium or format. You may also create and distribute modified versions of the work. This is on the condition that: you credit the author and do not use it, or any derivative works, for a commercial purpose. When reusing or sharing this work, ensure you make the licence terms clear to others by naming the licence and linking to the licence text. Where a work has been adapted, you should indicate that the work has been changed and describe those changes. Please seek permission from the copyright holder for uses of this work that are not included in this licence or permitted under UK Copyright Law.

Acknowledgements

Firstly I would like to sincerely thank my supervisors Dr James Harker and Prof Sejal Saglani, for the opportunity to conduct my PhD within your groups, for your constant support and guidance throughout the years and for helping me become the scientist that I am today. It has been a great pleasure learning from and with you. James, I could not have had a better supervisor. You constantly had an open door, no matter the time or the circumstances you were there to help me both scientifically and personally. You were always there to share a sarcastic, but full of knowledge comment, always positive and enthusiastic about every bit of data or idea that I would run by you (even when they didn't make any sense!). You were a great mentor and I am sure I have learned loads from you. I will always remember the Harker Lab socials, the Harker night hike, your wedding day and all the times when you would "casually" just come and say hi, thank you so much! Sejal, thank you for being a constant role model, thank you for showing this young female scientist what it takes to be a strong, successful, independent female scientist. Thank you for making me think about the fundamental questions of the project and for believing in me. I would also like to thank my early- and late-stage PhD assessors Fiona Culley and Paul Turner, for the constructive feedback and suggestions as well as for career advice.

I would also like to acknowledge the National Heart and Lung Foundation as well as the Rosetress Foundation for funding my PhD studies. On this line, I will like to thank my landlord Charles Kenyon for allowing me to live in central London with a PhD stipend, thank you so much for believing in PhD students and for being so reasonable and altruistic, I owe you a lot. Kunyuan, Will and Chloe, thank you a million for showing me all the techniques that I needed to know to complete this PhD and for always doing it with a smile, pretending that my questions were indeed very important and interesting. Simone, thank you for watching out for us and for always being on top of everything! You are amazing! Régis, Laura and particularly Franz, thank you so much for your constant career advice, for guiding me to become a better scientist and for doing so while being extremely approachable and fun. You definitely hold the department together! I will also like to thank all the people that when having a mice harvest would remember that I could probably use some of their spare organs. I won't list you because I think the whole of IRD will end up here. I don't think I let a single mediastinal lymph node, spleen or bone marrow go to waste and this couldn't have been done without you! Minerva and Lorena, than you for being such great MSc students. Thank you for helping me with the experiments and for pushing me to come up with ideas, I have probably learnt more from you than you would have learnt from me!

I would also like to express my gratitude to all the friends that supported me throughout this PhD, we made SAF feel like home (and that wasn't thanks to the commodities of the building!). Kunyuan, thank you so much! This PhD would be nothing without you! Thank you for dosing all the mice and

for making all the long days of harvest so much fun. I have a very fond and happy memory of all of them and I would repeat them all. Thank you for all the laughs, for the stories, for the Chinese food (I think I can cope up much better with spicy food now!) and for always keeping a positive attitude. Rafaela, Nico and Kornleija, thank you for adapting to my “Spanish eating schedule”, I know it wasn’t easy and I truly appreciate our lunches together. Rafaela, thank you for being a great support and for always giving on point and very rationalised advice (maybe I am not so grateful about your spotless desk, it made mine look extra messy!). Nico, thank you for being the sun that I needed in the very grey London weather, thank you for always wanting to meet up, cook and provide me with the constant activity that I needed to be happy (and probably cope with this PhD). No, I have not learnt anything, I will still accompany you to any movie or play that you could come up with. Kornelija, thank you for being my rock. Thank you for knowing with a simple quick look how I was feeling and what I needed, for being there all steps of the way, with either help in the lab, small presents, a laugh, a meme or a fun story. Thank you for opening my horizons and for letting me into your art world, allowing me to switch out from science from time to time and get a bit of a break.

Helen and Gesa, thank you for always being there, for equally providing me with a quick machinery fix (yes, including the bike!), great science advice or for feeding me, I will always remember your amazing cakes, pancakes, your German ketchup and yes, also the broccoli salad! Georgie, thank you for making IRD a great department! Thank you for the coffee mornings, for organising the Christmas and summer picnics and for always helping out in every small or big celebration. Your great taste (yes, in big champagne bottles as well!) and your organisation skills have clearly saved more than one party! I would also like to thank all the other people in the department Karim, Lola, Christina, Will, Minerva, Ciara, Sara, Leia, David, Emily, Garance, Martina, Elina, Krish, Sky, Kyle, Senthil, Shwetha and Sean for making me feel so welcome and for sharing such great moments!

També m’agradaria agrair a la Cris, la Laia i l’Ainoa, per sempre creure en mi i per saber que aconseguiré tots els reptes que em proposo. Gràcies per estar sempre al meu costat, per fer malabars perquè ens puguem veure el màxim possible i per estar sempre en contacte amb mi, no he notat gens que hem estat vivint en països diferents! Sara i Sasha, gràcies per estar sempre al meu costat, per utilitzar-vos com a psicòlegs i per sempre treure’m un somriure. Sara, Londres no hagués estat el mateix sense tu, gràcies per ser la meva família lluny de casa.

Marc, no puc ni començar a dir-te tot el que agraeixo el que hem viscut aquests últims anys. Gràcies per creure en mi i per ajudar-me en absolutament tot! Gràcies per les llargues converses telefòniques, per compartir tots els meus hobbies (si! La loqui dels teatres!) i per venir a Londres a fer-me el dinar i portar-me’l al laboratori. La setmana que venies era sens dubte la més feliç del mes! Gràcies per haver aguantat aquesta relació a llarga distància i per sempre creure en nosaltres. No pateixis, ja s’ha acabat!

También me gustaría agradecer profundamente a toda mi familia. Especialmente al Nono, la Tía Martita y la Tía Ele, por enseñarme que la ciencia es una carrera que, aunque difícil, maravillosa y excitante. A la abuelas y la Tía Marta, por siempre creer en mí y demostrarme que las mujeres podemos hacer todo lo que nos propongamos (las extraño tanto!). Y por último a los más importantes, gracias a Mamá, Papá, Lara y Blacky por acompañarme y mimarme siempre, por siempre creer en mí y por sacarme tantas carcajadas. Definitivamente no sería la persona que soy hoy ni hubiese conseguido esto sin su ayuda. Los re quiero!

Abstract

T follicular helper cell (T_{FH}) dependent antibody responses are critical for long term immunity, but are compromised early in life. Respiratory syncytial virus (RSV), the most common cause of viral bronchiolitis in infancy, promotes limited antibody responses in early life when compared to adults leading to increased susceptibility to reinfection. Using a murine model of RSV, I found that the decrease in neonatal T_{FH} differentiation was associated with differences in key components regulating the signalling of IL-2. These included increased secretion of IL-2 in early life and increased expression of IL-2 receptors on neonatal naïve $CD4^+$ T cells, which were also more prone to phosphorylate STAT5, a T_{FH} antagonist, when compared to adult counterparts. Continuous intranasal exposure of mice to the lyophilised farmyard microbe *Acinetobacter lwoffii F78* (*A.lwoffii)* during recurrent RSV infection was sufficient to bypass the early life IL-2 mediated suppression and augment T_{FH} and RSV-specific antibody responses both systemically and locally, but this was not observed with short-term exposure to the bacteria. Continuous *A.lwoffii* also boosted conventional dendritic cell type 2 (cDC2) proportions in mediastinal lymph nodes, increased cDC2 expression of CD25 (the secreted form of which can quench IL-2 from the microenvironment) and IL-6, a pro-T_{FH} cytokine. Likewise, *in vitro* stimulation of bone marrow derived DCs (BMDCs) with *A.lwoffii*, but not RSV, potently induced both CD25 and IL-6 secretion. This was partly replicated by LPS but not by TLR3, 7 or 9 agonists. Co-culture of *A.lwoffii*-stimulated BMDCs with naïve $CD4^+$ T cells promoted T_{FH}-like differentiation, a process RSV-stimulation of BMDCs inhibited. *A.lwoffii* exposure also enhanced IL-6 production by B cells both *in vivo* and *in vitro*. Together, this data highlights the ability of microbiota to overcome the IL-2-dependent restriction in early life, at least partially, by modulating cDC2s and B cells, and promote antigen-specific antibody mediated immunity.

Table of Contents

Statement of Originality ***2***

Copyright Declaration ***3***

Acknowledgements ***4***

Abstract ***7***

Table of Contents ***8***

List of Figures ***13***

List of Tables ***18***

List of Abbreviations ***19***

1 Introduction **24**

1.1 Overview of the early life immune system – a distinct immunological landscape 25

1.2. T_{FH} differentiation is a multistep, multifactorial and spatiotemporal process ***27***

1.2.1 B cell helper T cells at a glance 27

1.2.2 Transcriptional factors regulating T_{FH} differentiation 28

1.2.3 T_{FH} differentiation vs alternative T_{helper} pathways 30

1.3 Alternative T helper pathways differentiated by the cytokine microenvironment 39

1.4 High affinity B cell responses require T_{FH} cell help 42

1.4.1 B cell activation and differentiation 42

1.4.2 Generation of class-switch high affinity antibodies 44

1.5. Differences in T cell dependent antibody responses in early life and adulthood 45

1.5.1. Differences in T_{FH} and B cells in children and adults 45

1.5.2. Support cells and their alterations in early life 47

1.5.3. Anatomical Sites 48

1.6 Respiratory Syncytial Virus – a major pathogen in infancy 52

1.6.1 RSV viral structure 52

1.6.2 RSV viral replication 53

1.6.3 Risk factors for RSV infection 55

1.6.4 Clinical disease and treatment 56

1.6.5 Immune response to RSV infection 57

1.6.6 RSV immune evasion 61

1.6.7 Delayed sequelae of RSV bronchiolitis 64

1.6.8 Vaccination against RSV 65

1.7 Can microbial exposure shape the T cell-dependent humoral immune response in early life? 67

1.8 Hypothesis and Aims 68

2 Materials and Methods **70**

2.1 Animal experiments 71

2.2 Microbial and viral cultures 71

2.2.1 *Acinetobacter lwoffii F78 culture* 71

2.2.2 RSV culture 72

2.2.3 RSV Focus-forming Assay 72

2.3 Animal *in vivo* procedures 73

2.3.1 Exposure to inhaled *A.lwoffii* 73

2.3.2 Respiratory viral infection 73
2.4 Animal tissue harvest and cell recovery 73
2.4.1 Animal euthanasia 73
2.4.2 Blood 73
2.4.3 Bronchoalveolar Lavage (BAL) 74
2.4.4 Nasal Airway Lavage (NAL) 74
2.4.5 Mediastinal lymph node and Peyer's Patches (medLN & PP) 74
2.4.6 Lungs 74
2.4.7 Spleen 75
2.4.8 Bone Marrow (BM) 75
2.5 *Ex vivo* cultures 76
2.5.1 *Ex vivo* stimulation for lymphocyte intracellular staining 76
2.5.2 *Ex vivo* differentiation of bone marrow progenitors into matured DCs subsets 76
2.5.3 Stimulation of bone marrow derived DCs *in vitro* 77
2.5.4 Naïve $CD4^+$ T cell isolation from mouse tissue 78
2.5.5 *In vitro* DC and T cell co-culture 78
2.5.6 *In vitro* cytokine stimulation for phosphoflow cytometry 78
2.6 Human samples 78
2.6.1 Isolation of Human Peripheral Blood Naïve $CD4^+$ T Cells 78
2.6.2 Cell culture and T helper cell differentiation towards $CXCR5^{hi}PD\text{-}1^{hi}$ cells 79
2.7 Flow Cytometry Analysis 80
2.7.1 General staining protocol 80
2.7.2 Acquisition and analysis 85
2.8 RNA isolation, cDNA synthesis and real time quantitative PCR 85
2.8.1. RNA isolation and cDNA synthesis from single cell suspensions 85
2.8.2. RNA isolation and cDNA synthesis from lung tissue 85
2.8.3 Real Time Quantitative PCR (RT-qPCR) 86
2.9 Enzyme-Linked Immunosorbent Assay (ELISA) 88
2.9.1 Validation of RSV and *A.lwoffii* Antigen 88
2.9.2 Detection of antigen (Ag)-specific mouse antibodies in serum and BAL samples 88
2.9.3 Avidity assay for Ag-specific antibodies 89
2.9.4 Detection of human and mouse cytokines and receptors 89
2.10 Neutralization assay 89
2.11 Statistical Analysis 90
2.12 Diagram Figures 90

3 Results I: Early life T cell responses are characterised by increased IL-2/pSTAT5 signalling 91
3.1 Introduction 92
3.1.1 Anatomical organisation of the immune system 92
3.1.2 The T cell lifespan 92
3.1.3 The humoral immune response against respiratory syncytial virus is downregulated in early life 93
3.1.4 Hypothesis and Aims 94
3.2 Results 95
3.2.1 STAT5 phosphorylation is increased in naïve $CD4^+$ T cells from infant mice both after IL-2 and IL-6 stimulation 95
3.2.2 Early evidence of T_{FH} differentiation 3 days post RSV infection 97
3.2.3 The SLOs' microenvironment of early life mice is enriched in IL-2 103

3.2.4 IL-2 receptor expression on T cells is increased in 1wk old mice when compared to adult counterparts 107
3.2.5 IL-6 and IL-6 receptor expression in mediastinal LN are increased 3dpi in adult mice 110
3.2.6 T_{FH} responses in the lung are diminished in early life when compared to adulthood 3 days post RSV infection 113
3.2.7 The neonatal lung microenvironment is enriched in IL-2 and IL-6 production 115
3.2.8 T cell populations in the thymus differ from those found in peripheral organs 117
3.2.9 Both the IL-2 and IL-6 thymic signatures are upregulated in early life when compared to adult counterparts 120
3.2.10 The percentage of cells producing IL-2 is increased throughout the developmental pathway of $CD4^+FOXP3^-$T cells in early life when compared to adulthood 124
3.2.11 Human T_{FH} can be differentiated *in vitro* from adult peripheral blood naïve $CD4^+$ T cells 126
3.2.12 STAT3 signalling promotes $CD4^+$ T cell survival and T_{FH} effector function *in vitro* 128
3.2.13 Phosphorylation of STAT4 *in vitro* seems redundant for human T_{FH} differentiation 130
3.2.14 Human STAT5 phosphorylation limits T_{FH} differentiation 132
3.3 Discussion 134
3.3.1 Early life secondary lymphoid organs are enriched for IL-2 production 134
3.3.2 Neonatal $CD4^+$ T cells have an altered response to cytokine signalling 135
3.3.3 Biological implications for enhanced IL-2 signalling in early life 136
3.3.4 Early life increased IL-2 signature in the thymus is altered by infection 137
3.3.5 The increased T_{FR} signature could promote the GC inhibition observed in neonatal mice 138
3.3.6 STAT3 and STAT5 phosphorylation play a crucial role in driving human T_{FH} proliferation and differentiation 139
3.4 Concluding remarks 140

4 Results II: Recurrent exposure to *A.lwoffii* in early life promotes T_{FH}, B cell responses and RSV-specific antibody production in infant mice 141
4.1 Introduction 142
4.1.1 Investigating the role of farmyard microbes in promoting early life immune responses 142
4.1.2 *Acinetobacter lwoffii F78* – a key promoter of early life immunity? 143
4.1.3 Hypothesis and aims 144
4.2 Results 145
4.2.1 Inhaled recurrent exposure to *A.lwoffii* promotes an increased T_{FH} and $CD138^+$ cell signature in the SLOs of RSV infected infant mice 145
4.2.2 Early life *A.lwoffii* exposure enhances local and systemic RSV-specific antibody responses 154
4.2.3 Short exposure to *A.lwoffii* in early life is not sufficient to drive T_{FH} or antibody responses in RSV infected infant mice 163
4.2.4 Therapeutic *A.lwoffii* exposure in early life fails to boost RSV-specific antibody responses 175
4.2.5 Recurrent exposure to *A.lwoffii* in early life boosts local RSV-IgA responses upon adult re-challenge 185
4.3 Discussion: 200

4.3.1 *A.lwoffii* exposure at the time of RSV re-challenge promotes T_{FH} differentiation in infant mice 200
4.3.2 Enhanced RSV-specific antibody responses are observed after recurrent *A.lwoffii* exposure during early life 202
4.3.3 Short *A.lwoffii* exposure regimens fail to promote RSV-antibody mediated immunity 206
4.4 Concluding remarks: 207

5 Results III: *A.lwoffii* generates a pro-T_{FH} environment in cDC2s and B cells 208
5.1 Introduction: 209
5.1.1 cDC2 are the main primers of naïve $CD4^+$ T cell responses, while B cells promote a GC-T_{FH} signature 209
5.1.2 TLR signalling leads to enhanced mediator secretion and antigen presentation 210
5.1.3 Hypothesis and Aims 212
5.2 Results: 213
5.2.1 Soluble CD25 expression is increased in the SLOs of adult mice 213
5.2.2 *A.lwoffii* exposure promotes CD25 and IL-6 expression by mediastinal LN cDC2s and B cells 218
5.2.3 *A.lwoffii*, but not RSV, stimulation of bone marrow-derived cDC2s promotes a pro-T_{FH} environment 225
5.2.4 Live RSV exposure is required to promote cDC2 activation, CD25 and IL-6 production 234
5.2.5 LPS is a potent inducer of CD25 and IL-6 secretion by BM-cDC2s 239
5.2.6 TLR4 inhibition suppresses LPS, but not *A.lwoffii* or RSV, mediated production of IL-6 and CD25 by BMDCs 245
5.2.7 Non-proteolytic release of CD25 by BMDCs 247
5.2.8 *A.lwoffii* promotes B cell activation and IL-6 secretion 249
5.2.9 *A.lwoffii*-stimulated DCs promote Bcl6 upregulation of co-cultured naïve $CD4^+$ T cells 253
5.2.10 RSV-stimulated BMDCs promote mCD25 expression in co-cultured $CD4^+$ T cells 260
5.3 Discussion: 262
5.3.1 *A.lwoffii* promotes a more potent pro-T_{FH} environment by cDC2s when compared with RSV 262
5.3.2 *A.lwoffii* is able to promote IL-6 secretion by early life B cells 263
5.3.3 RSV-exposed DCs fail to drive T_{FH} differentiation and instead promote a T_{H2} signature 264
5.3.4 LPS can replicate some, but not all, of *A.lwoffii*'s pro-T_{FH} functions 265
5.4 Concluding remarks: 268

6 Discussion 269
6.1 Rationale of the project and summary of findings: 270
6.2. *A.lwoffii* promotes the generation of a pro-T_{FH} environment 272
6.2.1 *A.lwoffii* exposure is able to bypass the early life IL-2 dependent restriction and promote T_{FH} responses against RSV infection 272
6.2.2 *A.lwoffii* exposure in early life promotes IL-6 secretion, which contributes to increased T_{FH} differentiation 275
6.3 SLOs are specific microanatomical niches where IL-2 responses are tightly regulated 278
6.4 Limitations and future directions 278
6.4.1 Investigating the role of sCD25 in driving T_{FH} responses in early life 279

6.4.2 Investigating the role of IL-6 in driving T_{FH} responses in early life 279
6.4.3 Deciphering the molecular mechanisms of *A.lwoffii*-mediated antibody enhancement 280
6.5 Translating my findings 281
6.5.1 Effect of *A.lwoffii* exposure on RSV protection in the elderly 281
6.5.2 Clinical implications 282
6.6 Concluding remarks 283
7. References ***284***
Appendix I: Publications arising from this thesis ***342***
Appendix II: Conference presentations arising from this thesis ***343***

List of Figures

Fig 1.1. Factors affecting T-cell dependent antibody responses in infancy.....26

Fig 1.2. Cell interactions promoting pre-T_{FH} and GC-T_{FH} development.....28

Fig 1.3. Murine signals influencing T_{FH} differentiation vs alternative $T_{effector}$ pathways.....39

Fig 1.4. Alternative $CD4^+$ $T_{effector}$ subsets arising from activated T cells 42

Fig 1.5. High affinity antibody responses are reduced in early life 51

Fig 2.1. Depiction of supporting structures modified from pipette tips to help isolation of bone marrow cells by the centrifugation method 76

Fig 3.1. STAT5 phosphorylation is increased in naïve $CD4^+$ T cells from early life mice both after rmIL-2 and rmIL-6 stimulation 96

Fig 3.2. Early life is characterised by a Stat5/Stat3 signature.....97

Fig 3.3. Gating $CD4^+$ T cell subsets early after RSV infection 98

Fig 3.4. The T_{FH} differentiation programme in mediastinal lymph node has started 3dpi with RSV in both early life and adult mice.....100

Fig 3.5. T_{FH} responses 3dp RSV infection in spleen are more developed in adulthood when compared to early life mice 101

Fig 3.6. Neonatal antigen experienced $CD4^+$ T cells are more prone to phosphorylate STAT5 after RSV infection than their adult counterparts 102

Fig 3.7. Lymphocyte quantification in mediastinal LN and SP of steady state and after RSV infection in neonatal and adult mice 104

Fig 3.8. Increased IL-2 microenvironment in the mediastinal lymph node of early life mice when compared to adult counterparts.....105

Fig 3.9. Increased percentage of IL-2 producing cells in the early life spleen when compared to adult counterparts 106

Fig 3.10. Increased proportion of membrane CD25 expressing T cells in the mediastinal LN from 1wk old mice when compared to adult counterparts.....108

Fig 3.11. Increased IL-2R expression in $FOXP3^-$ naïve $CD4^+$ T cells of early life mice when compared to adult counterparts.....109

Fig 3.12. Increased percentage of $mCD25^+FOXP3^-CD4^+$ T cells in adult mice spleen when compared to neonatal counterparts after RSV infection 110

Fig 3.13. IL-6 and IL-6 receptor expression are increased in adult mediastinal LN..... 111

Fig 3.14. IL-6 receptor expression on naïve $CD4^+$ T cells peaks at 2wks of live 112

Fig 3.15. Stat3/Stat5 levels are increased in adult LN in the steady state, but this is reversed after 3dpi..... 113

Fig 3.16. T_{FH} responses are diminished in early life lung when compared to adulthood 3dp RSV infection 114

Fig 3.17. Increased IL-2 and IL-6 expression in lungs of neonatal mice when compared to adults 116

Fig 3.18. Stat3/Stat5 ratio in the lung doesn't change with age 117

Fig 3.19. T cell populations in the thymus differ to those found in the SLOs 119

Fig 3.20. Thymocyte quantification in neonatal and adult mice 120

Fig 3.21. Increased IL-2 microenvironment in the thymus of early life mice when compared to adult counterparts 121

Fig 3.22. Increased proportion of membrane CD25 expressing thymocytes in early life mice when compared to adult counterparts 123

Fig 3.23. IL-6 and IL-6 receptor expression is increased in neonatal thymus 124

Fig 3.24. Neonatal thymocytes have increased Stat3 and Stat5 124

Fig 3.25. IL-2 levels are increased throughout the development of $CD4^+$ T cell lymphocytes in early life when compared to adulthood 125

Fig 3.26. Human T_{FH} can be differentiated in vitro from peripheral blood naïve $CD4^+$ T cells. 127

Fig 3.27. STAT3 phosphorylation in humans controls in vitro $CD4^+$ T cell viability and T_{FH} effector function. 129

Fig 3.28. STAT4 phosphorylation is redundant for T_{FH} differentiation in humans 131

Fig 3.29. Human STAT5 phosphorylation limits T_{FH} differentiation 133

Fig 4.1. Recurrent A.lwoffii exposure reduces RSV viral load in the lung of early life mice 146

Fig 4.2. Investigation of T cell responses in recurrent A.lwoffii exposed RSV infected infant mice 147

Fig 4.3. Early life recurrent A.lwoffii exposure enhances T_{FH} and $CD138^+$ cell proportions in the lymph nodes of RSV infected mice 148

Fig 4.4. Similar B and T cell responses in the spleen of recurrent A.lwoffii exposed and unexposed mice 149

Fig 4.5. Recurrent A.lwoffii exposure promotes T_{FH}, GC-T_{FH} and $CD138^+$ cell frequency in the spleen of RSV infected 20d old mice 151

Fig 4.6. Similar B and T cell responses in the Peyer's Patches of A.lwoffii exposed and unexposed RSV infected mice 152

Fig 4.7. Lack of T_{FH} and antibody secreting cells in the Peyer's Patches of A.lwoffii exposed RSV infected infant mice 153

Fig 4.8. Determination of antigen concentrations used for in-house developed ELISAs against A.lwoffii and RSV 155

Fig 4.9. RSV infection decreases A.lwoffii-specific serum IgG1 antibody titre 156

Fig 4.10. Early life recurrent A.lwoffii exposure boosts the production of IgG2a antibodies in the serum of RSV-infected mice 157

Fig 4.11. Determination of urea concentration used for early life avidity assays 158

Fig 4.12. Establishment of RSV neutralization assays 160

Fig 4.13. Early life recurrent A.lwoffii exposure does not affect serum RSV-specific antibody avidity or neutralization 161

Fig 4.14. Trend to an increase BAL RSV-specific IgA responses in mice recurrently exposed to A.lwoffii *162*

Fig 4.15. Similar viral titre and B cell responses in RSV infected infant mice irrespective of prophylactic A.lwoffii exposure *164*

Fig 4.16. No difference in T cell responses is observed between RSV infected and prophylactically A.lwoffii exposed and unexposed mice *165*

Fig 4.17. Exposure to A.lwoffii prophylactically does not enhance the T_{FH} and $CD138^{+}$ response when compared to RSV infected infant mice alone *166*

Fig 4.18. No major splenic differences in B and T cell responses after short exposure to A.lwoffii *168*

Fig 4.19. A.lwoffii exposure prophylactically does not affect the splenic GC response of RSV infected infant mice *169*

Fig 4.20. Short A.lwoffii exposure regimens do not promote A.lwoffii-specific antibody secretion *170*

Fig 4.21. Short A.lwoffii regimens do not boost systemic RSV-specific antibody responses *171*

Fig 4.22. Early life short exposure to A.lwoffii does not affect serum RSV-specific antibody avidity or neutralization capacity *173*

Fig 4.23. Analysis of antibody avidity and neutralization capacity in BAL of prophylactic A.lwoffii exposed mice *174*

Fig 4.24. Similar B and T cell responses in the LN of therapeutic A.lwoffii exposed and unexposed RSV infected 20d old mice *176*

Fig 4.25. Exposure to A.lwoffii therapeutically in early life promotes mediastinal LN T_{FH} cells proportions and numbers *177*

Fig 4.26. Similar B and T cell responses in the spleen of late A.lwoffii exposed and unexposed RSV infected 20d old mice *178*

Fig 4.27. Exposure to A.lwoffii therapeutically in early life does not affect the splenic GC reaction *179*

Fig 4.28. Exposure to A.lwoffii therapeutically does not promote A.lwoffii-specific IgG1 or IgG2a antibody production *181*

Fig 4.29. Exposure to A.lwoffii therapeutically does not promote RSV-specific antibody production *182*

Fig 4.30. Analysis of serum antibody avidity and neutralization capacity after therapeutically A.lwoffii exposed mice *183*

Fig 4.31. No difference in BAL antibody titre, avidity or neutralization capacity with therapeutical exposure to A.lwoffii *184*

Fig 4.32. No difference in body weight or adult viral titre between A.lwoffii exposed and unexposed RSV infected mice *186*

Fig 4.33. Lymph node T cell responses in early life A.lwoffii exposed and unexposed mice re-challenged with RSV as adults *187*

Fig 4.34. Lymph node GC responses in early life A.lwoffii exposed and unexposed mice re-challenged with RSV as adults *188*

Fig 4.35. Splenic T cell responses in early life A.lwoffii exposed and unexposed mice re-challenged with RSV as adults *189*

Fig 4.36. Splenic GC responses in early life A.lwoffii exposed and unexposed mice re-challenged with RSV as adults *190*

Fig 4.37 Serum A.lwoffii-specific antibody levels are still increased in adult mice that received recurrent A.lwoffii exposure in early life *191*

Fig 4.38 No difference in RSV-specific antibody titre in adult mice irrespective of A.lwoffii exposure in early life *192*

Fig 4.39 No difference in RSV-specific antibody avidity in adult mice irrespective of A.lwoffii exposure in early life *193*

Fig 4.40 BAL A.lwoffii-specific antibody titres are still increased in adult mice that received A.lwoffii exposure in early life *194*

Fig 4.41 Increased adult RSV-IgA antibody titre in BAL of RSV infected mice exposed to A.lwoffii in early life *195*

Fig 4.42 No difference in avidity of adult BAL RSV-specific antibodies in mice exposed to A.lwoffii in early life *197*

Fig 4.43 NAL A.lwoffii-specific antibody titres are still increased in adult mice that received recurrent A.lwoffii exposure in early life *198*

Fig 4.44 No difference in adult RSV-specific antibody titres in NAL of RSV challenged mice exposed to A.lwoffii in early life *199*

Diagram 5.1. TLR signalling pathways *211*

Fig 5.1. Soluble CD25 is increased in the SLOs of adult mice *214*

Fig 5.2. Gating intracellular CD25 and membrane CD25 in cDC2s and B cells to investigate CD25 secretion in vivo *215*

Fig 5.3. Increased proportion of intracellular CD25 expression in adult cDC2s, but increased percentage of membrane CD25^{+} cDC2s in neonates *216*

Fig 5.4. Increased proportion of intracellular CD25 expression in adult B cells, but increased percentage of membrane CD25^{+} B cells in neonates *217*

Fig 5.5. Increased Il6 transcript production in the lymph node of A.lwoffii exposed mice during 2nd RSV infection when compared with RSV infected mice alone *219*

Fig 5.6. Increased cDC2s in the lymph nodes of recurrent A.lwoffii exposed infant mice *220*

Fig 5.7. Recurrent A.lwoffii exposure in early life increases cDC2s activation and their expression of CD25 and IL-6 during RSV infection *221*

Fig 5.8. Recurrent A.lwoffii exposure during early life in RSV infected mice increases B cells' CD25 and IL-6 expression *222*

Fig 5.9. Increased cDC2s in the spleen of recurrent A.lwoffii and RSV alone infected mice *223*

Fig 5.10. No difference in early life spleen cDC2s is observed between A.lwoffii exposed RSV infected mice and viral infected mice alone *224*

Fig 5.11. No difference in early life B cell CD25 or IL-6 production in the spleen of A.lwoffii exposed or unexposed RSV infected mice *225*

Fig 5.12. Centrifuge isolation of bone marrow progenitors is effective for the Flt3-L differentiation of bone marrow derived DCs in vitro *227*

Fig 5.13. The ability to differentiate matured cDC2s from BM progenitors in vitro is not influenced by mice age *228*

Fig 5.14. Similar CD86 expression after A.lwoffii or RSV-stimulation of BM-derived cDC2s *230*

Fig 5.15. Increased intracellular and soluble CD25 after A.lwoffii-stimulation of BM-cDC2s *231*

Fig 5.16. Elevated IL-6 after A.lwoffii-stimulation of BM-cDC2s *233*

Fig 5.17. Heat and UV inactivated RSV, unlike live RSV, do not promote BM-cDC2 activation .. *235*

Fig 5.18. Live RSV stimulation promotes BM-cDC2s CD25 expression when compared to inactivated counterparts *237*

Fig 5.19. Live RSV stimulation promotes BM-cDC2s IL-6 expression *239*

Fig 5.20. LPS, Poly(I:C) and Imiquimod-stimulation promote BM-cDC2s activation *240*

Fig 5.21. LPS-stimulation promotes CD25 expression by BM-cDC2s *242*

Fig 5.22. LPS-stimulation promotes IL-6 expression by BM-cDC2s *244*

Fig 5.23. sCD25 is affected by TLR4 inhibition in LPS and A.lwoffii-stimulated BMDCs *246*

Fig 5.24. Inhibition of proteases does not affect BM-cDC2s CD25 secretion *248*

Fig 5.25. A.lwoffii-stimulation promotes early life B cell activation and IL-6 production *250*

Fig 5.26. Stimulation of early life B cells with TLR-adjuvants has minimal effect on activation, CD25 or IL-6 expression *252*

Fig 5.27. Co-culture with BM-derived DCs is needed to promote naïve $CD4^+$ T cell proliferation and BCL6 expression in vitro *254*

Fig 5.28. A.lwoffii stimulation of BMDCs promotes Bcl6 expression in co-cultured naïve $CD4^+$ T cells *256*

Fig 5.29. After 5 days of co-culture naïve $CD4^+$ T cells have not fully differentiated into T_{FH} cells under any stimulating condition *257*

Fig 5.30. RSV-stimulated BMDCs promote Gata3 expression on $CD4^+$ co-cultured T cells *258*

Fig 5.31. Intermediate $CD4^+$ T cell phenotype in cells co-cultured with A.lwoffii+RSV-BMDCs .. *260*

Fig 5.32. Co-culture with RSV-stimulated BM-cDCs promotes mCD25 expression in $CD4^+$ T cells *261*

Fig 6.1. Recurrent A.lwoffii exposure promotes T_{FH} and RSV-specific antibody responses in early life *271*

Fig 6.2. The IL-2 microenvironment differs with age and stimulation leading to marked differences in $CD4^+$ T cell differentiation *274*

Fig 6.3. The IL-2 microenvironment might dictate IL-6 responses in naïve $CD4^+$ T cells *277*

List of Tables

Table 2.1. Stimulants, inhibitors and antagonists used in in vitro DC cultures.....77

Table 2.2. Chemical inhibitors, reference numbers, supplier, concentration, regime and matched vehicle controls used in cell culture.....79

Table 2.3. Surface and intracellular anti-mouse antibodies, clone, supplier and dilution used for flow cytometry 84

Table 2.4. Surface and intracellular anti-human antibodies, clone, supplier and dilution used for flow cytometry 84

Table 2.5. Mouse TaqMan™ probes used for RT-qPCR 86

Table 2.6. Human TaqMan™ probes used for RT-qPCR.....87

Table 2.7. Primers and probes used for detection of RSV-L RNA.....87

List of Abbreviations

Abbreviation	Term
A	
α	Anti
AAD	Allergic airway disease
ADAM	A desintegrine and metalloproteinase
ADCC	Antibody dependent cellular cytotoxicity
AEC	3 amino-ethylcarbazole
Ag	Antigen
AHR	Airway hyperresponsiveness
AID	Activation induced cytidine deaminase
Akt	Protein kinase B
ALRs	Absent in melanoma-2 like receptors
A.lwoffii	*Acinetobacter lwoffii F78*
AM	Airway macrophage
APC(s)	Antigen presenting cell(s)
ASCL2	Aschaete-scute homologue-2
B	
BAL	Bronchoalveolar lavage
BALT	Bronchus-associated lymphoid tissue
BCL6	B-cell lymphoma 6 protein
BCR	B cell receptor
BFA	Brefeldin A
BLIMP-1	B lymphocyte-induced maturation protein-1
BM	Bone marrow
BMDC	Bone marrow derived dendritic cell
B_{regs}	B regulatory cells
BSA	Bovine serum albumin
C	
cDC1	Conventional dendritic cell type 1
cDC2	Conventional dendritic cell type 2
CDP(s)	Common dendritic cell progenitor(s)
cfu	Colony forming units
CLRs	C-type lectin receptors
C-MAF	C-musculoaponeurotic fibrosarcoma
COPD	Chronic obstructive pulmonary disease
COVID-19	Coronavirus disease 19
cRPMI	Complete RPMI medium
CSR	Class switch recombination
C_T	Cycle threshold
CTV	Tag-it Violet™ Proliferation and Cell Tracking Dye
CXCR	C-C-C chemokine receptor
D	
d	Day(s)
DAMP(s)	Damage-associated molecular pattern(s)
DC	Dendritic cell

DMEM	Dulbecco's Modified Eagle Medium
DMSO	Dimethyl sulfoxide
DN	Double negative
DNA	Deoxyribonucleic acid
DP	Double positive
dpi	Days post-infection
E	
EDTA	Ethylenediaminetetraacetic acid
EF	Extra Follicular
EGFR	Epidermal growth factor receptor
ELISA	Enzyme-linked immunosorbent assay
F	
F	Fusion protein (from RSV)
FACS	Flow Cytometry Staining Buffer
FBS	Foetal bovine serum
FDCs	Follicular Dendritic Cells
FFU	Focus forming units
Flt3	FMS-like tyrosine kinase 3
Flt3-L	FMS-like tyrosine kinase 3 ligand
FOXP	Forkhead box protein
FRCs	Fibroblastic Reticular Cells
G	
G	Glycoprotein (from RSV)
GAGs	Glycosaminoglycans
GALT	Gut-associated lymphoid tissue
GATA3	GATA-binding protein 3
GC	Germinal Centre
γc	Common gamma chain
Ge	Gene end
GI	Gastrointestinal
GITR	Glucocorticoid-induced TNFR family-related protein
GM-CSF	Granulocyte-macrophage colony-stimulating factor
Gp	Glycoprotein
Gs	Gene start
H	
HDM	House dust mite
HEPES	4-(2-hydroxyethyl)-1-piperazineethanesulfonic acid
HRP	Horseradish peroxidase
I	
IAV	Influenza A virus
ICAM1	Intercellular adhesion molecule 1
iCD25	Intracellular CD25
ICOS	Inducible T cell co-stimulator
IFN(s)	Interferon(s)
Ig	Immunoglobulin
IGF1R	Insulin like growth factor 1 receptor
IL	Interleukin
ILC2	Type 2 innate lymphoid cells

i.n.	Intranasal
i.p	Intraperitoneal
IRF	Interferon regulatory factor
ISGs	Interferon-stimulated genes
L	
L	Large RNA-dependent RNA-polymerase (from RSV)
Le	Leader
LN(s)	Lymph node(s)
LPS	Lipopolysaccharide
LRTI	Lower respiratory tract infection
LTβR	Lymphotoxin-β receptor
Ly	Lymphocyte antigen
M	
M	Matrix protein (from RSV)
MALT	Mucosal-associated lymphoid tissue
MAVS	Mitochondrial antiviral signalling protein
mCD25	Membrane CD25
M-CSF	Macrophage colony-stimulating factor
MDA	Melanoma differentiation associated genome
medLN	Mediastinal lymph node
MFI	Mean Fluorescence intensity
mgp130	Membrane glycoprotein 130
MHC-II	Major histocompatibility complex class II
Mib1	Mind bomb1
mIL-6Rα	Membrane IL-6 receptor alpha
MLE	Muse lung epithelial cells
MOI	Multiplicity of infection
mTOR	Mammalian target of rapamycin
MyD88	Myeloid Differentiation primary response 88
N	
N	Nucleocapsid protein (from RSV)
NAL	Nasal airway lavage
NC	Nucleocapsid
NF-KB	Nuclear factor kappa-light-chain-enhancer of activated B cells
NK	Natural Killer cell
NKT	Natural Killer T cell
NLRs	Nucleotide oligomerization domain-like receptors
NS	Non-structural protein (from RSV)
O	
OASL	Oligoadenylate synthase-like proteins
OD	Optical density
OVA	Ovalbumin
P	
P	Phosphoprotein (from RSV)
PAMP(s)	Pathogen-associated molecular pattern(s)
PB(s)	Plasma blast(s)
PBMC	Peripheral blood mononuclear cells
PBS	Phosphate-buffered saline

PBS-T	Phosphate-buffered saline-0.05% Tween-20
PC(s)	Plasma cells(s)
PD-1	Programme cell death protein 1
pDC	Plasmacytoid dendritic cell
PD-L1	Programmed cell-death ligand 1
PLOs	Primary lymphoid organ(s)
PND	Post natal day
PFA	Paraphormaldehyde
PFU	Plaque-forming units
PI3K	Phosphoinositide 3-kinase
PP	Peyer's Patches
PRR	Pattern recognition receptor
PSGL1	P-selectin glycoprotein ligand 1
pSTAT	Phosphorylated signal transducer and activator of transcription
pTreg	Peripheral T regulatory cell
Q	
qPCR	Quantitative polymerase chain reaction
R	
RBC	Red blood cells
rh	Recombinant human
rm	Recombinant mouse
RT	Room temperature
RNA	Ribonucleic acid
RNA-seq	RNA sequencing
ROR-γt	Retinoic acid-related orphan receptor-t
RPMI	Rosewell Park Memorial Institute medium
RSV	Respiratory Syncytial Virus
S	
SARS-CoV 2	Severe acute respiratory syndrome coronavirus 2
SATB1	Special AT-rich sequence-binding protein-1
sCD25	Soluble CD25
sc-RNA-seq	Single cell RNA sequencing
sG	Soluble glycoprotein (from RSV)
sgp130	Soluble glycoprotein 130
SH	Small hydrophobic protein (from RSV)
SHM	Somatic hypermutation
sIL-6Rα	Soluble IL-6 receptor alpha
SIRPα	Signal regulatory protein α
SLOs	Secondary lymphoid organ(s)
SMAD	Small mothers against decapentaplegic
SOCS	Suppressor of cytokine signalling
SP	Spleen or Single positive
STAT	Signal transducer and activator of transcription
T	
TBK1	TANK-binding kinase 1
TCR	T-cell receptor
TdT	Terminal deoxynucleotidyl transferase
TGF-β	Transforming growth factor beta

T_{FH}	T follicular helper cell
T_{FR}	T follicular regulatory cell
T_H	T helper cell
TLR	Toll-like receptor
TLS	Tertiary lymphoid structure
T	Tween 20
TMB	3,3′,5,5′-Tetramethylbenzidine
TR	Trailer
TREC	T-cell receptor excision circles
T_{reg}	T regulatory cell
tTreg	Thymic T regulatory cell
U	
URTI	Upper respiratory tract infection
V	
VR	Viral replication
vRNA	Viral RNA
W	
WHO	World Health Organisation
wk	Week

1 Introduction

1.1 Overview of the early life immune system – a distinct immunological landscape

Despite efforts to enhance infant wellbeing, and a reduction in the global child mortality rate of 53% over the last three decades, six million children under five still die every year (1,2). Many of these deaths are due to infectious diseases and thus are potentially preventable through vaccination (3). Indeed, most infections are first encountered in early life, and children have historically been considered to be more susceptible to infections than adults in part due to the presence of an immature immune system (4–6). The reality is however much more nuanced; and in actuality the early life immune system is acutely adapted to recognise and differentiate the multitude of antigens being encountered for the first time. Therefore, rather than being an inert or immature version of its adult counterpart, the early life immune system is tuned to promote a tolerogenic response against self, microbiotal and environmental antigens, to avoid excess inflammation, and still provide rapid responses against pathogens to prevent fatal infection (7).

One cost of this distinct immunological poise in early life is a reduced capacity to generate strong and effective immune responses and immune memory against many common pathogens compared to adults, leading to more severe outcomes and potentially lifelong sequalae. For instance, respiratory syncytial virus (RSV) infection, while only producing mild upper respiratory tract infection in the majority of adults can cause severe bronchiolitis is infancy (8). Infants also fail to generate long-lasting immunity to RSV, with recurrent infections with the same serotype commonly seen during the first three years of life (9). Moreover, severe RSV infection in infancy is associated with an increased prevalence of wheeze and asthma in later life (10). Likewise, repeated malarial infections are commonplace in children younger than five years old, and this age group accounts for 80% of all malaria deaths in the World Health Organization (WHO) African malaria region (11). Importantly, vaccines designed to protect from RSV and malaria, while showing efficacy in adults, have had much more limited success in infants, with reduced antibody responses observed in early life (12,13).

The infant immune response is however capable of mounting sufficient antibody responses to provide protection against many agents, with vaccines against polio, tetanus, whooping cough, pneumococcus and haemophilus among others all administered in the first 12 months of life (14–19). Precisely why some stimuli, but not others, can generate protective antibody-mediated immunity in early life is complex, and like for like infant versus adult human studies are uncommon, with infants routinely receiving more booster vaccinations than adults for the equivalent vaccine. The nature of danger signals associated with immune activation does however appear to influence the outcome, and some adjuvants are more capable of reproducing some adult-like adaptive responses in neonatal mice than others (20–22). The nature of the antigen also seems to play a role, with those that promote T-independent antibody responses, like many bacterial antigens,

being relatively more effective in early life, than those that rely on T-dependent responses. Indeed, the ability to generate higher affinity antibodies, and the specialised $CD4^+$ T cell help these rely on is known to be more limited in early life compared to adults (13,23–26). At the level of the whole organism many environmental, microbiotal and genetic influences determine the quality of the T-cell dependent antibody response. At cellular level however it relies on tightly regulated interactions between $CD4^+$ T cells and B cells, supported by cells from the innate, myeloid and stromal compartments *(Fig 1.1)*.

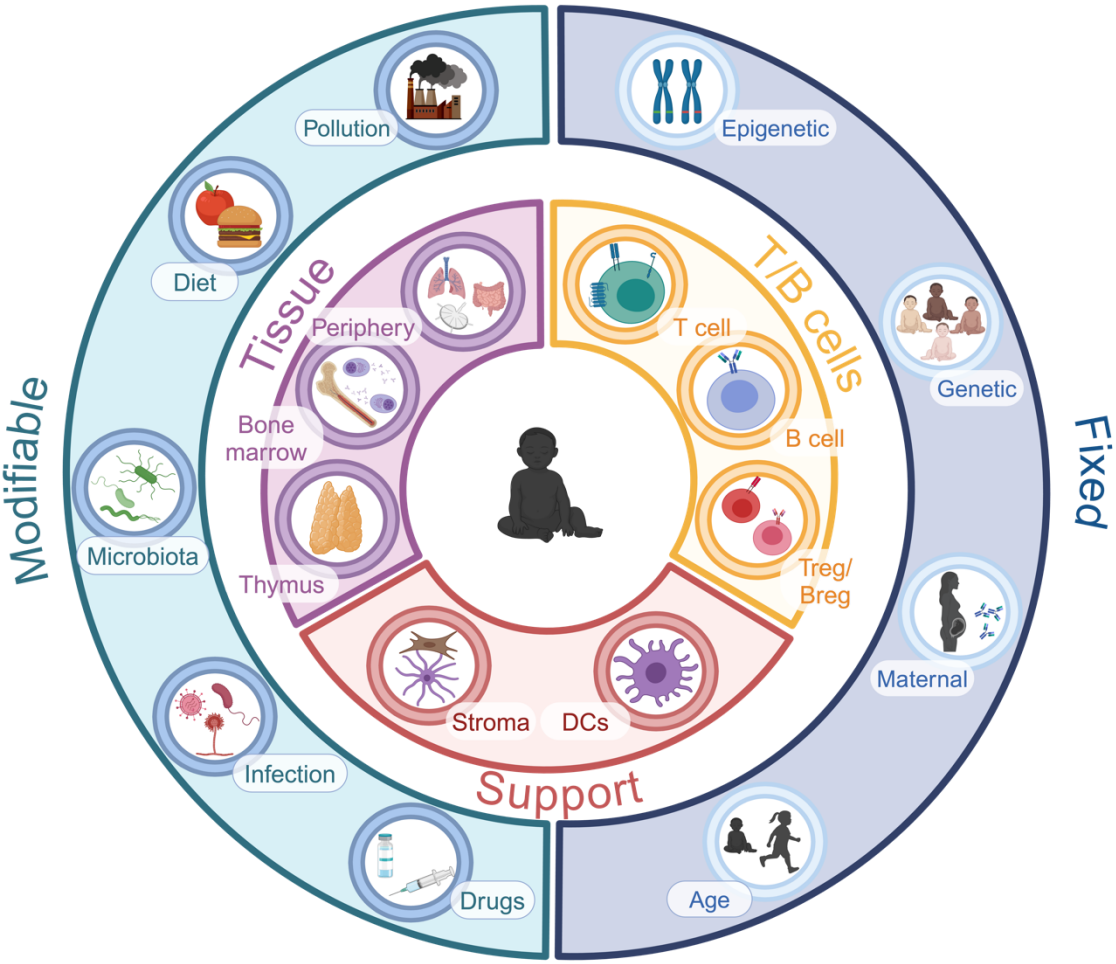


Fig 1.1. Factors affecting T-cell dependent antibody responses in infancy.

The generation of T-cell dependent antibody responses is regulated by multiple factors at both a molecular, cellular and whole organism level which are all altered in early life compared to adulthood. At the cellular and molecular level (depicted by the inner ring) there are intrinsic alterations in the T and B cells themselves, alongside the cells that support them during antibody generation including dendritic cells (DCs) and stroma (e.g. follicular dendritic cells). There are also fundamental differences in the tissues in which these processes take place (primary, secondary and tertiary lymphoid structures). At the level of the whole organism (depicted by the outer ring), factors fixed at birth, such as age, maternal, genetic and epigenetic background, and modifiable factors, such as drug, nutritional, infection and pollution exposure history, alongside the state of the microbiome, all feed into the development and function of the cells involved in the T-cell dependent antibody responses. *Adapted from Labeur-Iurman & Harker* (7).

1.2. T_{FH} differentiation is a multistep, multifactorial and spatiotemporal process

T follicular helper cells (T_{FH}) are a specialised subset of $CD4^+$ T cells that provide help to B cells. This T cell help is needed to promote B cell differentiation into plasma cells (PCs), able to produce antibodies, and memory B cells, long-lasting cells capable of rapidly mounting an immune response upon re-encountering an antigen (27,28).

To provide B cell help T_{FH} cells first need to differentiate from naïve $CD4^+$ T cells. T_{FH} differentiation is a complex process that accommodates a significant amount of heterogeneity. It requires the participation of different antigen presenting cells (APCs), the orchestration of several cytokine signals and transcriptional factors and the physical migration of cells inside the secondary lymphoid organs (SLOs) (27,28). SLOs are subdivided into distinct T cell and B cell zones, with the area in between known as the T:B border. The B cell zone is made up of primary follicles where B cells and follicular dendritic cells (FDCs) reside, while the T cell zone consists of T cells and dendritic cells (DCs). A chemokine gradient and fibroblastic reticular cells (FRCs) allow compartmentalization of these distinct zones (29,30).

1.2.1 B cell helper T cells at a glance

Expression of the transcriptional repressor B-cell lymphoma 6 protein (Bcl6) is necessary and sufficient to promote T_{FH} differentiation from naïve $CD4^+$ T cells (31–33). DCs, found in the T-cell zone of the SLOs promote the initial differentiation towards a pre-T_{FH} phenotype. High affinity TCR signalling (34–36), co-stimulation via CD28, ICOS and CD40 (37–39) and cytokine-induced STAT3 signalling (40) favour T_{FH} differentiation *in vivo*. Conversely, interleukin (IL)-2-STAT5 signalling exerts a strong inhibitory effect on T_{FH} differentiation by driving the transcription of the T_{FH}-repressor factor B lymphocyte-induced maturation protein-1 (Blimp-1) (41–43). Once differentiated, pre-T_{FH} cells are able to migrate to the T:B border of the SLOs via a chemokine gradient where a second interaction with the cognate antigen, this time presented on activated B cells, takes place. This interaction can trigger an extra-follicular (EF) response, driving rapid plasma blast (PB) differentiation and low affinity antibody responses; and it can also promote the migration of T-B cells into the B cell follicle where they continue to proliferate and become committed to the germinal centre (GC) fate. Canonical GC responses are often, but not always, preceded by a short phase of EF proliferation and differentiation, while there are also responses that don't generate a GC reaction and have prolonged interactions at EF sites (44).

GCs are the primary location for somatic hypermutation (SHM) and affinity maturation needed to create high affinity memory B cells and long-lived PCs producing high affinity antibodies (27,45). To drive this, GC B cells interact with GC-T_{FH} cells; with GC-T_{FH} numbers being 'rate limiting' for GC formation and frequency, promoting the survival, proliferation and affinity maturation of GC B

cells, and ultimately regulating their differentiation into high affinity antibody secreting PCs or memory B cells (27,28). Within the GC, T_{FH} are a major source of two canonical cytokines, IL-21 and IL-4. IL-21 acts on B cells to stimulate proliferation and survival and thus affinity maturation, immunoglobulin class switch recombination (CSR) and PC formation (46). IL-4 boosts antibody responses by promoting B cell selection and CSR, in particular IgG_1 and IgE and B cell memory formation (47,48). Human, but not mouse, T_{FH} are also a potent source of the CXCR5 agonist and B cell chemokine, CXCL13 (49,50) *(Fig 1.2)*.

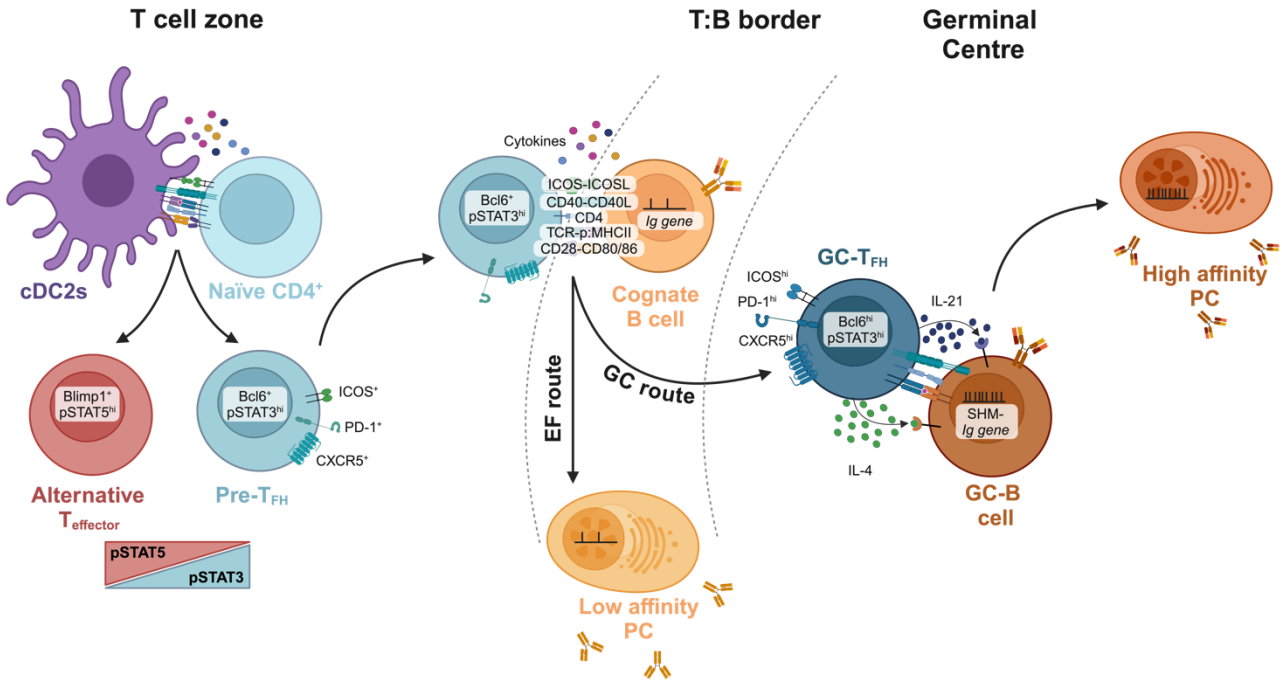


Fig 1.2. Cell interactions promoting pre-T_{FH} and GC-T_{FH} development

T_{FH} differentiation is a multistep, multifactorial and spatiotemporal process. DCs are the first primers of T_{FH} differentiation. T_{FH} poise is characterized by the high expression of phosphorylated STAT3 over STAT5, which drives the expression of the T_{FH}-defining transcription factor Bcl6 over the T_{FH}-repressor Blimp-1. Once activated pre-T_{FH} cells can migrate to the T:B cell border where a second interaction with the antigen, this time presented by cognate B cells takes place. This drives a bidirectional exchange of information between both lymphocytes that either promotes the generation of low affinity plasma blasts by the extrafollicular (EF) route or drives the formation of germinal centres (GC), where further help provided by GC-T_{FH} cells to B cells allows SHM of the immunoglobulin gene (Ig gene) and final differentiation to memory B cells or high affinity antibody-secreting plasma cells (PC).

1.2.2 Transcriptional factors regulating T_{FH} differentiation

T_{FH} have been considered a unique T helper cell subset since the identification of Bcl6 as their master transcription regulator by three independent studies (31–33). Prior to this, gene-expression profiling of human and mouse T cells found in the follicle indicated that they were a transcriptionally and functionally unique subset of T cells, different from the other major $CD4^+$ T cell subsets (49,51). These studies revealed a set of genes commonly upregulated in T_{FH} cells in both species including *BCL6, Aschaete-scute homologue-2 (ASCL2), Programme cell death protein 1 (PD-1), CXCR5 and*

Inducible T cell co-stimulator (ICOS). These have subsequently been shown to be key molecules for regulating T_{FH} cell development, migration, homeostasis, and function. Importantly, high expression of CXCR5 in combination with PD-1 on the cell membrane is a reliable way to identify T_{FH} cells, with expression of these markers increasing as T_{FH} develop; being at their highest in GC-T_{FH} cells (52–54).

1.2.2.1 Transcriptional promoters of T_{FH} differentiation

Bcl6, encoded by the *Bcl6* gene, is a transcriptional repressor, inhibiting the expression of other lineage defining transcription factors while simultaneously leading to downstream upregulation of T_{FH} effector molecules (55). Of note, by binding regulatory complexes of genes controlling cellular migration, Bcl6 can inhibit the expression of some genes, such as CCR7, which helps maintain T cells in the T cell zone; while indirectly upregulating others, like CXCR5, allowing early-T_{FH} migration towards the T:B cell zone border in response to its ligand, CXCL13, produced by FDCs (33,50,56–58). Bcl6 also indirectly promotes the expression of PD-1 in T_{FH} cells (59,60). PD-1, a co-inhibitory receptor, has garnered attention in recent years as a maker of T cell exhaustion. In T_{FH} cells however it is considered a pivotal molecule to promote T_{FH} cell migration and maintenance in the GC territory and provide T_{FH} help to B cells by maintaining the stringency of the GC affinity selection, controlling T_{FH} cytokine production and therefore regulating PC selection and survival (61–63). Initial differentiation towards T_{FH} lineage is marked by Bcl6 dependent downregulation of P-selectin glycoprotein ligand 1 (PSGL1), a T-cell zone retention ligand (64), accompanied by downregulation of Lymphocyte antigen 6C (Ly6C), which marks differentiation towards a T_{H1} fate (65,66).

While upregulation of Bcl6 is necessary and sufficient to promote T_{FH} differentiation, there are other transcription factors that also play a role including Ascl2 and c-musculoaponeurotic fibrosarcoma (c-Maf). Ascl2 regulates T_{FH} migration towards B cell follicles by collaborating with Bcl6 in promoting CXCR5 expression and CCR7 downregulation. It is also implicated in inhibiting T_{H1} and T_{H2} differentiation processes while dampening inhibitory T_{FH} pathways such as the one promoted by IL-2 (67). In parallel, c-Maf promotes T_{FH} effector functions by inducing IL-21 secretion (68) and is critical in determining the pre-T_{FH} to GC-T_{FH} transition (69) while driving T_{FH} fate away from a T_{H17} alternative pathway (70). Full differentiation of T_{FH} cells in humans requires c-MAF expression as BCL6 alone is not sufficient to promote all T_{FH} defining markers (71). These principal T_{FH} regulators are downstream of other transcription factors such as Tcf-1, Lef-1, Egr2, Egr3 and Batf which promote their transcription allowing T_{FH} cell commitment and growth (72–75).

1.2.2.2 Transcriptional inhibitors of T_{FH} differentiation

The existence of transcriptional inhibitors of T_{FH} differentiation has also been widely reported. Probably the most important is Blimp-1 encoded by the *Pr domain zinc finger protein 1* (*Prdm1*) gene. This repressor antagonises Bcl6 functions therefore promoting T cell differentiation towards T_{FH}-alternative fates (31,76). Krüppel-like factor 2 (Klf2) is another important inhibitor of T_{FH} differentiation. It is associated with the expression of typical naïve genes such as CD62L or CCR7 and therefore maintains T cells in the T cell zone, preventing their migration towards the B cell follicles. Similarly to Blimp-1, Klf2 promotes the transcription of other major T helper cell transcription factors such as Tbet or Gata3 and it also upregulates *Prdm1* transcription while preventing the expression of T_{FH}-defining markers such as PD-1, ICOS, IL-6Rα, IL-21 and IL-4 (60,77,78). Klf2 has however recently been proposed as a key transcription factor in regulating the differentiation of memory-like T_{FH} cells, which develop independently from T_{FH}-effector cells and B cell contact and are prone to circulate. These cells have long-term survival, express memory- and stemness-associated genes and are capable of giving rise to T_{FH}-effector cells in recall responses (79). Similarly, Forkhead box protein (Fox) O1 (Foxo1) also plays a dual role in T_{FH} differentiation. While its initial degradation is needed to prevent negative regulation of Bcl6, Foxo1 upregulation is required in the last stages to allow final GC-T_{FH} differentiation (80). Foxp1 expression also shows periodic fluctuations, while it is considered a negative regulator in initial T_{FH} differentiation from naïve T cells (81), its upregulation is needed to promote a more differentiated T_{FH} subset that is able to promote GC stabilization and B cell somatic hypermutation (82).

1.2.3 T_{FH} differentiation vs alternative T_{helper} pathways

T helper cell differentiation from naïve $CD4^+$ T cells canonically depends on initial interaction with conventional DCs type 2 (cDC2) and requires three signals. Initial interaction of the T cell receptor (TCR) with cognate antigen presented on major histocompatibility complex class II (MHC-II) on cDC2s allows the formation of an immunological synapse (signal 1). Further T cell activation is enabled through signals from co-stimulatory molecules including, but not limited to, B7 family members and ICOS (signal 2). The cytokine microenvironment is also key in driving the differentiation of naïve $CD4^+$ T cells into different T helper subsets (signal 3) (83).

1.2.3.1 Antigen presentation

The naïve T cell T_{FH} versus non-T_{FH} fate decision is the first one to take place and it can be made as early as the first two divisions after T cell priming, when Bcl6 and CXCR5 start to be expressed (37,43). The strength and duration of antigen presentation plays a critical role in determining the outcome of $CD4^+$ T cell responses with the ones with the strongest affinity and longer interaction

times preferentially differentiating towards a T_{FH} pathway (34,35,84). Antigen dose and sustained inflammation also positively correlate with both T_{FH} induction and the magnitude of the GC response (85,86).

1.2.3.2 Co-stimulatory signals

Co-stimulatory receptors and their ligands such as CD80/86, CD40, OX40L, ICOSL and NOTCHL in APC's and CD28/CTLA4, CD40L, OX40, ICOS and NOTCH in T cells also drive T_{FH} differentiation both by having unique and redundant roles. Early reports show that CD28-deficient mice have impaired GC and humoral immune responses (87,88). Similar results are observed after Cre-mediated deletion of CD80/86 counterparts in the membrane of DCs, indicating a critical role for CD28-CD80/86 signalling by DCs during pre-T_{FH} differentiation (89). Persistent CD28 stimulation is also required for total GC-T_{FH} cell differentiation and maintenance and to promote an adequate function of humoral responses (90), suggesting a role for B cell dependent signalling. CD80/86 can also bind the co-inhibitory receptor CTLA-4 (91). Deletion of this receptor in T_{FH} cells results in increased T_{FH} cell numbers and heightened B cell responses while the opposite is observed in CTLA-4 overexpressing conditions (88,92–95). Similar to CD28 signalling, the CD40 signalling is key in regulating T_{FH} differentiation both by DCs (93) and B cells (89).

OX40 is upregulated on naïve T cells following both CD28 and CD40 activation so the roles of these three molecules can also be intertwined and difficult to pull apart. As with CD28, OX40-deficient mice show impaired T_{FH} and humoral responses and blocking OX40L during and after T_{FH} cell differentiation leads to a significant reduction in T_{FH}, GC-T_{FH} and GC B cell frequencies, while constitutive expression of OX40L leads to the opposite observations (93,96–98). Interestingly however, administration of agonistic OX40 antibodies during LCMV infection diverts naïve $CD4^+$ T cell differentiation away from a T_{FH} pathway and instead promotes $T_{effector}$ alternative pathways by upregulating Blimp-1 expression (99), suggesting that the role of OX40 signalling might be context-dependent. When comparing the effects of all three co-stimulatory molecules on T_{FH} priming *in vivo,* CD28 and CD40 play a crucial role in promoting T_{FH} differentiation and GC B cell responses. Conversely, OX40 signalling role is strain- and immunization site-specific as an impairment in GC responses is observed in lymph nodes (LNs) of C57BL/6 mice when using OX40 blocking antibodies, but no effect is seen in the spleen of these mice nor in SLOs of Balb/c counterparts (88). Together these results suggest that CD28 and CD40 signalling both by DCs and B cells are important drivers of T_{FH} differentiation and while the requirement of OX40L might not be absolute, under specific conditions it could regulate certain aspects of the humoral immune response.

ICOS signalling plays a central role in T_{FH} cell priming and maintenance, so much so that blockage of ICOS results in relocation of fully developed T_{FH} cells back to the T-cell zone and reversion of

their phenotype to non-T_{FH} effector subsets (39). ICOS signalling promotes T_{FH} differentiation by inhibiting Klf2 and inducing Foxo1 degradation in the initial phases of T_{FH} polarisation (39,80). Similarly to CD28 and CD40, patients and mice with ICOS deficiency have impaired T_{FH}, GC B cell frequencies and compromised humoral responses (88,94,100). Concomitantly, overexpression of ICOS due to loss of its transcriptional repressors results in spontaneous accumulation of T_{FH} and GC B cells in mice (101–103). Early ICOS signalling by DCs is required for initial Bcl6 expression and T_{FH} commitment (37). Subsequent ICOSL signalling through TANK-binding kinase 1 (TBK1) by B cells is however key to promote GC-T_{FH} cell differentiation and antibody responses (37,104). ICOSL signalling by follicular bystander B cells enables T_{FH} cell migration from the T:B border to the follicle to form a GC (63). During antigen-specific interactions with GC B cells, an ICOS-CD40 intercellular positive feedback loop promotes T-B cell entanglement and facilitates rapid selection of high-affinity B cells (38). ICOS signalling is therefore crucial for multiple stages of T_{FH} differentiation, rendering both DCs and B cells, via their provision of ICOS-L, indispensable.

To a lesser extent, T_{FH} differentiation and function can also be regulated by NOTCH signalling. NOTCH signalling has an effect in early T_{FH} fate poise, as $CD4^+$ T cells deficient in NOTCH1 and 2 receptors fail to downregulate Blimp-1 and upregulate Bcl6, c-Maf, IL-4 and IL-21 leading to reduced T_{FH} cell frequencies and IL-4 dependent GC B cell responses such as IgE secretion (105,106). Simultaneously, DC-specific deletion of the NOTCH ligand E3 ubiquitin ligase Mind bomb1 (Mib1) also impairs early T_{FH} differentiation, but no difference in T_{FH} cell priming is observed if Mib1 is deleted in B cells or follicular DCs. T_{FH} cell frequencies in DC-specific $Mib1^{-/-}$ mice are eventually comparable to controls at later stages of the response, indicating that requirement for DC-derived NOTCH signals is redundant (106).

Overall, co-stimulation in the form of CD28-CD80/86, CD40L-CD40 and ICOS-ICOSL from both DCs and B cells are all crucial to promote and maintain T_{FH} differentiation. Additional co-stimulatory molecules, such as OX40-OX40L and the NOTCH pathway can further accentuate these responses and collaborate in T_{FH} differentiation and function.

1.2.3.3 Cytokine microenvironment

The cytokine microenvironment in the SLOs plays a fundamental role in directly driving naïve $CD4^+$ T cell polarization towards different $CD4^+$ T cell subsets and is also key to T_{FH} maintenance. Depending on the pathogen-associated molecular patterns (PAMPs) and danger-associated molecular patters (DAMPs) associated with the antigen encountered, DCs and B cells secrete cytokines that can significantly influence the outcome of the T cell response *(**Fig 1.3**)*.

Pro-T_{FH} cytokine microenvironment

Various cytokines can promote T_{FH} cell differentiation by binding to type 1 or type 2 cytokine receptors. These in turn mediate the activation of Janus kinase (JAK)-signal transducers that can phosphorylate, and therefore activate, several signaling molecules such as signal transducer and activator of transcription (STAT) proteins. As indicated by their name, once activated STAT proteins can migrate to the nucleus and recruit RNA polymerase II to promote the transcription of specific genes. The balance of these signals can dictate the transcription profile of $CD4^+$ T cells, with those upregulating Bcl6 over Blimp-1 becoming T_{FH} cells (107).

IL-6 is the main driving cytokine of T_{FH} differentiation in mice. IL-6 signalling through the IL-6 receptor promotes STAT3, and to a lesser extent STAT1, phosphorylation in activated T cells, inducing Bcl6 expression and therefore promoting T_{FH} differentiation (31,32,58,108). The IL-6 receptor is made up of two distinct subunits, the IL-6Rα subunit (CD126), that can bind IL-6, and the glycoprotein 130 (gp130) subunit (CD130), that, lacking affinity for IL-6, functions as the signalling component of the IL-6 receptor complex. Gp130 is expressed on nearly all cells, perhaps with the exception of granulocytes (109). IL-6Rα is however only expressed in hepatocytes and certain populations of myeloid cells and lymphocytes, including both T cells and canonical DCs (110). Both subunits of the IL-6 receptor complex, IL6Rα and gp130, exist in a membrane bound version and in a soluble form. Soluble IL-6Rα (sIL-6Rα) is predominantly produced through proteolytic shedding, while a minor fraction, less than 20%, in the serum is potentially derived from direct secretion following the translation of alternatively spliced mRNA (111–113). Soluble gp130 (sgp130) is generated by alternative splicing of the gp130 transcript (114,115).

IL-6 interacts not only with membrane bound IL-6Rα (mIL-6Rα) but also with its soluble form; thus multiple models of IL-6 signalling have been identified. In the canonical signalling pathway, IL-6 binds to mIL-6Rα, which then recruits membrane gp130 (mgp130), resulting in mgp130 homodimerization and signalling. Even cells without mIL-6Rα can respond to IL-6 through trans-signalling, the second signalling mechanism, where a preassembled soluble IL-6/sIL-6Rα complex engages mgp130 on target cells, triggering mgp130 dimerization and downstream signalling (110). The soluble receptor-ligand complex mainly forms when IL-6Rα is shed from the surface by metalloproteases such as a desintegrine and metalloproteinase (ADAM)10 and ADAM17 (116). The ubiquitously expressed mgp130 allows almost any cell to participate in IL-6 trans-signalling, despite the limited expression of mIL-6Rα. sgp130 can neutralize the IL-6/IL-6Rα complex, thereby inhibiting trans-signalling (117). The third mode of IL-6 signalling, known as IL-6 cluster signalling, consists of a donor cell presenting IL-6 through its membrane-bound IL-6Rα to a recipient cell. This interaction requires the recipient cell to be in close proximity to the donor cell to detect the IL-6/mIL-

6Rα complex via its mgp130, often requiring the formation of an immunological synapse. Similar to trans-signalling, the recipient cell therefore does not need to express mIL-6Rα to respond to IL-6 through cluster signalling (118). Whether sgp130 also interferes with IL-6 cluster signalling appears to depend on the specific context (118,119).

Both subunits of the IL-6 receptor complex are expressed in high quantities on naïve $CD4^+$ T cells (120). Upon sensing of IL-6, one of the earliest cytokines produced by DCs upon stimulation by PAMPs, DAMPs and CD40 activation (32,58), IL-6Rα is downregulated in naïve T cells. In fact, the expression level of IL-6Rα in T cells is linked to the expression of the naïve markers CCR7 and CD62L (121) as these proteins are also cleaved by ADAM metalloproteases (122). While shedding of IL-6Rα might be the main mechanism to downregulate mIL-6Rα expression (123), ligand dependent and independent mechanisms of IL-6Rα internalisation have also been described (124,125). IL-6 signalling however drives T_{FH} differentiation, thus due to the low expression of mIL-6Rα on recently activated T cells it is believed that, similar to T_{H17} priming, T_{FH} differentiation requires IL-6 trans-signalling and cluster signalling (118,121). In these mechanisms the IL-6/sIL-6Rα or IL-6/mIL-6Rα complexes could be generated by proximal DCs. It has been shown that $SIRP1\alpha^+$ DCs (cDC2s) can mediate cluster signalling by loading IL-6 onto their IL-6Rα before displaying it on the cell surface which can then be recognised by mgp130 on recently activated cognate T cells (118). Once IL-6 has been recognised by activated $CD4^+$ T cells, there is an intracellular activating cascade involving STAT1, and particularly STAT3, that will ultimately drive Bcl6 upregulation leading to pre-T_{FH} differentiation (31,32,58,108). Fitting with this, IL-6, IL6Rα, gp130, STAT3 and STAT1 have all been shown to be important in $CD4^+$ T_{FH} differentiation and function *in vivo* in a range of contexts (40,58,126–129). Sensing of IL-6 by T cells enhances ICOS expression, required for the DC-mediated initiation process of T_{FH} commitment (130).

IL-6 is however neither absolutely required, nor solely involved, in $CD4^+$ T_{FH} priming (64,127). IL-6 deficient mice show a strong reduction of T_{FH} cells upon protein immunization, but T cell conditional *Il6ra*$^{-/-}$ mice only have a slight reduction in T_{FH} cells; yet their function is fundamentally impaired resulting in reduced GC B cells and specific antibody titers (130). Consistent with this observation, the development and function of T_{FH} cells during the later stages of chronic LCMV relay on IL-6, as *Il6*$^{-/-}$ mice exhibit diminished antigen-specific IgG1 and IgG2 responses (127). IL-6 production by B cells is therefore necessary for GC T_{FH} final differentiation and T_{FH} long-term maintenance (127,131,132). In this scenario IL-6 produced by B cells is sensed by pre-T_{FH} that, in response to IL-6, generate IL-21 to further drive the differentiation of T_{FH} in an autocrine feedforward loop while simultaneously maintaining T_{FH} IL-2 hyporesponsiveness, thus leading to GC T_{FH} differentiation (131,132).

Other than IL-6, IL-21, IL-27, IL-1β and IFNs α/β/γ are all context-dependent positive regulators for $CD4^+$ T_{FH} cell differentiation. IL-21, apart from being one of the main cytokines produced by T_{FH} cells to induce B cell help, is one of the main drivers of T_{FH} differentiation by acting through Vav1, generating a positive-feedback loop that promotes T_{FH} differentiation (133). IL-6 accentuates this process as it promotes IL-21 production by T_{FH} cells acting through c-Maf (134) and simultaneous removal of IL-6 and IL-21 results in reduced T_{FH} differentiation after acute viral infection (135). IL-27, a cytokine critical in promoting survival of activated T cells, further promotes this loop, as it is also involved in enhancing Bcl6 and IL-21 secretion by $CD4^+$ T cells and ultimately supporting GC formation and B cell function (136–138). IL-1β production by monocytes also promotes T_{FH} differentiation by enhancing the expression of the adaptor protein Myeloid Differentiation primary response 88 (MyD88) which activates the protein complex nuclear factor kappa-light-chain-enhancer of activated B cells (NF-ΚB) allowing Bcl6 transcription (139). This process is accentuated by IL-1β acting through IL1R1 which in turn enhances not only Bcl6 expression but also CXCR5 and ICOS (139). Apart from being involved in clearance of intracellular pathogens, interferons (IFNs) also have pivotal roles in driving T_{FH} fate. Type I IFNs can induce Bcl6, CXCR5 and PD-1 through STAT1 signaling (140). Type I IFN involvement in T_{FH} differentiation has been linked to increased production of all of the aforementioned cytokines (i.e IL-6 (141), IL-21 (139), IL-27 (136) and IL-1β (139)) indicating that IFN molecules support the response generated by pro-T_{FH} cytokines. IFN–α/β receptor-deficient mice (*Ifnar*$^{-/-}$) have impaired T_{FH} and antibody responses (141). Likewise, type II IFN (IFN-γ) also play a positive role in T_{FH} differentiation by upregulating Bcl6 expression (142). Therefore, depending on the antigen encountered, different DC subsets can use alternative IFN-dependent pathways to prime T-dependent B cell responses.

Cytokines involved in T_{FH} differentiation in mice have also been shown to be important in humans. IL-6 can be involved in T_{FH} differentiation and IFNAR signalling in human DCs promotes IL-27 production which in turn drives T_{FH} differentiation (137). There are however some species-specific differences in the T_{FH} differentiation process, with IL-12 having greater relative importance than IL-6 in human T_{FH} poise (143,144). In mice, IL-12 mostly signals through phosphorylation of STAT4, although it can also promote STAT3 activation (145). Similar to mice in humans IL-12 can bind both STAT3 and STAT4, but the first one is more important in driving pro-T_{FH} responses. Thus, STAT3 by binding the *Bcl6* promoter and recruiting RNA polymerase II is the most potent inducer of Bcl6 in humans and mice alike (40,108,146,147); with patients with Hyper IgE syndrome, which present STAT3 deficiency, having impaired T_{FH} differentiation and B cell help (146). Patients with IL-12Rβ1 deficiency, an IL-12 and IL-23 receptor subunit, have decreased GC T_{FH} cell frequency and a downregulated antibody response (148) as also observed in an *in vitro* human T_{FH} differentiation model (149). Thus, IL-23 is also an important regulator of human T_{FH} polarisation (143,144,150). Despite IL-12's known role in driving human T_{FH} differentiation, its role in mice remains

controversial. Some studies show a positive relation between IL-12 signalling and T_{FH} differentiation both *in vitro* (145) and *in vivo* (149) while others show a dispensable effect (151). Surprisingly, IL-12 blocks T_{FH} cell differentiation and contributes to GC suppression in a mouse model of salmonella infection (152). Therefore, while the role played by IL-12 in T_{FH} cell differentiation in humans is widely accepted, IL-12 involvement in mouse T_{FH} differentiation remains controversial and might be context- and antigen-specific.

Transforming growth factor β (TGF-β) is also considered an important co-factor to promote early differentiation of human T_{FH} cells. T_{FH} differentiation requires TGF-β-mediated repression of genomic organizer special AT-rich sequence-binding protein-1 (SATB1) (153). TGF-β acts in synergy with IL-12 and IL-23 to induce the expression of BCL6, c-MAF, CXCR5, PD-1, ICOS and IL-21 through STAT3, STAT4 and via small mothers against decapentaplegic (SMAD)2 and SMAD3 signalling while downregulating BLIMP-1 *in vitro* by human naïve $CD4^+$ T cells; a process that is enhanced by IL-1β (147,154). Similar to IL-12, TGF-β's role on murine T_{FH} differentiation continues to be a subject of debate. TGF-β has been shown to induce apoptosis of T_{FH} cells and limit their ability to produce IL-21 and ICOS both *in vitro* and *in vivo* (134,147,155). As with humans however, Satb1 repression is important for T_{FH} differentiation in mice (153) and some studies link TGF-β signalling with decreased T_{H1} and T_{H17} differentiation and an increase poise towards murine T_{FH} fate (70,156). Therefore, TGF-β seems to play an important role in driving T_{FH} differentiation in humans while in murine models it has a complex role.

Activated $CD4^+$ T cells are able to secrete activin A following stimulation via the TCR (157). Activin A, either independently or in concert with other signals, promotes the expression of human T_{FH} associated genes via SMAD2 and SMAD3 dependent pathways (154). Activin A's ability to drive T_{FH} cell differentiation is not conserved in mice, but it is in non-human primates (154,158).

Several cytokines can therefore drive T_{FH} differentiation in both mice and humans, with some being conserved among species and some being species-specific. IL-6 and IL-12 are respectively the main drivers of mice and human T_{FH} poise through STAT3 phosphorylation and Bcl6 upregulation.

Anti-T_{FH} cytokine microenvironment

There are also negative signals that prevent BCL6 expression and therefore inhibit the T_{FH} differentiation process. Paradoxically, IL-2, which is considered the main promoter of T cell proliferation, is the principal inhibitor of T_{FH} differentiation (36,42); with exposure to low doses of IL-2 treatment in patients with autoimmunity reducing circulating T_{FH} frequencies (159). IL-2 production by $CD4^+$ T cells occurs following high-affinity TCR engagement on naïve T cells and thus *in vivo* selective IL-2 desensitization during T cell priming is required to promote T_{FH}

differentiation. Naïve $CD4^+$ T cells receiving high affinity TCR signalling produce high amounts of IL-2, but concomitantly reduce IL-2R on their membrane. This inability to recognise IL-2 poises them towards a T_{FH} fate. Low-affinity TCR cells in the vicinity instead express high amounts of IL-2 receptors and are able to recognise the paracrine IL-2 produced by T_{FH} cells becoming alternative $T_{effector}$ cells (36).

The high-affinity IL-2 receptor consists of three subunits, CD25 (IL2-Rα), CD122 (IL2-Rβ) and CD132 (the common gamma chain or γc). The three IL-2R subunits are not pre-formed as stable heterodimers, and the current model is that IL-2 recognition promotes assembly of the trimeric receptor. IL-2 is first captured by CD25 resulting in a weak interaction. The CD25-IL-2 binary complex leads to a small conformational change in IL-2 that promotes the association with CD122. The ternary complex CD25-CD122-IL-2 then recruits CD132 through a weak interaction with IL-2 and a stronger interaction with CD122 to produce a stable quaternary high affinity IL-2/IL-2R interaction. IL-2 can either only bind CD25, resulting in a low affinity interaction, bind both CD122 and CD132 resulting in an intermediate-affinity interaction, or it can bind the trimeric receptor thus providing high affinity interactions. It is both through CD122 and CD132 that the JAK-STAT5 signalling transduction pathway is activated, as only IL-2Rβ and the γc have transmembrane signalling domains (160).

Mechanistically, IL-2 signalling promotes STAT5 phosphorylation, that by preventing the binding of RNA polymerase II to the Bcl6 locus inhibits the expression of Bcl6 and the T_{FH} gene program while promoting Blimp-1 upregulation. Thus, STAT5 directly competes with STAT3 to prevent T_{FH} differentiation (41,161,162). Cells receiving IL-2 in a paracrine fashion are more prone to phosphorylate STAT5 (163), further suggesting a role for paracrine IL-2 sensing in driving differentiation away from a T_{FH} phenotype (36). The IL-2 inhibitory cascade also prevents the phosphorylation of SMADs proteins, therefore preventing activation of TGF-β and Activin A intracellular pathways (154). IL-2 mediated mammalian target of rapamycin complex 1 (mTORC1) activation of protein kinase B (AKT) also suppresses T_{FH} differentiation (164). IL-2 signalling also prevents T_{FH} differentiation into GC-T_{FH} cells, as IL-6-mediated prevention of STAT5 binding to the CD122 locus is required for GC-T_{FH} differentiation (131).

Recently activated $CD4^+$ T cells in the vicinity of T_{FH}-precursor cells are not the only cells capable of quenching IL-2 from the microenvironment (36). $CD25^+$ T_{reg} cells are also able to do so, therefore promoting T_{FH} differentiation and antigen-specific GC responses (165). cDC2s also express high levels of CD25 but minimal to no levels of CD122, making them unresponsive to IL-2 (166,167) and therefore suggesting a role for controlling the IL-2 microenvironment during T cell activation. Their role at affecting T_{FH} differentiation is however controversial. A murine study showed that cDC2s in the spleen are able to quench IL-2 from the milieu by expressing soluble CD25 upon TCR

stimulation that in turn promotes T_{FH} differentiation (166). Contrary to this observation, *in vitro* generated DCs from human peripheral blood mononuclear cells (PBMCs) are able to 'lend' their membrane bound CD25 in *trans* to antigen-experienced $CD25^-$ T cells expressing CD122 and CD132, thus facilitating early high-affinity IL-2 signalling on T cells which is crucial for their expansion. The role on T_{FH} differentiation in this study was however not assessed (167). Meanwhile, activated B cells are also able to express IL-2 receptors in their membranes (168–171) but their function at affecting T_{FH} differentiation through a CD25-IL-2 pathway has not yet been established. IL-2 is therefore a crucial cytokine in driving T cell proliferation while preventing T_{FH} differentiation. Thus, its presence in the microenvironment needs to be tightly controlled to allow both T_{FH} and alternative $T_{effector}$ pathway differentiation.

Similar to IL-2, direct IL-7 recognition by T cells mediates activation of STAT5 that contributes to the repression of T_{FH} associated genes including Bcl6 (172,173). IL-7 signaling *in vivo* however can have a pro-T_{FH} effect. IL-7 can increase CXCL13 expression in the LNs, thereby promoting activated B cell and T_{FH} recruitment and therefore differentiation (174,175). It can also drive plasmacytoid DCs (pDCs) homing to the lymph node, which by secreting IFNs, can also promote T_{FH} differentiation (176). Moreover, a recent study has proposed a role for IL-7 recognition in the formation of memory-like T_{FH} cells which are able to give rise to effector T_{FH} cells in recall responses (79). Like IL-7, IL-15 can also have anti- and pro-T_{FH} roles. *In vitro* IL-15 *trans*-signalling to activated mouse $CD4^+$ T cells can repress Bcl6 expression while promoting Blimp-1-STAT5 signalling, which is capable of driving T_{H1} differentiation at the expense of the T_{FH} pathway (177). Interestingly however, direct IL-15 signalling by T cells has the opposite effect, as it allows an increased Bcl6 expression and the upregulation of a T_{FH}-like profile (177). Treatment of mice with IL-15 *in vivo* enhances T_{FH} differentiation, antigen-specific antibody levels and improves survival by signalling through NK-cell derived IL-10 (178). IL-10 is known to signal through STAT3 (179), but the exact mechanisms describing how IL-10 could drive T_{FH} differentiation are not known and require further investigation.

Overall, this data highlights that an IL-2 enriched microenvironment prevents T_{FH} differentiation and their maintenance. Conversely, IL-7 and IL-15 signalling can have an anti- or pro-T_{FH} response depending on the cell they are acting through.

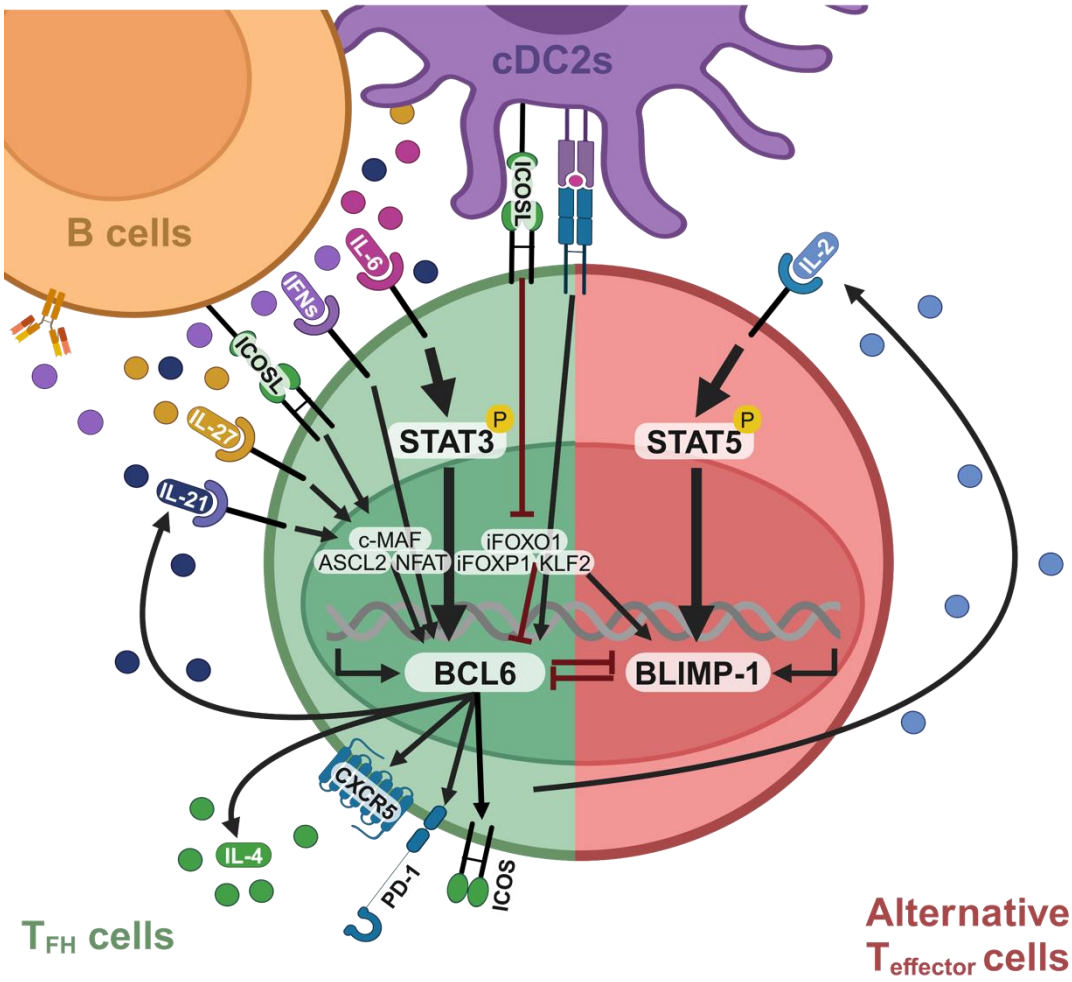


Fig 1.3. Murine signals influencing T_{FH} differentiation vs alternative $T_{effector}$ pathways.

Naïve $CD4^+$ T cells require of three signals to differentiate into $T_{effector}$ cells: Ag-TCR recognition, co-stimulatory signals and the presence of a specific cytokine milieu. pStat3/Stat5 balance affects this decision with signals promoting Stat3 phosphorylation leading to Bcl6 expression and therefore T_{FH} differentiation. Conversely, signals leading to Stat5 phosphorylation, most notably IL-2, lead to the upregulation of Bcl6's antagonist Blimp-1 promoting naïve $CD4^+$ T cells differentiation towards alternative $T_{effector}$ pathways at the expense of T_{FH} differentiation.

T_{FH} differentiation therefore requires the participation of multiple cell types, a high TCR and co-stimulatory signalling and a tight control of the cytokine microenvironment; with pro-STAT3 cytokines, such as IL-6 and IL-12, inducing T_{FH} differentiation while pro-STAT5 cytokines, such as IL-2, prevent it.

1.3 Alternative T helper pathways differentiated by the cytokine microenvironment

After the initial decision to a T_{FH} or alternative $T_{effector}$ fate is decided, those activated cells that upregulate Blimp-1 differentiate into alternative T helper pathways mostly depending on the

cytokine milieu encountered. The different T helper fates these cells can develop into are briefly described below *(**Fig 1.4**)*.

T helper 1 (T_{H1})

T_{H1} cells were, together with T_{H2}, the first subsets of $CD4^+$ T cells identified using murine models (180). IL-12 through phosphorylation STAT4, but also IL-18 and IFN-γ are the major drivers of T_{H1} differentiation. These signals upregulate the expression of the master transcription factor T-box transcription factor (T-bet) in mouse and humans. Once differentiated, T_{H1} cells produce IFN-γ and TNF-α which, through the activation of other immune cells including macrophages, NK cells and $CD8^+$ T cells, mediate intracellular infection clearance (181).

T helper 2 (T_{H2})

T_{H2} cells are considered the counterpart of T_{H1} cells. They are generated in an IL-4 enriched environment which through the phosphorylation of STAT6 promotes GATA-binding protein 3 (GATA-3) upregulation (181). IL-1β can also promote T_{H2} differentiation (182) and T_{H2} cells are also more prone to develop in an IL-2 enriched environment (183). As a result, these cells produce high amounts of IL-4, IL-5 and IL-13 which are key to mount an immune response against extracellular pathogens activating cells such as mast cells and eosinophils, therefore T_{H2} cells are also key contributors to allergic disease (184).

T helper 9 (T_{H9})

IL-4 and TGF-β, through phosphorylation of STAT6 and SMAD proteins, drive T_{H9} differentiation (185). In the absence of TGF-β, IL-1β can also promote T_{H9} differentiation (186). The primary master regulator for this subset is still ambiguous as it seems that a complex network of different transcription factors, most of which are also co-expressed in other T cell populations, play an important role. PU.1 however, which is encoded by the *SPI1* gene (187) and interferon regulatory factor 4 (IRF4), encoded by the *IRF4* gene (188) are normally chosen as the T_{H9} lineage defining factors. Although other cell types such as T_{H2}, T_{H17} and even T_{FH} can secrete IL-9, this is the classical interleukin expressed by T_{H9} cells which mediates allergic inflammation and responses against intestinal parasites (189).

T helper 17 (T_{H17})

T_{H17} cells are preferentially differentiated in the presence of IL-6 and IL-1β or TGF$-\beta$ through the phosphorylation of STAT3 and inhibition of Suppressor of cytokine signalling 3 (SOCS3)

respectively. In the absence of IL-6, IL-21 in combination with TGF−β can also drive T_{H17} differentiation through similar mechanisms (190). IL-23 is necessary for T_{H17} expansion and it also stabilises the T_{H17} phenotype, however it is not crucial to promote differentiation. Through these pathways the *RORC* gene is activated promoting the expression of the key T_{H17} molecule retinoic acid-related orphan receptor-γt (ROR-γt). T_{H17} cells produce IL-17A, IL-17F, IL-22 and Granulocyte-macrophage colony-stimulating factor (GM-CSF) which enhance neutrophil production and recruitment to the zone of infection (191). T_{H17} participate in inflammation disorders and they also counteract extracellular infections. Moreover, they maintain the human microbiota (192).

Regulatory T Cells (T_{regs})

In their attempt to counteract the infection and inflammatory processes, $T_{effector}$ cells produce mediators that can result in tissue damage. Regulatory T cells (T_{regs}) suppress $T_{effector}$ cells and are therefore involved in tissue repair (193). There are two main types of T_{regs}. Thymic T_{regs} (tT_{regs}) originate in the thymus as a single population of $CD4^+$ T cells. Conversely, the peripheral T_{regs} (pT_{regs}) arise from naïve T cells that encounter antigen in the periphery in the presence of IL-2 and TGF-β (194). Both cell types express high amounts of the IL-2 receptor CD25 as well as the co-stimulatory molecule Glucocorticoid-induced TNFR family-related protein (GITR) (195). FOXP3 is the transcription factor that designates T_{regs} fate. Once activated, T_{regs} secrete inhibitory cytokines such as IL-10, TGF-β and IL-35 (196).

T follicular regulatory cells (T_{FR})

As with T_{FH} cells T_{FR} are located within the B cell zone of the SLOs, they however have a regulatory role and therefore share aspects of the T_{reg} and T_{FH} subsets. They normally develop from tT_{regs}, although under specific circumstances they can also arise from pT_{regs}. As T_{FH} cells they require IL-6 for their differentiation into T_{FR} cells, a process that occurs in the periphery irrespective of T_{reg} origin. They express both BCL6 and FOXP3 as transcriptional regulator factors and, similarly to T_{regs}, act to suppress T_{FH}-mediated B cell help (197–199).

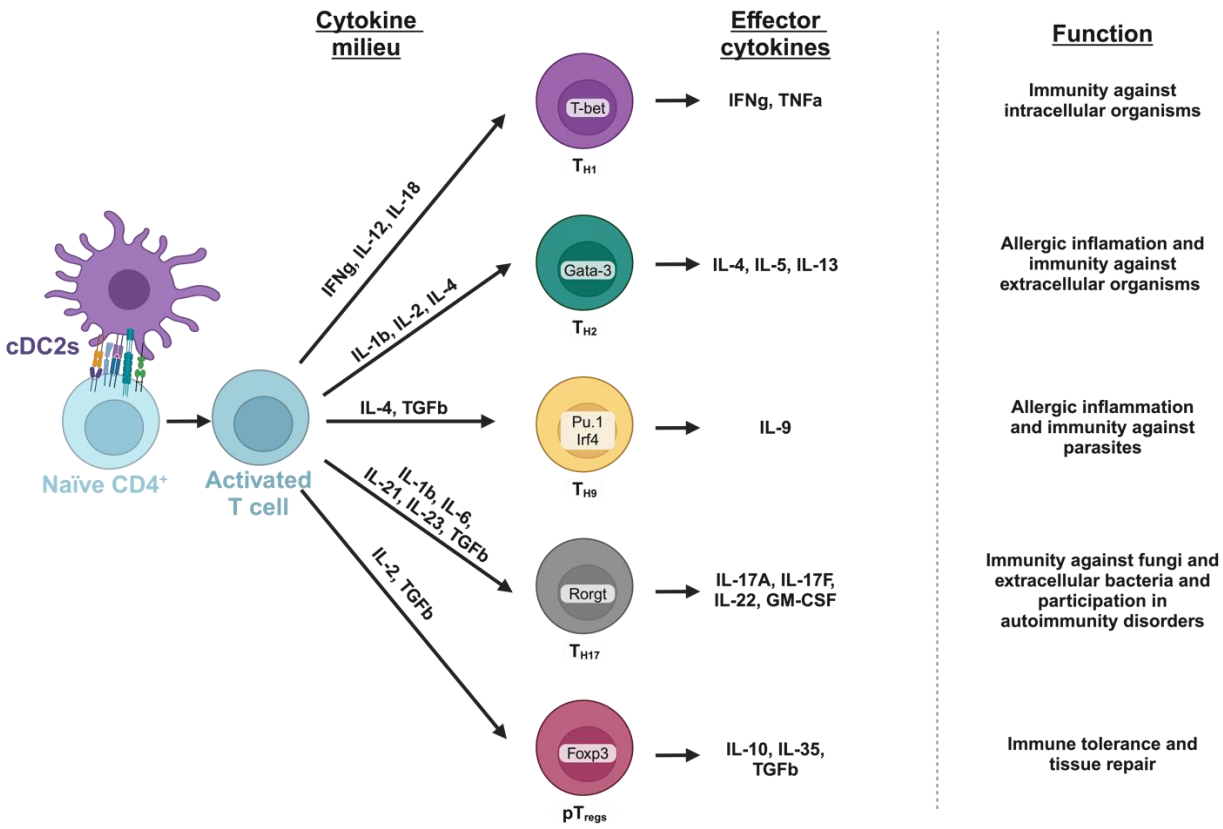


Fig 1.4. Alternative CD4⁺ $T_{effector}$ subsets arising from activated T cells

Naïve CD4⁺ T cells can be activated by cDC2s through TCR:MHC-II engagement of cells carrying cognate antigen and co-stimulation molecules. The differentiation into different T helper subsets is highly dependent on the cytokine milieu they encounter at the time of differentiation promoting their poise towards T_{FH} or alternative $T_{effector}$ subsets like T_{H1}, T_{H2}, T_{H9}, T_{H17} or peripheral $T_{regulatory}$ cells (pT_{regs}). Once activated these T cells will express lineage defining transcription factors which will allow them to secrete different effector cytokines to induce a specific immune response.

1.4 High affinity B cell responses require T_{FH} cell help

Similar to T_{FH} differentiation, B cell differentiation and production of high affinity class-switch antibodies is also a multi-step process requiring the participation of several cell types and a coordinated spatiotemporal migration inside the SLOs.

1.4.1 B cell activation and differentiation

B cell activation occurs when circulating naïve B cells encounter an antigen specific for their BCR. B cells can either recognise soluble antigen (200) or immune complexes associated to macrophages in the lymph node subcapsular sinus or to FDCs (201–204). Co-ligation of the BCR signalling with co-receptors including CD19 and CD21 further promote B cell activation (205). These B cells can then internalise their antigen/BCR complexes into the immunoproteosome and

process the antigen to be presented on MHC-II (206). B cells then upregulate CCR7 and migrate to the T:B cell border to present their peptide/MHC-II complexes to cognate pre-T_{FH} cells (207). Upon antigen recognition T_{FH} cells can provide B cell help driving full B cell activation and differentiation into GC B cells that can mature into memory B cells or PCs (208). As T_{FH} cells, GC B cells express high levels of Bcl6 which is critical for their development (209,210)

The GC is split into two distinct zones: the light zone (LZ) and the dark zone (DZ). DZ GC B cells are $CXCR4^{hi}CXCR5^{low}CD86^{low}$ cells known as centroblasts. Centroblasts undergo rapid proliferation and go through the process of somatic hypermutation (SHM) allowing them to accumulate mutations in the variable region of their BCR locus. Centroblasts can downregulate CXCR4 while upregulating CXCR5, becoming centrocytes ($CXCR4^{low}CXCR5^{hi}CD86^{hi}$ cells), which allows them to migrate from the CXCL12 enriched environment of the DZ into the CXCL13 high environment of the LZ. Centrocytes are non-dividing cells that can interact with FDCs, a source of continuous antigen and CXCL13, and present antigen to GC-T_{FH} (208). GC-T_{FH} being 'rate-limiting' will only provide survival and differentiation signals to those B cells carrying the highest affinity BCR receptors for their cognate antigen within the LZ. Thus, B cells carrying low affinity BCRs can undergo apoptosis, those with high affinity meanwhile re-enter the DZ to accumulate more mutations, while some of those with the highest affinities undergo further differentiation into antibody secreting PCs or memory B cells, leaving the GC (208,211–213).

PBs are the rapidly produced and short-lived effector cells that generate an early antibody response. It is thought that PBs can represent an early stage of PC differentiation as they undergo limited to no SHM (214). By upregulating expression of Blimp-1, PCs downregulate the GC B cell program, become larger, and no longer express surface BCR, CD19, B220 or MHC-II molecules, instead possessing extensive endoplasmic reticulum allowing enhance antibody production capacity (214). PCs also upregulate bone marrow homing receptors that allow them to migrate to the bone marrow niche, where transition from a short-lived PC to a long-lived PC occurs, but they can also be found in other body sites, both lymphoid and non-lymphoid organs (214–216).

Unlike GC B cells and PCs there is no known master regulator for memory B cell differentiation and thus their differentiation pathway is currently less well understood. Chronologically the majority of memory B cells exit the GC earlier after initiation of an immune response than PCs (217). As a result, memory B cells have generally undergone less SHM, and thus have lower affinity compared to PCs (218). Upon exiting the GC, memory B cells can be retained within the lymphoid tissues or migrate to the site of inflammation. There, they can either terminally differentiate into antibody-secreting cells, re-enter GCs accumulating more specificity, or become a long-lasting source of immune memory ready to respond to antigen re-encounters (219).

1.4.2 Generation of class-switch high affinity antibodies

The process of class switch recombination (CSR), that allows the formation of antibodies of multiple isotypes, commences upon T cell priming and it normally occurs outside of GCs (45). The GC is however essential for the generation of antibodies of high affinity via the processes of somatic hyper mutation (SHM) (45). Both CSR and SHM are initiated by the enzyme activation induced cytidine deaminase (AID), which is expressed in B cells and converts deoxycytidine nucleotides to deoxyuracil. As deoxyuracil is not normally found in DNA, its presence initiates repair processes that drive CSR and SHM (220–222)

1.4.2.1 Class switch recombination (CSR)

CSR is a process by which the isotype of the antibody is changed, therefore altering antibody function, while their antigen affinity is maintained (45). The gene locus of the Ig constant region contains multiple constant domains referring to different antibody subtypes. In mice, the order of the heavy chain exons is IgM, IgD, IgG3, IgG1, IgG2b, IgG2a/c, IgE, IgA. Naïve B cells produce both IgM and IgD, which are the first two heavy chain segments in the immunoglobulin locus. During CSR, portions of the antibody heavy chain are permanently removed from the chromosome and the gene segments surrounding the deleted portion are re-joined to retain a functional antibody gene that, upon transcription, produces antibodies of a different subtype (IgA, IgG or IgE). With the exception of IgM and IgD, only one antibody class is expressed by a B cell at one point in time (223).

Cytokine signalling from T_{FH} is important for promoting CSR, with specific cytokines determining the resulting isotype. For example, in mice, IL-4 drives IgG1 and IgE switch, while IFN-γ promotes IgG2a production and TGF$-\beta$ promotes an IgA switch (47). IgA is the main antibody isotype found in mucosal surfaces and plays a critical role in providing protection from inhaled and ingested pathogens. It is also important in maintaining commensal bacterial populations (224,225). IgG is the predominant isotype within serum, with different IgG subclasses driving distinct immune functions. IgG1 is the most prevalent of the different isotypes and it is involved in mediating responses to soluble and membrane antigens. Since allergies are associated with an increased IL-4 microenvironment, an IgG1 subclass is also prevalent in these diseases. A high IFN-γ environment drives the production of IgG2a/c antibodies. Thus, they are linked with T_{H1} responses and intracellular pathogen (such as viral) clearance (226–229). IgG2b and IgG3 are generated early in the immune response and increase pathogen clearance by activating complement, allowing antibody opsonization for phagocytosis and inducing antibody dependent cellular cytotoxicity (228,230). Finally, IgE mediates allergic responses by binding to Fc receptors on basophils and mast cells driving their activation upon antigen recognition (231,232). Overall, CSR allows

antibodies to change their isotype from IgM and IgD to IgA, IgG or IgE, allowing context specific effector functions, while maintaining their BCR affinity and specificity.

1.4.2.2 Somatic hypermutation (SHM)

SHM occurs within DZ centroblasts and here AID introduces mutations into the variable region of the Ig heavy and light chains of the BCR. This is then repaired using terminal deoxynucleotidyl transferase (TdT), an error-prone polymerase resulting in point mutations, insertions or deletions, that can increase, decrease or have no impact on BCR affinity while the isotype of the antibody remains unchanged (233,234). These B cells then move to the LZ where B cells bearing high affinity BCRs are selected via cognate interactions with T_{FH} cells. Thus, it is through the process of SHM that B cells acquire high affinity for antigen.

1.5. Differences in T cell dependent antibody responses in early life and adulthood

1.5.1. Differences in T_{FH} and B cells in children and adults

As introduced above the generation, expansion and functional differentiation of antigen-specific T and B cells is the central hallmark of adaptive immunity, and appropriate help from antigen-specific $CD4^+$ T cells is essential for the generation of high-quality, long-lasting B cell responses. T_{FH} and B cell differentiation and the humoral response they generate are however diminished in early life when compared to adults, this section therefore focuses on these two cell types and how are they altered in early life.

1.5.1.1 T_{FH} function is reduced in early life

In both humans and mice T_{FH} differentiation, and the subsequent GC B cell response they promote, are reduced in early life after vaccination or infection (13,25,235,236). T_{FH} cells that do differentiate are also functionally distinct from those seen in adults, with altered cytokine production and increased regulatory functions (235,237,238).

The capacity of antigen-specific $CD4^+$ T cells to differentiate into T_{FH} is reduced in infancy when compared to adulthood after respiratory virus infection (25). Studies in mice show that neonatal T_{FH} fail to display the same fully matured GC-T_{FH} phenotype observed in adulthood, appearing to be lodged in a pre-T_{FH} stage that limits their ability to fully promote B cell survival and differentiation (238). Adoptive transfer experiments indicate these changes are dependent on both T-cell intrinsic and extrinsic factors (21,239). Specifically, neonatal T cells fail to upregulate Bcl6 to levels observed

in adult T_{FH}, along with a host of T_{FH}-related genes including *Cxcr5, Tbk1, Ascl2* and c-*Maf*, hindering both differentiation, homing to the GC and appropriate interactions with GC B cells (235,238).

T_{FH} that do differentiate in early life also display altered functionality. While adult T_{FH} can support GCs that are sustained for months, which allows multiple rounds of SHM and increased affinity maturation (44), neonatal T_{FH} are shorter-lived, as are other neonatal $CD4^+$ T cell subsets, hindering this cycle (238). Cytokine production by T_{FH} cells is also altered in early life, with reduced expression of IL-4 and IL-21, but increased expression of IL-13 (235,238). While both IL-4 and IL-13 are canonical T_{H2} cytokines located within the T_{H2} locus, in adult LNs T_{FH} are the major source of IL-4 across a range of inflammatory stimuli but do not produce IL-13 (47,240–242); Specifically IL-4 is produced by T_{FH} in a Gata3 independent fashion through use of a distinct upstream element, that does not result in the production of IL-13 (242,243). In neonates, reduced T_{FH} IL-4 and IL-21 production is accompanied by a decreased expression of the IL-4R and IL-21R by neonatal GC B cells impacting B cell survival, proliferation and differentiation (237). While less is known about the impact of increased IL-13 production in neonates, aberrant production of IL-13 by adult T_{FH} has been associated with IgE-mediated anaphylaxis in mice and humans (244,245).

1.5.1.2 Reduced somatic hypermutation by B cells in early life

As with neonatal T cells, neonatal B cells display distinct qualities to those observed in adults. Murine B cells can be subdivided into B1 and B2 cells, with B1 cells being predominant in early life (246). B1 cells appear to represent a more innate-like subset of B cells with a limited BCR repertoire, probably due to low TdT and reduced expression of AID leading to diminished SHM and CSR (247). As a result, B1 cells produce more polyreactive IgMs (248). B2 cells on the other hand readily enter the GC and are capable of producing high titre, antigen-specific, high-affinity antibodies (249). The existence of B1 cells in humans is a subject of debate (reviewed in (250)), but reduced antibody production, enhanced IgM secretion and poor SHM are features commonly seen in human neonatal B cells (251–253).

1.5.1.3 Impaired T-B cell crosstalk in early life

Affinity maturation within the GC relies on tight cognate interactions between T and B cells facilitated by MHC:TCR, co-stimulation and soluble mediators. Murine neonatal B cells express both lower levels of MHC-II and co-stimulatory proteins compared to adult B cells (254,255). CD40 expression in particular is reduced in neonatal B cells (256), and concomitantly neonatal murine and human $CD4^+$ T cells have reduced CD40L expression (257,258). CD40 regulates PC precursor development in a dose-dependent manner (259) and CD40-CD40L interaction promotes ICOS-L

expression by B cells (38), which in turn induces PI3K signalling in T_{FH} (68) allowing nuclear exclusion of Foxo1 and maintaining T_{FH} phenotype and function (80). CD21, a complement receptor, and TACI, a receptor for trophic factors, are also decreased in neonatal B cells (260,261). The above, alongside likely, as yet, unidentified differences between neonatal and adult T and B cells, all contribute to the distinct output of neonatal GCs compared to adult GCs.

1.5.1.4 Neonatal GCs display enhanced regulation

The early life immune system is poised towards tolerogenic responses, this age is therefore often characterized by an increased T_{reg}:$T_{effector}$ ratio (262,263). Neonatal T_{regs} possess a distinct phenotype to those found in adults, with an increased ability to proliferate and a more potent suppressive activity (264) including those located within the B cell zone, T_{FR}. As with T_{regs}, neonatal T_{FR} are preferentially positioned to exert higher inhibitory functions than their adult counterparts. They are located in the interfollicular regions of the B cells zone and GCs, rather than in the T:B border, as observed in adulthood (237). There are also increased numbers of T_{FR} compared to T_{FH} in early life SLOs (237), and the low IL-21 production by neonatal T cells is linked with increased T_{FR} proliferation (265).

IL-10 producing regulatory B cells (B_{regs}) are also enriched in human cord blood and neonatal mouse spleen when compared to adult tissue (266,267). Indeed, while neonatal human and mouse B cells have a similar expression of pattern recognition receptors to their adult counterparts, their activation promotes an anti-inflammatory environment, rather than the pro-inflammatory environment seen in adult B cells (268,269). Overall GC intrinsic changes in differentiation, cross-talk, effector and regulatory functions in the neonatal T and B cell compartments could explain most of the differences observed in T-cell dependent antibody production between neonates and adults.

1.5.2. Support cells and their alterations in early life

T and B cells may represent the “output” of the adaptive immune response, but their generation and maintenance rely on regulation and support by a network of other hematopoietic and mesenchymal cells; “support” cells that are equally as distinct in early life compared to adulthood, and which can alter the generation of antibody-mediated immunity.

1.5.2.1 Neonatal dendritic cells fail to promote complete T_{FH} differentiation in early life

Conventional dendritic cells (cDCs) can be sub-classified into cDC1s, the main drivers of $CD8^+$ T cell responses, and cDC2s, efficient at promoting $CD4^+$ T cell activation (270); cDC2s being particularly critical for T_{FH} differentiation, with *Zbtb46*, *Dock8* and *Irf4* deficiencies all resulting in the absence of T_{FH} and abrogated antibody responses (271,272). Ongoing immune development in

early life means identifying distinct cDC subsets is challenging (summarized in (270)). The DC pool is however clearly highly dynamic in early life with the frequency of murine DCs dramatically increasing with age (273); a process at least partially modulated by maternal diet. For instance, a high-fibre maternal diet can promote Flt3L expression in newborn pups, a growth factor needed for the final development of cDC2s (274,275). In mice there is also an increased cDC1:cDC2 ratio in the first 3 weeks of life (276,277); however in humans cDC distribution, maturation and migration are largely maintained from infancy through old age with tissue sites determining the difference in cDC1:cDC2 ratio (278).

Both murine and human neonatal DCs appear to have decreased expression of surface markers (collected in (270)) such as MHC-II alongside co-stimulatory ligands for CD28 and ICOS (277). Similarly to B cells, cDCs promote an anti-inflammatory environment in response to PAMPs; resulting in T_{reg} differentiation at the expense of alternative T helper pathways (279). Early life DCs also produce less cytokines when compared to adults (277) with decreased IL-12, a key T_{H1} and T_{FH} differentiation signal in humans, having been reported (Sun et al. 2005; Renneson et al. 2009; Kleer et al. 2016).

1.5.2.2 Impaired micro-organization of the secondary lymphoid organs in early life due to differences in the follicular stroma

The stroma of the SLOs also plays a critical role in shaping GCs. FRCs organise the SLOs' microarchitecture by allowing compartmentalization of T and B cells while directing the leukocyte traffic to promote antigen encounter (29). Follicular dendritic cells (FDCs) meanwhile are the first primers of B cell responses, as B cells can recognise antigens presented on the surface of FDCs, and FDCs sustain B cell survival through the secretion of trophic factors (204) as well as organising lymphocyte trafficking (284). In infancy there is a reduced frequency of both FRCs and FDCs in SLOs, compromising the organization and B cell response (247). A lack of lymphotoxin-β receptor (LTβR) signalling in FRCs during early life, but not adulthood, can compromise the capacity of GCs to support CSR and PC homing to peripheral organs, affecting antibody production (285). In line with other approaches that seem to circumvent the poise of the neonatal immune response, immunization with a suitable adjuvant, such as CTA1-DD or LT-K63, can overcome these deficits and promote FDCs function in neonatal mice, enhancing GC responses (286,287).

1.5.3. Anatomical Sites

While the generation and maintenance of high affinity antibody-mediated immunity has historically focused on activities within the SLOs, it is increasingly apparent that other tissue sites are vitally important in these processes.

1.5.3.1 Generation of ectopic germinal centre structures at the forefront of antigen exposure in infancy

GC reactions routinely seen in the SLOs, are also seen within peripheral tissues in certain circumstances. For instance, a recent study of human paediatric and infant tissue found that in early life the human immune system may rely more on the formation of ectopic GCs within sites such as the lungs (288). Indeed, the formation of bronchus-associated lymphoid tissue (BALT), where ectopic GCs in the lung are found, develops during the first years of life and declines through age, coincident with the maturation of the SLOs as the primary site for antibody production and the rise of immunological memory (288,289). BALT can support GC formation, B cell differentiation and CSR but with a reduced level of SHM when compared to SLOs (288). B cells from these ectopic structures have a distinct BCR repertoire, and are more activated, when compared with lung-draining lymph node B cells, further suggesting *in situ* development and expansion of these structures independent from the SLOs (288). Indeed, murine studies have shown that inducible BALT (iBALT) can form in the absence of SLOs, with this being particularly pronounced when mice are exposed to local microbial signals, such as LPS, in early life (290,291). Of note, the type of T_{FH} present in both iBALT and tertiary lymphoid structures (TLS) in other sites such as the gastro-intestine (292), is also distinct from that found in the SLOs, with those in the TLS closely resembling T_{H17} cells (293,294). Overall indicating that the tissue location of T-cell dependent help to B cells alters as we age, and with it the functional output from these interactions.

1.5.3.2 Growth-dependent thymic involution

The thymus is the organ responsible for generating immunocompetent and self-tolerant T cells. Despite its significant function most mammals undergo thymic involution, which consists of a loss in thymic epithelial cells that are replaced with adipose tissue therefore reducing thymic output. Human thymic involution is thought to begin as early as one year of age and continue throughout adolescence (295). Involution in mice starts from 4-6 weeks after birth (296,297) which corresponds to pre-puberty in humans (7-11.5 years) (298). Due to the earlier onset of thymic involution in humans a more pronounced phenotype is expected, but in both humans and mice thymic involution has been measured by decreased thymic cellularity, changes in thymic epithelial space and a reduced number of recent thymic emigrants (299). Because at these ages most other organs don't show evidence of immunoaging, thymic involution has been subdivided into two phases in both human and mice. Growth-dependent and age-dependent thymic involution with the first one associated with early life and the second one with senescence. The early phase of thymic involution might be explained by a bioenergetic trade-off in which the thymus is forced to rapidly develop to accommodate for the high demand of naïve $CD4^+$ T cells needed to fill the empty T cell pool as newborns. T cell production however comes with a high energetic demand used for T cell

differentiation and selection, especially when considering the high elimination rate of inadequate T cells. Thus, once the T cell repertoire is established and because T cells are long-lived, the bioenergy is redistributed to alternative organs leading to thymic involution (299). This distinct need of thymic output between children and adults is observed in historic thymectomy's experiments (300). Thus, differences in $CD4^+$ T cells between early life and adulthood could be explained by recent thymic emigration during childhood.

1.5.3.3 Compromised B cell niches in early life

Long-lived PCs, differentiated from activated B cells, produce and maintain serum antibody levels (214). Therefore, alongside a reduced generation of PC differentiation from GCs, regulation and maintenance of PCs in early life also influences the antibody responses seen in infants.

B cell development begins in the bone marrow, with pro-B cells arising from a common lymphoid progenitor population (301). In humans the total number of B cells peaks in the first year of life, with a high B cell production rate in the bone marrow, resulting in a B cell landscape dominated by those with a naïve phenotype when compared to adults (302); precursor B cells then rapidly decrease during the first two years of a child's life, with decline continuing, albeit less rapidly, until adulthood (303). Likewise, generation of PCs is also greater in infants (6-11 months old), approximately tenfold higher than that seen in adults (18-39 years old) (253). Total circulating IgD and IgM however only reach adult-like concentrations by two years of age. Meanwhile, the class-switched antibody pool, mostly comprised of IgAs and IgGs, is only 60 to 70% of adult concentrations by three years of age (304). Some antibody effector functions, such as NK cell activation, are still reduced in four-year-olds and require more time to develop (236). While other classes of antibody stabilise and peak in adulthood, IgE concentrations go up over the first few years of life, peaking in later childhood, before reducing in adulthood (305).

One explanation for the contrast between PC numbers and antibody concentration in infancy is likely the reduced homing of neonatal PCs to the bone marrow (BM) (306) combined with a failure to maintain long-lived PCs within the neonatal BM niche (307); recently differentiated PCs are highly pro-apoptotic (308) and neonatal BM has reduced expression of macrophage derived pro-survival factors (309). Alongside reduced concentrations of antibody there is also a shift in antibody subclass with age. The relative abundance of IgA1, IgG1 and IgG3 is higher in early life, while peak concentrations of their isotype counterparts IgA2, IgG2 and IgG4, which also display greater levels of SHM and higher antigen affinity, are only reached during adulthood (253,310). Indeed, reduced SHM is frequently observed in infancy probably due to the compromised GC response highlighted above (251,252,311).

The immune system is therefore distinctly poised in early life compared to adulthood, to meet the distinct demands of perinatal life. One outcome of this is a reduced ability to generate T-cell dependent, class-switched, high affinity antibody responses; which limits the ability of infants to form long-term protective immunity rendering them more vulnerable to infections *(Fig 1.5)*.

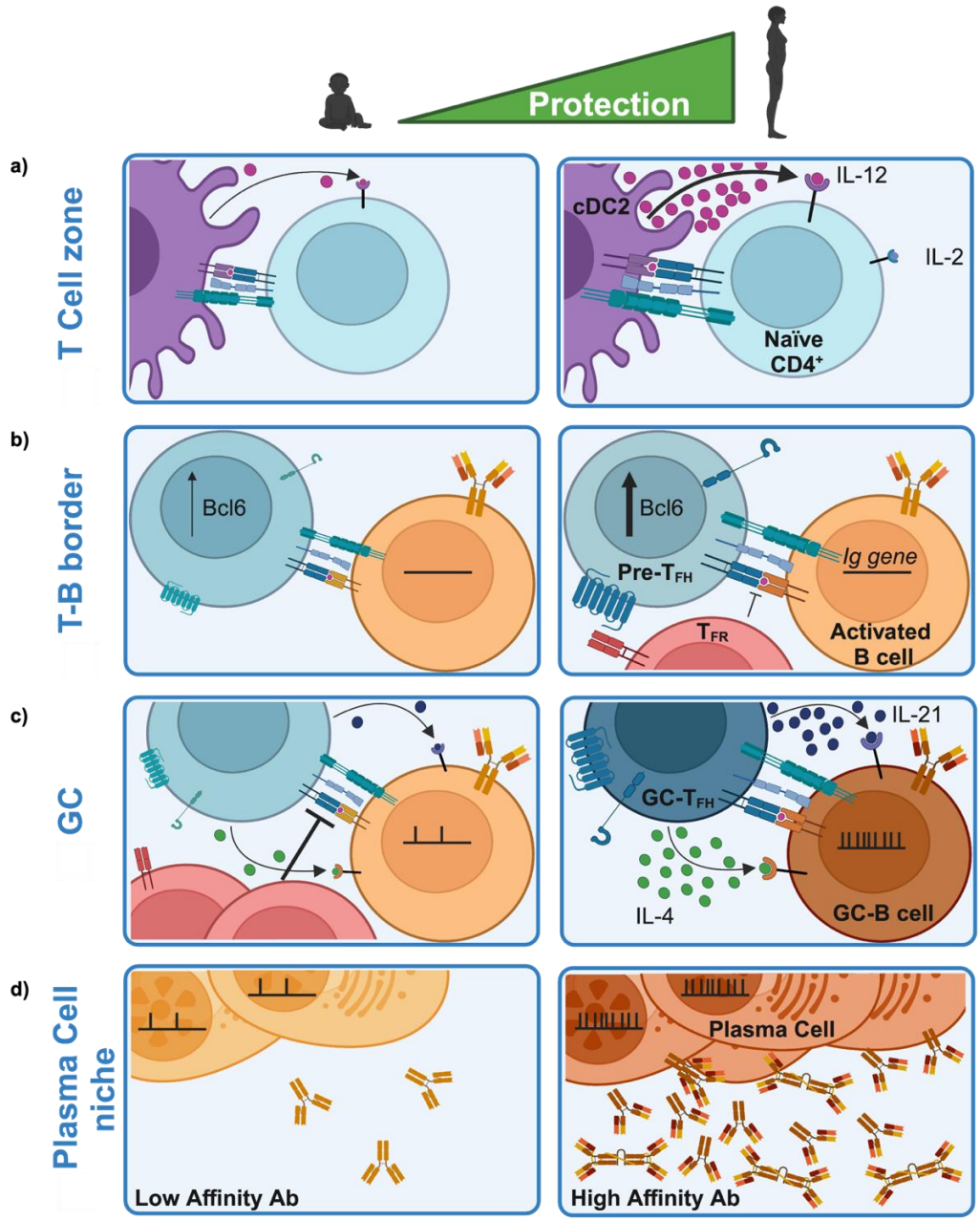


Fig 1.5. High affinity antibody responses are reduced in early life

The production of T-dependent antibody responses starts in the T-cell zone of secondary lymphoid organs. **(a)** Naïve $CD4^+$ T cells interact with cDC2s. In early life a low abundance of pro-T_{FH} factors generated by cDC2s prevents naïve $CD4^+$ T cell differentiation towards pre-T_{FH} cells. **(b)** These pre-T_{FH} fail to effectively migrate towards the T-B border where in adults a second interaction with the antigen presented by B cells further promotes the differentiation of both T and B cells and initiation of a GC. **(c)** Within the GC early life T_{FH} provide altered, and more limited, help to GC B cells. The low GC response observed in infancy is accentuated by the increased presence of regulatory T_{FR} within the GC. **(d)** Overall, there is therefore a reduced frequency of high affinity plasma cells within plasma cell niches and reduced production of antibody, alongside an altered antibody subclass profile. *Adapted from Labeur-Iurman & Harker* (7).

1.6 Respiratory Syncytial Virus – a major pathogen in infancy

RSV infections mostly result in mild or asymptomatic disease, but especially in infants and the elderly, RSV can cause severe disease resulting in hospitalization or even death. RSV infection has an estimated global incidence of over 30 million cases in children younger than 5 years, with hospitalization for RSV-associated respiratory tract infection of an estimated 3.6 million and 101,400 deaths in 2019 (312). RSV-associated deaths therefore represent 1 in every 50 deaths in children younger than 5 years and 1 in 28 deaths in children aged 28 days to 6 months (312). These numbers are probably an underestimation as most of RSV infection and death occurs in low-income countries, and RSV is estimated to be the 2nd biggest infectious killer in children under one year of age (4). Almost seven decades after its discovery, it still remains the commonest viral cause of serious respiratory illness in children under one year of age and the major cause of infantile bronchiolitis (4). Children can be re-infected with the same serotype of virus even within one cold season and re-infection is common even in adults (313–315). There is no specific treatment for RSV infection. Two vaccines have recently been licensed for use in the elderly and during pregnancy and are now being trialled for use in infants. It is therefore vital to better understand the early life immune response against RSV to promote the development of efficient vaccines targeted to this age group.

1.6.1 RSV viral structure

RSV belongs to the family of *Paramyxoviridiae*, order *Mononegavirales* and it is an enveloped, non-segmented negative-strand RNA virus. It's 15.2Kb genome comprises 10 genes that encode 11 proteins, as the M_2 mRNA contains two overlapping open reading frames resulting in $M_{2\text{-}1}$ and $M_{2\text{-}2}$ (316). RSV is classified into two distinct subgroups dependent on antigen variability, type A (RSVA) and type B (RSVB) (316). Unlike influenza, being non-segmented, RSV cannot reassort genome segments and undergo rapid antigenic shifts (317). Despite this, RSV has a mutable genome due to its dependence on RNA polymerase that lacks the capacity for RNA proofreading and editing. Nevertheless, RSV has remained stereotypically stable and, in fact, the relative antigenic stability of RSV makes the apparent lack of effective immunological memory all the more striking.

The outer envelope of RSV contains the surface glycoprotein (G), the fusion (F) protein and the small hydrophobic protein (SH). The G protein is the most varying structure among RSV strains and dictates the antigenic nature between RSVA and B. It is involved in the attachment of the virus to host cells. There is a soluble version of the G protein (sG) that acts as an antigen decoy mechanism that can bind antibodies and prevent their attachment to viral particles (318). The F protein is highly conserved between RSV subtypes and thus is the focus of pharmaceutical treatments and vaccine development. It is involved in viral membrane fusion and syncytium

formation (319). The SH protein is a viroporin, capable of forming ion channels in cellular membranes. It is not involved in viral entry, but by interfering with the normal function of the host cell, it allows infection to be possible (320). The matrix (M) protein is located underneath the envelope and is involved in the assembly of viral particles as well as in reducing the transcriptional activity of host cell genes (321). The nucleocapsid (N) protein, the phosphoprotein (P), the transcription factor M_2 and the large RNA-dependent RNA-polymerase (L) are all found in an inner nucleocapsid that wraps the genomic RNA and collectively constitute the viral replication (VR) complex (322). The non-structural proteins NS_1 and NS_2 are virulence factors that can inhibit the host immune response by blocking the type I interferon response and delaying apoptosis of infected cells (323,324).

1.6.2 RSV viral replication

Transcription and replication of viral genomes occur within cytoplasmatic virus-induced spherical inclusions, commonly referred as inclusion bodies. The viral replication cycle can be divided into three steps: entry, replication and assembly and budding. The final outcome of viral replication is the production of mature virions which can infect subsequent cells (325).

1.6.2.1 Entry steps:

RSV infectious cycle starts with the attachment of the virion to host cell mediated by the two viral F and G proteins. G would mediate initial RSV attachment through interactions between its two mucin-like domains with glycosaminoglycans (GAGs), which are unbranched disaccharide polymers linked to transmembrane glycoproteins (326,327). Another host cell attachment factor thought to interact with G is the fractalkine receptor CX3C-chemokine receptor 1 (CX3CR1) (328). RSV can also activate toll-like receptors (TLRs) 2 and 6 through the recognition of the RSV G protein (329,330). The initial contact with the G protein to the host membrane allows the engagement of a secondary receptor causing the activation of the F protein and allowing membrane fusion. Several host proteins have been proposed to interact with F to facilitate RSV entry and cell activation. These include nucleolin and the co-receptor candidates epidermal growth factor receptor (EGFR), insulin like growth factor 1 receptor (IGF1R), intercellular adhesion molecule 1 (ICAM1), TLR4 and C-type lectins (331–340).

The F protein is synthetized as an inactive F_0 precursor and is cleaved intracellularly by furin-like host proteases (341). The proteases generate two subunits: F_1 and F_2, which are covalently linked to create a heterodimeric structure called protomer. Three of these protomers associate to form the mature trimeric form of the F protein in the prefusion conformation (319). Membrane fusion is triggered by a major transconformation of the F protein, a process that is believed to be catalysed by binding to the host cell receptors (342). There are thus two forms of this protein: a pre-fusion

form, which is the form present on the surface of the virion, and a post-fusion form, which is the most stable form that allows membrane-membrane interaction. The structures of both forms are extremely different (343,344). The prefusion F conformation has a spheroidal shape with the fusion subunits buried inside the central cavity of the protein. In this conformation the F protein is unstable and has a low energy barrier to refolding. During the refolding process, the fusion subunits are withdrawn from the central spherical cavity of the protein and are projected away from the viral membrane forming a long α-helix. If another membrane, such as a host cell membrane, is in close proximity, the fusion subunits will insert into the adjacent membrane. The F protein continues to refold in the amino termini and carboxyl termini of the F_1 subunit, forming a trimer of hairpins that brings the two membranes together and facilitates fusion. The number of F proteins required to form a fusion pore has not yet been determined. The refolding process of F is irreversible, and the postfusion conformation of F is extremely stable allowing pore formation to persist through time (319).

Despite eliciting neutralising antibodies in people that have been infected, RSV F does not undergo substantial antigenic drift. In fact, and unlike the G protein, the sequences of F ectodomains differ by ~5% between RSVA and RSVB making it an ideal target for vaccine development. A vaccine against RSV should promote the production of antibodies against specific antigenic sites in the prefusion form of F, which would be able to neutralise the F protein before it promotes fusion; therefore inhibiting viral entry and propagation between cells. Most of the drugs in development or on the market are in fact fusion inhibitors, targeting the prefusion F protein with several of them being validated in humans. This is the case of Nirsevimab, a stable monoclonal antibody given to children during their first RSV season (345), or the newly developed RSV vaccine for pregnant women (346).

1.6.2.2 Viral RNA synthesis

The fusion between the viral envelop and cell membranes ensures the release of the virion into the cytoplasm. Viral RNA synthesis occurs in the cytoplasm of the infected cell. The polymerase L together with its co-factors P and $M_{2\text{-}1}$ ensures both transcription and replication using the encapsulated viral RNA (vRNA) as a template (325). The vRNA is tightly encapsulated by the N protein forming an helicoidal ribonucleocapsid (NC) (347). P functions as a chaperone, stabilizing N in its monomeric, RNA-free state and ensuring its competence for encapsulation of newly synthesized vRNA. The L polymerase is a large 250kDa protein that possesses RNA-dependent RNA polymerase activity, as well as polyribonucleotide transferase and methyltransferase functions, which facilitate the capping of viral mRNA (348). $M_{2\text{-}1}$, a viral transcription elongation factor enables the synthesis of full-length mRNAs and it also has a role involving cellular RNA

interactions. The biological significance of these interaction is however still poorly understood (349).

The viral particle contains the RSV genome, that is 15.2 kb in length and consists of 10 genes encoding 11 proteins. At the 3´ and 5´extremes of the genome there are non-coding, regulating regions known as Leader (le) and Trailer (tr) that recruit the viral polymerase. Moreover, each gene within the viral RNA genome is flanked by a promoter (Gene start, gs) and a terminator (Gene End, ge) sequence for the viral polymerase (350). Transcription of viral mRNAs commences with the binding of L protein, in conjunction with its cofactors P and the $M_{2\text{-}1}$, to its template at the le region. According to the current model, the polymerase complex would transcribe each gene sequentially initiating at the gs signal. Once the gene transcription is completed, the ge signals cause the polymerase to polyadenylate and release the mRNA transcript. After completing the transcription of a gene, the polymerase can either scan for the next gs signal or detach from the NC. This sequential transcription would result in a transcriptional gradient, where the mRNA of the genes closer to the le region are the most abundant transcripts (325,350). The L genome is the last gene transcribed, as it is the one closer to the tr signal. Thus, it is normally used in qPCR as a surrogate to define viral titre; since only a complete sequence of RNA containing the 10 genes will be able to be encapsulated to form a virion.

1.6.2.3 Assembly and export

The newly synthetized and encapsulated viral genomes will then associate with the viral internal proteins to form new virions. The structural proteins are synthetised in the Golgi body and deposited in the host membrane. Published data suggests that the M protein facilitates virion assembly, likely through interactions with the cytoplasmic tail of the F protein. The P protein acts as a cofactor facilitating the process and directing particle morphology (351). From the plasma membrane RSV is proposed to bud, forming elongated membrane filaments (352). The exact mechanisms of virions release from inclusion bodies to the cytosol and of their transport to the plasma membrane however remain particularly elusive (325).

1.6.3 Risk factors for RSV infection

Age remains the most significant risk factor; as RSV severely infects individuals at the extreme of life (<5 years and >65 years). Children have smaller diameter airways, impaired respiratory capacity, and a lower respiratory reserve than adults. Thus, obstruction of the small airways in infants has a greater clinical significance than an obstruction in the peripheral airways of an older child or adult. Concomitantly, RSV illness is more severe in male infants due to the smaller diameter of their airways (8). Preterm birth is another risk factor due to the underdevelopment of the immune system and the lack of passive immunity provided by the mother’s antibodies, which are crucial to

protect against infections in the first few months of life and are transferred during late pregnancy (353–355). The household environment can become a risk factor, particularly if older children that attend daycare or school are living in the same house or if there are crowded living conditions. Exposure to passive smoke also increases the risk of suffering from RSV disease. RSV infection can also be contracted as a nosocomial infection and children suffering from underlying conditions like malnutrition, congenital or acquired immunodeficiencies, trisomy 21 or respiratory conditions, among others, also have an increased risk factor for RSV infection (8). Despite the known predictors of severe disease, most infants hospitalized with RSV bronchiolitis are previously healthy and without known risk factors other than young age, the biggest risk factor for severe bronchiolitis (356,357).

1.6.4 Clinical disease and treatment

RSV is transmitted through respiratory droplets via direct contact with an infected individual or with contaminated surfaces. Infection is normally confined to the respiratory mucosa and does not usually disseminate to other organs or appear in the blood. By the age of two, over 80% of children have experienced at least one RSV infection, 2/3 of these occurring in the first year of life (358); and by the age of 3 years virtually all children have been infected with RSV at least once (9,236). RSV infects airway epithelial cells in the upper respiratory system. From there, it spreads to the lower respiratory system and reaches the bronchioles, where viral replication is more effective (359,360). Adults will typically experience mild to moderate nasal congestion and low-grade fever within a few days of exposure and transmission, followed by a productive cough. Whilst most infants display only mild upper respiratory tract infection (URTI) or occasionally otitis media, around one-third will develop an infection of the lower respiratory tract (LRTI), usually bronchiolitis, with 10% of them requiring hospitalization (361). This is caused by an infiltration of inflammatory cells into the airspaces, mucus hyper-production, shedding of necrotic airway epithelial cells, and oedema of the airway wall. These processes lead to a narrowing of the airway lumen, airflow obstruction, overinflation, and impaired gas exchange. In more severe RSV disease crackles and wheeze occur with laboured breathing, tachypnoea and hypoxia (362).

Once virion particle replication has occurred, the virus can be shed. The host is considered infectious, with the ability to infect others, as long as the virus is being shed. Shedding of the virus begins within approximately a day from infection, before the onset of major symptoms (8). The median time from symptom onset for presentation to hospital with RSV LRTI is of 4 days (363). Thus, as the first symptoms arise, the virus has already begun rapidly disappearing from the host due to the action of the immune system (364). This explains why antivirals, such as aerosolized ribavirin which inhibits viral replication, are normally not administered to immunocompetent children; as by the time children present symptoms and arrive to the hospital the virus titre is already

in decline. These drugs are instead recommended for severe immunocompromised patients where the virus can replicate for months after initial infection due to their ineffective immune response (8). Thus, due to the nature of the viral infection, the effect of ribavirin and similar drugs depends on how long after initial infection the drug is administered.

Adult human challenge models of participants inoculated with RSV have successfully demonstrated both antiviral effect and improvement in (upper) respiratory tract symptoms when treatment commences within 12h of RSV detection on nasal swabs, which is 24-48h before the onset of clinical symptoms (364–366). In contrast, administration of nanobodies (nebulised ALX-0171), a therapeutic protein designed to neutralise RSV in the airways reducing available infectious virions, to children after symptom onset only lead to a decline in RSV viral load, without this being associated with improved clinical outcomes when compared to placebo (367). Thus, while these drugs are able to decrease viral titre, they do not prevent the symptoms of RSV associated disease in immunocompetent individuals if these have already started. Since ribavirin can have potent side effects, it is best to limit its administration to patients for whom the risk of infection is greater than the risk of suffering from adverse drug effects, such as immunocompromised children (368). The clinical management of RSV therefore consists mostly of supportive therapy. This includes supplemental oxygen, intravenous fluids, mechanical ventilation and nasal suction and lubrication (8).

1.6.5 Immune response to RSV infection

RSV predominantly infects the superficial ciliated cells of the upper airway, the epithelium of the small bronchioles and type-I alveolar pneumocytes (359,360). Compared to other respiratory viruses, RSV is only weakly cytopathic, causing comparatively little cell lysis in human airway epithelial cells (369). Nevertheless, it undergoes cell-to-cell transmission in infected airways and fuses cells to form syncytia; giving this virus its name (370). The virus's ability to complete its life cycle in superficial airway cells may facilitate immune evasion, as the immune system typically has limited access to epithelial tissue. The exact contributions of the virus and the host immune system to the pathogenesis of bronchiolitis remains a subject of debate, as there are both protective and pathological responses associated with the participation of the immune system (358,359,371).

1.6.5.1 Innate immunity to RSV infection in early life

Early viral detection is mediated through PRRs expressed by epithelial cells, fibroblasts, and APCs of the respiratory tract. Alveolar macrophages (AMs) are specialized macrophages found in the alveoli that have an important role in clearing debris and promoting lung homeostasis. They are also ideally placed to sense pathogens, such as viruses, and have a protective role in RSV infection

(372,373). Thus, once RSV enters the respiratory tract it will be recognised by AMs. Both AMs and epithelial cells, by the secretion of cytokines and chemotactic factors recruit a series of innate immune cells such as neutrophils, natural killer (NK) cells, DCs (including both cDCs and pDCs), γδ T cells, eosinophils, type 2 innate lymphoid cells (ILC2s) and natural killer T cells (NKT) to the site of infection. These innate immune cells act in concert to promote an antiviral immune response and attract cells from the adaptive immune system which will help clear the infection. The recruitment and function of all these cells is reduced in early life when compared to adulthood making the antiviral response less effective, starting with AMs which have an underdeveloped phenotype in infants (374).

Neutrophils and monocytes are the first immune cells recruited to the site of infection. Neutrophils are the dominant cell type in the bronchioalveolar lavage of RSV infected children (375,376). It is unclear if they have a beneficial or detrimental role in clearing the infection; since they have been linked with both killing of the infected cells, but also with the secretion of enzymes that can damage the healthy surrounding tissue (377,378). γδ T cells, by producing IL-17, can also help recruit neutrophils to the infection site, and their depletion is linked with attenuated RSV-induced inflammation in mice, suggesting that they may have an immunopathogenic role (379,380). Monocytes are able to phagocytose viral particles, making them central cells in helping reduce viral load, control RSV infection and lessen disease severity in murine models (377,381). It is thought that treatments to promote monocyte production may provide new paths to control RSV infection, particularly in high risk individuals. For example, *Heligmosomoides polygyrus* infection prior to RSV challenge in mice protects from RSV infection by inducing bone marrow monopoiesis, increasing circulatory monocytes and elevating lung mononuclear phagocytes; all factors contributing to reduced RSV load (381). NK cells are also recruited to the lung. As indicated by their name NK cells can kill infected cells leading to viral clearance (382). They are also an early source of IFNγ which is important in activating DCs and priming T_{H1} responses, which are anti-viral (382). An increase frequency of NK cells is observed in the lung of children ventilated due to severe bronchiolitis (383), but NK cells are sparse in the lung tissue from fatal cases (384).

Upon recognition of viral particles by PRRs, and additional signalling cues, several cells can produce IFNs such as AMs or NK cells, which mainly produce type II interferons (385,386). AM activation tightly correlates with IFNγ exposure in a neonatal murine model of RSV infection (387). In some circumstances, such as infection with RNA viruses, AMs can also produce type I IFNs like IFNα (388) and AMs are the major source of type I IFNs upon RSV infection in mice (377). AM derived type I IFNs contribute to inflammatory monocyte recruitment to the lung (377). Upon antigen challenge, pDCs are also high producers of type I IFNs (389–391). By producing type I IFNs, pDCs can induce an antiviral state on the cells of the immune system while helping avoid excessive

immunopathology (392,393). Neonates have a suboptimal type I and type II IFN response probably due to the low frequency of pDCs in this age group, as observed in neonatal RSV infected murine lungs (394,395), and due to an underdeveloped phenotype of infant AMs (374). Moreover, the RSV NS_1 and NS_2 proteins can block type I IFNs, like IFNα and β signalling; further accentuating this reduced response and helping in virus immunoevasion (396).

cDCs are also recruited to the site of infection and their activation is dependent on PRR signalling both in the cell surface and in endosomes after phagocytosis or infection with virus particles (397–401). RSV can infect cDCs, but their secretion of virions is substantially lower than the amount produced by infected epithelial cells (402). cDCs are the bridge between innate and adaptive responses. In adulthood, there is a sustained increase in the number of pulmonary DCs after RSV infection, which also express higher co-stimulatory markers (403). DCs are however found less frequently and have a distinct phenotype in early life as previously highlighted. RSV infection of neonatal mice shows an increased ratio of $CD103^+$:$CD11b^+$ DCs in the mediastinal LN, which is associated with a reduced ability to transport antigen and express co-stimulation factors by DCs, that leads to reduced $CD8^+$ T cell responses (276). The $NS_{1/2}$ RSV proteins also inhibit DC maturation accentuating the diminished DC responses observed in early life (401).

1.6.5.2 Adaptive immunity to RSV infection in early life

In mice, RSV infection in early life results in a more limited adaptive immune response associated with lower levels of pro-inflammatory mediator release by the innate immune system (404). This appears to result in the generation of a more limited T_{H1} response, and upon antigen re-encounter eosinophils, NKT cells, ILC2s and T_{H2} cells generate a cytokine environment enriched in IL-4 (404–408).

<u>$CD8^+$ T cell responses</u>

$CD8^+$ T cells play a crucial role in RSV viral clearance by killing infected cells (409,410). As with cells of the innate response, and probably due to their dysregulation as observed in DC capacity to produce IL-12 (276), $CD8^+$ T cell responses are decreased in RSV-infected infants (411,412). The same phenotype is seen in murine models (413). Notably, $CD8^+$ T cells are absent in children suffering from fatal RSV infection (358). Depletion of $CD8^+$ T cells in a mouse model of RSV infection is associated with increased eosinophilia; suggesting $CD8^+$ T cells play a key role in preventing excess T_{H2} bias as well as their known role in killing infected cells (414).

CD4+ T cell responses

RSV may actively suppress T_{helper} immunity when compared with other respiratory viruses, since both nasal washes and lung tissue from post-mortem RSV infected individuals have lower cytokine levels than those infected with influenza (358). Concomitant with the innate immune system response, those T_{helper} that differentiate in RSV infection are skewed towards a T_{H2} phenotype, as observed by their ability to potently secrete IL-4, while failing to promote IFNγ responses, when compared to healthy controls (415–419). Age at the time of RSV infection also influences $CD4^+$ T cell responses, with greater recruitment of T_{H2} cells and eosinophils in younger mice (405). Children whose cord blood monocytes are less able to produce IFNγ in response to RSV, have an increased frequency of upper respiratory tract infections and respiratory related hospitalizations (420). The delayed development of IL-12 producing cDCs further compromises the differentiation of T_{H1} cells (421). The increased T_{H2}/T_{H1} balance might be associated with the development of bronchiolitis, as an increased T_{H2}-skewed environment is reported in children suffering from severe bronchiolitis when compared with milder URTI cases (406). Moreover, neonatal mice infected with RSV develop a T_{reg} population with a compromised suppressive function, but an increased ability to secrete T_{H2} cytokines (422). T_{H17} responses have also been associated with pathology in RSV (423), with local IL-17A driving increased neutrophilia to the infected respiratory tract (424) which might lead to increased inflammation and inhibit the $CD8^+$ T cell response (425,426).

T cell dependent antibody responses

As highlighted above, the T-cell dependent humoral immune response is downregulated in early life due to both T and B cell intrinsic and extrinsic factors. This is particularly true in the case of RSV infection, a virus that repeatedly infects children, even within the same cold season (313,314). Re-infection with the same strain of RSV can even occur in adults as soon as two months after the previous infection (315). Virtually all children and adults have RSV-specific antibodies, indicating the high prevalence of RSV infection in early life. These antibodies are however insufficient to prevent re-infection even in adulthood, despite a lifetime of repeated infection, since the local and systemic antibody titres generated after RSV infection and re-infection are only partially protective and limited in duration (9). This is a highly unusual response since most acute viral responses, like the ones caused by influenza or rhinovirus, induce robust homotypic long-lasting immunity following natural infection (427–429). Re-infection symptoms are however normally milder than the ones caused by the first contact with RSV and are generally limited to the upper respiratory tract.

Natural RSV infection in early life can promote the production of IgG and IgA antibodies, but due to the age differences in immune cells described above, the neonatal antibody response is weak, poorly functional and short lived; declining to pre-infection levels within three to four months

(236,353,430–432). During the third trimester of pregnancy, maternal IgG is actively transported across the placenta endowing term, and near-term infants with a full variety of maternal derived antibodies that are capable of providing immediate protection from life-threatening infections. This allows the transmission of adult-derived, high-affinity, RSV-specific antibodies that have developed from repeated exposure to, and infection with RSV over many years (433). Maternally derived antibodies have a half-life of approximately 38 days. The exact duration of these antibodies in the babies' bloodstream would depend on the mother's ability to generate RSV-specific antibodies, the neonatal gestational age at birth – with premature babies having lower to no levels of maternally derived antibodies -, the efficacy of active transport of antibodies across the placenta and the timing of the birth related to the onset of the RSV season (434). It is important to notice that preexisting maternal antibodies may interfere with the generation of neonatal antibody responses, but they are the most likely explanation for the neonatal resistance to RSV induced bronchiolitis during the first weeks of life (353–355).

Many aspects of the innate and adaptive immune system therefore display age-dependent differences that predispose infants to a more severe RSV infection. The RSV virus, despite only possessing 11 proteins, further compromises the infant immune response and prevents the generation of long-lasting protective responses.

1.6.6 RSV immune evasion

RSV employs diverse strategies to evade host immune defences, facilitating unimpeded replication of viral particles that culminate in tissue damage and the onset of clinical manifestations of the disease.

The non-structural proteins NS_1 and NS_2 are the main drivers of immune evasion mainly by preventing the IFN-I response, the recognition of viral RNA by the host cell and the apoptosis of infected cells. NS_1 and NS_2 are the first proteins produced by the virus upon infection, facilitating a rapid suppression of the immune response (323,324). A549 cells are an immortalised cell line extracted from a human alveolar basal epithelial carcinoma which are typically used in the study of respiratory physiology. The infection of A549 cells and human derived macrophages with rh-RSV variants with single or double deletions of the NS genes promotes the production of higher levels of IFN-I compared to WT virus, with both RSV proteins exhibiting a cumulative inhibitory effect (396). The antiviral effects of IFN-I are triggered when IFN-α/β binds to type I interferon receptors, composed of the IFNAR1 and IFNAR2 subunits. This interaction activates downstream signalling pathways, particularly the JAK/STAT pathway, leading to the expression of a wide range of interferon-stimulated genes (ISGs). Viral RNA can also be detected in the cytoplasm by specific cytoplasmic PRRs, including RIG-I-Like receptors. NS proteins can block the IFN-I signalling

response by preventing interferon regulatory factor 3 (IRF3), a regulatory factor needed for the transcription of type I IFN and ISGs, translocation to the nucleus (435,436). The NS proteins, singly or in combination can also affect the JAK/STAT signalling pathway, specifically by interacting with STAT2 (323,437). These RSV proteins can also prevent viral RNA recognition by the host cell by reducing the presence of adaptor proteins downstream of RIG-I-like receptors (438,439).

NS_1 can also inhibit IFNAR synthesis by a viral-replication dependent system. Data from a dual-luciferase reporter assay in A549 cells confirmed that during RSV replication NS_1 upregulates the expression of the host derived microRNA miR-29a, which in turn targets the mRNA of the *IFNAR* gene for degradation, preventing IFNAR protein translation (440). NS_1 can also prevent viral degradation by interacting with further aspects of the innate immune response. The oligoadenylate synthase-like proteins (OASL) are ISGs thar modulate the antiviral response. The NS_1 RSV protein can promote the degradation of OASL in a proteosome-dependent manner, therefore allowing RSV immunoevasion (441). NS_1 can also affect the T cell response by preventing human DC maturation upon infection; affecting T cell activation and differentiation. Moreover, by a process that is only partly dependent on IFN-I-signalling, NS_1 can reduce the number and activation of anti-viral $CD8^+$ T cells and T_{H17} cells, needed to attract neutrophils, while simultaneously promoting the proliferation and activation of T_{H2} cells, which are associated with enhanced RSV disease (442). NS_2 on the other hand is able to prevent apoptosis of infected cells in a murine model by an IFN-I dependent pathway, leading to enhanced cell survival by preventing the action of $CD8^+$ T cells (443). In the human A549 cell line, both NS_1 and NS_2 individually and in combination can prevent cell death by interacting with TNF-α (324). RSV infection of human bronchial epithelial cells also upregulates PD-L1, therefore enabling infected cells to evade $CD8^+$ T cell-mediated cytotoxicity (444). RSV thus employs various molecular strategies to limit the IFN-I response and cell death; with all of these processes increasing viral infectivity as they allow continuous replication of the virus in host cells.

The G protein does not only participate in viral attachment to the host cells, but it also has an immunomodulatory function both through IFN-dependent and independent pathways. The G protein impedes ISG15 expression on mouse lung epithelial (MLE)-15 cells, a type II pneumocyte cell line representing the distal bronchial and alveolar epithelium (445). Moreover, due to the similarities of the G protein with the CX3C chemokine fractalkine, G can bind the CX3C receptor, impairing the production of IFN-I and III and therefore the innate immune response against RSV (446). As previously mentioned, the RSV's CX3C motif also allows the attachment of viral particles through the CX3C receptor, promoting RSV infectivity (328). Glycosylation is a widespread viral tactic used to shield antigenic proteins from antibody recognition by altering the glycan structures (447,448). Using this process, the RSV virus can modify the macrostructure of G, concealing its protein backbone thus reducing antibody binding affinity and given the G protein its name. Extensive glycosylation also impairs antigen acquisition and presentation to T cells, diminishing T

cell activation (447). To further evade the adaptive immune response, the G protein contains two hypervariable regions within its ectodomain, which facilitate frequent mutation of antigenic epitopes. Additionally, G protein variability is enhanced by frameshifts, point mutations and premature stop codons that are observed across seasonal strains. These changes hinder RSV recognition by antibodies generated during prior infections, undermining immune memory and complicating immune defense (449,450).

In addition to its membrane form, the G protein can also be generated as a secreted isoform, secreted G (sG). The sG form arises owing to a translation initiation at an alternative AUG codon, which, in the full-length protein, is located in the middle of the transmembrane domain. A subsequent proteolytic event removes the remaining portion of the transmembrane region that normally anchors the G protein to the viral capsid. This shorter, truncated version has a hydrophobic amino terminus that allows its traffic out of the infected cell into the adjacent culture medium (451). As for NS_1 and NS_2, the sG protein is produced in large quantities at the beginning of the viral life cycle, acting as an antigen decoy for G-directed antibodies; thus limiting the effectiveness of G-specific antibodies upon the actual RSV virion (318,452). sG also impairs the production of pro-inflammatory modulators in human lung A549 epithelial cells, such as chemokines CCL5 and IL-8, suggesting a role for sG in blocking the recruitment of immune cells, specifically T cells and neutrophils, to the site of infection (453).

The F protein is also involved in RSV immunoevasion as it has a special tropism for neonatal B_{regs}. Recognition of F through the polyreactive BCR promotes the upregulation of CX3CR1 on B_{regs}, which by binding the G protein through its CX3C domain allow infection of these cells. RSV infection of neonatal B_{regs} causes an increase production of the anti-inflammatory cytokine IL-10, which in turn suppresses T_{H1} activity (454). Interestingly, the increased F recognition was specifically observed by early life B_{regs} found in both cord blood an neonatal blood immediately after birth. The amount of B_{regs} however significantly decreases with age, with less than 2% of $CD19^+$ regulatory cells found in one year old babies (454). This observation may help explain why young age is such a significant risk factor for severe RSV infection.

The SH protein, a pentameric ion channel, also has immunoevasion mechanisms as it is involved in delaying apoptosis of infected cells (320,455). The exact mechanism leading to its impaired cell death is incompletely understood. Murine experiments have shown that SH deletion mutants, despite possessing a similar ability to enter cells and replicate, are less virulent than their WT counterparts (320,456). The presence of SH also influences cytokine production, with virus with intact SH proteins having an impaired IL-1β and TNF expression, both pivotal proteins involved in the antiviral defence (320,457).

Together with its key structural role, the N protein also has immunomodulatory functions. Early after infection of DCs and epithelial cells, the N protein can be found in the membrane of the host cells (458). In this location the N protein is able to prevent the formation of mature immunological synapses, leading to a reduction in T cell activation, as shown in a murine model. This impaired activation also affects T_{FH} differentiation, therefore leading to an impaired humoral immune response (458). The N protein can also limit the anti-viral IFN response by modulating the RIG-1 and melanoma differentiation associated gene 5 (MDA5) at the biggening of the infection and the mitochondrial antiviral signalling protein (MAVS) and MDA5, later during infection. These are all crucial signalling molecules that when inhibited lead to a more efficient and undisturbed RSV replication, as shown in experiments with human cell lines (459).

Collectively these studies indicate an intricate relationship of RSV with the immune system, with several RSV proteins involved in immunoevasion mechanisms all contributing to the impaired response against this viral pathogen.

1.6.7 Delayed sequelae of RSV bronchiolitis

In addition to acute disease, RSV bronchiolitis is associated with long-term respiratory problems. These long-term effects normally involve recurrent wheezing and asthma, diseases that are associated with an aberrant T_{H2} response (460–465). About 1/3 of cases of early childhood asthma diagnoses come from children that have experienced bronchiolitis earlier in life (466,467). In a study using a small cohort of patients it was found that childhood bronchiolitis accounted for approximately 40% of cases of clinical allergy and atopic sensitization with the risk of asthma and allergies increasing with the severity of infant bronchiolitis (467). These results however would need to be performed with a larger patient cohort to be confirmed and found applicable to the broad population.

RSV associated bronchiolitis in infancy may increase the risk of allergic sensitization by generating a local environment enriched in IL-4 at a time when airborne allergens are first encountered; a signature that has been linked with pro-allergenic rather than innocuous responses (417,468,469). In another small study, researchers found that treatment with the α-RSV monoclonal antibody palivizumab causes a substantial reduction in wheeze in preterm babies during the first year of life (470). A 6-year follow-up of the same patient population however indicated that RSV prevention during the first year of life does not affect the risk of physician-diagnosed asthma or results of lung function test at an age of 6 years, when analysing either the whole patient cohort (471) or specific high-risk subpopulations (472). In contrast, an alternative study using a similar number of participants, in which palivizumab was administered in preterm babies during the first 6 months of life, did report a significant lower incidence of physician-diagnosed recurrent wheezing during the

first 3 years of life (473). A third independent 2 years follow-up study also performed in a small cohort of individuals showed that RSV prophylaxis can decrease the relative risk of recurrent wheezing by 80%, but this was only seen in a nonatopic subgroup of premature infants while no difference in recurrent wheezing was reported for children with an atopic family history (474). Thus, early life RSV bronchiolitis may have at least a short continuing causal impact beyond acute infection, particularly in nonatopic children.

Overall, these studies indicate that RSV infection in early life does not only lead to acute symptoms but it may also lead to respiratory problems later in life. In line with these observations, in adult murine models, the T_{H2} bias inflammation and airway sensitization induced by OVA or cockroach allergen is exacerbated when preceded by RSV infection (475–477). Importantly however, further studies with a high number of enrolled participants with longitudinal follow-ups need to be conducted before a causal association between RSV infection and asthma can be definitely stablished.

1.6.8 Vaccination against RSV

Childhood and old age are the two periods which are more affected by RSV. Concomitantly, these age groups also respond poorly to vaccination due to the inability to potently activate the adaptive immune system (478,479).

In the 1960s, trials of formalin-inactivated alum-adjuvanted RSV vaccines proved disastrous, since the vaccine did not only induce poorly neutralizing antibodies, but also enhanced disease upon natural infection in children younger than 2 years. Several causes can lead to this enhanced response such as the formation of immune complexes in conjunction with a pro-T_{H2} and deficient T_{reg} response (480–482). The difference in response between children and adults clearly highlights the existence of a distinct immunological landscape in early life that needs to be accounted for when designing vaccine strategies.

Maternal immunization, by promoting the generation of RSV-specific antibodies that can cross the placenta, offer a way to promote early life RSV immune responses without the need to directly vaccinate the neonate. A recent clinical trial showed efficacy of an RSVpreF vaccine administered during pregnancy without the identification of safety concerns (483). Maternally derived antibody however has a half live of approximately 38 days, so even if they are found at high levels early after birth it is unlikely that they will protect throughout the most vulnerable first six months of life. There is even a hypothetical risk that maternally derived antibodies will skew or prevent the antibody responses generated by the neonate.

Nirsevimab, a neutralising human monoclonal antibody against the RSV pre-fusion F protein, is currently recommended as a prophylactic for infants during their first winter (484). A modification in the Fc region of this monoclonal antibody extends its serum half-life which allows a single administration to protect infants during their first cold season (484). Initial studies with Nirsevimab show that it substantially reduces infant hospitalisations for RSV-associated LRTI and severe RSV-associated LRTI requiring oxygen (485–487). Contrary to protein vaccine strategies, administration of passive antibodies like Nirsevimab do not promote the activation of the infant's adaptive immune system with its ability to give rise to memory B cells and long lived plasma cells able to produce antigen-specific antibody responses against subsequent infections. Therefore, once the monoclonal antibody is waned from the system it does not provide future protection against infection. It is true however, that infant's receiving passive immunisation are still naturally infected with RSV, albeit the clinical response is milder. Thus, not unlike passive immunisation from maternally-derived antibodies, administration of Nirsevimab does not prevent the generation of the infant antibody response but there is a hypothetical risk that it might skew it. Due to the recently approved use of Nirsevimab, long-lasting longitudinal studies analysing the serologic response in children are lacking. Similar seroresponse rates to the post-fusion form of the RSV F protein are however reported in Nirsevimab recipients when compared to the placebo group during the first RSV season, suggesting that while Nirsevimab protects from RSV disease, it still allows an active immune response able to generate similar natural levels of α-RSV-specific antibodies (486).

Palivizumab is another humanised monoclonal α-RSV antibody used as passive immunisation, but unlike Nirsevimab it requires the administration of several doses to maintain its functionality. Administration of Palivizumab also promotes the production of infant α-RSV neutralising antibodies when compared to the placebo group beyond what is expected from its pharmacokinetics, suggesting that naturally acquired α-RSV neutralising antibodies are being generated in children receiving Palivizumab, albeit the antibody titres are lower when compared to untreated adults (488). A recent study shows that Nirsevimab prophylaxis in children confers $\sim$10-fold higher and more sustained RSV neutralizing antibodies relative to Palivizumab during the first two RSV cold seasons and that neutralizing RSV antibodies are still present after a year of monoclonal antibody administration (345), indicating that Nirsevimab is even better than Palivizumab at promoting protection. Overall these recent studies show that Nirsevimab can protect from severe RSV disease while still allowing the generation of naturally arising α-RSV neutralising antibodies. Future research on the neutralization capacity and affinity of naturally arising RSV-specific antibodies as well as their ability to counteract RSV infection and disease in longitudinal cohorts would help provide a better understanding on the role played by Nirsevimab in affecting the children adaptive immune response.

Importantly, various vaccines aiming to protect vulnerable groups via vaccination of infants/children, pregnant women, or older adults are in late-stage clinical development and several have recently been approved for marketing (483,489,490). An RSV vaccine (MRESVIA) has recently been approved by the FDA for the prevention of LRTD in individuals of 60 years of age or older, but it has not been yet approved for infants (491). There is currently no licensed RSV vaccine approved in the EU for childhood immunization. The generation of a future neonatal RSV vaccine will need to use appropriate adjuvants to overcome the RSV T_{H2} bias and promote a potent T_{FH} response able to provide help in the generation of high affinity, high titre antibody both systemically and in the respiratory tract.

1.7 Can microbial exposure shape the T cell-dependent humoral immune response in early life?

Identifying new methods to improve responses to immunity and vaccination in infancy is clearly highly desirable; both to provide protection against pathogens for which there are currently no licenced vaccines and improve the efficacy and durability of protection against pathogens for which there are. The cell intrinsic nature of some of the alterations in early life immunity, such as the altered maternally and paternally derived epigenetic background and the functional state of recently generated naïve $CD4^+$ T and B cells, makes them less susceptible to modification. Some cell-extrinsic alterations however do appear modifiable, largely through age-specific use of adjuvants to promote a pro-T_{FH} cytokine microenvironment, DC phenotype or both during antigen exposure.

Likewise, as highlighted in figure 1.1, at the level of the whole organism some factors that influence antibody responses in early life are fixed, such as genetics, developmental age and parental history. Some factors are, however, modifiable, with the host microbiome and diet garnering the most current interest. Indeed, it is clear from the use of germ-free mice, broad-spectrum antibiotic treatments and dietary interventions that appropriate microbiotal colonization, diversification and metabolite generation are essential to allowing antibody-mediated immunity (492–497). Studies in infants also highlight the importance of diet and microbiome on vaccine responses (498–500). The precise role of specific microbes and metabolites is however unclear; likely due to the complex interplay between diet, microbiota and the host's genetic background, meaning the optimal conditions may well be highly personalized. Prophylactic supplementation with certain "beneficial" bacterial species and their metabolites has however proved capable of modifying T cell and antibody responses in mouse models (501–505), suggesting a mechanism by which early life immune responses could be boosted.

In the last ten years several studies have highlighted a distinct group of bacteria, referred to as "farmyard microbes", for playing a significant role in promoting immune system development in infants. Early-life exposure to farm environments correlates with a lower incidence of severe respiratory diseases, wheezing and asthma in later life; an effect predominantly attributed to bacteria exposure specific to these environments (506–509). *Acinetobacter lwoffii F78* (*A.lwoffii*) is among the most prevalent bacterial species identified within cowshed microflora (510). This gram-negative, aerobic bacillus that forms part of the microbiota of 20-25% of healthy individuals has been linked with protection against asthma and allergies. Several studies using murine models have associated intranasal administration of *A.lwoffii* with protection against allergic inflammation (510,511). A study from our group shows that early life *A.lwoffii* exposure can protect mice against house dust mite allergen-induced airway hyperresponsiveness by reducing the frequency of IL-13^{+}CD4^{+} T cells (503).

Numerous studies have linked exposure to *A.lwoffii* with protective effects against asthma, wheezing and allergic conditions, but its specific role in mitigating early life viral-induced airway diseases, which often lead to wheezing and asthma later in life, remains poorly understood. Similarly, although microbial exposure has been shown to induce antibodies capable of neutralising viral respiratory infections in adult mouse models (492,501), the potential for enhancing this system during early life remains to be elucidated.

1.8 Hypothesis and Aims

Our understanding of the early life immune system has progressed substantially in the last decade, and we therefore no longer see it as just an immature version of the immune system found in adults. Precisely how it differs, especially in humans, and how we can selectively modify certain aspects of it without detrimental outcomes to other aspects, still requires substantial future research. It is increasingly clear however that we can use age-specific approaches to enhance antibody mediated immunity in early life. To try to understand the process of T cell dependent antibody mediated immunity during early life RSV infection and evaluate mechanisms to boost it, the overarching hypothesis and aims of this thesis are:

Overarching Hypothesis

Early life is characterised by an increased IL-2 microenvironment that prevents T_{FH} differentiation during RSV infection, but can be overcome by exposure to farmyard microbes to promote antibody mediated immunity.

Overarching Aims

- To investigate the mechanism(s) leading to reduced T_{FH} differentiation in early life RSV infection when compared to adulthood

- To analyse if exposure to *Acinetobacter lwoffii F78,* a farmyard microbe, can promote a RSV-specific T cell-dependent antibody response in early life

- To evaluate the ability of *Acinetobacter lwoffii F78* in promoting a pro-T_{FH} cytokine microenvironment by interacting with APCs

2 Materials and Methods

2.1 Animal experiments

Animal work was conducted in accordance with the UK Home Office and the local Animal Welfare Ethical Review Body (AWERB) committee (UK Home Office project licence P996A24e1) as well as in accordance with the Animals (Scientific Procedures) Act 1986. Specific pathogen-free 6- to 8-week old BALB/c and C57BL/6 mice were purchased from Charles River Laboratories *(Margate, UK)*. Tlr4$^{-/-}$ mice were kindly provided by Dr Alice Denton *(Imperial College London, London UK)*. Mice were housed at Imperial College Central Biomedical Services (CBS) where in-house breeding was also performed. Mice were maintained in specific pathogen-free conditions with *ad libitum* food and water. Experimental animals and studs used for breeding were fed a general maintenance diet ("RM1"), whereas female breeders received a highly nutritious diet specifically used for breeding, lactation and growth of young animals ("RM3").

Pregnant females were singly housed approximately two weeks into gestation. Litters were housed with their dams until weaning at 3 weeks of life, when animals were separated by sex. For each group in individual experiments, mice were age-matched and randomly selected. In models of viral infection and/or microbial exposure, weight of mice was monitored throughout the experiment to analyse differences between groups and ensure health of the animals.

2.2 Microbial and viral cultures

2.2.1 *Acinetobacter lwoffii F78 culture*

The initial stock of lyophilized *A.lwoffii* was a gift from Prof Erika von Mutius *(Ludwig-Maximilians Univeristy of Munich, Germany)* and was cultured as previously described (510). Briefly, lyophilized *A.lwoffii* was rehydrated, transferred onto an agar plate made with Trypticase Soy Broth media *(Sigma-Aldrich)* containing 0.3% yeast extract *(Sigma-Aldrich)* and cultured overnight at 37ºC. A single *A.lwoffii* colony was selected, transferred to 5mL liquid media, and incubated overnight at 30ºC with constant rotation at 220rpm for initial expansion. Optical density (OD) at 600nm was determined by spectrometer SpectraMax® i3x microplate reader *(Molecular Devices)* and propagation of *A.lwoffii* in large quantities was performed at 30ºC with a starting OD600 at 0.1. Following 6 hours of incubation, final OD600 was measured and *A.lwoffii* was centrifuged at 3000rpm for 20 minutes, lyophilised, resuspended in pre-determined volumes of PBS, aliquoted and stored at -20ºC for future use. Cell purity was checked by PCR and bacterial concentration was determined using a BCA assay *(Thermo Fisher Scientific)* as per manufacturer's instructions.

2.2.2 RSV culture

Plaque purified RSV A2 was kindly provided by Dr. Cecilia Johansson *(Imperial College London, London UK)*. RSV A2 was grown in HEp-2 cells (American Type Culture Collection [ATCC] number CCL-23) and viral titre was then determined by focus forming assay (refer to 2.2.3) as previously described (512).

Briefly, HEp-2 cells were maintained in GlutaMAX™ supplemented Dulbecco's Modified Eagle Medium (DMEM) *(Gibco, Invitrogen)* with 10% Foetal Bovine Serum (FBS) *(Invitrogen)* and 100U/mL penicillin/streptomycin *(Invitrogen)* at 37ºC and 5% CO_2 conditions. Enough HEp-2 cells were seeded to allow 60-80% confluency overnight (10^7 cells in T150 flask *(Corning)*) and then RSV infection was performed by inoculating 0.1 focus forming unit (ffu)/cell RSV for 2h in serum-free media and intermittently rotating the flasks every 15 minutes to account for unevenness in the incubator surface. After 2h, serum content was supplemented to reach 10%. After 24h cultures were serum-reduced again to 2% FBS for 24-48h. Cells were monitored using an inverted light microscope every day until the cytopathic effect reached approximately 80%, when cells were harvested. Virions were released from HEp-2 cells by mechanically detaching cells form the flask and sonicating them in an ice-cold water bath for 90 seconds. Finally, virions were aliquoted in cryovials, snap frozen and maintained in liquid nitrogen until further use. A non-infected flask was treated in the same conditions to have as control.

2.2.3 RSV Focus-forming Assay

RSV concentration was assessed by focus-forming assay by titrating it on monolayers of HEp-2 cells in tissue culture treated, 96-well, flat-bottom plates *(Corning Incorporated).* Infection was performed as described above starting at 1:100 dilution and then performing consecutive 1:2 dilutions of the cryovial content. After 24h plates were washed and fixed with methanol containing 2% hydrogen peroxide (both from Sigma-Aldrich) for 20 minutes at room temperature (RT). Plates were then washed and kept in Phosphate-buffered saline (PBS) (Gibco, Invitrogen) with 1% bovine serum albumin (BSA) (Sigma-Aldrich) and 0.1% Azide (G. Biosciences) at 4ºC in the dark until further staining. RSV staining was performed by 1 hour incubation with biotinylated α-RSV antibody (Polyclonal, Catalogue PA1-73019) *(Invitrogen)*, followed by 1 hour incubation with ExtrAvidin®-Peroxidase *(Sigma-Aldrich)* at RT. Infected cells were detected with 3 amino-ethylcarbazole (AEC) substrate with peroxidase *(Vector Laboratories),* made according to manufacturer's instructions and reaction was stopped by washing wells with deionised water when an orange/brown colour developed (usually 20 minutes). Infectious units were enumerated by light microscopy, following the formula:

Dilution factor x average cell count x (1mL/ initial volume (mL) of virus added to plate)

2.3 Animal *in vivo* procedures

2.3.1 Exposure to inhaled *A.lwoffii*

Following heat inactivation of *A.lwoffii* at 70ºC for 15 minutes, BALB/c mice were intranasally (i.n) exposed to $1.3x10^8$ colony-forming units (cfu) lyophilized *A.lwoffii* in 10µL of PBS for the first 2 weeks of life (from post-natal day (PND) PND3 to PND14) three times a week. From PND14 onwards mice were exposed to $2x10^8$ cfu *A.lwoffii* in 15µL of PBS three times a week until indicated timepoints. Mice were always exposed to *A.lwoffii* 48h and 6h before RSV-infection, but for RSV infection as adults (PND61) where *A.lwoffii* exposure was finished on PND26. From PND13, exposure to the bacteria was performed under isoflurane-induced anaesthesia. The dosing regime was established following a previously published study (503). Mice from control groups received PBS instead of *A.lwoffii* at respective dates.

2.3.2 Respiratory viral infection

WT BALB/c neonatal mice were infected at PND5 i.n. with 15µL $1.5x10^5$ ffu of RSV A2. RSV re-infection in early life was undertaken using isoflurane-induced anaesthesia followed by inhalation of 35µL $3.5x10^5$ ffu RSV A2 at PND15 and 100uL $8x10^5$ ffu RSV A2 as adults (PND61). The amount of virus used for infection was kept consistent at $0.5x10^5$ ffu per gram body weight, as previously published (25,405). Mice from control groups received PBS at respective dates.

1 week and 8 week old WT C57BL/6 mice were infected with $2.5x10^5$ ffu RSV A2 or PBS i.n. in 20 and 100µL respectively. Control mice received PBS at respective dates. Adult mice were infected under isoflurane-induced anaesthesia.

2.4 Animal tissue harvest and cell recovery

2.4.1 Animal euthanasia

WT BALB/c and C57/BL6 mice received a euthanising dose of sodium pentobarbital *(Animalcare)* intraperitoneally (i.p.) followed by exsanguination in accordance with Schedule 1 of the Animals (Scientific Procedures) Act 1986.

2.4.2 Blood

Blood was collected from mice by terminal exsanguination immediately after euthanasia using heparinised capillaries. After centrifugation for 10 minutes at 1800rpm and 4ºC to separate blood layers, the upper plasma layer was collected and stored at -70ºC for subsequent analysis by Enzyme-Linked ImmunoSorbent Assay (ELISA).

2.4.3 Bronchoalveolar Lavage (BAL)

The trachea was exposed and cannulated using a blunt-ended needle secured by surgical sutures. A 1mL syringe was attached to the needle. Lungs were carefully flushed with PBS three times and lavage was recovered in the syringe. A volume of 0.2mL per wash was used in animals from 2 weeks to 3 weeks of age, an increased volume of 0.4mL per wash was used in animals between 4 and 6 weeks of age and 1mL per wash was used for adult mice as previously published (25,513). Recovered BAL fluid was centrifuged at 1500rpm and 4ºC and supernatant was stored at -70°C for subsequent analysis by ELISA.

2.4.4 Nasal Airway Lavage (NAL)

The upper airway was isolated by scissor dissection and the mouse head was separated at the level of the larynx. A canulated 1mL syringe was inserted through the pharyngeal opening into the choana. 1mL of PBS was instilled and the fluid was collected into 1.5mL microcentrifuge tubes positioned at the extreme of the mice nostrils. Recovered NAL fluid was centrifuged at 1500rpm and 4ºC and supernatant was stored at -70°C for subsequent analysis by ELISA.

2.4.5 Mediastinal lymph node and Peyer's Patches (medLN & PP)

Mediastinal lymph nodes (medLN) were exposed, by gently displacing the lung towards the heart and avoiding the thymus, and scooped into microcentrifuge tubes containing 1mL of complete Roswell Park Memorial Institute media (cRPMI) consisting of RPMI1 1640 *(Gibco)*, 2mM L-glutamine *(Life technologies),* 10% FBS *(Life technologies)* and 100U/mL penicillin/streptomycin. Peyer's Patches (PP) were isolated from the mice gastrointestinal tract and resuspended in 1mL cRPMI. To obtain a single-cell suspension for flow cytometry analysis, medLN and PP were passed through 70µm cell strainers *(Greiner Bio-One)* with 1mL of cRPMI. Then they were centrifuged and resuspended in 0.5mL cRPMI and counted using trypan blue *(Sigma-Aldrich)* exclusion staining and FastRead 102 counting slides *(Kova International).* Cells were used for flow cytometry analysis and or stored at -70ºC in RLT buffer *(Qiagen)* containing 1% 2-β-mercaptoethanol *(Sigma-Aldrich)* for RNA isolation. In some experiments, the 1mL used to flush the medLN was recovered after centrifugation and stored at -70ºC for ELISA analysis.

2.4.6 Lungs

Lungs were removed as a whole and lobes were separated and used according to downstream applications. Lung tissue from animal studies was allocated according to project focus.

2.4.6.1 Left lobes and middle right lobe (Flow cytometry)

The left lobe and middle right lobe were used for flow cytometry analysis of lung immune cells. Lobes were weighed, finely chopped and digested for 45 minutes at 37°C in a solution containing 150µg/mL collagenase D and 25µg/mL DNase I *(both Roche)* in cRPMI. Following digest, tissue was passed through 70µm cell strainers and erythrocytes were lysed by incubation in red blood cell (RBC) lysis buffer for five minutes at RT. RBC lysis buffer was quenched and lung cells were centrifuged, resuspended in 1mL cRPMI, counted and used for analysis.

2.4.6.2 Bottom right lung lobe (viral load measurements)

The bottom lung lobe was snap frozen in liquid nitrogen or preserved in 300µL of RNAlater™ Stabilization Solution *(Invitrogen)* and stored at -70ºC. Whole homogenate was used to determine viral load by Real Time Quantitative PCR (RT-qPCR) *RSV L* gene quantification.

2.4.7 Spleen

Spleen was collected from animals and inflated with 0.5mL of 0.15mg/mL collagenase D in RPMI for early life spleen, or 1mL 0.15mg/mL collagenase D in RPMI for adults and incubated for 20 minutes at 37ºC. Following digest, tissue was passed through 70µm cell strainers using the same media in which they were incubated for those experiments in which immune mediators were analysed from spleen supernatants (plus 0.5mL of new RPMI for early life spleens). Supernatants were stored at -70ºC for future analysis. Erythrocytes were lysed from the cell pellet by incubation in RBC lysis buffer for five minutes at RT. Finally, RBC lysis was quenched and splenocytes were centrifuged and resuspended in 1mL cRPMI, counted and used for further experiments (see naïve $CD4^+$ T cell isolation 2.5.4), flow cytometry or pelleted and stored at -70ºC in RLT buffer containing 1% 2-β-mercaptoethanol for RNA isolation.

2.4.8 Bone Marrow (BM)

Bone Marrow (BM) was obtained from femur and tibia of mice after removal of the surrounding muscle tissue. After disinfection with 70% ethanol and 2 washes of cRPMI, the distal and proximal epiphysis of each bone were cut. Two methods were used for cell isolation: a flushing method and a centrifugation method. In the flushing method, cRPMI was introduced with a syringe into the bone. Flushing was performed several times until the bone presented a white colour. In the centrifugation method, cut bones were placed in a microcentrifuge tube with supporting structures modified from pipette tips *(**Fig. 2.1**)* that held the bones upright. Bone marrow cells were then pelleted by centrifugation at 13000rpm for 30 seconds. The obtained pellet, which ended up in a different tube compartment after centrifugation, was resuspended in 1mL cRPMI. In both methods, bone marrow

cells were passed through a 70µm cell strainer and red blood cells were lysed using 1mL RBC Lysis Buffer for 5 minutes at RT followed by neutralization with 5mL cRPMI. Cells were then centrifuged and counted for subsequent experiments.

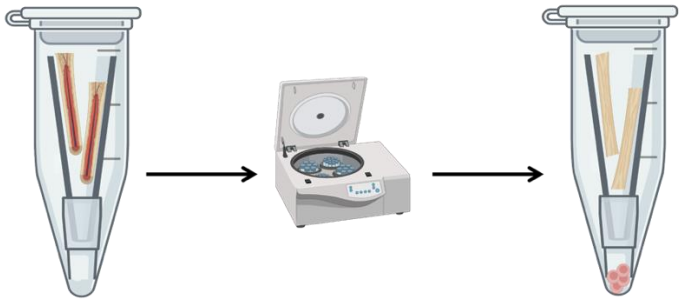


Fig 2.1. Depiction of supporting structures modified from pipette tips to help isolation of bone marrow cells by the centrifugation method.
Supporting structures are built by using the upper part of a p10 tip (bottom) and the lower part of a p200 tip (top). Bones are introduced into the upper pipette tip structure which maintains them upright and separates them from the cell pellet obtained after centrifugation.

2.5 *Ex vivo* cultures

2.5.1 *Ex vivo* stimulation for lymphocyte intracellular staining

To assess the potential of lymphocytes to produce intracellular mediators, single-cell suspensions from murine tissues or human cultures were seeded in 96-well round-bottom plates and stimulated with 20ng/mL PMA and 1.5µg/mL ionomycin in the presence of 10µg/mL Brefeldin A (BFA) *(all from Sigma-Aldrich)* in cRPMI for 4 hours at 37°C in a humidified incubator containing 5% CO_2. As a control, cells were also exposed to 10µg/mL of BFA alone.

2.5.2 *Ex vivo* differentiation of bone marrow progenitors into matured DCs subsets

2-3x10^6 bone marrow cells/well were cultured in cRPMI supplemented with 1% HEPES (4-(2-hydroxyethyl)-1-piperazineethanesulfonic acid) *(Sigma-Aldrich)*, 50µM 2-β-mercaptoethanol, 1% MEM Non-essential amino acids *(Gibco)*, 1% Sodium Pyruvate *(Gibco)* and 50ng/mL recombinant mouse FMS-like tyrosine kinase 3 ligand (Flt3L) *(Preprotech),* unless otherwise stated, in 6 well flat bottom plates *(Corning Incorporated)* for 8 to 11 days at 37ºC and 5% CO_2. This protocol was adapted from (514) to promote differentiation of bone marrow progenitors towards a cDC2 phenotype.

2.5.3 Stimulation of bone marrow derived DCs *in vitro*

Differentiated BMDCs were harvested on top of ice by mechanical dissociation of the plate, centrifuged at 1200rpm for 7 minutes at 4ºC and seeded at $1x10^5$ cells/well in 1% HEPES, 50μM 2-β-mercaptoethanol, 1% Non-essential amino acids and 1% sodium pyruvate in serum-free RPMI onto 96 round-bottom plates (515). Cells were left to rest for at least 2h and then pulsed with different stimulants or treated with inhibitors and antagonists *(**Table 2.1**)*. In specific experiments, bone marrow progenitors from $TLR4^{-/-}$ C57BL/6 mice with respective WT controls were used. After 2h cells were supplemented with 50μL 40% FBS enriched cRPMI media. Collection of supernatants, for ELISA analysis, were taken at 6h, 24h, 48h and 72h post-pulsation. A 24h timepoint of cell harvesting was used for cell counting, flow cytometry and RT-qPCR.

Stimuli, antagonists & inhibitors	Concentration used	Inactivation method	Supplier	Additional information
RSV	1 Multiplicity of infection (MOI)		Cultured in house as per methods 2.2.2	
Heat Inactivated RSV		60ºC for 30 minutes		
UV Inactivated RSV		999.900μJ for 5 minutes		
A.lwoffii	$2.5x10^8$cfu/mL	70ºC for 15 minutes	Cultured in house as per methods 2.2.1	
***A.lwoffii* + RSV**	$2.5x10^8$cfu/mL + 1 MOI respectively	70ºC for 15 minutes for *A.lwoffii*	Cultured in house as per methods 2.2.1 and 2.2.2	*A.lwoffii* was given 6h prior to RSV
LPS fom *E.coli* K12	0.3μg/mL for B cell cultures 0.85μg/mL for BMDC cultures 8.5μg/mL, equivalent to LPS present in *A.lwoffii, in TLR4 inhibitor or* $Tlr4^{-/-}$ *cultures*		*InvivoGen*	
CpG ODN (2006)	1μg/mL		*InvivoGen*	
Poly(I:C)	100ng/mL		*InvivoGen*	
Imiquimod	1μg/mL		*InvivoGen*	
TLR4 Antagonist (TAK-242)	2μM		*Merck*	Was left to act for 10 minutes at 37ºC and 5% CO_2 before adding the stimulants.
Protease inhibitor (P1860) and DMSO control	1:50		*Merck*	Specific for serines, cysteines, aspartic proteases and aminopeptidases. Stimulants were added at the same time

Table 2.1. Stimulants, inhibitors and antagonists used in in vitro DC cultures. *The table includes the concentration of the different molecules used as well as their supplier and additional specifications.*

2.5.4 Naïve CD4⁺ T cell isolation from mouse tissue

Following preparation of single cell suspension from spleen (see 2.4.7) naïve CD4⁺ T cells were isolated using specialized EasySep™ isolation kits according to manufacturer's instructions *(StemCell).* For BMDC-CD4⁺ T cell co-cultures (see 2.5.5), naïve CD4⁺ T cells were labelled with Tag-it Violet™ Proliferation and Cell Tracking Dye (CTV) *(Biolegend)* for 20 minutes at 37ºC as per manufacturer's recommendations to track cell division. For phosphoflow cytometry analysis cells were cultured *in vitro* (see 2.5.6). Cells were also stored at -70ºC in RLT buffer containing 1% 2-β-mercaptoethanol for RNA isolation.

2.5.5 *In vitro* DC and T cell co-culture

CTV labelled naïve CD4⁺ T cells from 3 pooled RSV-infected 2 week old Balb/c mice (see above 2.5.4) were co-cultured with preconditioned BMDCs 24h after stimulation (refer to 2.5.3). Cells were cultured at 1:1 ratio for 5 days in AIM-V media *(Gibco)* containing 5µg/ml purified α-mouse CD28 antibody *(Clone 37.51, Biolegend)* and supplemented with 50mM β-mercaptoethanol in 96-well round bottom plates precoated with 5µg/ml purified α-mouse CD3ε antibody *(Clone 145-2C11, Biolegend)*.

2.5.6 *In vitro* cytokine stimulation for phosphoflow cytometry

For detection of STAT phosphorylation following *in vitro* cytokine stimulation, isolated naïve CD4⁺ T cells from spleen (refer to 2.5.4) were rested in serum-free RPMI supplemented with 100U/mL penicillin/streptomycin at 37ºC 5% CO_2 overnight as per (25). Then, cells were stimulated with 100ng/mL rIL-2 or 50ng/mL rIL-6 *(both from Biolegend)* for 30 minutes. Cells were then fixed with prewarmed 1% paraformaldehyde (PFA) *(Sigma-Aldrich).* All steps were performed at 37ºC and 5% CO_2. Cells were subsequently frozen in True-Phos Perm Buffer (BioLegend) for 2h at -20 and then moved to −70°C until processed as described for flow cytometry.

2.6 Human samples

2.6.1 Isolation of Human Peripheral Blood Naïve CD4⁺ T Cells

35-50mL whole blood was obtained from healthy adult volunteers following approval by the National Research Ethics Committee (15/LO/1399 and 17/WA/0161). Peripheral blood mononuclear cells (PBMCs) were purified by density separation using Lymphoprep™ *(Stemcell™ Technologies).* Then, the EasySep™ Negative selection human naïve CD4⁺ isolation kit *(Stemcell™ Technologies)* was used as per manufacturer's instructions to isolate naïve CD4⁺ T cells. A day 0 input sample was reserved for flow cytometry and RT-qPCR analysis. Surface staining for the flow cytometry

samples was performed immediately. RT-qPCR samples were centrifuged at 2000rpm for 2 minutes, resuspended in RLT buffer and stored at -70ºC for future use.

2.6.2 Cell culture and T helper cell differentiation towards CXCR5^{hi}PD-1^{hi} cells

Following a protocol previously designed by Dr. W.Foster (516) 0.5x10^6 cells/mL of peripheral blood naïve CD4$^+$ T cells were first exposed to plate-bound 5ug/mL of ICOS-L-Fc *(rhB7-H2/Fc chimera, R&D Systems)* and/or soluble α-CD3/α-CD28 Dynabeads™ *(Thermo Fisher Scientific)* (1μL per 7.5 x10^4 cells) in AIM-V® media for 24 hours prior to addition of cytokines.

On the following day, cells exposed to ICOS-L-Fc received the whole T_{FH} skewing cocktail: 25ng/mL rhIL-6, 1ng/mL rhIL-12, 10ng/mL rhIL-1β, 5ng/mL rhTGF-β *(all from R&D Systems)* and 100ng/mL rhActivin A (*PeproTech Inc.,)*. Control cells that were not exposed to ICOS-L-Fc received 4ng/mL of rhIL-7 *(PeproTech)* instead of the T_{FH} cocktail. Cells were incubated for 5 days at 37ºC, 5% CO_2. Flow cytometry analysis was performed immediately after cell harvest whereas RT-qPCR samples were resuspended in 100μL of RLT buffer and stored at -70ºC for future use.

2.6.2.1 Culture of T Helper Cells with Intracellular Chemical Inhibitors

Peripheral blood naïve CD4$^+$ T cells were cultured as above (refer to 2.6.2), but in the presence of specific chemical inhibitors *(**Table 2.2**)*. Cells were then incubated for 5 days at 37ºC and 5% CO_2. Flow cytometry analysis was performed immediately after cell harvest whereas RT-qPCR samples were resuspended in 100μL of RLT buffer and stored at -70ºC for future use.

Inhibitor	Ref. num.	Supplier	Concentration	Regime	Vehicle control
α-pSTAT3	XIII C188-9	*Calbiochem*	0.2μM, 1μM, 5μM or 50μM	1h prior to cytokine stimulation	5μM or 50μM DMSO (Matching the highest concentration used in the experiment)
α-pSTAT4	CAS 6493-06-7	*Santa Cruz Biotechnologies*	100μM	1h prior to α-CD3/α-CD28 and 1h prior to cytokine stimulation	100μM or 50μM DMSO (Matching the highest concentration used in the experiment)
α-pSTAT5	CAS285986-31-4	*Calbiochem*	50μM		

Table 2.2. Chemical inhibitors, reference numbers, supplier, concentration, regime and matched vehicle controls used in cell culture.

2.7 Flow Cytometry Analysis

2.7.1 General staining protocol

Flow cytometry was performed following previous guidance (517). Staining of $0.5x10^6$-$2x10^6$ cells was carried out in 96-well V-bottom plates *(Corning Incorporated).* Cells were washed at least once between individual staining steps, except after live/dead dye, in the buffer last used for staining.

For discrimination of cells based on viability, cells were incubated for 20 minutes at 4ºC, in the dark, in 50µL of LIVE/DEAD™ Fixable Blue Dead Cell Stain e780 *(Thermo Fisher Scientific)* or with Zombie UV fixable viability dye *(Biolegend)* diluted to working concentration in PBS (1:5000 for tissue cell isolation and 1:1000 for *in vitro* cell cultures).

For staining of extracellular antigens, cells were incubated with 25µL of fluorescently-labelled antibodies (refer to ***Table 2.3*** and ***Table 2.4***) diluted in FACS buffer (PBS containing 2% FBS and 2mM EDTA *(Promega)*) for 30 minutes at 4°C in the dark, unless otherwise stated. 1:200 dilution of TruStain FcX antibody *(Biolegend)* was included in all stains to block non-specific binding.

Cells were then fixed either with 1% PFA diluted in PBS for 10 minutes at RT or, where fixation was followed by transcription factor staining, Foxp3/Transcription Factor Fixation/Permeabilization working solution *(Thermo Fisher Scientific)* for 30 minutes at 4ºC in the dark. In some cases, cells were stored in FACS buffer at 4°C at this point.

When intracellular staining was performed, cells were resuspended in 100µl Permeabilization buffer *(Thermo Fisher Scientific)* at RT and centrifuged at 2500rpm for 3 minutes. Then, cells were resuspended in 25µL of intracellular antibody mix prepared in permeabilization buffer in the presence of TruStain FcX antibody for 30minutes to 1h either at 4ºC or RT depending on the antibodies present in the cocktail and their specifications (refer to ***Table 2.3*** and ***Table 2.4***). Finally, cells were resuspended in 200µL of FACS buffer and acquired immediately.

On the day of staining cells for phospho STAT detection, plates were removed from the -70ºC and left to acclimatise at RT for 10 minutes. Then, cells were permeabilized with 100µl of permeabilization buffer and incubated with a 1:200 dilution of TruStain FcX antibody for 15 minutes at 4ºC. Cells were then stained with 25µl of mouse α-Stat3 *(pS727; BD)* or α-Stat5 *(pY694, BD)* alongside surface-stain antibodies in permeabilization buffer *(eBioscience)* for 1h at RT. Finally, cells were resuspended in FACS buffer and acquired immediately.

Single stains for compensation were prepared using Anti-Rat and Anti-Hamster Igκ/Negative Control Compensation Particles *(BD)*, except for the single stain of the viability dye, for which a mixture of live and dead cells, killed by heating them at 70ºC for 10 minutes, was used.

α – **Mouse antibodies**	**Clone**	**Supplier**	**Dilution Used**	**Specific considerations**
Brilliant Violet™ 421 anti-mouse CD11c	N418	*BioLegend*	1:200	
Brilliant Violet™ 421 anti-mouse CD64	X54-5/7.1	*BioLegend*	1:100	
Brilliant Violet™ 421 anti-mouse CXCR5	L138D7	*BioLegend*	1:50	30min @ RT
Brilliant Violet™ 421 anti-mouse IA/IE	M5/114.15.2	*BioLegend*	1:300	
Brilliant Violet™ 421 anti-mouse IgG1 Isotype	MOPC-21	*BioLegend*	1:50	
Brilliant Violet™ 421 anti-mouse IL-2	JES6-5H4	*BioLegend*	1:50	30min @ RT
Brilliant Violet™ 421 anti-mouse pSTAT3 (Tyr705)	13A3-1	*BioLegend*	1:50	
Brilliant Violet™ 421 anti-mouse pSTAT5 (pY694)	47/Stat5	*BD Biosciences*	1:50	
Brilliant Violet™ 510 anti-mouse B220	RA3-6B2	*BioLegend*	1:200	
Brilliant Violet™ 510 anti-mouse CD25 (IL-2Rα)	PC61	*BioLegend*	1:100	
Brilliant Violet™ 510 anti-mouse CD4	RM4-5	*BioLegend*	1:200	
Brilliant Violet™ 510 anti-mouse Ly6G	1A8	*BioLegend*	1:200	
Brilliant Violet™ 605 anti-mouse CD11b	M1/70	*BioLegend*	1:100	
Brilliant Violet™ 605 anti-mouse CD11c	N418	*BioLegend*	1:200	
Brilliant Violet™ 605 anti-mouse CD19	6D5	*BioLegend*	1:200	
Brilliant Violet™ 605 anti-mouse CD62L	MEL-14	*BioLegend*	1:200	
Brilliant Violet™ 605 anti-mouse CD8a	53-6.7	*BioLegend*	1:200	
Brilliant Violet™ 605 anti-mouse CD90.2	53-2.1	*BioLegend*	1:400	
Brilliant Violet™ 605 anti-mouse CXCR5	L138D7	*BioLegend*	1:50	
Brilliant Violet™ 605 anti-mouse Ly6G	1A8	*BioLegend*	1:200	
Brilliant Violet™ 605 anti-mouse Nkp46	29A1.4	*BioLegend*	1:100	
Brilliant Violet™ 605 anti-mouse PSGL1	2PH1	*BD Biosciences*	1:50	
Brilliant Violet™ 711 anti-mouse CD11b	M1/70	*BioLegend*	1:100	
Brilliant Violet™ 711 anti-mouse CD138	281-2	*BioLegend*	1:100	
Brilliant Violet™ 711 anti-mouse CD45.1	A20	*BioLegend*	1:100	
Brilliant Violet™ 711 anti-mouse CD8a	53-6.7	*BioLegend*	1:200	

Brilliant Violet™ 711 anti-mouse F4/80	BM8	*BioLegend*	1:200	
Brilliant Violet™ 711 anti-mouse GITR	DTA-1	*BD Biosciences*	1:100	
Brilliant Violet™ 711 anti-mouse PD-L1	10F.9G2	*BioLegend*	1:200	
Brilliant Violet™ 711 anti-mouse Tbet	4B10	*BioLegend*	1:50	
Brilliant Violet™ 785 anti-mouse CD19	6D5	*BioLegend*	1:100	
Brilliant Violet™ 785 anti-mouse CD86	GL-1	*BioLegend*	1:100	
Brilliant Violet™ 786 anti-mouse Rorγt	Q31-378	*BD Biosciences*	1:50	
FITC anti-mouse CD103	2E7	*BioLegend*	1:100	
FITC anti-mouse CD4	GK1.5	*BioLegend*	1:100	
FITC anti-mouse FOXP3	FJK-16s	*eBioscience*	1:100	
FITC anti-mouse GL7	GL7	*BioLegend*	1:100	
FITC anti-mouse IFN-γ	XMG1.2	*BioLegend*	1:50	
FITC anti-mouse IL-2	JES6-5H4	*BioLegend*	1:50	
FITC anti-mouse Ly6G	1A8	*BD Biosciences*	1:100	
FITC anti-mouse PDCA-1	927	*BioLegend*	1:100	
FITC anti-mouse TNF-α	MP6-XT22	*BioLegend*	1:50	
PerCpCy 5.5 anti-mouse CD11b	M1/70	*BioLegend*	1:100	
PerCpCy 5.5 anti-mouse CD19	eBio1D3	*eBiosciences*	1:200	
PerCpCy 5.5 anti-mouse CD25 (IL-2Rα)	3C7	*BioLegend*	1:100	Extracellularly or intracellularly
PerCpCy 5.5 anti-mouse CD44	IM7	*BioLegend*	1:100	
PerCpCy 5.5 anti-mouse IA/IE	M5/114.15.2	*BioLegend*	1:200 or 1:100	
PerCpCy 5.5 anti-mouse TCRVβ5.1,5.2	MR9-4	*BioLegend*	1:100	
PerCpCy 5.5 anti-mouse TCRβ	H57-597	*BioLegend*	1:100	
PerCP-eFluor 710 anti-mouse Gata3	TWAJ	*eBioscience*	1:50	
PE anti-mouse Bcl-6	K112-91	*BD Biosciences*	1:25	
PE anti-mouse CD122 (IL-2Rβ)	5H4	*BioLegend*	1:50	
PE anti-mouse CD25 (IL-2Rα)	PC61	*BioLegend*	1:100	
PE anti-mouse CD69	H1. 2F3	*BD Pharmigen*	1:100	
PE anti-mouse CD8a	53-6.7	*eBioscience*	1:100	
PE anti-mouse CD80	16-10A1	*eBioscience*	1:100	

PE anti-mouse CD86	GL-1	*BioLegend*	1:100	
PE anti-mouse CXCR5	L138D7	*BioLegend*	1:50	
PE anti-mouse FOXP3	FJK-16s	*BioLegend*	1:100	
PE anti-mouse IL-6	MP5-20F3	*BioLegend*	1:100	
PE anti-mouse SiglecF	E50-2440	*BD Biosciences*	1:100	
PE/Dazzle™ anti-mouse CD44	IM7	*BioLegend*	1:300	
PE/Dazzle™ anti-mouse TCRβ	H57-597	*BioLegend*	1:100	
PE/Dazzle™ anti-mouse Sirpα	P84	*BioLegend*	1:200	
PE-Cy5 anti-mouse CD3	17A2	*BD Biosciences*	1:300	
PE-Cy7 anti-mouse CD11c	N418	*BioLegend*	1:200	
PE-Cy7 anti-mouse IFNγ	XMG1.2	*BioLegend*	1:100	
PE-Cy7 anti-mouse F4/80	BM8	*BioLegend*	1:50	
PE-Cy7 anti-mouse PD-1	RMP1-30	*BioLegend*	1:200	
Alexa Fluor 647 anti-mouse CD11b	M1/70	*BioLegend*	1:200	
APC anti-mouse CD132 (common γ chain)	TUGm2	*BioLegend*	1:50	
APC anti-mouse CD19	ID3/CD19	*BioLegend*	1:100	
APC anti-mouse CD25 (IL-2Rα)	PC61.S	*eBioscience*	1:100	Extracellularly or intracellularly
APC anti-mouse CD4	RM4-5	*BioLegend*	1:200	
APC anti-mouse CD45	30-F11	*eBioscience*	1:200	
APC anti-mouse CD90.2	30-H12	*BioLegend*	1:100	
APC anti-mouse FOXP3	FJK-16s	*eBioscience*	1:50	
APC anti-mouse RORγT	AFKJS-9	*eBioscience*	1:50	
APC anti-mouse TCRβ	H57-597	*BioLegend*	1:100	
APC anti-mouse TCRγ/δ	GL3	*BioLegend*	1:100	
APC anti-mouse TNF-α	MP6-XT22	*BioLegend*	1:100	
eFluor Tbet	eBio4B10	*Invitrogen*	1:25	
AF647 anti-mouse CD11b	M1/70	*BioLegend*	1:200	
APC/Cy-7 anti-mouse CD11c	N418	*BioLegend*	1:100	
APC/Cy-7 anti-mouse CD45	30-F11	*BioLegend*	1:200	
Alexa Fluor® 700 anti-mouse CD19	6D5	*BioLegend*	1:50	

Alexa Fluor® 700 anti-mouse CD38	90	*BioLegend*	1:100
Alexa Fluor® 700 anti-mouse CD4	RM4-5	*BioLegend*	1:100
Alexa Fluor® 700 anti-mouse CD45	30-F11	*BioLegend*	1:100
Alexa Fluor® 700 anti-mouse CD90.2	30-H12	*BioLegend*	1:100
Alexa Fluor® 700 anti-mouse FOXP3	FJK-16s	*Invitrogen*	1:50
Alexa Fluor® 700 anti-mouse Ly6C	HK1.4	*BioLegend*	1:100
Alexa Fluor® 700 anti-mouse Ly6G	1A8	*BioLegend*	1:100
APC efluor 780 Live/Dead dye	L23105	*Invitrogen*	1:1000
TruStain FcX™ antibody	93	*BioLegend*	1:200
Zombie UV L/D	423108	*BioLegend*	1:1000

Table 2.3. Surface and intracellular anti-mouse antibodies, clone, supplier and dilution used for flow cytometry
Antibodies used for intracellular staining are marked in grey.

α – **Human antibodies**	**Clone**	**Supplier**	**Dilution Used**
Brilliant Violet™ 421 anti-human pSTAT3	13A3-1	*BioLegend*	1:50
Brilliant Violet™605 anti-human CD4	OKT4	*BioLegend*	1:100
Brilliant Violet™ 650 anti-human CD25	BC96	*BioLegend*	1:50
Brilliant Violet™ 711 anti-human CCR7	G043H7	*BioLegend*	1:50
Brilliant Violet™ 785 anti-human CD19	HIBC19	*BioLegend*	1:50
Brilliant Violet™ 785 anti-human CD45RA	HI 100	*BioLegend*	1:100
BB515 Rat anti-human CXCR5 (CD185)	RF8B2	*BD Horizon™*	1:25
PerCpCy 5.5 anti-human CD3	UCHT1	*BioLegend*	1:50
PerCpCy 5.5 anti-human CD4	RPA-T4	*BioLegend*	1:50
PerCpCy 5.5 anti-human CD19	HIB19	*BioLegend*	1:50
PE anti-human BCL6	K112-91	*BD Biosciences*	1:25
PE/Dazzle™ 594 anti-human CD25	M-A251	*BioLegend*	1:50
PE/Cy7 anti-human CD279 (PD-1)	EH12.2H7	*BioLegend*	1:50
Alexa Fluor® 647 anti-human GITR	A18	*BioLegend*	1:50
APC anti-human CCR7	G043H7	*BioLegend*	1:50
APC efluor 780 Live/Dead dye	L23105	*Invitrogen*	1:1000

Table 2.4. Surface and intracellular anti-human antibodies, clone, supplier and dilution used for flow cytometry
Antibodies used for intracellular staining are marked in grey.

2.7.2 Acquisition and analysis

Samples were acquired on LSRFortessa™ machines with either four or five lasers running FACSDiva™ software *(both BD)*. Data analysis was performed in Version 10 FlowJo software *(BD)*. All analyses were restricted to non-debris, live, single cells. Representative gating strategies for each panel are depicted in the results section prior to the quantification of the results using such panels.

2.8 RNA isolation, cDNA synthesis and real time quantitative PCR

2.8.1. RNA isolation and cDNA synthesis from single cell suspensions

After adding an equal volume of 70% ethanol to the samples stored at -70ºC in RLT buffer and 1% 2-β-mercaptoethanol, the RNeasy Mini kit *(QiAGEN)* was used for extraction of RNA from cell suspensions as per manufacturer's instructions. RNA quantity and quality were measured using the NanoDropTM 1000 spectrophotometer *(Thermo Fisher Scientific).* RNA was transcribed into cDNA using the GoScriptTM Reverse Transcription System *(Promega)* as per manufacturer's recommendations using random hexamers.

2.8.2. RNA isolation and cDNA synthesis from lung tissue

On the day of RNA extraction, the top right lung lobe stored at -70ºC in RNAlater™ stabilization solution was thawed on ice and placed in homogenization tubes with lysing matrix D *(MP Biomedicals)* in RLT lysis buffer. Tissue homogenizations were performed using FastPrep®-24 Homogeniser *(MP Biomedicals)* at max speed (6.5 m/s) for 40 seconds. Homogenised samples were then centrifuged at 10000rpm for 10 minutes and supernatants were collected for RNA extraction using the RNeasy Micro kit. As before, quantity and quality of RNA were measured using NanoDropTM 1000 spectrophotometer. RNA conversion to cDNA was prepared using High-Capacity cDNA Reverse Transcription Kit *(Applied Biosystems)* and run in VeritiTM 96-Well Fast Thermal Cycler *(Applied Biosystems)* as per manufacturer's instructions.

Lung lobes that were snap frozen in liquid nitrogen were disrupted in cRPMI using a handheld homogenizer *(Stuart SHM1).* RNA isolation was then performed in the same way as per single cell suspensions of alternative tissue sites (refer to 2.8.1).

2.8.3 Real Time Quantitative PCR (RT-qPCR)

RT-qPCR reaction mixes were prepared from TaqMan™ FAM probes and Fast Advanced Master Mix at 1:10 dilution *(both from Thermo Fisher Scientific)*. A list of all TaqManTM probes used in this thesis can be found in ***Table 2.5*** *and* ***Table 2.6***. Per reaction, 3.3µL of this mix was added to 2.7µL of 1:10 diluted cDNA per well in nuclease-free, deionized and distilled water *(Thermo Scientific)*. All conditions were run in triplicates in 384-well plates on a ViiA 7 Real-Time PCR system *(Thermo Fisher Scientific)* set at 40 cycles and using manufacturer-recommended settings. QuantStudio Real-Time PCR software *(Thermo Fisher Scientific)* was used to determine cycle threshold (CT) values. Relative expression of genes was calculated using the following formula:

$$\text{Relative Expression} = 2^{\Delta CT} \ ,$$

$$\text{Where } \Delta CT = CT \text{ (housekeeping genes)} - CT \text{ (gene of interest)}$$

The RT-qPCR limit of detection was calculated as:

$$\text{Limit of detection} = 2^{\Delta CT \text{ housekeeping genes}},$$

$$\text{Where } \Delta CT \text{ housekeeping genes} = CT(\text{housekeeping gene}) - 40$$

Results were plotted as relative expression ($2^{\Delta CT}$).

Actb and *Gapdh* or *ACTB* and *18S* were used as housekeeping genes for mouse or human samples respectively and CT values were averaged before calculation of relative expression.

Gene Name	Assay ID
Actb	Mm01205647_g1
Cd122	Mm00434264_m1
Cd132	Mm00442885_m1
Cd25	Mm01340213_m1
Gapdh	Mm03302249_g1
Il2	Mm00442486_m1
Il6	Mm00446190_m1
IL6ra	Mm01211445_m1
Il6st	Mm00439665_m1
Stat3	Mm01219775_m1
Stat5a	Mm00839861_m1

Table 2.5. Mouse TaqMan™ probes used for RT-qPCR.

Gene Name	Assay ID
ACTB	Hs01060665_g1
18S	Hs99999901_s1
BCL6	Hs00153368_m1
CXCR5	Hs00173527_m1
GAPDH	Hs02758991_g1
ICOS	Hs00359999_m1
IL9	Hs00174125_m1
IL17A	Hs00174383_m1
IL21	Hs00222327_m1
IRF4	Hs00180031_m1
PDCD1	Hs00169472_m1
PRDM1	Hs00153357_m1
RORC	Hs01076112_m1
SPI1	Hs02786711_m1
TGFB1	Hs00998133_m1

Table 2.6. Human TaqMan™ probes used for RT-qPCR.

For the detection of RSV-L viral RNA, RT-qPCR was carried out on lung RNA using the following *(**Table 2.7**)*.

	Concentration	Sequence
Forward primer	900nM	5′-GAACTCAGTGTAGGTAGAATGTTTGCA-3′
Reverse primer	300nM	5′-TTCAGCTATCATTTTCTCTGCCAAT-3′
Probe	100nM	5′- FAM-TTTGAACCTGTCTGAACAT-TAMRA-3′

***Table 2.7. Primers and probes used for detection of RSV-L RNA**. Includes concentration and sequence of the primers and probes used.*

2.9 Enzyme-Linked Immunosorbent Assay (ELISA)

2.9.1 Validation of RSV and *A.lwoffii* Antigen

RSV antigens grown as per *section 2.2.2* were validated through ELISA by comparing them to a previous stock made and validated in the lab. RSV antigen was diluted at 1:100, 1:500 and 1:1000 for binding to titrations of poly-Igs in serum of RSV-infected adult Balb/c mice. The wells of high binding, half-area, 96 well flat-bottom plates *(Corning)* were coated with RSV antigen (50µL/well) at the three different concentrations and incubated at 4°C overnight. Coating with HEp2 antigen (50µL/well) instead of RSV was used as a control. After coating, wells were washed once with PBS-0.05% Tween-20 (PBS-T) and free binding sites were blocked with PBS containing 1% BSA (100µL/well) for 2 hours at RT. For antigen testing, serum from RSV infected and uninfected adult Balb/c mice were diluted (also at 1:100, 1:500, 1:1000) in PBS–Tween 20–BSA, and 35µL of each dilution was added to the plate wells and incubated for 2 hours at RT. After sample incubation, plates were washed three times with PBS-T. Following the addition of anti-immunoglobulin (Ig) secondary antibody conjugated with Horseradish peroxidase (HRP from the SBA Clonotyping System-HRP (35µL/well) *(Southern-Biotech)*, plates were incubated for 1h at RT. Plates were then washed with PBS-T 5 times. HRP activity was measured through addition of H_2O_2- 3,3′,5,5′-Tetramethylbenzidine (TMB) (35µL/well). The reaction was permitted to continue in the dark until the colour had developed well, at which point it was quenched with H_2SO_4 (0.18M; 35µL/well). Light absorption was determined at 450nm using a SpectraMax® i3x microplate reader *(Molecular Devices)*. Dilution of the RSV antigen at 1:100 proved to be best at reaching plateau and giving a distinctive separation between samples when analysing the RSV antigen and HEp2 control. Therefore, 1:100 dilution was used for subsequent ELISAs and avidity assays.

The same procedure was used for *A.lwoffii* antigen validation with a few adjustments. The obtained antigen from culture (refer to section 2.2.1) was sonicated and diluted to 100ug/mL, followed by 1:10 subsequent dilutions in PBS. In this case, serum from 3wk old *A.lwoffii*+RSV and PBS exposed Balb/c mice were used as samples for comparison. A distinctive response between the *A.lwoffi*+RSV and PBS treated mice was observed at a 1:100 dilution, so this combination was used for subsequent ELISAs and avidity assays.

2.9.2 Detection of antigen (Ag)-specific mouse antibodies in serum and BAL samples

For quantification of Ag-specific total Ig, IgA, IgG, IgG1 and IgG2a/c in serum, BAL and NAL, ½ area ELISA microplates *(Corning)* were coated with RSV A2 antigen, or previously sonicated *A.lwoffii* antigen for 10 minutes grown in house, and left overnight at 4ºC (see 2.2.1 and 2.2.2). The same protocol as per RSV or *A.lwoffii* validation was used (see above, 2.9.1) where bound antibody

was detected using the SBA Clonotyping System-HRP and absorbance was measured at 450nm using the SpectraMax® i3x microplate reader.

2.9.3 Avidity assay for Ag-specific antibodies

For avidity assays, the same procedure as before was repeated (see above, 2.9.1), but after sample incubation, plates were washed three times for 5 minutes with either 4M of urea, for early life samples, or 8M of urea, for adult samples, unless otherwise stated, or PBS as control. As before, bound antibody was detected using the SBA Clonotyping System-HRP and absorbance was measured at 450nm using the SpectraMax® i3x microplate reader.

2.9.4 Detection of human and mouse cytokines and receptors

Commercial kits for detection of cytokines in serum, BAL, tissue and culture supernatants were purchased for mouse IL-6 Uncoated ELISA kit *(Invitrogen)* and CD25/IL-2Rα kit *(R&D systems)* and human CXCL13 *(R&D Systems)* and IL-21 *(Invitrogen)*. Assays were performed following manufacturer's recommendations but reducing the volumes by 50% as ½ area ELISA microplates were used. All samples were incubated overnight at 4ºC to maximise results. Absorbance was measured using the SpectraMax® i3x microplate reader.

2.10 Neutralization assay

To analyse the neutralization capacity of α-RSV antibodies in infected and uninfected mouse serum and BAL, first a monolayer of HEp2 cells was grown. To that end, $3x10^4$ HEp2 cells/well in DMEM 10% FBS, 1% penicillin/streptomycin were transferred into a 96 well flat-bottomed plate (100µL/well) and incubated for 24h at 37ºC and 5% CO_2. The next day, having checked that there was a confluent monolayer in the plate, serum and BAL samples were diluted with serum-free DMEM, 1% penicillin/streptomycin and inactivated by incubation at 56ºC for 30 minutes. For serum samples 1:20 dilution of serum followed by 1:3 subsequent dilutions were used, whereas 1:4 dilutions were used for BAL with a final volume of 50µL/well. Once inactivated, mouse samples were mixed with RSV to a final concentration of $1.98x10^6$pfu/mL of RSV. Serum samples were combined with viral particles and shaken for 30 minutes at RT to give them time to interact before carefully adding them on top of the HEp2 monolayer. After 2h at 37ºC and 5% CO_2, 150µL of 10% FBS, 1% penicillin/streptomycin was added to the wells, which were incubated at 37ºC and 5% CO_2 for an extra 18h. Following this incubation, media was expelled from the wells and washed once with 100µL of PBS/well. Cells were then fixed with 100µL of absolute methanol with 2% hydrogen peroxide per well for 20 minutes at RT. HEp2 cells were then washed with 150µL of PBS with 1% BSA and incubated with biotinylated α-RSV antibody *(Invitrogen)* diluted 1:200 in PBS 1% BSA for 1h at RT. Wells were then washed twice with PBS 1% BSA for 5 minutes and then a 1:500

dilution of extravidin-peroxidase *(Sigma-Aldrich)* was added to each well for 1h at RT. Plates were washed twice again with PBS 1% BSA for 5 minutes and then stained with 50µL/well of AEC substrate with peroxidase made according to manufacturer's instructions. Wells were checked regularly for colour change under an inverted light microscope until plaques of an orange/brown colour were developed (usually 20 minutes). The reaction was then stopped by discarding the AEC substrate and filling the wells with deionised water. Finally, plaques were counted manually using an inverted light microscope *(Olympus CK40* and *Leica DMi1* microscopes).

2.11 Statistical Analysis

Statistics and graphs were analysed in GraphPad Prism 10.0 *(Graphpad Software Inc)*. Data is depicted as median with interquartile range. Each symbol represents a unique biological sample unless otherwise stated. Since normality of data could not be assumed, non-parametric analyses were conducted unless otherwise indicated. Two groups were compared by calculating exact p values using a two-sided Mann-Whitney test. Significance between more than two groups was determined using a Kruskal-Wallis Test with Dunn's multiple comparisons. For matched, non-parametric two group data Willcoxon signed ranked test was employed and for matched, multiple group data Fridman with Dunn's multiple comparisons test was used. For correlation analysis simple linear regression with Pearson analysis was performed. In all cases p values < 0.05 were considered statistically significant and are depicted as: *$p < 0.05$, **$p < 0.005$, *** $p < 0.001$, **** $p < 0.0001$.

2.12 Diagram Figures

Diagram figures were created using BioRender.com

3 Results I: Early life T cell responses are characterised by increased IL-2/pSTAT5 signalling

3.1 Introduction

3.1.1 Anatomical organisation of the immune system

The immune system, comprising an array of cells, organs and tissues, is distributed throughout the entire organism. The blood and lymphatic vessels connect lymphoid organs and tissues and unite them into a functional whole. The lymphoid organs and tissues can be classified into two main categories: the primary lymphoid organs (PLOs) and the secondary lymphoid organs (SLOs). Lymphocytes are generated in the PLOs, where they also undergo development and maturation; with the main PLOs being bone marrow and thymus. The SLOs meanwhile are where matured immunocompetent lymphocytes interact with antigens and therefore they are where the adaptive immune responses are initiated. They include the lymph nodes and spleen, where canonical GC structures are generated. GCs are also seen in mucosal-associated lymphoid tissues (MALT) such as the bronchus-associated lymphoid tissue (BALT) in the lung and the gut-associated lymphoid tissue (GALT) in the gastrointestinal tract. The formation of organised MALT, alongside initiation of adaptive immune responses and the formation of GC structures, in the mucosa is dependent on local inflammatory insults. The generation of immune responses is not the primary role of these tissues; these regions are therefore referred to as tertiary lymphoid structures (TLS) or ectopic germinal centres. The initial priming of naïve B cells and T cells that eventually become memory B cells, antibody secreting cells, cytotoxic T cells or helper T cells, occurs within the SLOs (518).

3.1.2 The T cell lifespan

Lymphocyte location is not restricted to lymphoid organs, as T cells can be found in virtually every organ and tissue. They can populate mucosal and barrier sites, exocrine organs, fat, skin and even the central nervous system. The majority of T cells are however found in the aforementioned lymphoid organs, particularly in the gastrointestinal tract, with 2-3% of them found in blood (519–521).

The yolk sac is the first hematopoietic site in the mouse and human embryo followed by liver production of foetal T cell progenitors from day 14.5 of gestation in mice and day 23 antenatal in humans. Just before birth in mice and after birth in humans, T lymphocytes originating from hematopoietic stem cells (HSCs) in the BM migrate to the thymus for maturation and selection and are subsequently exported to the periphery in the form of naïve T cells or natural T_{regs} (522–524). Naïve T cells travel through the different SLOs and the interconnecting vessels until encountering a cognate antigen presented by APCs in the SLOs. It is in the SLOs where naïve T cells will differentiate into effector T cells which are capable of generating specific immune functions. In general, both effector $CD4^+$ and $CD8^+$ T cells will migrate to the site of infection to promote pathogen clearance through the production of cytokines or cytotoxic mediators. Activated effector

cells are short-lived, although a proportion survive as memory T cells that persist as heterogeneous subsets based on migration, tissue localization, and self-renewal capacities (525).

In this regard T_{FH} cells are the exception to the norm as instead of migrating to the site of infection and/or inflammation, the majority remain in the SLOs, migrating into the B cell zone to initiate a humoral immune response and promote GC formation (526). T_{FH}, and the GCs they generate, are therefore primarily found within the SLOs to which the primary site of inflammation drains, but GC responses are also seen in both the TLS of the inflamed tissue and distal SLOs. Indeed analysis of antigen-specific B cell clones and SHM frequencies in humans shows that there is some overlap in the response between the different SLOs indicating that they might be interconnected (288,527). Circulatory T_{FH} cells (cT_{FH}), generated prior to GC entry, can be isolated from peripheral blood of both mice and humans, possess a memory-like phenotype, and can likely seed these distal SLOs, however their exact function and relationship to either draining LNs or tissue-resident T_{FH} remains unclear (79,528,529). B cell responses between SLOs however aren't entirely identical, indicating that there is at least a partial compartmentalization of the humoral immune response, which could be explained by the response being highly dependent on the migration of DCs carrying cognate antigen from the infected tissue sites (288,530). This is observed in the context of organ-specific pathogens as well as cancer tissue (288,530). Therefore, local responses against specific pathogens can be studied by analysing the BALT or GALT, in the case of respiratory and intestinal tract infections respectively, as well as the immune response initiated in the lymph node located closer to the site of infection from a network of 500-700 lymph nodes found in the human body (531). In mice, spleen responses are also frequently studied since the spleen is both the largest SLO and the one that filters circulating blood for aging red blood cells as well as foreign antigens or pathogens that have gained access to the bloodstream, and thus combines responses across many anatomical sites (531).

3.1.3 The humoral immune response against respiratory syncytial virus is downregulated in early life

As outlined in the main introduction, antibody-mediated immunity is essential for long-term protection following infection or vaccination but is often defective in early life probably due to the decreased differentiation of T_{FH} cells and associated B cell responses (13,21,25,235,532). This is particularly true in the case of RSV infection, the most common cause of infant bronchiolitis that can cause re-infection in children even within the same cold season while it normally causes mild URTI in adults (9).

Studies in adult models of infection and immunization show that T_{FH} differentiation depends on the pSTAT3/pSTAT5 balance, with cytokines that promote the activation of STAT3 in both mice and

humans being T_{FH}-promoters and cytokines driving STAT5 phosphorylation, most notably IL-2, preventing T_{FH} differentiation (526). T_{FH}-deficient adult mice highlight the importance of T_{FH} cells in the development of protective immunity during RSV infection; as Bcl6-deficient adult mice are unable to mount protective responses against RSV re-challenge (25). Similarly, while T_{FH}-sufficient RSV infected adult mice generate robust antibody responses, those infected in early life have a limited ability to do so, characterized by reduced levels of both RSV-specific systemic IgG and mucosal IgA (25,533). This failure to produce antibody is associated with limited differentiation of T_{FH} and GC B cells in the lung draining LNs and enhanced susceptibility to secondary infection (25).

3.1.4 Hypothesis and Aims

Despite several studies suggesting a reduced ability to form T cell dependent humoral immune responses in early life (13,23–26,237,533,534), little is known about the mechanisms leading to impaired T_{FH} differentiation during the neonatal period.

Thus, the hypothesis of this chapter is that:

Early life promotes an IL-2 enriched environment that prevents T_{FH} differentiation and hinders the infant immune response against RSV infection.

To address this hypothesis, the aims of this chapter are:

1. To analyse if IL-2/STAT5 signalling is upregulated in early life
2. To analyse the mechanism(s) leading to an increase in IL-2 signalling in early life in distinct lymphoid organs
3. To investigate the role of pSTAT3 and pSTAT5 in human T_{FH} differentiation using an *in vitro* model

The experimental work presented here forms part of a bigger published work (25) and also extends on it *(refer to appendix I.1)*

3.2 Results

3.2.1 STAT5 phosphorylation is increased in naïve CD4$^+$ T cells from infant mice both after IL-2 and IL-6 stimulation

T_{FH} differentiation depends on pSTAT3/pSTAT5 balance with phosphorylation of STAT3 giving rise to Bcl6 upregulation leading to T_{FH} differentiation and pSTAT5 promoting Blimp-1 upregulation and differentiation towards alternative $T_{effector}$ cells (526). The ability of early life and adult naïve CD4$^+$ T cells to recognise T_{helper} differentiation-driving cytokines and phosphorylate these transcription factors was first analysed. To this end, naïve CD4$^+$ T cells were isolated from splenocytes of young and adult mice and were exposed to recombinant mouse (rm)IL-2 or rmIL-6 *in vitro* (***Fig 3.1a***). In response to the same dose of IL-2, naïve CD4$^+$ T cells from 1wk old mice showed an increased predisposition to phosphorylate STAT5 when compared with naïve CD4$^+$ T cells from 8wk old mice (***Fig 3.1b***). No difference in STAT3 phosphorylation upon rmIL-6 stimulation was observed between both ages (***Fig 3.1c***). Similar results were obtained for naïve splenic CD4$^+$ T cells isolated from 3wk old mice compared to 6wk old mice (***Fig 3.1d,e***). In addition it was noted that naïve CD4$^+$ T cells from younger mice also showed an increased phosphorylation of STAT5 after rmIL-6 stimulation (***Fig 3.1d***), while again no difference according to age was seen in pSTAT3 after rmIL-2 or rmIL-6 exposure *in vitro* (***Fig 3.1e***).

To determine if the differential activation of STAT5 resulted from altered STAT3/STAT5 balance, *Stat3* and *Stat5* transcript from naïve CD4$^+$ T cells of different ages were analysed by RT-qPCR. *Stat3* levels increased with age (***Fig 3.2a***) while *Stat5* levels remained constant (***Fig 3.2b***). The *Stat3/Stat5* ratio was therefore increased later in life when compared to neonatal counterparts as observed by a significant increase in 3wk and 8wk old mice when compared to 3d old animals (***Fig 3.2c***). This data overall indicates that STAT5 activation is enhanced in early life, while STAT3 activation remains similar, potentially explaining the reduced T_{FH} differentiation seen in young mice.

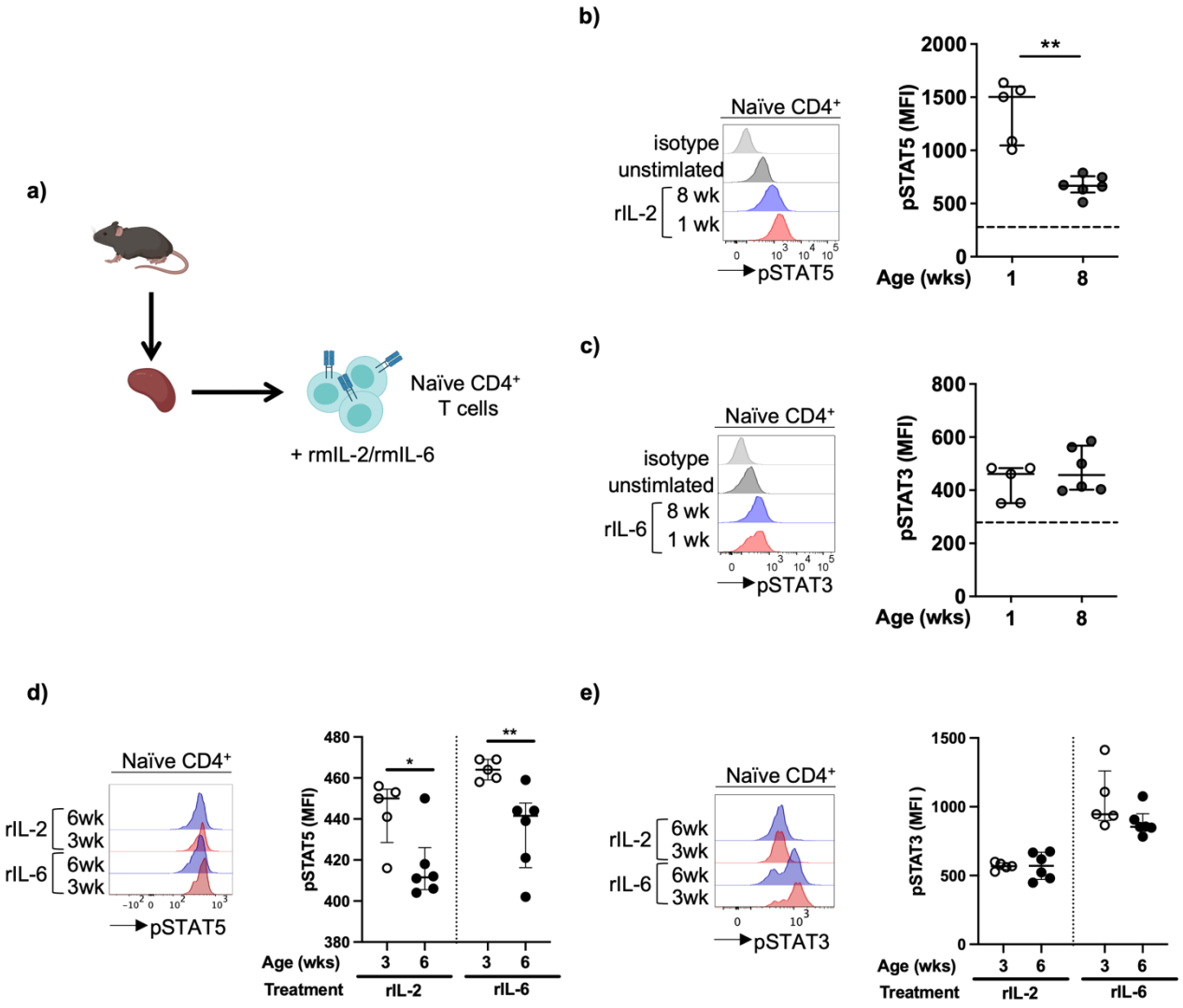


Fig 3.1. STAT5 phosphorylation is increased in naïve CD4⁺ T cells from early life mice both after rmIL-2 and rmIL-6 stimulation

(a) Naïve CD4⁺ T cells were isolated from spleens of adult and young C57BL/6 mice and stimulated with either recombinant mouse IL-2 or IL-6 for 30 minutes at 37ºC and 5% CO_2. **(b)** pSTAT5 after rm-IL-2 stimulation and **(c)** pSTAT3 after rm-IL-6 stimulation was measured in naïve CD4⁺ T cells isolated from spleens of 1 and 8wk old mice. **(d)** pSTAT5 after rm-IL-2 and rm-IL-6 stimulation and **(e)** pSTAT3 after rm-IL-2 and rm-IL-6 stimulation were measured in naïve CD4⁺ T cells isolated from spleens of 3 and 6wk old mice. Data from two independent experiments with n= 4-6 mice per group (b,c) or one independent experiment with n = 5-6 mice per group (d,e). Data shown with median and interquartile range. Each dot represents one mouse. Mann-Whitney test was performed in which *, $p < 0.05$; **, $p < 0.01$; and ***, $p < 0.001$.

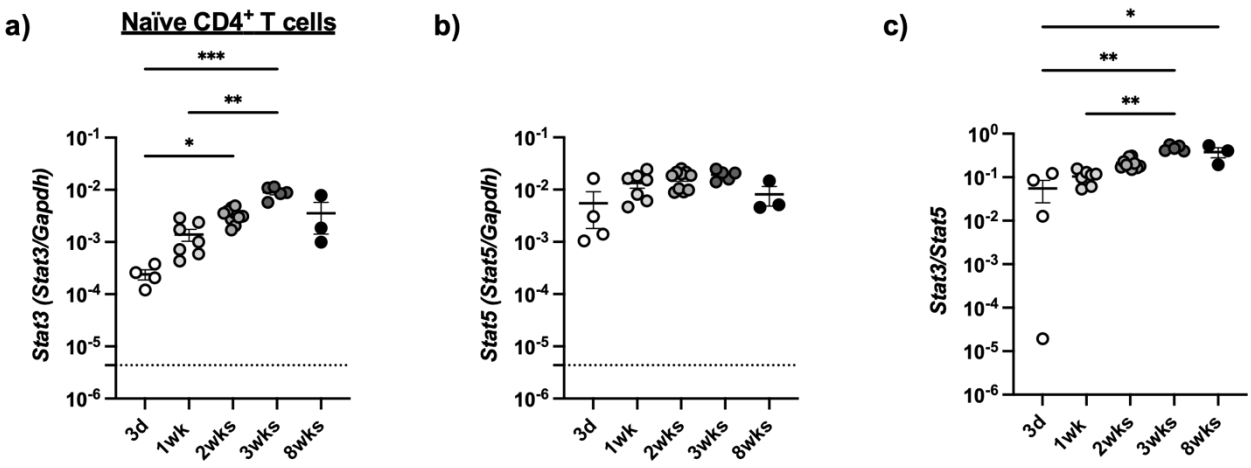


Fig 3.2. Early life is characterised by a Stat5/Stat3 signature

(a) Naïve CD4⁺ T cells were isolated from spleens of C57BL/6 mice of different ages and *Stat3* and **(b)** *Stat5* were analysed by RT-qPCR. **(c)** The ratio of *Stat3/Stat5* was calculated. Data from two independent experiments with n = 3-14 mice per group. Data shown with median and interquartile range. Each dot represents one mouse. Bottom dotted line represents the limit of detection for the given assay. Kruskal-Wallis test with multiple comparisons was performed in which *, $p < 0.05$; **, $p < 0.01$; and ***, $p < 0.001$.

3.2.2 Early evidence of T_{FH} differentiation 3 days post RSV infection

In vivo T_{FH} differentiation, GC reactions and antigen-specific antibody responses are decreased in early life (1 and 2wk old mice) when compared to adult counterparts (8wk old mice), 14 days post RSV infection (25). In adult mice, the T_{FH} differentiation programme starts as early as day 2-3 post systemic viral infection (57). I therefore sought to determine if early evidence of T_{FH} differentiation by CD4⁺ T cells could also be observed at this timepoint in neonatal and adult mice following RSV infection.

1 and 8wk old mice were infected i.n. with the same dose of RSV and culled 3dpi, when SLOs and lungs were harvested. A group of 8wk old mice, an age that readily allows T_{FH} differentiation, was exposed to PBS i.n as controls (***Fig 3.3a***). A flow cytometry strategy was used to identify different populations of CD4⁺ T cells (***Fig 3.3b***).

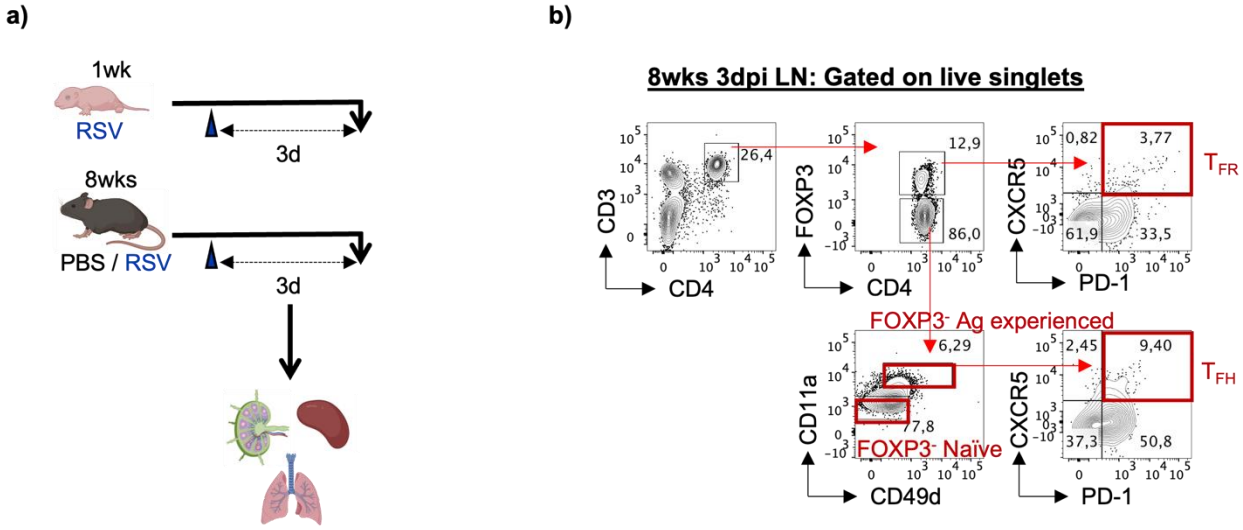


Fig 3.3. Gating CD4⁺ T cell subsets early after RSV infection

(a) 1wk and 8wk-old C57BL/6 mice were infected with 2.5 × 10^5 PF RSV A2 i.n. A group of 8wk old mice was exposed to PBS i.n as controls. Mediastinal lymph node, spleen and lung were harvested 3dpi and the T cells subsets were analysed. **(b)** Representative flow cytometry gating strategy for T cell subsets. From total cells doublets were excluded and live cells were selected as e780 live/dead negative cells. Lymphoid cells were gated and $CD4^+$ T cells were defined as $CD3^+CD4^+$ cells. FOXP3 expression distinguished between $FOXP3^-$ and $FOXP3^+$ (T_{reg}) cells. $FOXP3^-$ cells further co-expressing CD11a and CD49d were classified as antigen experienced cells with cells negative for these markers being $FOXP3^-$ naïve cells. Co-expression of CXCR5 and PD-1 markers were used to select T_{FH} or T_{FR} cells depending on their cells of origin.

No significant difference in proportion or cell numbers was observed in mediastinal LN antigen (Ag) experienced $CD4^+$ T cells ($CD11a^+CD49d^+$) or T_{FH} cells ($CD11a^+CD49d^+FOXP3^-CXCR5^+PD\text{-}1^+$) with age between 3dpi mice at this early timepoint, but infected adults showed a trend to an increased Ag experienced and T_{FH} cell numbers when compared to both infected neonates and naïve adult counterparts (***Fig 3.4a-e***). A trend to an increase percentage of T_{FH} cells in both neonatal and adult infected mice was observed when compared with 8wk old naïve animals (***Fig 3.4d***). CXCR5 expression was increased in 1wk and 8wk old infected animals when compared to controls; with CXCR5 expression being significantly increased in infected 8wk old mice T_{FH} cells when compared to young counterparts (***Fig 3.4f***). No difference in PD-1 expression was observed between groups (***Fig 3.4g***). One limitation of this study is the low n number included for control mice, which makes interpretation of results more challenging, particularly when there is a big spread between both data points. Nevertheless, the T_{FH} programme seems to be initiated in the LN of both 1wk and 8wk old mice 3dp infection as indicated by the lack of Ly6C and the lower expression of PSGL1 in T_{FH} cells when compared to naïve cells in these animals (64), which was significant in neonates (***Fig 3.4g***).

A trend to an increase T_{FR} ($FOXP3^+CXCR5^+PD\text{-}1^+$) proportion was observed in infected neonates when compared with infected adults (***Fig 3.4i***), but similar numbers of T_{FR} were seen in LN of all mice ages and infection status (***Fig 3.4j***). A trend to an increase T_{FH}/T_{FR} ratio was observed in 3dpi

animals when compared to naïve mice and this was more pronounced in adulthood when compared to early life *(**Fig 3.4k**)*.

More pronounced responses were observed in the spleen of infected mice, with significantly increased proportions and numbers of antigen-experienced and T_{FH} cells in 8wk old mice *(**Fig 3.5a-d**)*. A trend to an increase CXCR5 and PD-1 MFI was also seen in T_{FH} of adult mice *(**Fig 3.5e,f**)*. Differentiation of splenic T_{FH} cells in adult mice was confirmed by their low PSGL1 expression, while this was not observed in neonatal mice *(**Fig 3.5g**)*. In 1wk old mice T_{FR} proportions were upregulated *(**Fig 3.5h**)* but T_{FR} cell numbers were significantly increased in 8wk counterparts *(**Fig 3.5i**)*. All these factors are probably contributing to the significant increase in T_{FH}/T_{FR} ratio observed in adult when compared to neonatal spleen *(**Fig 3.5j**)*.

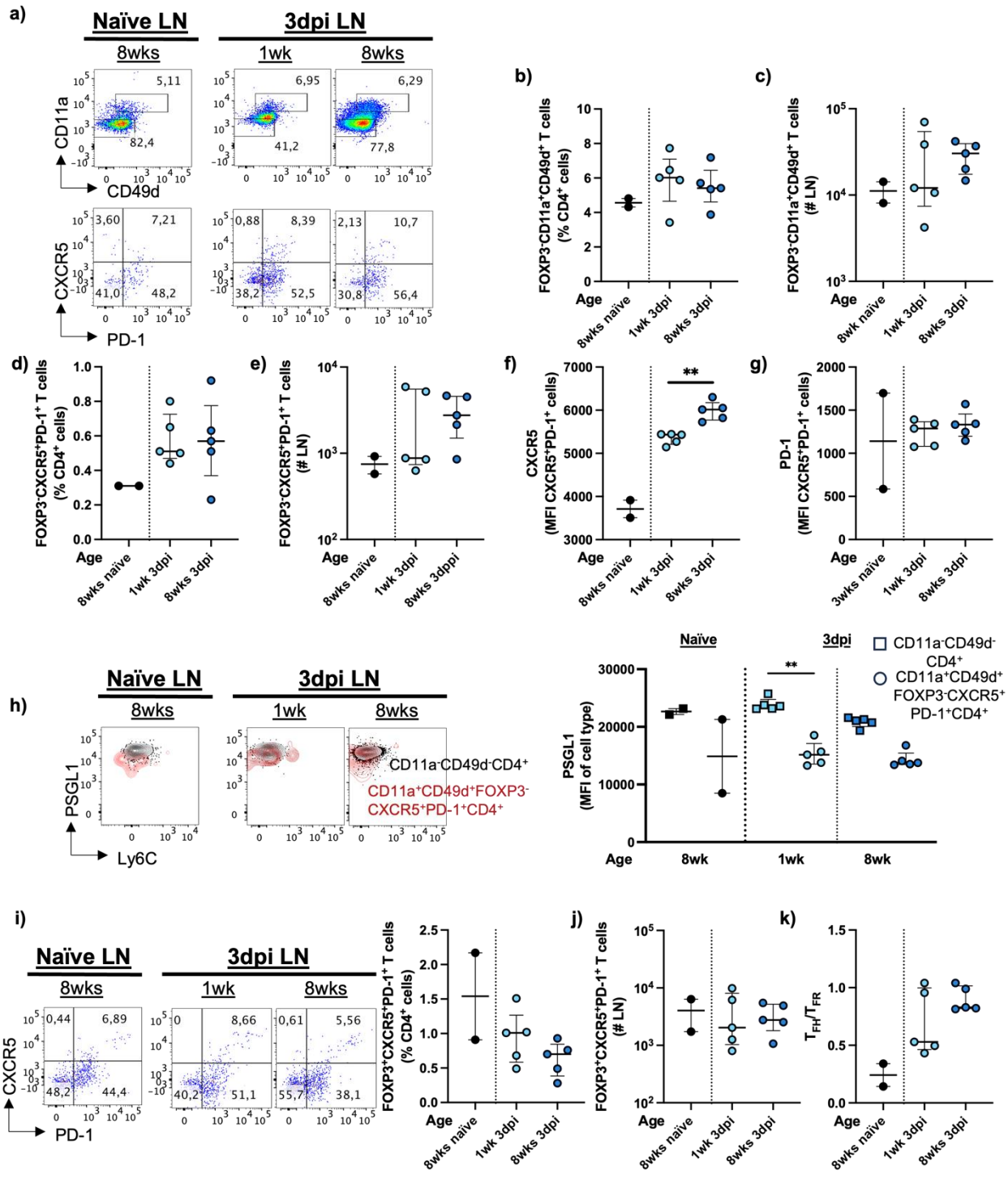


Fig 3.4. The T_{FH} differentiation programme in mediastinal lymph node has started 3dpi with RSV in both early life and adult mice

1wk and 8wk-old C57BL/6 mice were infected with 2.5 × 10^5 PFU RSV A2 i.n. A group of 8wk old mice was exposed to PBS i.n as controls. Mediastinal lymph node was harvested and flow cytometry was used to determine the proportion and number of different T cell subsets 3dpi. **(a)** Representative flow plots for FOXP3$^-$ antigen experienced cells (FOXP3$^-$CD11a$^+$CD49d$^+$) and T_{FH} (FOXP3$^-$CD11a$^+$CD49d$^+$CXCR5$^+$PD-1$^+$) cells. **(b)** Proportion and **(c)** quantification of FOXP3$^-$ antigen experienced cells and **(d,e)** T_{FH} cells. **(f)** CXCR5 and **(g)** PD-1 MFI on T_{FH} cells. **(h)** PSGL1 MFI on naïve (CD11a$^-$CD49d$^-$CD4$^+$) cells and T_{FH} cells. **(i)** Flow plots, percentage and **(j)** cell number of T_{FR} (FOXP3$^+$CXCR5$^+$PD-1$^+$) cells. **(k)** T_{FH} to T_{FR} ratio. Data from one independent experiment with n = 2-5 mice per group. Data shown with median and interquartile range. Each dot represents one mouse. Mann-Whitney test (a-f,h-j) between 3dpi groups or Kruskal-Wallis with multiple comparisons test for 3dpi groups (g) were performed in which *, $p < 0.05$; **, $p < 0.01$; and ***, $p < 0.001$.

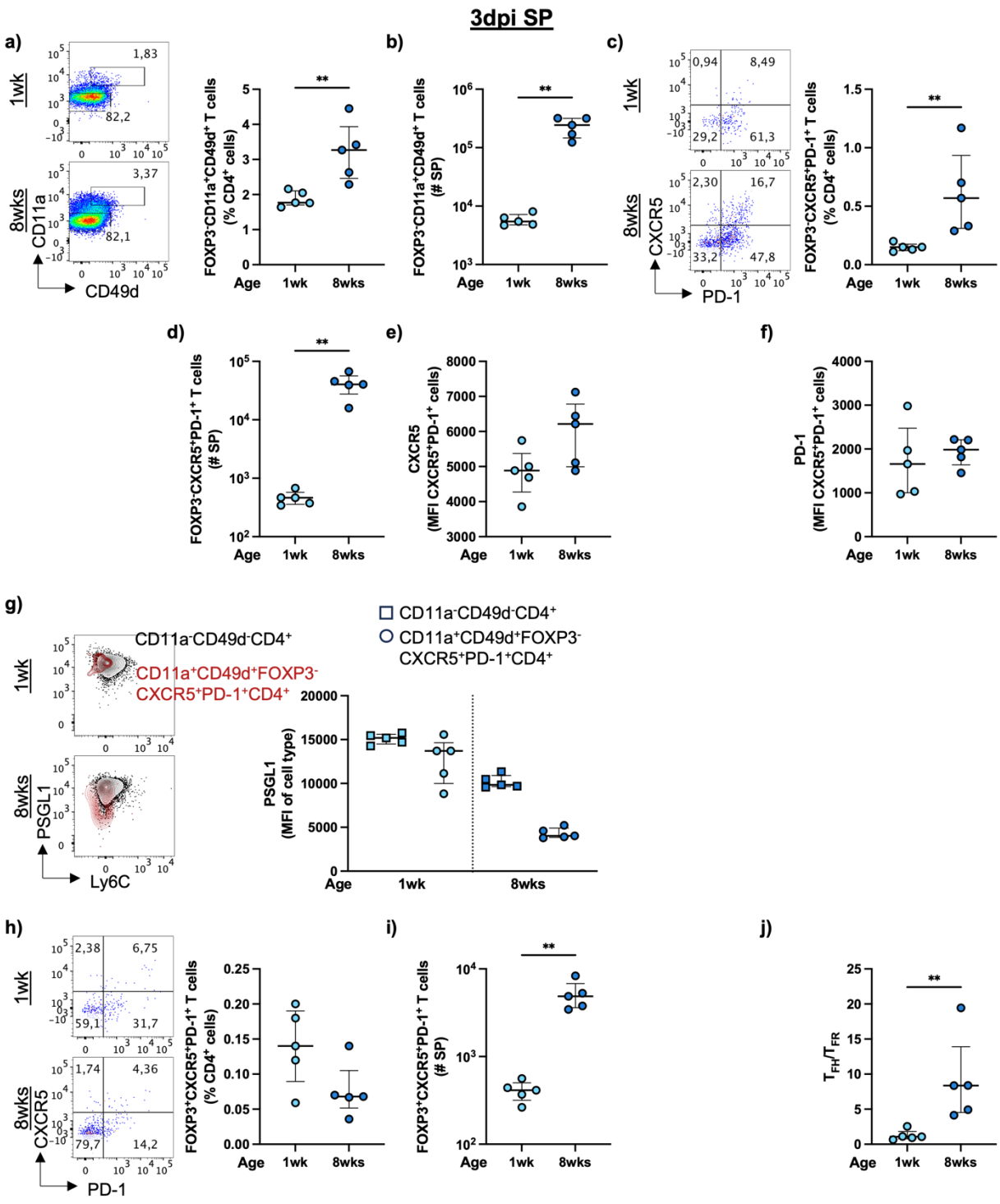


Fig 3.5. T_{FH} responses 3dp RSV infection in spleen are more developed in adulthood when compared to early life mice

1wk and 8wk-old C57BL/6 mice were infected with 2.5 × 10^5 PFU RSV A2 i.n. Spleen was harvested and flow cytometry was used to determine the proportion and number of different T cell subsets 3dpi. **(a)** Representative flow plots, proportion and **(b)** quantification of FOXP3⁻ antigen experienced cells (FOXP3⁻CD11a⁺CD49d⁺) and **(c,d)** T_{FH} (FOXP3⁻CD11a⁺CD49d⁺CXCR5⁺PD-1⁺ cells). **(e)** CXCR5 and **(f)** PD-1 MFI from T_{FH} cells. **(g)** PSGL1 MFI from naïve (CD11a⁻CD49d⁻CD4⁺) cells and T_{FH} cells. **(h)** Flow plots, percentage and **(i)** cell number of T_{FR} (FOXP3⁺CXCR5⁺PD-1⁺) cells. **(j)** T_{FH} to T_{FR} ratio. Data from one independent experiment with n = 5 mice per group. Data shown with median and interquartile range. Each dot represents one mouse. Mann-Whitney test (a-f, h-j) or Kruskal-Wallis with multiple comparisons test (g) were performed in which *, $p < 0.05$; **, $p < 0.01$; and ***, $p < 0.001$.

Adult murine responses in the SLOs confirmed that T_{FH} development has started by 3dp RSV infection. Thus, this timepoint was used to analyse the cytokine microenvironment of the SLOs to examine T_{FH} differentiation in early life and adulthood. To this end, STAT3 and STAT5 phosphorylation were directly assessed in naïve ($CD44^-Foxp3^-GITR^-$) and antigen-experienced cells ($CD44^+Foxp3^-GITR^-$) from 1 and 8 week old mice 3 days post RSV infection (*Fig 3.6a*). Antigen-experienced, but not naïve, $CD4^+$ T cells in the mediastinal LN of 1wk old mice showed a significant increase in pSTAT5 when compared with adult counterparts while the opposite was true for pSTAT3 (*Fig 3.6b*). In the spleen, a significant increase in pSTAT5 in 1wk $CD44^+$ cells was observed, but there was no significant difference in pSTAT3 (*Fig 3.6c*).

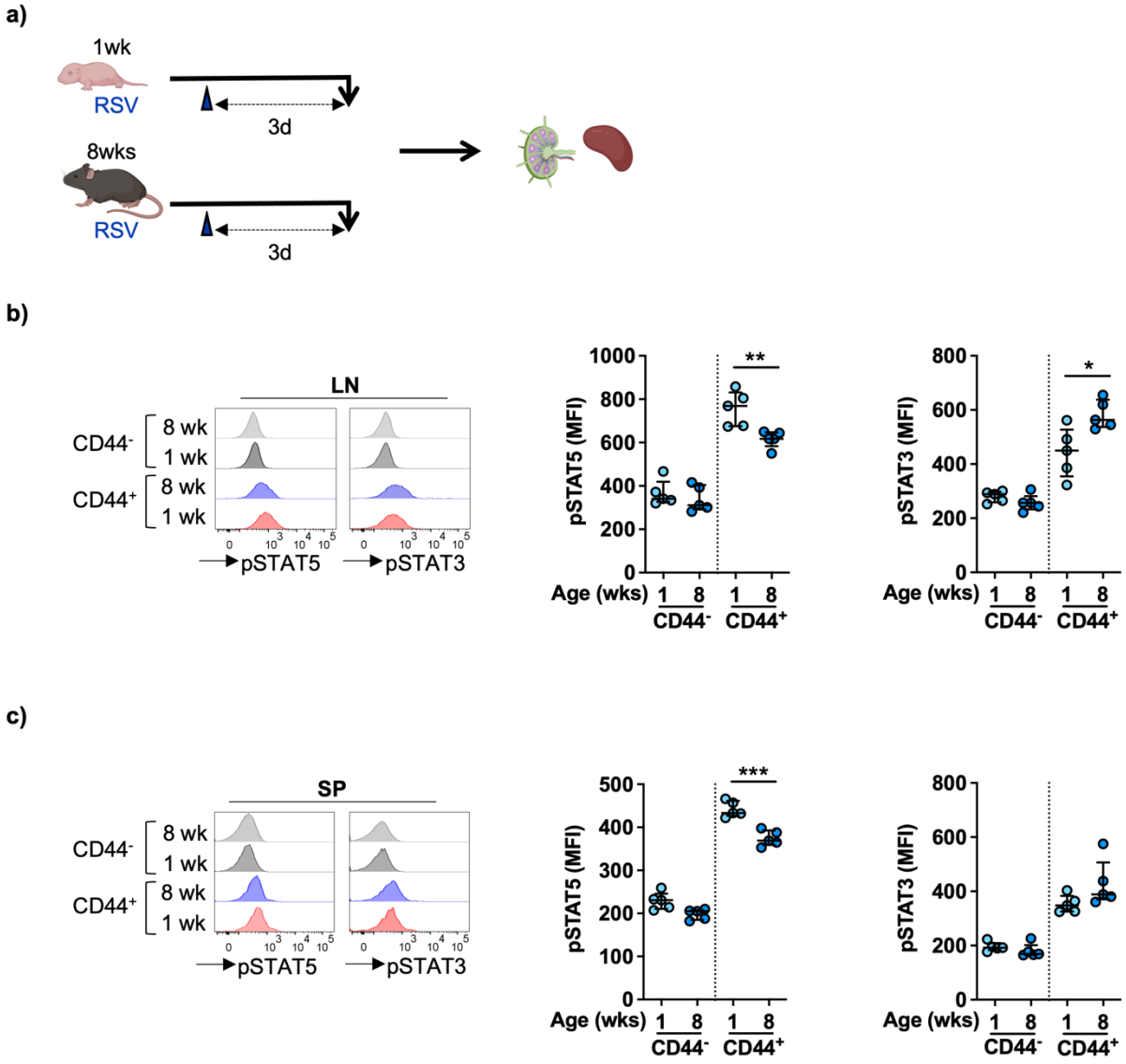


Fig 3.6. Neonatal antigen experienced CD4⁺ T cells are more prone to phosphorylate STAT5 after RSV infection than their adult counterparts

(a) 1wk and 8wk old C57BL/6 mice were infected with $2.5x10^5$ pfu RSV A2, lymph node and spleen were extracted 3dpi. **(b)** Phosphorylation of STAT5 and STAT3 was measured directly *ex vivo* in naïve ($CD44^-Foxp3^-GITR^-$) and antigen-experienced ($CD44^+Foxp3^-GITR^-$) $CD4^+$ T cells in the medLN and **(c)** spleen. STAT phosphorylation was quantified by flow cytometry. Data from two independent experiment with n =5 mice per group. Data shown with median and interquartile range. Each dot represents one mouse. Mann-Whitney test was performed in which *, $p < 0.05$; **, $p < 0.01$; and ***, $p < 0.001$.

Overall, these results indicate that there is an increased predisposition of $CD4^+$ T cells for enhanced STAT5 over STAT3 signalling in early life when compared to adults, potentially limiting T_{FH} differentiation in this life period.

3.2.3 The SLOs' microenvironment of early life mice is enriched in IL-2

As shown in the above experiments, the reduced T_{FH} differentiation observed in neonatal mice following RSV infection is associated with increased STAT5 phosphorylation in activated $CD4^+$ T cells within the SLOs early during infection. This effect could result from enhanced pSTAT5 sensitivity by early life $CD4^+$ T cells, but could also be the result of elevated STAT5 signalling cytokines, in particular IL-2.

To test this, flow cytometry was used to determine age specific differences in the ability of different cell types to produce IL-2 when stimulated with PMA and Ionomycin *(**Fig 3.7a,b**)*. The proportions of immune cells in the SLOs differed in neonatal versus adult mice. Specifically the proportion of $FOXP3^-CD4^+$ T cells, T_{reg} cells ($FOXP3^+CD4^+$) and $CD3^-CD19^-$ cells were all significantly increased in 1wk old mice when compared to the adult counterpart in the medLN of steady state mice. The opposite was observed with B cells ($CD19^+$), as they were upregulated in adulthood *(**Fig 3.7c**)*. The same trends were observed 3dpi with a significant increase in neonatal T_{reg} and $CD3^-CD19^-$ cells and an enhanced B cell proportion in adult medLN *(**Fig 3.7d**)*. In the spleen however the proportions of T and B cells were significantly reduced in neonates, associated with a significant increase in the proportion of non-T and B cells ($CD3^-CD19^-$), compared to adults *(**Fig 3.7e,f**)*.

Following PMA/Ionomycin stimulation, all the cell types analysed showed the capacity to produce IL-2, but to differing extents *(**Fig 3.8a**)*; $FOXP3^-CD4^+$ T cells showing the greatest proportion of cells able to produce IL-2 when compared to all other cell populations analysed *(**Fig 3.8a,b**)*. The percentage of cells able to produce IL-2 after mitogen stimulation was greatly enhanced when taken from 1 week old mice compared to 8 week old mice, especially for the $FOXP3^-CD4^+$ T cell population *(**Fig 3.8b**)*. Infection with RSV did not appear to affect the proportion of cells able to produce IL-2 in either neonatal or adult mice and the percentage of cells able to produce IL-2 was still increased in young mice when compared to adult counterparts after infection *(**Fig 3.8c**)*. In naïve mice, *Il2* expression was poorly detected in either neonatal or adult uninfected LN *(**Fig 3.8d**)*, but following RSV infection there was an overall increase in *Il2* expression in the LN of 1wk old mice, which was significantly higher than that observed in 8 week old mice *(**Fig 3.8e**)*.

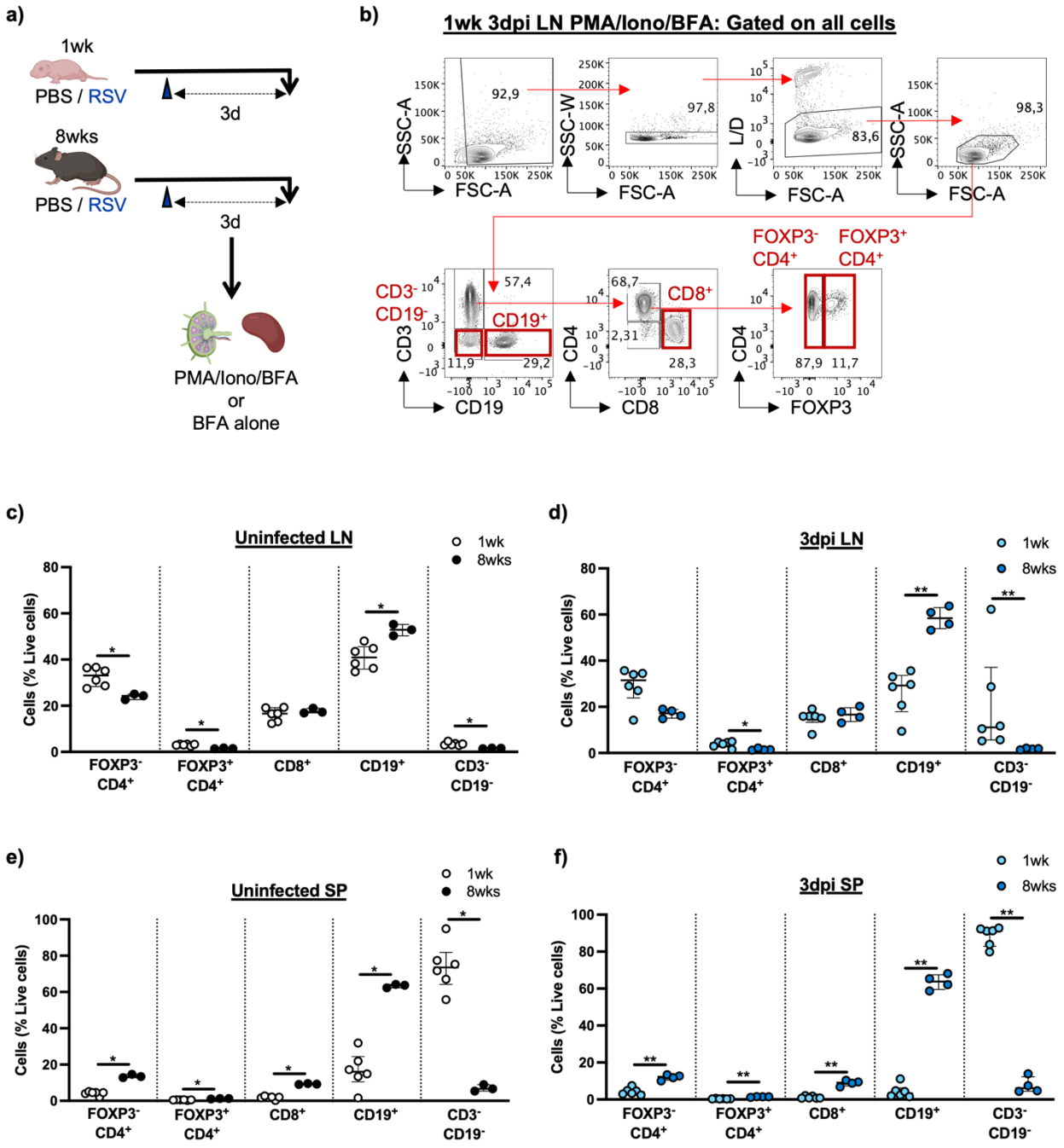


Fig 3.7. Lymphocyte quantification in mediastinal LN and SP of steady state and after RSV infection in neonatal and adult mice

(a) 1wk and 8wk-old C57BL/6 mice were infected with 2.5 × 10^5 PFU RSV A2 or PBS i.n,. Mediastinal lymph node and spleen were harvested 3dpi and stimulated with PMA, Ionomycin and BFA or BFA alone for 4h at 37ºC, 5% CO2. **(b)** Representative flow cytometry gating strategy for lymphoid subsets. From total cells doublets were excluded and live cells were selected as e780 live/dead negative cells. Lymphoid cells were gated and $CD4^+$ T cells were defined as $CD3^+CD4^+CD8^-$. T_{regs} and $FOXP3^-$ cells were classified according to their FOXP3 expression. $CD8^+$ T cells were defined as $CD3^+CD4^-CD8^-$ cells and B cells as $CD19^+$ cells. The remaining cells were classified as $CD3^-CD19^-$ cells. **(c)** Proportion of the above cell types in uninfected and **(d)** 3dpi conditions in the mediastinal LN and **(e)** in uninfected and **(f)** infected spleen. Data from one independent experiment with n = 3-6 mice per group. Data shown with median and interquartile range. Each dot represents one mouse. Mann-Whitney test was performed in which *, $p < 0.05$; **, $p < 0.01$; and ***, $p < 0.001$

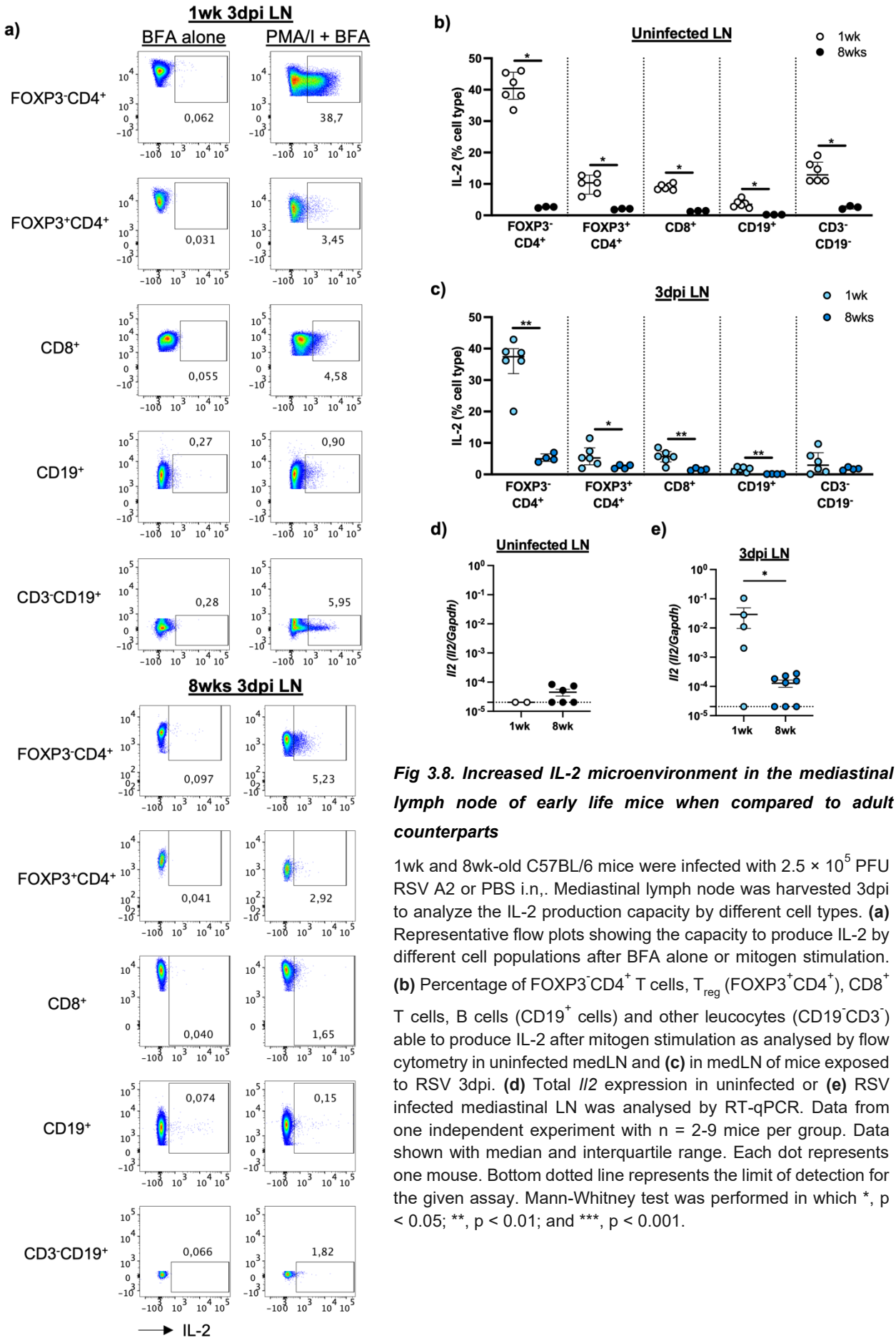


Fig 3.8. Increased IL-2 microenvironment in the mediastinal lymph node of early life mice when compared to adult counterparts

1wk and 8wk-old C57BL/6 mice were infected with 2.5 × 10^5 PFU RSV A2 or PBS i.n,. Mediastinal lymph node was harvested 3dpi to analyze the IL-2 production capacity by different cell types. **(a)** Representative flow plots showing the capacity to produce IL-2 by different cell populations after BFA alone or mitogen stimulation. **(b)** Percentage of $FOXP3^-CD4^+$ T cells, T_{reg} ($FOXP3^+CD4^+$), $CD8^+$ T cells, B cells ($CD19^+$ cells) and other leucocytes ($CD19^-CD3^-$) able to produce IL-2 after mitogen stimulation as analysed by flow cytometry in uninfected medLN and **(c)** in medLN of mice exposed to RSV 3dpi. **(d)** Total *Il2* expression in uninfected or **(e)** RSV infected mediastinal LN was analysed by RT-qPCR. Data from one independent experiment with n = 2-9 mice per group. Data shown with median and interquartile range. Each dot represents one mouse. Bottom dotted line represents the limit of detection for the given assay. Mann-Whitney test was performed in which *, $p < 0.05$; **, $p < 0.01$; and ***, $p < 0.001$.

Similar to LNs, the potential to produce IL-2 in the spleen after mitogen stimulation was increased in early life compared to adults *(**Fig 3.9a-e**);* with a significantly higher percentage of FOXP3$^-$CD4$^+$ T cells, T_{regs} and CD3$^-$CD19$^-$ leucocytes able to produce IL-2 than adult counterparts in uninfected conditions *(**Fig 3.9a**)*. Similar trends were observed in 3dpi splenocytes with an increased percentage of 1wk FOXP3$^-$CD4$^+$ T cells and CD3$^-$CD19$^-$ cells able to produce IL-2 than the 8wk old mice analogues after mitogen stimulation *(**Fig 3.9b**)***.*** Again, the FOXP3$^-$CD4$^+$ T cell population contained the greatest proportion of cells able to produce IL-2 in the neonatal spleen. No difference in *Il2* transcript was however observed in whole splenocytes either in uninfected *(**Fig 3.9c**)* or infected conditions *(**Fig 3.9d**)*. Isolation of naïve splenic CD4$^+$ T cells from uninfected mice at different ages did however show that while *Il2* was undetectable at 3 days of age, by 1 week it was readily detectable, and peaked at 2 weeks of age, before declining again between 3 and 8 weeks of life *(**Fig 3.9e**)*.

Overall, this data shows that the early life SLOs are an IL-2 enriched microenvironment, a cytokine reported to hinder T_{FH} differentiation responses. In particular naïve CD4$^+$ T cells, the source of effector cells such as T_{FH}, are a potent source of IL-2 in 2wk old mice but much less so in adults.

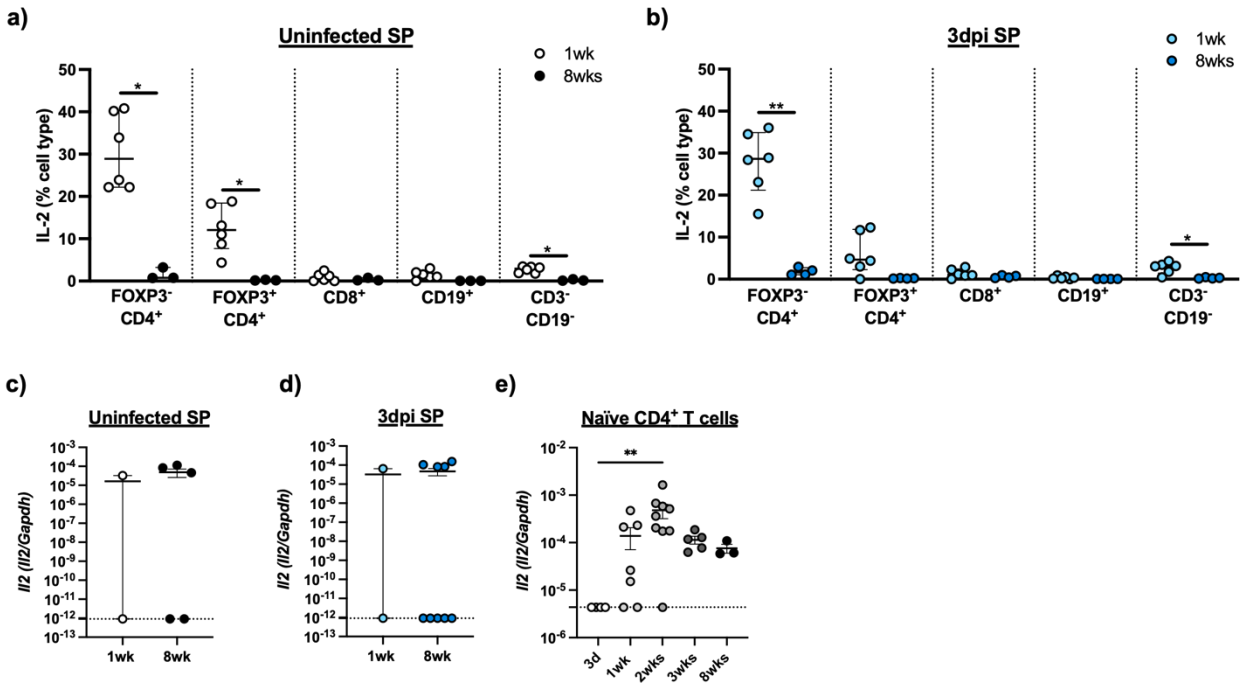


Fig 3.9. Increased percentage of IL-2 producing cells in the early life spleen when compared to adult counterparts

1wk and 8wk-old C57BL/6 mice were infected with 2.5 × 10^5 PFU RSV A2 or PBS i.n,. Spleen was harvested 3dpi to analyze the IL-2 production by different cell types. **(a)** Percentage of IL-2 producing FOXP3$^-$CD4$^+$ T cells, T_{reg} (FOXP3$^+$CD4$^+$), CD8$^+$ T cells, B cells (CD19$^+$ cells) and other leucocytes (CD19$^-$CD3$^-$) was analysed by flow cytometry in uninfected and **(b)** 3dp RSV infection after mitogen stimulation. **(c)** Total *Il2* expression in uninfected or **(d)** RSV infected spleen was analysed by RT-qPCR. **(e)** Naïve CD4$^+$ T cells were isolated from spleens of C57BL/6 mice of different ages and *Il2* production was analysed by RT-qPCR**.** Data from one (a-d) or two (e) independent experiments with n = 2-9 mice per group. Data shown with median and interquartile range. Each dot represents one mouse. Bottom dotted line represents the limit of detection for the given assay. Mann-Whitney test (a-d) or Kruskal-Wallis with multiple comparisons test (e) were performed in which *, $p < 0.05$; **, $p < 0.01$; and ***, $p < 0.001$.

3.2.4 IL-2 receptor expression on T cells is increased in 1wk old mice when compared to adult counterparts

To analyse if the recognition of IL-2 was also altered with age, IL-2 receptor expression by T cells was investigated. The percentage of lymph node FOXP3$^-$CD4$^+$ T cells expressing membrane CD25 (mCD25), the high affinity IL-2Rα subunit, was significantly upregulated in 1wk old mice when compared to adult counterparts both in steady state and 3dpi with RSV *(**Fig 3.10a,b**)*. mCD25 is a typical marker of T_{reg} differentiation (535). The percentage of mCD25 expressing cells was elevated in early life T_{reg} cells at the steady state when compared to adult samples, but this significant difference was lost at 3dpi *(**Fig 3.10a,b**)*. The proportion of mCD25$^+$ CD8$^+$ T cells was significantly increased in 1wk old mice when compared to 8wk old mice, but only after RSV infection *(**Fig 3.10a,b**)*. Opposite results were obtained when analysing the different IL-2R subunits (*Cd25, Cd122* and *Cd132)* transcripts from overall LN cells with an increase in 8wk old mice when compared to neonates that was significant for *Cd132,* the common γ chain receptor, expression in infected conditions *(**Fig 3.10c,d**)*.

Early life splenic naïve FOXP3$^-$CD4$^+$ T cells (CD44$^-$CD62L$^-$FOXP3$^-$) showed a significant increase in membrane expression of both CD25 and CD122 (IL-2Rβ) when compared with adult analogues *(**Fig 3.11a,b**)*. The common γ chain receptor CD132 was however not readily detected by flow cytometry in either 1 or 8 week old mice *(**Fig 3.11c**)*. In comparison, FOXP3$^+$CD4$^+$ naïve T cells (CD44$^-$CD62L$^-$FOXP3$^+$) showed similar levels of CD25 and also had increased levels of CD122 in 1wk old mice, while CD132 was again not readily detectable *(**Fig 3.11d-f**)*. At a transcriptional level, *Cd25* was similarly expressed by splenic naïve CD4$^+$ T cells irrespective of age *(**Fig 3.11g**)*. Increased *Cd122* was however observed in 2 and 3wks old mice, where expression peaked, when compared to 3d old mice *(**Fig 3.11h**)*. *Cd132* displayed a similar pattern, expression peaking in 2wks old mice, and was significantly increased compared to 1wk and 3d old pups *(**Fig 3.11i**)*. When analysing the whole spleen however, a trend to an increase in all IL-2R subunits was observed in 8wk old mice when compared with 1wk old counterparts *(**Fig 3.11j**)*. After RSV infection there was an increase in the percentage of mCD25$^+$ cells of the adult FOXP3$^-$CD4$^+$ and CD8$^+$ T cell populations when compared with young mice counterparts *(**Fig 3.12a**)* and again a trend to an increase *Cd25, Cd122* and *Cd132* was observed in adult whole spleen after infection *(**Fig 3.12b**)*.

This data indicates that CD4$^+$ T cells within mediastinal LN of neonatal mice and naïve CD4$^+$ T cells in the spleen not only have the ability to produce more IL-2, but are also more prone to recognise it, as shown by their elevated protein expression of membrane IL-2 receptors.

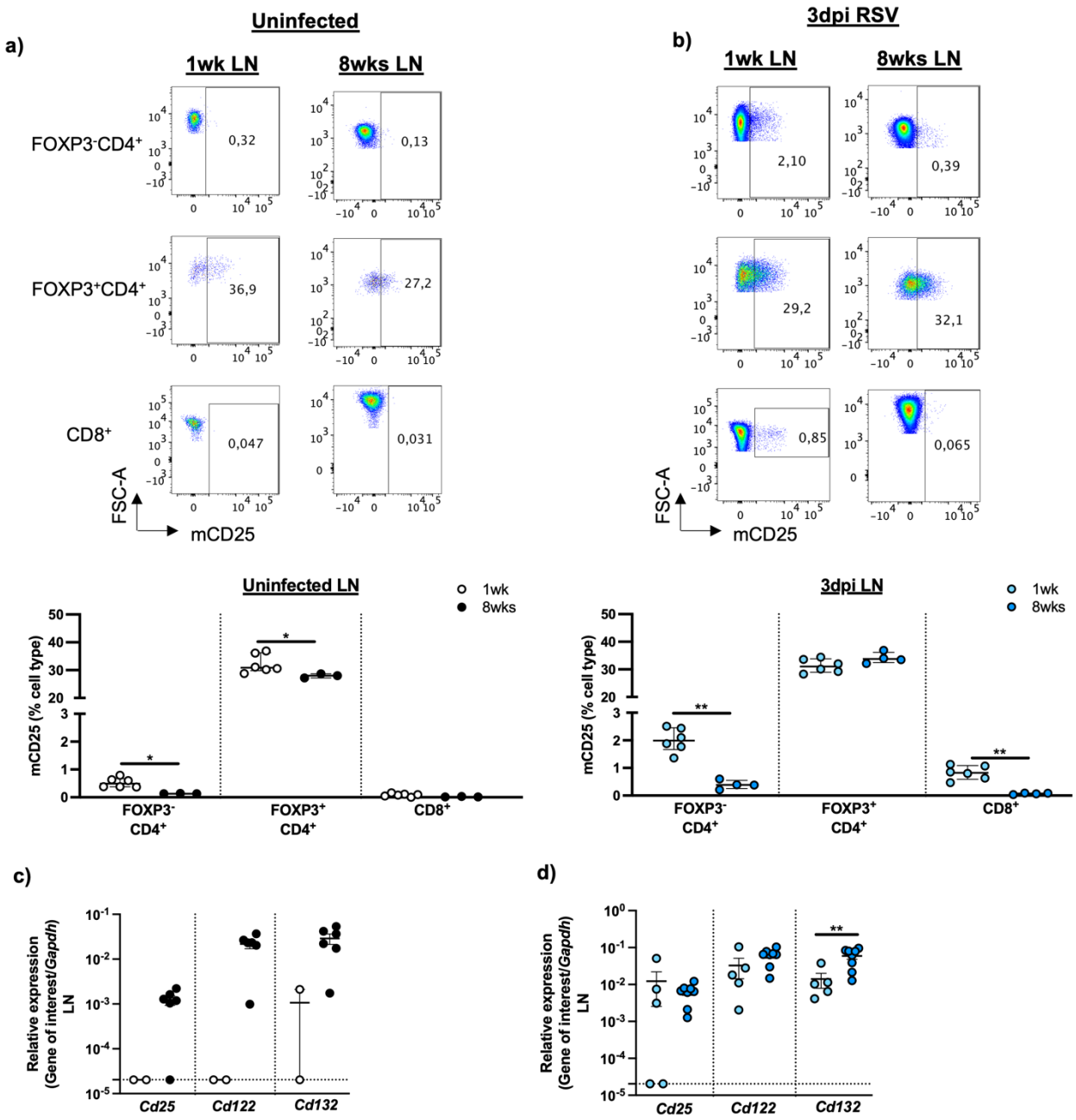


Fig 3.10. Increased proportion of membrane CD25 expressing T cells in the mediastinal LN from 1wk old mice when compared to adult counterparts

1wk and 8wk-old C57BL/6 mice were infected with 2.5 × 10^5 PFU RSV A2 or PBS i.n,. Mediastinal lymph node was harvested 3dpi. **(a)** Representative flow plots and proportion of FOXP3$^-$CD4$^+$ T cells, T_{reg} (FOXP3$^+$CD4$^+$) and CD8$^+$ T cells expressing membrane CD25 analysed by flow cytometry in uninfected and **(b)** 3dp RSV infection**. (c)** *Cd25*, *Cd122* and *Cd132* levels detected by RT-qPCR in mediastinal LN of uninfected or **(d)** 3dpi mice. Data from one (a,b) or two (c,d) independent experiments with n = 2-9 mice per group. Data shown with median and interquartile range. Each dot represents one mouse. Mann-Whitney test was performed in which *, $p < 0.05$; **, $p < 0.01$; and ***, $p < 0.001$.

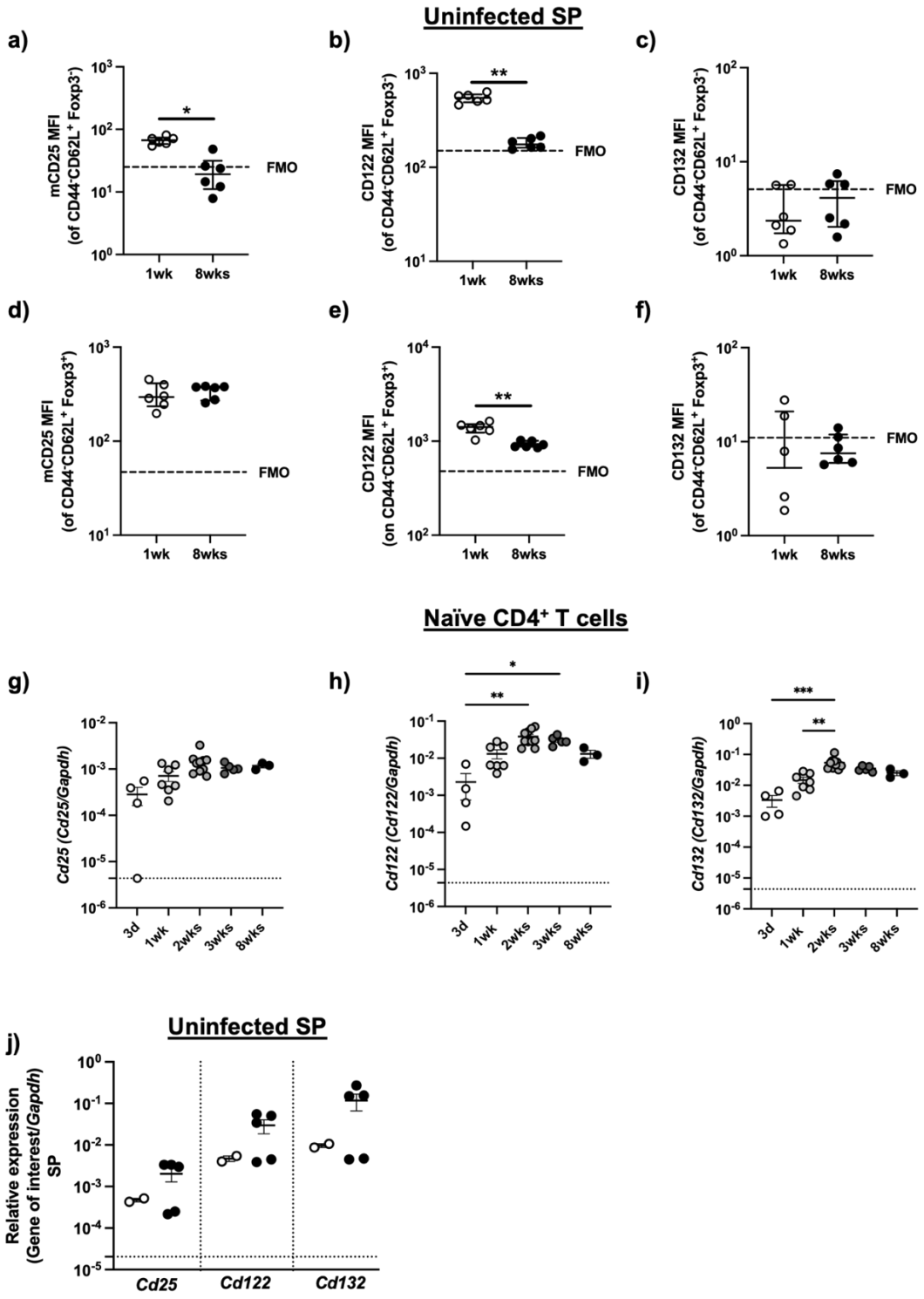


Fig 3.11. Increased IL-2R expression in FOXP3⁻ naïve CD4⁺ T cells of early life mice when compared to adult counterparts

(a) Membrane CD25 (IL-2Rα), **(b)** CD122 (IL-2Rβ) and **(c)** CD132 (common γ chain) MFI expression by splenic FOXP3⁻ naïve CD4⁺ T cells (CD44⁻CD62L⁻FOXP3⁻) and by **(d,e,f)** FOXP3⁺ naïve CD4+ T cells (CD44-CD62L-FOXP3+) of 1 and 8wk uninfected C57BL/6 mice analysed by flow cytometry. **(g)** *Cd25*, **(h)** *Cd122* and **(i)** *Cd132* transcript from splenic naïve CD4⁺ T cells isolated from uninfected C57BL/6 mice of different ages analysed by RT-qPCR. **(j)** *Cd25*, *Cd122* and *Cd132* transcript analysed by RT-qPCR in total spleen of uninfected mice. Data from one (a-f) or two (g-i) independent experiments with n = 2-8 mice per group. Data shown with median and interquartile range. Each dot represents one mouse. Bottom dotted line represents the limit of detection for the given assay and dash line signals FMO. Mann-Whitney test (a-f,j) and Kruskal-Wallis with multiple comparisons test (g-i) was performed in which *, $p < 0.05$; **, $p < 0.01$; and ***, $p < 0.001$.

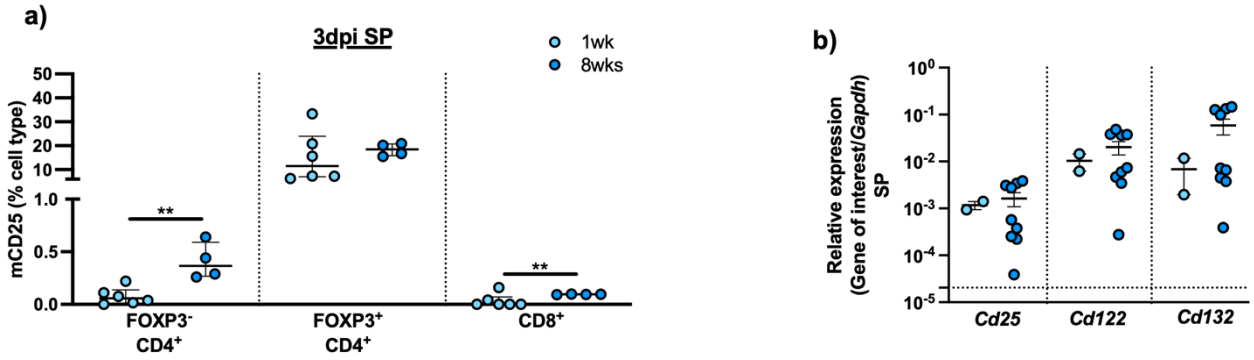


Fig 3.12. Increased percentage of mCD25$^+$FOXP3$^-$CD4$^+$ T cells in adult mice spleen when compared to neonatal counterparts after RSV infection

1wk and 8wk-old C57BL/6 mice were infected with 2.5 × 10^5 PFU RSV A2 or PBS i.n,. Spleen was harvested 3dpi. **(a)** Proportion of FOXP3$^-$CD4$^+$ T cells, T_{reg} (FOXP3$^+$CD4$^+$) and CD8$^+$ T cells expressing mCD25 analysed by flow cytometry. **(b)** *Cd25*, *Cd122* and *Cd132* transcript in 3dp RSV infection. Data from one independent experiment (a) or two independent experiments (b) with n = 2-9 mice per group. Data shown with median and interquartile range. Each dot represents one mouse. Mann-Whitney test was performed in which *, $p < 0.05$; **, $p < 0.01$; and ***, $p < 0.001$.

3.2.5 IL-6 and IL-6 receptor expression in mediastinal LN are increased 3dpi in adult mice

In contrast to IL-2, IL-6 signalling, via phosphorylation of STAT3, is a pro-T_{FH} factor in a range of adult models (57,128,131,536). To understand if alterations in the IL-6 pathway might be playing a role in preventing T_{FH} differentiation in early life, systemic IL-6 levels in serum in steady state or after 3dpi conditions were analysed. No detectable IL-6 was found in either 1 or 8 wk old mice *(**Fig 3.13a**)*. Expression of IL-6 cytokine and transcript in LN was undetected in naïve mice of all analysed ages, while *Il6ra* and *Il6st* were elevated in the LN of 8wk old mice *(**Fig 3.13b,c**)*. 3dpi IL-6 in the LN supernatant was also undetectable *(**Fig 3.13d**)*. *Il6* transcript expression was increased in adult infected mice and both neonatal and adults showed elevated *Il6ra*, which showed no difference according to age. *Il6st* transcript levels were significantly elevated in adulthood after infection *(**Fig 3.13e**)*.

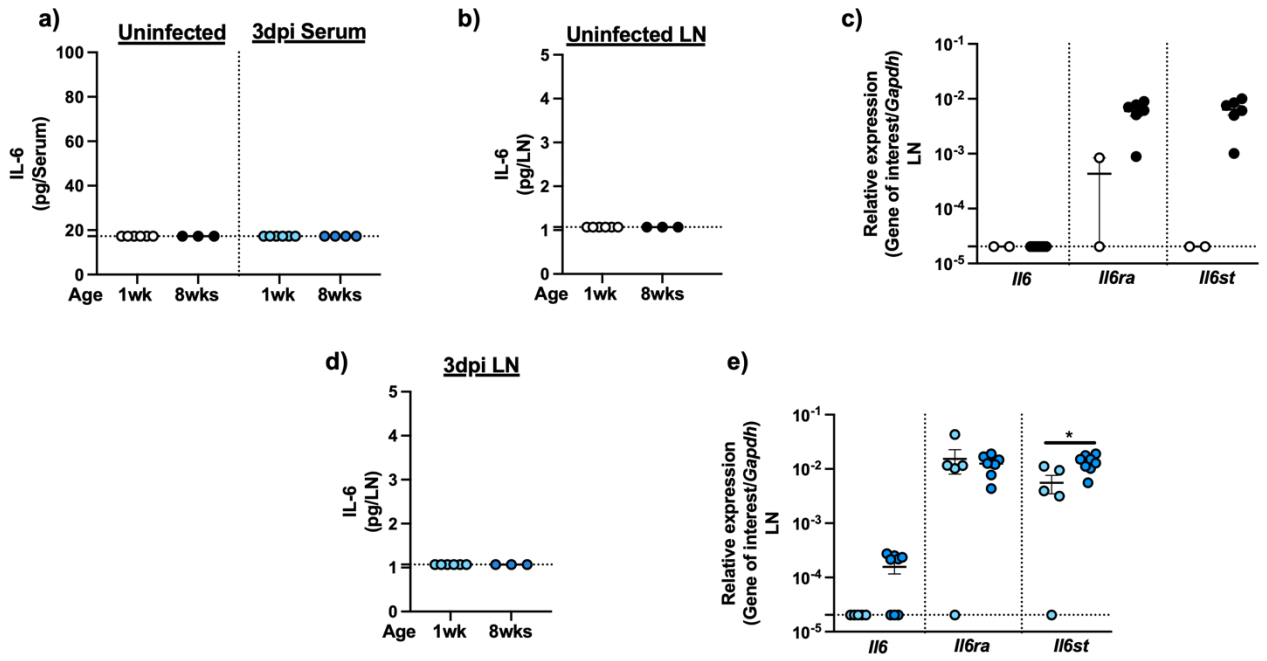


Fig 3.13. IL-6 and IL-6 receptor expression are increased in adult mediastinal LN

1wk and 8wk-old C57BL/6 mice were infected with 2.5 × 10^5 PFU RSV A2 or PBS i.n,. **(a)** Serum was extracted, and IL-6 levels were quantified by ELISA. Mediastinal LN was harvested 3dpi. **(b)** IL-6 levels in LN were analysed by ELISA. **(c)** *Il6, Il6ra* and *Il6st* levels were analysed by RT-qPCR in LN of uninfected mice. **(d)** IL-6 and **(e)** *Il6, Il6ra* and *Il6st* transcripts were analysed in 3dpi LN. Data from one (a,b,d) or two (c,e) independent experiments with n = 2-9 mice per group. Data shown with median and interquartile range. Each dot represents one mouse. Bottom dotted line represents the limit of detection for the given assay. Mann-Whitney test was performed in which *, $p < 0.05$; **, $p < 0.01$; and ***, $p < 0.001$.

Next, IL-6 receptor expression was analysed in naïve $CD4^+$ T cells isolated from spleen of uninfected mice of different ages. As with IL-2 receptors, both *Il6ra* and *Il6st* transcripts peaked at 2 wks of life and were significantly upregulated when compared to 3d and 7d old pups but remained constant during adulthood *(Fig 3.14a,b)*. IL-6 protein levels were undetected in spleen of uninfected and infected mice and while transcript levels of *Il6* were significantly elevated in neonatal mice 3d post RSV infection, no differences according to age were observed in its receptors in either steady state or infected conditions *(Fig 3.14c-f)*.

Overall, IL-6 levels were mostly undetected in mediastinal LN of 1wk and 8wk old mice, but there were indications that *Il6* and IL-6 receptor RNA expression might be elevated in the adult mice LN following infection. This was not, however, the case in the spleen, where IL-6 receptor levels were similar between 1wk and 8wk old mice.

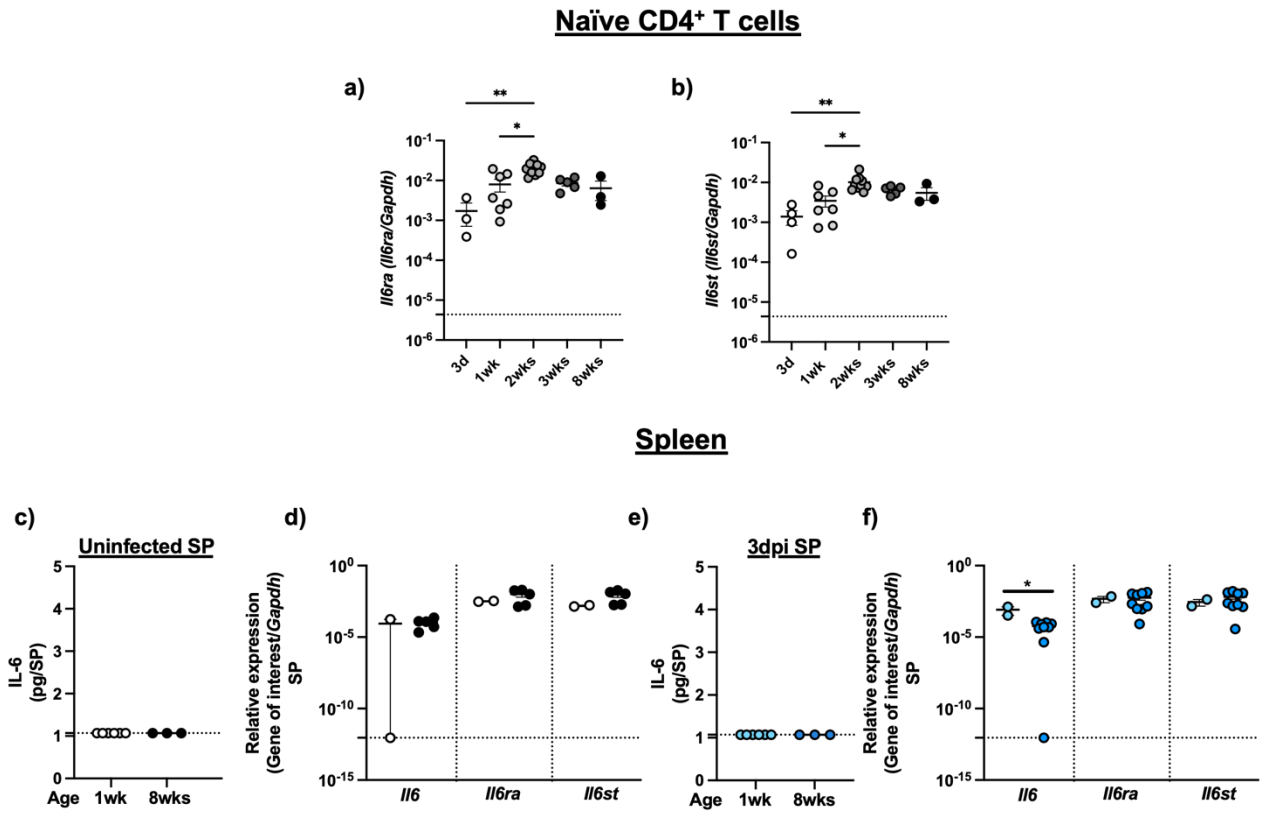


Fig 3.14. IL-6 receptor expression on naïve CD4⁺ T cells peaks at 2wks of live

1wk and 8wk-old C57BL/6 mice were infected with 2.5 × 10^5 PFU RSV A2 or PBS i.n,. **(a)** Naïve CD4⁺ T cells were isolated from spleens of uninfected C57BL/6 mice of different ages and *Il6ra* and **(b)** *Il6st* were analysed by RT-qPCR. 1wk and 8wk-old C57BL/6 mice were infected with 2.5 × 10^5 PFU RSV A2 or PBS i.n,. Spleen was harvested 3dpi. **(c)** IL-6 levels in spleen were analysed by ELISA. **(d)** *Il6*, *Il6ra* and *Il6st* levels were analysed by RT-qPCR in spleen of uninfected mice. **(e)** IL-6 and **(f)** *Il6*, *Il6ra* and *Il6st* transcripts were analysed in 3dpi spleen. Data from one (c,e) or two (a,b,d,f) independent experiments with n = 2-9 mice per group. Data shown with median and interquartile range. Each dot represents one mouse. Bottom dotted line represents the limit of detection for the given assay. Mann-Whitney (c-f) or Kruskal-Wallis test with multiple comparisons (a,b) were performed in which *, p < 0.05; **, p < 0.01; and ***, p < 0.001.

Next, *Stat3* and *Stat5* transcript were analysed in the SLOs to determine if the difference in phosphorylation observed with age could be explained by a difference in Stat expression. *Stat3* and *Stat5* transcripts were increased overall in adult uninfected LN leading to an increased *Stat3/Stat5* in 8wks old mice relative to 1wk old mice *(**Fig 3.15a,b**)*. No difference according to age was observed in *Stat3* levels in 3dpi conditions, but a significant upregulation in *Stat5* levels were observed in 8wk old mice *(**Fig 3.15c**)*; so a significant increase in the *Stat3/Stat5* ratio was identified in the LN of 1wk old mice in comparison with adult analogues *(**Fig 3.15d**)*. Similar levels of *Stat3*, *Stat5* and their ratio were observed for 1wk and 8wk mice spleen both in uninfected and infected conditions *(**Fig 3.15e-h**)*. Overall, the balance of *Stat3/Stat5* expression was upregulated in the LN of 8wk old uninfected mice, similarly to what was observed for naïve CD4⁺ T cells. This balance seems to flip during infection, but no difference according to age or infection are seen in the spleen.

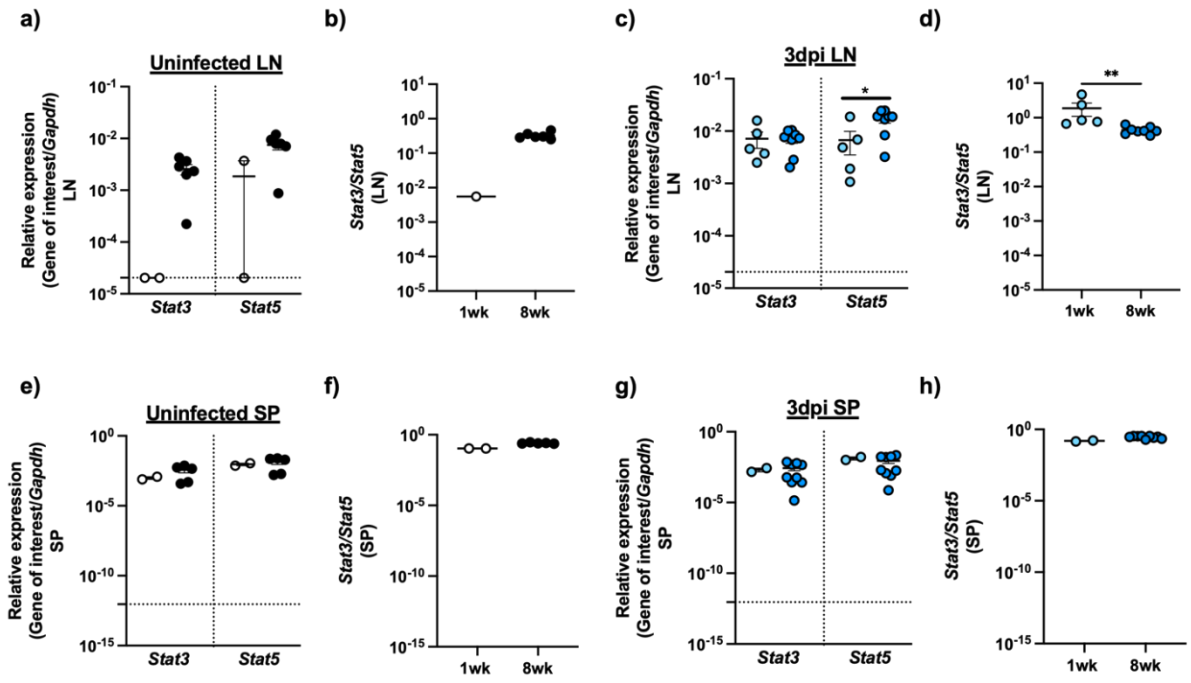


Fig 3.15. Stat3/Stat5 levels are increased in adult LN in the steady state, but this is reversed after 3dpi

1wk and 8wk-old C57BL/6 mice were infected with 2.5 × 10^5 PFU RSV A2 or PBS i.n,. Mediastinal LN and spleen were harvested 3dpi. **(a)** *Stat3* and *Stat5* were analysed by RT-qPCR and **(b)** the *Stat3/Stat5* ratio was calculated in both uninfected and **(c,d)** infected conditions in mediastinal LN or **(e,f)** uninfected or **(g,h)** infected spleen. Data from two independent experiments with n = 2-9 mice per group. Data shown with median and interquartile range. Each dot represents one mouse. Bottom dotted line represents the limit of detection for the given assay. Mann-Whitney test was performed in which *, $p < 0.05$; **, $p < 0.01$; and ***, $p < 0.001$.

3.2.6 T_{FH} responses in the lung are diminished in early life when compared to adulthood 3 days post RSV infection

Humoral immune responses normally develop in SLOs, but GC-like structures can be observed in peripheral organs such as the lung or the gut; known as ectopic GCs. Because recent literature has shown that ectopic GC are enhanced during human infections in early life when compared to adulthood (10), a feature replicated in mice (290,291), the T_{FH} differentiation response after RSV infection was analysed in the lungs of neonatal and adult mice. To this end, 1wk and 8wk old C57/BL6 mice were infected with RSV and the T cell response in the lung were analysed 3dpi. Antigen experienced $CD4^+$ T cells, both proportion and number, were significantly increased in the lungs of 8wk old mice *(**Fig 3.16a,b**)* as was the proportion in T_{FH} cells *(**Fig 3.16c**)*. A trend to an increase T_{FH} cell numbers was also observed in 8wk old mice when compared with younger analogues *(**Fig 3.16d**)*. The low frequency of T_{FH} cells in both neonates and adults made the study of T_{FH} characteristics more difficult, but no difference in CXCR5, PD-1 or PSGL1 was seen according to mouse age *(**Fig 3.16e-g**)*. No reduction in PSGL1 was observed when comparing naïve $CD4^+$ T cells and the low detectable T_{FH} cells in either 1wk or 8wk old cells *(**Fig 3.16g**)*. A trend to an increase T_{FR} proportion was observed in lungs of infected 1wk old mice, but no difference in absolute number was seen *(**Fig 3.16h,i**)*. An increased T_{FH}/T_{FR} ratio was therefore

seen in adult mice when compared to young animals (*Fig 3.16j*). In summary, this data indicates that T_{FH} responses in the lungs are limited, but elevated in adult mice 3dp RSV infection.

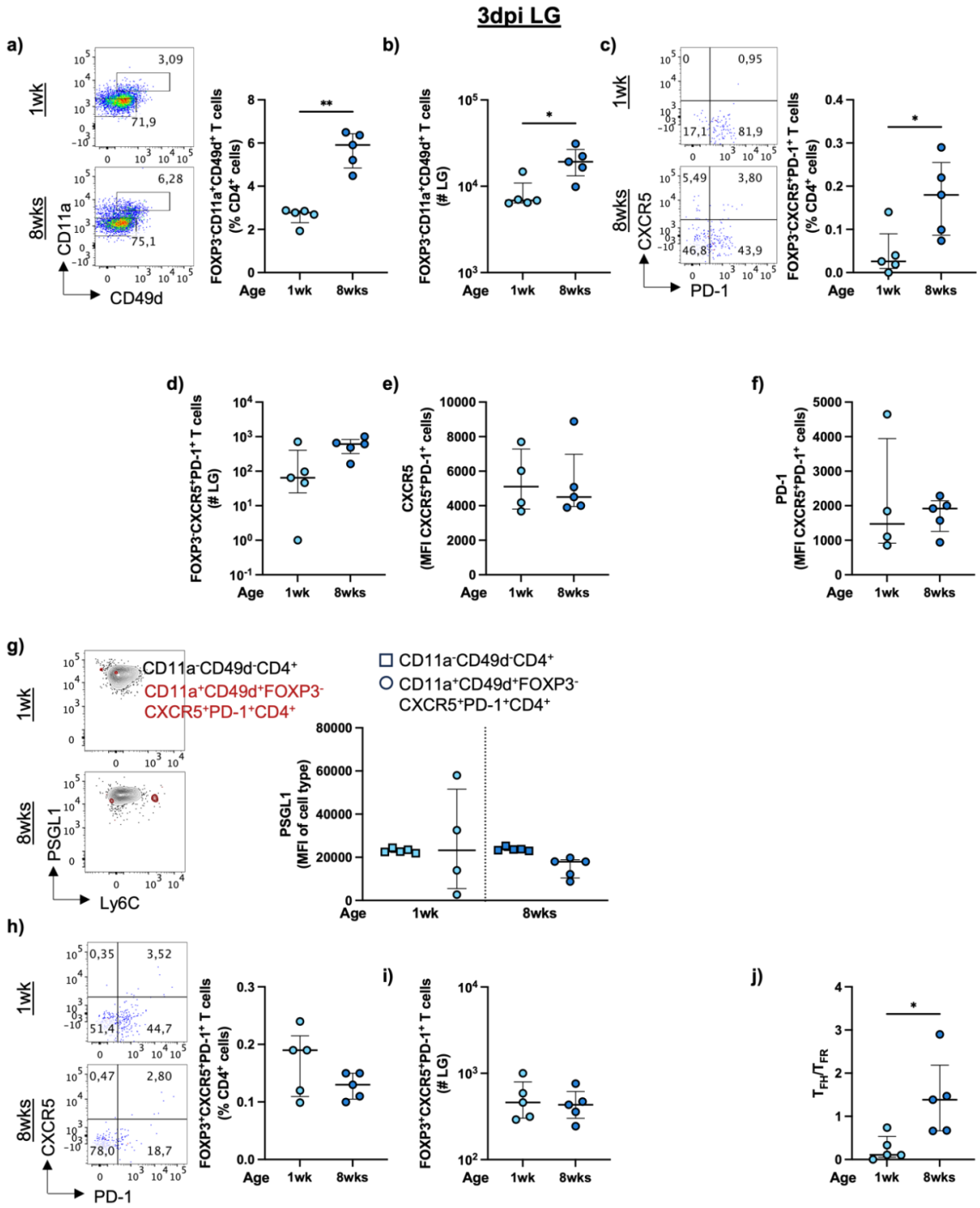


Fig 3.16. T_{FH} responses are diminished in early life lung when compared to adulthood 3dp RSV infection

1wk and 8wk-old C57BL/6 mice were infected with 2.5 × 10^5 PFU RSV A2 i.n. The right lung lobe was harvested and flow cytometry was used to determine the proportion and number of different T cell subsets 3dpi. **(a)** Representative flow plots, proportion and **(b)** quantification of FOXP3$^-$ antigen experienced cells (FOXP3$^-$ CD11a$^+$CD49d$^+$) and **(c,d)** T_{FH} (FOXP3$^-$CD11a$^+$CD49d$^+$CXCR5$^+$PD-1$^+$ cells). **(e)** CXCR5 and **(f)** PD-1 MFI from T_{FH} cells. **(g)** PSGL1 MFI from naïve (CD11a$^-$CD49d$^-$CD4$^+$) cells and T_{FH} cells. **(h)** Flow plots, percentage and **(i)** cell number of T_{FR} (FOXP3$^+$CXCR5$^+$PD-1$^+$) cells. **(j)** T_{FH} to T_{FR} ratio. Data from one independent experiment with n = 5 mice per group. Data shown with median and interquartile range. Each dot represents one mouse. Mann-Whitney test (a-f, h-j) or Kruskal-Wallis with multiple comparisons test (g) were performed in which *, $p < 0.05$; **, $p < 0.01$; and ***, $p < 0.001$.

3.2.7 The neonatal lung microenvironment is enriched in IL-2 and IL-6 production

As with SLOs, the lung microenvironment was enriched in IL-2 as shown by a significant increased expression of *Il2* transcripts in uninfected conditions *(**Fig 3.17a**)*. Concomitantly, IL-2R expression was increased in the lung of naïve neonatal mice as observed by a significant elevated expression of *Cd25* and *Cd132* in 1wk old mice when compared to 8wk old mice *(**Fig 3.17b**)*. A similar trend was observed in the lungs of infected neonatal mice, with increased IL-2 levels in young mice when compared to adults *(**Fig 3.17c**)*. The lung IL-2R expression was however similar between both 1 and 8wk old animals after infection *(**Fig 3.17d**)*.

A significant increase in *Il6* and IL-6 receptor RNA was seen in 1wk old mice when compared to adult counterparts at the steady state, but as with SLOs, IL-6 protein levels in the BAL were undetected *(**Fig 3.17e-g**)*. *Il6* transcript level was also increased in 1wk old mice when compared with 8wk old animals after RSV infection *(**Fig 3.17h**)*. IL-6 levels were however not detected by ELISA *(**Fig 3.17i**)* and IL-6R transcript was similar between both age groups after viral challenge *(**Fig 3.17j**)*.

Both *Stat3* and *Stat5* transcripts were upregulated in early life steady state conditions, but their ratio was maintained throughout life and no difference in lung transcripts was observed after viral infection *(**Fig 3.18a-d**)*. Overall, this data indicates that the lungs of neonatal mice have enhanced expression of factors involved in IL-2 and IL-6 signalling both before and after infection with RSV.

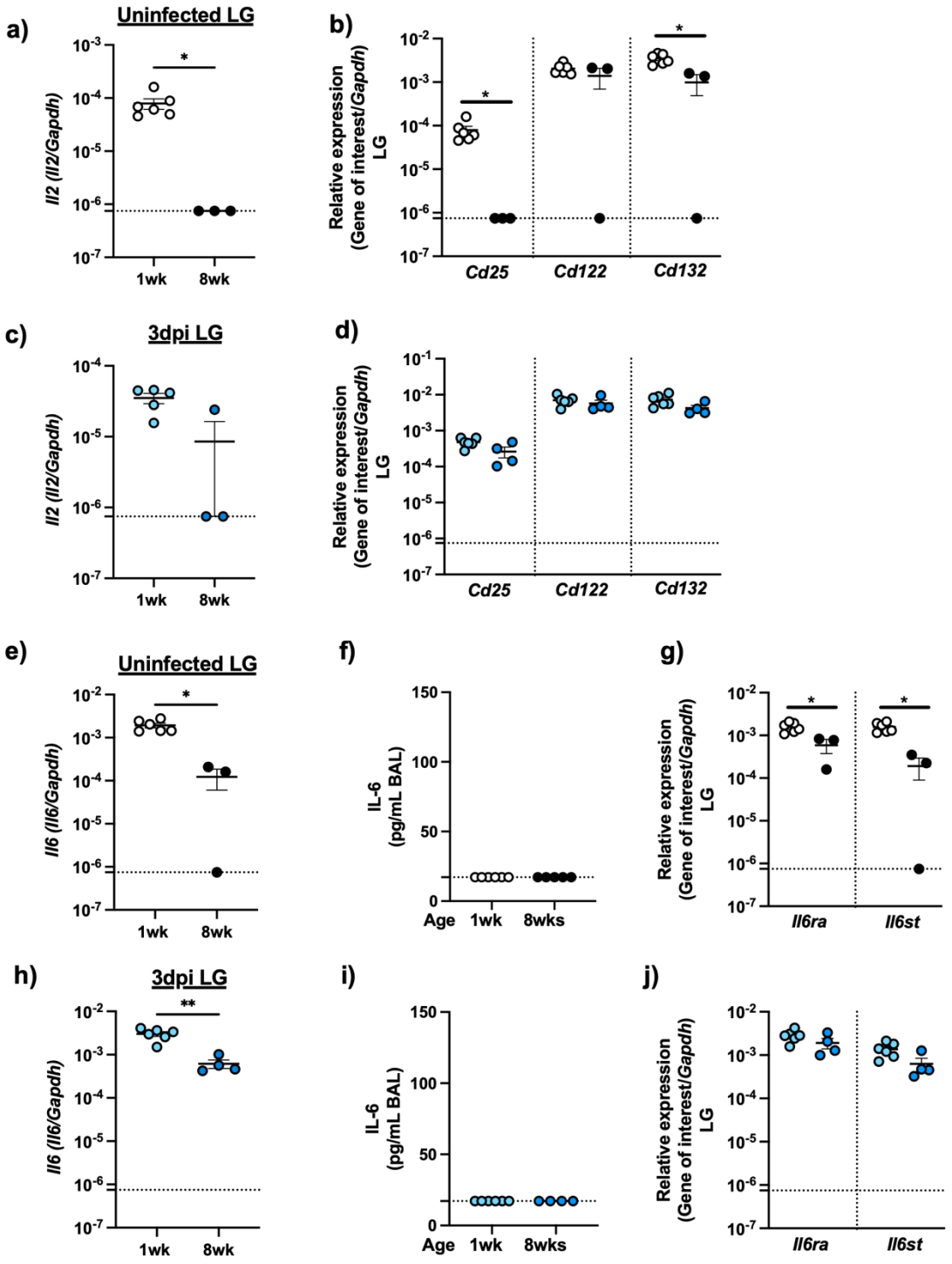


Fig 3.17. Increased IL-2 and IL-6 expression in lungs of neonatal mice when compared to adults

1wk and 8wk-old C57BL/6 mice were infected with 2.5 × 10^5 PFU RSV A2 or PBS i.n,. **(a,b)** Lung was harvested 3dpi. and *Il2* levels were analysed by RT-qPCR together with **(c)** *Cd25*, *Cd122* and *Cd132* transcripts in uninfected or **(c,d)** 3dpi conditions. **(e)** IL-6 levels by RT-qPCR in the lung and **(f)** ELISA in the BAL together with **(g)** *Il6ra* and *Il6st* transcription were analysed in uninfected and **(h-j)** 3dpi conditions. Data from one independent experiment with n = 3-6 mice per group. Data shown with median and interquartile range. Each dot represents one mouse. Bottom dotted line represents the limit of detection for the given assay. Mann-Whitney test was performed in which *, $p < 0.05$; **, $p < 0.01$; and ***, $p < 0.001$.

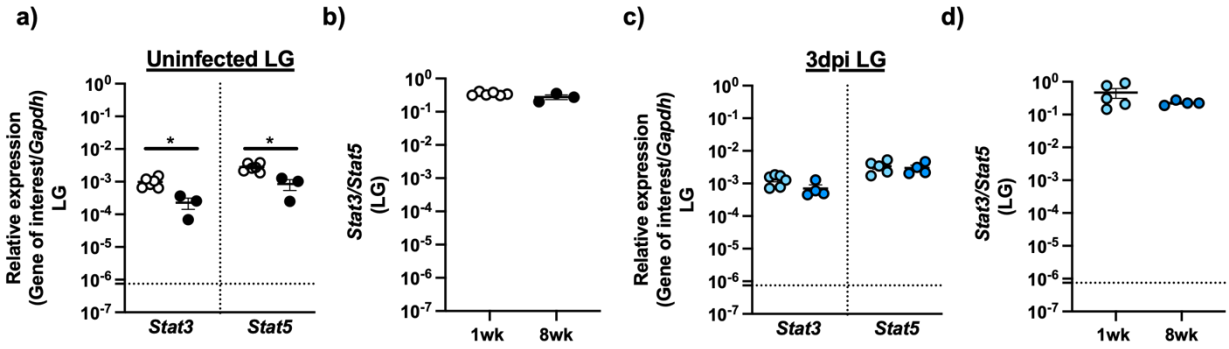


Fig 3.18. Stat3/Stat5 ratio in the lung doesn't change with age

1wk and 8wk-old C57BL/6 mice were infected with 2.5 × 10^5 PFU RSV A2 or PBS i.n,. Lung lobes were harvested 3dpi. **(a)** *Stat3* and *Stat5* were analysed by RT-qPCR and the **(b)** *Stat3/Stat5* ratio was calculated in both uninfected and **(c,d)** infected conditions. Data from one independent experiment with n = 3-6 mice per group. Data shown with median and interquartile range. Each dot represents one mouse. Bottom dotted line represents the limit of detection for the given assay. Mann-Whitney test was performed in which *, $p < 0.05$; **, $p < 0.01$; and ***, $p < 0.001$.

3.2.8 T cell populations in the thymus differ from those found in peripheral organs

The thymus is the source of all mature naïve $CD4^+$ T cells. Alterations in thymic development, therefore, can affect T cell responses in the periphery. Indeed, the thymus undergoes age-dependent involution both in humans and mice, a process that starts as early as in one year old humans and by 4-6wks of age in mice (295–297). Whether changes in the thymus, and the mature $CD4^+$ T cells it generates, may also underlie the altered IL-2 signalling capacity of $CD4^+$ T cells in neonates compared to adults was therefore assessed.

The thymus contains a number of immature subsets of T cells that eventually differentiate into mature $CD4^+$ and $CD8^+$ T cells *(summarized in Fig 3.19a)* (537). Immature T cells are $CD3^-CD4^-CD8^-$ T cells, also known as double negative (DN) T cells due to their lack of CD4 and CD8 surface markers. These cells undergo several maturation stages that are marked by antigen recognition to end up expressing stable high CD3/TCR and either CD4 or CD8 on their membranes, at which point they are considered matured and able to leave the thymus for the periphery. The synthetization and expression of CD3, TCR, CD4 and CD8 molecules occurs in parallel, stabilizing the membrane expression of the TCR complex. CD4 and CD8 markers are first co-expressed in the cell membrane of immature thymocytes, cells at this stage are known as double positive (DP) cells. Upon upregulation of a lineage-defining transcriptional signature, thymocytes then become single positive (SP) CD4 or CD8 T cells. These changes in surface marker expression coincide with positive and negative selection; positive selection requiring a thymocyte's TCR to bind MHC class I or II molecules with at least a weak affinity. Negative selection on the other hand is the process by which thymocytes that have a TCR able to bind MHC and/or self-peptides with high affinity are eliminated. As a result, only functional and non-self-reacting T cells will be selected in the thymus (524).

To analyse how T cell thymus maturation and thymus involution affects IL-2 and IL-6 responses in mice of different ages, 1wk and 8wk old mice were left uninfected or they were infected with an equal dose of RSV, the thymus was extracted and stimulated with PMA/Ionomycin/BFA or with BFA alone 3d post infection *(**Fig 3.19b**)*. Lymphocyte populations were divided into $CD3^{low}$ and $CD3^{high}$ and pools of all the different combinations of CD4 and CD8 markers were analysed *(**Fig 3.19c**)*. $CD3^{low}$ populations at the steady state remained constant with age except for DP $CD3^{low}$ cells which were significantly increased in proportion in infancy and SP $CD3^{low}CD4^{+}$ cells which were increased in adulthood *(**Fig 3.20a**)*. $CD3^{high}$ populations were predominantly observed in adult thymus in uninfected conditions as observed by the significant increase proportion of DP $CD3^{high}$ cells, $CD4^{+}FOXP3^{-}$ cells and $CD8^{+}$ cells *(**Fig 3.20b**)*. Natural T_{regs} ($CD4^{+}FOXP3^{+}$ cells differentiated in the thymus) and $CD3^{high}$ DN cells remained constant across both mice ages *(**Fig 3.20b**)*. A similar pattern was observed in infected conditions, where $CD3^{low}CD8^{+}$, $CD3^{high}$DP, $CD3^{high}CD4^{+}FOXP3^{-}$, $CD3^{high}CD4^{+}FOXP3^{+}$ and $CD3^{high}CD8^{+}$ cells were increased in adulthood *(**Fig 3.20c,d**)*.

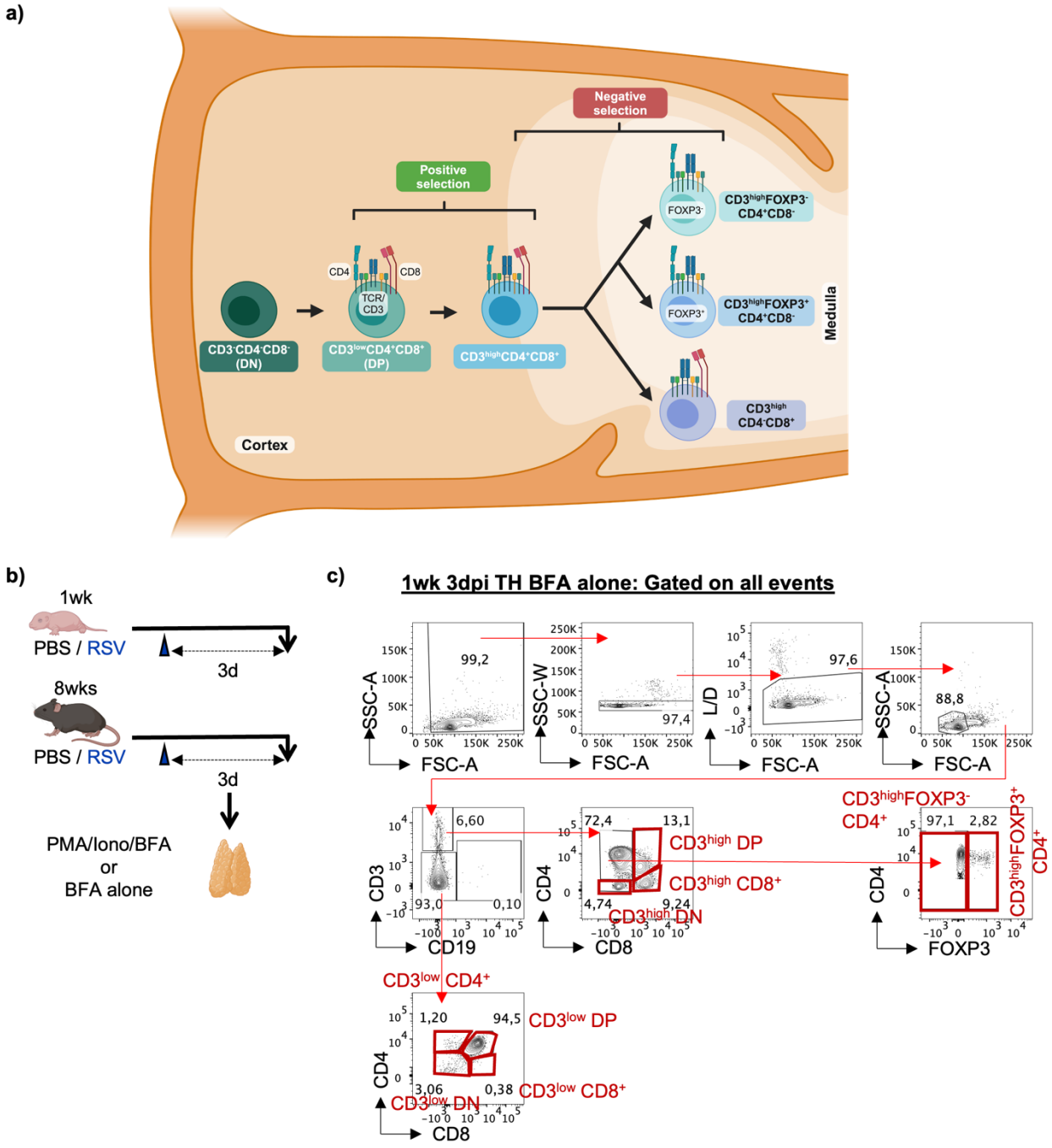


Fig 3.19. T cell populations in the thymus differ to those found in the SLOs

(a) Schematic of T cell maturation in the thymus. **(b)** 1wk and 8wk-old C57BL/6 mice were infected with 2.5 × 10^5 PFU RSV A2 or PBS i.n,. Thymus was harvested 3dpi and stimulated with PMA, Ionomycin and BFA or BFA alone for 4h at 37ºC, 5% CO2. **(c)** Representative flow cytometry gating strategy for lymphoid subsets. From total cells doublets were excluded and live cells were selected as e780 live/dead negative cells. Lymphoid cells were gated and $CD3^{high}$ or $CD3^{low}$ cells where selected. From these parental gates T cells were classified into double negative (DN), double positive (DP), $CD4^+$ or $CD8^+$ according to their expression of CD4 and CD8 markers. $CD3^{high}CD4^+$ singlets were then classified into $FOXP3^-$ or $FOXP3^+$ cells according to their expression of this transcriptional marker.

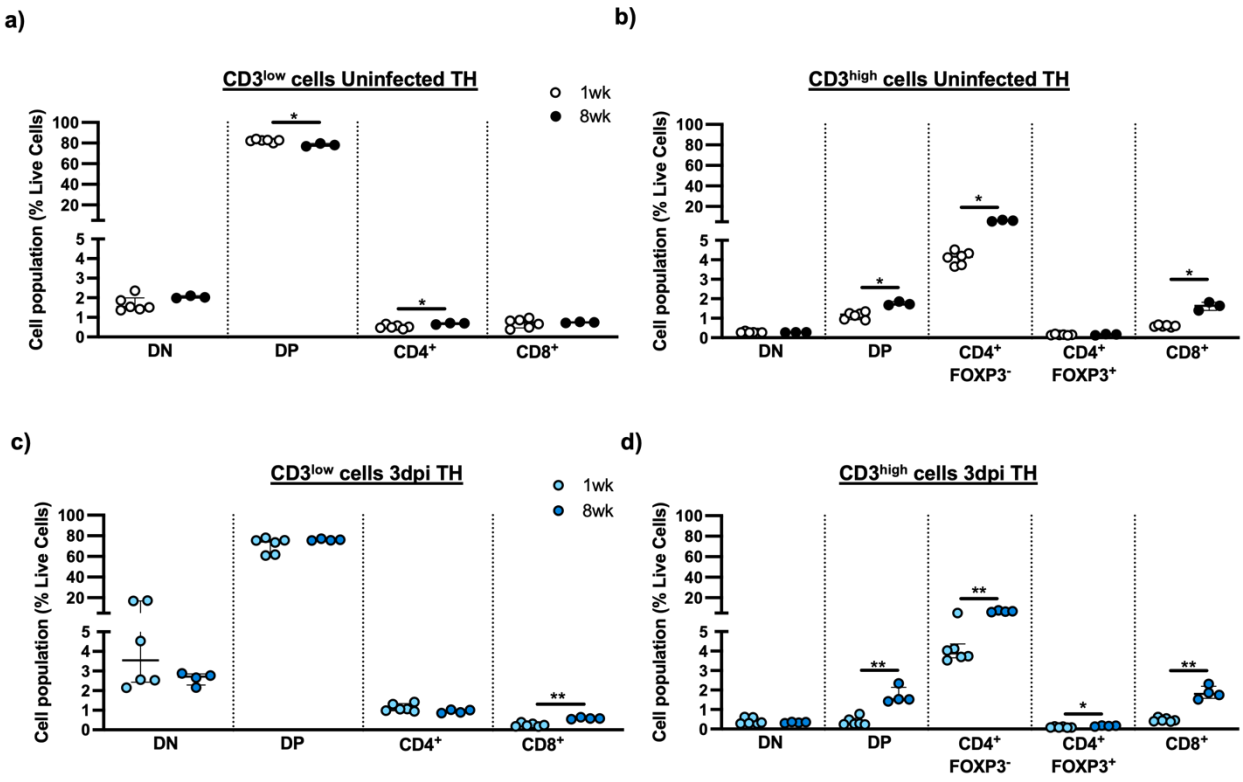


Fig 3.20. Thymocyte quantification in neonatal and adult mice

1wk and 8wk-old C57BL/6 mice were infected with 2.5 × 10^5 PFU RSV A2 or PBS i.n,. Thymus was harvested 3dpi. **(a)** Proportion of Double Negative (DN, $CD4^-CD8^-$), Double Positive (DP, $CD4^+CD8^+$), $CD4^+(CD4^+CD8^-)$ and $CD8^+$ ($CD4^-CD8^+$) $CD3^{low}$ and **(b)** $CD3^{high}$ cells from total live cells in uninfected conditions and **(c)** $CD3^{low}$ cells and **(d)** $CD3^{high}$ cell types from total live cells 3dpi. Data from one independent experiment with n = 3-6 mice per group. Data shown with median and interquartile range. Each dot represents one mouse. Mann-Whitney test was performed in which *, $p < 0.05$; **, $p < 0.01$; and ***, $p < 0.001$.

3.2.9 Both the IL-2 and IL-6 thymic signatures are upregulated in early life when compared to adult counterparts

The percentage of all thymocyte populations able to produce IL-2 after mitogenic stimulation was significantly elevated in early life steady state conditions when compared to adulthood with the exception of $CD3^{low}CD8^+$ cells *(Fig 3.21a,b)*. The proportion of neonatal cells that produced increased IL-2 was similar between all $CD3^{low}$ and $CD3^{high}$ cell populations, without one cell type having an increased proportion of cells able to produce IL-2 when compared with the rest. The percentage of adult immature $CD8^+$ T cells ($CD3^{low}CD8^+$ T cells) able to produce IL-2, the only cell type that had an increased proportion of cells able to produce IL-2 in 8wk old mice, was diminished when compared with the percentage of IL-2 producing neonatal T cells *(Fig 3.21a)*. The percentage of mature $CD8^+$ T cells ($CD3^{high}CD8^+$ T cells) able to produce IL-2 was increased in neonates when compared to adults, but again this was reduced when compared with all other $CD3^{low}$ and $CD3^{high}$ cell types *(Fig 3.21a,b)*. The percentage of IL-2 producing thymocytes was reduced after infection, but again the proportion of neonatal $CD3^{low}$ and $CD3^{high}$ cells able to produce IL-2 was elevated when compared to their adult counterparts as observed by the significantly increased proportion of

IL-2 producing cells by neonatal CD3^{low} DN and DP populations and CD3^{high} DN, DP, CD4^{+}FOXP3^{-} and CD4^{+}FOXP3^{+} populations *(Fig 3.21c,d)*. As with the steady state, after infection, the percentage of immature CD8^{+} T cells that produced IL-2 was increased in adult mice when compared to their early life counterpart, but this was reversed, albeit not significantly, after maturation *(Fig 3.21c,d)*. Concomitant with this result, the *Il2* transcript was also increased in 1wk old mice when compared with 8wk old mice in both uninfected and infected conditions *(Fig 3.21e-f)*.

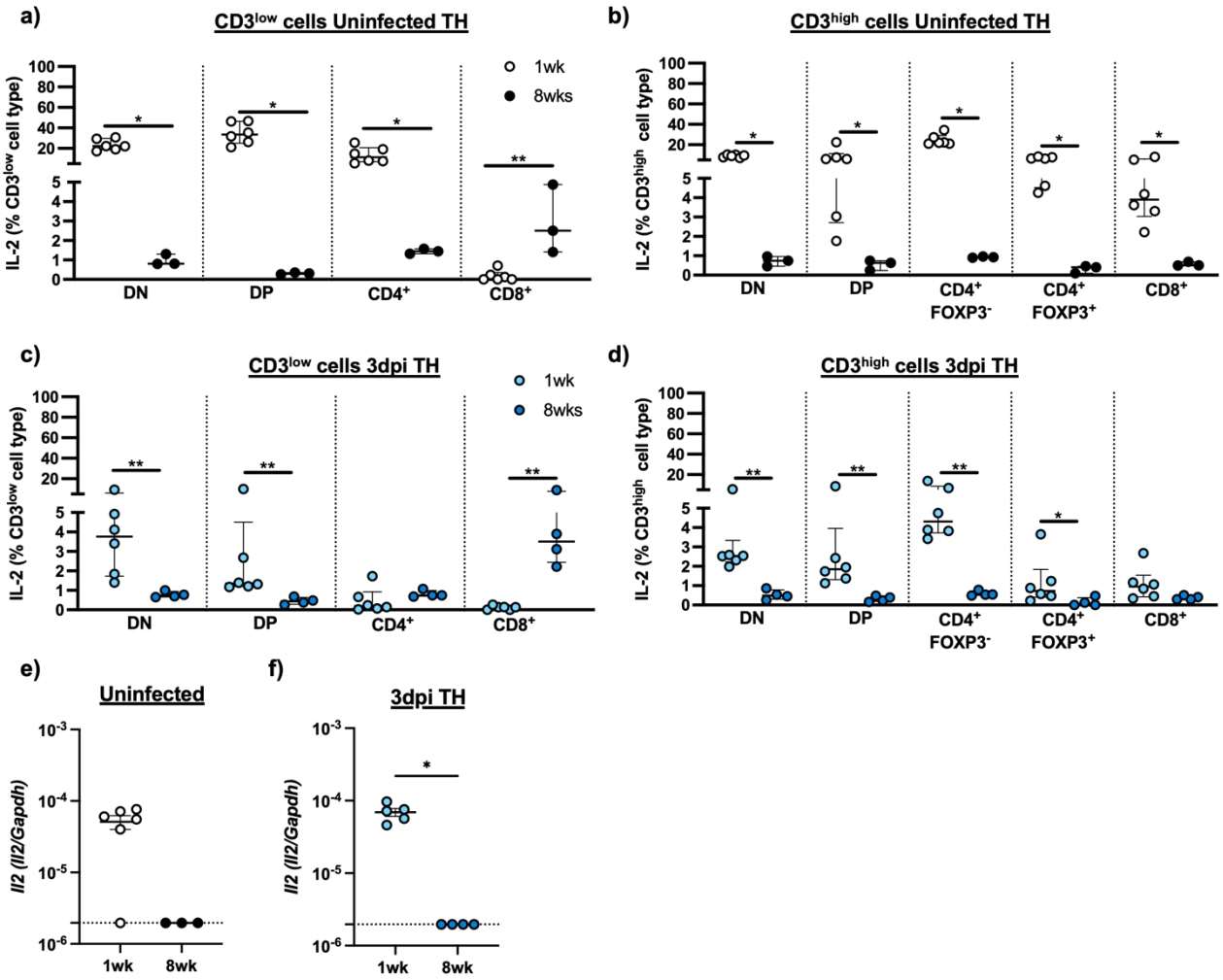


Fig 3.21. Increased IL-2 microenvironment in the thymus of early life mice when compared to adult counterparts

1wk and 8wk-old C57BL/6 mice were infected with 2.5 × 10^{5} PFU RSV A2 or PBS i.n,. Thymus was harvested 3dpi to analyze the IL-2 production by different cell types. **(a)** IL-2 production by Double Negative (DN, CD4^{-}CD8^{-}), Double Positive (DP, CD4^{+}CD8^{+}), CD4^{+}(CD4^{+}CD8^{-}) and CD8^{+} (CD4^{-}CD8^{+}) CD3^{low} and **(b)** CD3^{high} cells in uninfected or **(c,d)** infected conditions after mitogen stimulation. **(d)** Total *Il2* expression in uninfected or **(e)** RSV infected thymus was analysed by RT-qPCR. Data from one independent experiment with n = 3-6 mice per group. Data shown with median and interquartile range. Each dot represents one mouse. Bottom dotted line represents the limit of detection for the given assay. Mann-Whitney test was performed in which *, $p < 0.05$; **, $p < 0.01$; and ***, $p < 0.001$.

The percentage of thymic cells expressing CD25 was next analysed. The thymus of naïve neonatal mice contained a significant greater proportion of $CD3^{low}$ DN, $CD4^{+}$ and $CD8^{+}$ cells expressing mCD25 than adult counterparts *(**Fig 3.22a**)*. The percentage of $mCD25^{+}CD3^{low}$DP cells was minimal when compared to the percentage of all other $mCD25^{+}CD3^{low}$ thymocyte populations, and no difference according to age was observed *(**Fig 3.22a**)*. The percentage of $CD3^{low}$ DN expressing mCD25 was higher when compared to all other cell types *(**Fig 3.22a**)*. The proportion of mCD25 expressing $CD3^{high}CD4^{+}FOXP3^{-}$ cells and $CD3^{high}CD8^{+}$ T cells was also significantly elevated in neonates when compared to adults *(**Fig 3.22b**)*. In accordance to their lineage defining CD25 expression, $CD3^{high}CD4^{+}FOXP3^{+}$ cells contained the greatest proportion of $mCD25^{+}$ cells when compared to the other $CD3^{high}$ thymic populations analysed and no difference in this population was observed with age *(**Fig 3.22b**)*. After RSV infection there was an increased proportion of adult $CD3^{low}$DN and DP CD25 expressing cells when compared to neonatal counterparts, with the percentage of $CD3^{low}$DN cells still containing the greatest proportion of $mCD25^{+}$ cells *(**Fig 3.22c**)*. As in uninfected conditions, the proportion of neonatal $CD3^{high}CD4^{+}FOXP3^{-}$ and $CD3^{high}CD8^{+}$ T cells expressing mCD25 was increased when compared with thymocytes from 8wk old mice and again the population of $CD3^{high}CD4^{+}FOXP3^{+}$ cells contained the greatest proportion of mCD25 expressing $CD3^{high}$ thymocytes with no difference according to age *(**Fig 3.22d**)*. Transcript levels for *Cd25*, *Cd122* and *Cd132* were significantly upregulated in the thymocytes of 1wk naïve and RSV infected mice when compared to 8wk counterparts *(**Fig 3.22e,f**)*.

IL-6 protein and transcript expression as well as *Il6ra* and *Il6st* receptor subunits were also upregulated in early life when compared to adulthood in both uninfected and infected conditions *(**Fig 3.23a-d**)*. *Stat3* and *Stat5* levels were significantly elevated in neonates in steady state and RSV infected conditions leading to non-significant differences in the *Stat3/Stat5* ratio between neonates and adults *(**Fig 3.24a-d**)*. Both IL-2 and IL-6 signalling are therefore upregulated in early life murine thymocytes when compared to adult counterparts probably affecting the local and systemic T cell immune response in SLOs and peripheral organs.

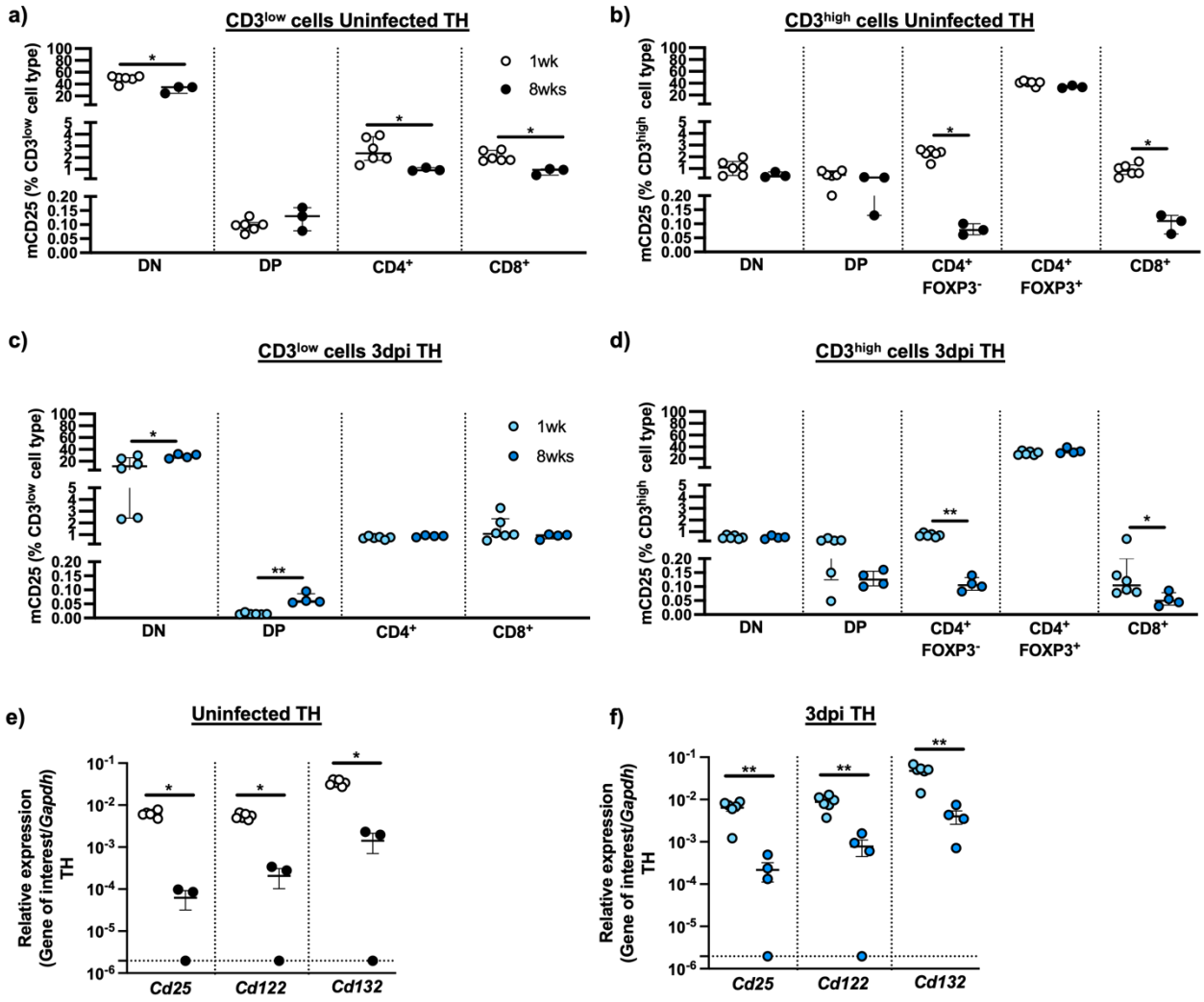


Fig 3.22. Increased proportion of membrane CD25 expressing thymocytes in early life mice when compared to adult counterparts

1wk and 8wk-old C57BL/6 mice were infected with 2.5 × 10^5 PFU RSV A2 or PBS i.n,. Thymus was harvested 3dpi. **(a)** Proportion of Double Negative (DN, $CD4^-CD8^-$), Double Positive (DP, $CD4^+CD8^+$), $CD4^+$ ($CD4^+CD8^-$) and $CD8^+$ ($CD4^-CD8^+$) $CD3^{low}$ and **(b)** $CD3^{high}$ cells expressing mCD25 in uninfected or **(c,d)** infected conditions. **(e)** *Cd25*, *Cd122* and *Cd132* transcripts in thymus extracts from uninfected or **(f)** infected mice. Data from one independent experiment with n = 3-6 mice per group. Data shown with median and interquartile range. Each dot represents one mouse. Bottom dotted line represents the limit of detection for the given assay. Mann-Whitney test was performed in which *, $p < 0.05$; **, $p < 0.01$; and ***, $p < 0.001$.

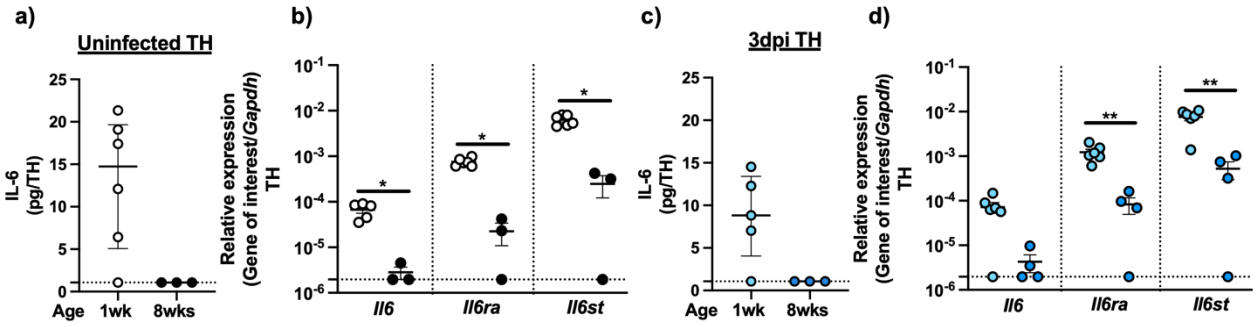


Fig 3.23. IL-6 and IL-6 receptor expression is increased in neonatal thymus

1wk and 8wk-old C57BL/6 mice were infected with 2.5 × 10^5 PFU RSV A2 or PBS i.n,. Thymus was harvested 3dpi. **(a)** IL-6 protein and **(b)** *Il6*, *Il6ra* and *Il6st* RNA detected in uninfected or **(c,d)** 3dpi conditions. Data from one independent experiment with n = 3-6 mice per group. Data shown with median and interquartile range. Each dot represents one mouse. Bottom dotted line represents the limit of detection for the given assay. Mann-Whitney test was performed in which *, p < 0.05; **, p < 0.01; and ***, p < 0.001.

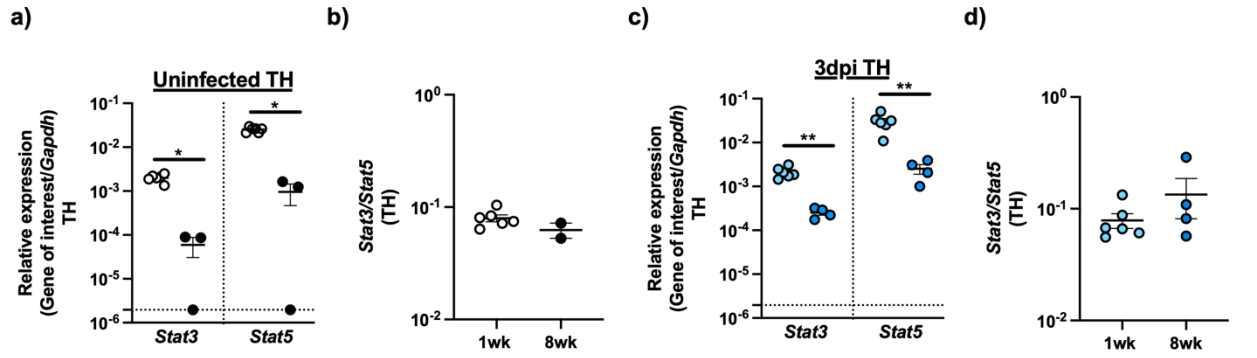


Fig 3.24. Neonatal thymocytes have increased Stat3 and Stat5

1wk and 8wk-old C57BL/6 mice were infected with 2.5 × 10^5 PFU RSV A2 or PBS i.n,. Thymus was harvested 3dpi. **(a)** *Stat3* and *Stat5* were analysed by RT-qPCR and **(b)** the Stat3/Stat5 ratio was calculated in both uninfected and **(c,d)** infected conditions. Data from one independent experiment with n = 3-6 mice per group. Data shown with median and interquartile range. Each dot represents one mouse. Bottom dotted line represents the limit of detection for the given assay. Mann-Whitney test was performed in which *, p < 0.05; **, p < 0.01; and ***, p < 0.001.

3.2.10 The percentage of cells producing IL-2 is increased throughout the developmental pathway of CD4$^+$FOXP3$^-$T cells in early life when compared to adulthood

Naïve CD4$^+$ T cells can be thought of as progressing through the stages of thymic development until they differentiate into fully mature cells that can migrate to the SLOs. One hypothesis might be that neonatal enrichment for immature thymocytes explains some of the altered state of neonatal versus adult CD4$^+$ T cells. Analysis of adult CD4$^+$ T cells however showed a reduced percentage of IL-2 producing cells even from immature thymocytes which is sustained throughout T cell development *(**Fig 3.25a**)*. Conversely, the proportion of neonatal CD4$^+$ T cells able to produce IL-2 was elevated at all developmental stages, with particularly the proportion of thymocytes with a non-regulatory fate able to produce IL-2 already increased in the thymus *(**Fig 3.25a**)*. This was slightly reduced in CD4$^+$ SP thymocytes but elevated again in mature CD4$^+$ T cells in the LNs and spleen

of uninfected mice *(Fig 3.25a)*. Intriguingly, infection resulted in a reduced thymic proportion of early life IL-2 producing non-regulatory $CD4^+$ T cells, but the percentage of IL-2 producing T cells in the SLOs was not affected by infection *(Fig 3.25b)*.

The proportion of T_{reg} cells able to produce IL-2 when stimulated with PMA and Ionomycin was diminished when compared to $FOXP3^-CD4^+$ T cells in both neonates and adults, with no marked increase in the proportion of IL-2 producing T_{regs} cells at the last stages of thymus maturation nor once the T_{regs} reached the peripheral organs. Nevertheless, the proportion of T_{regs} able to produce IL-2 after mitogen stimulation was elevated in 1wk old mice when compared to 8wk old mice in steady state conditions *(Fig 3.25c)*, but this difference was no longer notable in viral infected animals *(Fig 3.25d)*.

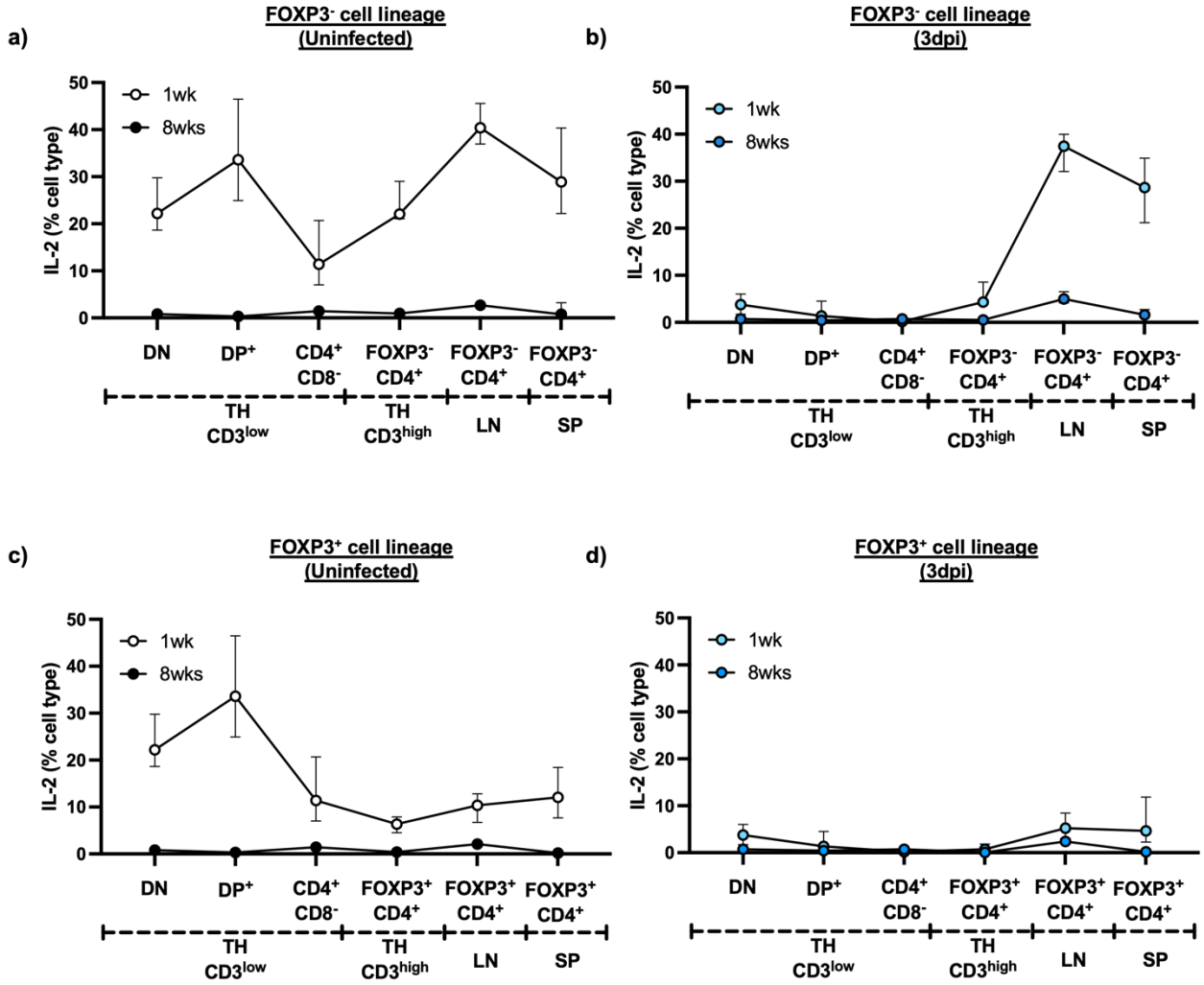


Fig 3.25. IL-2 levels are increased throughout the development of $CD4^+$ T cell lymphocytes in early life when compared to adulthood

1wk and 8wk-old C57BL/6 mice were infected with 2.5 × 10^5 PFU RSV A2 or PBS i.n,. **(a)** IL-2 expression by $FOXP3^-$ $CD4^+$ T cell lymphocytes through different organs in steady state and **(b)** infected conditions**. (c)** IL-2 expression by T_{regs} ($FOXP3^+$ CD4+) through different organs in steady state and **(d)** infected conditions. Re-ploted data from previous graphs. Data from one independent experiment with n = 3-6 mice per group. Data shown with median and interquartile range. Each dot represents one group of mice.

In summary this data indicates that the proportion of IL-2 producing cells in early life is upregulated at the earliest stages of thymocyte development, a feature retained throughout T cell maturation and when reaching the periphery.

3.2.11 Human T_{FH} can be differentiated *in vitro* from adult peripheral blood naïve $CD4^+$ T cells

The cytokine microenvironment also plays a significant role in human $CD4^+$ T cell differentiation. Thus, to evaluate the role of IL-2 and IL-6 signalling in T_{FH} differentiation in humans, an *in vitro* T_{FH} differentiation protocol developed by a previous student in the lab was used (516). To confirm that naïve $CD4^+$ T cells isolated from human whole peripheral blood can be differentiated into $CXCR5^+PD\text{-}1^+$ cells *in vitro* in my hands, undifferentiated $CD4^+$ T cells were cultured with a skewing T_{FH} cytokine cocktail, consisting of rhIL-6, rhIL-12, rhTGF-β, Activin A and rhIL-1β, and exposed to ICOS-L for 5 days (*in vitro* T_{FH}) and data was compared with naïve $CD4^+$ T cells treated with rhIL-7 alone (control) by flow cytometry *(**Fig 3.26a,b**)*.

A significant proportion of naïve $CD4^+$ T cells cultured with the T_{FH}-skewing cocktail upregulated CXCR5 and PD-1 when compared to control cells *(**Fig 3.26c**)*. Their T_{FH} signature was further confirmed by an increased expression of the canonical T_{FH} transcriptional factor BCL6 *(**Fig 3.26d**)*. Fitting with this, the ratio of *BCL6* to *PRDM1* (the gene for BLIMP-1, the natural BCL6 repressor (31,76)), was also increased in *in vitro* T_{FH} when compared to the control counterparts *(**Fig 3.26e**)*.

Cells cultured in T_{FH} favouring and neutral conditions were equally viable (**Fig 3.26f**) and presented a similar proliferation index (**Fig 3.26g**). CXCL13 and IL-21, canonical cytokines secreted by human *in vivo* T_{FH} (71), were however only detectable in supernatants from the *in vitro* T_{FH} culture *(**Fig 3.26h,i**)*. Overall, this supports the conclusion that cells with a T_{FH} phenotype can be generated *in vitro* from human peripheral blood naïve $CD4^+$ T cells.

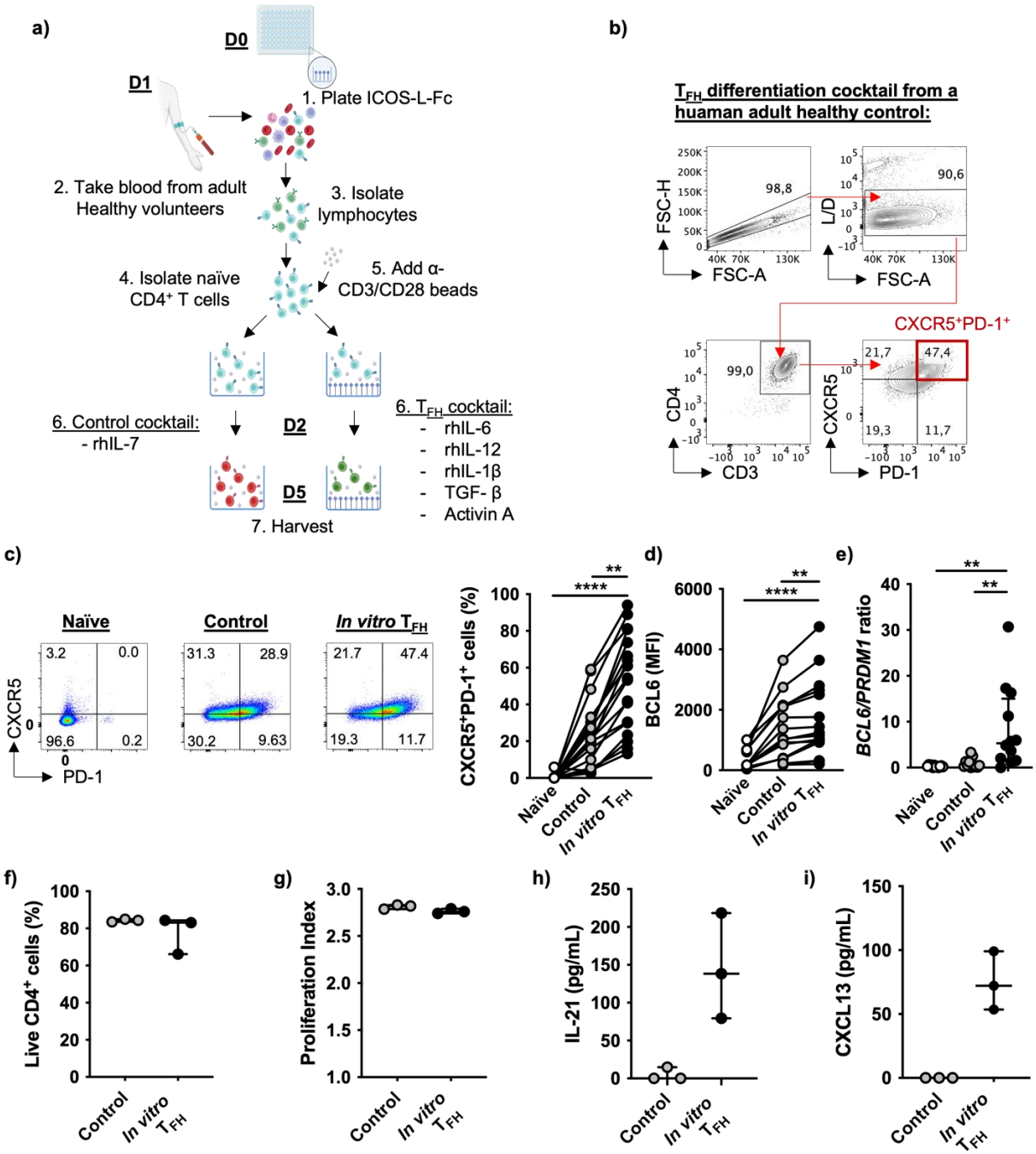


Fig 3.26. Human T_{FH} can be differentiated in vitro from peripheral blood naïve CD4⁺ T cells.

(a) Naïve CD4⁺ T cells *(Naïve)* isolated from adult healthy donor's PBMCs were stimulated with a-CD3/28 magnetic beads and rhIL-7 (*Control*) or a T_{FH}-skewing cocktail (*in vitro* T_{FH}) consisting of ICOS-L-Fc, rhIL-6, rhIL-12, rhIL-1β, rhTGF-β and rhActivin A for 5 days. **(b)** Representative flow cytometry gating strategy. From total cells cultured doublets were excluded and live cells were selected as e780 live/dead negative cells. Cultured cells were confirmed as $CD3^+CD4^+$ cells and T_{FH} cells were defined as $CXCR5^+PD\text{-}1^+$ cells. **(c)** The percentage of T_{FH} at day 0 (*Naïve*) or after 5 days' culture (*control* and *in vitro* T_{FH}) was analysed by flow cytometry. **(d)** The effect of T_{FH} differentiation on the MFI for BCL6 and **(e)** the ratio between *BCL6* and *PRDM1* gene expression were analysed by flow cytometry and RT-qPCR respectively. **(f)** Viability and **(g)** proliferation index of one independent experiment with three biological replicates was analysed by flow cytometry. **(h)** IL-21 and **(i)** CXCL13 present in the supernatants of naïve $CD4^+$ T cells cultured in the presence of neutral conditions or the T_{FH}-skewing cocktail were measured by ELISA in the representative experiment. Data are representative of seven independent experiments with eighteen biological replicates (c-e) or of one representative experiment with three biological replicates (f-i). Data shown with median and interquartile range. Each dot represents an individual donor. Friedman test with Dunn's multiple comparison test (c-e) or the Wilcoxon ranked test (f-i) was performed in which *, $p < 0.05$; **, $p < 0.01$; and ***, $p < 0.001$; ****, $p < 0.0001$.

3.2.12 STAT3 signalling promotes CD4$^+$ T cell survival and T_{FH} effector function *in vitro*

In order to evaluate the importance of STAT3 phosphorylation in human T_{FH} differentiation, *in vitro* T_{FH} were generated as described above and were exposed to increasing concentrations of an α-STAT3 phosphorylation inhibitor (XIII C188-9). The highest concentration of DMSO for each experiment was used as a vehicle control. First, naïve CD4$^+$ T cells were inhibited for 1 hour both prior to TCR activation and cytokine stimulation. While the vehicle control culture responded normally, all cells treated with inhibitor were not viable at 5 days *(data not shown).* Therefore, a more conservative approach was chosen in which cells were exposed to a single inhibitor dose 1h prior to cytokine exposure. In this case, cells treated with low concentrations of the drug (0.2 and 1μM) were viable, but inhibition of pSTAT3 at high concentrations (5 and 50μM) caused a significant decrease in T_{FH} cell culture viability. This was not observed in the matched 50μM vehicle controls *(**Fig 3.27a**)*. In control cultures, cultured with rhIL-7 alone, the presence of 5μM α-pSTAT3 also had decreased viability when compared with their vehicle counterpart, but this effect was less pronounced than in the *in vitro* T_{FH} culture and not significant *(**Fig 3.27b**)*.

Surprisingly, an increase in the proportion of CXCR5$^+$PD-1$^+$ cells was observed in the presence of the α-pSTAT3 inhibitor *(**Fig 3.27c**)*. Due to the significant cell death associated with the 5μM culture, the number of CXCR5$^+$PD1$^+$ cells per well was lower, but this did not happen in the cultures treated with lower concentrations of the drug (*Fig 3.27d*). Efficiency of STAT3 phosphorylation inhibition was confirmed through pSTAT3 phospho-flow staining. To mimic the differentiation protocol, naïve CD4$^+$ T cells extracted from PBMCs were incubated for 1h with α-pSTAT3 followed by a 30 minutes' exposure to the T_{FH} skewing cocktail, STAT3 phosphorylation was then analysed by flow cytometry. 5μM and 50μM, but not 0.2μM and 1μM, resulted in reduced pSTAT3 at this time point *(**Fig 3.27e**)*.

Lower concentrations of the pSTAT3 inhibitor did not appear to suppress peak phosphorylation of STAT3 nor CXCR5 or PD-1 expression. Viability and cell number were also unchanged. Interestingly however, both 0.2μM and 1μM of the inhibitor were sufficient to prevent secretion of both IL-21 and CXCL13 *(**Fig 3.27f,g**)*. Taken together, this data indicates that STAT3 is essential for T_{FH} survival during differentiation and secretion of CXCL13 and IL-21, but not for the production of CXCR5 or PD-1.

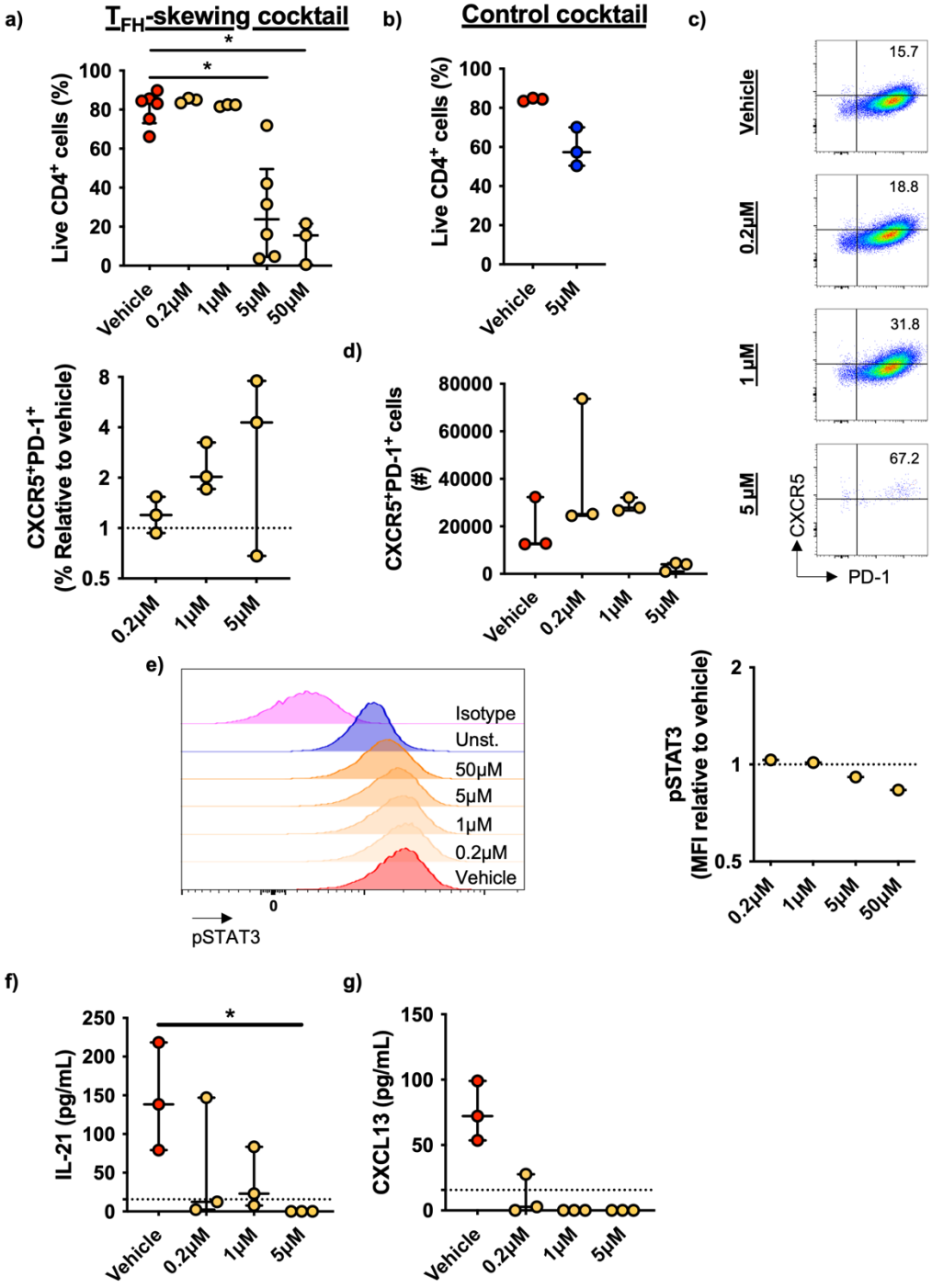


Fig 3.27. STAT3 phosphorylation in humans controls in vitro CD4⁺ T cell viability and T_{FH} effector function.

(a) Proportion of live CD4⁺ cells after 5 days' culture of naïve CD4⁺ T cells activated with α-CD3/α-CD28 magnetic beads and treated with DMSO (vehicle) or decreasing concentrations of XIII C188-9 (α-pSTAT3) 1h prior to T_{FH} skewing cocktail (yellow) or **(b)** neutral conditions (blue)**. (c)** Percentage relative to vehicle and **(d)** number of CXCR5⁺PD-1⁺ cells when exposed to increasing concentrations of XIII C188-9. **(e)** Effect on STAT3 phosphorylation**, (f)** IL-21 and **(g)** CXCL13 production by cells exposed to the T_{FH}-skewing cocktail and increasing concentrations of XIII C188-9. Each dot represents an individual donor. Bottom dotted line represents the limit of detection for the given assay. Data are representative of two (a, c-h) or one (b) independent experiments with three biological replicates each. Friedman test with Dunn's multiple comparison test (a, c-g) or the Wilcoxon ranked test (b) was performed in which *, $p < 0.05$; **, $p < 0.01$; and ***, $p < 0.001$; ****, $p < 0.0001$.

3.2.13 Phosphorylation of STAT4 *in vitro* seems redundant for human T_{FH} differentiation

IL-12 is the main driver of T_{FH} polarisation in humans (143), because in mice this cytokine mainly acts through the phosphorylation of STAT4 (145), the role of pSTAT4 in human T_{FH} differentiation was analysed using the previously stablished *in vitro* system. To this end, cells receiving the T_{FH}-skewing cocktail were exposed to 100μM of CAS 6493-06-7, a pSTAT4 chemical inhibitor, both 1h prior to TCR stimulation and cytokine cocktail and compared to PBS treated cells as a vehicle control.

Although there was a subtle decline in the amount of $CXCR5^{+}PD\text{-}1^{+}$ cells in cultures inhibited with α-pSTAT4 when compared to the vehicle control, this was not significant *(**Fig 3.28a**)* and both cultures contained the same number of *in vitro* T_{FH} cells *(**Fig 3.28b**)*. Consistently, there was no significant difference in any of the analysed T_{FH} related genes *(**Fig 3.28c**)* and no change in the *BCL6*/*PRDM1* ratio was observed when both culture conditions were compared *(**Fig 3.28d**)*. Inhibition of STAT4 did cause a significant upregulation of *IRF4* and *IL9* RNA transcripts as well as a decrease in *IL17A* *(**Fig 3.28e**)*. Although one limitation of the study is the lack of data supporting the inhibition of pSTAT4 by the reagent used, these experiments show that STAT4 inhibition has a limited effect on human T_{FH} differentiation; pointing that maybe both STAT3 and STAT4 play redundant roles in driving T_{FH} differentiation using this particular *in vitro* system.

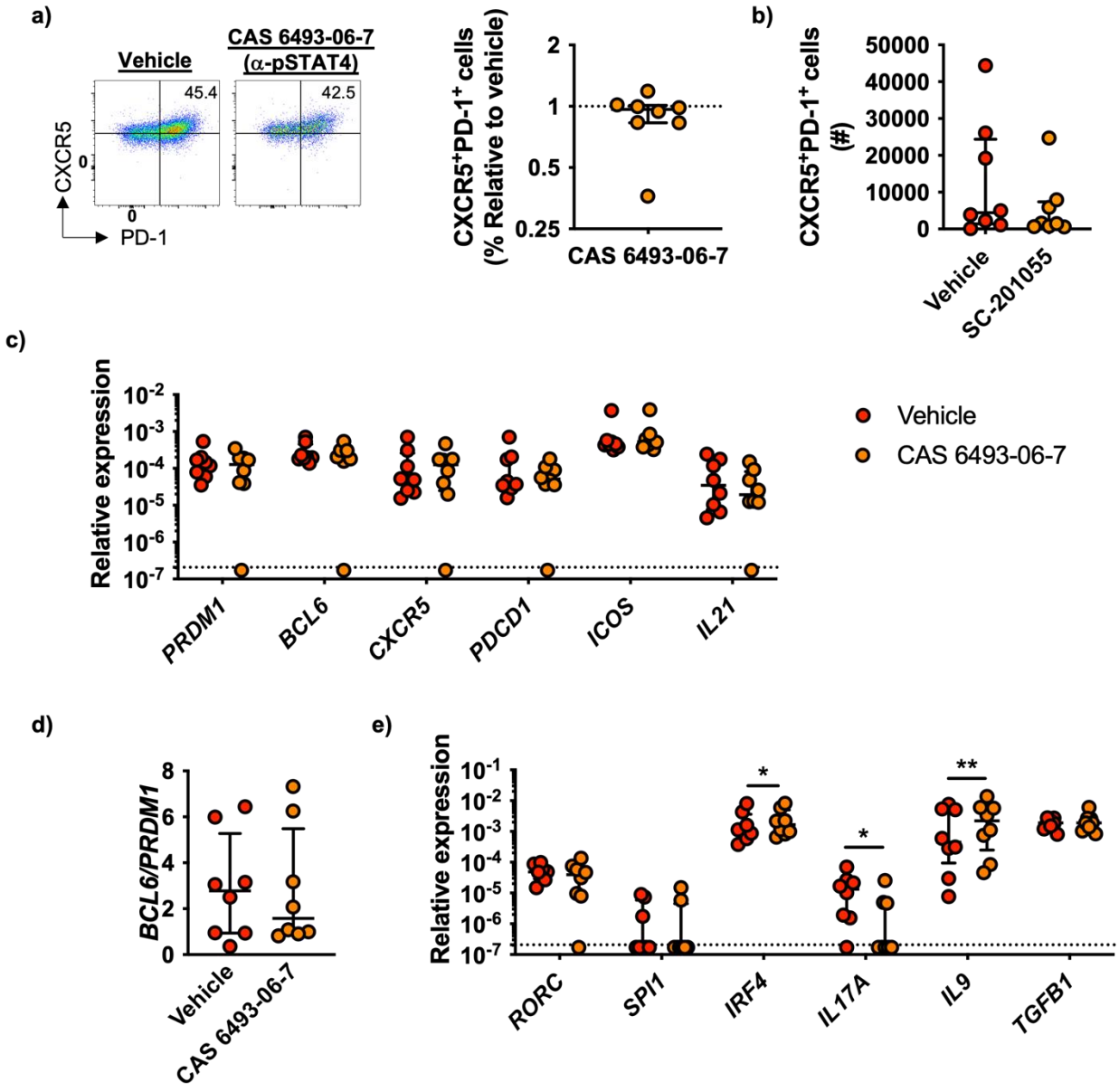


Fig 3.28. STAT4 phosphorylation is redundant for T_{FH} differentiation in humans

(a) Proportion and **(b)** number of CXCR5$^+$PD-1$^+$ cells relative to vehicle after 5 days' culture of naïve CD4$^+$ T cells inhibited for 1h prior to α-CD3 and α-CD28 activation and 1h prior to T_{FH}-skewing cocktail addition with DMSO (vehicle) or 100μM of CAS 6493-06-7 (α-pSTAT4). **(c)** Effect of STAT4 inhibition on T_{FH} related genes where relative expression is quantified as gene of interest/average of housekeeping genes (ACTB and 18S). **(d)** Ratio between BCL6 and PRDM1 gene expression. **(e)** Effect of chemical pSTAT4 inhibition on T helper defining genes' transcription where relative expression is quantified as gene of interest/average of housekeeping genes (*ACTB* and *18S*). Each dot represents an individual donor. Bottom dotted line represents the limit of detection for the given assay. Data are representative of three independent experiments with three biological replicates each. Friedman test with Dunn's multiple comparison test was performed in which *, $p < 0.05$; **, $p < 0.01$; and ***, $p < 0.001$; ****, $p < 0.0001$.

3.2.14 Human STAT5 phosphorylation limits T_{FH} differentiation

Next, to analyse the role played by STAT5 signalling in human T_{FH} polarisation, a chemical inhibitor of STAT5 phosphorylation, CAS285986-31-4, was used 1h prior to TCR activation and cytokine stimulation in the human T_{FH} differentiation system.

Concomitant to the observations in mice, the percentage of $CXCR5^{+}PD\text{-}1^{+}$ cells was significantly increased in the inhibited culture when compared with the DMSO-treated control *(**Fig 3.29a**)*, although the number of T_{FH} cells was similar in both conditions *(**Fig 3.29b**)*. A significant upregulation of CXCR5 and BCL6 was observed at a protein level in the treated cultures, while no difference in PD-1 was seen *(**Fig 3.29c-e**)*. No difference in T_{FH} related RNA levels were observed between the chemically inhibited group and the control *(**Fig 3.29f**)*, but the *BCL6/PRDM1* ratio was significantly downregulated in the group exposed to the chemical, contradicting the protein results *(**Fig 3.29g**)*.

Given the role of IL-2 mediating STAT5 phosphorylation in the differentiation of other T helper subsets (31), the effect of STAT5 inhibition in T helper polarisation towards alternative T_{FH} fates was assessed at a transcript level. No statistical differences or major trends were observed in T helper transcriptional factors or cytokines in the depicted genes *(**Fig 3.29h**)*.

An important limitation of the experiment is the lack of data supporting the inhibition of pSTAT5 by the reagent used. If the premise of pSTAT5 inhibition is accepted, the protein data shown here confirms that pSTAT5 is a negative regulator of the human T_{FH} differentiation process, but its inhibitory effect does not directly promote polarisation towards other T helper fates when submitted to T_{FH} polarising conditions.

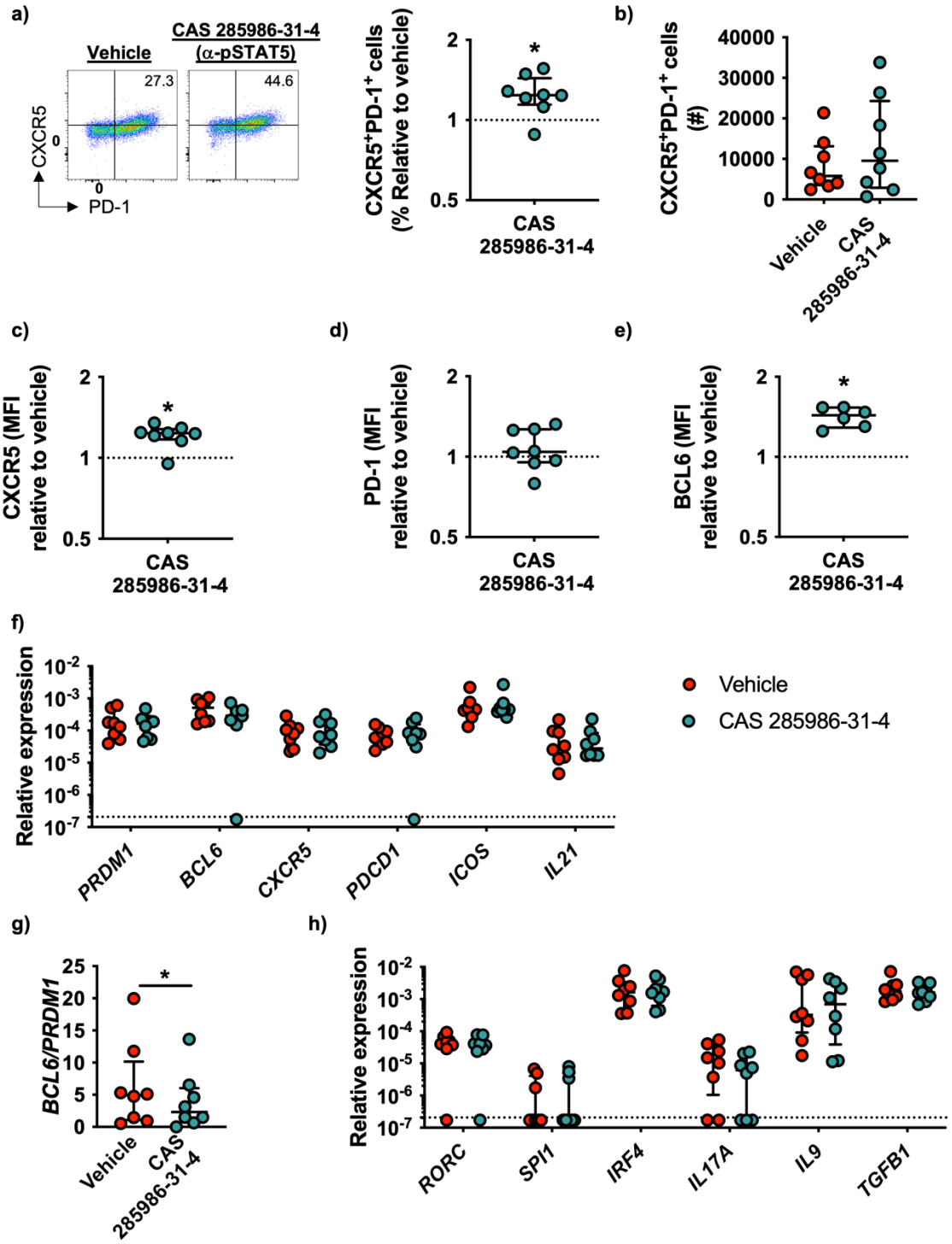


Fig 3.29. Human STAT5 phosphorylation limits T_{FH} differentiation

(a) Proportion and **(b)** cell number of CXCR5$^+$PD-1$^+$ cells relative to vehicle after 5 days' culture of naïve CD4$^+$ T cells inhibited for 1h prior to α-CD3/28 activation and 1h prior to T_{FH}-skewing cocktail with DMSO (vehicle) or 50mM of a STAT5 chemical inhibitor (CAS285986-31-4) analysed by flow cytometry. **(d)** Effect of STAT5 inhibition on the MFI of CXCR5, **(e)** PD-1 and **(f)** BCL6 by flow cytometry. **(g)** Effect of STAT5 inhibition on T_{FH} related genes where relative expression is quantified as gene of interest/average of housekeeping genes (*ACTB* and *18S*) and **(h)** ratio between BCL6 and PRDM1 gene expression by RT-qPCR. (i) Gene expression of classical transcription factors and cytokines from T helper subsets by RT-qPCR where relative expression is quantified as gene of interest/average of housekeeping genes (ACTB and 18S). Each dot represents an individual donor. Bottom dotted line represents the limit of detection for the given assay. Data are representative of three independent experiments with three biological replicates each. Wilcoxon ranked test was performed in which *, $p < 0.05$; **, $p < 0.01$; and ***, $p < 0.001$; ****, $p < 0.0001$.

3.3 Discussion

Humoral responses mediate essential long-term protection following infection or vaccination, but are often diminished in early life. The low antibody production is linked with a reduced T_{FH} differentiation capacity in neonates when compared to adulthood. Most of our understanding of the T_{FH} differentiation pathways however comes from adult mouse studies and human *in vitro* systems using adult samples, but much less is investigated in early life, the period where the humoral immune responses are first established. This chapter aimed to characterise the unique immunological landscape in neonates when compared to adults, early after infection with RSV when T cell responses are developing, to identify mechanisms that might affect T_{FH} differentiation.

As well as antigen recognition and co-stimulation signalling, the cytokine microenvironment plays a critical role in driving $CD4^+$ T cell differentiation. In adulthood, STAT3-phosphorylating cytokines, such as IL-6 in mice and IL-12 in humans, are linked with pro-T_{FH} differentiation while STAT5 signalling molecules, as IL-2 in both murine models and humans, are associated with reduced T_{FH} fate (526). In this chapter I found that the percentage of lymphocytes able to produce IL-2 after mitogenic stimulation is increased in neonates when compared to adults. This observation is true in all organs analysed (thymus, mediastinal LN, spleen and lung). Early life naïve $CD4^+$ T cells, which can go on to become T_{FH} upon antigen encounter, also have a higher ability to recognise and respond to IL-2 both *in vitro* and *in vivo*. Indeed, *in vivo,* we have shown that neutralising IL-2 in neonates is sufficient to induce T_{FH} dependent protective immunity (25).

3.3.1 Early life secondary lymphoid organs are enriched for IL-2 production

T_{FH} differentiation is reduced in early life when compared to adults, but the precise mechanisms driving this age-dependent difference in T_{FH} polarization remain unclear. In this chapter I found that following stimulation with PMA, Ionomycin and BFA the percentage of lymphoid cells able to produce IL-2 is enhanced in early life when compared to adulthood. The $Foxp3^-CD4^+$ T cell population contained the greatest proportion of cells able to produce IL-2 after mitogen stimulation, but an increased percentage of IL-2 producing cells was seen in all other cell types analyzed including $CD8^+$ T cells, T_{regs} and B cells. While the extent of this difference could partially be the result of the mitogen stimulation used, enhanced *Il2* expression is also observed directly in LN tissue, especially after infection. Likewise, directly isolated naïve $CD4^+$ T cells have enhanced *Il2* expression compared to adult counterparts. Fitting with these observations, a number of murine studies have shown that $Foxp3^-CD4^+$ T cells are the major source of IL-2 in adult lymphoid tissues (535,538). Some early murine studies using mixed lymphocyte cultures found that neonatal cells produced less IL-2 than their adult counterparts (539). More recent studies in mice however have suggested, that at least after antigen-encounter, neonatal $CD4^+$ T cells have an equal or

accelerated ability to produce IL-2 (540). Indeed, using IL-2 reporter mice, IL-2 producing $CD4^+$ T cells are seen by day 3 of life (541). Fate-mapping of IL-2 producing murine cells revealed that approximately 10% of $Foxp3^-CD4^+$ T cells in the spleen have produced IL-2 by 10 days of life (542). One of the main limitations of my study is the inability to capture IL-2 in serum or organ supernatants, since the ELISA methods used previously in the lab could not detect any measurable IL-2, probably due to the high IL-2 uptake by immune cells. The flow cytometry and transcript data however support the observation that IL-2 production is elevated in early life. Fitting with this, if IL-2 is neutralized during the neonatal period, T_{FH}, GC B cells and RSV-specific antibody responses are elevated in early life (25). Together this supports the conclusion that there is an enhanced capacity to produce IL-2 during the neonatal period, especially in the case of naïve non-regulatory $CD4^+$ T cells. It is from this pool of $CD4^+$ T cells that T_{FH}, and other effector cells, are generated upon antigenic stimulation, likely affecting their ability to differentiate in early life.

3.3.2 Neonatal $CD4^+$ T cells have an altered response to cytokine signalling

Early life $CD4^+$ T cells are not only able to produce more IL-2, but they also show an increased ability to recognise it and respond to it. This is observed by increased expression of CD25 (IL-2Rα) and CD122 (IL-2Rβ) in neonatal naïve $FOXP3^-CD4^+$ T cells when compared with adult counterparts. Early life naïve $CD4^+$ T cells are also more prone to phosphorylate STAT5 upon IL-2 recognition, as higher pSTAT5 levels are detected in early life cells than adult analogues when exposed to the same dose of IL-2 *in vitro*. An increased pSTAT5 is also observed in neonatal recently activated antigen-experienced cells after RSV infection *in vivo.* In accordance with my observations, data in both mice and humans shows that neonatal naïve $CD4^+$ T cells are transcriptionally and functionally distinct from their adult naïve counterparts (543–546). Human cord blood naïve $CD4^+$ T cells have increased expression of IL-2R components and appear more sensitive to IL-2 signalling when compared to adult cells (545). One mouse study observed that neonatal naïve $CD4^+$ T cells are intrinsically more prone to acquiring an effector phenotype, providing rapid immune responses at the cost of reduced long lasting immunity (239). Interestingly, even IL-6 signalling, predominantly thought to activate STAT3 (58,127,128,131), and to a lesser extent STAT1 (58), is able to induce STAT5 phosphorylation in $CD4^+$ T cells from 2wk, but not 6wk, old mice. This suggests that while IL-2R components might partially explain the enhanced STAT5 signalling seen in infancy there are also alterations in the signal transduction pathways between early life and adult $CD4^+$ T cells. Indeed, another group recently reported that IL-6 induces STAT5 activation in neonatal murine T_{FH} upon pneumococcal conjugate vaccination, limiting their differentiation and function (534). In part they found this was through the regulation of IL-2R expression, at odds with the observation in adult mice that IL-6 acts to suppress IL-2R signalling in germinal centre T_{FH}, allowing their ongoing function (127). The precise mechanism for this is unclear. In my hands, $CD4^+$ T cells from 2-3wk old mice did display a slightly higher ratio of STAT5

than STAT3 at the transcript level, which might impact which is preferentially activated. This data combined suggests that early life naïve $CD4^+$ T cells are intrinsically different to those observed in adulthood with enhanced pSTAT5 that could hinder their differentiation towards a T_{FH} phenotype.

3.3.3 Biological implications for enhanced IL-2 signalling in early life

Several mechanisms could be involved in driving the enriched IL-2 microenvrionment observed in 1wk old mice. Early life is the period when we interact with multiple antigens, both innocuous and infectious, for the first time (547). This age has historically been described as a period of immune immaturity, and while the reality is more complex, it is clear that the functions of the neonatal immune system differ from those seen in adulhood in both humans and murine models (7,548). In order to generate sufficient peripheral T cells to meet the distinct demands of perinatal life, i.e encounering pathogens for the first time and establishing immune tolerance, thymic output peaks in infancy and the adolescent period, before declining due to thymic involution from about 4-6 weeks old in mice and as early as 1 year old in humans albeit it continues throughout adolescence (295–297). The pool of peripheral T cells in infants is therefore dominated by recent thymic emigrants (263), and due to the lack of cumulative exposure to both environmental and pathogenic antigens in early life the pool is also primarily naïve (549). Memory responses are developed throughout life upon antigen encounter and therefore are decreased in infancy (288). Recent thymic emigrants display a higher proliferative capacity which is dependent on gamma c cytokines, such as IL-2 (550). IL-2 is one of the first cytokines produced upon antigen recognition by $CD4^+$ T cells (551). Concomitantly, human neonatal T cells are poised for rapid proliferation when compared to adult counterparts (239,550,552). Cord blood $CD4^+$ T cells express elevated amounts of miR-181, leaving them more sensitive to TCR activation and calcium signalling (543,553). Likewise, neonatal $CD4^+$ T cells from human newborns express complement receptors, CR1 and CR2, whose engagement further accentuate the $CD4^+$ T cell activation initiated by TCR signalling (12). All of these mechanisms suggest that neonatal $CD4^+$ T cells can readily be activated upon antigen/TCR recognition leading to high IL-2 production.

Apart from driving proliferation, IL-2 signalling is important for T_{reg} cell differentiation and maintenance (554). IL-2 secretion by autoreactive T cells in the thymus is important for scaling T_{reg} generation, with a significant proportion of this IL-2 production occurring in the first 10 days of mice life (542,554). This is consistent with findings that human foetal $CD4^+$ T cells have a bias for T_{reg} differentiation at the expense of alternative helper fates (545,555). In early life 10-30% of all $CD4^+$ T cells in human blood, lymphoid tissue and mucosal sites are T_{regs}, whereas in adults this subset represents less than 5% of total $CD4^+$ T cells (263). Concomitant with these observations, the let-7 family of miRNAs is downregulated in human foetal-derived T cells, creating a metabolic profile highly conducive to rapid growth and T_{reg} differentiation (556). IL-2 production from non-T_{reg} cells

is essential for T_{reg} peripheral maintenance (535). T cells are thought to participate in quorum sensing, coordinated by IL-2, to regulate their own proliferation (557). In this scenario IL-2-producing $CD4^+$ T cells are kept in check by both activated T cells and T_{regs} recognising the secreted IL-2 (557,558). Therefore, the increased ability to produce IL-2 and respond to it in early life could be explained by the importance of this cytokine at promoting T cell proliferation at the time when a naïve $CD4^+$ T cell pool needs to be established and when quick effector responses, that require both rapid $T_{effector}$ and T_{reg} proliferation, are needed. This allows the infant's immune system to counteract pathogenic antigens encountered for the first time, when the system cannot rely on memory responses, while simultaneously establishing peripheral tolerance to self-reactive and microbial antigens. IL-2 signalling is however detrimental for T_{FH} differentiation (526), leading to the reduced T cell dependent antibody responses observed in early life.

3.3.4 Early life increased IL-2 signature in the thymus is altered by infection

Thymic output is upregulated in early life, probably explaining the differences observed between neonates and adults. Similar to the responses observed in the SLOs, the percentage of thymocytes able to produce IL-2 after mitogen stimulation is increased in early life when compared to adult counterparts. The increased IL-2 signature is observed at all stages of $CD4^+$ T cell development, both by immature and mature thymocytes. Strikingly, the proportion of IL-2 producing thymocytes is abrogated 3dpi with RSV, to similar levels to those observed in adulthood, but no major difference is observed in the percentage of IL-2 producing cells by peripheral $CD4^+$ T cells after infection. The mechanisms driving this observation remain unclear. Importantly, proportions of both $CD3^{low}$ and $CD3^{high}$ thymic T cell populations remain constant before and after infection in both 1wk and 8wk old mice, as do $CD4^+$ T cells in the SLOs. Thus, an accentuated thymic output after infection, as observed in HIV infected individuals (559), could not explain the differences in the percentage of IL-2 producing thymocytes.

A phenomenon known as infection-associated thymic atrophy has been previously reported in the literature after viral infection in both mice and humans (560). Viruses such as SARS-CoV-2 can directly infect human thymus medullary epithelial cells and alter thymic function in a disease-severity dependent manner (561). To my knowledge a direct RSV infection of thymocytes has not been experimentally demonstrated so far. A significant reduction of T-cell receptor excision circles (TREC) counts, an episomal DNA generated during re-arrangement of thymic T-cell receptors and as such a reliable marker for thymus activity, is however observed in children hospitalized with RSV infection as opposed to healthy individuals (562). The reduction in TREC correlates with disease severity clearly suggesting a direct role for RSV infection on thymus impact (562). Therefore, similar to SARS-CoV-2, RSV infection could alter thymic functionality and IL-2 production by thymocytes.

Contrary to the response in the thymus, no reduction in the percentage of IL-2 producing $CD4^+$ T cells is observed in peripheral organs after RSV infection. One hypothesis could be that by analyzing the percentage of IL-2 producing cells only 3d post RSV infection, the responses observed in the SLOs and the lung are mostly generated by T cells matured in the thymus before infection onset, and therefore before infection-associated thymic atrophy. Further experiments using T cell tracker systems and longer time periods between infection and IL-2 production analysis could be used to investigate this. A study in humans shows a reduced IL-2 production by PBMC-derived $CD4^+$ T cells from RSV infected infants when compared to controls (563), highlighting that the blood compartment and longer infectious periods, such as the ones required to hospitalize young children, could be more reflective of the thymus response. Thus, RSV infection in early life clearly affects IL-2 production by thymocytes through currently unclear mechanisms. The SLOs, where T cells are activated and poised towards distinct $T_{effector}$ fates, seem however unaffected at least during the first stages of infection, when T_{FH} fate is decided (57), indicating that a possible infection-associated thymic atrophy after RSV infection has little repercussion on T_{FH} differentiation.

3.3.5 The increased T_{FR} signature could promote the GC inhibition observed in neonatal mice

As highlighted previously, early life is characterized by an increased T_{reg} signature (545,555). Similar to T_{reg} cells, T_{FR} cells inhibit GC B cell responses (564). Therefore, the decreased GC signature observed in early life could also be the result of enhanced T_{FR} responses. T_{FR} cells share characteristics of both T_{FH} and T_{reg} cells as they reside in the SLOs and express classical T_{FH} markers such as CXCR5, ICOS, PD-1 and even Bcl6, but are typically defined by the co-expression of the transcriptional marker Foxp3 (197). These $CXCR5^+Bcl6^+T_{reg}$ cells are absent in the thymus but can be generated *de novo* from $CXCR5^-Foxp3^+$ natural T_{reg} precursors (198). Here, an increased T_{FR} differentiation and decreased T_{FH}/T_{FR} ratio is observed in neonatal mice when compared with adult counterparts in both LN, spleen and lung. These results are consistent with a previous study showing an increased T_{FR} response in neonatal mice (237). Since T_{FR} cells co-express Bcl6, their dependence on IL-2 is limited when compared to T_{reg} counterparts as observed by the downregulation of CD25 expression in T_{FR} cells from both mice and humans (565). IL-2 production at the peak of infection is shown to limit T_{FR} differentiation in adult mice (566), making the enrichment of the IL-2 microenvironment observed in early life an unlikely promoter of T_{FR} responses. Instead, neonatal T_{FR} upregulation is linked with an increased recognition of IL-6 when compared to both neonatal T_{FH} cells and adult T_{FR} cells (237). These findings point to increased IL-6 activity on neonatal T_{FR} cells as an underlying mechanism of the increased T_{FR}/T_{FH} ratio observed in infected neonatal mice. An increase in T_{FR} proportion when compared to T_{FH} cells in neonates could therefore also explain the low GC response observed after RSV infection and most likely

both mechanisms, increased T_{FR} differentiation and reduced T_{FH} generation, are parallelly taking place in early life.

3.3.6 STAT3 and STAT5 phosphorylation play a crucial role in driving human T_{FH} proliferation and differentiation

As with murine models, the cytokine microenvironment is key in driving T_{FH} differentiation in humans (27). The precise signalling pathways that drive human T_{FH} differentiation after cytokine recognition, particularly in infancy, however remain elusive. Here I showed that human T_{FH} analogues, with the ability to upregulate BCL6, CXCR5 and PD-1 and secrete IL-21 and CXCL13 while downregulating BLIMP-1, can be generated *in vitro.* Conversely, T_{FH} proliferation, IL-21 and CXCL13 cytokine production are hindered in the presence of an α-pSTAT3 chemical inhibitor, indicating a crucial role for STAT3 signalling in promoting T_{FH} survival and function. Interestingly, higher concentrations of the inhibitor caused widespread cell death in the T_{FH} differentiating culture, but not in control T cell conditions. This indicates that sustained STAT3 signalling is a requirement for T_{FH} survival, but less so for other $CD4^+$ T cell subsets. My results are in accordance with a previous mouse study showing that compared with wild-type (WT), Stat3-deficient T_{FH} cells develop at a lower rate in Peyer's patches, spleen and bone marrow (567).

The use of α-pSTAT5 inhibitors on the other hand promotes increased T_{FH} differentiation; as shown by elevated CXCR5 and BCL6. This highlights the pivotal nature of IL-2 mediated antagonism in regulating human T_{FH} differentiation and function as previously described (159). Probably the high-affinity antibodies used here to promote TCR signalling *in vitro*, combined with the homogeneous nature of naïve $CD4^+$ T cell cultures, results in a high proportion of IL-2 producing cells in the absence of any quenching or competition for IL-2 by bystanding immune cells. A previous study in the lab showed that reducing IL-2 signalling in this pro-T_{FH} environment results in increased T_{FH} differentiation with upregulated CXCR5 expression and an increased *BCL6/PRDM1* ratio (516), replicating the observation of using an α-pSTAT5 inhibitor. Thus, similarly to what is observed in mice, IL-2 signalling through STAT5 phosphorylation prevents T_{FH} differentiation in humans. These results suggest that T_{FH} differentiation in humans infants, as observed here in mice, could also be hindered by high IL-2/pSTAT5 signalling.

Caution should be applied when translating the findings of the mice studies presented here into human RSV disease. Mice require a significantly higher dose of RSV to become infected when compared to humans and mice do not develop severe bronchiolitis upon RSV exposure, which contrasts with the response seen in a proportion of children (512,568). Besides having many conserved mechanisms, both the postnatal lung development and the immunological development in mice do not exactly mirror that observed in humans. 1d old mice resemble a premature newborn

human infant while mice at 1wk of age more closely resemble human infants at term. Mice rapidly mature, with weaning taking place at 3-4wks of age, as opposed to approximately 1-2 years in infants, and puberty starting at 6-8wks when compared with 11.5-15.5 years in humans (298,569–571). As observed in mice however, human infants have reduced circulating T_{FH} and plasmablast frequencies compared with older children, rendering them to develop a poorer response to the RTS,S malaria vaccine (13) and in infection (572). Likewise, lower antibody titres have been reported in response to live attenuated RSV vaccines in infants compared with older age groups (12) and RSV-specific antibodies responses from young children are attenuated when compared to adult counterparts (236), indicating that the mechanisms reported here are likely translatable. Due to ethical restrictions only serum samples from adults could be included in this study. The use of this *in vitro* system with human cord blood derived naïve $CD4^+$ T cells could however provide a novel system to help do an in-depth dissection of the role played by cytokine signalling in neonatal human T_{FH} differentiation using a controlled environment.

3.4 Concluding remarks

This chapter sought to investigate the mechanisms driving a reduced T_{FH} differentiation during early life RSV infection. At the time of publication of this work (25), it was reported for the first time that T_{FH} differentiation is hindered in early life due to an elevated IL-2 microenvironment in the SLOs and an increased ability of early life naïve $CD4^+$ T cells to express IL-2 receptors and phosphorylate STAT5. These results have since been confirmed by another group (534). The elevated IL-2 response observed in early life at all stages of T cell development suggests that this is an organism-orchestrated event probably associated with the high proliferation of naïve, $T_{effector}$ and T_{reg} cell generation and maintenance needed to survive the perinatal life. Confirming my hypothesis, the data showed here clearly highlights that early life is dominated by a unique immunological landscape that differs from the one observed in adulthood. This information should be taken into consideration when designing drugs and vaccines tailored to this specific age group. Some of the alterations observed in early life are of cell intrinsic nature. Other factors are however modifiable, such as the microbiome. In the following chapter therefore, the ability to boost GC responses during early life RSV infection after early respiratory tract bacteria exposure will be analysed.

4 Results II: Recurrent exposure to *A.lwoffii* in early life promotes T_{FH}, B cell responses and RSV-specific antibody production in infant mice

4.1 Introduction

4.1.1 Investigating the role of farmyard microbes in promoting early life immune responses

RSV infection, despite possessing multiple PAMPs and DAMPs, can't promote a strong humoral immune response in neonates, even though it does so in adults (chapter 3 and (25)). Defective T_{FH} differentiation after immunization in early life can however be partially overcome by the use of a suitable adjuvant (238,532,573). One of the key drivers of immunological development in early life is thought to be establishment and diversification of the microbiome, with disruption associated with pathology (547). Although the respiratory tract is one of the least colonised mucosal surfaces in the human body (574), sustaining a rich and healthy respiratory microbiota is instrumental for the development of a balanced immune system (575). Microbial and immunological development in human airways go hand in hand, and gestational age is a key determinant of immune maturation; as such the human lower airway microbiome forms within the first 2 postnatal months (576). Chronic lung disorders, such as asthma, are strongly associated with airway dysbiosis (577). Onset of wheezing and progression to asthma in humans is associated with early life respiratory viral infections such as RSV and colonization with particular bacterial species such as Moraxella, Haemophilus, Streptococcus and Staphylococcus (467,578,579).

Respiratory health and the immune system are also highly dependent on distal signals associated with the gastrointestinal microbiome. Research involving germ-free mice, broad-spectrum antibiotics, and dietary modifications clearly indicates that suitable microbiotal colonization, diversification, and metabolite production are vital for the development of antibody-mediated immunity (492,497,502). One study showing that adult mice treated with antibiotics prior to influenza A virus (IAV) infection have a higher viral load in the lungs, reduced $CD4^+$ T cell responses and fewer influenza-specific antibody titres; with administration of commensal bacteria or Toll-like receptor agonists required to clear the infection (492). Further, oral administration of OM-85, a lyophilized extract derived from a mixture of bacterial respiratory pathogens, to adult mice, is sufficient to promote the release of polyclonal antibodies with broad specificity that are capable of neutralizing IAV infection in the respiratory tract (501). Whether the provision of microbiota is effective at enhancing antibody-mediated immunity in children is currently unknown, but murine infant exposure to probiotics can modify T and B cell responses in early life (503–505). Clinical trials testing the impact of OM-85 on human paediatric respiratory tract infections have however yielded mixed results (580–584). The dosing regimen (continuous or intermittent), route of administration (oral, intranasal or sublingual) and preparation method (whole-cell bacteria or mechanically disrupted) did vary between OM-85 studies, and undoubtedly contribute to optimal efficacy, making interpretation more challenging. Prophylactic studies in children are also difficult to carry out due to the high number of participants needed to have statistical power, the need for

long follow-up studies that last years with the associated withdrawal risk and the high amount of confounding factors (584,585). Therefore, the use of animal models, in which group numbers and the environment can be controlled, can be crucial in helping elucidate the mechanisms linking microbiota colonization and protective immune function.

A specific group of bacteria, known as farmyard microbes, has gained interest in the last decade regarding their beneficial role in promoting children's immune system. Farm exposure in early childhood is associated with a reduced risk of developing severe respiratory illnesses, wheezing and asthma in later life, an effect narrowed to bacterial exposure within these environments (506–509). An influential study found reduced asthma prevalence in Amish children, who are frequently directly exposed to livestock, when compared to children from the Hutterite community, with whom they share a common European ancestry but instead have modernised farming practices (586). Living in a farm environment is associated with an increased variety of microorganisms in home dust, with microbial diversity and/or specific composition of bacteria being protective against respiratory disorders (586–589). Importantly, introduction of farm-like indoor micriobiota in non-farm homes protected children from asthma development with an inverse relationship between asthma risk and similarity to farm-home bacteria composition (589).

4.1.2 *Acinetobacter lwoffii F78* – a key promoter of early life immunity?

One of the most abundant bacteria in the cowshed microflora is *Acinetobacter lwoffi F78* (*A.lwoffii*) (510). *A.lwoffii* is a gram-negative aerobic bacillus that is a component of normal flora on the skin, oropharynx and perineum of about 20–25% of healthy individuals and in steady-state conditions is not pathogenic (590). In fact, the skin and nasal microbiota in the Russian Karelian population, which is characterized by living in traditional rural environments and have low prevalence of asthma and allergy, is enriched in *Acinetobacter* species (591). Several studies have highlighted a crucial role for *A.lwoffii* in protecting against asthma and allergies, with murine models linking intranasal administration of *A.lwoffii,* and other microbial strains derived from cowsheds such as *Lactococcus lactis* and *Staphylococcus scurii,* with protection against allergic airway inflammation (510,511). Exposure to *A.lwoffii* has also been associated with protection against airway hyperresponsiveness (AHR) in adult mouse models (586). Exposure to inhaled inactivated *A.lwoffii* reduces airway eosinophilia and mucus hypersecretion in mouse models of ovalbumin (OVA) challenge (510). Many *A.lwoffii* effects have been linked with increased innate immunity, however a study from our group shows that early life *A.lwoffii* exposure can protect infant mice against house dust mite (HDM) allergen-induced AHR by reducing the frequency of IL-13^{+}CD4^{+} T cells in the lungs (503). Some studies have also shown that exposure to inhaled *A.lwoffii* in mouse models of OVA challenge can induce proinflammatory cytokines and chemokines, namely TNFα, IL-6 and IL-12p40, thereby promoting T_{H1} responses (592,593). A recent paper has highlighted the role of live exposure to

A.lwoffii in IL-6 dependent protection against murine OVA allergic airway inflammation (594). The effects of *A.lwoffii* on protection from viral infection and/or production of T-dependent B cell responses have however not been analysed.

4.1.3 Hypothesis and aims

Despite the plethora of studies associating *A.lwoffii* exposure with protection from asthma, wheezing and allergies, little is known about *A.lwoffii*'s role in the protection of viral induced airway disease in early life. Furthermore, while microbial stimuli are important in shaping antibody responses to vaccines and infections in adult mice, the ability of farmyard microbes such as *A.lwoffii* to shape infant antibody responses has not been evaluated.

Therefore, the hypothesis for this chapter is that:

Intranasal exposure to lyophilised, heat-inactivated A.lwoffii in early life boosts the GC response and RSV-specific antibody production in an infant mouse model of RSV infection.

To address this hypothesis, the aims of this chapter are:

1. To investigate the role of recurrent exposure to *A.lwoffii* in promoting a GC-dependent humoral immune response in RSV infected infant mice

2. To evaluate if recurrent exposure to farmyard microbes is needed to promote such an effect or if shorter exposures to the bacteria can have similar prophylactic outputs

3. To evaluate if exposure to *A.lwoffii* could have a therapeutic effect during second re-infection with RSV antigen

4. To investigate if *A.lwoffii* exposure in early life confers life-long protection against RSV infection

4.2 Results

4.2.1 Inhaled recurrent exposure to *A.lwoffii* promotes an increased T_{FH} and CD138$^+$ cell signature in the SLOs of RSV infected infant mice

T_{FH} are crucial to drive protection upon RSV re-infection (25) and microbiota colonization is important for the generation of high-quality antibodies in adult models (501), but whether this is true in infancy is currently unknown. To answer this question, I tested the role of *A.lwoffii* exposure on the generation of GC responses in an early life RSV re-challenge mice model. To this end, a recurrent RSV infection model that produces high viral replication, with the associated lung damage and type 2 biased inflammation in early life, was used (595). In my studies, 3d old Balb/c mice were intranasally (i.n) exposed to heat inactivated lyophilized *A.lwoffii* or PBS three times a week for 3 weeks ("recurrent *A.lwoffii")* and i.n infected with RSV, or given an equal dose of PBS, on day 5 and 15 of life. Mice were culled 5d post RSV re-infection and lung, lung draining lymph nodes (LN), spleen (SP), Peyer's patches (PP), blood and bronchoalveolar lavage (BAL) were collected *(**Fig 4.1a**).* Recurrent *A.lwoffii* exposure in early life decreased the viral load in the lungs, as measured by *RSV L* gene *(**Fig 4.1b**).* Flow cytometry was used to analyse the different B and T cell populations in the LN, spleen and PP *(**Fig 4.1c**).* LN cell numbers were increased in mice receiving either RSV or *A.lwoffii* when compared with PBS, with mice receiving both *A.lwoffii* and RSV being the most significant *(**Fig 4.1d**)*. B cell proportions were increased in RSV alone infected mice when compared with PBS controls and all mice treated with either the farmyard microbe, the virus or both showed increased B cell numbers when compared with PBS control counterparts *(**Fig 4.1e**)*. No difference between RSV and *A.lwoffii* exposed RSV infected mice was observed in the lung draining LN B cell response *(**Fig 4.1e**).*

A.lwoffii exposure alone led to an increase in the proportion of $\gamma\delta$ T cells *(**Fig 4.2a**).* No difference in TCRβ proportion was observed between groups *(**Fig 4.2b**)*, but *A.lwoffii* or RSV exposure alone resulted in an increased CD8$^+$ T cell proportion, accompanied by a reduced CD4$^+$ T cell percentage, but this was not the case for mice exposed to the bacteria in addition to the virus *(**Fig 4.2c-e**).* Total numbers of each T cell population in the LNs were significantly increased in mice infected with RSV alone, *A.lwoffii* alone or in RSV combined with *A.lwoffii* compared to PBS *(**Fig. 4.2a-e**);* Exposure to both however resulted in a more significant increase compared to control mice than when exposed to RSV or *A.lwoffii* alone *(**Fig. 4.2a-e**)*. RSV infection did however result in a significant increase of the activation marker CD69 expression on CD8$^+$ T cells compared to RSV and *A.lwoffii* exposed mice *(**Fig 4.2d**),* but no difference in CD69 expression on CD4$^+$ T cells was observed between groups *(**Fig 4.2f**).*

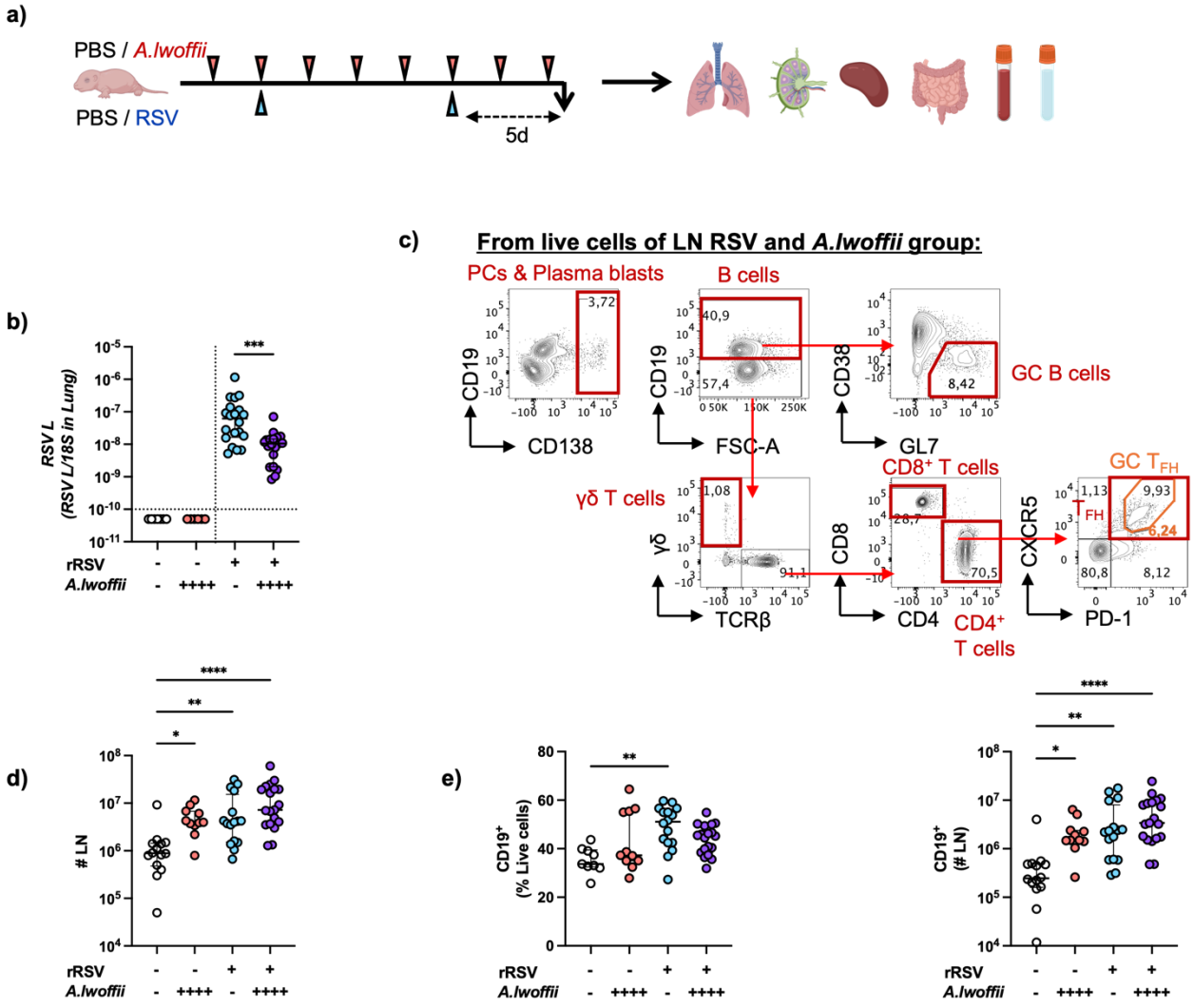


Fig 4.1. Recurrent A.lwoffii exposure reduces RSV viral load in the lung of early life mice

(a) 3d old Balb/c mice were intranasally exposed to *A.lwoffii* or PBS three times a week and infected with RSV or saline on day 5 and 15 of life. Lymph node, spleen, Peyer's patches, blood and BAL were collected 5d post RSV re-infection and 24h after the last *A.lwoffii* dose. **(b)** *RSV L* relative to *18S* in lung tissue measured by RT-qPCR. **(c)** Flow cytometry strategy to gate B and T cell populations. From live cells, Plasma cells and Plasma blasts were gated as $CD19^{all}CD138^{+}$ cells, B cells as $CD19^{+}$ cells and from there germinal centre B cells were gated as $CD38^{low}GL7^{high}$ cells. From $CD19^{-}$ cells T cells were split into γδ T cells and $TCR\beta^{+}$ T cells with the last split into $CD8^{+}$ and $CD4^{+}$ T cells. $CD4^{+}$ T cells were further classified according to their CXCR5 and PD-1 expression into $CXCR5^{+}PD\text{-}1^{+}$ cells as T_{FH} cells or germinal centre T_{FH} cells as $CXCR5^{hi}PD\text{-}1^{hi}$ cells. **(d)** Lymph node (LN) cell count. **(e)** B cells percentage and frequency. Data from three independent experiments with n = 14-19 mice per group. Data shown with median and interquartile range. Each dot represents one mouse. Horizontal doted line indicates limit of detection. Mann-Whitney (b) and Kruskal-Wallis with multiple comparisons test (d,e) was performed in which *, $p < 0.05$; **, $p < 0.01$; and ***, $p < 0.001$.

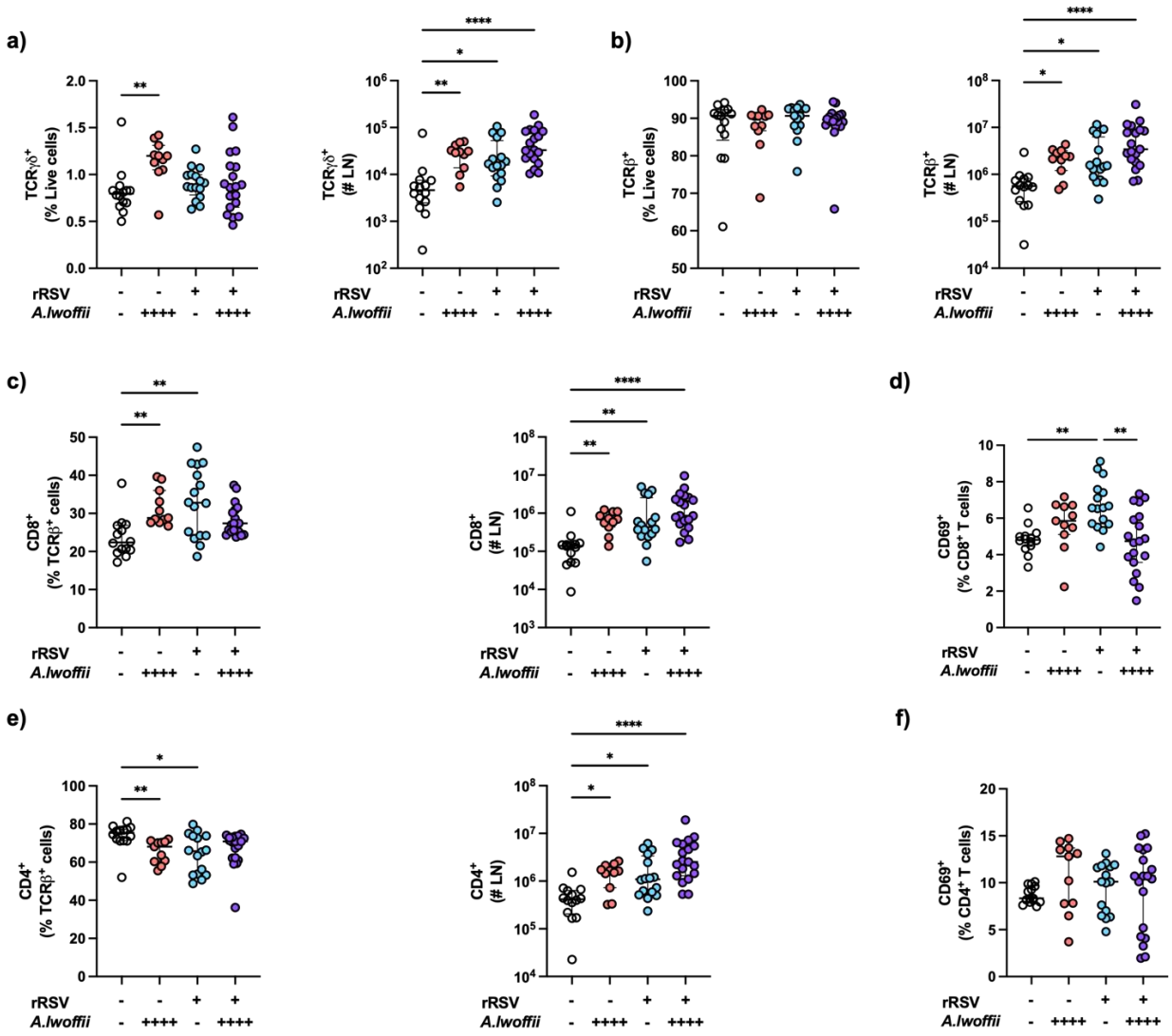


Fig 4.2. Investigation of T cell responses in recurrent A.lwoffii exposed RSV infected infant mice

3d old mice were intranasally exposed to *A.lwoffii* or PBS three times a week and infected with RSV or saline on day 5 and 15 of life. **(a)** Proportion and quantification of TCRγδ and **(b)** TCRβ T cells, **(c)** $CD8^+$ T cells and **(d)** their expression of CD69 as well as **(e)** $CD4^+$ T cells and their **(f)** CD69 expression. Data from three independent experiments with n = 14-19 mice per group. Data shown with median and interquartile range. Each dot represents one mouse. Kruskal-Wallis with multiple comparisons test was performed in which *, $p < 0.05$; **, $p < 0.01$; and ***, $p < 0.001$.

Next the effect of *A.lwoffii* in GC responses was assessed by analysing the proportion and frequency of T_{FH} ($CXCR5^+PD\text{-}1^+CD4^+$ T cells), GC T_{FH} ($CXCR5^{hi}PD\text{-}1^{hi}$ $CD4^+$ T cells), GC B cells ($CD38^-GL7^+$ B cells) and $CD138^+$ antibody-secreting cells (containing both plasma cells (PCs) and plasmablasts (PBs)) *(**Fig 4.3a**)*. Early life recurrent *A.lwoffii* exposure significantly increased the proportion of T_{FH} cells in the LNs compared to RSV infected mice (***Fig 4.3b***). *A.lwoffii* exposure also promoted a higher increase in GC T_{FH} proportion when compared with PBS mice than RSV alone treated animals and the same trend was observed in GC T_{FH} frequency for *A.lwoffii*+RSV treated mice *(**Fig 4.3c**)*. Both *A.lwoffii* and RSV promoted the formation of GC B cells, the proportion did not differ in those mice that received both, although the highest increase in GC B cell numbers was seen in mice receiving the microbe and virus (***Fig 4.3d***). Mice who received both RSV and *A.lwoffii*

also had a statistical significant increase in the proportion of antibody secreting cells in their LNs compared to any other group, with the frequency of CD138^{+} cells being statistically more increased in these mice when compared with PBS mice *(Fig 4.3e)*.

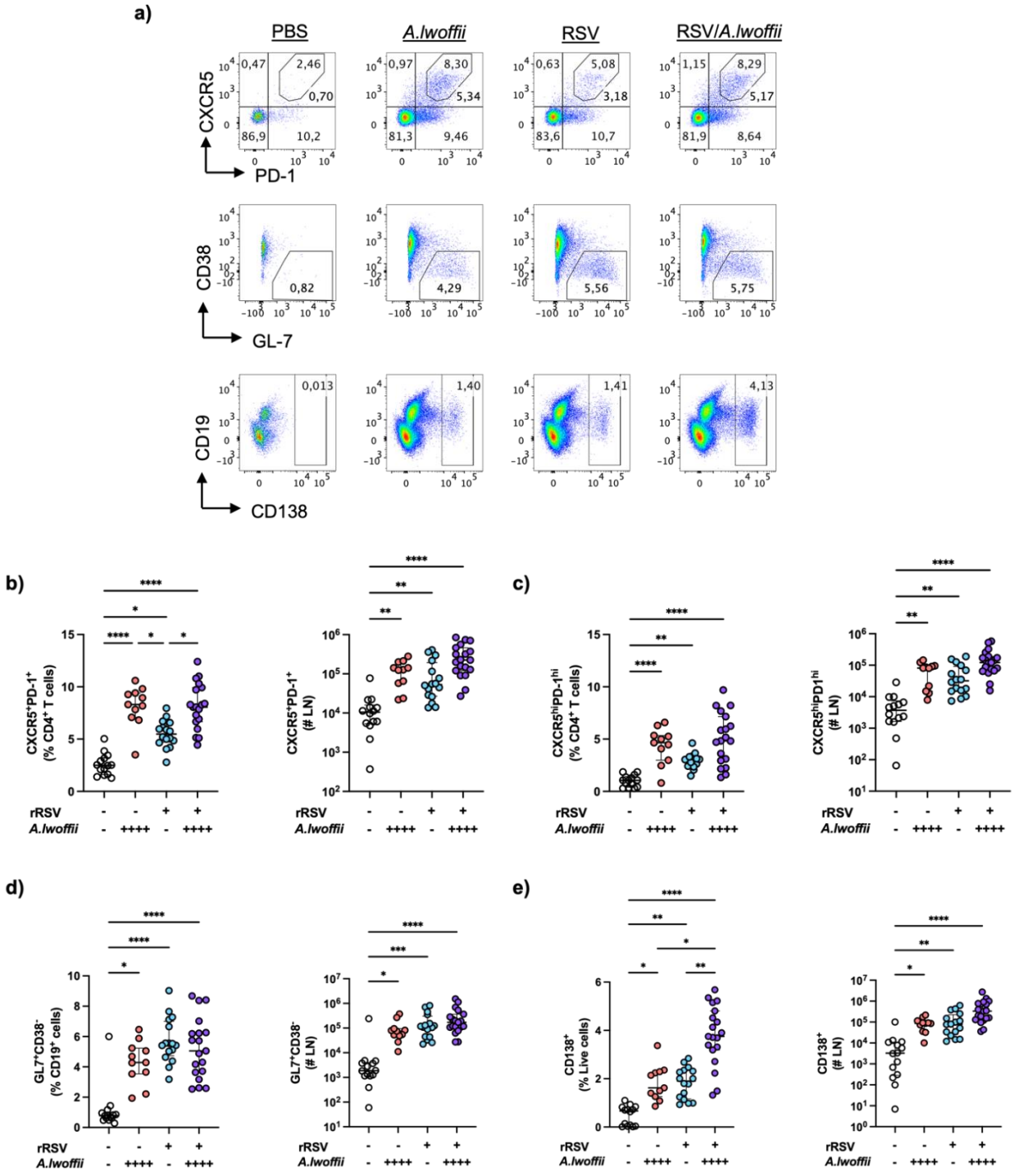


Fig 4.3. Early life recurrent A.lwoffii exposure enhances T_{FH} and CD138^{+} cell proportions in the lymph nodes of RSV infected mice

3d old mice were intranasally exposed to *A.lwoffii* or PBS three times a week and infected with RSV or saline on day 5 and 15 of life. **(a)** Representative flow plots for cell populations involved in the GC reaction. **(b)** Lymph node proportion and quantification of T_{FH} cells (CXCR5^{+}PD-1^{+}), **(c)** GC T_{FH} cells (CXCR5^{hi}PD-1^{hi}), **(d)** GC B cells (GL7^{+}CD38^{-}) and **(e)** Plasma cells & Plasma blasts (CD138^{+}). Data from three independent experiments with n = 14-19 mice per group. Data shown with median and interquartile range. Each dot represents one mouse. Kruskal-Wallis with multiple comparisons test was performed in which *, $p < 0.05$; **, $p < 0.01$; and ***, $p < 0.001$.

Unlike in the lung draining LNs, in the spleen there were no substantial differences in the total numbers or proportions of T or B cell populations when comparing RSV alone and *A.lwoffii* exposed RSV infected 3wk old mice *(**Fig 4.4a-h**)*.

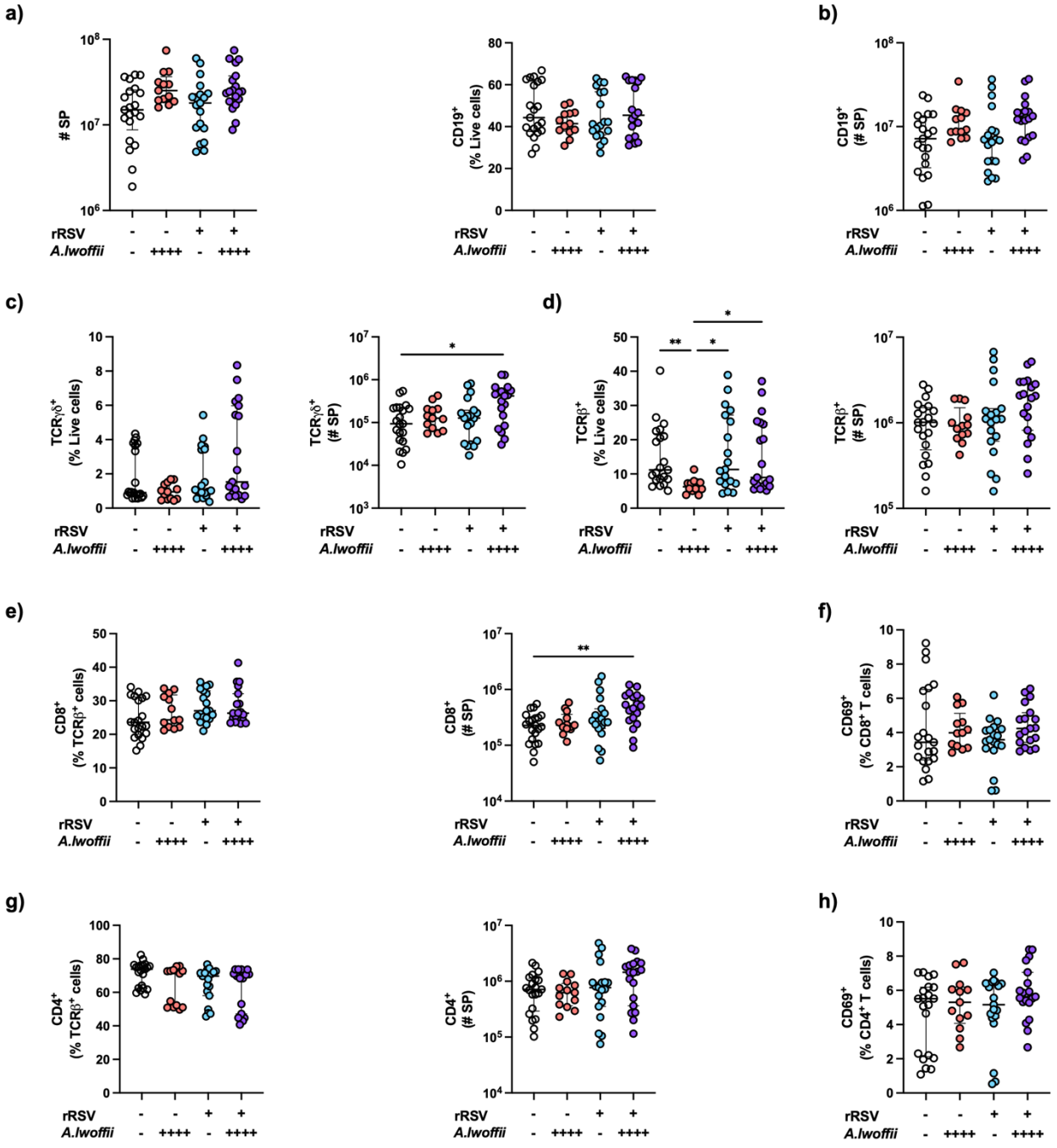


Fig 4.4. Similar B and T cell responses in the spleen of recurrent A.lwoffii exposed and unexposed mice

3d old mice were intranasally exposed to *A.lwoffii* or PBS three times a week and infected with RSV or saline on day 5 and 15 of life. **(a)** Spleen (SP) cell numbers. **(b)** Spleen proportion and quantification of B cells, **(c)** TCRγδ, **(d)** TCRβ T cells, **(e)** $CD8^+$ T cells and **(f)** percentage of $CD8^+CD69^+$ cells as well as **(g)** $CD4^+$ T cells and their **(h)** CD69 expression. Data from three independent experiments with n = 14-19 mice per group. Data shown with median and interquartile range. Each dot represents one mouse. Kruskal-Wallis with multiple comparisons test was performed in which *, $p < 0.05$; **, $p < 0.01$; and ***, $p < 0.001$.

A significant increase in γδ T cell numbers was however observed in the RSV+*A.lwoffii* group when compared with the control group *(Fig 4.4c)*. A decreased proportion in TCRβ$^+$ T cells was observed in the *A.lwoffii* alone exposed group when compared with all other groups, but no difference was seen in cell number *(Fig 4.4d)*. A significant increase in CD8$^+$ T cell number was seen in mice that were exposed to both RSV and *A.lwoffii* when compared to PBS exposed mice *(Fig 4.4e)*.

There was also no significant increase in splenic T_{FH}, GC B cells or antibody secreting cells in mice infected with RSV alone compared to control mice *(Fig 4.5a-e)*. The addition of *A.lwoffii* however did significantly increase both the proportion and number of T_{FH} and GC T_{FH} both when compared with the PBS animals and mice treated with RSV alone *(Fig 4.5a-c)*. The proportion of GC B cells was not increased in these animals, although both *A.lwoffii* and *A.lwoffii*+RSV treated mice had significant increases in the total number of GC B cells when compared with PBS control mice *(Fig 4.5d)*. The proportion of CD138$^+$ cells in the spleen was similarly unaffected by any treatment group, however *A.lwoffi*+RSV had a significant increase in the total numbers of these cells compared to RSV infected or control mice *(Fig 4.5e)*. Taken together the data from the LNs and spleen indicates that *A.lwoffii* can enhance T_{FH} and antibody secreting cell frequencies after RSV infection, although the effect is more pronounced in the LNs, likely due to their proximity to the site of infection.

As introduced in this chapter, previous studies have shown the capacity of gastrointestinal (GI) microbial exposure to alter antibody-mediated immunity. While *A.lwoffii* was delivered i.n., it is known that a certain proportion of the inoculum is swallowed, especially in infancy. Therefore, PP were also analysed to look for any GI-associated effects. As with the other SLOs, limited variations were seen in the B cell or T cell response in PP in any treatment group *(Fig 4.6a-h)*, except for an increase in CD69 expression by CD8$^+$ T cells in mice exposed to *A.lwoffii* alone when compared with control mice *(Fig 4.6f)*. In adult specific-pathogen free mice PP are rich in GC-associated immune cells due to the presence of dietary and microbiotal antigens (596). Interestingly however, PBS-treated mice at day 20 of life had very few T_{FH} or GC B cells in their PP *(Fig 4.7a)*. No difference in T_{FH} cell proportion or number was observed between groups *(Fig 4.7b)*. Although there was a modest, but significant, increase in the proportion of GC T_{FH} for *A.lwoffii* exposed groups when compared to PBS controls, this did not affect the total number of these cells *(Fig 4.7c)*, nor were there any other observable changes in the proportion or number of PP GC-associated immune cells after either RSV or *A.lwoffii* exposure *(Fig 4.7a-e)*. Overall, this observations suggest that 20 day old mice have not yet developed the PP associated GCs seen in adulthood. This is likely linked to the absence of a substantial microbiome and limited intake of solid food. It also shows that *A.lwoffii* treatment has limited impact on this, while altering lung-draining responses.

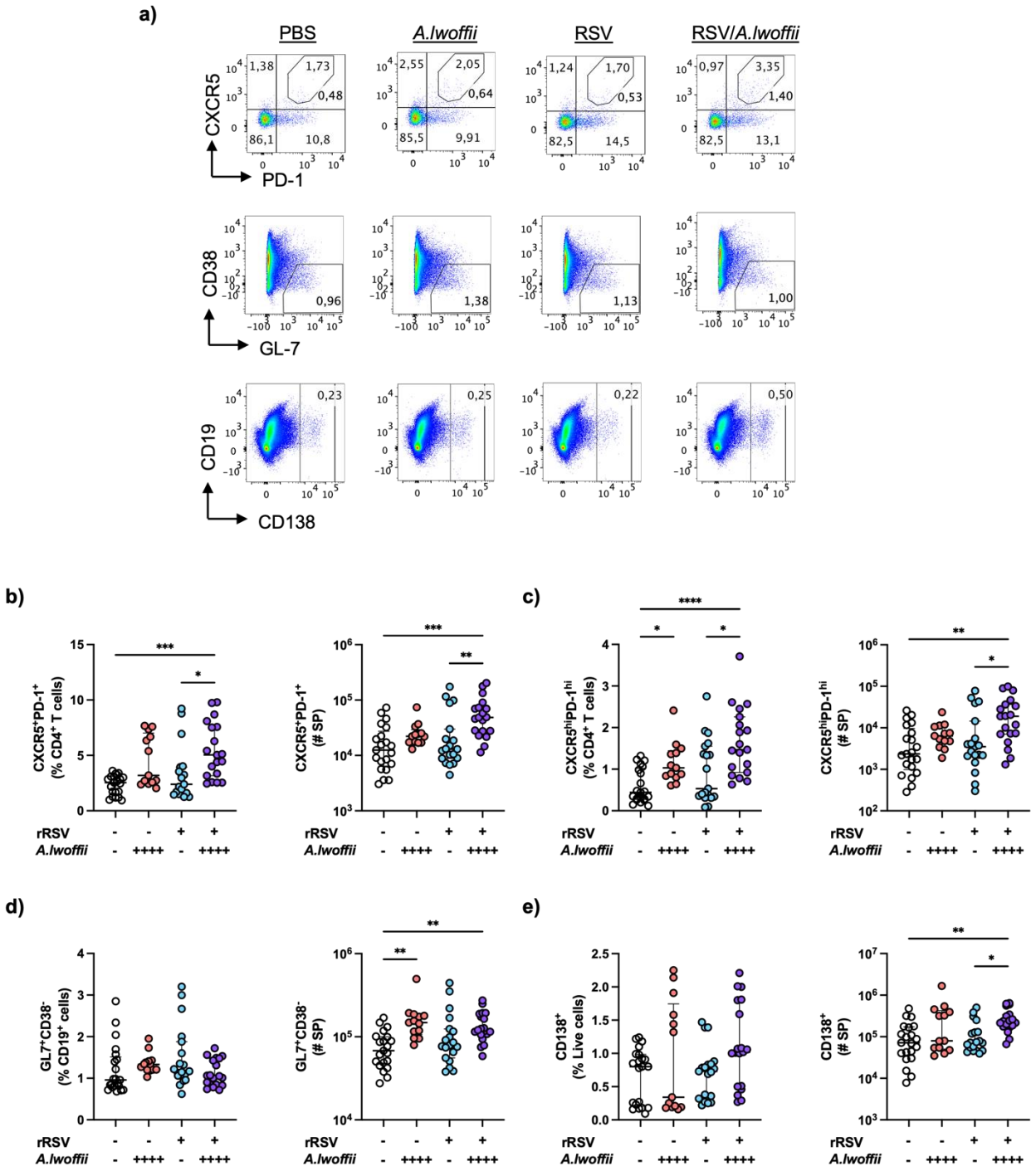


Fig 4.5. Recurrent A.lwoffii exposure promotes T_{FH}, GC-T_{FH} and CD138⁺ cell frequency in the spleen of RSV infected 20d old mice

3d old mice were intranasally exposed to *A.lwoffii* or PBS three times a week and infected with RSV or saline on day 5 and 15 of life. **(a)** Representative flow plots for cell populations involved in the GC reaction. **(b)** Spleen proportion and quantification of T_{FH} cells, **(c)** GC T_{FH} cells, **(d)** GC B cells and **(e)** Plasma cells & Plasma blasts. Data from three independent experiments with n = 14-19 mice per group. Data shown with median and interquartile range. Each dot represents one mouse. Kruskal-Wallis with multiple comparisons test was performed in which *, $p < 0.05$; **, $p < 0.01$; and ***, $p < 0.001$.

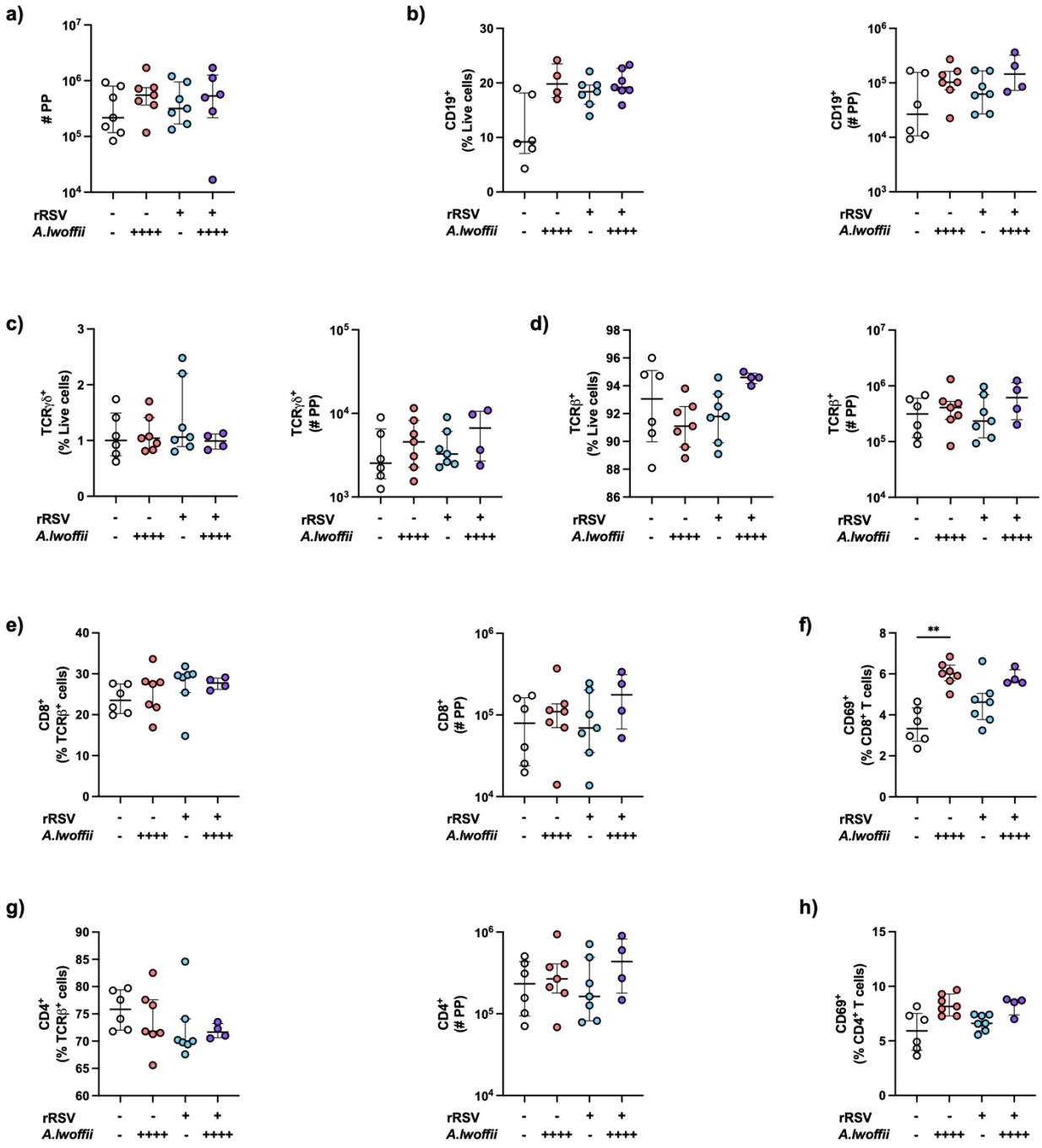


Fig 4.6. Similar B and T cell responses in the Peyer's Patches of A.lwoffii exposed and unexposed RSV infected mice

3d old mice were intranasally exposed to *A.lwoffii* or PBS three times a week and infected with RSV or saline on day 5 and 15 of life. **(a)** Payer's Patches (PP) cell numbers. **(b)** Payer's Patches proportion and quantification of B cells, **(c)** TCRγδ, **(d)** TCRβ T cells, **(e)** $CD8^+$ T cells and **(f)** percentage of $CD8^+CD69^+$ cells as well as **(g)** $CD4^+$ T cells and their **(h)** CD69 expression. Data from one independent experiments with n = 4-7 mice per group. Data shown with median and interquartile range. Each dot represents one mouse. Kruskal-Wallis with multiple comparisons test was performed in which *, $p < 0.05$; **, $p < 0.01$; and ***, $p < 0.001$.

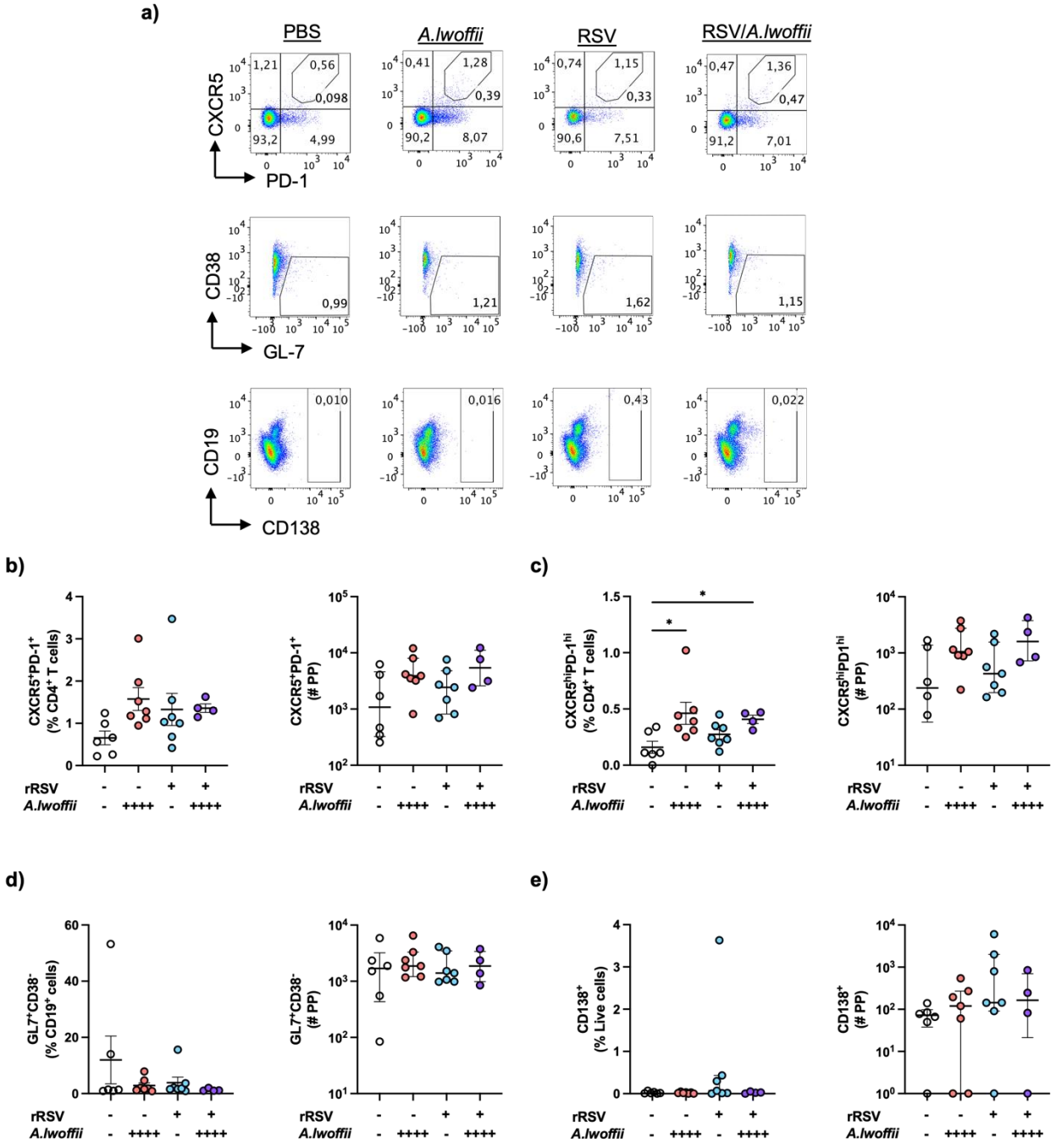


Fig 4.7. Lack of T_{FH} and antibody secreting cells in the Peyer's Patches of A.lwoffii exposed RSV infected infant mice

3d old mice were intranasally exposed to *A.lwoffii* or PBS three times a week and infected with RSV or saline on day 5 and 15 of life. **(a)** Representative flow plots for cell populations involved in the GC reaction. **(b)** Payer's Patches proportion and quantification of T_{FH} cells, **(c)** GC T_{FH} cells, **(d)** GC B cells and **(e)** Plasma cells & Plasma blasts. Data from three independent experiments with n = 4-7 mice per group. Data shown with median and interquartile range. Each dot represents one mouse. Kruskal-Wallis with multiple comparisons test was performed in which *, $p < 0.05$; **, $p < 0.01$; and ***, $p < 0.001$.

4.2.2 Early life *A.lwoffii* exposure enhances local and systemic RSV-specific antibody responses

Recurrent *A.lwoffii* exposure promotes the production of T_{FH} and antibody secreting cells in the SLOs of RSV infected 20 day old mice. To identify if this correlates with an increase in *A.lwoffii*- and RSV-specific antibody responses, *A.lwoffii* and RSV-specific in house ELISAs were developed based on previous protocols used in the lab (25). To detect *A.lwoffii*-specific antibodies a range of concentrations of *A.lwoffii* were coated onto ELISA plates as an antigen. Then, a serial dilution of serum from *A.lwoffii* exposed RSV infected or naïve infant mice were used to identify the optimal antigen concentration for the assay. 100ug/mL of *A.lwoffii* antigen was found to give the highest resolution between *A.lwoffii* exposed and naïve serum and therefore it was used for subsequent studies *(**Fig 4.8a**)*. Similarly, a range of concentrations of RSV antigen were tested to determine the optimal concentration required to identify poly-Igs found in serum of RSV-infected adult Balb/c mice. The highest resolution, between RSV antigen and HEp2 control antigen, being seen at a 1:100 dilution of both *(**Fig 4.8b**)*.

To determine *A.lwoffii* and RSV-specific antibody concentrations, serum and BAL from *A.lwoffii* exposed or unexposed mice were collected 5d post-secondary infection with RSV/PBS *(**Fig 4.9a**)*. As would be predicted, only mice exposed to *A.lwoffii* showed increased serum levels of *A.lwoffii*-specific antibodies, with total, IgG1 and IgG2a antibodies all being identified *(**Fig 4.9b-d**)*. While *A.lwoffii*-specific total and IgG2a were similar in the presence or absence of RSV infection, *A.lwoffii*-IgG1 was significantly reduced in RSV infected mice when compared with uninfected mice *(**Fig 4.9c**)*.

Analogous to *A.lwoffii*-specific antibody responses, RSV-specific antibody titres were observed only in mice that were infected with RSV (**Fig 4.10a-d**). Total RSV-specific Igs were not affected by *A.lwoffii* exposure *(**Fig 4.10a**)*. Total RSV-specific IgG was however increased in mice receiving recurrent early life *A.lwoffii* exposure compared to RSV alone *(**Fig 4.10b**)*. This was associated with a significant increase in RSV-specific IgG2a, but not IgG1 *(**Fig 4.10c,d**)*. Environments enriched for IFN-γ promote an antibody switch towards IgG2a in B cells (597,598), while an IL-4 enriched environment instead promotes IgG1 secretion (47,599). Therefore, both *Ifnγ* and *Il4* transcripts in mediastinal LN were measured. No significant difference in either of the transcripts was observed between groups, but mice exposed to *A.lwoffii* showed a trend to an increase *Ifnγ/Il4* ratio when compared with RSV infected mice alone *(**Fig 4.10e,f**)*.

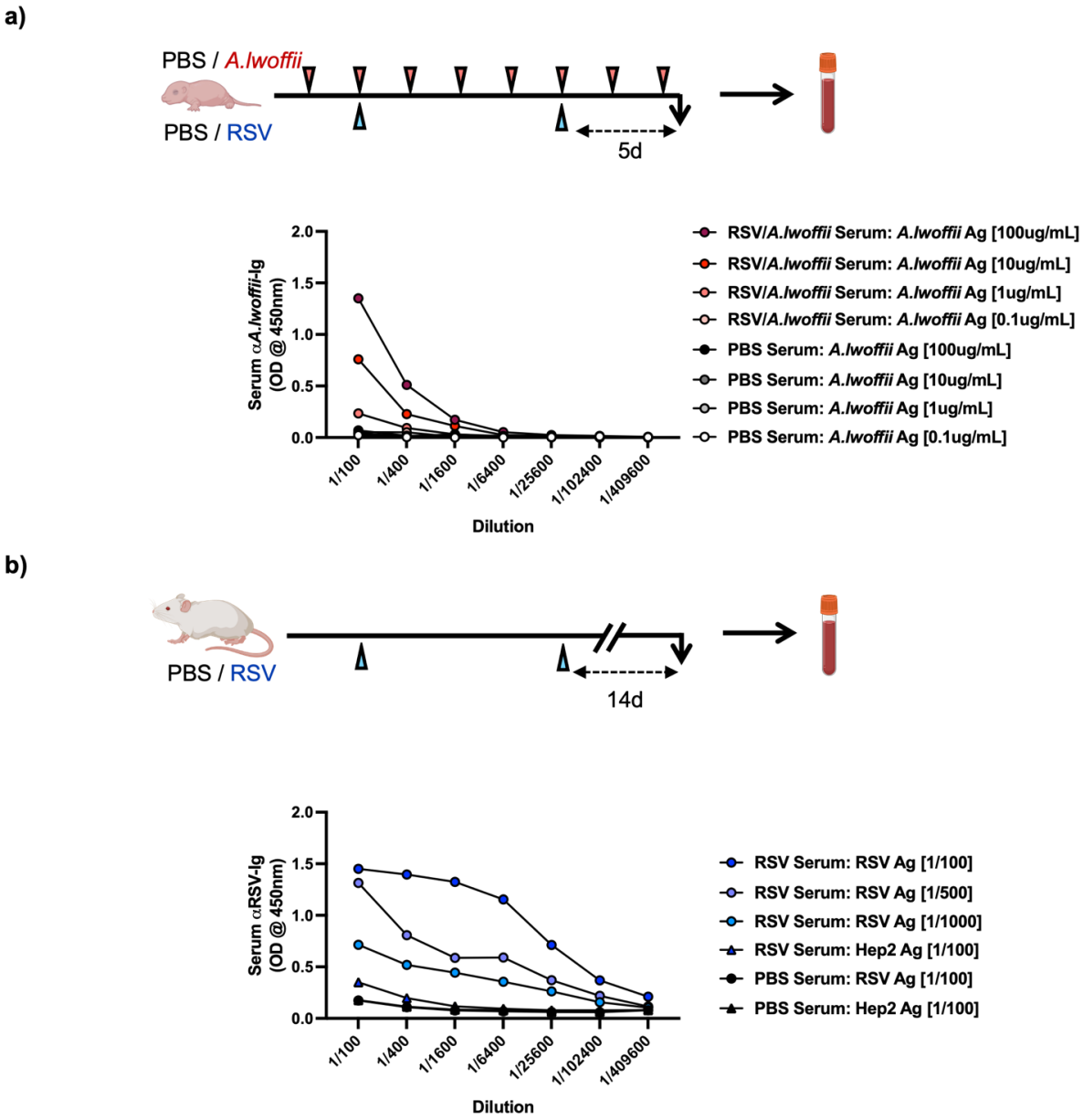


Fig 4.8. Determination of antigen concentrations used for in-house developed ELISAs against A.lwoffii and RSV

(a) 3d old Balb/c mice were intranasally exposed to *A.lwoffii* or PBS three times a week and infected with RSV or saline on day 5 and 15 of life. Serum from *A.lwoffii* exposed RSV infected or control infant mice were used to test different antigen concentrations (100, 10, 1 and 0.1ug/mL) for binding to titrations of poly-Igs. **(b)** ELISA validation assay testing dilutions (1:100, 1:500, 1:1000) of RSV antigen for binding to titrations of poly-Igs from serum of adult Balb/c mice infected twice with RSV separated by 10 days and serum collected 14d post infection. Serum from PBS exposed mice and Hep2 antigen were used as controls. Optical density (OD) was measured at 450nm in both ELISA protocols. Data from one experiment with n = 1 mice per group. Each dot represents one serum titration.

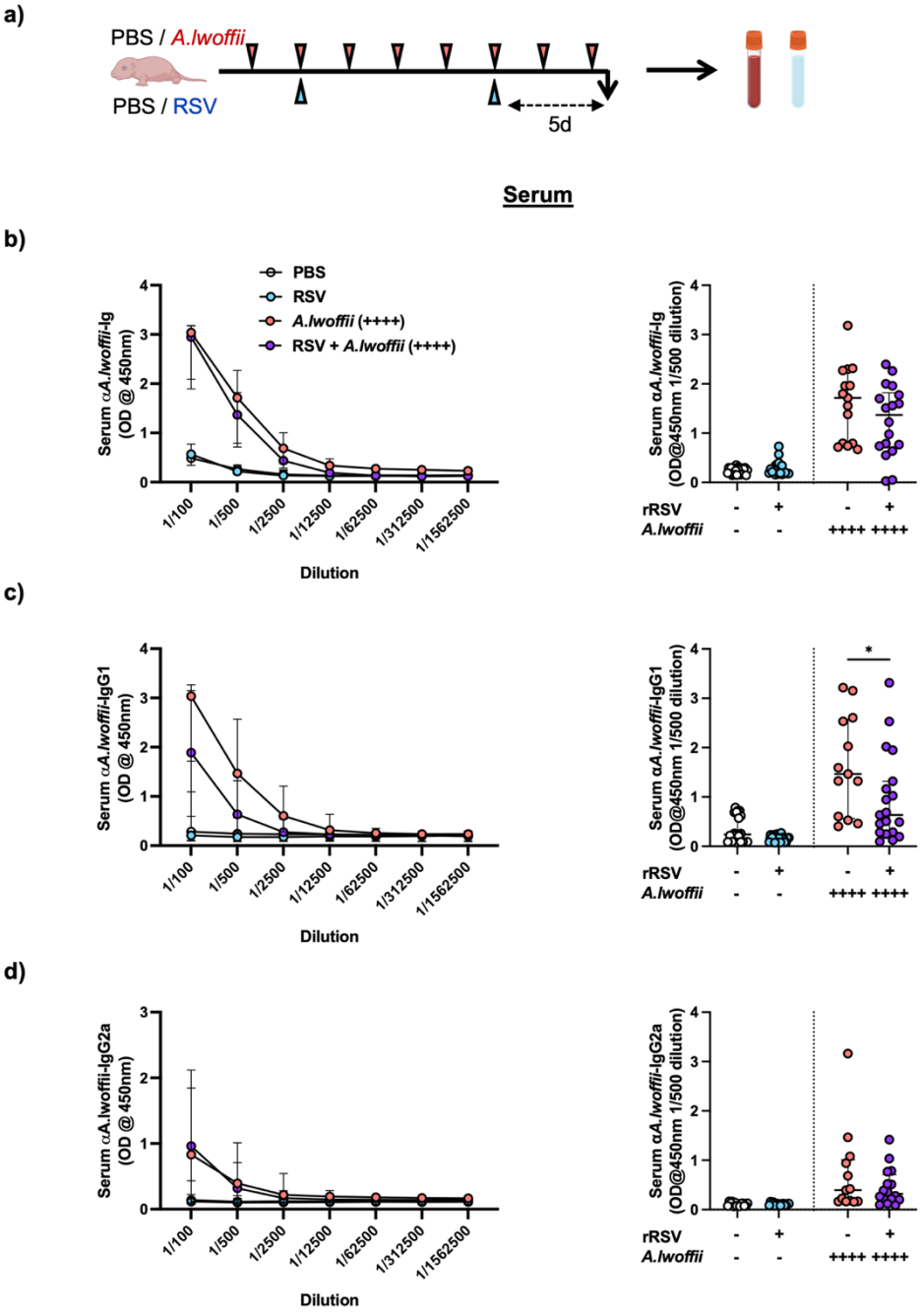


Fig 4.9. RSV infection decreases A.lwoffii-specific serum IgG1 antibody titre

(a) 3d old Balb/c mice were intranasally exposed to *A.lwoffii* or PBS three times a week and infected with RSV or saline on day 5 and 15 of life. Serum and BAL were extracted on 5d post re-infection. **(b)** Titration of serum *A.lwoffii*-specific poly-Igs, **(c)** IgG1 and **(d)** IgG2a. Data from three independent experiments with n = 14-19 mice per group. Data shown with median and interquartile range. In titration experiments each dot represents the mean of the group. For antibody quantification each dot represents one mouse. Mann-Whitney test between *A.lwoffii* and RSV + *A.lwoffii* groups was performed in which *, $p < 0.05$; **, $p < 0.01$; and ***, $p < 0.001$.

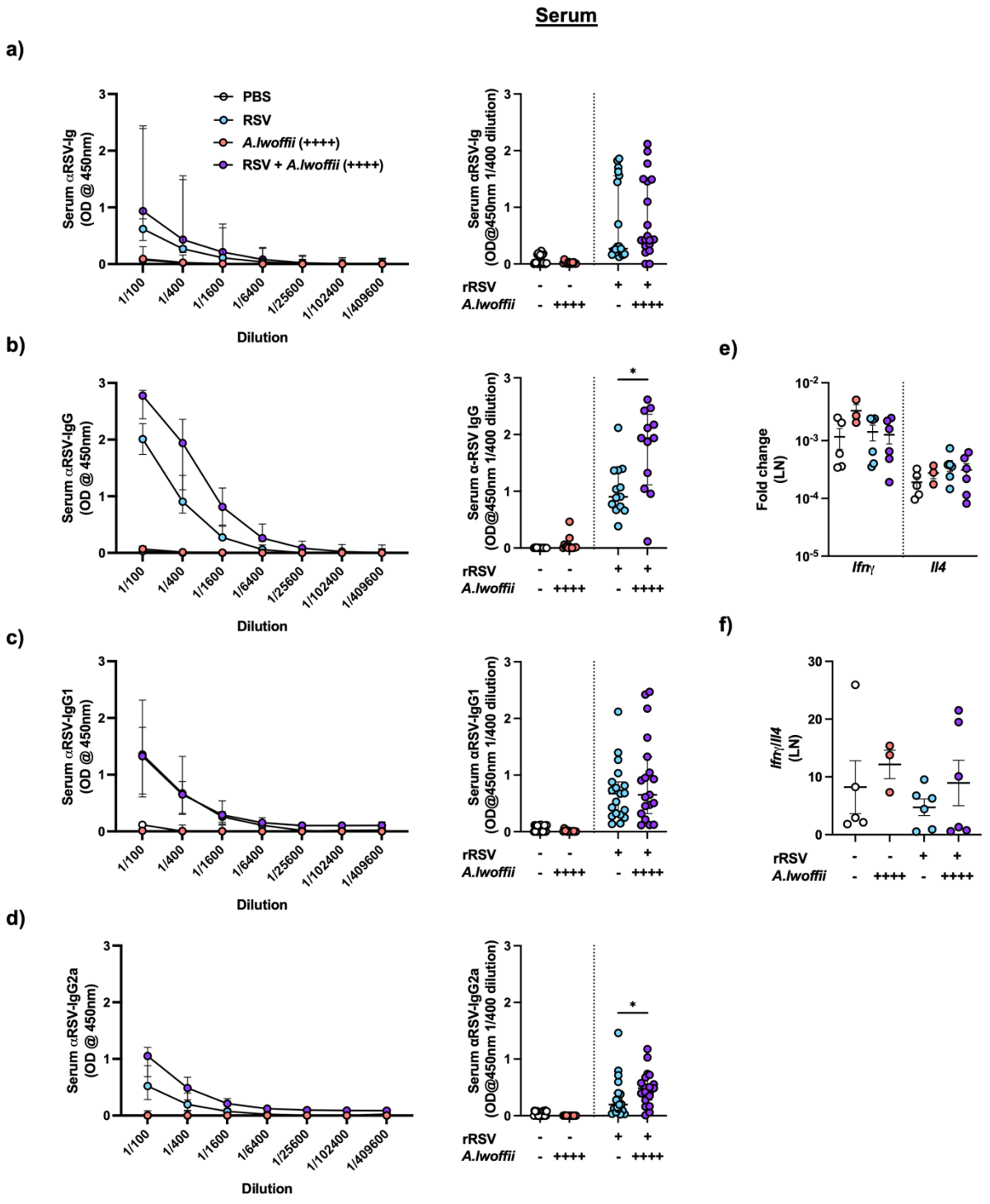


Fig 4.10. Early life recurrent A.lwoffii exposure boosts the production of IgG2a antibodies in the serum of RSV-infected mice

3d old Balb/c mice were intranasally exposed to *A.lwoffii* or PBS three times a week and infected with RSV or saline on day 5 and 15 of life. Serum and BAL were extracted 5d post re-infection. **(a)** Titration of serum RSV-specific poly-Igs, **(b)** total IgG, **(c)** IgG1 and **(d)** IgG2a. **(e)** Transcript quantification of *Infg* and *Il4* in LN of experimental mice as well as **(f)** *Infg/Il4* ratio measured by RT-qPCR. Data from three independent experiments with n = 14-19 mice per group (a-d) or two independent experiments with n= 3-6 mice per group (e,f). Data shown with median and interquartile range. In titration experiments each dot represents the mean of the group. For antibody quantification and transcript titres each dot represents one mouse. Mann-Whitney test between RSV and RSV + *A.lwoffii* groups was performed in which *, $p < 0.05$; **, $p < 0.01$; and ***, $p < 0.001$.

Alongside the concentration and class of antibody produced, its ability to bind and neutralize a target function, and the affinity of these interactions, are important aspects of antibody function that can be enhanced through affinity maturation within the GC. While affinity is challenging to measure in polyclonal sera against multiple pathogens with a large number of potential epitopes, avidity can be measured as a surrogate. This is often done by looking at binding before and after treatment with a denaturing agent such as urea, which can disrupt antibody-antigen complexes (600). Therefore, to determine antibody avidity, the in-house ELISA technique was used but antibody-antigen complexes were washed with either PBS or urea after sample addition and incubation. First, the published concentration of 8M urea was used for the assay (127,128), however no avidity index could be calculated for antibodies generated in early life; as 8M urea was sufficient to remove all detectable antibody binding at all serum dilutions analysed *(data not shown).* Therefore, different concentrations of urea (10mM to 8M) were tested in the early life context, compared to mice infected as adults, to determine suitable concentration for use in infant serum *(Fig 4.11a,b).*

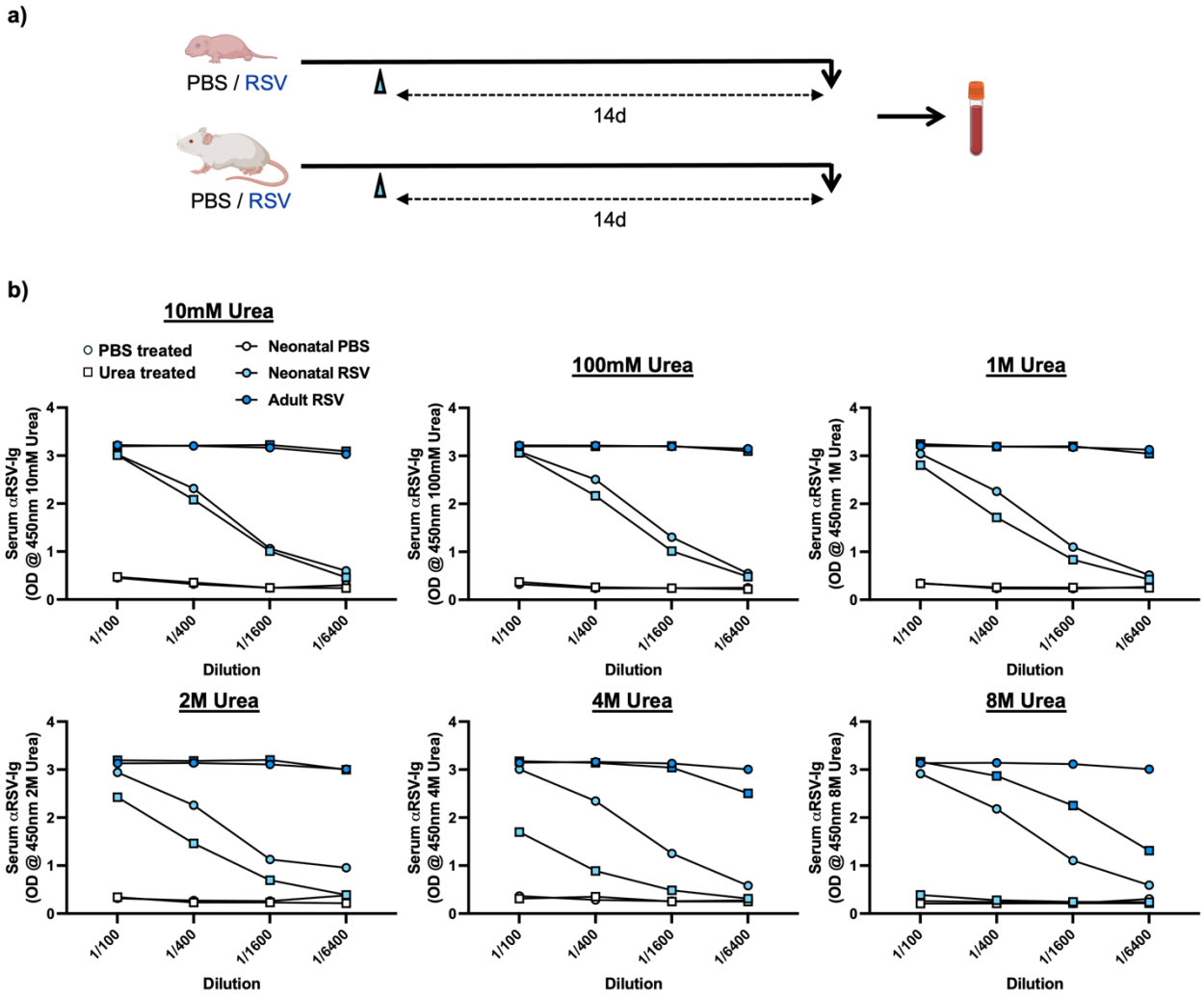


Fig 4.11. Determination of urea concentration used for early life avidity assays

(a,b) 1 and 8wk old mice were infected with the same dose of RSV or left uninfected. Different concentrations of urea (10mM, 100mM, 1M, 2M, 4M and 8M) were used in an avidity assay against RSV-specific poly-Igs found in the serum of 1wk and 8wk Balb/c mice 14dpi. Data from one experiment with n = 1 mice per group. Each dot represents one serum titration.

4M urea was selected, as in both adult and early life sera it was sufficient to denature some, but not all, antibody-antigen interactions at at least one dilution of serum *(**Fig 4.11b**)*. A viral neutralization assay was also established, in which serum and live RSV were pre-mixed, to allow for antigen-antibody binding, prior to infection of HEp2 cells and enumeration of infectious particles by plaque assay. As a preliminary confirmation, serum and BAL from adult RSV infected mice were used for this assay *(**Fig 4.12a**)*. Serum from RSV infected adult mice resulted in a reduced plaque count compared to serum from an uninfected mouse or no serum controls *(**Fig 4.12b**)*. When BAL from T_{FH}-sufficient and deficient animals was tested, reduced plaque counts were only observed in a mouse with T_{FH} *(**Fig 4.12c**)*.

When avidity in experimental samples was assessed, 4M urea was still sufficient to remove all detectable Ig, IgG1 or IgG2a binding, in both RSV and *A.lwoffii*+RSV groups, even at the highest concentration of serum analyzed *(**Fig 4.13a-c**)*. While this made avidity impossible to calculate, it indicated that any change in avidity was likely modest *(**Fig 4.13a-c**)*. As before, a decrease in plaque count was seen between the no serum control and serum from adult RSV infected animals. There was however no reduction in plaque count, compared to serum from uninfected mice, in either RSV or RSV+*A.lwoffii* treated infant mice suggesting not detectable neutralizing antibodies were present at the serum concentration used *(**Fig 4.13d**)*.

Given the importance of local mucosal antibodies in preventing respiratory infections, BAL antibody titers were also measured. *A.lwoffii*-specific IgA was detected in both *A.lwoffii* treated groups, and unaffected by RSV infection *(**Fig 4.14a**)*. There was meanwhile a trend to an increase RSV-IgA in the BAL of *A.lwoffii* exposed RSV infected mice when compared with the RSV alone group *(**Fig 4.14b**)*. There was however no difference in RSV-IgA antibody avidity *(**Fig 4.14c**)*, nor was there any evidence of neutralizing antibodies in the BAL sufficient to prevent viral infection *(**Fig 4.14d**)*.

These results indicate that alongside promoting T_{FH} and B cell responses in SLOs, recurrent intranasal exposure to *A.lwoffii* also enhances serum RSV-specific IgG, IgG2a and potentially mucosal IgA antibody concentrations in early life.

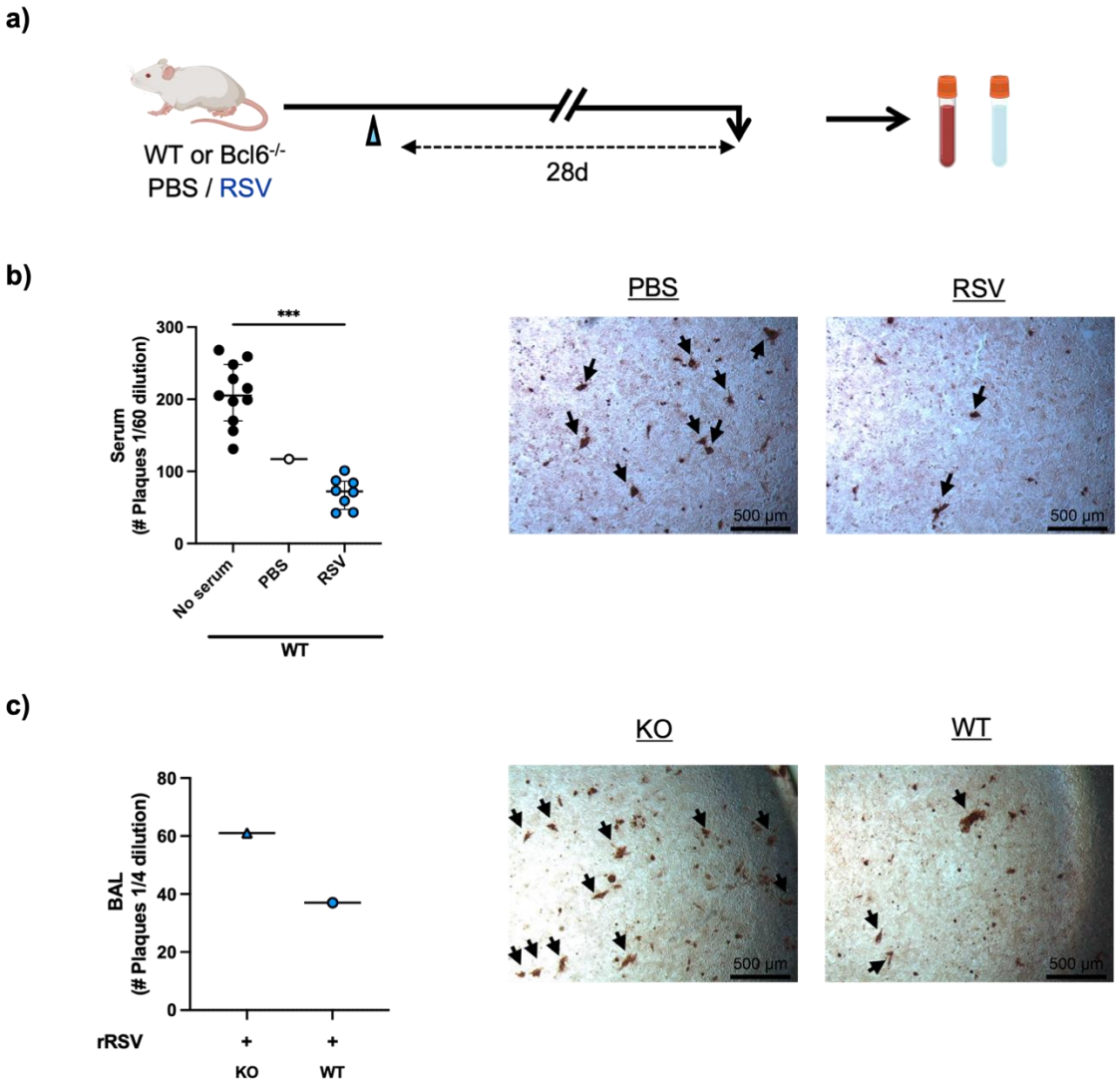


Fig 4.12. Establishment of RSV neutralization assays

(a) 8wk old WT or Bcl6$^{-/-}$ mice were infected with RSV, serum and BAL were collected 28d post-infection. **(b)** Neutralization assay performed with serum or **(c)** BAL of WT RSV infected or control mice. Data shown with median and interquartile range. Arrows indicate position of RSV plaques. Each symbol represents one mouse, but for the no-serum control where each symbol is one well. Data from one independent experiment with n= 1-8. Kruskal-Wallis with multiple comparisons test was performed in which *, $p < 0.05$; **, $p < 0.01$; and ***, $p < 0.001$.

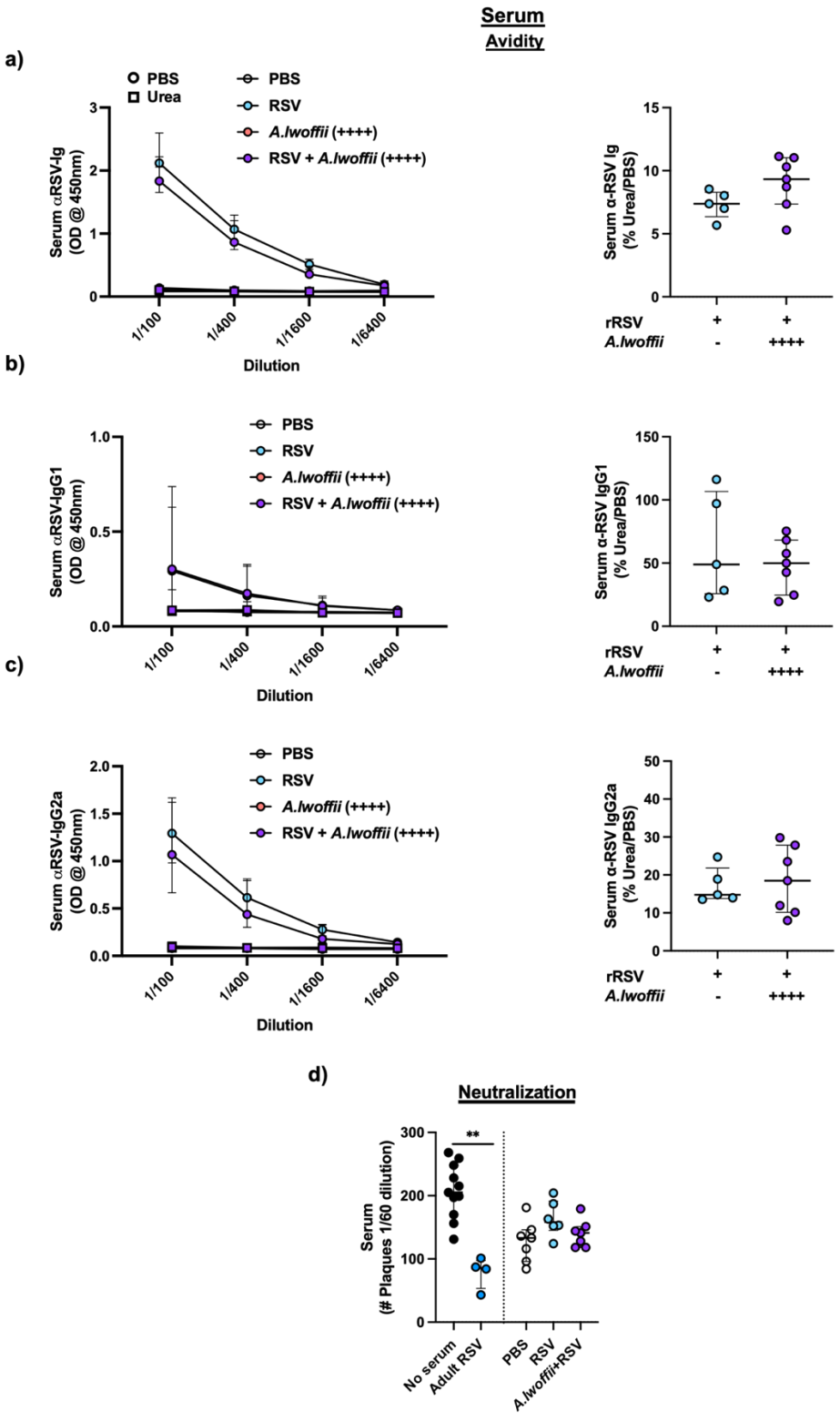


Fig 4.13. Early life recurrent A.lwoffii exposure does not affect serum RSV-specific antibody avidity or neutralization

3d old Balb/c mice were intranasally exposed to *A.lwoffii* or PBS three times a week and infected with RSV or saline on day 5 and 15 of life. Serum and BAL were extracted on 5d post re-infection. **(a)** Avidity quantification of serum RSV-specific poly-Igs, **(b)** IgG1 and **(c)** IgG2a. **(d)** Neutralization assay on serum of experimental mice. Data from one independent experiment with n = 4-7 mice per group. Data shown with median and interquartile range. In titration experiments each dot represents the mean of the group. For antibody quantification and neutralization each dot represents one mouse. Mann-Whitney test (a-c) or Kruskal-Wallis with multiple comparisons test (d) were performed in which *, $p < 0.05$; **, $p < 0.01$; and ***, $p < 0.001$.

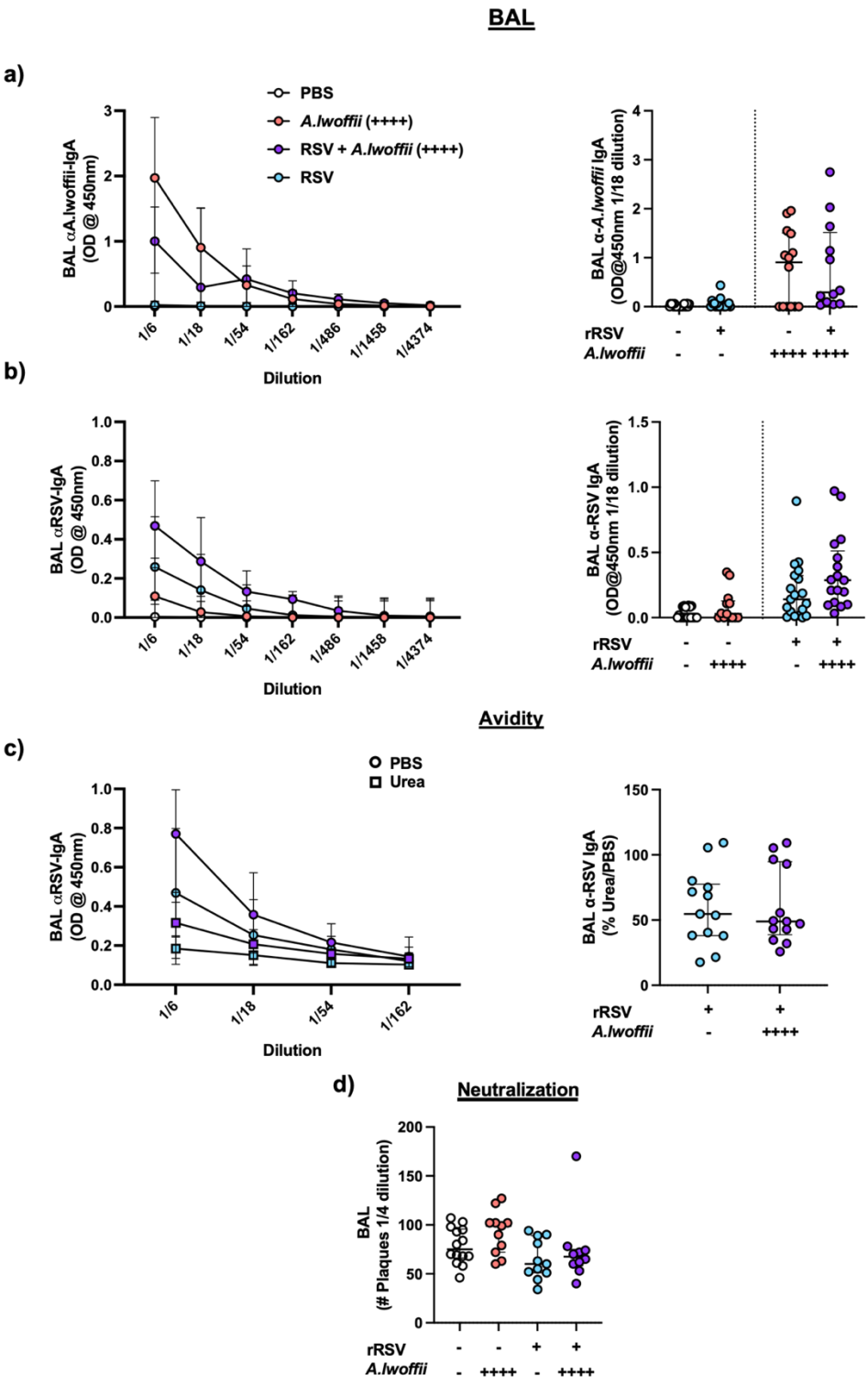


Fig 4.14. Trend to an increase BAL RSV-specific IgA responses in mice recurrently exposed to A.lwoffii

3d old Balb/c mice were intranasally exposed to *A.lwoffii* or PBS three times a week and infected with RSV or saline on day 5 and 15 of life. Serum and BAL were extracted on 5d post re-infection. **(a)** Titration of BAL *A.lwoffii*-specific IgA, **(b)** RSV-specific IgA and **(c)** avidity index for RSV-IgA antibodies. **(d)** BAL neutralization assay. Data from two independent experiments with n = 14-19 mice per group. Data shown with median and interquartile range. In titration experiments each dot represents the mean of the group. For antibody quantification, avidity and neutralization capacity each dot represents one mouse. Mann-Whitney test between pertinent groups (a-c) or Kruskal-Wallis with multiple comparisons test (d) were performed in which *, $p < 0.05$; **, $p < 0.01$; and ***, $p < 0.001$.

4.2.3 Short exposure to *A.lwoffii* in early life is not sufficient to drive T_{FH} or antibody responses in RSV infected infant mice

The first years of life are a crucial time when the microbiota is establishing and when the immune system is developing that represents a "window of opportunity" to prevent microbiome and immune alterations, such as asthma, severe respiratory infections and autoimmune diseases (601). Since recurrent exposure to *A.lwoffii* in early life promotes a T-cell dependent antibody response against RSV infection, shorter exposures to the bacteria were then used to determine if they could have a similar effect. To this end, 3d old Balb/c mice were i.n exposed to *A.lwoffii* or PBS twice (+), four times (++) or five times (+++) before RSV re-infection ("prophylactic *A.lwoffii")*. RSV challenge was maintained at 5 and 15d of life *(**Fig 4.15a**)*. Mice were culled 5d post RSV re-infection and lung, lung draining lymph nodes, spleen, blood and BAL were collected. No difference in viral load, quantified as *RSV L* gene in the lung, was observed between RSV infected mice and mice exposed to four doses of *A.lwoffii (**Fig 4.15b**)*. LN cell numbers were increased in those mice receiving two and four doses of *A.lwoffii* on top of RSV when compared with control mice *(**Fig 4.15c**)*. Increased B cell proportions were observed in mice receiving RSV and this was accompanied by an increased B cell number in mice that were exposed to two and four doses of *A.lwoffii* when compared to control counterparts *(**Fig 4.15d**)*.

Exposure to two and four doses of *A.lwoffii* led to increased $\gamma\delta$ and $\alpha\beta$ T cell numbers, but no difference in cell proportion was observed by any group *(**Fig 4.16a,b**)*. Both RSV infection alone and combined with two doses of *A.lwoffii* exposure led to an increased $CD8^+$ T cell proportion in the mediastinal LN, but an increased $CD8^+$ T cell frequency was observed both after exposure to two and four doses of the farmyard microbe *(**Fig 4.16c**)*. Increased CD69 expression on $CD8^+$ T cells was observed in the three groups, namely, mice challenged with RSV alone and exposed to few doses of the bacteria *(**Fig 4.16d**)*. No difference in $CD4^+$ T cell proportion was observed, but mice that were exposed to two doses of the bacteria showed increased $CD4^+$ T cell numbers when compared to PBS exposed mice *(**Fig 4.16e**)*. All RSV infected mice significantly increased CD69 on $CD4^+$ T cells when compared with PBS controls *(**Fig 4.16f**)*.

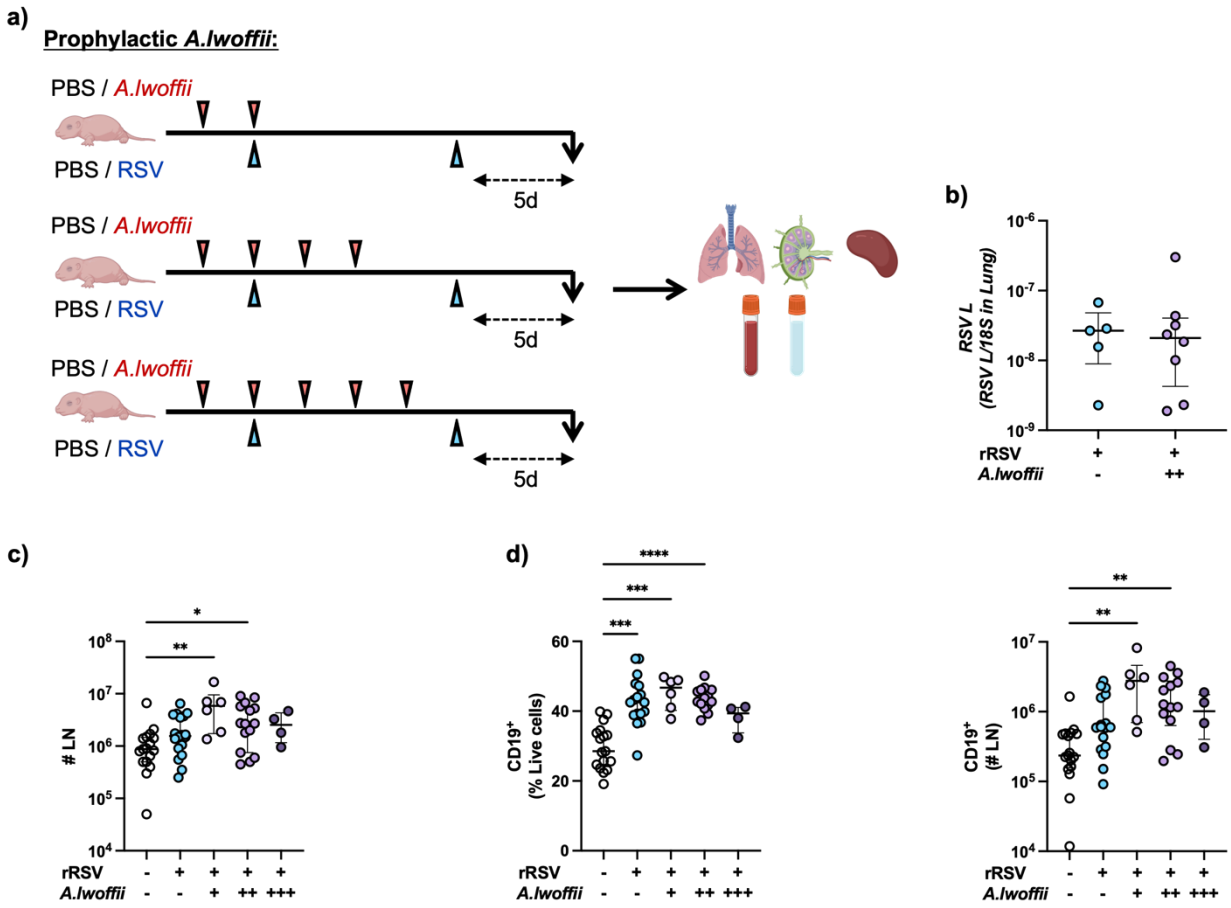


Fig 4.15. Similar viral titre and B cell responses in RSV infected infant mice irrespective of prophylactic A.lwoffii exposure

(a) Balb/c mice were infected with RSV on day 5 and 15 of life and intranasally exposed to different doses of *A.lwoffii* or PBS from d3 of life stopping before RSV re-infection. Lymph node, spleen, blood and BAL were collected 5d post 2nd dose with RSV. **(b)** *RSV L* relative to *18S* in lung tissue measured by RT-qPCR. **(c)** Lymph node (LN) cell count. **(d)** B cells percentage and frequency. Data from one independent experiment (b) with n= 5-8 mice per group or three independent experiments (c,d) with n = 4-20 mice per group. Data shown with median and interquartile range. Each dot represents one mouse. Mann-Whitney (b) and Kruskal-Wallis with multiple comparisons test (c,d) were performed in which *, $p < 0.05$; **, $p < 0.01$; and ***, $p < 0.001$.

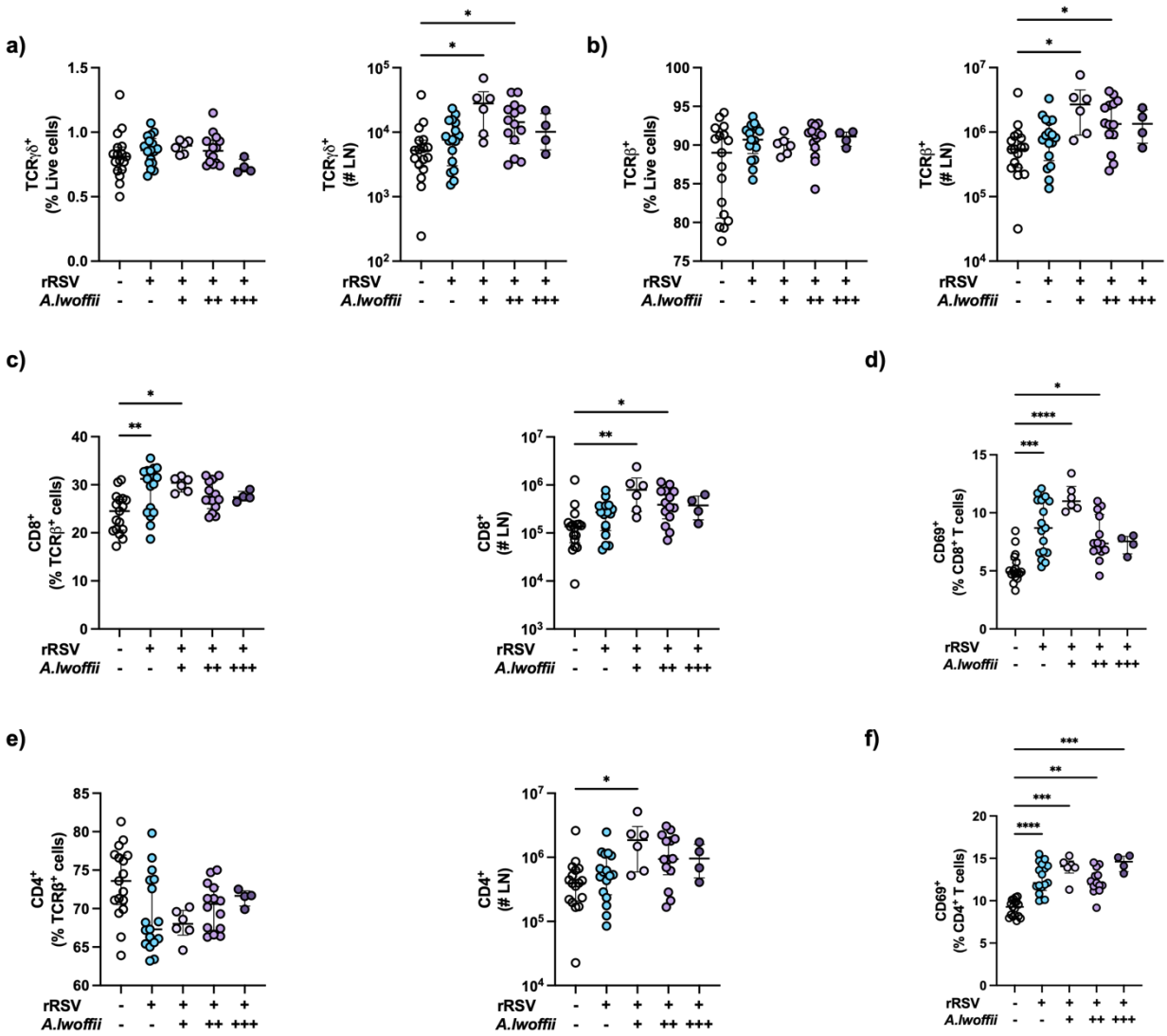


Fig 4.16. No difference in T cell responses is observed between RSV infected and prophylactically A.lwoffii exposed and unexposed mice

Balb/c mice were infected with RSV on day 5 and 15 of life and intranasally exposed to different doses of *A.lwoffii* or PBS from d3 of life stopping before RSV re-infection. **(a)** Proportion and quantification of TCRγδ and **(b)** TCRβ T cells, **(c)** $CD8^+$ T cells and **(d)** their expression of CD69 as well as **(e)** $CD4^+$ T cells and their **(f)** CD69 expression. Data from three independent experiments with n = 4-20 mice per group. Data shown with median and interquartile range. Each dot represents one mouse. Kruskal-Wallis with multiple comparisons test was performed in which *, $p < 0.05$; **, $p < 0.01$; and ***, $p < 0.001$.

Cells involved in the GC reaction were also analysed after short exposure to the farmyard microbe. An increase in T_{FH} cells was observed in all infected groups, with mice exposed to two and four doses of the bacteria showing the greatest difference when compared to control counterparts; but only mice exposed to *A.lwoffii* showed an increase in T_{FH} cell numbers *(**Fig 4.17a**)*. The same trend was observed in GC T_{FH} proportion, with mice that received four doses of *A.lwoffii* having a significant increase when compared with RSV infected mice alone *(**Fig 4.17b**)*. All RSV infected groups had increased GC T_{FH} numbers and, as with T_{FH} responses, the greatest significance was seen in mice exposed to two and four doses of the bacteria *(**Fig 4.17b**)*. The formation of GC B cells was promoted in mice infected with RSV alone or exposed to four or five doses of *A.lwoffii*,

with mice that received five doses of the farmyard microbe showing the highest trend and being significantly upregulated when compared with mice exposed to *A.lwoffii* only twice *(Fig 4.17c)*. All infected groups however showed an increase in GC B cell numbers when compared with control mice *(Fig 4.17c)*. An increased CD138^{+} cell response was observed in mice infected with the virus alone or accompanied by four and five doses of *A.lwoffii*, with cell numbers again being elevated in all infected groups *(Fig 4.17d)*.

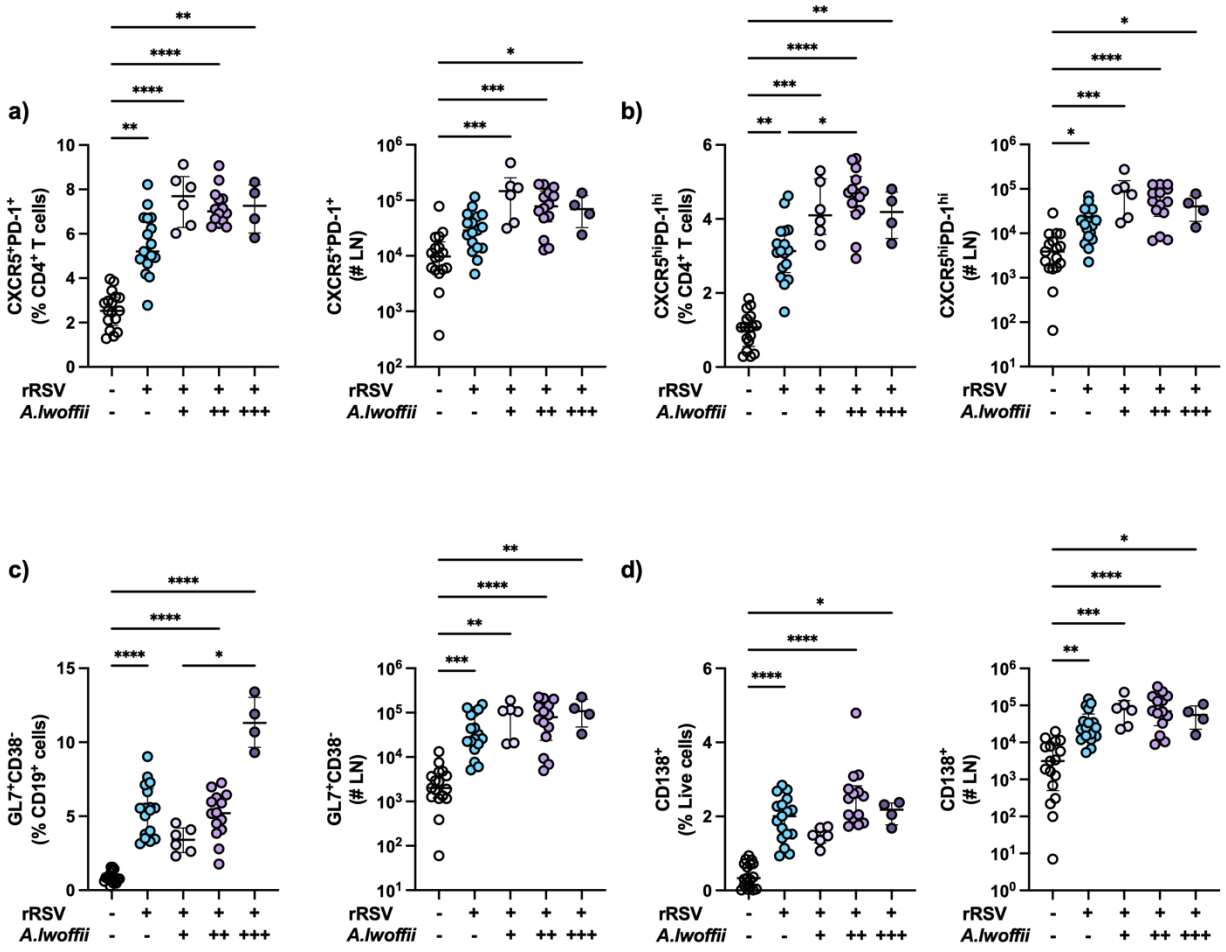


Fig 4.17. Exposure to A.lwoffii prophylactically does not enhance the T_{FH} and CD138^{+} response when compared to RSV infected infant mice alone

Balb/c mice were infected with RSV on day 5 and 15 of life and intranasally exposed to different doses of *A.lwoffii* or PBS from d3 of life stopping before RSV re-infection. **(a)** Lymph node proportion and quantification of T_{FH} cells, **(b)** GC T_{FH} cells, **(c)** GC B cells and **(d)** Plasma cells & Plasma blasts. Data from three independent experiments with n = 4-20 mice per group. Data shown with median and interquartile range. Each dot represents one mouse. Kruskal-Wallis with multiple comparisons test was performed in which *, $p < 0.05$; **, $p < 0.01$; and ***, $p < 0.001$.

The B and T cell response was also analysed in the spleen. No difference in spleen cell counts was seen among groups *(Fig 4.18a)*. An increased CD19^{+} cell proportion when compared with RSV infected mice alone was observed for mice receiving four doses of *A.lwoffii,* which also showed a significant increase when compared with mice exposed to five doses of the bacteria *(Fig 4.18b)*. Elevated B cell numbers were seen in mice receiving both two and four doses of *A.lwoffii* when

compared with mice receiving five doses *(**Fig 4.18b**)*. An increase in γδ T cell proportion was observed in mice exposed to four doses of *A.lwoffii* when compared with PBS, RSV alone mice or mice exposed to five doses of the bacteria; but increased cell numbers were only observed with the control group and mice exposed to the highest dose of *A.lwoffii* *(**Fig 4.18c**)*. No difference in αβ T cell proportion or cell number was apparent between groups *(**Fig 4.18d**)*. Mice receiving two and four doses of the farmyard microbe had increased $CD8^+$ T cell proportion accompanied by a reduction in $CD4^+$ T cell percentage *(**Fig 4.18e,g**)*. Increased $CD8^+$ T cell numbers were observed after exposure to two and four doses of the bacteria when compared with PBS mice *(**Fig 4.18e**)*. An increase in CD69 expression by these cells was seen between PBS and mice receiving two doses of *A.lwoffii* when compared with mice exposed to five doses *(**Fig 4.18f**)*. CD69 expression by $CD4^+$ T cells was elevated in animals exposed to two and five doses of the bacteria when compared with RSV infected mice alone and mice receiving four doses of *A.lwoffii* *(**Fig 4.18h**)*.

In the spleen there were no major differences in the proportion and frequency of cells involved in the GC when comparing PBS controls and RSV infected groups *(**Fig 4.19a-d**)*. No difference in T_{FH} cell proportion or frequency was observed between groups *(**Fig 4.19a**)*. An increase in GC T_{FH} cell proportion and cell number was only seen in mice treated with four doses of *A.lwoffii* when compared with PBS controls *(**Fig 4.19b**)*. GC B cell proportions were increased in mice exposed to the five doses of *A.lwoffii* when compared with all other RSV infected groups, but no difference in GC B cell frequency was apparent *(**Fig 4.19c**)*. Proportion and cell number of $CD138^+$ cells also remained constant between groups *(**Fig 4.19d**)*. Overall, this data suggests that short exposure to *A.lwoffii* does not promote T_{FH} nor B cell responses in the mediastinal LN or spleen of RSV infected mice.

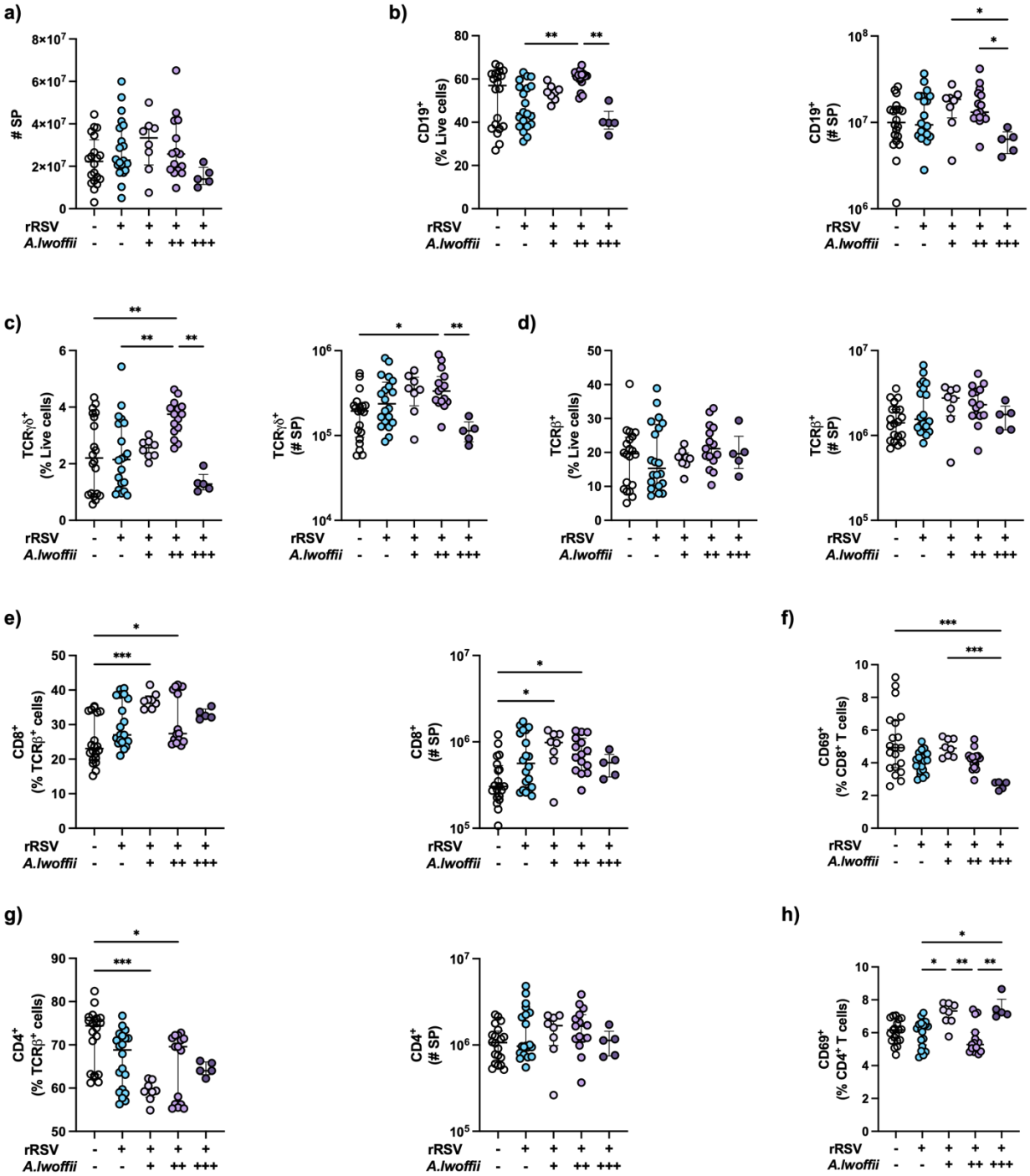


Fig 4.18. No major splenic differences in B and T cell responses after short exposure to A.lwoffii

Balb/c mice were infected with RSV on day 5 and 15 of life and intranasally exposed to different doses of *A.lwoffii* or PBS from d3 of life stopping before RSV re-infection. **(a)** Spleen (SP) cell numbers. **(b)** Spleen proportion and quantification of B cells, **(c)** TCRγδ, **(d)** TCRβ T cells, **(e)** $CD8^+$ T cells and **(f)** percentage of $CD8^+CD69^+$ cells as well as **(g)** $CD4^+$ T cells and their **(h)** CD69 expression. Data from three independent experiments with n = 5-20 mice per group. Data shown with median and interquartile range. Each dot represents one mouse. Kruskal-Wallis with multiple comparisons test was performed in which *, $p < 0.05$; **, $p < 0.01$; and ***, $p < 0.001$.

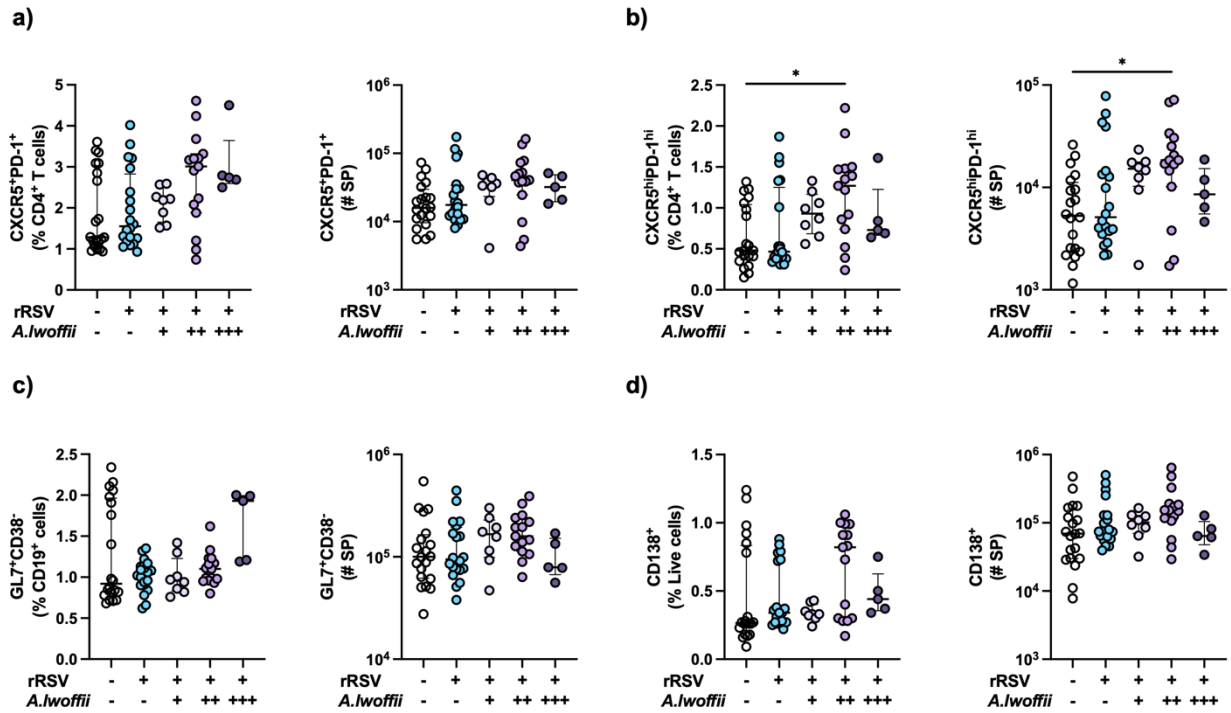


Fig 4.19. A.lwoffii exposure prophylactically does not affect the splenic GC response of RSV infected infant mice

Balb/c mice were infected with RSV on day 5 and 15 of life and intranasally exposed to different doses of A.lwoffii or PBS from d3 of life stopping before RSV re-infection.**(a)** Spleen proportion and quantification of T_{FH} cells, **(b)** GC T_{FH} cells, **(c)** GC B cells and **(d)** Plasma cells & Plasma blasts. Data from three independent experiments with n = 5-20 mice per group. Data shown with median and interquartile range. Each dot represents one mouse. Kruskal-Wallis with multiple comparisons test was performed in which *, $p < 0.05$; **, $p < 0.01$; and ***, $p < 0.001$.

Concomitant with the SLO results, short exposure to *A.lwoffii* in early life also failed to upregulate *A.lwoffii*-specific serum antibody titres, as only mice who received five doses of the bacteria showed a trend to an increase serum *A.lwoffii*-specific total Igs, IgG1 and IgG2a antibodies *(**Fig 4.20a-c**)*. Albeit an increase in RSV-specific total Igs, IgG1 and IgG2a antibodies was observed in all RSV treated groups, there was no difference between them *(**Fig 4.21a-c**)*. While no significant difference was observed in *Ifnγ* or *Il4* transcript in the mediastinal LN, an increased *Ifnγ* and reduced *Il4* signature was observed in mice exposed to five doses of *A.lwoffii* when compared with the RSV alone group, showing a trend to an increase *Ifnγ/Il4* ratio *(**Fig 4.21d,e**)*.

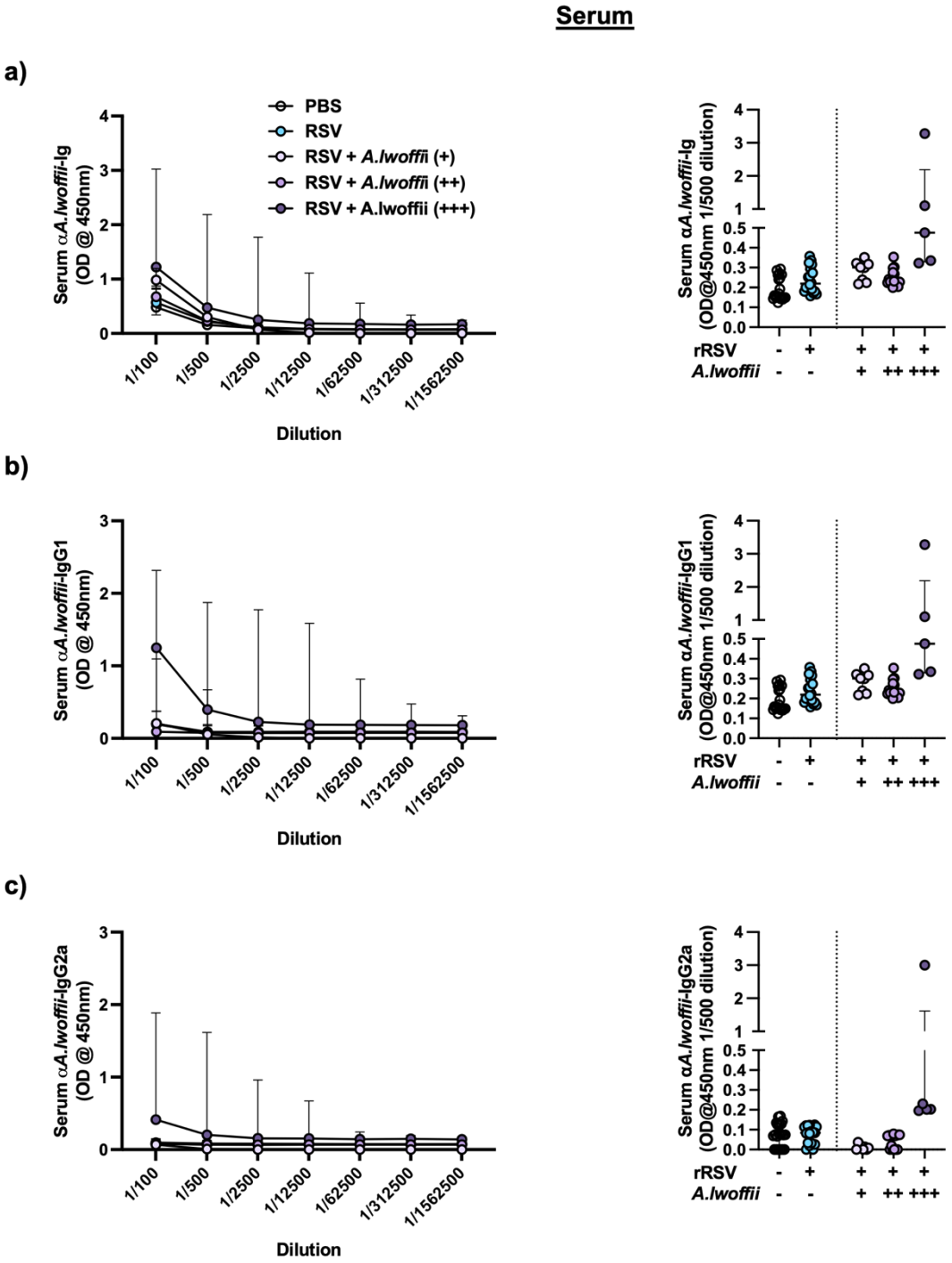


Fig 4.20. Short A.lwoffii exposure regimens do not promote A.lwoffii-specific antibody secretion

Balb/c mice were infected with RSV on day 5 and 15 of life and intranasally exposed to different doses of *A.lwoffii* or PBS from d3 of life stopping before RSV re-infection. Serum and BAL were extracted 5d post re-infection. **(a)** Titration of serum *A.lwoffii*-specific poly-Igs, **(b)** IgG1 and **(c)** IgG2a. Data from three independent experiments with n = 5-20 mice per group. Data shown with median and interquartile range. In titration experiments each dot represents the mean of the group. For antibody quantification each dot represents one mouse.

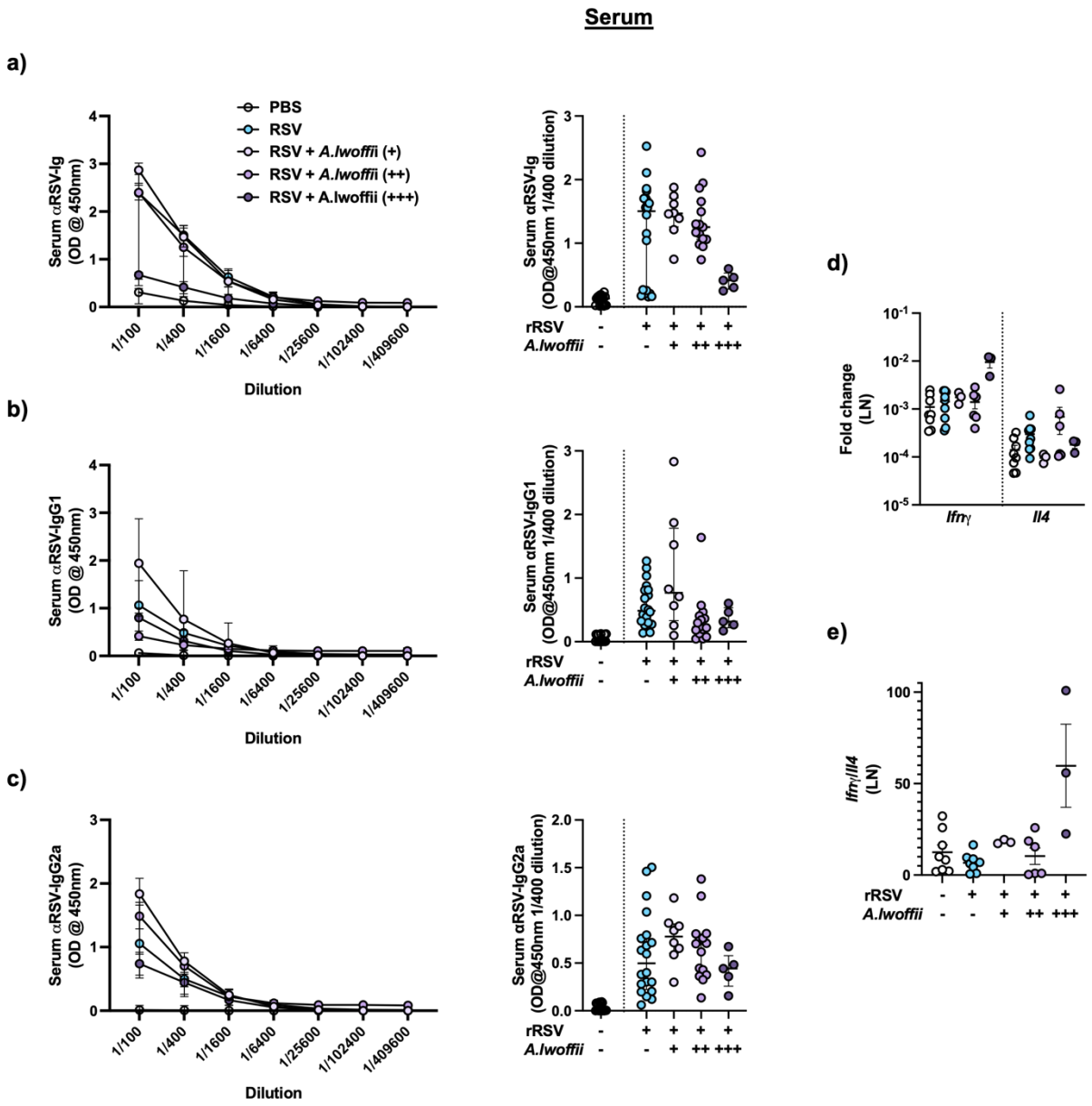


Fig 4.21. Short A.lwoffii regimens do not boost systemic RSV-specific antibody responses

Balb/c mice were infected with RSV on day 5 and 15 of life and intranasally exposed to different doses of *A.lwoffii* or PBS from d3 of life stopping before RSV re-infection. Serum and BAL were extracted 5d post re-infection. **(a)** Titration of serum RSV-specific poly-Igs, **(b)** IgG1 and **(c)** IgG2a. **(d)** Transcript titre for *Infg* and *Il4* in LN of experimental mice as well as **(e)** *Infg/Il4* ratio measured by RT-qPCR. Data from three independent experiments with n = 5-20 mice per group (a-d) or with n= 3-8 mice per group (e,f). Data shown with median and interquartile range. In titration experiments each dot represents the mean of the group. For antibody quantification and transcript titres each dot represents one mouse. Kruskal-Wallis with comparisons against RSV group (a-c) or multiple comparisons (d,e) was performed in which *, $p < 0.05$; **, $p < 0.01$; and ***, $p < 0.001$.

As with recurrent *A.lwoffii* exposure, use of 4M urea was sufficient to remove all detectable Ig, IgG1 or IgG2a binding, in both RSV alone infected mice and mice exposed to four doses of *A.lwoffii* *(**Fig 4.22a-c**).* While again this made avidity impossible to calculate, it indicated that any change in avidity was likely modest *(**Fig 4.22a-c**).* Similarly, when performing a neutralization assay, there was no reduction in plaque count, when compared to PBS mice, in any RSV infected group analyzed irrespective of *A.lwoffii* exposure. Likewise, there was no difference between the RSV alone group and the mice treated with four doses of *A.lwoffii* on top of RSV, suggesting no detectable neutralizing antibodies were present in these samples at the serum concentration used *(**Fig 4.22d**).*

As with serum responses, a trend to an increase *A.lwoffii*-specific IgA was only observed in the BAL of RSV infected mice that were exposed to five doses of the farmyard microbe *(**Fig 4.23a**).* RSV-IgA antibody responses were detected in the BAL of all mice infected, with RSV alone mice showing a statistically significant increase in RSV-IgA production when compared with mice exposed to four doses of *A.lwoffii* *(**Fig 4.23b**).* On measurement of avidity, exposure to five doses of *A.lwoffii* appeared to cause a slight increase in IgA compared to RSV alone *(**Fig4.23c**).* This was however likely an artifact caused by the lower titres of RSV-specific IgA in this group compared to the RSV only group, while after urea treatment no antibody was detectable in either group. As with recurrent exposure to *A.lwoffii*, no difference in plaque cell number was observed between groups when a neutralization assay was performed, suggesting that neutralizing antibodies were not present in the BAL of infant RSV infected mice even after four or five doses of *A.lwoffii* exposure *(**Fig4.23d**).* Combined, this data indicates that shorter exposures to *A.lwoffii* are not sufficient to generate RSV specific T cell-dependent antibody responses.

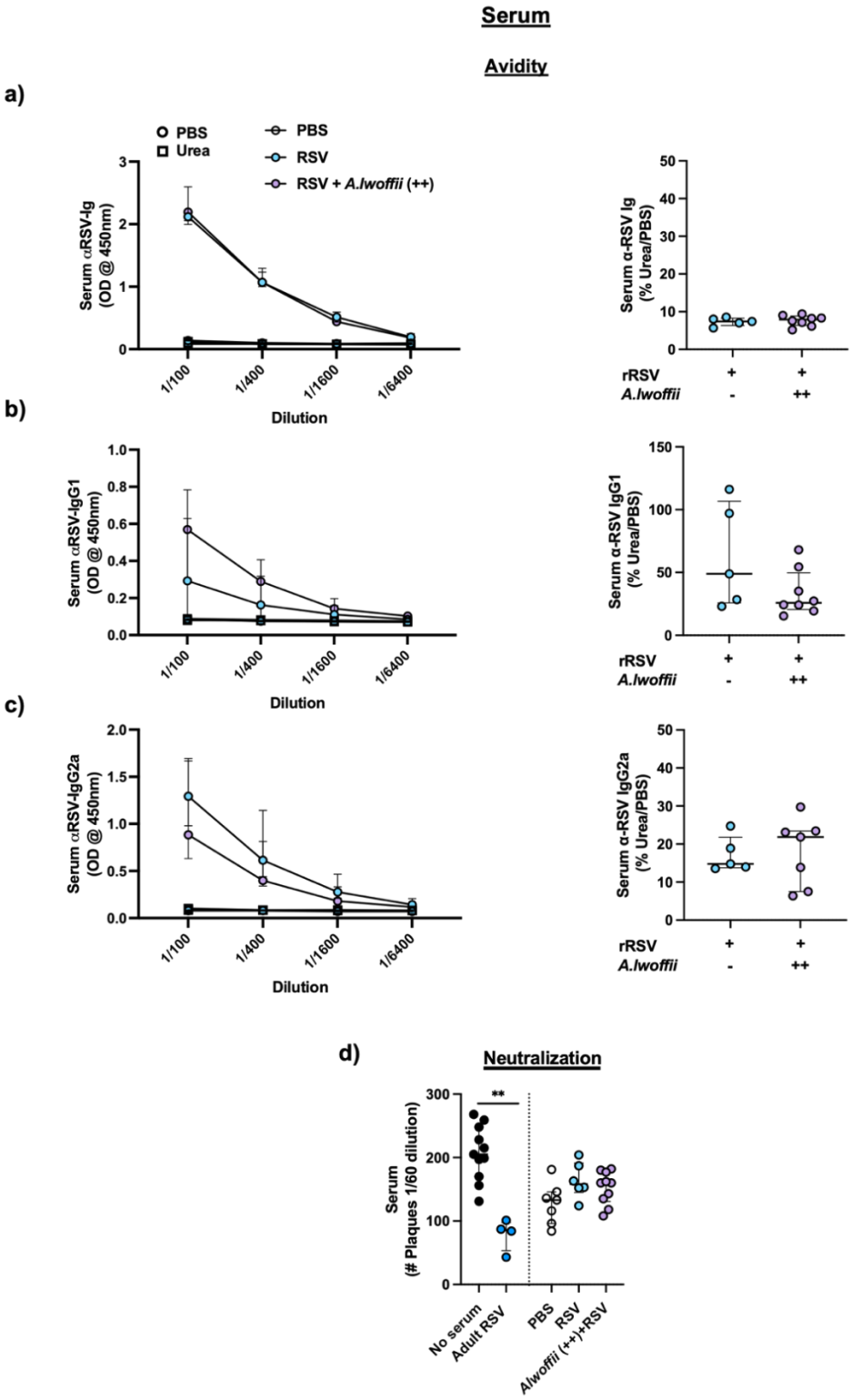


Fig 4.22. Early life short exposure to A.lwoffii does not affect serum RSV-specific antibody avidity or neutralization capacity

Balb/c mice were infected with RSV on day 5 and 15 of life and intranasally exposed to different doses of *A.lwoffii* or PBS from d3 of life stopping before RSV re-infection. Serum and BAL were extracted on 5d post re-infection. **(a)** Avidity quantification of serum RSV-specific poly-Igs, **(b)** IgG1 and **(c)** IgG2a. **(d)** Neutralization assay on serum of experimental mice. Data from one independent experiment with n = 4-10 mice per group. Data shown with median and interquartile range. In titration experiments each dot represents the mean of the group. For antibody quantification and neutralization each dot represents one mouse. Mann-Whitney test (a-c) or Kruskal-Wallis with multiple comparisons test (d) were performed in which *, $p < 0.05$; **, $p < 0.01$; and ***, $p < 0.001$.

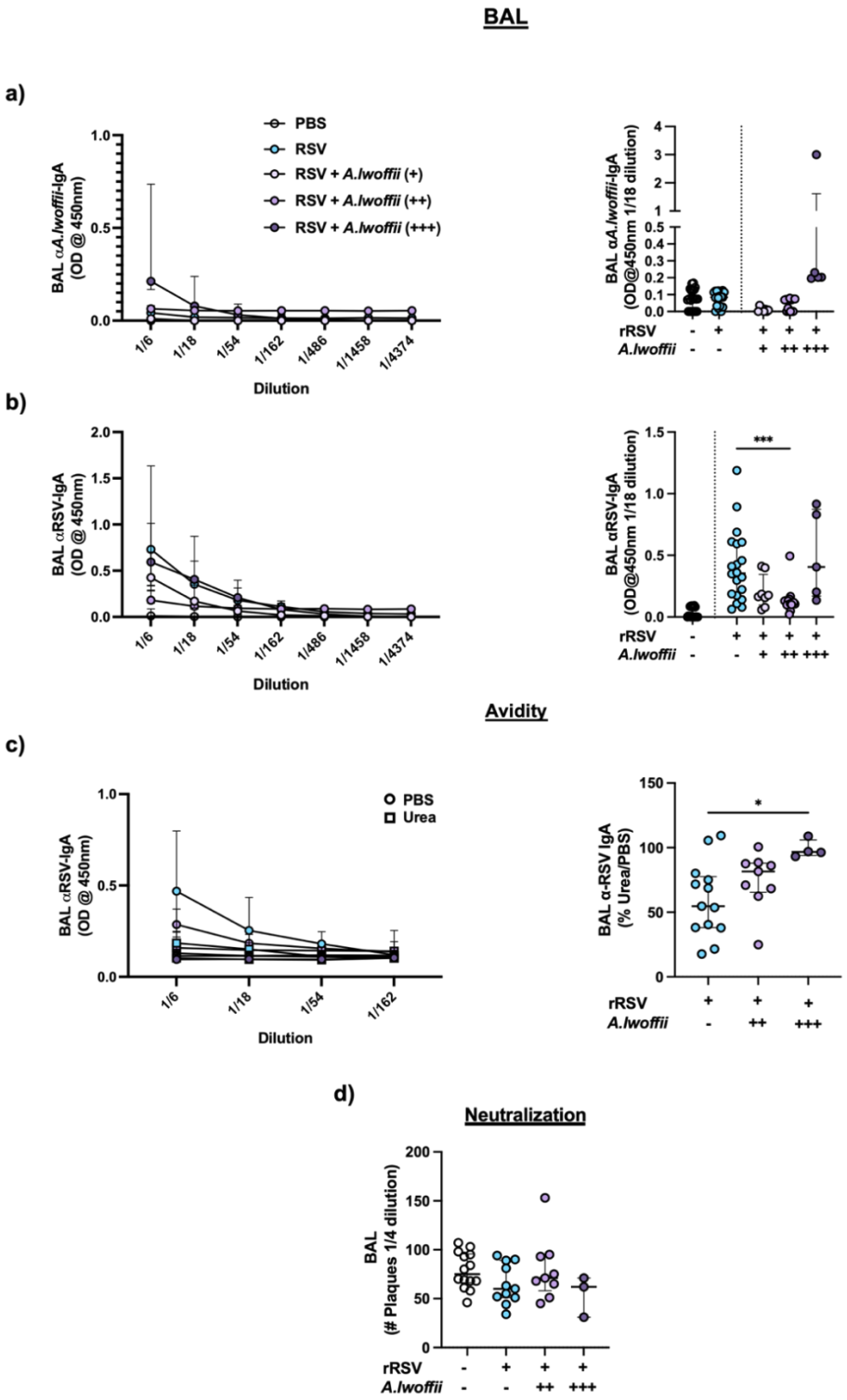


Fig 4.23. Analysis of antibody avidity and neutralization capacity in BAL of prophylactic A.lwoffii exposed mice

Balb/c mice were infected with RSV on day 5 and 15 of life and intranasally exposed to different doses of *A.lwoffii* or PBS from d3 of life stopping before RSV re-infection. Serum and BAL were extracted 5d post re-infection **(a)** Titration of BAL *A.lwoffii*-specific IgA, **(b)** RSV-specific IgA and **(c)** avidity index of RSV-IgA antibodies. **(d)** BAL neutralization assay. Data from three independent experiments (a,b) with n = 5-20 mice per group or one independent experiment (c,d) with n= 3-14 mice per group. Data shown with median and interquartile range. In titration experiments each dot represents the mean of the group. For antibody quantification, avidity and neutralization capacity each dot represents one mouse. Kruskal-Wallis with comparisons against RSV alone group (b,c,d) was performed in which *, $p < 0.05$; **, $p < 0.01$; and ***, $p < 0.001$.

4.2.4 Therapeutic *A.lwoffii* exposure in early life fails to boost RSV-specific antibody responses

Recurrent *A.lwoffii* exposure in early life promotes a T cell dependent antibody response in RSV infected infant mice, but this is not the case when shorter *A.lwoffii* regimens are used. Mice treated with recurrent *A.lwoffii* are however exposed to the bacteria at the time of re-infection, indicating that *A.lwoffii* might be acting therapeutically. To test this hypothesis, mice were infected with RSV at d5 and 15 of life and exposed to *A.lwoffii* or PBS during RSV re-challenge, i.e. 3 times a week from d13 of life ("therapeutic *A.lwoffii")*, to test if this timing was crucial in boosting the GC reaction *(**Fig 4.24a**)*.

As with prophylactic doses of the bacteria, no differences in therapeutically used *A.lwoffii* and RSV alone group were observed in lung viral load measured by *RSV L (**Fig 4.24b**)*. An increase in mediastinal LN cell counts was however seen in mice treated with four doses of *A.lwoffii* therapeutically when compared with PBS animals *(**Fig 4.24c**)*. The proportion of B cells was increased in RSV alone infected mice when compared with control mice, but higher B cell numbers were seen in *A.lwoffii* exposed animals relative to the PBS group *(**Fig 4.24d**)*. An increase in $\gamma\delta$ T cell proportion and frequency was observed for *A.lwoffii* treated mice when compared with mice that were only infected with RSV *(**Fig 4.24e**)*. No difference in proportion of TCRβ^+ T cells was observed between groups *(**Fig 4.24f**)*. An increase in $CD8^+$ T cells was seen in RSV treated mice which was accompanied by a reduction in $CD4^+$ T cell proportion when compared with PBS animals *(**Fig 4.24g,i**)*. Elevated $\alpha\beta$ T cell numbers, in total and for $CD8^+$ and $CD4^+$ T cell subsets, were seen in the *A.lwoffii* exposed group *(**Fig 4.24f-i**)*. CD69 expression on $CD8^+$ T cells was increased in mice infected with RSV alone, while both RSV infected groups showed an increase in the CD69 marker in $CD4^+$ T cells *(**Fig 4.24h,j**)*.

T_{FH} proportion and numbers in mediastinal LN were increased in *A.lwoffii* exposed mice when compared with PBS or RSV infected mice alone *(**Fig 4.25a**)*. GC T_{FH} cell proportions were increased in both RSV infected groups when compared with PBS mice, but the difference between the control and *A.lwoffii* exposed group was more statistically significant; concomitant with the elevated GC T_{FH} numbers observed only in this group when compared with PBS mice *(**Fig 4.25b**)*. The proportion of GC B cells was increased in mice only infected with RSV, but increased numbers were observed only after *A.lwoffii* exposure *(**Fig 4.25c**)*. $CD138^+$ cells were elevated in both groups infected with the virus, with again the highest increase observed in mice exposed to the farmyard microbe *(**Fig 4.25d**)*.

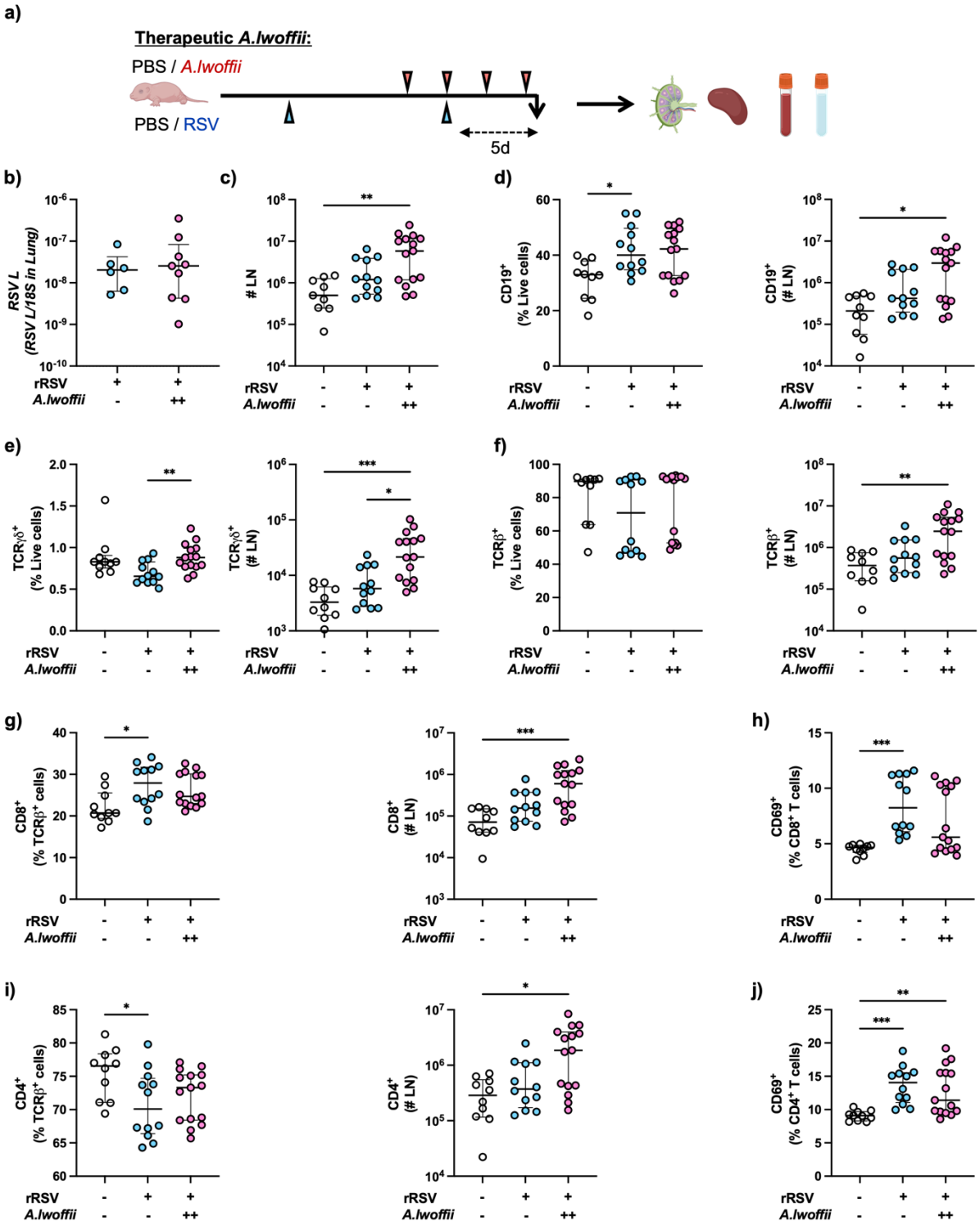


Fig 4.24. Similar B and T cell responses in the LN of therapeutic A.lwoffii exposed and unexposed RSV infected 20d old mice

(a) Balb/c mice were infected with RSV on day 5 and 15 of life and intranasally exposed to *A.lwoffii* or PBS 3 times a week from d13 of life. Lymph node, spleen, blood and BAL were collected 5d post 2nd dose with RSV. **(b)** *RSV L* relative to *18S* in lung tissue measured by RT-qPCR. **(c)** Lymph node (LN) cell count. **(d)** Percentage and frequency of B cells, **(e)** TCRγδ, **(f)** TCRβ T cells, **(g)** $CD8^+$ T cells and **(h)** percentage of $CD8^+CD69^+$ cells as well as **(i)** $CD4^+$ T cells and their **(j)** CD69 expression. Data from two independent experiments with n = 10-15 mice per group. Data shown with median and interquartile range. Each dot represents one mouse. Mann-Whitney (b) Kruskal-Wallis with multiple comparisons test (c-j) was performed in which *, $p < 0.05$; **, $p < 0.01$; and ***, $p < 0.001$.

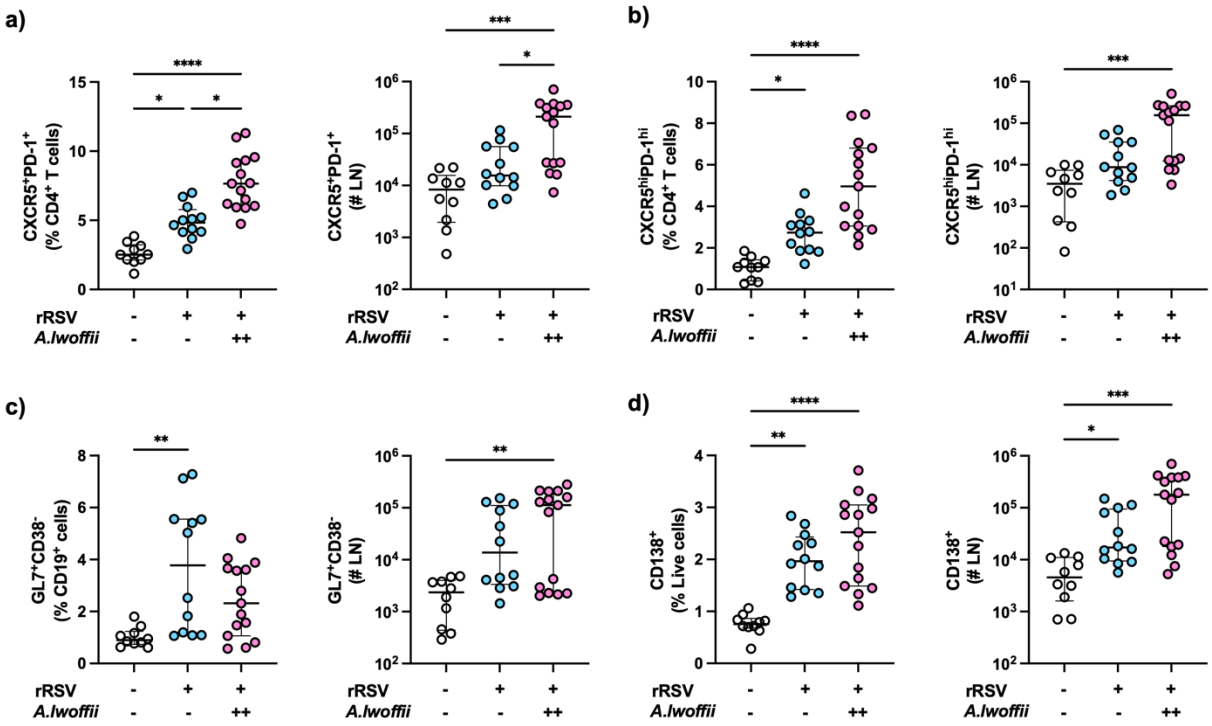


Fig 4.25. Exposure to A.lwoffii therapeutically in early life promotes mediastinal LN T_{FH} cells proportions and numbers

Balb/c mice were infected with RSV on day 5 and 15 of life and intranasally exposed to *A.lwoffii* or PBS 3 times a week from d13 of life. **(a)** Lymph node proportion and quantification of T_{FH} cells, **(b)** GC T_{FH} cells, **(c)** GC B cells and **(d)** Plasma cells & Plasma blasts. Data from three independent experiments with n = 10-15 mice per group. Data shown with median and interquartile range. Each dot represents one mouse. Kruskal-Wallis with multiple comparisons test was performed in which *, $p < 0.05$; **, $p < 0.01$; and ***, $p < 0.001$.

When compared with the lung draining LN response, a more uniform response between groups was observed in the spleen. Spleen cell numbers *(**Fig 4.26a**)* and B cells proportion and frequency remained constant between groups *(**Fig 4.26b**)*. An increase $\gamma\delta$ T cell proportion was however observed after therapeutic *A.lwoffii* exposure both when comparing it with PBS or RSV alone treated animals; but an increase frequency was only observed when compared to PBS exposed mice *(**Fig 4.26c**)*. The $\alpha\beta$ T cell response remained constant between groups, but RSV infection was associated with an increased $CD8^+$ T cell and a decreased $CD4^+$ T cell proportion when compared with control mice *(**Fig 4.26d-g**)*. No difference in $TCR\beta^+$ T cell or $CD4^+$ T cell numbers was seen in spleen; a significant increase in $CD8^+$ T cell frequency was however observed for the RSV treated mice when compared to control animals *(**Fig 4.26d-g**)*. Reduced expression of CD69 was observed in $CD8^+$ T cells of RSV infected animals when compared with PBS or *A.lwoffii* exposed mice *(**Fig 4.26f**)*, but no difference in CD69 expression was seen in the $CD4^+$ T cell subset *(**Fig 4.26h**)*.

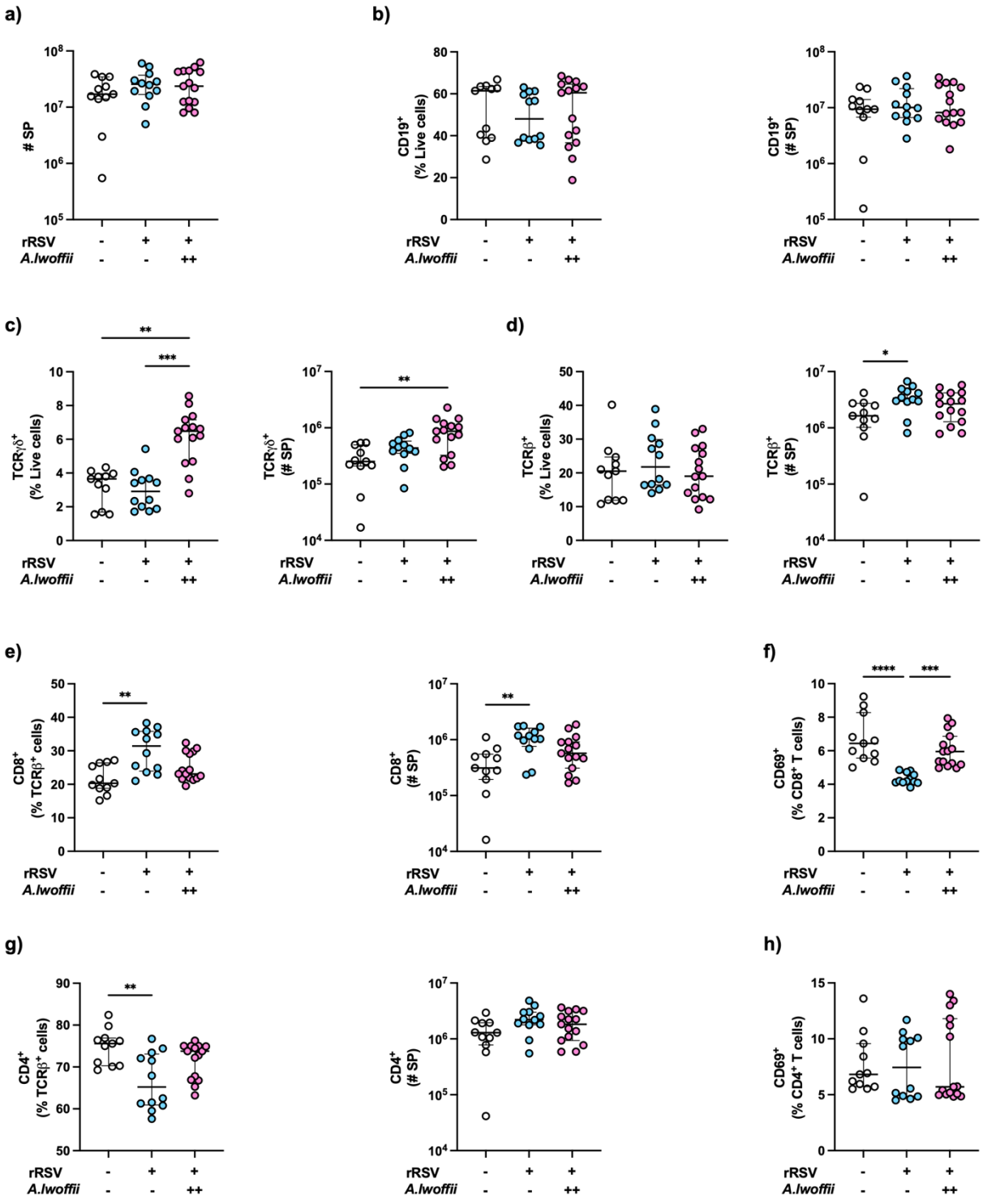


Fig 4.26. Similar B and T cell responses in the spleen of late A.lwoffii exposed and unexposed RSV infected 20d old mice

Balb/c mice were infected with RSV on day 5 and 15 of life and intranasally exposed to *A.lwoffii* or PBS 3 times a week from d13 of life. **(a)** Spleen (SP) cell count. **(b)** Percentage and frequency of B cells, **(c)** TCRγδ, **(d)** TCRβ T cells, **(e)** $CD8^+$ T cells and **(f)** percentage of $CD8^+CD69^+$ cells as well as **(g)** $CD4^+$ T cells and their **(h)** CD69 expression. Data from two independent experiments with n = 10-15 mice per group. Data shown with median and interquartile range. Each dot represents one mouse. Kruskal-Wallis with multiple comparisons test was performed in which *, $p < 0.05$; **, $p < 0.01$; and ***, $p < 0.001$.

Similarly, no enhancement in the cells involved in the GC response was observed in the spleen of RSV and RSV+*A.lwoffii* exposed mice treated therapeutically; as proportion and frequency of T_{FH}, GC T_{FH}, GC B cells and $CD138^+$ cells remained constant between groups *(Fig 4.27a-d)*. Collectively, this data suggests that while *A.lwoffii* exposure therapeutically increases mediastinal LN T_{FH} cell proportion, it doesn't promote $CD138^+$ cell responses.

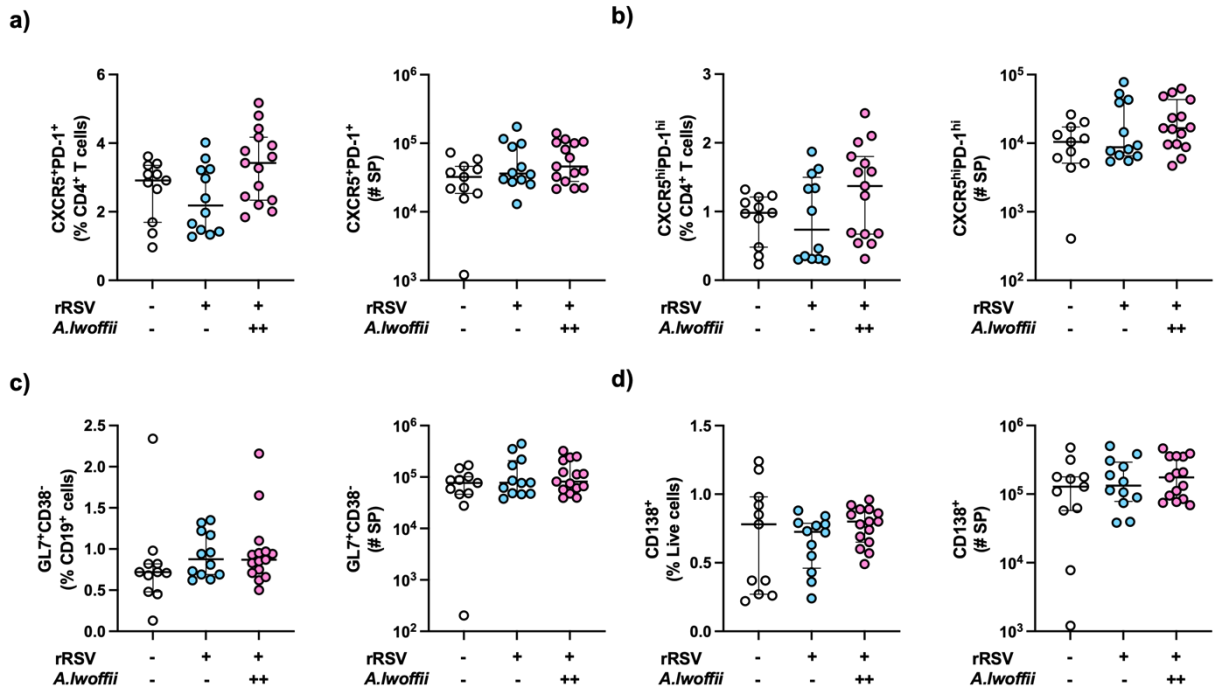


Fig 4.27. Exposure to A.lwoffii therapeutically in early life does not affect the splenic GC reaction

Balb/c mice were infected with RSV on day 5 and 15 of life and intranasally exposed to *A.lwoffii* or PBS 3 times a week from d13 of life. **(a)** Spleen proportion and quantification of T_{FH} cells, **(b)** GC T_{FH} cells, **(c)** GC B cells and **(d)** Plasma cells & Plasma blasts. Data from three independent experiments with n = 10-15 mice per group. Data shown with median and interquartile range. Each dot represents one mouse. Kruskal-Wallis with multiple comparisons test was performed in which *, $p < 0.05$; **, $p < 0.01$; and ***, $p < 0.001$.

Next, the systemic and local antibody response after therapeutic *A.lwoffii* exposure was analysed. Mice exposed to *A.lwoffii* therapeutically in early life showed a trend to an increase *A.lwoffii*-specific serum poly-Igs, but this was not dependent on *A.lwoffii*-specific IgG1 or IgG2a, as mice exposed to the farmyard microbe showed similar levels of these antibody subtypes when compared with controls *(Fig 4.28a-c)*. A trend to a decrease RSV-specific poly-Igs, IgG1 and IgG2a was observed in mice that received late exposure to *A.lwoffii* when compared to RSV alone infected animals, but this was not significant *(Fig 4.29a-c)*. Interestingly however, mice exposed to *A.lwoffii* during RSV re-challenge had a significant increased expression of *Ifnγ* when compared to PBS mice and they showed a trend to an increase *Ifnγ/Il4* when compared to both PBS and RSV alone treated groups *(Fig 4.29d,e)*. On measurement of avidity, late-treatment with *A.lwoffii* appeared to cause a slight increase in Ig compared to RSV alone, but no effect on IgG1 or IgG2a *(Fig4.30a-c)*. The Ig response was however likely an artifact caused by the lower titres of RSV-specific Ig in the *A.lwoffii*

exposed group when compared to the RSV only group, while after urea treatment no antibody was detectable in either group. Conversely, serum from farmyard microbe exposed animals had a significantly lower ability to neutralize RSV virions, as shown by an increased plaque count in this group when compared with PBS animals in a neutralization assay *(**Fig4.30d**)*.

Similar to the serum response, no increase in BAL *A.lwoffii*-IgA was observed in mice exposed to the bacteria therapeutically *(**Fig 4.31a**)*. While RSV-IgA was detected in BAL of both RSV infected groups, no difference between bacteria exposed animals and RSV alone treated mice was observed *(**Fig 4.31b**)*. Additionally, no difference in BAL RSV-IgA avidity or general BAL neutralization capacity was seen *(**Fig 4.31c,d**)*. Overall, this data suggests that exposure to *A.lwoffii* at the time of RSV re-infection is insufficient to enhance RSV-specific antibody responses.

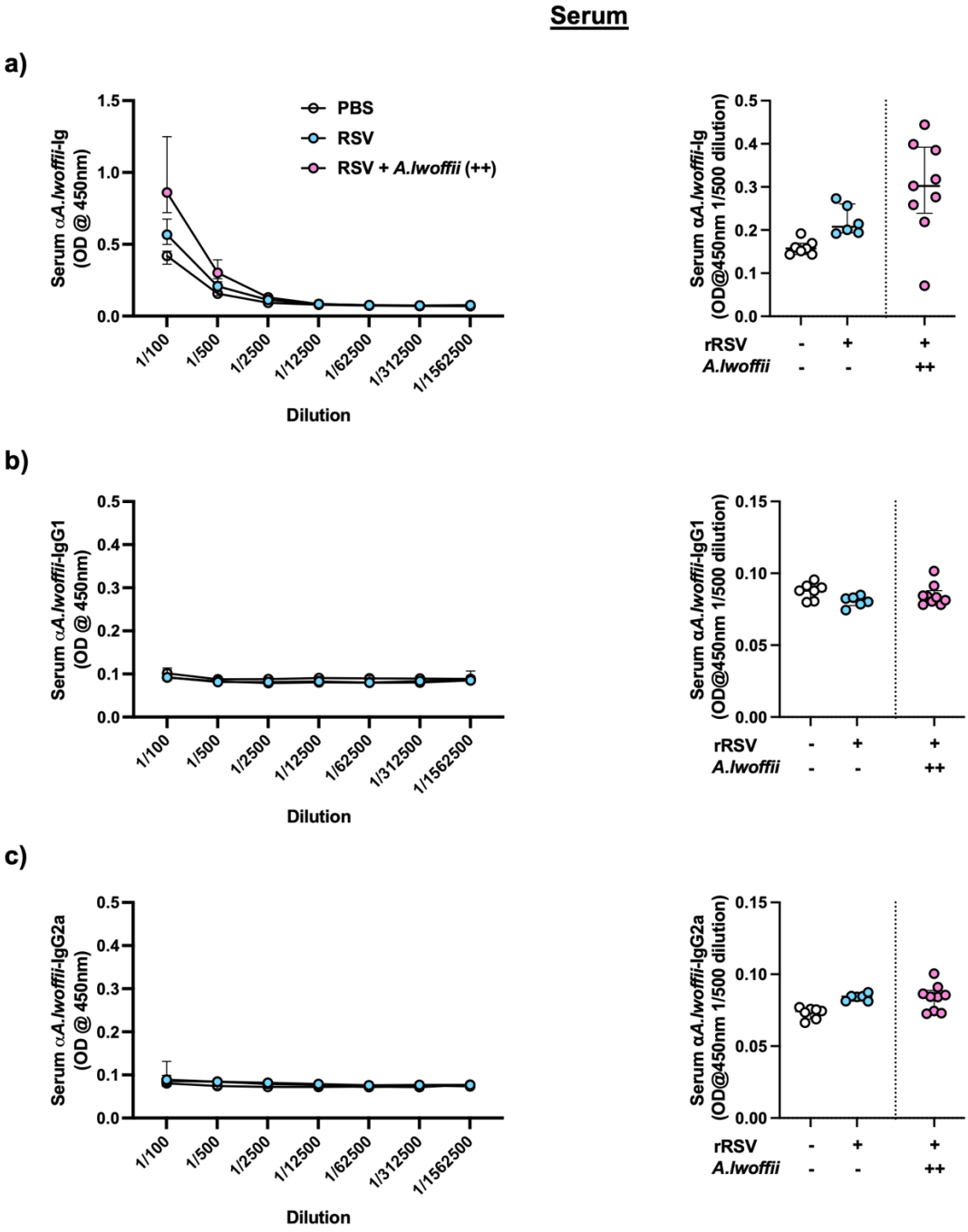


Fig 4.28. Exposure to A.lwoffii therapeutically does not promote A.lwoffii-specific IgG1 or IgG2a antibody production

Balb/c mice were infected with RSV on day 5 and 15 of life and intranasally exposed to *A.lwoffii* or PBS 3 times a week from d13 of life. Serum and BAL were extracted on 5d post re-infection. **(a)** Titration of serum *A.lwoffii*-specific poly-Igs, **(b)** IgG1 and **(c)** IgG2a. Data from one independent experiments with n = 6-9 mice per group. Data shown with median and interquartile range. In titration experiments each dot represents the mean of the group. For antibody quantification each dot represents one mouse.

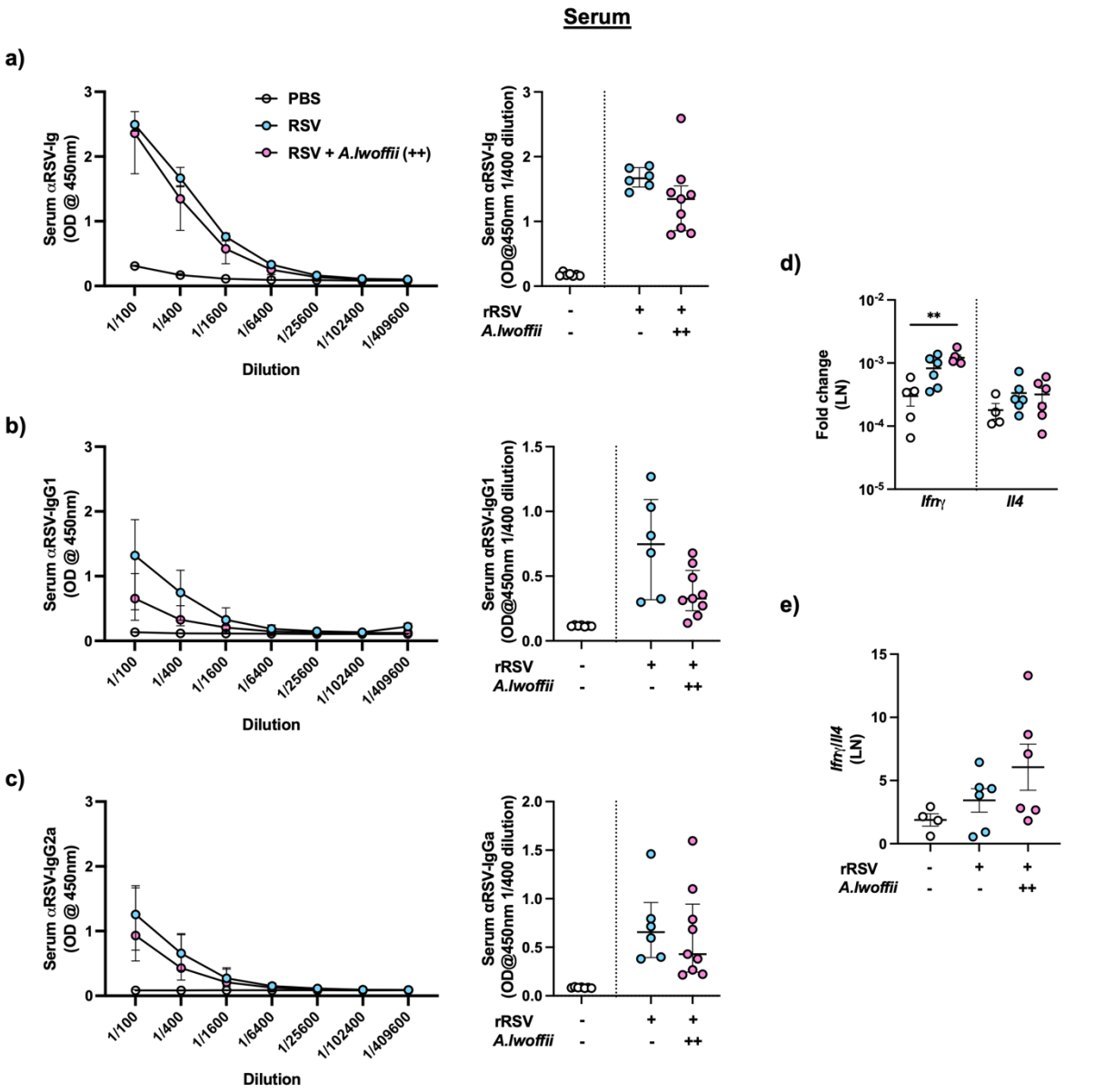


Fig 4.29. Exposure to A.lwoffii therapeutically does not promote RSV-specific antibody production

Balb/c mice were infected with RSV on day 5 and 15 of life and intranasally exposed to *A.lwoffii* or PBS 3 times a week from d13 of life. Serum and BAL were extracted on 5d post re-infection. **(a)** Titration of serum RSV-specific poly-Igs, **(b)** IgG1 and **(c)** IgG2a. **(d)** *Infγ* and *Il4* in LN of experimental mice as well as **(e)** *Infg/Il4* ratio measured by RT-qPCR. Data from two independent experiments with n = 6-9 mice per group (a-d) or with n= 4-6 mice per group (e,f). Data shown with median and interquartile range. In titration experiments each dot represents the mean of the group. For antibody quantification and transcript titres each dot represents one mouse. Mann-Whitney test between RSV treated and *A.lwoffii* exposed mice (a-c) or Kruskal-Wallis with multiple comparisons were performed in which *, $p < 0.05$; **, $p < 0.01$; and ***, $p < 0.001$.

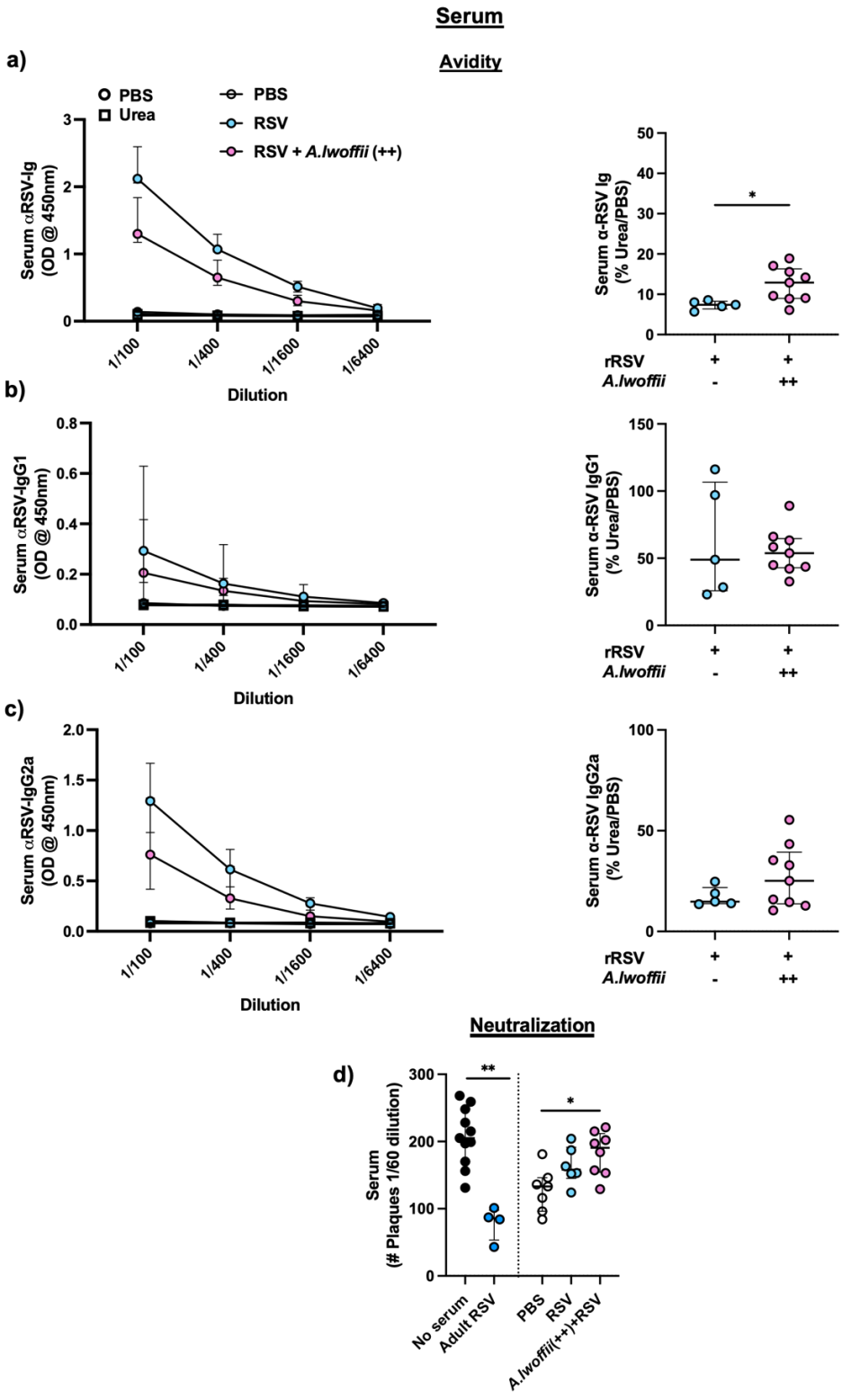


Fig 4.30. Analysis of serum antibody avidity and neutralization capacity after therapeutically A.lwoffii exposed mice

Balb/c mice were infected with RSV on day 5 and 15 of life and intranasally exposed to *A.lwoffii* or PBS 3 times a week from d13 of life. Serum and BAL were extracted 5d post re-challenge. **(a)** Avidity quantification of serum RSV-specific poly-Igs, **(b)** IgG1 and **(c)** IgG2a. **(d)** Neutralization assay on serum of experimental mice. Data from one independent experiment with n = 4-8 mice per group. Data shown with median and interquartile range. In titration experiments each dot represents the mean of the group. For antibody quantification and neutralization each dot represents one mouse. Mann-Whitney test (a-c) or Kruskal-Wallis with multiple comparisons test (d) were performed in which *, $p < 0.05$; **, $p < 0.01$; and ***, $p < 0.001$.

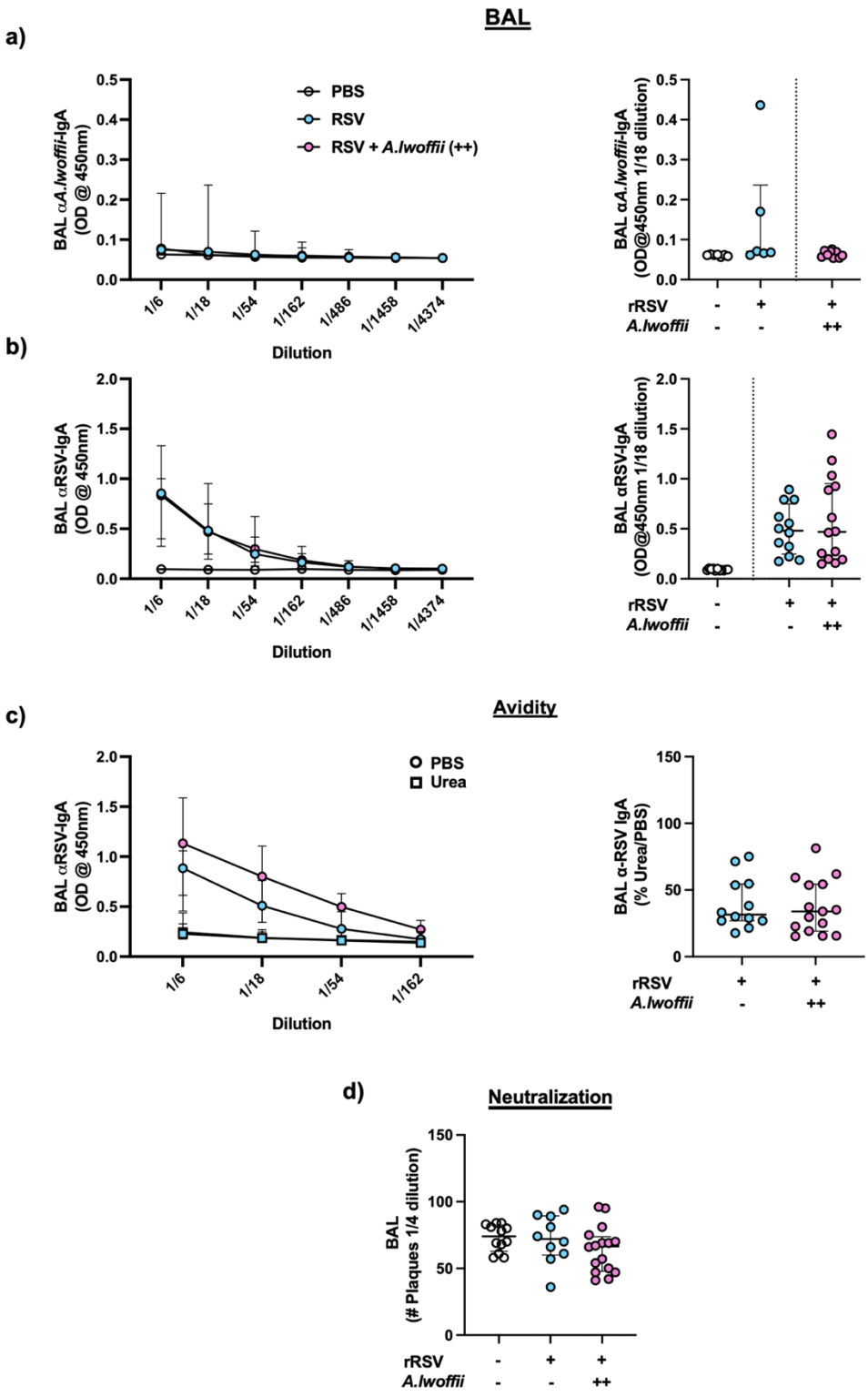


Fig 4.31. No difference in BAL antibody titre, avidity or neutralization capacity with therapeutical exposure to A.lwoffii

Balb/c mice were infected with RSV on day 5 and 15 of life and intranasally exposed to *A.lwoffii* or PBS 3 times a week from d13 of life. Serum and BAL were extracted on 5d post re-infection. **(a)** Titration of BAL *A.lwoffii*-specific IgA, **(b)** RSV-specific IgA and **(c)** avidity index of RSV-IgA antibodies. **(d)** BAL neutralization assay. Data from two independent experiments with n = 10-15 mice per group. Data shown with median and interquartile range. In titration experiments each dot represents the mean of the group. For antibody quantification, avidity and neutralization each dot represents one mouse. Mann-Whitney test (b,c) or Kruskal-Wallis with multiple comparisons (d) were performed in which *, $p < 0.05$; **, $p < 0.01$; and ***, $p < 0.001$.

4.2.5 Recurrent exposure to *A.lwoffii* in early life boosts local RSV-IgA responses upon adult re-challenge

So far, the data collected here shows that recurrent *A.lwoffii* exposure in early life can boost the T_{FH} generation and the production of RSV-specific infant antibodies. Moreover, a paper from our group shows that boosting T_{FH} in early life provides protective immunity against re-infection in adulthood (25). Therefore, next I investigated if recurrent *A.lwoffii* exposure in early life had a similar effect. To this end, mice were exposed to *A.lwoffii* three times per week from d3 of life until 10d post 2nd RSV challenge, point at which GC responses for the 2nd infection should be stablished. As before, mice were infected with RSV at day 5 and 15 of life. At 8.5wks of life, when mice are considered adults, they were infected with a high dose of RSV that is sufficient to induce weight loss in the absence of enhanced antibody titres, as previously shown (25).

After 4 days of adult RSV infection, when mice got to the humane end point, lymph node, spleen, blood, BAL and NAL were collected *(**Fig 4.32a**)*. These final *in vivo* studies coincided with a 12-month period of construction within our animal facilities. Associated with this, we encountered a significant increase in the frequency of failed mattings, reduced litter sizes and loss of pups pre-weaning. This greatly affected the final n number in this study, and thus results should only be taken as preliminary indications and definitive conclusions cannot be drawn from the limited set of data presented here. Unfortunately, due to the difficulties highlighted above a single animal (one data point) was included in one of the groups, the RSV infected alone group to be precise. The following description of the data and preliminary interpretations extracted from it are done assuming this single data point is truly representative of the group and acknowledging that the main limitation of this study is the lack of enough n numbers and experimental repeats. The preliminary observations extracted from this dataset are however important to discuss the role of early life *A.lwoffii* exposure in protecting from RSV re-infection in adulthood and to highlight some potential areas to follow up, overall adding value to this thesis.

With this preliminary set of data, no difference in body weight was seen between RSV alone and RSV+*A.lwoffii* group after adult RSV infection *(**Fig 4.32b**)*. No difference in *RSV L* gene in the lung was observed between both groups *(**Fig 4.32c**)*. A slight trend to an increase in LN numbers was however seen in *A.lwoffii* exposed animals *(**Fig 4.32d**)*. Similar T and B cell responses in the mediastinal LN were observed between both groups. Both the mouse that received RSV alone and those exposed to recurrent *A.lwoffii* in early life had similar B cell proportions, but a trend to an increase B cell frequency was observed in *A.lwoffii* exposed mice *(**Fig 4.32e**)*. A trend to a decrease TCR$\gamma\delta^+$ cells was observed in *A.lwoffii* exposed mice, while similar proportions of TCRβ^+ cells were seen for both groups *(**Fig 4.33a,b**)*. This response was accompanied by similar proportions of CD8$^+$ and CD4$^+$ T cells, but CD69 expression on both subsets seemed to be elevated in the RSV alone

challenge mouse *(Fig 4.33c-f)*. Concomitant with the elevated total medLN cell numbers in the *A.lwoffii* treated group, a trend to an increase cell number in mice exposed to the bacteria was observed for all T cell populations analysed *(Fig 4.33a-f)*.

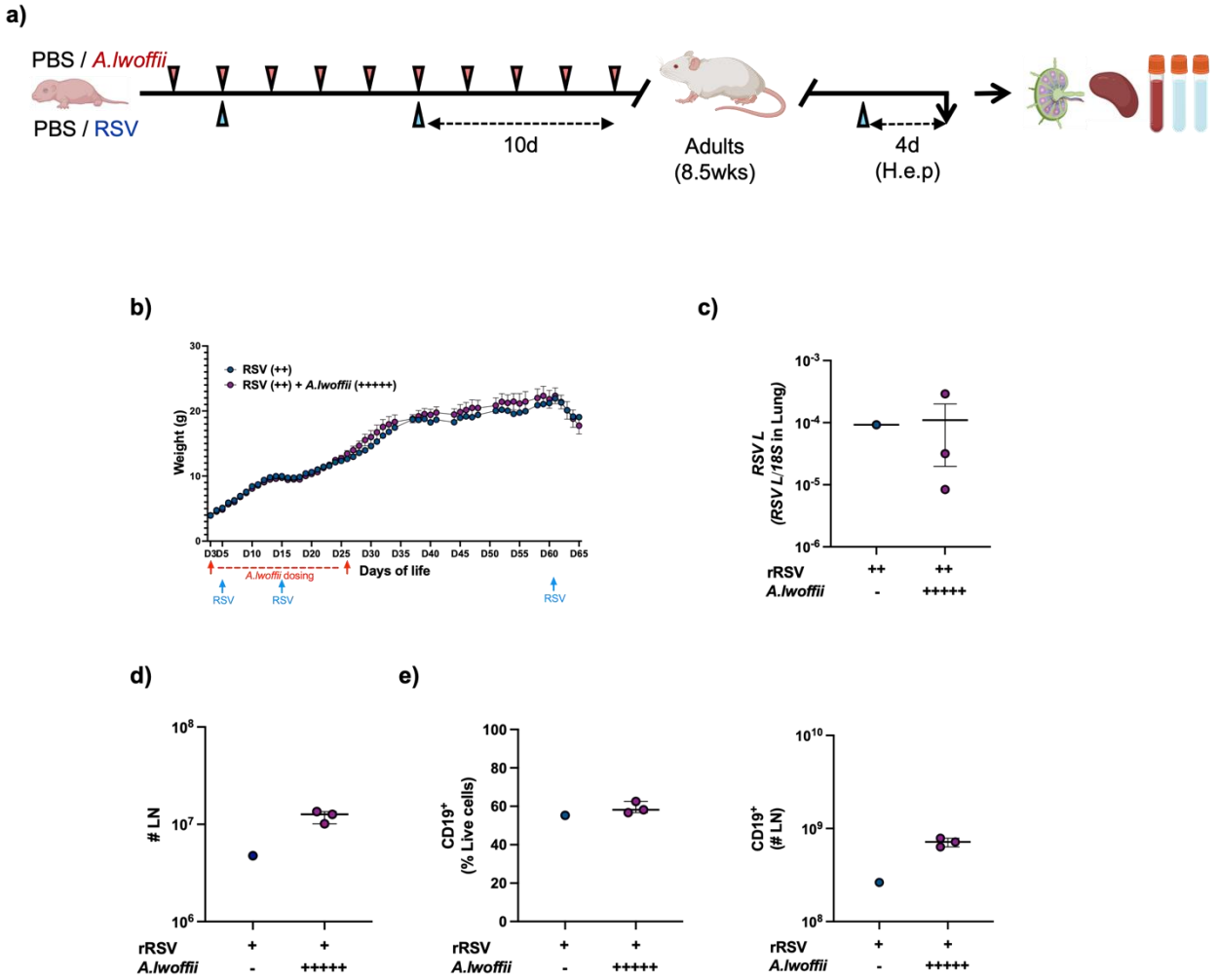


Fig 4.32. No difference in body weight or adult viral titre between A.lwoffii exposed and unexposed RSV infected mice

(a) Balb/c mice were infected with RSV on day 5 and 15 of life and later as adults (8.5wks of life). They were intranasally exposed to *A.lwoffii* or PBS from d3 of life until after 10d post 2nd dose of RSV infection. Lymph node, spleen, blood, BAL and NAL were collected 4d post RSV infection as adults. **(b)** Weight curve of mice with the different treatments. **(c)** *RSV L* relative to *18S* in lung tissue measured by RT-qPCR. **(d)** Lymph node (LN) cell count. **(e)** Percentage and frequency of B cells. Data from one independent experiment with n = 1-3 mice per group. Data shown with median and interquartile range. Each dot represents one mouse. H.e.p = humane end point.

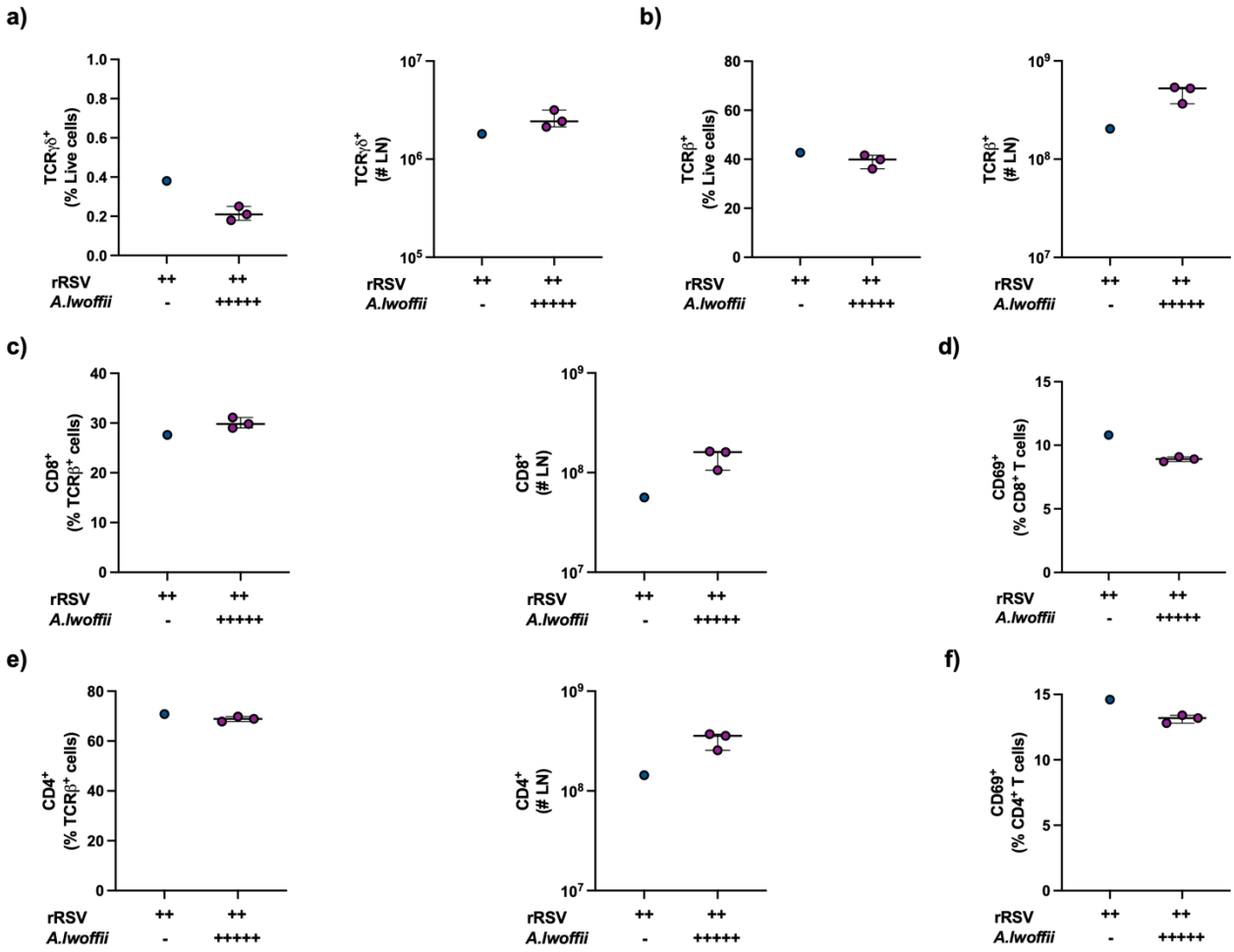


Fig 4.33. Lymph node T cell responses in early life A.lwoffii exposed and unexposed mice re-challenged with RSV as adults

Balb/c mice were infected with RSV on day 5 and 15 of life and later as adults (8.5wks of life). They were intranasally exposed to *A.lwoffii* or PBS from d3 of life until after 10d post 2nd dose of RSV infection. **(a)** Proportion and quantification of TCRγδ and **(b)** TCRβ T cells, **(c)** $CD8^+$ T cells and **(d)** their expression of CD69 as well as **(e)** $CD4^+$ T cells and their **(f)** CD69 expression. Data from one independent experiment with n = 1-3 mice per group. Data shown with median and interquartile range. Each dot represents one mouse

Similar proportions in T_{FH} and GC T_{FH} cells were observed between groups *(Fig 4.34a,b)*, but a trend to a decrease GC B cell and $CD138^+$ proportions were seen in *A.lwofffii* exposed mice when compared with RSV alone treated animals *(Fig 4.34a-d)*. As before, a trend to an increase in cell numbers was observed in bacteria exposed mice for all analysed populations *(Fig 4.34a-d)*.

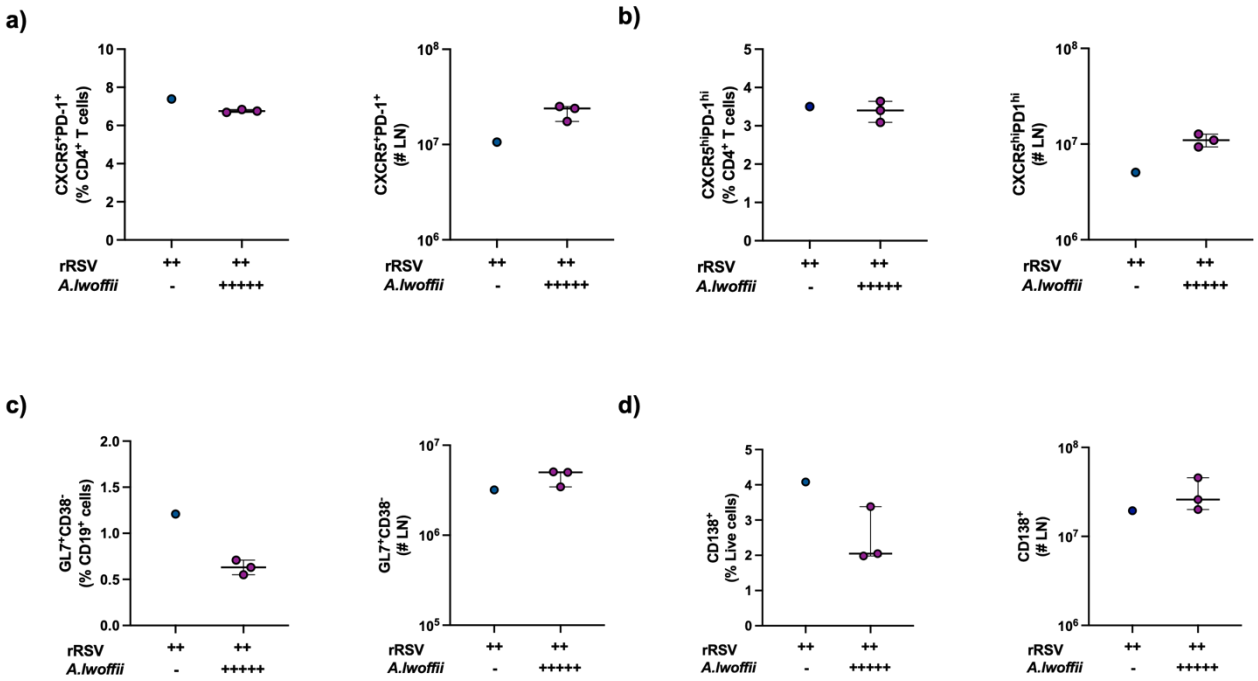


Fig 4.34. Lymph node GC responses in early life A.lwoffii exposed and unexposed mice re-challenged with RSV as adults

Balb/c mice were infected with RSV on day 5 and 15 of life and later as adults (8.5wks of life). They were intranasally exposed to *A.lwoffii* or PBS from d3 of life and until 10d post 2nd dose of RSV infection. **(a)** Lymph node proportion and quantification of T_{FH} cells, **(b)** GC T_{FH} cells, **(c)** GC B cells and **(d)** Plasma cells & Plasma blasts. Data from one independent experiment with n = 1-3 mice per group. Data shown with median and interquartile range. Each dot represents one mouse.

The T and B cell responses were also analysed in spleen. Similar spleen cell numbers were observed for both groups *(**Fig 4.35a**)*. Concomitantly, no difference in B cell proportion and frequency was seen between *A.lwoffii* exposed and unexposed RSV infected mice *(**Fig 4.35b**)*. A trend to an increase $\gamma\delta$ T cells was however seen in mice treated with *A.lwoffii*, but no difference in cell number was observed *(**Fig 4.35c**)*. Similar to the B cell response, no difference in $\alpha\beta$ T cell proportion or frequency, nor in the $CD4^+$ and $CD8^+$ subtypes, or their expression of CD69 was observed between groups in the spleen *(**Fig 4.35d-h**)*. Concomitantly, similar proportions and frequency of T_{FH}, GC T_{FH}, GC B cells and $CD138^+$ cells were observed in the spleen of RSV infected animals when compared with the RSV+*A.lwoffii* group *(**Fig 4.36a-d**)*.

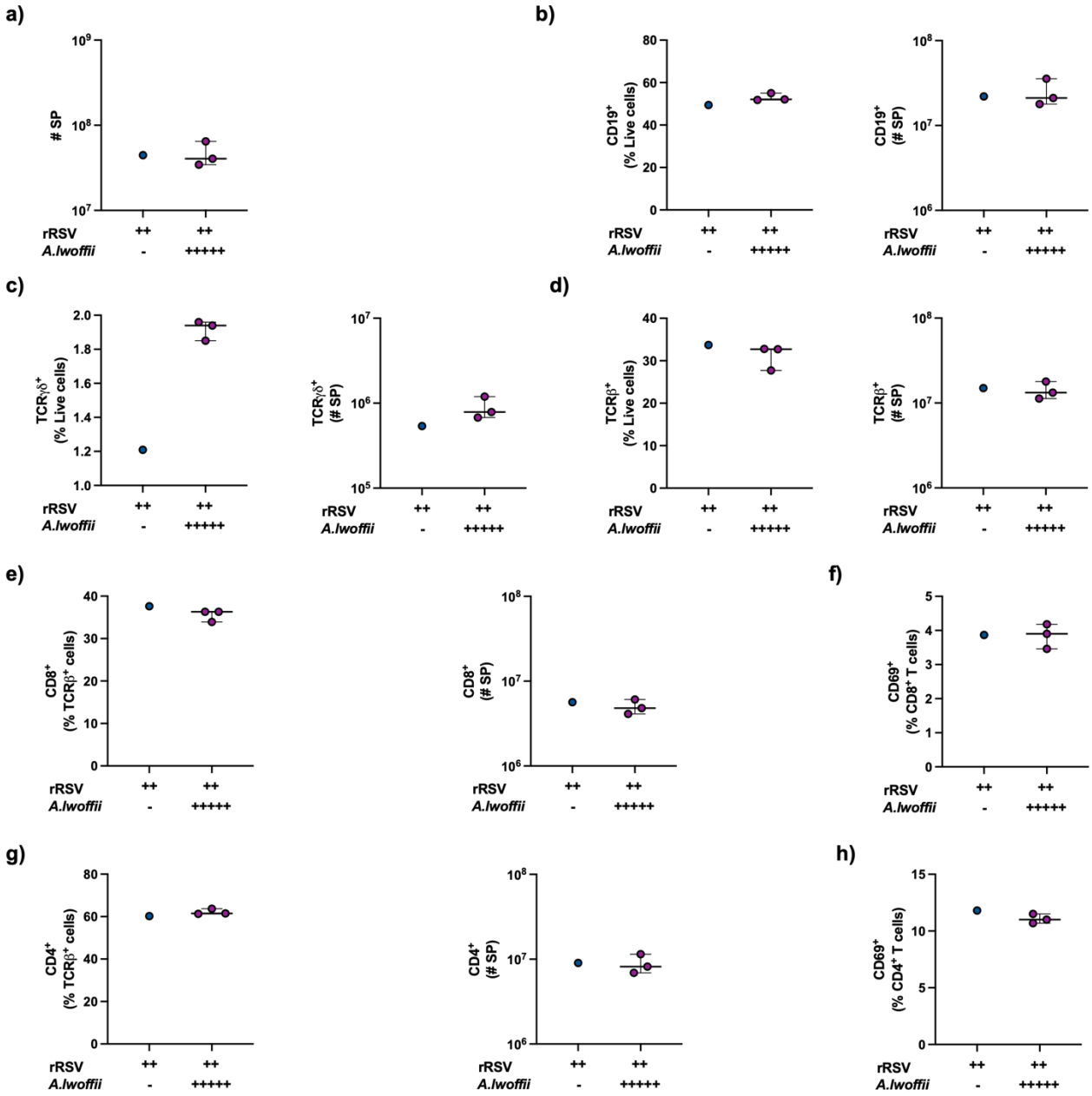


Fig 4.35. Splenic T cell responses in early life A.lwoffii exposed and unexposed mice re-challenged with RSV as adults

Balb/c mice were infected with RSV on day 5 and 15 of life and later as adults (8.5wks of life). They were intranasally exposed to *A.lwoffii* or PBS from d3 of life until after 10d post 2nd dose of RSV infection. **(a)** Spleen (SP) cell count. **(b)** Percentage and frequency of B cells, **(c)** TCRγδ, **(e)** TCRβ T cells, **(f)** $CD8^+$ T cells and **(g)** percentage of $CD8^+CD69^+$ cells as well as **(h)** $CD4^+$ T cells and their **(i)** CD69 expression. Data from one independent experiment with n = 1-3 mice per group. Data shown with median and interquartile range. Each dot represents one mouse.

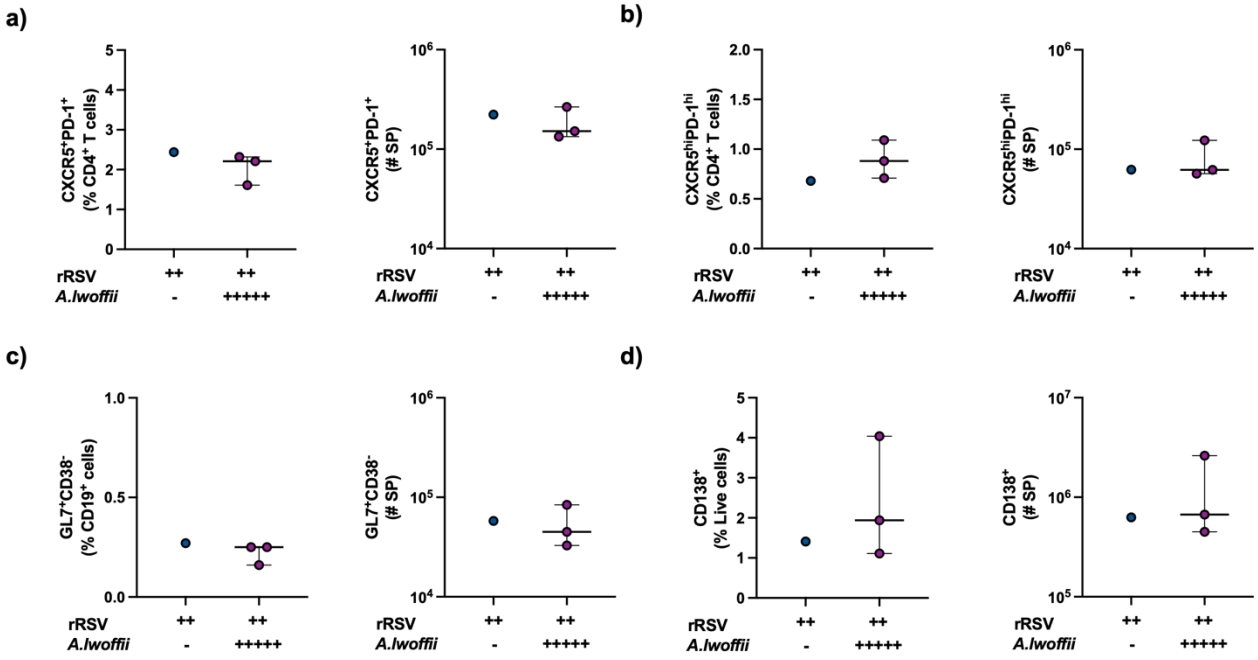


Fig 4.36. Splenic GC responses in early life A.lwoffii exposed and unexposed mice re-challenged with RSV as adults

Balb/c mice were infected with RSV on day 5 and 15 of life and later as adults (8.5wks of life). They were intranasally exposed to *A.lwoffii* or PBS from d3 of life and until 10d post 2nd dose of RSV infection. **(a)** Spleen proportion and quantification of T_{FH} cells, **(b)** GC T_{FH} cells, **(c)** GC B cells and **(d)** Plasma cells & Plasma blasts. Data from one independent experiment with n = 1-3 mice per group. Data shown with median and interquartile range. Each dot represents one mouse.

To analyse if *A.lwoffii* exposure in early life boosts antibody production after adult challenge, both *A.lwoffii*- and RSV-specific antibodies were also analysed. Serum *A.lwoffii*-specific antibody concentrations were still increased in mice that received recurrent *A.lwoffii* exposure in early life, as indicated by increased *A.lwoffii*-Igs, IgG1, IgG2a and IgA *(**Fig 4.37a-d**)*. This was however not translated into an increase in serum RSV-specific antibody titre as mice from both groups showed similar concentrations of RSV-Ig, IgG1, IgG2a and IgA *(**Fig 4.38a-d**)*. Since at the time of sacrifice these were adult mice, 8M of urea were used in the avidity assay. Since use of 8M of urea was sufficient to denature some, but not all, antibody-antigen interactions, particularly at high serum dilutions, an avidity index was calculated. No difference in serum avidity for either RSV-Ig, IgG1, IgG2a or IgA was however observed between groups *(**Fig 4.39a-d**)*.

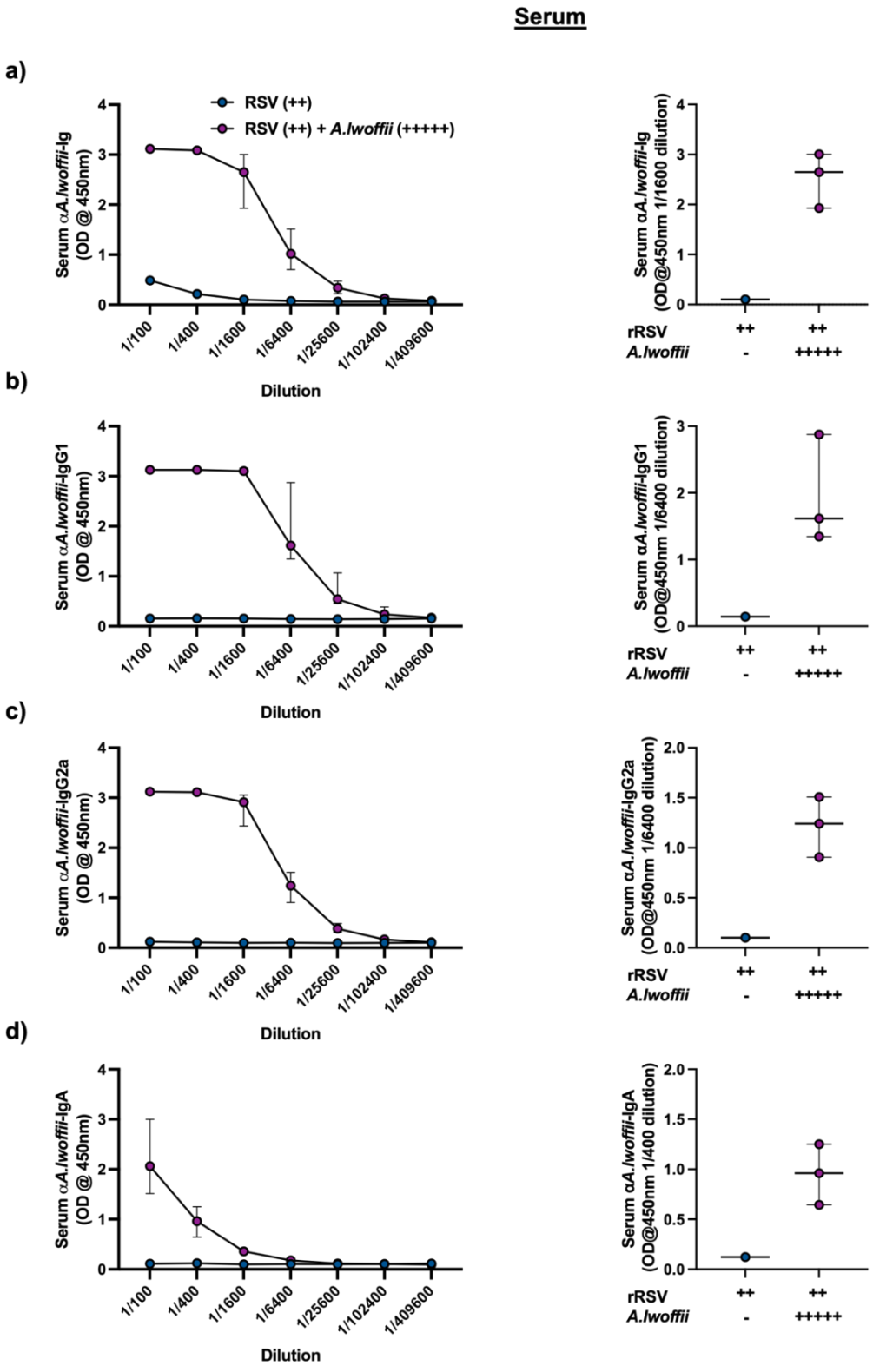


Fig 4.37 Serum A.lwoffii-specific antibody levels are still increased in adult mice that received recurrent A.lwoffii exposure in early life

Balb/c mice were infected with RSV on day 5 and 15 of life and later as adults (8.5wks of life). They were intranasally exposed to *A.lwoffii* or PBS from d3 of life until after 10d post 2nd dose of RSV infection. **(a)** Titration of serum *A.lwoffii*-specific poly-Igs, **(b)** IgG1, **(c)** IgG2a and **(d)** IgA. Data from one independent experiment with n = 1-3 mice per group. Data shown with median and interquartile range. In titration experiments each dot represents the mean of the group. For antibody quantification each dot represents one mouse.

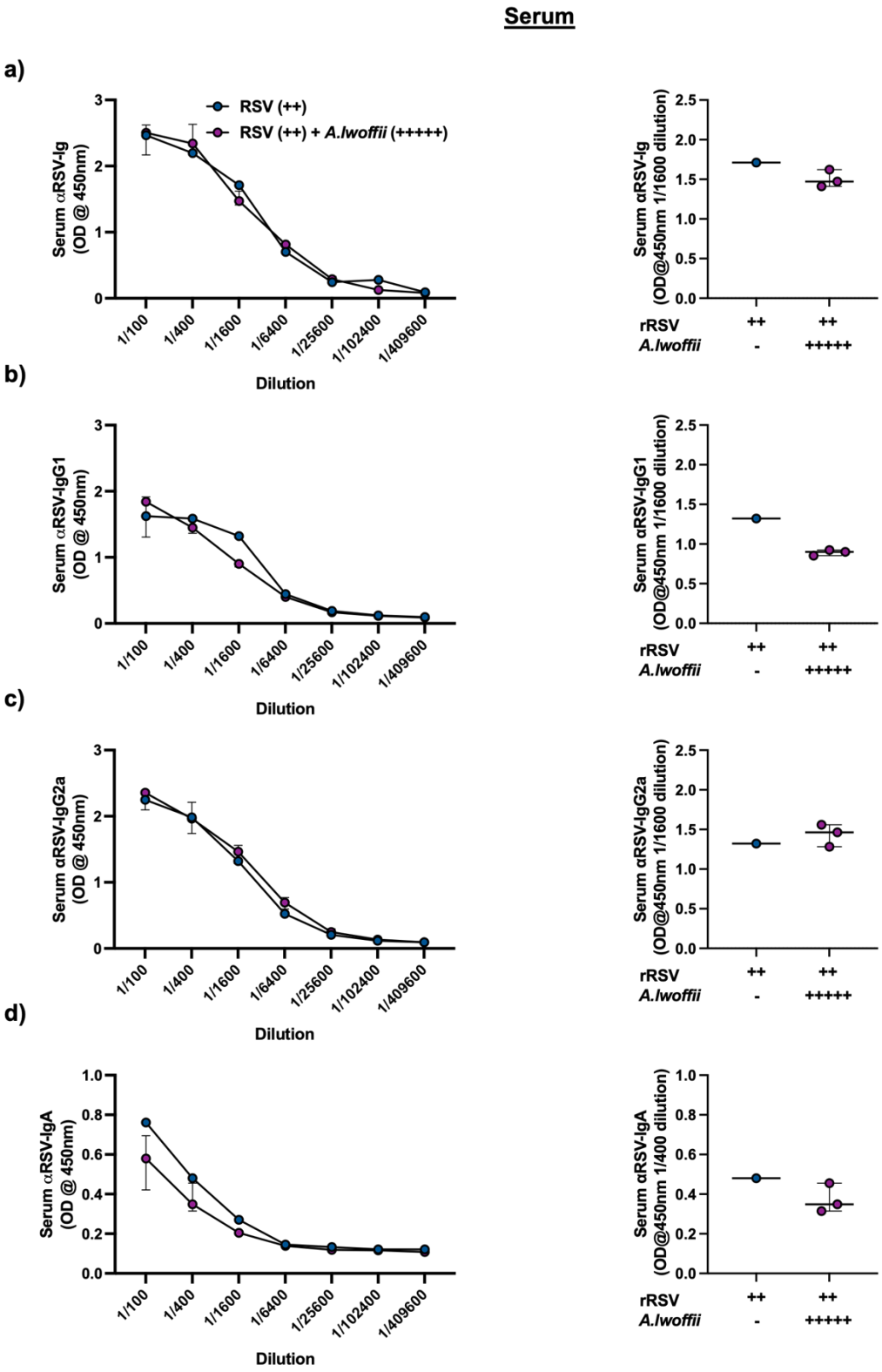


Fig 4.38 No difference in RSV-specific antibody titre in adult mice irrespective of A.lwoffii exposure in early life

Balb/c mice were infected with RSV on day 5 and 15 of life and later as adults (8.5wks of life). They were intranasally exposed to *A.lwoffii* or PBS from d3 of life until after 10d post 2nd dose of RSV infection. **(a)** Titration of serum RSV-specific poly-Igs, **(b)** IgG1, (c) IgG2a and (d) IgA. Data from one independent experiment with n = 1-3 mice per group. Data shown with median and interquartile range. In titration experiments each dot represents the mean of the group. For antibody quantification each dot represents one mouse.

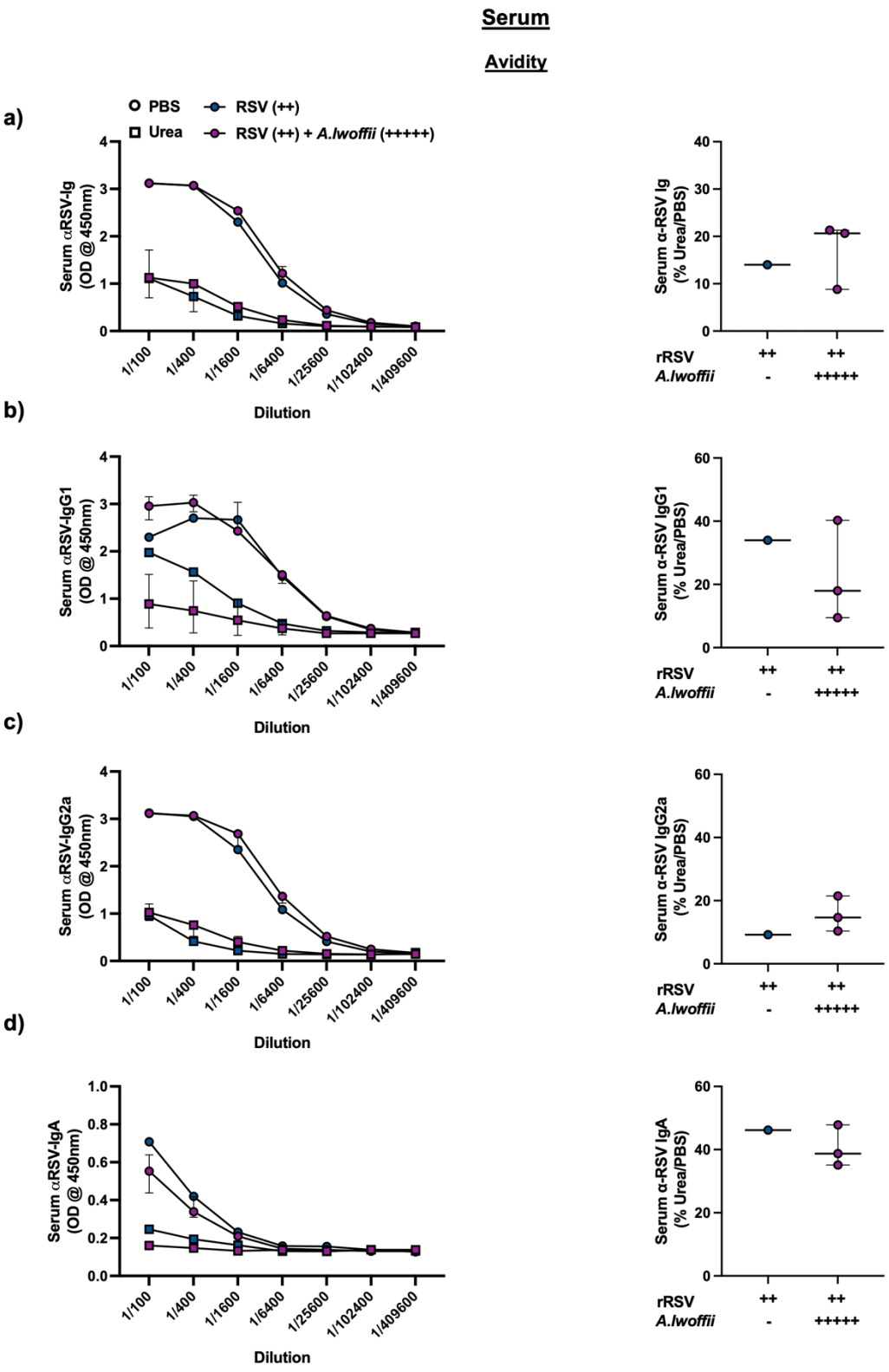


Fig 4.39 No difference in RSV-specific antibody avidity in adult mice irrespective of A.lwoffii exposure in early life

Balb/c mice were infected with RSV on day 5 and 15 of life and later as adults (8.5wks of life). They were intranasally exposed to *A.lwoffii* or PBS from d3 of life until after 10d post 2nd dose of RSV infection. **(a)** Avidity quantification of serum RSV-specific poly-Igs, **(b)** IgG1 **(c)** IgG2a and **(d)** IgA. Data from one independent experiment with n = 1-3 mice per group. Data shown with median and interquartile range. In titration experiments each dot represents the mean of the group. For antibody quantification each dot represents one mouse.

Concomitant with the serum response, an increase in BAL *A.lwoffii*-specific antibody titres, for both *A.lwoffii*-Ig, IgG1 and IgG2, was observed in the *A.lwoffii* treated animals when compared with the RSV alone challenged mouse *(**Fig 4.40a-c**)*.

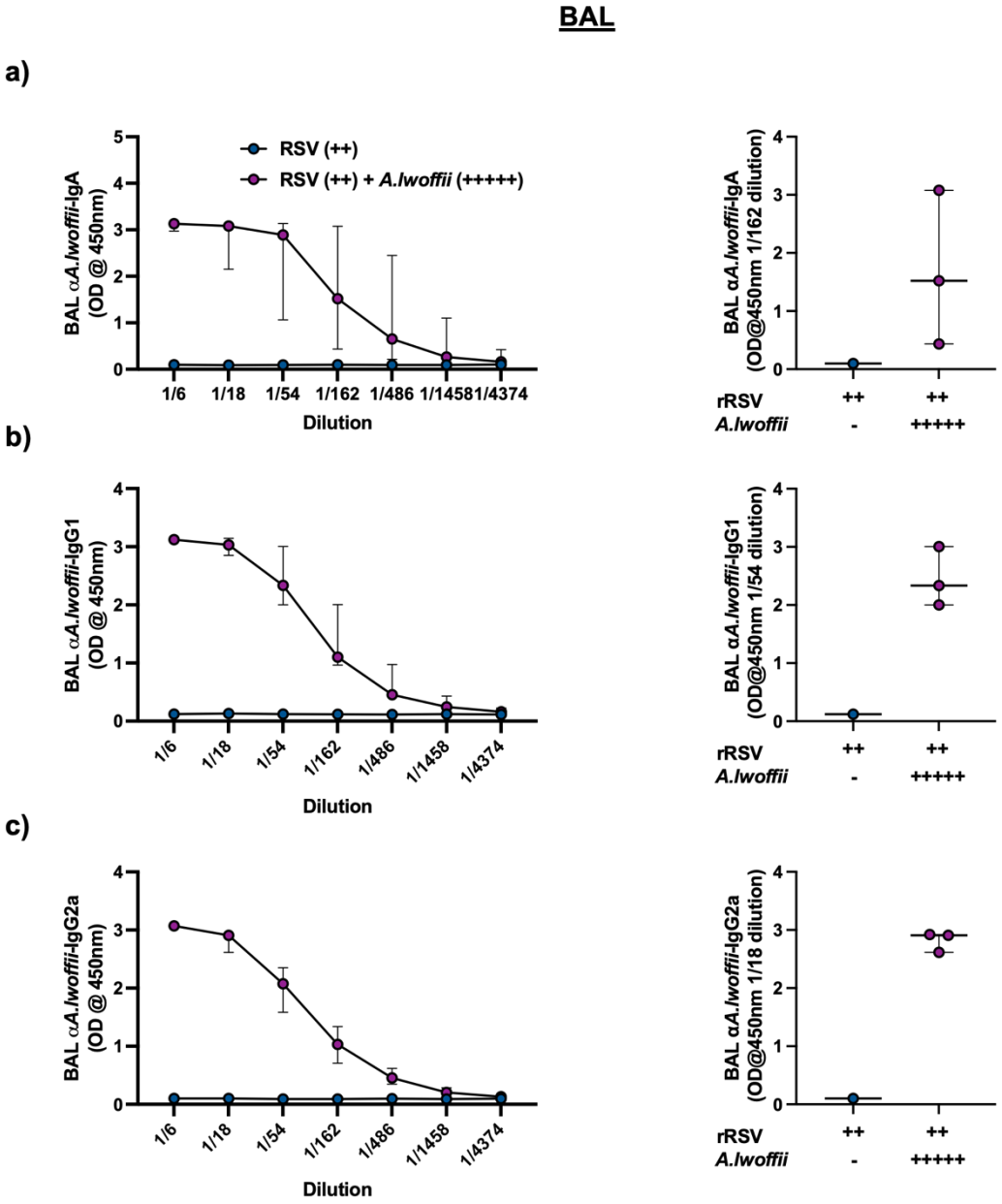


Fig 4.40 BAL A.lwoffii-specific antibody titres are still increased in adult mice that received A.lwoffii exposure in early life

Balb/c mice were infected with RSV on day 5 and 15 of life and later as adults (8.5wks of life). They were intranasally exposed to *A.lwoffii* or PBS from d3 of life until after 10d post 2nd dose of RSV infection. **(a)** Titration of BAL *A.lwoffii*-specific IgA, **(b)** IgG1 and **(c)** IgG2a. Data from one independent experiment with n = 1-3 mice per group. Data shown with median and interquartile range. In titration experiments each dot represents the mean of the group. For antibody quantification each dot represents one mouse.

Interestingly, a trend to an increase BAL RSV-IgA titre was observed in mice exposed to the farmyard microbe in early life when compared with mice only challenged with the virus *(Fig 4.41a)*. This difference was however not replicated for BAL RSV-IgG1 or IgG2a subtypes *(Fig 4.41b,c)*.

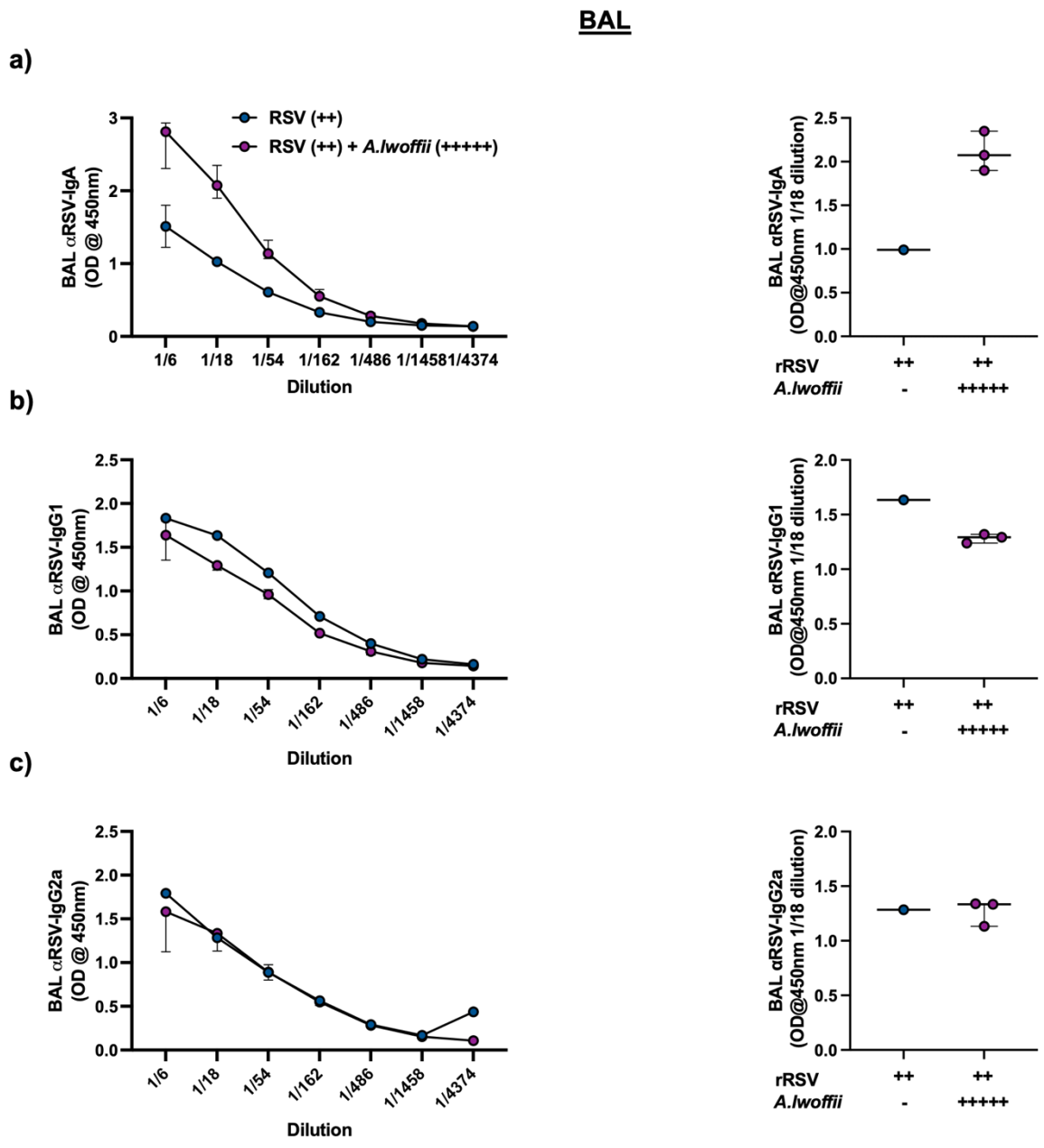


Fig 4.41 Increased adult RSV-IgA antibody titre in BAL of RSV infected mice exposed to A.lwoffii in early life

Balb/c mice were infected with RSV on day 5 and 15 of life and later as adults (8.5wks of life). They were intranasally exposed to *A.lwoffii* or PBS from d3 of life until after 10d post 2nd dose of RSV infection. **(a)** Titration of BAL RSV-specific IgA, **(b)** IgG1 and **(c)** IgG2a. Data from one independent experiment with n = 1-3 mice per group. Data shown with median and interquartile range. In titration experiments each dot represents the mean of the group. For antibody quantification each dot represents one mouse.

Despite the increased BAL RSV-IgA titre, no difference in BAL avidity for any antibody subtype, RSV-IgA, IgG1 or IgG2a, was seen between groups *(Fig 4.42a-c)*. Mice were intranasally exposed

to RSV and *A.lwoffii*; Thus, to analyse the antibody response in the nasal cavity, NAL was collected. As with the lung and systemic response, NAL IgA, IgG1 and IgG2a *A.lwoffii*-specific antibody levels were still increased in adult mice exposed to *A.lwoffii* in early life *(**Fig 4.43a-c**)*. No difference in RSV-specific antibody responses, when looking at both RSV-specific IgA, IgG1 or IgG2a, were however observed between groups *(**Fig 4.44a-c**)*.

Overall, this preliminary experiment suggests the generation of similar responses in the SLOs of adult mice challenged with RSV irrespective of *A.lwoffii* exposure in early life. Local RSV-IgA enhancement is however seen in mice exposed to the bacteria in early life, which may indicate the promotion of TLS by *A.lwoffii*. Nevertheless, properly powered studies, as well as analysis of the lung immune response, need to be carried out before any definitive conclusions can be drawn.

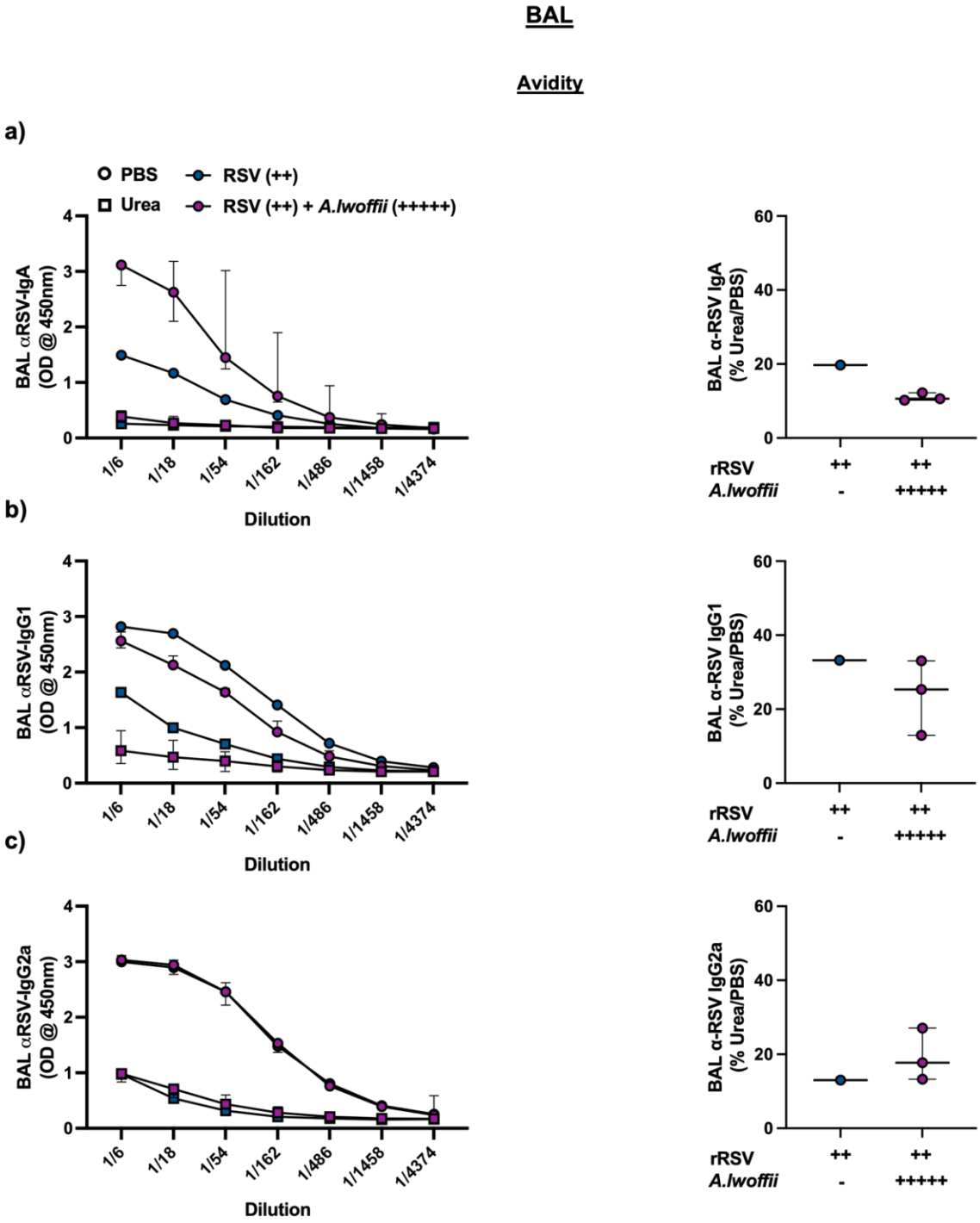


Fig 4.42 No difference in avidity of adult BAL RSV-specific antibodies in mice exposed to A.lwoffii in early life

Balb/c mice were infected with RSV on day 5 and 15 of life and later as adults (8.5wks of life). They were intranasally exposed to *A.lwoffii* or PBS from d3 of life until after 10d post 2nd dose of RSV infection. **(a)** Avidity quantification of BAL RSV-specific IgA, **(b)** IgG1 and **(c)** IgG2a. Data from one independent experiment with n = 1-2 mice per group. Data shown with median and interquartile range. In titration experiments each dot represents the mean of the group. For antibody quantification each dot represents one mouse.

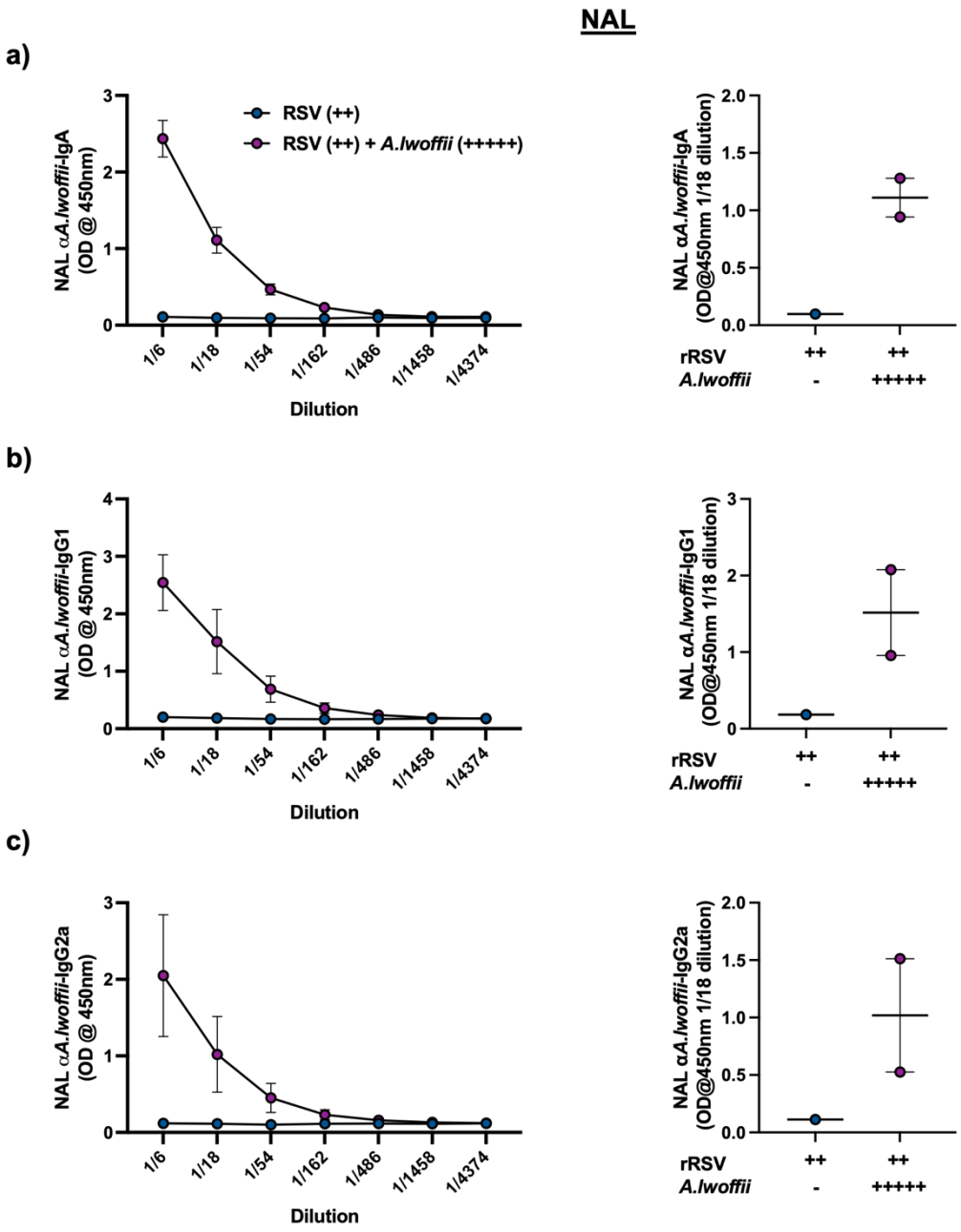


Fig 4.43 NAL A.lwoffii-specific antibody titres are still increased in adult mice that received recurrent A.lwoffii exposure in early life

Balb/c mice were infected with RSV on day 5 and 15 of life and later as adults (8.5wks of life). They were intranasally exposed to *A.lwoffii* or PBS from d3 of life until after 10d post 2nd dose of RSV infection. **(a)** Titration of NAL *A.lwoffii*-specific IgA, **(b)** IgG1 and **(c)** IgG2a. Data from one independent experiment with n = 1-2 mice per group. Data shown with median and interquartile range. In titration experiments each dot represents the mean of the group. For antibody quantification each dot represents one mouse.

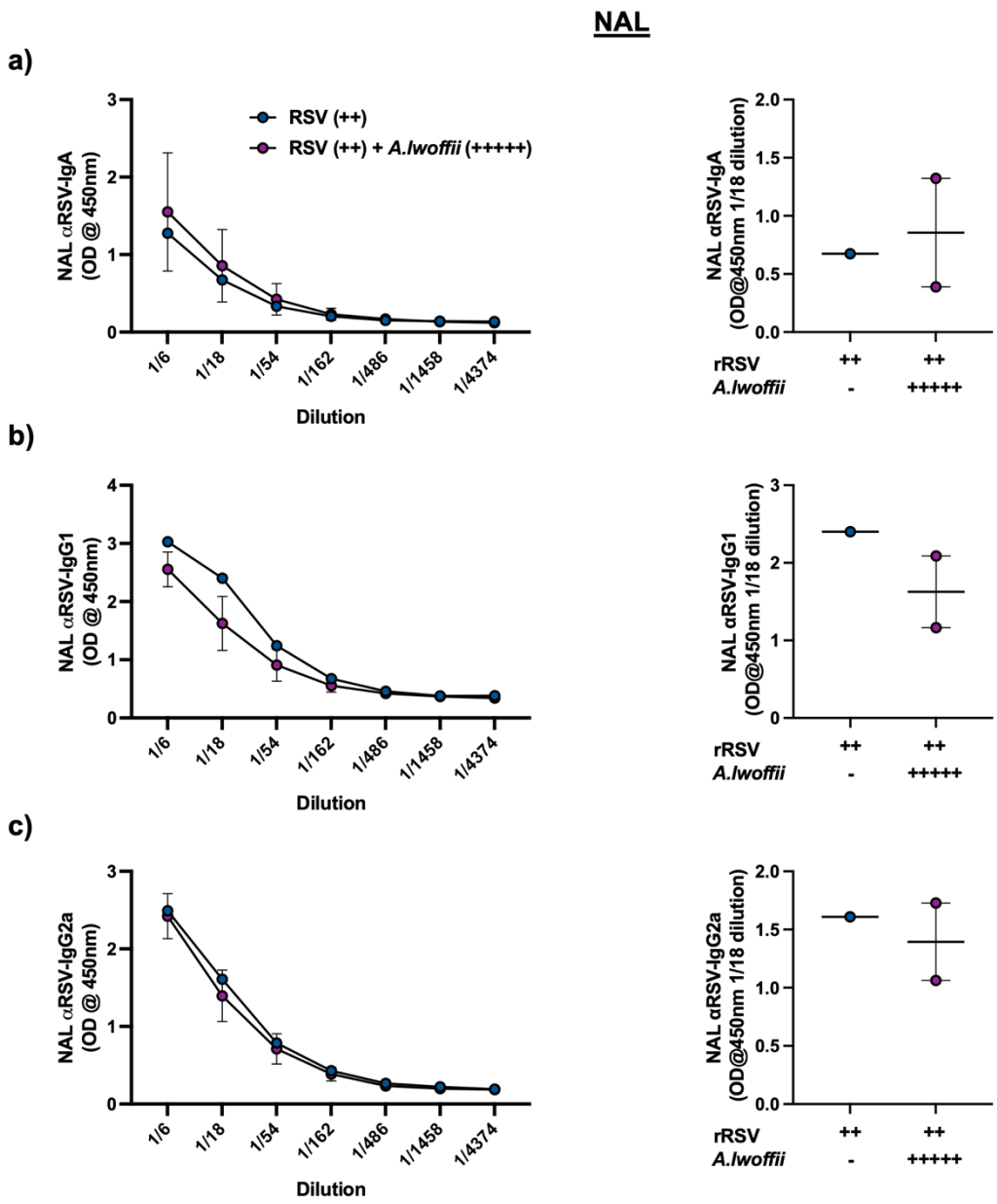


Fig 4.44 No difference in adult RSV-specific antibody titres in NAL of RSV challenged mice exposed to A.lwoffii in early life

Balb/c mice were infected with RSV on day 5 and 15 of life and later as adults (8.5wks of life). They were intranasally exposed to *A.lwoffii* or PBS from d3 of life until after 10d post 2nd dose of RSV infection. **(a)** Titration of NAL RSV-specific IgA, **(b)** IgG1 and **(c)** IgG2a. Data from one independent experiment with n = 1-2 mice per group. Data shown with median and interquartile range. In titration experiments each dot represents the mean of the group. For antibody quantification each dot represents one mouse.

4.3 Discussion:

Due to an increase in IL-2/pSTAT5 signalling in neonates, T_{FH} differentiation is reduced in early life (refer to chapter 3). Adjuvants however can promote humoral responses in infant mice and have a beneficial effect when co-administered with vaccines (21,573,602,603). Likewise, prophylactic exposure to microbes promotes responses against a variety of infections, including respiratory viral infections, in adult mice (501). Exposure to farmyard microbes in children in particular being associated with a reduced risk of suffering from respiratory diseases, clearly suggesting a protective mechanism for specific bacteria found in farm environments (587,588). While exposure to cowshed-derived microorganisms has a protective effect in the establishment of murine early life AHR (503) and childhood wheeze in humans (509), little is known about the role of these bacteria in the protection against respiratory early life infections, particularly in the context of T-dependent antibody responses.

The data in this chapter supports a beneficial role for recurrent exposure to inhaled cowshed-derived bacteria strain *A.lwoffii* in promoting a protective response against RSV infection in early life; with decreased viral load and increased proportion of T_{FH} and $CD138^+$ cells. Recurrent *A.lwoffii* exposure also increases serum RSV-specific total IgGs and IgG2a levels and there is a trend to an increase RSV-specific IgA in the airways. Indeed, in a preliminary study elevated airway RSV-specific IgA is also seen in adult mice infected with RSV which had been exposed to *A.lwoffii* in early life*,* suggesting that a sustained enhancement of local antibodies can be achieved. Recurrent exposure to the farmyard bacteria in early life is however crucial, since shorter dosing regimens used both prophylactically or therapeutically do not promote the same effects.

In parallel to the work presented here, another PhD student in the lab investigated murine local lung responses generated by *A.lwoffii* after RSV infection in early life. In brief, she confirmed that recurrent exposure to *A.lwoffii* is also able to abrogate RSV-induced eosinophilia, mucus hypersecretion and T_{H2} responses in the lung, in particular those generated by $IL\text{-}13^+CD4^+$ T cells. As with humoral responses, the effect is maximal with recurrent *A.lwoffii* exposure, since short-term exposure to the bacteria, both during primary or recurrent RSV infection, only result in partial protection against T_{H2}-associated pathologies (604).

4.3.1 *A.lwoffii* exposure at the time of RSV re-challenge promotes T_{FH} differentiation in infant mice

Living in a farm environment is associated with a reduced risk of suffering from recurrent wheeze in childhood and asthma in later life (503,509). RSV infection in humans is one of the risk factors leading to wheeze (467,578,579). The role of farmyard microbes in promoting protective T cell dependent antibody responses against RSV infection is however unknown. Here recurrent *A.lwoffii*

exposure of RSV infected mice in early life is able to increase the proportion of T_{FH} cells both in the mediastinal LN and spleen, but this is not achieved when fewer doses of the bacteria are used prophylactically. Consistent with my results, sustained inflammation resulting from continuous antigen exposure favours T_{FH} accumulation, as reported in murine models of repeat protein immunisation (85), repeat infection (35), chronic infections like chronic LCMV (127,605), and allergic airway disease driven by OVA (606) or HDM exposure (100). Chronic disease in humans also leads to an increase in T_{FH} frequency as observed during rhinosinusitis (607), rheumatoid arthritis (608), hepatitis B and C (609,610), HIV infection (611) and chronic obstructive pulmonary disease (COPD) (612). Likewise, T_{FH} numbers are increased and positively correlate with the total IgE level in patients suffering from allergic asthma (613,614).

Similar to recurrent *A.lwoffii* exposure, increased mediastinal LN T_{FH} cell proportions and numbers are observed after therapeutic exposure to the farmyard microbe. Several factors could contribute to an increased T_{FH} cell response when *A.lwoffii* is given therapeutically rather than prophylactically. One of them is mouse age. As mice age their T_{FH} and GC B cell responses are increased (25). Thus, exposure to *A.lwoffii* during the third week of life might promote increased T_{FH} responses when compared with exposure during the first week of life, when the ability to generate GCs is decreased. Secondly, antigen dose affects T_{FH} differentiation, with the amount of antigen positively correlating with T_{FH} and GC B cell frequency (85). To try to compensate for age and the associated lung growth, different doses of *A.lwoffii* are given during the first two weeks of life when compared with the third week of life ($1.3x10^8$cfu vs $2x10^8$cfu, refer to chapter 2) as previously described (503). Thus, the increased *A.lwoffii* dose given during therapeutic exposure could help explain the increased T_{FH} proportion. The increase in dose is however minimal and it is accompanied by an increase in lung growth, indicating that per lung area mice would have received similar doses of *A.lwoffii* at one and three weeks of life; making it unlikely to affect T_{FH} differentiation. Thirdly, the timing between *A.lwoffii* exposure and the culling of the mice also needs to be considered. T_{FH} responses precede GC B cell responses, consistent with T_{FH} driving GC development (50,100). The use of IL-21 reporter mice, shows that mediastinal LN T_{FH} cells peak at 7d post immunization to then decrease slightly and be maintained through time (615), suggesting that time post immunisation can alter T_{FH} differentiation dynamics. The study of T_{FH} differentiation over time in this mice model is however complex, as mice are exposed to several doses of both *A.lwoffii* and RSV that can influence and potentiate each other. Therefore, memory T_{FH} cell responses should also be considered when comparing the two *A.lwoffii* dosing regimens as therapeutic *A.lwoffii* is given at the time of RSV re-infection. T_{FH} can accumulate after secondary challenge both when exposed to infection agents or protein immunisation models by arising from memory T cells through a B-cell dependent mechanism (527,616). *A.lwoffii* exposure could therefore be promoting the memory response to RSV.

T_{FH} cells in this model are characterised as CXCR5^{+}PD-1^{+} cells, but their Foxp3 expression is not determined, suggesting that they could also be T_{FR} cells. T_{FR} cells are regulatory cells that co-express T_{FH} and T_{reg} markers and inhibit the GC response (197). T_{FR} cells however normally develop from natural T_{regs} generated in the thymus and therefore are specific for self-antigen and do not expand upon foreign antigen exposure (197–199), making it unlikely for *A.lwoffii* to promote their accumulation. Moreover, here an increase in CD138^{+} cells and *A.lwoffii*- and RSV-specific antibody titre is observed after recurrent *A.lwoffii* exposure, suggesting that the increase in CXCR5^{+}PD-1^{+} cells is driven by T_{FH} accumulation, which promote the GC reaction, rather than T_{FR}, that inhibit it.

Together these results indicate that *A.lwoffii* exposure during RSV re-infection is key in promoting mediastinal LN T_{FH} responses. Several factors may contribute to this observation including continuous antigen exposure, mouse age, timing from *A.lwoffii* exposure and T_{FH} analysis, and promotion of recall responses; most likely a combination of several or all factors leads to the increase in T_{FH} proportion observed.

4.3.2 Enhanced RSV-specific antibody responses are observed after recurrent *A.lwoffii* exposure during early life

In a murine adult model, exposure to a microbial extract promotes the generation of low affinity cross-reactive antibodies that clear viral infection (501), but whether the same mechanism is active in early life is unclear. Recurrent exposure to *A.lwoffii* is not only able to increase T_{FH} proportions, but it can also increase the percentage of CD138^{+} cells, containing both PBs and PCs, in the SLOs. Concomitantly, an increase in RSV-specific IgG and IgG2a response is observed systemically, and locally in the form of RSV-IgA, after continuous exposure to the bacteria. Contrary to the observations in adult mice receiving oral OM-85 (501) however, *A.lwoffii* exposure does not promote the generation of antibodies with broad specificity able to recognise RSV, as shown by the lack of RSV-antibodies expressed by the recurrent *A.lwoffii* alone treated group. Exposure to the farmyard microbe instead enhances the production of RSV-specific, class-switched antibodies. The age of the mice (adult vs early life), the amount and diversity of microbial antigens (OM-85 containing antigens from 21 microbial pathogens vs *A.lwoffii*), the route of administration (oral vs intranasal) and the nature of the viral pathogen (influenza PR8 vs RSV A2) could all be contributing to the difference in the observed antibody response.

Importantly, as shown here, murine *A.lwoffii* exposure increases systemic RSV-IgG antibodies. Levels of early life serum IgG in humans positively correlate with protection against RSV infection, and negatively with severity of infection and risk of hospitalization, suggesting a protective role for *A.lwoffii* exposure in RSV infection (355,617,618). Moreover, recurrent *A.lwoffii* exposure

preferentially promotes RSV-IgG2a production. IgG2a antibodies are linked with T_{H1} responses and viral infection clearance by the mechanism of antibody-dependent cellular cytotoxicity; indicating a mechanism by which *A.lwoffii* exposure could counteract the T_{H2} RSV infection and reduce viral load (226–228). This observation is consistent with a previous report using monoclonal antibodies to protect against RSV infection in Balb/c mice, in which the RSV-IgG2a subtype is also elevated when compared with IgG1, decreasing viral load (619). An environment rich in IFN-γ promotes B cell switch towards IgG2a secretion while IgG1 production is elevated in an IL-4 dependent manner (597–599). A trend to an increase *Ifnγ/Il4* is observed in the mediastinal LN of mice treated recurrently with *A.lwoffii* when compared with PBS and RSV alone. The same trend is observed in mice receiving five doses of the bacteria as well and four doses therapeutically further corroborating these results.

Upon immunization or infection T cell dependent antibody responses can be generated by two different routes: canonical responses, that feature a GC reaction, and non-canonical responses, that lack the formation of GCs and instead promote B cell proliferation and differentiation into $CD138^+$ at extrafollicular (EF) sites (44). As with the GC route, B cell priming for EF antibody responses against protein antigens also requires T_{FH} cells (620). Canonical GC responses are often, but not always, preceded by a short phase of EF proliferation and differentiation, while non-canonical reactions typically have prolonged responses at EF sites (44). Here, recurrent exposure to *A.lwoffii* alone and in combination with RSV is able to drive T_{FH}, GC-T_{FH} and GC B cell differentiation when compared with PBS controls. Concomitantly, recurrent *A.lwoffii* exposure in early life promotes the production of *A.lwoffii*-specific antibodies, that are still upregulated in adult mice, ~40 days post last *A.lwoffii* dose. These observations confirm that *A.lwoffii* exposure can generate a GC response, as long-lasting PCs (LLPCs), able to produce antigen-specific antibody responses long after antigen clearance, are specifically generated though the canonical route (217,621–624).

A trend to an increase mediastinal LN GC-T_{FH} proportion and number is observed in recurrent *A.lwoffii* exposed RSV infected infant mice when compared with mice only challenged with the virus, which was significant in spleen, also suggesting an enhancement of RSV-specific responses by a GC route. No difference in GC B cell proportion or frequency is however observed between these two groups in either of the SLOs, pointing towards an EF route. It is true however that GC responses, unlike EF responses, do not clonally expand in terms of overall cell number once reaching peak production. There is extensive proliferation among GCs but this is accompanied by high apoptosis rates of GC B cells. Thus, GC reach peak cell numbers early, typically 9-12d after antigen recognition, after which they start to involute, potentially explaining the similar GC B cells numbers observed among groups (625–628). Due to the timings of these experiments, with the cull being 15d post primary RSV infection and 5d post re-challenge, we could have missed peak GC

production. Responses at extrafollicular sites peak at 4-6 days post immunization, when $CD138^+$ have differentiated and are able to produce antigen-specific antibodies (44,620). Thus, the elevated RSV-specific antibody response observed after RSV re-challenge in both early life and adulthood could be the result of both LLPCs generated after the first infection by the canonical route or produced by newly differentiated PCs though the non-canonical route and thus are not helpful at discerning which route is promoted by *A.lwoffii* exposure.

A.lwoffii-specific class-switched antibodies, as well as an increase in RSV-IgG2a antibodies are observed after *A.lwoffii* exposure. Historically it was thought that isotype-switched, affinity-matured B cells could only be generated by the GC route, but recent data proves that both these processes can also be generated by an EF response, with some, like class-switching, predominantly occurring outside of GCs (45,629–631). Due to the repeated cycles of SHM, PCs derived from B cells that have undergone the GC differentiation route however have higher affinity and neutralization capacity (211,622,632,633). Neither avidity nor neutralization capacity of RSV-specific antibodies is upregulated after *A.lwoffii* exposure, supporting an EF route for *A.lwoffii* promotion of RSV-specific antibodies. Human RSV re-infection in adulthood, a system that can readily generate GC responses, is however common (568), indicating that antibody affinity maturation and neutralization capacity are specifically downregulated during RSV infection. In both adulthood and early life antibody avidity increases over time for both humans and murine models (20,634), so maybe a longer time between RSV exposure and cull of mice would have allowed for maturation of avidity and neutralization responses. The use of α-CD40L chemicals, that disrupt the GC (217), or mice deficient in Bcl6 expression specifically on B cells, a key marker for GC B cells differentiation (621), as well as analysis of RSV-antibodies over time without RSV re-challenge could help differentiate which precise mechanism is being used by *A.lwoffii* to promote RSV-specific antibody responses.

A.lwoffii exposure can also be promoting protection from RSV infection by enhancing the production of local antibodies. Recurrent *A.lwoffii* exposure in early life promotes BAL RSV-IgA responses in both infants and adults. Similarly, i.n administration of monoclonal RSV-IgA antibodies protects against upper and lower respiratory tract infection in mice (635) and non-human primates (636), indicating a role for IgA mucosal responses at counteracting RSV infection. This increase in IgA titre could be explained by an enhanced homing of SLO generated PCs an circulating memory B cells into the lung where they can secrete IgA (637,638). Memory B cell switch towards IgA-secreting PCs can be promoted at this mucosal site by the high abundance of cognate antigen, activation markers and TGFβ (639,640). Despite the increased BAL RSV-IgA response, similar RSV-IgA titres are observed in the circulation and in the NAL of *A.lwoffii* exposed and unexposed mice, suggesting that most likely local responses are driving the increased lung antibody response. Similar to an influenza re-infection murine model, *A.lwoffii* could be promoting the production of resident memory B cells in the lung, which require local antigen exposure to develop and are quick

to differentiate into IgA producing PCs due to their low activation threshold and their position directly near the infected alveoli (216,641). *A.lwoffii* exposure could also be promoting the formation of TLS (641–643). TLS are upregulated in early life when compared to adulthood both in murine models and infants (288–291,293). TLS can form in lungs during viral respiratory infections, such as influenza (644–646), as well as in other respiratory disorders such as COPD (647). Structures suggestive of iBALT are also present in the bronchi of asthmatic patients, with these structures being more frequent and larger than those seen in healthy individuals (648). RSV infection however does not promote the generation of TLS, but they can be generated in RSV-infected mice treated with IL-21 (649). Thus, similar to IL-21 treatment, frequent *A.lwoffii* exposure could promote TLS formation that in turn could enhance the local immune response. Exposure to microbial signals, such as LPS, promotes the formation of TLS structures in mice (290) which have also been associated with reduced eosinophilia, mucus production and T_{H2} responses (291). Prolonged infection at tissue sites also enhances the production of TLS (650,651), further explaining why these structures could be generated in recurrent exposure to *A.lwoffii* when compared with shorter exposures to the bacteria. Immunohistochemistry staining for CXCR5 and GL-7 on lung sections of these animals could be performed to corroborate this hypothesis.

Despite the increased RSV-IgA response in the lung, no difference in GC responses is seen in the PP of *A.lwoffii* treated mice. In adult mice TLR signaling by commensal intestinal microbiota is associated with increased airway immunity, highlighting the importance of a gut-lung axis (492,501,652). Whether such a strong gut-lung axis exists in infancy, is currently unknown. Concomitant with the intranasal exposure of both *A.lwoffii* and RSV, and the respiratory nature of RSV infection, T_{FH} responses are upregulated in the lung draining lymph node, followed by a reduced, albeit still present, response in the spleen in mice that receive both recurrent *A.lwoffii* and RSV. This is however not observed in the gut, indicating an absence of GCs in the PP of infant mice. This observation is most likely reflective of the young age of the animals and their developing microbiome as exemplified by use of germ-free or antibiotic-treated mice were PP are underdeveloped (653–655). Adult recurrent intranasal exposure to *A.lwoffii* however does not promote any substantial microbiome change both in the lung and gut of WT exposed animals suggesting that *A.lwoffii* protective effects are independent of microbiome composition (656). Dietary antigens also contribute to the induction of T_{FH} and GC B cells in the PP (596). Mice younger than 3wks of age, such as the ones used in these experiments have not yet been weaned, and therefore are most likely exposed to a very limited set of dietary antigens. The antigen delivery route could further affect the production of antibodies in different body sites. In humans, antigen specific IgA antibodies are produced in the upper respiratory tract and gut in cholera toxin B (CTB) intramuscularly vaccinated individuals. Intranasal vaccination with CTB however results in specific IgA production in both upper and lower respiratory tract and genital tract, but not in the gut while rectally vaccinated individuals only produce specific IgA locally (657,658).

In conjunction these observations indicate that i.n recurrent exposure to *A.lwoffii* significantly promotes the secretion of RSV-specific antibodies systemically and locally probably by enhancing both the generation of EF, GC and TLS responses. The proximity to the site of infection and bacteria exposure is however key in promoting *A.lwoffii* dependent responses; highlighting that inhaled, rather than oral, exposure to probiotics may be probably best to promote infant respiratory immunity.

4.3.3 Short *A.lwoffii* exposure regimens fail to promote RSV-antibody mediated immunity

Recurrent *A.lwoffii* exposure promotes the production of T_{FH} and $CD138^{+}$ cells in the mediastinal LN and spleen of infant mice which is associated with an increased RSV specific antibody response. Conversely, shorter doses of the bacteria, both given at the time of initial infection or during re-challenge, fail to promote PB and PC differentiation and to initiate both a systemic and/or local RSV-specific response. Of note, mice exposed to short *A.lwoffii* regimens also fail to increase *A.lwoffii*-specific antibody titres, indicating a role between strong *A.lwoffii* responses and enhancement of RSV-specific antibodies. These results are in accordance with previous studies in human children and adults that evaluate the relationship between a farming environment and asthma and allergy prevalence. As observed here, early exposure to farming environment is crucial in conferring protection against allergies, as highlighted by the lower occurrence of asthma, hay fever and atopic sensitization in children exposed to a farming environment when they are younger than one year of age when compared to children exposed between one and five years (659). As evidenced by our findings, frequent exposure to the farming environment proves to be more effective at conferring protection, since full-time farming activities have a higher protective effect when compared with part-time farming (660).

RSV can cause re-infection throughout human life and even during the same cold season, indicating that memory B cell responses both in early life and adulthood are limited (9). Defective RSV-IgA B cell memory formation is observed after human adult RSV infection, a process that is linked with RSV ability to cause recurrent symptomatic infections (568). The preliminary data of this thesis shows that RSV-IgA responses are upregulated in the BAL of adult mice exposed to *A.lwoffii* in early life, indicating a role for *A.lwoffii* at promoting either long-lasting or rapid local antibody responses. No difference in body weight after RSV re-challenge, nor in RSV viral load or antibody avidity or neutralization capacity is however observed in these mice, suggesting that the increased local antibody response is unable to counteract viral infection and protect from RSV re-infection in adulthood. One of the caveats of the data presented here is the lack of study of memory B cell responses. The preliminary adult experiment however indicates that early life exposure to *A.lwoffii* does not protect from RSV re-infection in adulthood, suggesting that the T and B cell memory generated by *A.lwoffii* in early life would be at best limited and rapidly waning. Concomitantly,

continuous exposure to the farm environment in humans, and particularly life-long exposure from childhood until adulthood, proved to be most optimal at reducing asthma risk (659,661). This data combined suggests that recurrent exposure to the farmyard microbe *A.lwoffii* from early life is crucial to promote a strong immune response against RSV infection.

4.4 Concluding remarks:

Consistent with the original hypothesis, the data of this chapter indicates a protective role for recurrent *A.lwoffii* exposure in infant RSV disease. Recurrent exposure to the farmyard microbe in early life promotes viral clearance and an increase in T_{FH} and $CD138^{+}$ responses in both mediastinal lymph nodes and spleen of infant mice while no response is observed in PP. Probably both by promoting EF and GC responses as well as the formation of TLS, continuous *A.lwoffii* exposure enhances the RSV-specific antibody response both systemically, by driving the production of RSV-IgG2a antibodies that are crucial at counteracting viral infections, and locally, in the form of RSV-IgA. While fewer doses of *A.lwoffii* can replicate some of the signatures of the recurrent model, the complete phenotype is not observed; indicating that, not unlike microbial protection provided in the context of asthma, early and repeated exposure to farmyard microbes is crucial to promote protection against RSV infection. Since recurrent *A.lwoffii* exposure is sufficient to promote T_{FH} responses in early life, the pro-T_{FH} environment generated by the bacteria will be further analysed in the following chapter.

5 Results III: *A.lwoffii* generates a pro-T_{FH} environment in cDC2s and B cells

5.1 Introduction:

5.1.1 cDC2 are the main primers of naïve CD4$^+$ T cell responses, while B cells promote a GC-T_{FH} signature

DCs are professional APCs bridging the innate and adaptive immune system (662). DCs are a heterogenous cell population originating from bone marrow progenitor cells that can be characterized by their ontogeny and function. Monocyte progenitor cells can differentiate into two populations: monocytes or common dendritic cell progenitors (CDPs); with macrophage colony-stimulating factor (M-CSF) promoting differentiation towards the first and fms-like tyrosine kinase 3 (FLT-3) the latter. CDPs can be further subdivided into conventional DCs (cDCs) and non-conventional DCs. cDCs are characterized by expressing the transcription factor ZBTB46 as well as CD45, CD135 (FLT3) and CD11c on their membranes. They can be further subtyped into type 1 (cDC1s), induced by BATF3 and IRF8 and expressing CD8a/CD103, and type 2 (cDC2s), induced by IRF4 and predominantly expressing CD11b and SIRPα. Plasmacytoid DCs (pDCs) are characterised by the E2-2 transcription factor and the expression of PDCA-1 on their surface (663).

Given the right experimental conditions, most DC subsets can prime T_{FH} cells (reviewed in (83)). Due to their preferential expression of MHC-II however, cDC2s are the major DC subset in priming CD4$^+$ T cell responses (271,664–666). Similarly, and probably also due to their unique location proximal to the B cell zone of the SLOs, cDC2s are also considered the dominant T_{FH}-priming DCs with *Zbtb46* and *Irf4* deficiencies resulting in the absence of T_{FH} and humoral responses (166,271,272,667). Relevantly, cDC2s play a dominant role in driving T-cell dependent antibody responses against inhaled antigens (272) and during chronic lung injury (612). Selective migration of RSV F-HLA-DR$^+$ DCs to the nasal mucosa, but not monocytes, highlights their likely role as primary APCs during RSV infection in humans (397). cDC2s can produce pro-T_{FH} cytokines, such as IL-6, and limit IL-2 signalling by quenching it from the microenvironment through the production of soluble CD25, thereby promoting T_{FH} differentiation from naïve CD4$^+$ T cells (141,166,668,669).

The function of B cells as professional APCs has been largely understudied. DCs have the structural and membrane capacity to engage in the mechanisms of endocytosis of large particles, including phagocytosis. The membrane structure of B cells limits their antigen uptake mostly to BCR-mediated endocytosis (670). Specific B cell subsets, such as B1-B cells, can however phagocyte pathogens but this mechanism is also dependent on BCR signalling (671). When BCR is involved in antigen detection and capture, antigen is recognised as foreign and processed through the MHC-II loading pathway that can then be presented to cognate T_{FH} cells (206). This makes B cells usually incapable of priming CD4$^+$ T cells due to the rarity of antigen-specific, and thus antigen-presenting, B cells early in the immune response. Localizing in the follicles, B cells

are also not strategically positioned to sample antigens from the site of infection nor to prime T cells (672). Under specific experimental conditions, such as high antigen load, however B cells can prime T_{FH} responses (673).

Despite B cell relative inability to prime T_{FH} responses, they are crucial in driving full maturation of pre-T_{FH} into fully effector GC-T_{FH} (38,674,675). B cell antigen presentation to T_{FH} cells occurs in a competitive environment, in which only B cells with high affinity BCRs are able to enhance expression of antigen/MHC-II on their membranes to efficiently interact with cognate T_{FH} cells; promoting both T_{FH} and B cell survival and differentiation (50,676–678). As with DCs, the promotion of a GC-T_{FH} phenotype is dependent on B cell production of a pro-T_{FH} microenvironment characterized by high affinity antigen presentation, strong co-stimulatory interactions and the presence of IL-6 (132,679). Moreover, constant GC B cell interaction with GC-T_{FH} is required to maintain T_{FH} GC phenotype, as disruption of B cell signalling by CD40 or ICOS-L blockage leads to T_{FH} de-differentiation (85).

5.1.2 TLR signalling leads to enhanced mediator secretion and antigen presentation

While antigen recognition through BCR is key in driving antigen-specific B cell responses, similar to innate immune cells, both DCs and B cells can recognise signals from the environment through PRRs that are able to recognise DAMPS and PAMPs (680). In contrast to antigen-recognition receptors, expression of PRRs allows APCs to recognize broad molecule types and induce a nonspecific immune response against infection or tissue damage (681). PRRs can generally be subdivided into five main subtypes, based on their location, structure and function: Absent in melanoma-2 (AIM2)-like receptors (ALRs), C-type lectin receptors (CLRs), Nucleotide oligomerization domain (NOD)-like receptors (NLRs), Retinoic acid-inducible gene-I (RIG-I)-like receptors (RLRs) and Toll-like Receptors (TLRs) (681).

The activation of TLR signalling is crucial to the induction of antigen-specific adaptive immune responses by promoting DC activation and maturation (680). Likewise, B cells express TLRs and use them in concert with BCR-cell signalling during adaptive immunity (682). Non-specific endocytosis and BCR-dependent endocytosis leads to antigen/MHC-II loading on immunoproteasomes in cDC2s and B cells respectively (670). TLR signalling on APCs however can lead to an increased activation and maturation state that is able to enhance their antigen presentation abilities linking innate immunity to enhanced adaptive immune responses (680–684).

To date, 10 TLRs have been identified in humans (TLR1-10) and 12 in mice (TLR1-9 and TLR11-13). TLRs 1-9 are conserved between both species, but TLR8 is non-functional in mice (680,685). TLRs are found in distinct cellular locations to give response to the high variability of infection agents. Cell surface TLRs (TLR1, 2, 4, 5 and 6) mainly recognize membrane components of

microorganisms, such as lipids, proteins and lipoproteins. Intracellular TLRs found in endosomes (TLR3, 7, 8 and 9) recognise nucleic acids derived from pathogens or self-nucleic acids in a disease condition. TLR4 localizes in the plasma cell membrane, but can be endocytosed upon activation. This change in cell location also promotes a switch in intracellular signalling. TLRs can form homo or hetero-dimers, but all share a similar cytoplasmic portion which by activating different intracellular pathways culminate in the production of pro-inflammatory cytokines and/or type I IFNs. TLR signalling can also alter the expression of chemokine receptors, promoting cell migration towards the SLOs, and co-stimulatory markers, leading to enhanced antigen presentation (680–682). Moreover, TLR signalling promotes the crosstalk between different endosomal vesicles allowing antigen/MHC-II loading and membrane expression (683) (*Diagram 5.1*). Due to TLRs ability to promote activation of immune cells, TLR-stimulating adjuvants are routinely used in vaccination strategies (686).

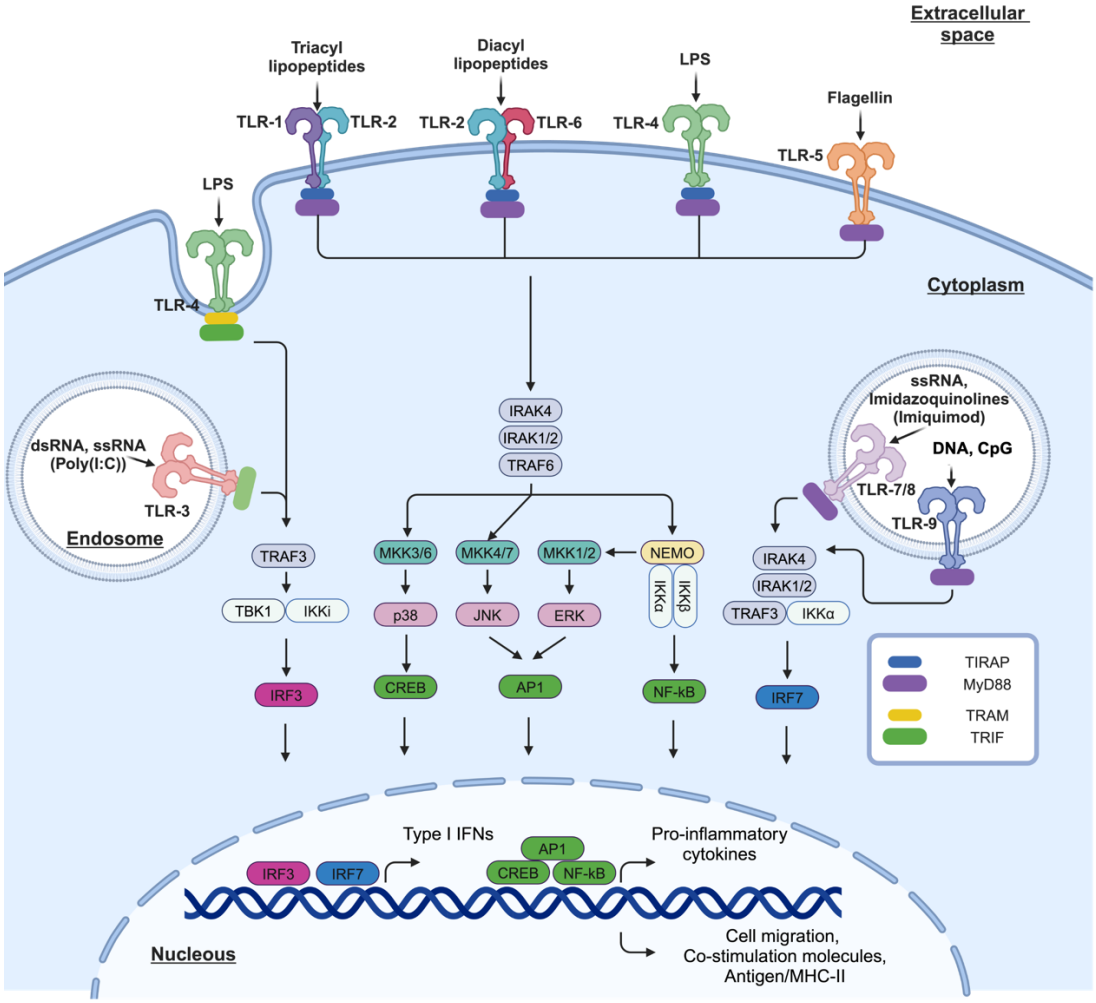


Diagram 5.1. TLR signalling pathways

9 TLRs are shared between mice and humans. TLRs can be located in different cellular compartments which allows them to recognise different DAMPS and PAMPs. Through activation of several signalling pathways TLRs can promote the secretion of type I interferons and pro-inflammatory cytokines as well as enhance cell migration, upregulate cell surface co-stimulation molecules and orchestrate antigen/MHC-II loading; thereby promoting APCs antigen presentation abilities. Adapted from (680).

5.1.3 Hypothesis and Aims

cDC2s are the main primers of T_{FH} cell responses while B cells promote terminal T_{FH} cell differentiation towards a GC-T_{FH} phenotype, and are required to maintain it. In the previous chapter a farmyard microbe, *Acinetobacter lwoffii F78*, was able to promote T_{FH} responses *in vivo* during an early life RSV infection (refer to chapter 4). The mechanisms leading to this enhanced T_{FH} and antibody response, are however unknown.

Therefore, the hypothesis of this chapter is that:

Direct recognition of A.lwoffii by cDC2s and B cells promotes a pro-T_{FH} environment via TLR-sensing that can drive T_{FH} responses in early life.

To address this hypothesis, the aims of this chapter are:

1. To analyse the difference in cDC2s and B cell secretion of a pro-T_{FH} factor between early life and adulthood

2. To investigate the production of a pro-T_{FH} signature by early life cDC2s and B cells in *A.lwoffii* exposed and unexposed RSV infected mice

3. To assess the ability of BM-derived cDC2s and B cells *in vitro* to generate a pro-T_{FH} environment when exposed to *A.lwoffii*, RSV and different TLR ligands

4. To determine the ability of *A.lwoffii*- and RSV-exposed DCs to drive T_{FH} differentiation *in vitro*

5.2 Results:

5.2.1 Soluble CD25 expression is increased in the SLOs of adult mice

Neonatal mice are characterised by having an enriched IL-2 microenvironment when compared to adults, contributing to the reduced T_{FH} differentiation observed in early life (refer to chapter 3, (25)). Given IL-2 potent ability to promote T cell proliferation and T_{reg} differentiation while suppressing T-cell dependent antibody responses, adult mouse models have suggested the existence of multiple mechanisms to tightly regulate IL-2 availability (36,165–167). One such mechanism is via CD25, the IL-2Rα subunit that possesses high affinity for IL-2, which has a secretory form that can quench IL-2 from the microenvironment; a process that is associated with increased T_{FH} differentiation (166). To investigate soluble CD25 (sCD25) expression in early life and adulthood, sCD25 concentration was analysed in different tissues from mice of different ages and RSV infection status.

First, serum from naïve mice at different ages was extracted and sCD25 concentration was determined by ELISA. Serum sCD25 concentration was reduced in young pups, peaked at 2-3wks of life and significantly decreased in adulthood *(**Fig 5.1a**)*. To analyse the expression of sCD25 in an infection context, 1wk and 8wk C57/BL6 mice were infected with $2.5x10^5$ pfu of RSV and were culled 3d post infection, a timepoint when T_{FH} responses are starting to develop *(**Fig 5.1b**)*. Serum from these mice was collected and an increased sCD25 concentration was detected in 1wk old RSV infected animals when compared with 8wk old mice *(**Fig 5.1c**)*. Likewise, sCD25 was increased in the BAL of young mice in the steady state, but similar levels of the receptor were seen after neonatal and adult RSV infection *(**Fig 5.1d,e**)*.

A previous study reported quantification of sCD25 in spleen supernatant by analysing sCD25 expression after spleen disruption to generate a splenocyte single-cell suspension (166). Thus, to investigate organ-specific sCD25 expression in early life and adulthood, thymus, mediastinal LN and spleen from naïve and RSV infected neonatal and adult mice were collected. Mirroring the systemic response, thymus of 1wk old mice showed increased sCD25 expression when compared to adults both in the steady state and after viral infection *(**Fig 5.1f,g**)*. The response was however opposite in the SLOs, since in both mediastinal LN and spleen sCD25 expression was increased in naïve and RSV infected adult mice *(**Fig 5.1h-k**)*. The thymus involutes with age, shrinking in size (295–297), spleen and lymph node are however bigger in an adult mouse when compared to a neonatal counterpart which might explain the differences in sCD25 observed between age.

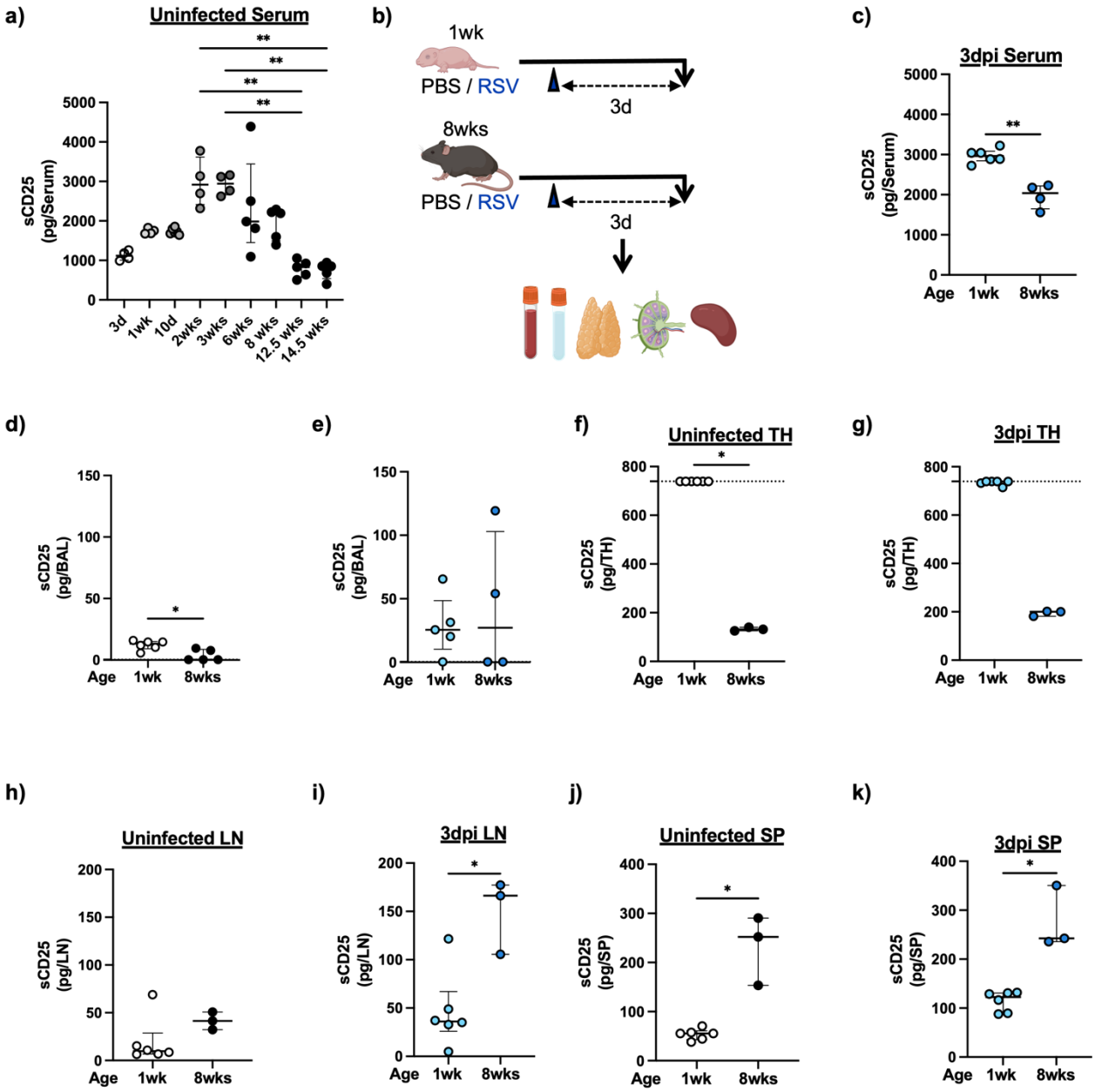


Fig 5.1. Soluble CD25 is increased in the SLOs of adult mice

(a) Serum from uninfected C57BL/6 mice of different ages was harvested and sCD25 levels were quantified by ELISA. **(b)** 1wk and 8wk old C57BL/6 mice were infected with RSV and harvested 3dpi when blood, BAL, thymus, mediastinal and spleen were obtained. **(c)** sCD25 levels on the serum of RSV infected neonatal and adult mice. **(d)** sCD25 levels on the BAL of uninfected and **(e)** RSV infected neonatal and adult mice. **(f)** sCD25 levels on the thymus supernatant of uninfected and **(g)** RSV infected neonatal and adult mice. **(h)** sCD25 levels on the mediastinal lymph node supernatant of uninfected and **(i)** RSV infected neonatal and adult mice. **(j)** sCD25 levels on the spleen supernatant of uninfected and **(k)** RSV infected neonatal and adult mice. Data from one (b-k) or two (a) independent experiments with n = 3-6 mice per group. Data shown with median and interquartile range. Each dot represents one mouse. Top dotted line represents top limit of detection for the given assay. Kruskal-Wallis with multiple comparisons test (for a) and Mann-Whitney test (for c-k) was performed in which *, $p < 0.05$; **, $p < 0.01$; and ***, $p < 0.001$.

sCD25 production in spleen occurs in a cDC2-dependent and T cell-independent manner (166). Differences in cDC2s ability to produce sCD25 between neonates and adults could therefore explain the altered concentrations of sCD25 observed with age. To investigate this, 1wk and 8wk old mice were infected with RSV, or left uninfected, and spleen was harvested 3d post infection. The ability of cDC2s to express membrane CD25 (mCD25) and intracellular CD25 (iCD25), as a surrogate to determine sCD25, were analysed by flow cytometry *(Fig 5.2a,b)*.

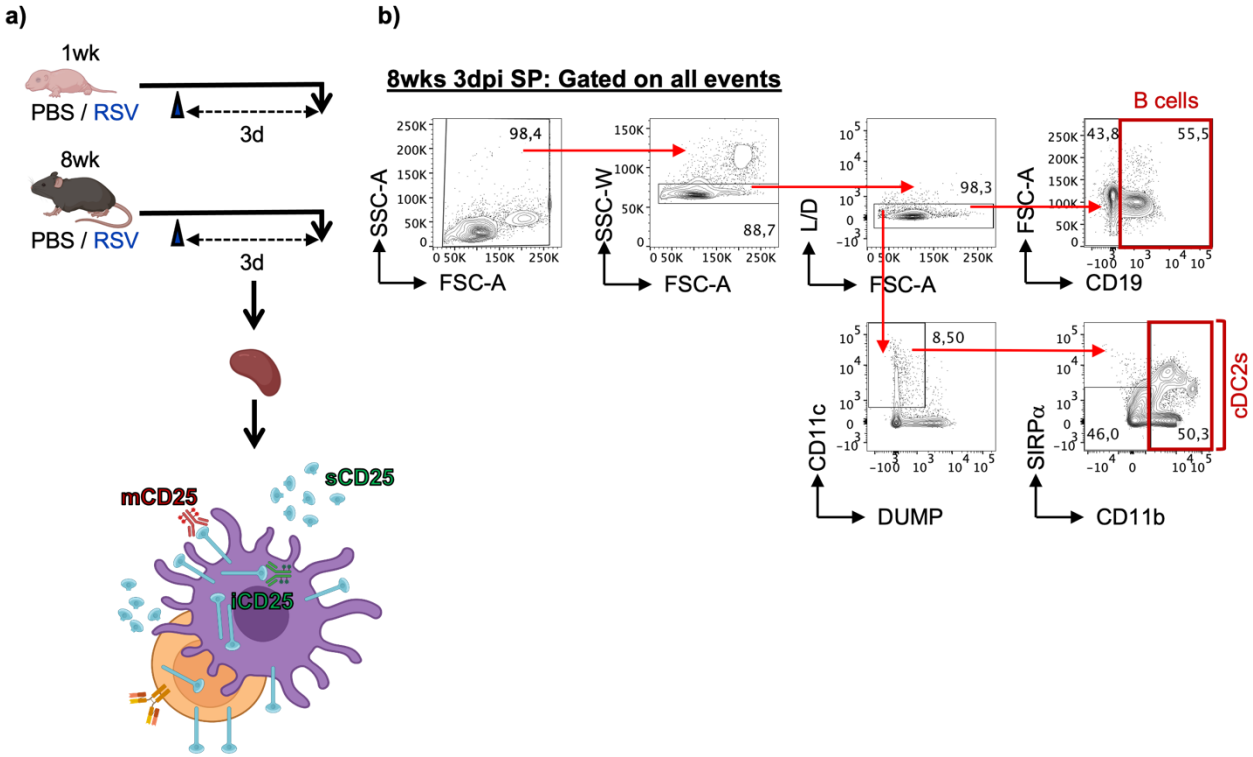


Fig 5.2. Gating intracellular CD25 and membrane CD25 in cDC2s and B cells to investigate CD25 secretion in vivo

(a) 1wk and 8wk-old C57BL/6 mice were infected with 2.5 × 10^5 PFU RSV A2 or PBS i.n. Spleen was harvested 3d post infection, splenocytes were isolated and stimulated with PMA and Ionomycin in the presence of BFA. cDC2s and B cell production of intracellular CD25 (iCD25) and membrane CD25 (mCD25) were analysed as a surrogate way to investigate CD25 secretion *in vivo*. **(b)** Representative flow cytometry strategy for cDC2 and B cell isolation. From all events doublets were excluded and live cells were selected as UV live/dead negative cells. B cells were gated as $CD19^+$ cells while cDC2s were selected as $CD11c^+CD11b^+DUMP^-$ cells. DUMP channel consists of CD90.2 and Nkp46 markers.

The percentage of cDC2s expressing iCD25 in the steady state was significantly increased in 8wk old mice when compared with 1wk old mice, while the opposite was observed for mCD25 *(Fig 5.3a-c)*. These differences were maintained after RSV infection *(Fig 5.3d-f)*.

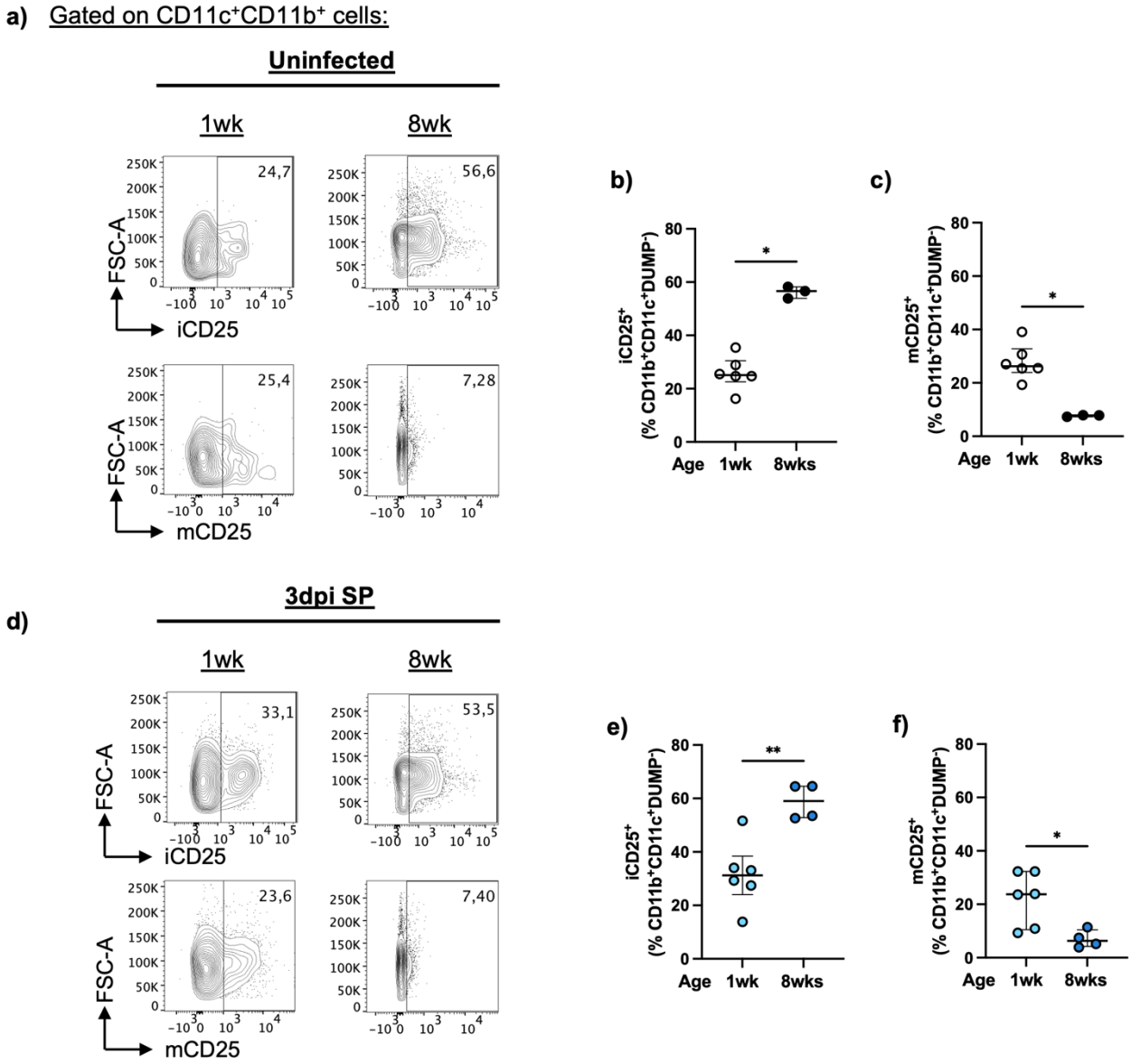


Fig 5.3. Increased proportion of intracellular CD25 expression in adult cDC2s, but increased percentage of membrane CD25⁺ cDC2s in neonates

1wk and 8wk-old C57BL/6 mice were infected with 2.5 × 10^5 PFU RSV A2 or PBS i.n. Spleen was harvested 3d post infection, splenocytes were isolated and stimulated with PMA and Ionomycin in the presence of BFA. **(a)** Representative flow plots and proportion of **(b)** intracellular and **(c)** membrane CD25 expressing cDC2s cells in uninfected and **(d,e,f)** infected conditions. Data from one independent experiment with n = 3-6 mice per group. Data shown with median and interquartile range. Each dot represents one mouse. Mann-Whitney test was performed in which *, $p < 0.05$; **, $p < 0.01$; and ***, $p < 0.001$.

B cells are also involved in dictating T_{FH} differentiation responses and have been shown to express CD25 (171). Hence, B cells ability to produce intracellular and membrane CD25 was also investigated. As with cDC2s, the percentage of B cells able to produce iCD25 was increased in uninfected and RSV infected adults when compared to neonates, but the proportion of mCD25 expressing B cells was upregulated in neonatal naïve and infected mice *(Fig 5.4a-f)*. The high production of iCD25 by adult cDC2s and B cells, combined with their low expression of mCD25, led me to hypothesise that most of the CD25 produced in adulthood by APCs is being secreted.

Overall this data shows an increased expression of sCD25 in the SLOs of adult mice associated with an increased capacity of adult cDC2s and B cells to produce iCD25, but not mCD25, upon stimulation.

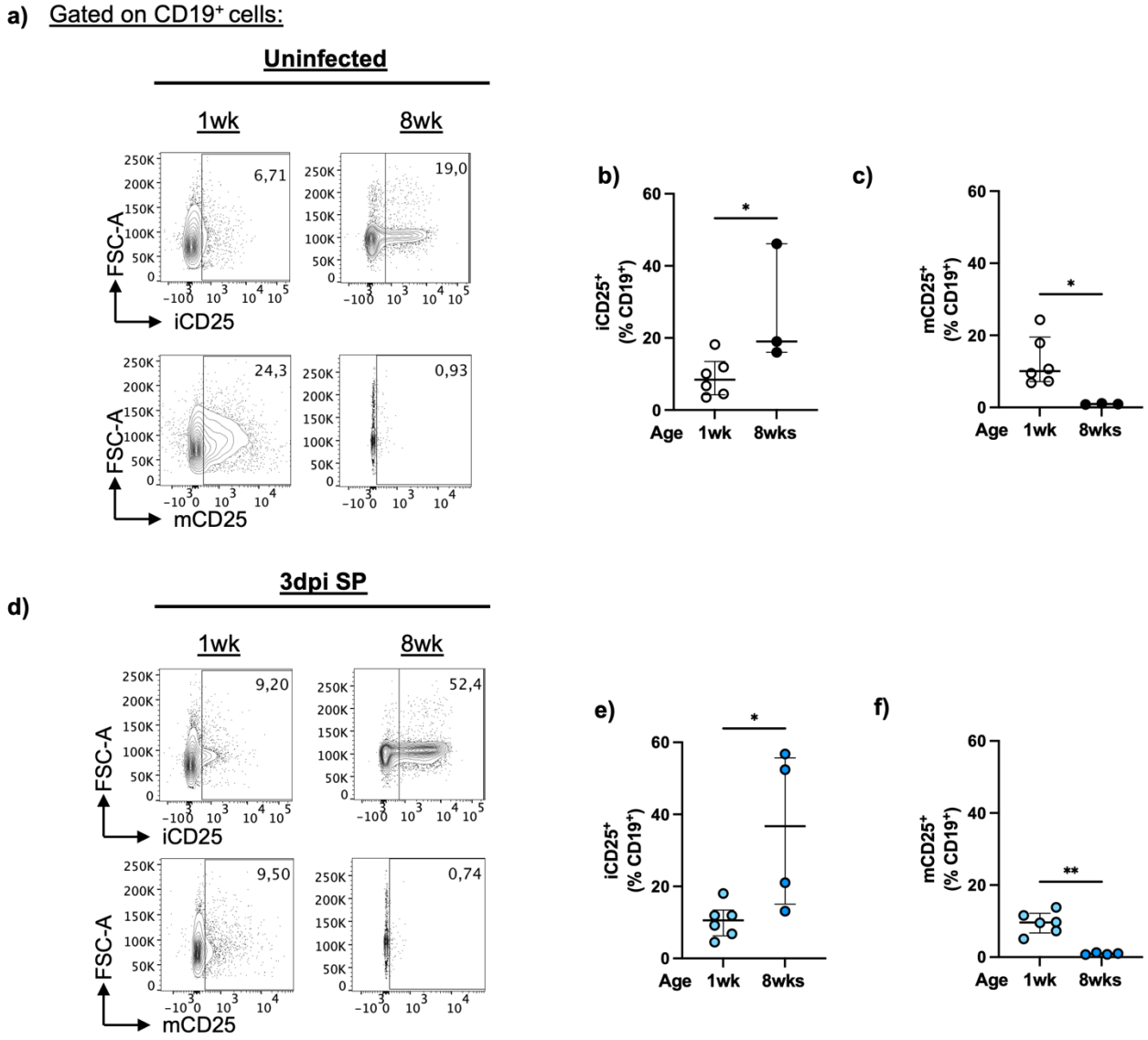


Fig 5.4. Increased proportion of intracellular CD25 expression in adult B cells, but increased percentage of membrane CD25⁺ B cells in neonates

1wk and 8wk-old C57BL/6 mice were infected with 2.5 × 10^5 PFU RSV A2 or PBS i.n. Spleen was harvested 3d post infection, splenocytes were isolated and and stimulated with PMA and Ionomycin in the presence of BFA. **(a)** Representative flow plots and proportion of **(b)** intracellular and **(c)** membrane CD25 expressing B cells in uninfected and **(d,e,f)** infected conditions. Data from one independent experiment with n = 3-6 mice per group. Data shown with median and interquartile range. Each dot represents one mouse. Mann-Whitney test was performed in which *, $p < 0.05$; **, $p < 0.01$; and ***, $p < 0.001$.

5.2.2 *A.lwoffii* exposure promotes CD25 and IL-6 expression by mediastinal LN cDC2s and B cells

Recurrent *A.lwoffii* exposure promotes T_{FH}, plasmablasts and RSV-specific antibody responses in early life (refer to chapter 4). Thus, differences in CD25 expression and cytokines involved in T_{FH} differentiation were analysed 5d post RSV re-challenge in mice exposed to different doses of *A.lwoffii* (***Fig 5.5a***). No difference in serum sCD25 expression nor in mediastinal LN *Cd25* transcript were observed in mice exposed to recurrent *A.lwoffii* when compared with mice infected with RSV alone or PBS control mice (***Fig 5.5b,c***). Similar levels of *Il2* transcript were also observed in medLN of these animals, but an increased *Il6* signature was seen in mice receiving constant exposure to the bacteria when compared with RSV infected mice alone (***Fig 5.5c***). No difference in transcript levels of *Cd25, Il2* or *Il6* were however found in the medLN of infant mice receiving early exposure to *A.lwoffii* alone (***Fig 5.5d***). Mice exposed to the farmyard microbe therapeutically, i.e. only during RSV re-infection, however showed increased mediastinal LN *Cd25* expression when compared with PBS control mice and an elevated production of *Il6* RNA in comparison to control and RSV alone groups, while no difference in *Il2* was observed (***Fig 5.5e***)

cDC2s play a crucial role in priming $CD4^+$ T cell responses and their maturation and activation can be modified with microbial interaction (reviewed in (687)). Therefore, it was hypothesised that exposure to *A.lwoffii* in early life could be promoting a pro-T_{FH} environment in a cDC2-dependent manner. To investigate differences in DC activation and cytokine production during *A.lwoffii* exposure, 3d old Balb/c mice were exposed to *A.lwoffii* or PBS three times a week and infected with RSV, or exposed to an equal volume of saline, on day 5 and day 15 of life. To capture differences in DC phenotype at the initial phase of $CD4^+$ T cell priming, mice were culled 24h after RSV re-infection and last *A.lwoffii* exposure (36). cDC2 responses were analysed by flow cytometry in the mediastinal LN and spleen (***Fig 5.6a,b***).

Mediastinal LN cell numbers were increased in mice exposed to *A.lwoffii*, RSV or both when compared with PBS control mice, but no differences between exposed groups were observed (***Fig 5.6c***). cDC1 ($CD8a^+CD11b^-SIRPa^-$) cell proportion was decreased in the mLN of mice exposed to *A.lwoffii*+RSV when compared with PBS mice (***Fig 5.6d***) while an increased cDC2 ($CD11b^+$ $CD11c^+DUMP^-$) signature was observed in mice exposed to the bacteria (***Fig 5.6e***). pDCs (PDCA-$1^+CD11b^-SIRP\alpha$) proportion was reduced in *A.lwoffii*, RSV and *A.lwoffii*+RSV groups in comparison with control mice (***Fig 5.6f***) and B cell percentages were increased in RSV infected animals (***Fig 5.6g***).

.

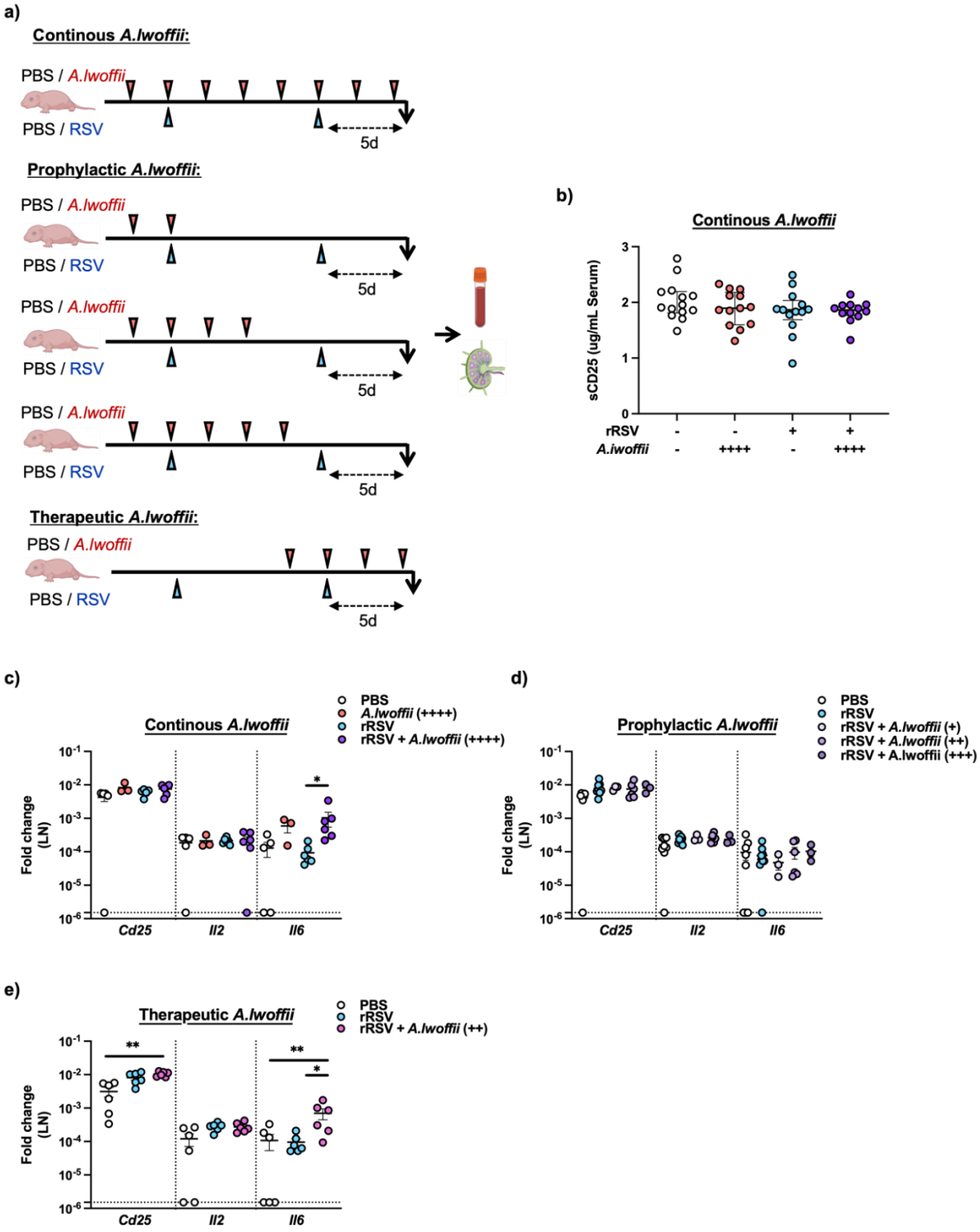


Fig 5.5. Increased Il6 transcript production in the lymph node of A.lwoffii exposed mice during 2nd RSV infection when compared with RSV infected mice alone

(a) Balb/c mice were intranasally exposed to *A.lwoffii* or PBS at indicated timepoints (red arrows) and infected with RSV or saline on day 5 and 15 of life (blue arrows). Serum and mediastinal lymph node were harvested 5d post viral re-infection. **(b)** Soluble CD25 was quantified by ELISA in the mice serum. **(c,d,e)** *Cd25, Il2* and *Il6* transcript were quantified in the mediastinal LN. Data from two independent experiments (b) with n = 12-14 mice per group or representative samples from two independent experiments (c-e) with n= 3-6. Data shown with median and interquartile range. Each dot represents one mouse. Kruskal-Wallis with multiple comparisons test was performed in which *, $p < 0.05$; **, $p < 0.01$; and ***, $p < 0.001$.

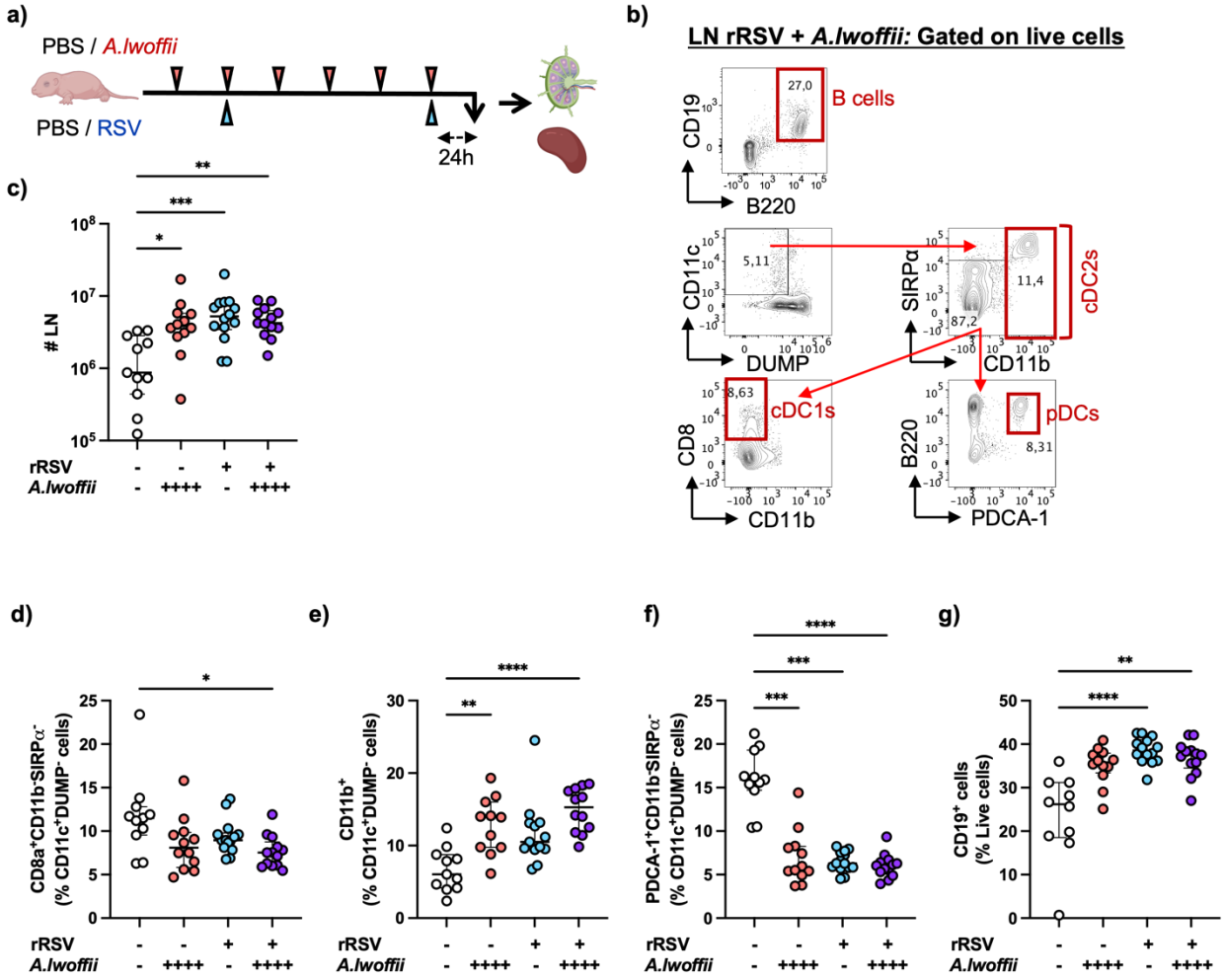


Fig 5.6. Increased cDC2s in the lymph nodes of recurrent A.lwoffii exposed infant mice

(a) 3d old Balb/c mice were intranasally exposed to *A.lwoffii* or PBS three times a week and infected with RSV or saline on day 5 and 15 of life. Lymph node and spleen were harvested 24h post re-challenge. **(b)** Representative gating strategy. **(c)** Mediastinal LN cell numbers for all treatment groups. **(d)** Mediastinal LN proportion of cDC1 ($CD8a^+CD11b^-SIRPa^-$), **(e)** cDC2 ($CD11b^+$), **(f)** pDC ($PDCA\text{-}1^+CD11b^-SIRPa^-$) and **(g)** B cells ($CD19^+$). DUMP channel consists of CD90.2 and Nkp46 markers. Data from two independent experiments with n = 11-13 mice per group. Data shown with median and interquartile range. Each dot represents one mouse. Kruskal-Wallis with multiple comparisons test was performed in which *, $p < 0.05$; **, $p < 0.01$; and ***, $p < 0.001$.

No difference in the activation marker CD86 was observed between cDC2s of different treatment groups *(**Fig 5.7a**)*, but decreased MHC-II expression was seen in RSV infected mice when compared with bacteria exposed pups *(**Fig 5.7b**)*. Signal regulatory protein α (SIRPα) is predominantly expressed in cDC2 cells (688). Sirpα interaction with its ligand, CD47, plays an essential role in promoting cDC2 SLO homing and function (689,690). Sirpα was upregulated in mice receiving recurrent *A.lwoffii* exposure, with mice receiving RSV+*A.lwoffii* showing a statistical increase when compared with RSV mice alone *(**Fig 5.7c,d**)*. Similarly, administration of recurrent *A.lwoffii* in early life seemed sufficient to increase both mCD25 and iCD25 expression in cDC2s *(**Fig 5.7e-i**)*, with mCD25 cDC2 MFI being significantly upregulated in *A.lwoffii*+RSV when compared with the RSV alone infected group *(**Fig 5.7f**)*. IL-6 production by

cDC2s was significantly elevated in the *A.lwoffii*+RSV group when compared with infected mice alone and PBS controls *(Fig 5.7j,k)*.

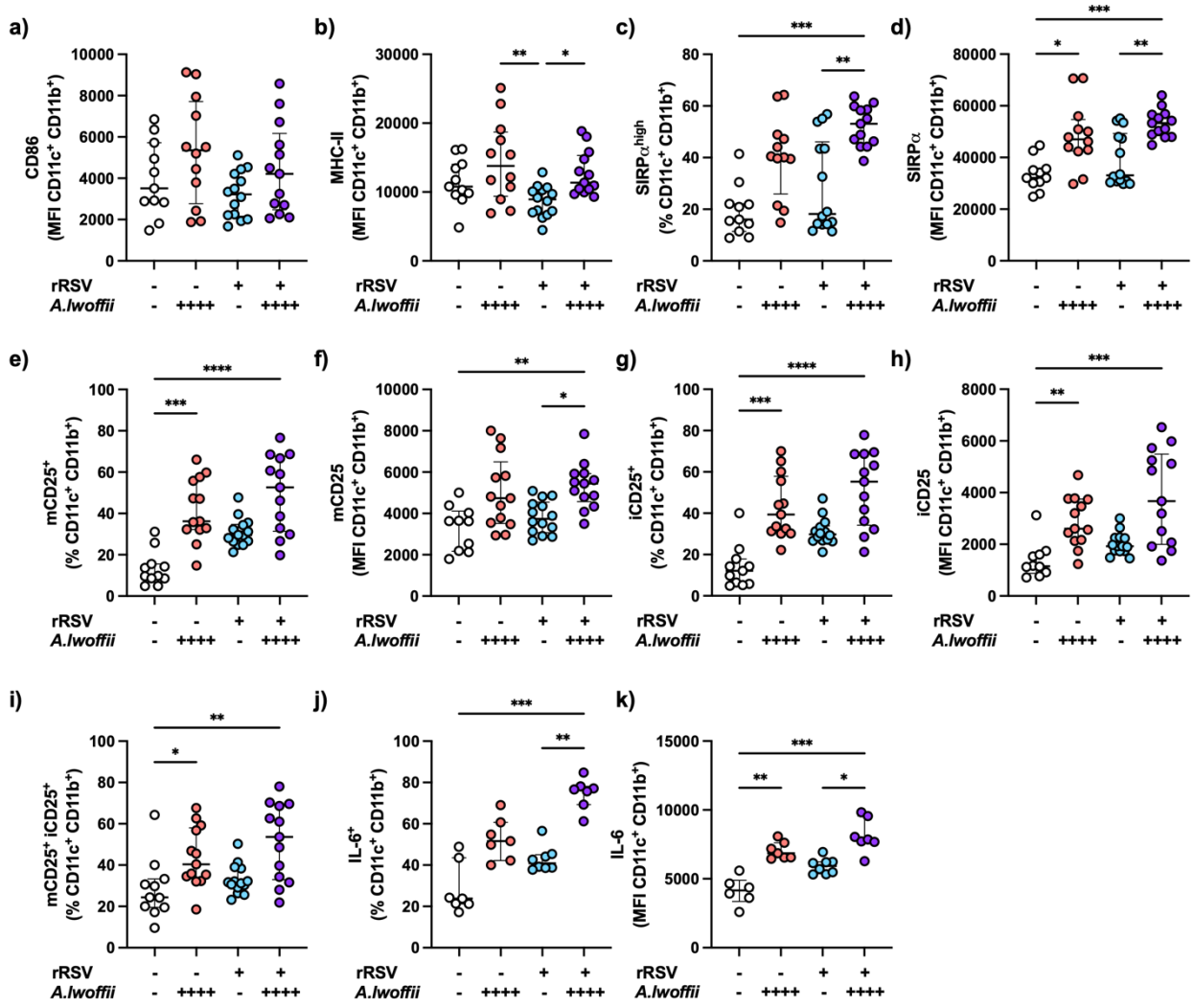


Fig 5.7. Recurrent A.lwoffii exposure in early life increases cDC2s activation and their expression of CD25 and IL-6 during RSV infection

3d old Balb/c mice were intranasally exposed to *A.lwoffii* or PBS three times a week and infected with RSV or saline on day 5 and 15 of life. Lymph node was harvested 24h post re-challenge. **(a)** CD86 and **(b)** MHC-II MFI of cDC2s. **(c)** Proportion and **(d)** MFI of SIRPα on cDC2 cells. **(e)** Proportion and **(f)** MFI of mCD25 and **(g,h)** iCD25 on cDC2s. **(i)** Proportion of $mCD25^{+}iCD25^{+}$ cDC2s. **(j)** Proportion and **(k)** MFI of IL-6 on cDC2 cells. DUMP channel consists of CD90.2 and Nkp46 markers. Representative data from two independent experiments with n = 11-13 mice per group (a-i) or data from one representative experiment (j,k) with n= 7-8 mice per group. Data shown with median and interquartile range. Each dot represents one mouse. Kruskal-Wallis with multiple comparisons test was performed in which *, $p < 0.05$; **, $p < 0.01$; and ***, $p < 0.001$.

B cells are involved in T_{FH} cell differentiation and microbial exposure can also shape B cell responses (691). Thus, B cell phenotype was next analysed in the mediastinal LN of these mice. B cells from mice infected with RSV alone promoted B cell CD86 expression when compared with *A.lwoffii* only exposed pups, but no difference was observed between both groups infected with the virus *(Fig 5.8a)*. B cell MHC-II expression was reduced in mice exposed to the virus or the bacteria

when compared with PBS control mice *(Fig 5.8b)*. Increased mCD25, iCD25, double positive cells and IL-6 producing B cells were increased in *A.lwoffii* exposed RSV infected infant mice when compared with the RSV alone group *(Fig 5.8c-i)*. RSV alone infected mice also showed a reduced ability to produce IL-6 when compared with control animals *(Fig 5.8h,i)*.

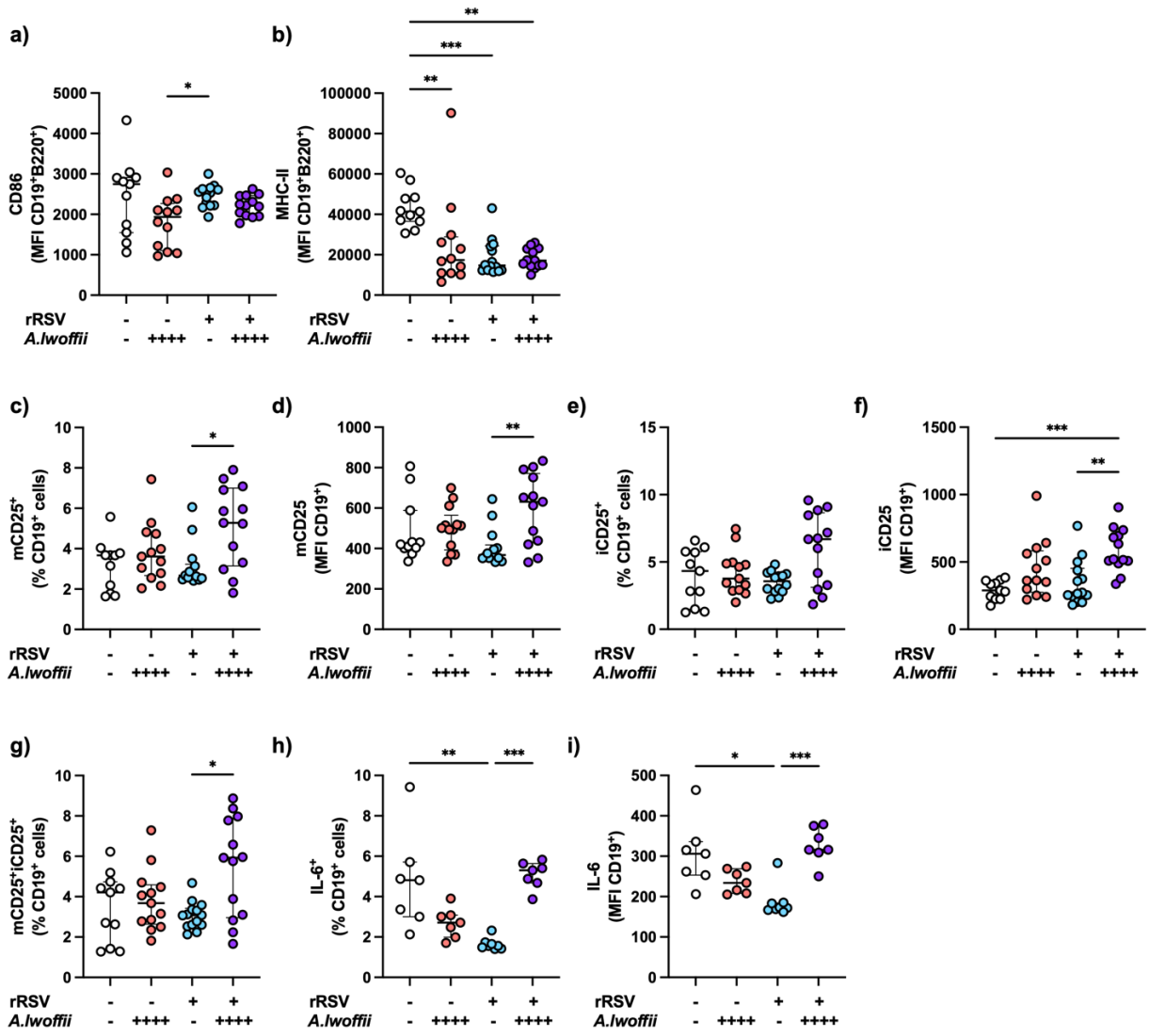


Fig 5.8. Recurrent A.lwoffii exposure during early life in RSV infected mice increases B cells' CD25 and IL-6 expression

3d old Balb/c mice were intranasally exposed to *A.lwoffii* or PBS three times a week and infected with RSV or saline on day 5 and 15 of life. Lymph node was harvested 24h post re-challenge. **(a)** CD86 and **(b)** MHC-II MFI of B cells. **(c)** Proportion and **(d)** MFI of mCD25 and **(e,f)** iCD25 on B cells. **(i)** Proportion of $mCD25^{+}iCD25^{+}$ B cells. **(j)** Proportion and **(k)** MFI of IL-6 on B cells. Representative data from two independent experiments with n = 11-13 mice per group (a-g) or data from one representative experiment (h,i) with n= 7-8 mice per group. Data shown with median and interquartile range. Each dot represents one mouse. Kruskal-Wallis with multiple comparisons test was performed in which *, $p < 0.05$; **, $p < 0.01$; and ***, $p < 0.001$.

cDC2 and B cell CD25 and IL-6 production were also analysed in the spleen, where a less pronounced response was observed. Splenocyte cell numbers were maintained among all groups analysed *(Fig 5.9a)*. cDC1 proportion was similar between groups and while an increased cDC2 cell signature was observed in mice exposed to *A.lwoffii* or RSV alone when compared with control

mice, no difference was seen in mice that received a combination of both *(Fig 5.9b,c)*. pDCs and B cell proportions were also maintained after RSV and *A.lwoffii* exposure *(Fig 5.9d,e)*.

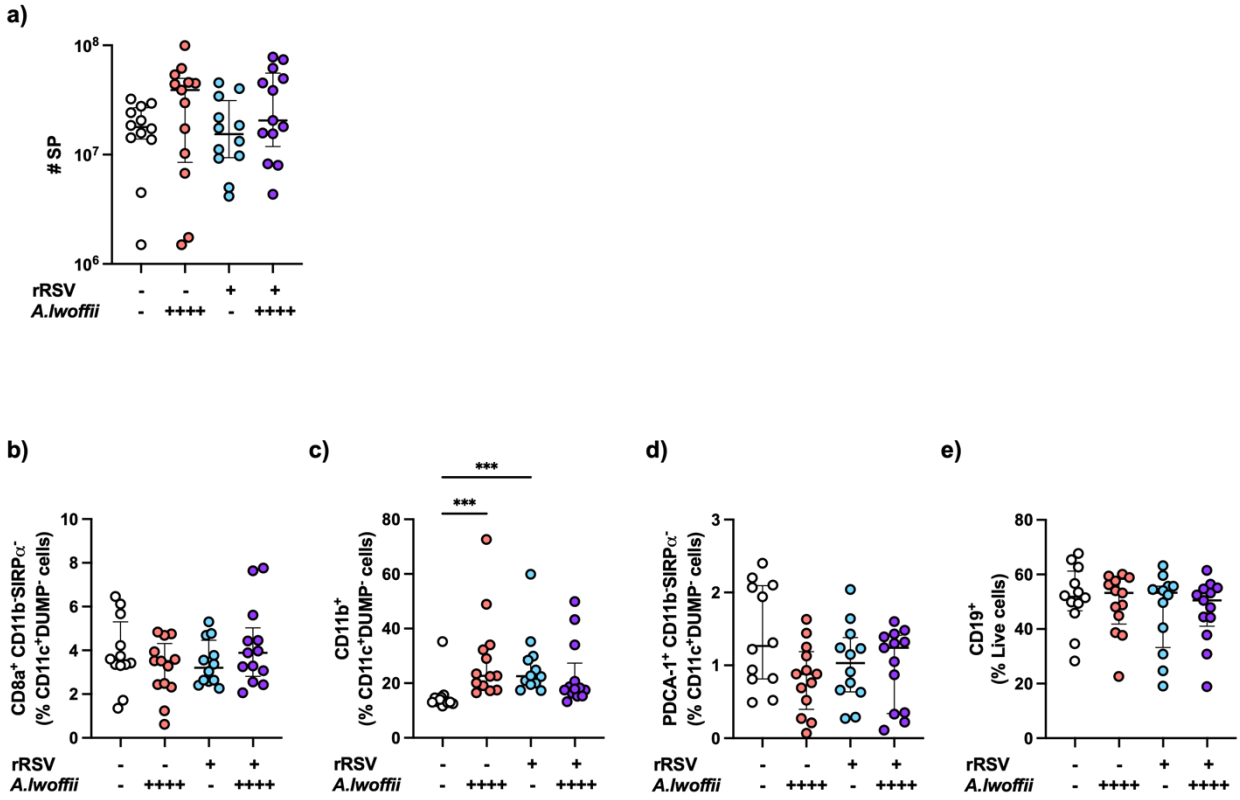


Fig 5.9. Increased cDC2s in the spleen of recurrent A.lwoffii and RSV alone infected mice

3d old Balb/c mice were intranasally exposed to *A.lwoffii* or PBS three times a week and infected with RSV or saline on day 5 and 15 of life. Spleen was harvested 24h post re-challenge. **(a)** Spleen cell numbers for all treatment groups. **(b)** Spleen proportion of cDC1 ($CD8a^+CD11b^-SIRP\alpha^-$), **(c)** cDC2 ($CD11b^+$), **(d)** pDC ($PDCA\text{-}1^+CD11b^-SIRP\alpha^-$) and **(e)** B cells ($CD19^+$). DUMP channel consists of CD90.2 and Nkp46 markers. Data from two independent experiments with n = 11-13 mice per group. Data shown with median and interquartile range. Each dot represents one mouse. Kruskal-Wallis with multiple comparisons test was performed in which *, $p < 0.05$; **, $p < 0.01$; and ***, $p < 0.001$.

Similar levels of CD86 were observed on splenic cDC2s, but RSV infection led to decreased expression of MHC-II and the percentage of SIRPα expressing cDC2s when compared to PBS mice, a phenotype that was rescued after *A.lwoffii* exposure *(Fig 5.10a-c)*. No difference in SIRPα MFI was seen between groups *(Fig 5.10d)*. Likewise, similar levels of both membrane and iCD25 proportions and MFI were observed *(Fig 5.10e-i)*. No difference in IL-6 percentage was seen in *A.lwoffii*, RSV or control mice, but an increased IL-6 MFI was seen in mice exposed to either the bacteria or the virus alone when compared with PBS controls. A similar increase was however not observed for mice in the *A.lwoffii*+RSV group *(Fig 5.10j,k)*.

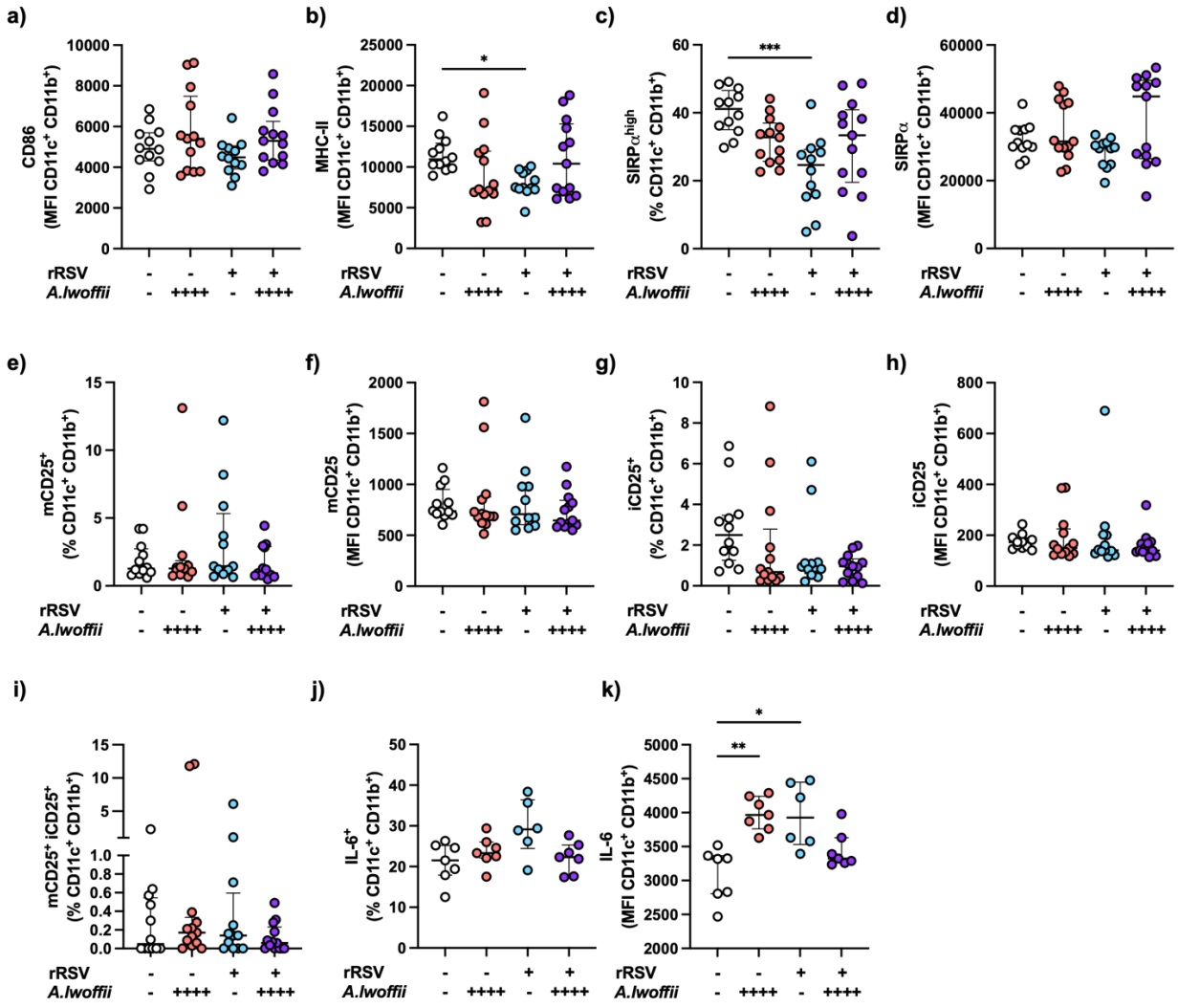


Fig 5.10. No difference in early life spleen cDC2s is observed between A.lwoffii exposed RSV infected mice and viral infected mice alone

3d old Balb/c mice were intranasally exposed to *A.lwoffii* or PBS three times a week and infected with RSV or saline on day 5 and 15 of life. Spleen was harvested 24h post re-challenge. **(a)** CD86 and **(b)** MHC-II MFI of cDC2s. **(c)** Proportion and **(d)** MFI of SIRPα on cDC2 cells. **(e)** Proportion and **(f)** MFI of mCD25 and **(g,h)** iCD25 on cDC2s. **(i)** Proportion of $mCD25^{+}iCD25^{+}$ cDC2s. **(j)** Proportion and **(k)** MFI of IL-6 on cDC2 cells. DUMP channel consists of CD90.2 and Nkp46 markers. Representative data from two independent experiments with n = 11-13 mice per group (a-i) or data from one representative experiment (j,k) with n= 7-8 mice per group. Data shown with median and interquartile range. Each dot represents one mouse. Kruskal-Wallis with multiple comparisons test was performed in which *, $p < 0.05$; **, $p < 0.01$; and ***, $p < 0.001$.

Splenic B cells from RSV alone infected mice showed upregulated CD86 expression when compared with control or *A.lwofffii* exposed animals *(Fig 5.11a)*, but no other differences in splenic B cells were observed for membrane or intracellular CD25 expression or IL-6 production *(Fig 5.11b-i)*. Overall, this data shows that recurrent exposure to *A.lwoffii* in early life promotes mediastinal LN cDC2 and B cell CD25 expression and IL-6 production, but no major differences are seen in spleen probably due to its more distal location from the *A.lwoffii* and RSV exposure route.

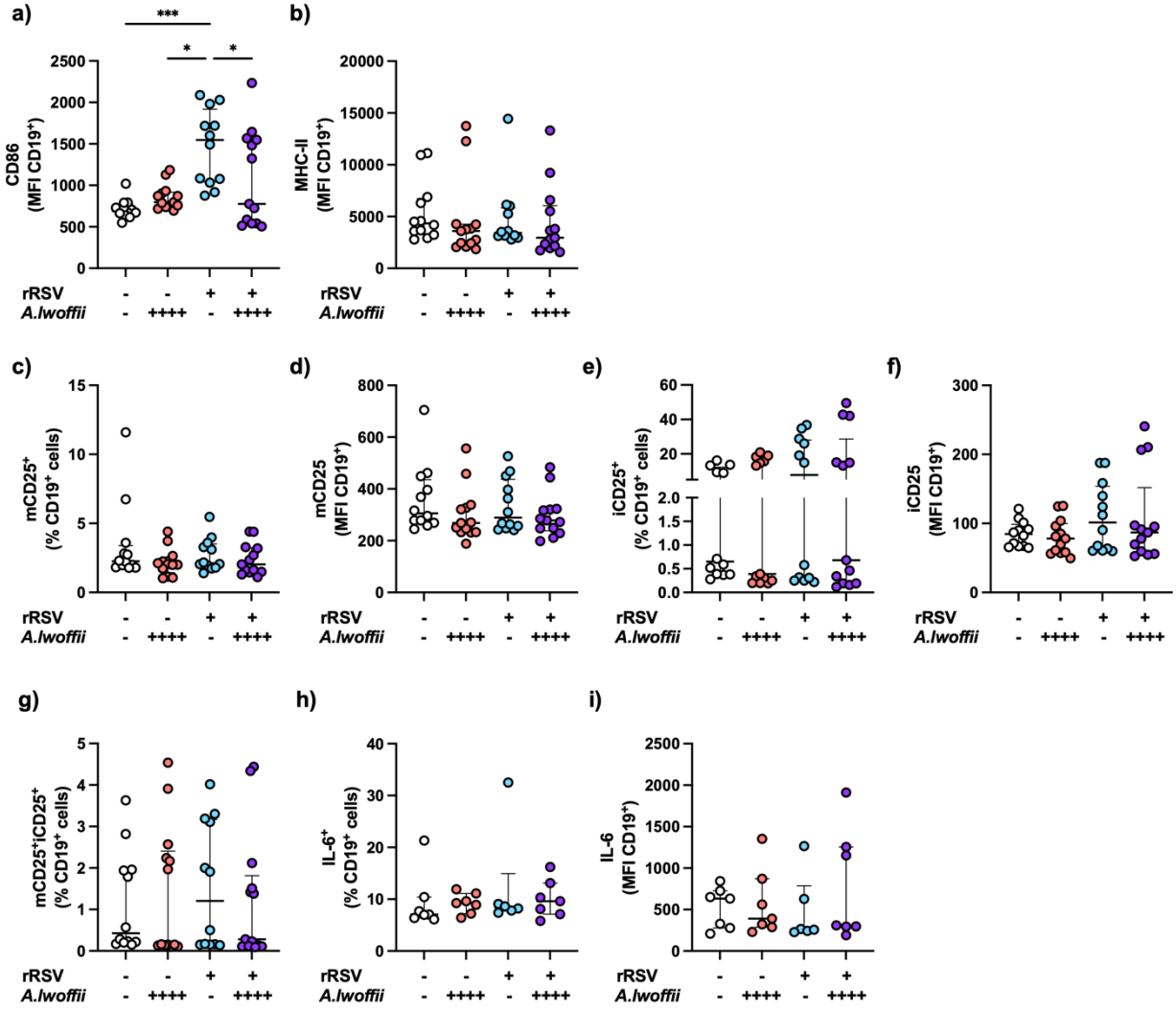


Fig 5.11. No difference in early life B cell CD25 or IL-6 production in the spleen of A.lwoffii exposed or unexposed RSV infected mice

3d old Balb/c mice were intranasally exposed to *A.lwoffii* or PBS three times a week and infected with RSV or saline on day 5 and 15 of life. Spleen was harvested 24h post re-challenge. **(a)** CD86 and **(b)** MHC-II MFI of B cells. **(c)** Proportion and **(d)** MFI of mCD25 and **(e,f)** iCD25 on B cells. **(i)** Proportion of $mCD25^{+}iCD25^{+}$ B cells. **(j)** Proportion and **(k)** MFI of IL-6 on B cells. Representative data from two independent experiments with n = 11-13 mice per group (a-g) or data from one representative experiment (h,i) with n= 7-8 mice per group.. Data shown with median and interquartile range. Each dot represents one mouse. Kruskal-Wallis with multiple comparisons test was performed in which *, $p < 0.05$; **, $p < 0.01$; and ***, $p < 0.001$.

5.2.3 *A.lwoffii*, but not RSV, stimulation of bone marrow-derived cDC2s promotes a pro-T_{FH} environment

To better understand the production of a pro- or anti-T_{FH} microenvironment generated by cDC2 cells stimulated with RSV or *A.lwoffii,* a controlled, *in vitro* system consisting of stimulation of bone-marrow (BM) derived DCs was used. First, a method to isolate BM-progenitors and promote their differentiation towards cDC2 cells was established. Bone marrow cell isolation can be accomplished using two methods. Both methods require isolation of mouse femur and tibia by

cleaning the surrounding tissue and cutting the bone epiphyses. The more laborious flushing method, using a 1mL syringe to manually flush media into the tibia and femur to allow bone marrow isolation, has traditionally been used by our group (128,692). This isolation process can however be accelerated by centrifugation as previously done by another group (693) (refer to chapter 2) *(**Fig 5.12a**)*. Culture of BM-progenitors with Flt3-L *in vitro* has been shown to promote DC differentiation towards *in vivo*-like DCs preferentially promoting cDC2 over cDC1 maturation (663,694,695). To analyse cell viability and DC differentiation by the two isolation methods and to determine an optimal dose for Flt3-L, a flow cytometry strategy containing markers for all major DC subsets was used *(**Fig 5.12b**)*. The use of the centrifuge method and 50ng/mL or 200ng/mL of Flt3-L showed the highest cell viability *(**Fig 5.12c,d**)* together with an increased production of cDC2 and SIRPα^+cDC2 cells *(**Fig 5.12e-g**)*. Minimal differentiation of BM-progenitors towards cDC1s was seen in either of the conditions *(**Fig 5.12h**)* and a reduced pDC differentiation was observed in the centrifuge method combined with high concentrations of Flt3-L *(**Fig 5.12i**)*. Due to its higher efficiency the centrifuge method combined with 50ng/mL of Flt3-L was used for all future BM-progenitor cell isolation and differentiation protocols.

Next, to analyse the differential production of a pro-T_{FH} environment by *A.lwoffii* and RSV, early life and adult murine BM-progenitors were isolated by the centrifugation method and exposed to 50ng/mL of Flt3-L *in vitro* for 8 to 11 days. Cells were then left unstimulated or were stimulated with *A.lwoffii* or RSV. 24h later cDC2 activation, CD25 and IL-6 production were analysed by flow cytometry and RT-qPCR. Culture supernatants were collected 6, 24, 48 and 72h post BMDC stimulation to evaluate sCD25 and IL-6 secretion *(**Fig 5.13a**)*. First, DC phenotype and activation status from unstimulated early life and adult BM-derived DCs were analysed to evaluate if there were age intrinsic differences in the maturation process. Similar proportions of major DC populations, namely cDC2s, SIRPα^+cDC2s, cDC1s and pDCs, were observed in BM cultures from early life and adult samples *(**Fig 5.13b-e**)*. Again, an increased proportion of cDC2s when compared with cDC1s or pDCs was observed in Flt3-L treated cultures at both ages *(**Fig 5.13b-e**)*. CD86 and MHC-II, markers of cDC2 activation and maturation, as well as SIRPα were all equally expressed in BM-derived cDC2s of early life and adult cultures *(**Fig 5.13f-h**)*.

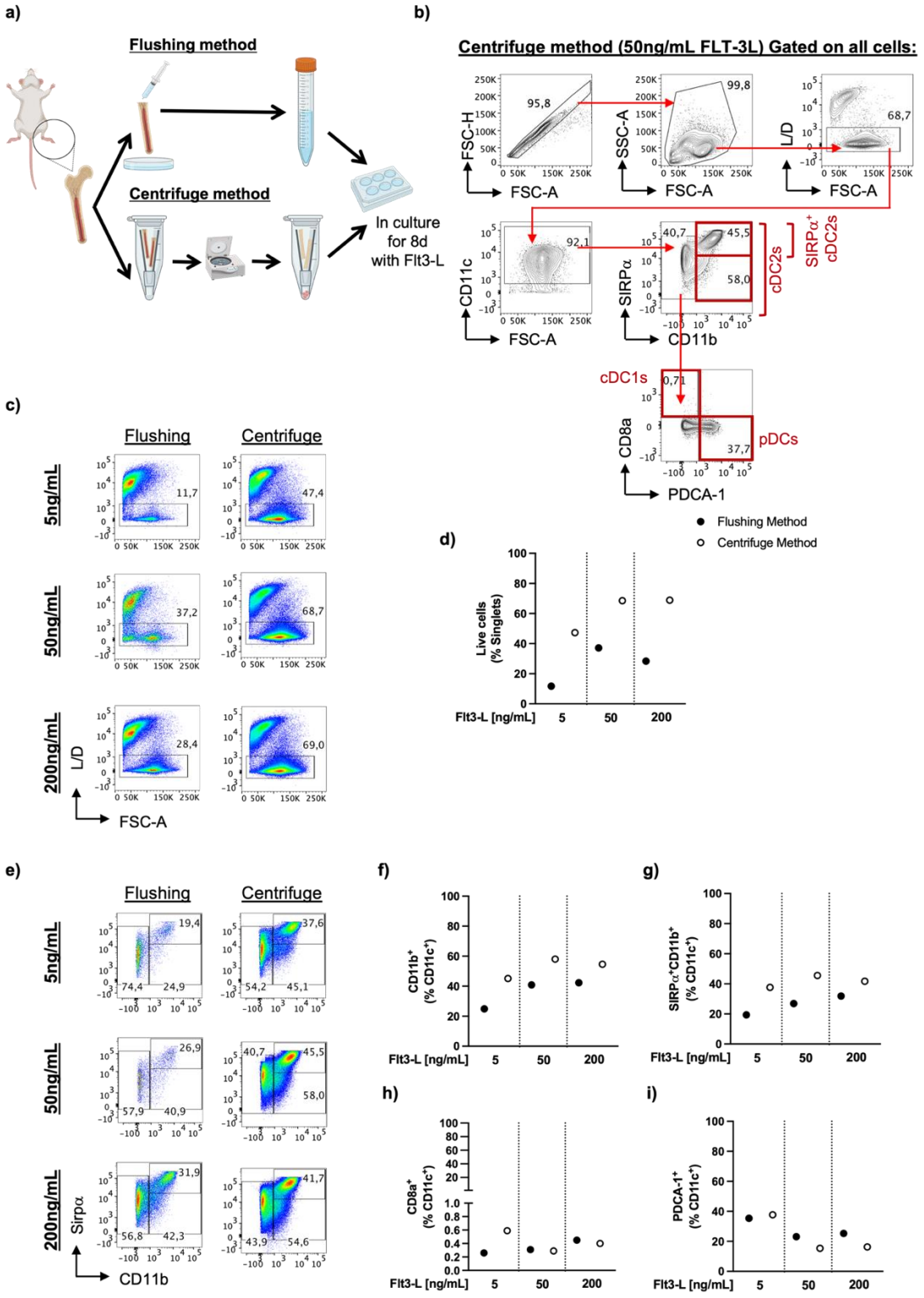


Fig 5.12. Centrifuge isolation of bone marrow progenitors is effective for the Flt3-L differentiation of bone marrow derived DCs in vitro

(a) Bone marrow progenitor cells were isolated from adult mice by the flushing or centrifugation method and cultured with different doses of Flt3-L for 8 days. **(b)** Representative flow gating strategy. **(c,d)** Representative flow plots and proportion of live cells per flushing and centrifugation isolation method when using different concentrations of Flt3-L. **(e)** Representative flow plots and proportion of **(f)** cDC2s (CD11b$^+$), **(g)** SIRPα^+ cDC2s (SIRPα^+CD11b$^+$), **(h)** cDC1s (CD8a$^+$) and (i) pDCs (PDCA-1$^+$) according to isolation method and dose of Flt3-L. Data from one independent experiment with n = 1 mice per group.

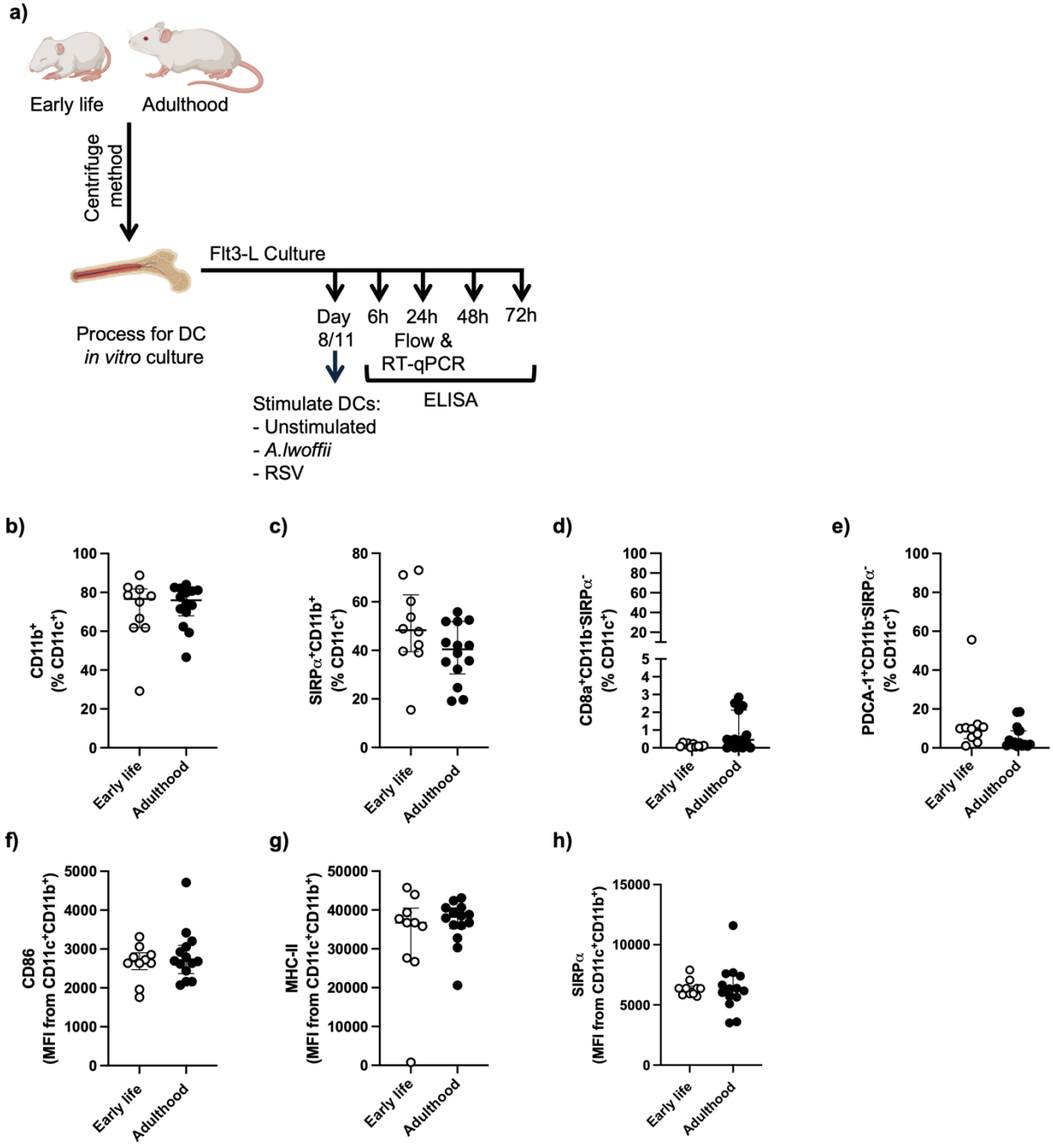


Fig 5.13. The ability to differentiate matured cDC2s from BM progenitors in vitro is not influenced by mice age

(a) Early life and adult BM progenitors were isolated from Balb/c mice by the centrifugation method and cultured with FLt3-L for 8 to 11 days. Then they were stimulated with *A.lwoffii*, RSV or left unstimulated. Flow cytometry analysis and RT-qPCR were performed 24h post-stimulation while supernatants were collected at 6,24, 48 and 72h post stimulation for ELISA. **(b)** Proportion of cDC2s, **(c)** Sirpα^+ cDC2s, **(d)** cDC1s and **(e)** pDCs. **(f)** CD86, **(g)** MHC-II and **(h)** SIRPα MFI on cDC2 cells. Data from five independent experiments with n = 10-14 mice per group. Data shown with median and interquartile range. Each dot represents one mouse. Mann-Whitney test was performed in which *, $p < 0.05$; **, $p < 0.01$; and ***, $p < 0.001$.

As with unstimulated conditions, BM-derived DC cultures used in *A.lwoffii* and RSV treated experiments were enriched for cDC2 cells both in early life and adulthood *(**Fig 5.14a,b**)*. A minimal, but statistically significant, increased proportion of cDC1s was seen in early life *A.lwoffii*-stimulated conditions when compared to other groups, but no difference was observed in adulthood *(**Fig 5.14c,d**)*. Increased pDCs percentages were observed in RSV-treated *in vitro* cultures, compared to those treated with *A.lwoffii*, at both ages *(**Fig 5.14e,f**)*. cDC1 and pDCs percentages were however minimal when compared to cDC2 proportions in all treatment groups, indicating that the analysed responses are mostly dependent on cDC2 cell behaviour upon stimulation. *A.lwoffii* or RSV stimulation promoted similar levels of CD86 membrane upregulation by both early life and adult BM-cDC2s when compared with unstimulated conditions *(**Fig 5.14g,h**)*. A trend to an increase MHC-II was observed in RSV-treated early life cDC2s *(**Fig 5.14i**)*, which was significant when compared with control in adulthood *(**Fig 5.14j**)*. Limited changes in SIRPα expression were observed, but it was slightly upregulated in *A.lwoffii* exposed early life *(**Fig 5.14k**)* and adult cultures *(**Fig 5.14l**)*. SIRPα MFI was significantly upregulated in adult *A.lwoffii*-cDC2s when compared with RSV, but not control cDC2s *(**Fig 5.14l**)*.

mCD25 expression was equally upregulated in *A.lwoffii* and RSV stimulated-cDC2s both in early life and adulthood *(**Fig 5.15a,b**)*, but iCD25 was preferentially increased in bacteria exposed conditions *(**Fig 5.15c,d**)*. Concomitantly, sCD25 was significantly upregulated in *A.lwoffii* stimulated cultures, with early life conditions showing a significantly increased sCD25 production when compared with RSV-treated or control DCs *(**Fig 5.15e,f**)*. A similar effect was seen over time, with CD25 upregulated in the supernatant of early life *A.lwoffii*-cultures, and to a lesser extent adult BMDCs, up to 72 hours post stimulation compared with RSV and control-treated cells *(**Fig 5.15g,h**)*.

To determine if the differential effects of RSV and *A.lwoffii* were simply a result of a distinct capacity to activate DCs *in vitro,* correlation analysis at a per culture level was performed. Examining adult BMDC cultures, where a higher n number of cultures had all parameters measured, a significant positive correlation between mCD25 and CD86 expression was observed in RSV-stimulated cDC2s, but not for *A.lwoffii* or control conditions *(**Fig 5.15i**)*. iCD25 production however showed a significant positive correlation with CD86 expression in both stimulated conditions, being strongest in *A.lwoffii*-exposed cDC2s *(**Fig 5.15j**)*. iCD25 also positively correlated with sCD25 in *A.lwoffii* exposed conditions, but after RSV-stimulation there was a significant negative correlation between the two parameters *(**Fig 5.15k**)*. *Cd25* transcript level was upregulated in both bacteria and virus-stimulated cultures when compared with early life control groups. No difference was observed in *Cd122* levels and the common γ receptor was preferentially expressed by cells from RSV-stimulated conditions *(**Fig 5.15l**)*. Adult cultures followed an exact pattern to the one seen in early life for IL-2 receptor RNA expression, but *Cd132* was also significantly upregulated in RSV treated conditions when compared with *A.lwoffii* cultures *(**Fig 5.15m**)*.

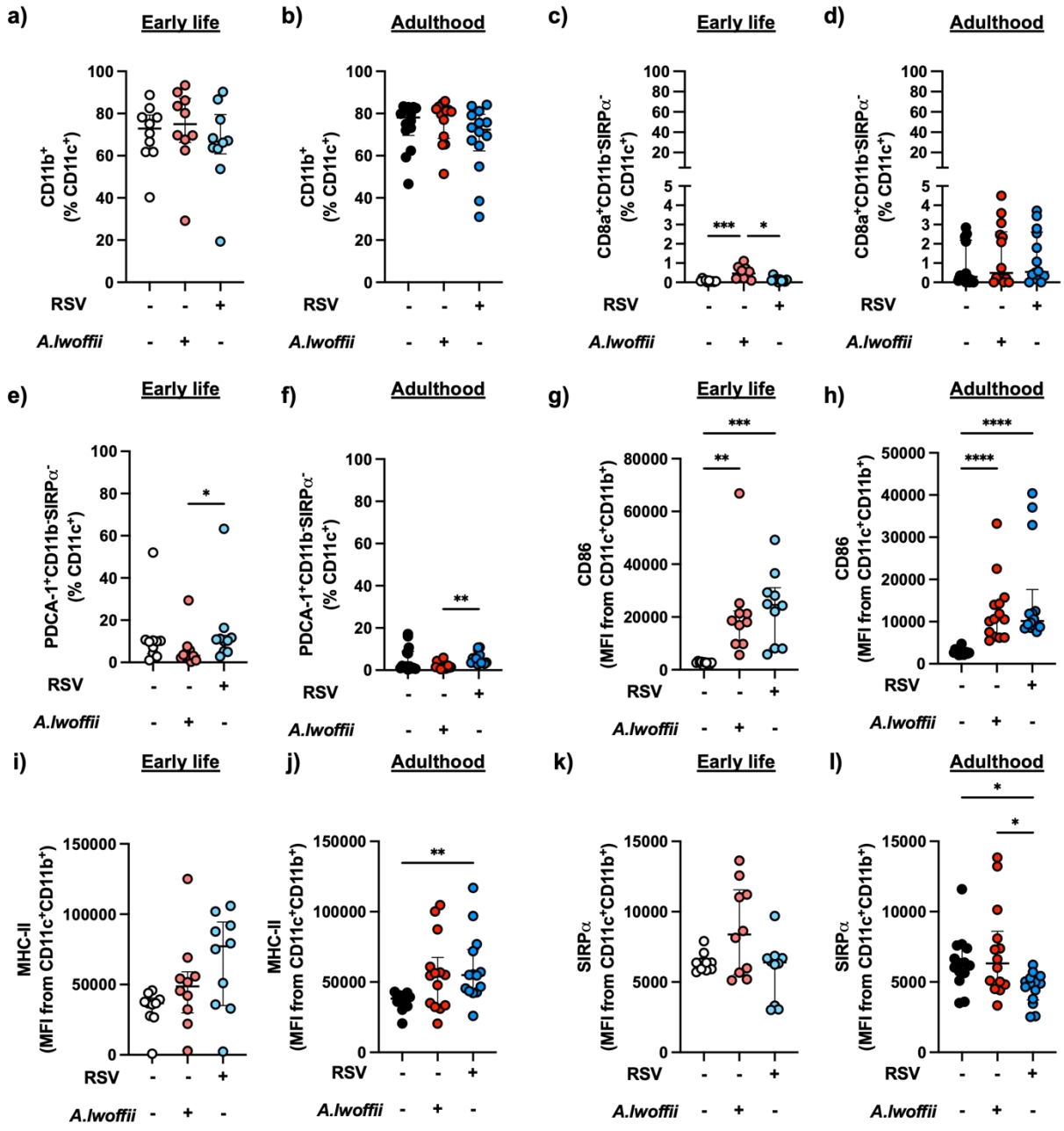


Fig 5.14. Similar CD86 expression after A.lwoffii or RSV-stimulation of BM-derived cDC2s

Early life and adult BM progenitors were isolated from Balb/c mice by the centrifugation method and cultured with FLt3-L for 8 to 11 days. Then they were stimulated with *A.lwoffii* ($2.5x10^8$cfu/mL) or RSV (1 MOI) or left unstimulated. Flow cytometry analysis was performed 24h post-stimulation. **(a)** Early life and **(b)** adult proportion of cDC2, **(c,d)** cDC1s and **(e,f)** pDCs. **(g)** Early life and **(h)** adult CD86, **(l,j)** MHC-II and **(k,l)** SIRPα MFI. Data from five independent experiments with n= 10-14 mice per group. Data shown with median and interquartile range. Each dot represents one mouse. Kruskal-Wallis with multiple comparisons test was performed in which *, $p < 0.05$; **, $p < 0.01$; and ***, $p < 0.001$.

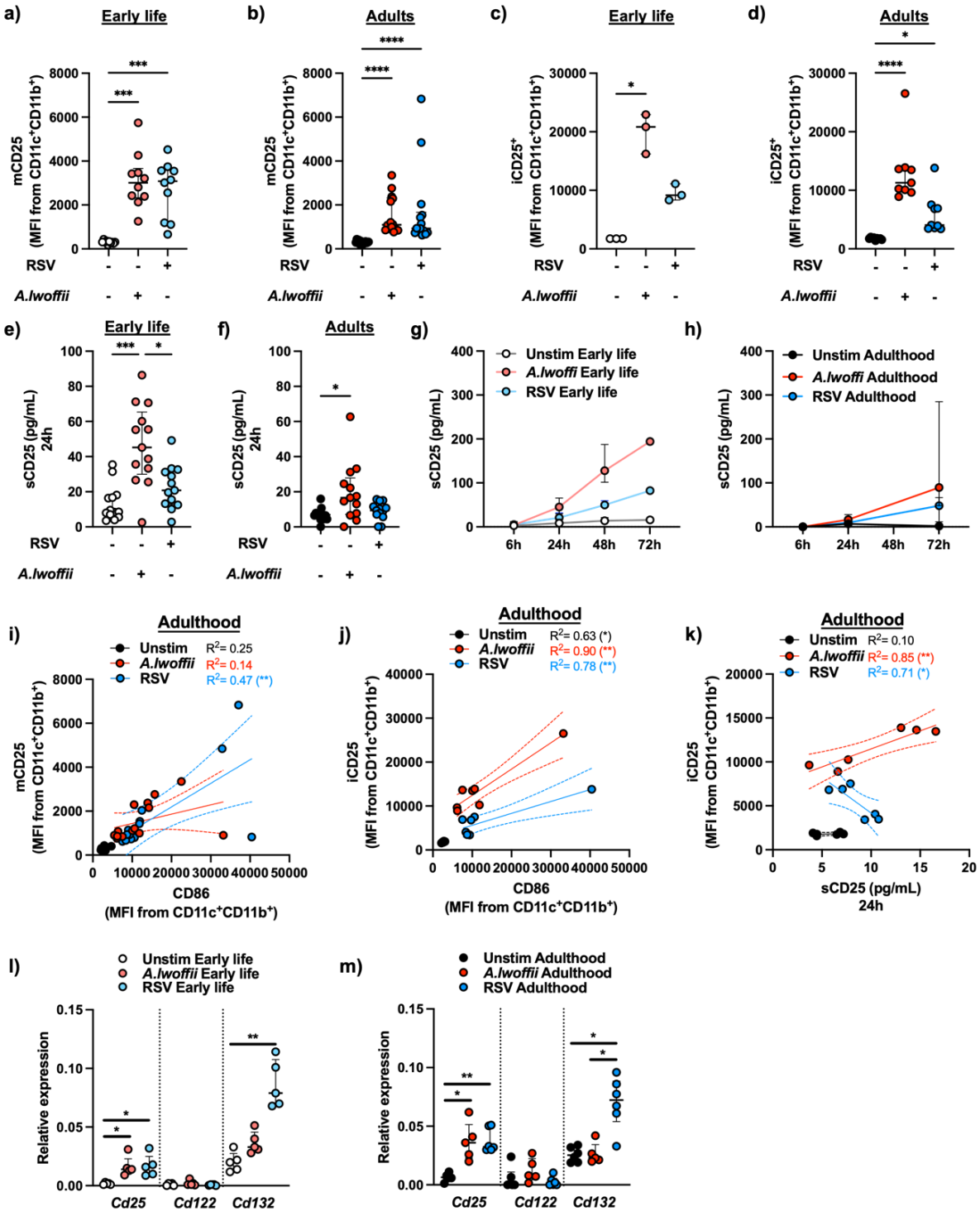


Fig 5.15. Increased intracellular and soluble CD25 after A.lwoffii-stimulation of BM-cDC2s

Early life and adult BM progenitors were isolated from Balb/c mice by the centrifugation method and cultured with FLt3-L for 8 to 11 days. Then they were stimulated with *A.lwoffii* ($2.5x10^8$cfu/mL) or RSV (1MOI) or left unstimulated. Flow cytometry analysis and RT-qPCR were performed 24h post-stimulation while supernatants were collected at 6,24, 48 and 72h post stimulation for ELISA. **(a)** Early life and **(b)** adult mCD25 and **(c,d)** iCD25 MFI on cDC2s. **(e)** Early life and **(f)** adult sCD25 production 24h post stimulation. **(g)** Early life and **(h)** adult sCD25 production 6,24,48 and 72h post-stimulation. **(i)** Correlation between mCD25 and CD86 on adult cDC cells. **(j)** Correlation between iCD25 and CD86 on adult cDC cells. **(k)** Correlation between iCD25 and sCD25 on two representative adult experiments. **(l)** Early life and **(m)** adult relative expression of *Cd25, Cd122* and *Cd132* when compared with an average of housekeeping genes (*Gapdh* and *Actb*) on samples from 5 representative BMDC cultures. Unless otherwise stated data from one (c) with n=3 mice per group or five (a,b, d-m) independent experiments with n=10-14 mice per group. Data shown with median and interquartile range. Each dot represents one mouse but for g and h where dots represent the mean of a group. Kruskal-Wallis with

multiple comparisons test (a-f,l,m) and simple linear regression with Pearson analysis (i-k) were performed in which *, $p < 0.05$; **, $p < 0.01$; and ***, $p < 0.001$.

The proportion of IL-6 expressing cDC2 cells was increased in *A.lwoffii* treated samples *(**Fig 5.16a,b**)* and so was IL-6 MFI on cDC2 cells *(**Fig 5.16c,d**)*. IL-6 production was significantly elevated in adult *A.lwoffii* cultures when compared with RSV ones *(**Fig 5.16b,d**)*. Concomitantly, IL-6 secretion in *in vitro* culture supernatants was increased in cultures exposed to the bacteria when compared with media or RSV-treated conditions 24h post stimulation *(**Fig 5.16e,f**)*. As with sCD25, IL-6 secretion by farmyard exposed BM-derived DC cultures was increased through time *(**Fig 5.16g,h**)*. IL-6 MFI by cDC2s did not correlate with either CD86 or iCD25 expression in adult *A.lwoffii*-exposed cultures, but IL-6 positively correlated with both CD86 and iCD25 expression in RSV-treated conditions *(**Fig 5.16i,j**)*. IL-6 and CD25 secretion positively correlated in *A.lwoffii* exposed cells, but no significant correlation was observed in control or viral treated conditions *(**Fig 5.16k**)*. As with the protein data, *Il6* transcript was increased in cells exposed to the farmyard microbe in both early life and adulthood *(**Fig 5.16l,m**)*.

Together this highlights the ability of *A.lwoffii,* but not RSV, to stimulate DCs to secrete IL-6 and CD25, despite both causing similar DC activation and mCD25 upregulation. Overall suggesting *A.lwoffii*-stimulated DCs may provide an enhanced pro-T_{FH} environment when compared with RSV-stimulated DCs.

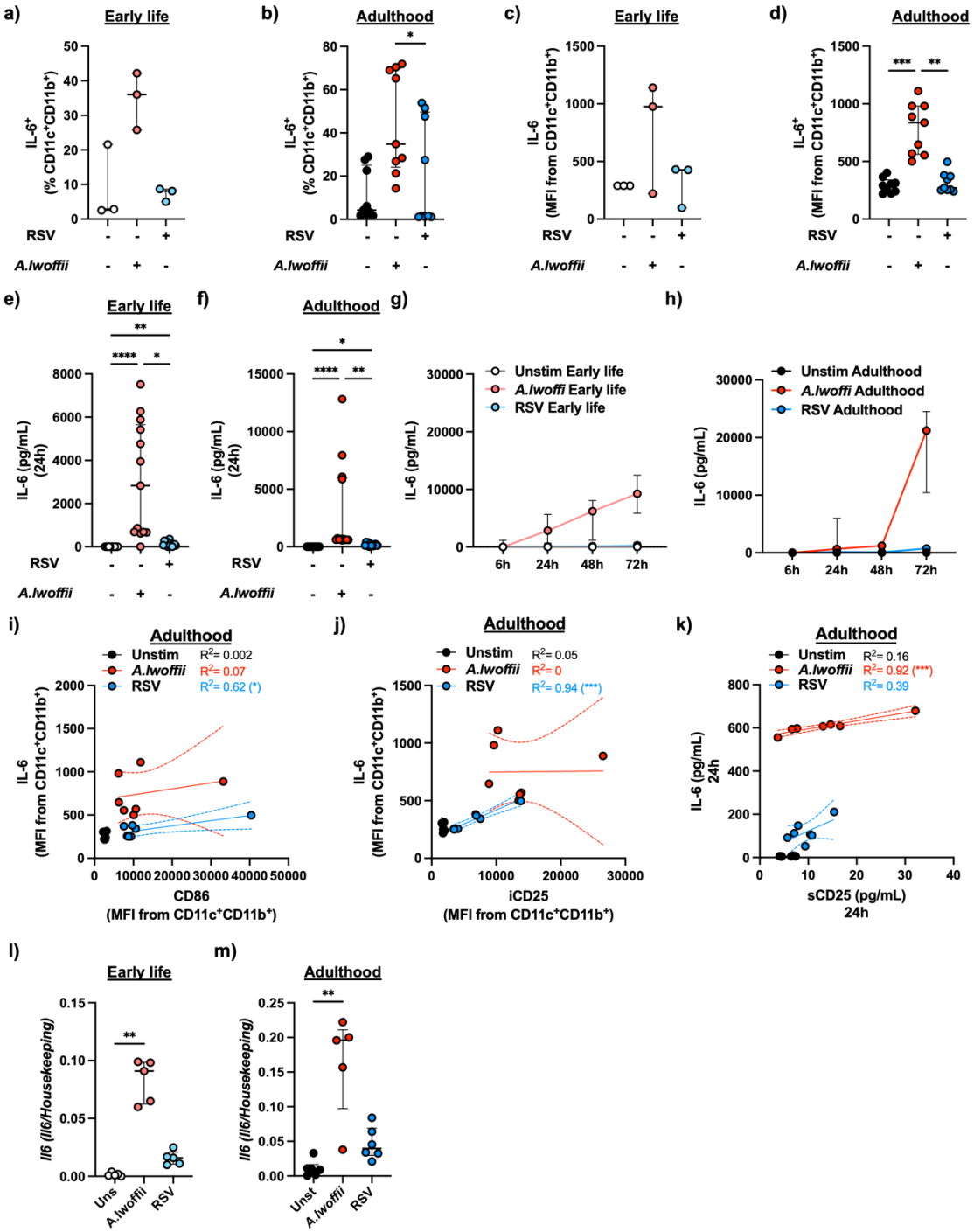


Fig 5.16. Elevated IL-6 after A.lwoffii-stimulation of BM-cDC2s

Early life and adult BM progenitors were isolated from Balb/c mice by the centrifugation method and cultured with FLt3-L for 8 to 11 days. Then they were stimulated with *A.lwoffii* (2.5x10^{8}cfu/mL) or RSV (1 MOI) or left unstimulated. Flow cytometry analysis and RT-qPCR were performed 24h post-stimulation while supernatants were collected at 6,24, 48 and 72h post stimulation for ELISA. **(a)** Early life and **(b)** adult IL-6 proportion and **(c,d)** MFI of cDC2 cells. **(e)** Early life and **(f)** adult IL-6 production 24h post stimulation. **(g)** Early life and **(h)** adult IL-6 production 6,24,48 and 72h post-stimulation. **(i)** Correlation between IL-6 and CD86 on adult cDC2 cells. **(j)** Correlation between IL-6 and iCD25 on adult cDC cells. **(k)** Correlation between IL-6 and sCD25 on two representative adult experiments. **(l)** Early life and **(m)** adult *Il6* relative expression when compared with an average of housekeeping genes (*Gapdh* and *Actb*) in 5 representative BMDC cultures. Unless otherwise stated data from one (a,c) with n= 3 mice per group or five independent experiments (b, d-m) with n= 10-14 mice per group. Data shown with median and interquartile range. Each dot represents one mouse, but for g and h where dots represent the mean of a group. Kruskal-Wallis with multiple comparisons test (a-f,l,m) and simple linear regression with Pearson analysis (i-k) were performed in which *, $p < 0.05$; **, $p < 0.01$; and ***, $p < 0.001$.

5.2.4 Live RSV exposure is required to promote cDC2 activation, CD25 and IL-6 production

I next sought to determine which components of RSV or *A.lwoffii* may be involved in promoting specific molecules in cDC2s. RSV can be inactivated by exposure to heat (RSV HI) or to UV light (RSV UV) (696). Heat inactivation results in protein denaturation, limiting attachment to host cells compared to UV. Both HI and UV inactivation degrade the RSV RNA genome preventing viral transcription and replication (697). Thus, to analyse the effect of viral replication, virion protein structure and viral RNA recognition, early life and adult BM-derived DCs were exposed to live RSV, RSV HI and RSV UV for 24h; after which cDC2 cell responses were analysed. No difference in cDC2 cell proportion was seen between early life cultured groups, but an increased $CD11b^{+}CD11c^{+}$ expression was observed in adult cultures stimulated with RSV UV when compared with the other RSV treated groups *(**Fig 5.17a,b**)*. There was an increase in cDC1s in RSV treated cultures when compared with RSV HI conditions in early life cells while no difference was observed in adulthood *(**Fig 5.17c,d**)*. Elevated proportions of pDCs were also seen in RSV-stimulated conditions when compared with RSV UV cultures in adulthood *(**Fig 5.17e,f**)*. As before however cDC2s represented the most abundant cell type in these *in vitro* cultures *(**Fig 5.17a-f**)*. Expression of CD86 was only significantly elevated in live RSV-treated conditions of both age groups *(**Fig 5.17g,h**)* as was MHC-II *(**Fig 5.17i,j**)*. A trend to a decrease SIRPα expression was seen in RSV-exposed early life cDC2s that was significantly downregulated when compared with control and RSV UV conditions in adulthood *(**Fig 5.17k,l**)*.

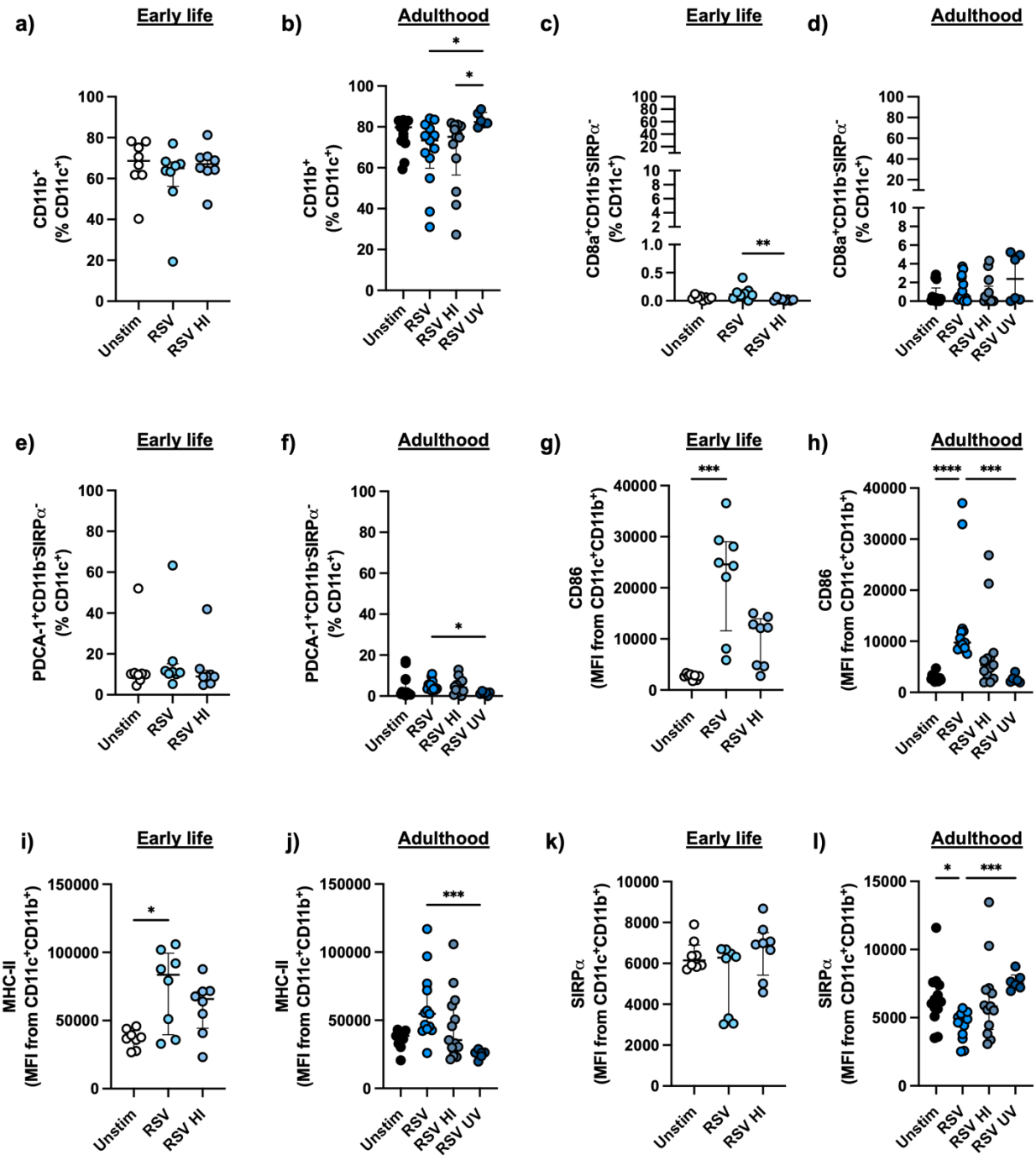


Fig 5.17. Heat and UV inactivated RSV, unlike live RSV, do not promote BM-cDC2 activation

Early life and adult BM progenitors were isolated from Balb/c mice by the centrifugation method and cultured with FLt3-L for 8 to 11 days. Then they were stimulated with 1MOI of RSV, RSV heat inactivated (RSV-HI), RSV exposed to UV light (RSV-UV) or left unstimulated. Flow cytometry analysis was performed 24h post-stimulation. **(a)** Early life and **(b)** adult proportion of cDC2, **(c,d)** cDC1s and **(e,f)** pDCs. **(g)** Early life and **(h)** adult CD86, **(I,j)** MHC-II and **(k,l)** SIRPα MFI. Data from three (early life) with n= 8 mice per group or four (adulthood) independent experiments with n= 13 mice per group. Data shown with median and interquartile range. Each dot represents one mouse. Kruskal-Wallis with multiple comparisons test was performed in which *, $p < 0.05$; **, $p < 0.01$; and ***, $p < 0.001$.

mCD25 expression by cDC2s was likewise increased in live virus-exposed cultures when compared with control cells in early life *(**Fig 5.18a**)* and adulthood *(**Fig 5.18b**);* where upregulation was also observed when compared with RSV UV treated cultures. A trend to a decrease mCD25 was seen in RSV HI when compared with live RSV treated conditions, but expression of mCD25 was significantly elevated in HI cultures when compared with UV treated ones *(**Fig 5.18b**).* iCD25 was also preferentially elevated in conditions treated with live RSV, when compared to both media and RSV UV treated cells, but RSV HI cDC2s also showed an increased ability to produce iCD25 when compared with control wells *(**Fig 5.18c,d**).* No difference in CD25 secretion was seen between control and live RSV exposed cultures in any age group at 24h post-stimulation *(**Fig 5.18e,f**).* UV viral-inactivation lead to decreased sCD25 when compared with live RSV *(**Fig 5.18f**).* sCD25 production did increase over time in all RSV-treated cultures analysed with no major differences observed between RSV and RSV HI treated groups *(**Fig 5.18g,h**).* mCD25 and CD86 significantly correlated with each other in all RSV-treated adult cultures *(**Fig 5.18i**)*, but no correlation was observed between iCD25 and CD86 *(**Fig 5.18j**)*. As before, an inverse correlation was seen for iCD25 and sCD25 in RSV-treated cultures and a negative correlation was also observed in RSV HI conditions. No association between both molecules was however seen in unstimulated or RSV UV treated conditions *(**Fig 5.18k**).* The upregulated expression of *Cd25* and *Cd132* by DCs in response to RSV was dependent on live virus, with neither HI-RSV or UV-RSV resulting in increased transcript levels *(**Fig 5.18l,m**).*

The proportion of IL-6^{+} cDC2s and IL-6 MFI in cDC2 populations was similar between all RSV treated conditions *(**Fig 5.19a-d**).* IL-6 production 24h post stimulation was however upregulated in the supernatant of BM-derived live RSV-treated cultures when compared with media or RSV HI conditions in early life *(**Fig 5.19e**)* and unstimulated conditions in adulthood *(**Fig 5.19f**).* IL-6 production by RSV-treated cells increased over time and was elevated when compared with unstimulated or RSV HI conditions *(**Fig 5.19g,h**).* No correlation between IL-6 and CD86 MFI on adult cDC2 cells was observed for any RSV culture *(**Fig 5.19i**)*. A positive correlation between IL-6 and iCD25 was observed for live RSV stimulated cultures, but not for RSV inactivated conditions *(**Fig 5.19j**)*. No correlation was however seen for the secreted forms of IL-6 and CD25 in any culture supernatant *(**Fig 5.19k**). Il6* transcript expression was elevated in live RSV treated BMDC cultures, but this was not observed when cells were treated with RSV HI virus *(**Fig 5.19l,m**).*

In summary, this data indicates that replication-sufficient RSV is needed to promote cDC2 activation, CD25 and IL-6 production. Live virus also appeared to be involved in the decrease in SIRPα on cDC2s within the culture.

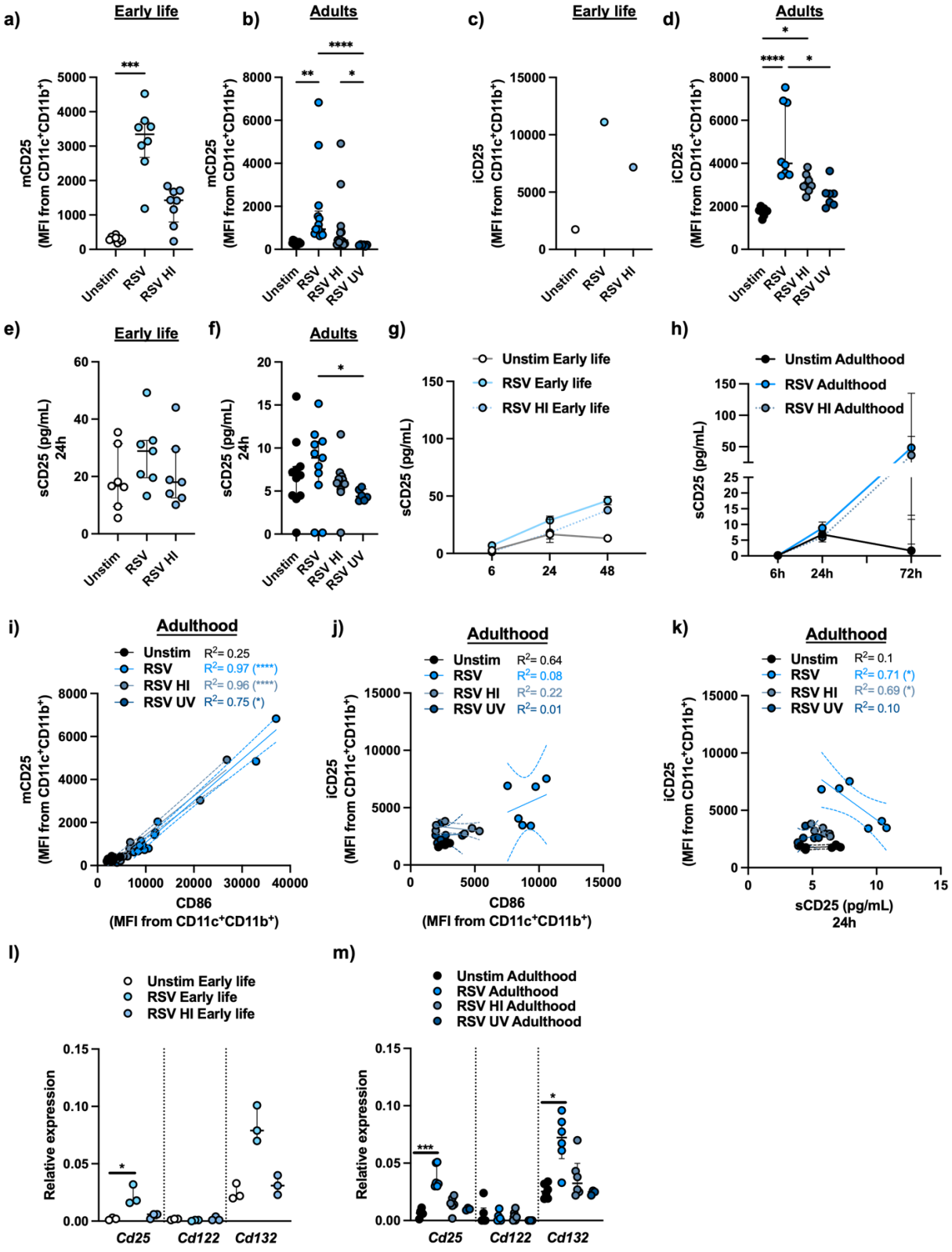


Fig 5.18. Live RSV stimulation promotes BM-cDC2s CD25 expression when compared to inactivated counterparts

Early life and adult BM progenitors were isolated from Balb/c mice by the centrifugation method and cultured with FLt3-L for 8 to 11 days. Then they were stimulated with 1MOI of RSV, RSV heat inactivated (RSV-HI), RSV exposed to UV light (RSV-UV) or left unstimulated. Flow cytometry analysis and RT-qPCR were performed 24h post-stimulation while supernatants were collected at 6,24, 48 and 72h post stimulation for ELISA. **(a)** Early life and **(b)** adult mCD25 and **(c,d)** iCD25 MFI on cDC2s. **(e)** Early life and **(f)** adult sCD25 production 24h post stimulation. **(g)** Early life and **(h)** adult sCD25 production 6,24,48 and 72h post-stimulation. **(i)** Correlation

between mCD25 and CD86 on adult cDC cells. **(j)** Correlation between iCD25 and CD86 on adult cDC cells. **(k)** Correlation between iCD25 and sCD25 on two representative adult experiments. **(l)** Early life and **(m)** adult relative expression of *Cd25, Cd122* and *Cd132* when compared with an average of housekeeping genes (*Gapdh* and *Actb*) in 3-6 representative BMDC cultures. Unless otherwise stated data from one (c) n= 1, three (a,e,g,l) n= 8 or four (b,f,h) independent experiments n=11 mice per group. Data shown with median and interquartile range. Each dot represents one mouse but for g and h where dots represent the mean of a group. Kruskal-Wallis with multiple comparisons test (a-f,l,m) and simple linear regression with Pearson analysis (i-k) were performed in which *, $p < 0.05$; **, $p < 0.01$; and ***, $p < 0.001$.

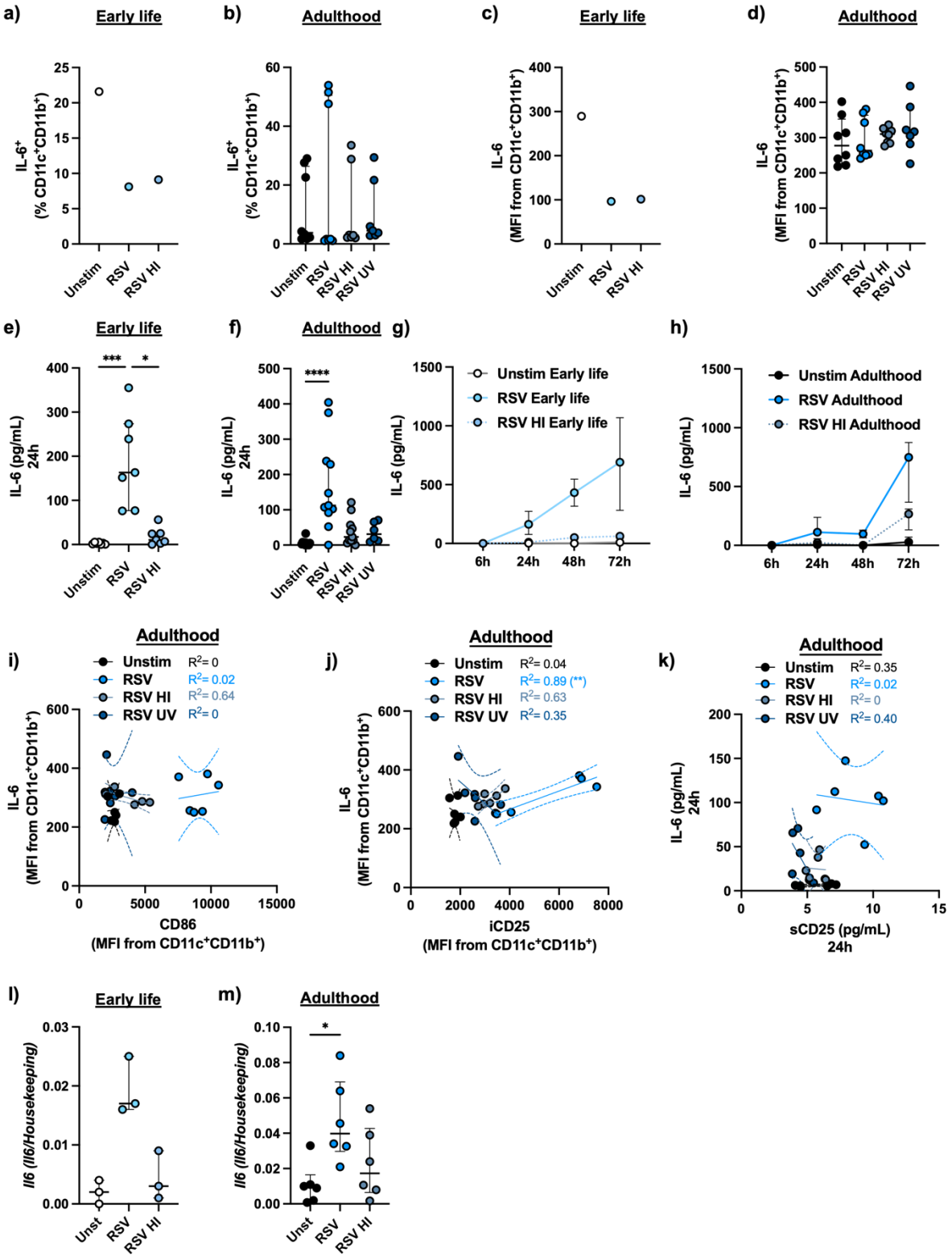


Fig 5.19. Live RSV stimulation promotes BM-cDC2s IL-6 expression

Early life and adult BM progenitors were isolated from Balb/c mice by the centrifugation method and cultured with FLt3-L for 8 to 11 days. Then they were stimulated with 1MOI of RSV, RSV heat inactivated (RSV-HI), RSV exposed to UV light (RSV-UV) or left unstimulated. Flow cytometry analysis and RT-qPCR were performed 24h post-stimulation while supernatants were collected at 6,24, 48 and 72h post stimulation for ELISA. **(a)** Early life and **(b)** adult IL-6 proportion and **(c,d)** MFI of cDC2 cells. **(e)** Early life and **(f)** adult IL-6 secretion 24h post stimulation. **(g)** Early life and **(h)** adult IL-6 secretion 6,24,48 and 72h post-stimulation. **(i)** Correlation between IL-6 and CD86 on adult cDC2 cells. **(j)** Correlation between IL-6 and iCD25 on adult cDC2 cells. **(k)** Correlation between IL-6 and sCD25 on two representative adult experiments. **(l)** Early life and **(m)** adult *Il6* relative expression when compared with an average of housekeeping genes (*Gapdh* and *Actb*) on 3-6 representative BMDC cultures. Unless otherwise stated data from one (a,c,l) n= 1, three (e,g) n=7, or four (b,d,f,h,m) independent experiments n= 11 mice per group. Data shown with median and interquartile range. Each dot represents one mouse, but for g and h where dots represent the mean of a group. Kruskal-Wallis with multiple comparisons test (a-f,l,m) and simple linear regression with Pearson analysis (i-k) were performed in which *, $p < 0.05$; **, $p < 0.01$; and ***, $p < 0.001$.

5.2.5 LPS is a potent inducer of CD25 and IL-6 secretion by BM-cDC2s

A.lwoffii recognition can be dependent on TLR2, TLR3, TLR4, TLR7 and TLR9 signalling (510,592). RSV also possesses multiple PAMPs that can be recognised by several TLR such as TLR2/6, TLR3, TLR4 and TLR7 (329,330,338,698,699). Therefore, I next sought to determine whether activation of specific TLR pathways elicited distinct effects on cDC2 activation and expression of CD25 and IL-6, which might explain differences between cDC2 responses to RSV and *A.lwoffii*. To this end, BMDCs were stimulated with Poly(I:C) (a TLR3 agonist), LPS (TLR4), Imiquimod (TLR7) and CpG (TLR9) for up to 72h and responses were analysed by flow cytometry, ELISA and qPCR.

Proportions of cDC2s, cDC1s and pDCs were maintained in all stimulated conditions at 24 hours, with cDC2s representing the most abundant cell type *(**Fig 5.20a-f**)*. Upregulation of cDC2 CD86 expression was observed in Poly(I:C)-, LPS- and Imiquimod-, but not in CpG-stimulated cultures when compared with unstimulated conditions in both age groups *(**Fig 5.20g,h**)*. LPS recognition by cDC2s also significantly upregulated CD86 compared to CpG *(**Fig 5.20g,h**)*. Similarly, Poly(I:C) and Imiquimod promoted MHC-II expression in early life cDC2 cells while this was also the case for LPS exposure in adults, but not CpG *(**Fig 5.20i,j**)*. SIRPα expression was significantly upregulated in LPS and CpG treated conditions when compared with Poly(I:C) and Imiquimod cultures, but not unstimulated cells in early life BM-derived cDC2s *(**Fig 5.20k**)*. No difference in SIRPα expression was observed in adult cultures *(**Fig 5.20l**)*.

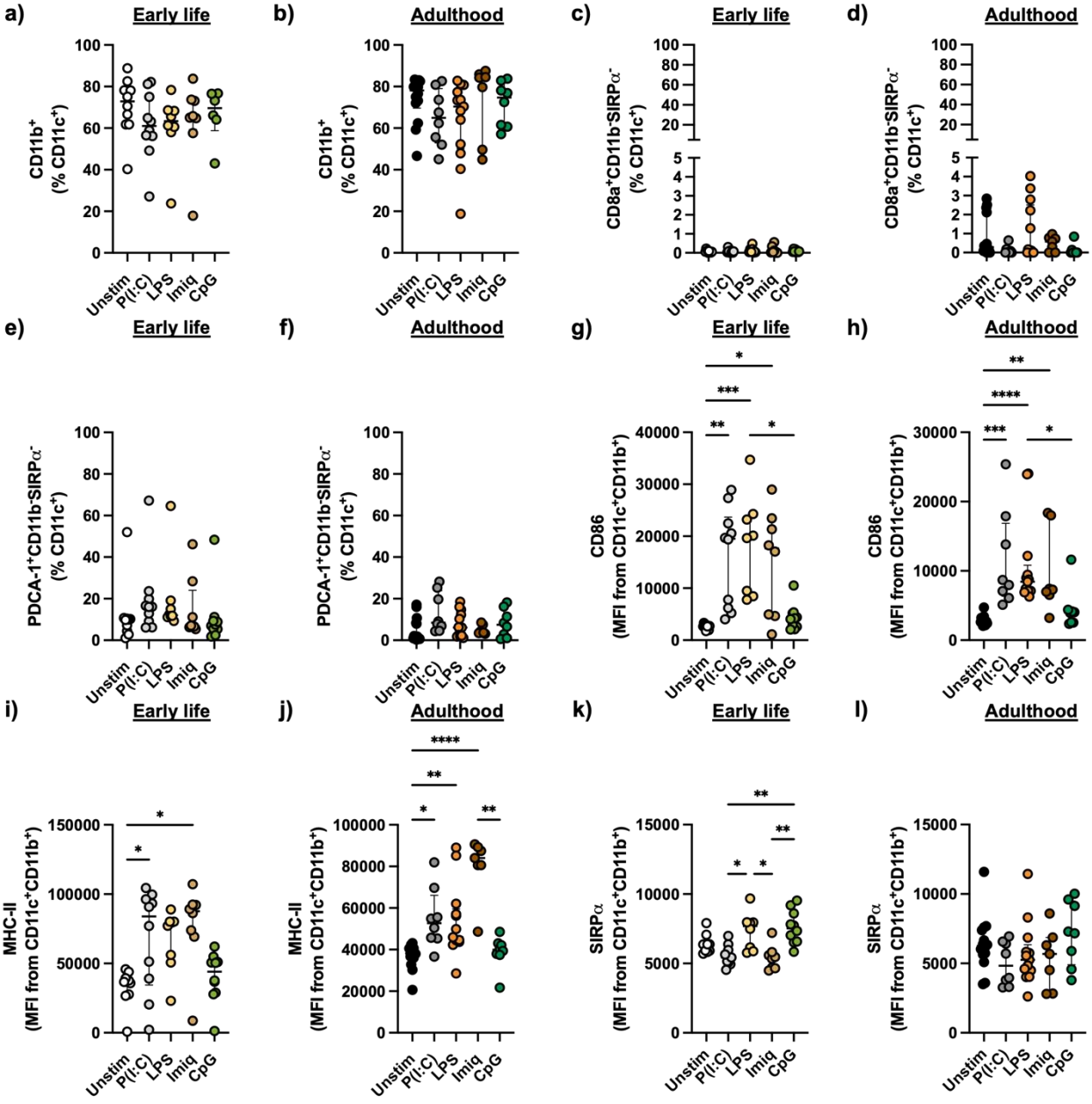


Fig 5.20. LPS, Poly(I:C) and Imiquimod-stimulation promote BM-cDC2s activation

Early life and adult BM progenitors were isolated from Balb/c mice by the centrifugation method and cultured with FLt3-L for 8 to 11 days. Then they were stimulated with Poly(I:C) (100ng/mL), LPS (0.85µg/mL), Imiquimod (1µg/mL), CpG (1µg/mL) or left unstimulated. Flow cytometry analysis and RT-qPCR was performed 24h post-stimulation **(a)** Early life and **(b)** adult proportion of cDC2, **(c,d)** cDC1s and **(e,f)** pDCs. **(g)** Early life and **(h)** adult CD86, **(l,j)** MHC-II and **(k,l)** SIRPα MFI. Data from five independent experiments with n=8-14 mice per group. Data shown with median and interquartile range. Each dot represents one mouse. Kruskal-Wallis with multiple comparisons test was performed in which *, $p < 0.05$; **, $p < 0.01$; and ***, $p < 0.001$.

Membrane CD25 expression was significantly upregulated in Poly(I:C)-, LPS- and Imiquimod-stimulated cultures when compared with unstimulated and CpG treated conditions, with LPS recognition promoting the highest mCD25 expression at the doses of agonists used *(**Fig 5.21a,b**)*. The same trend was observed for iCD25 production, with Poly(I:C), LPS and Imiquimod significantly promoting iCD25 MFI in cDC2 cells *(**Fig 5.21c,d**)*. Again, LPS exposure promoted the highest iCD25 expression at the doses used, being significantly upregulated when compared with CpG cultures *(**Fig 5.21c,d**)*. CD25 secretion was increased in supernatants of LPS treated cultures when compared with CpG treated ones in early life, while a reduced sCD25 signature with no difference between groups was observed in adults 24h post stimulant exposure *(**Fig 5.21e,f**)*. sCD25 increased over time in the culture supernatants with no major differences observed between stimulants in both age groups *(**Fig 5.21g,h**)*. mCD25 positively correlated with CD86 expression in LPS-, Imiquimod- and CpG- treated conditions *(**Fig 5.21i**)*. On average, Poly(I:C), LPS and Imiquimod activated cDC2 cells to a similar extent, as observed by their similar CD86 MFI, but LPS exposure promoted the highest iCD25 production *(**Fig 5.21j**)*. iCD25 and sCD25 seemed to correlate in LPS treated cultures, followed by Poly(I:C) cultures *(**Fig 5.21k**)*. Upregulated *Cd25* and *Cd132* levels were detected for neonatal Poly(I:C) cultures, but no significant difference in IL-2R transcripts was observed in other conditions *(**Fig 5.21l**)*. LPS-exposure however promoted an increase in *Cd25* transcript when compared to unstimulated or CpG adult treated cultures with no difference observed for Poly(I:C) *(**Fig 5.21m**)*.

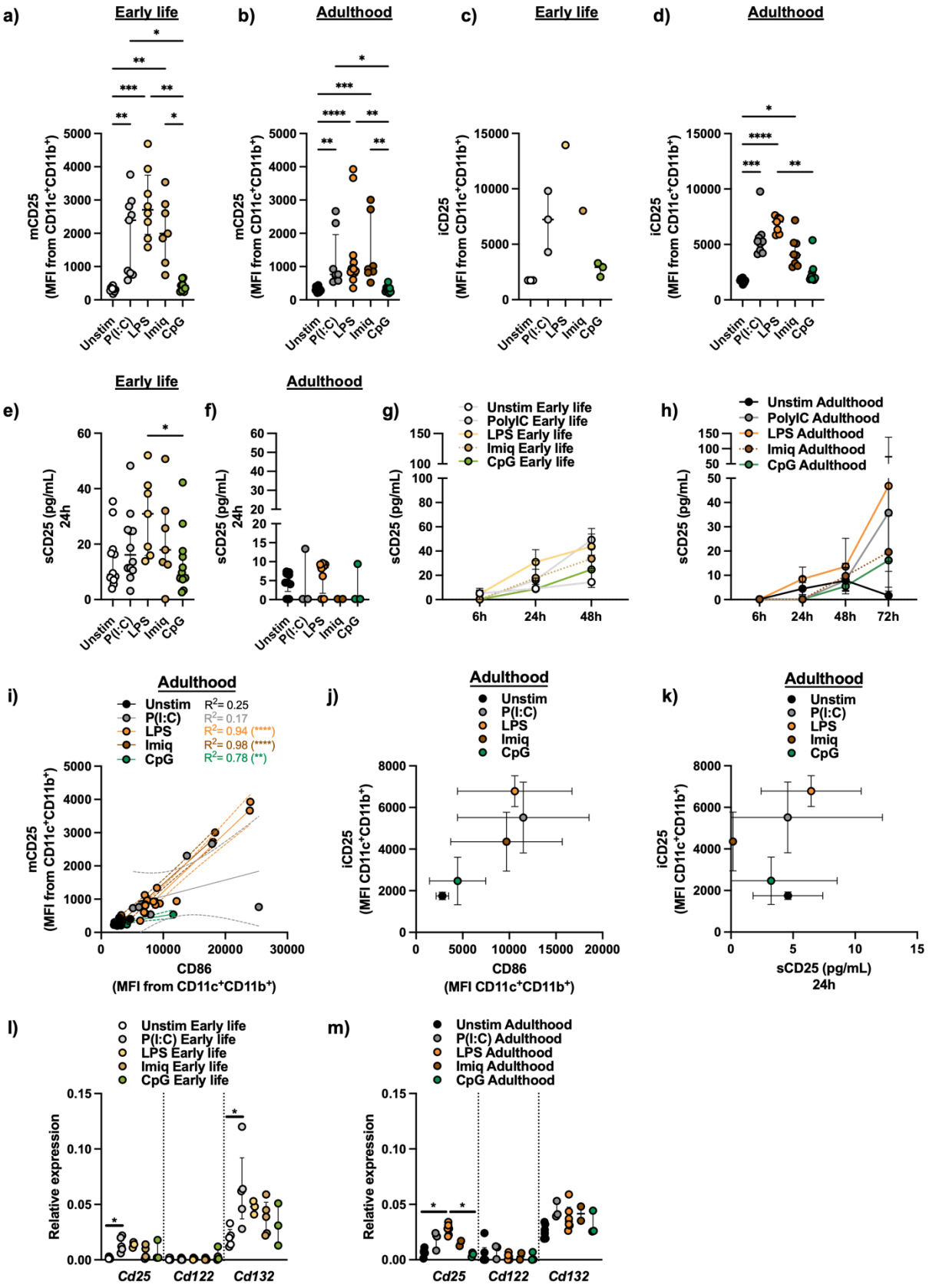


Fig 5.21. LPS-stimulation promotes CD25 expression by BM-cDC2s

Early life and adult BM progenitors were isolated from Balb/c mice by the centrifugation method and cultured with FLt3-L for 8 to 11 days. Then they were stimulated with Poly(I:C) (100ng/mL), LPS (0.85µg/mL), Imiquimod (1µg/mL), CpG (1µg/mL) or left unstimulated. Flow cytometry analysis and RT-qPCR were performed 24h post-stimulation while supernatants were collected at 6,24, 48 and 72h post stimulation for ELISA. **(a)** Early life and

(b) adult mCD25 and **(c,d)** iCD25 MFI on cDC2s. **(e)** Early life and **(f)** adult sCD25 production 24h post stimulation. **(g)** Early life and **(h)** adult sCD25 production 6,24,48 and 72h post-stimulation. **(i)** Correlation between mCD25 and CD86 on adult cDC cells. **(j)** Association between iCD25 and CD86 on adult cDC cells. **(k)** Association between iCD25 and sCD25. **(l)** Early life and **(m)** adult relative expression of *Cd25, Cd122* and *Cd132* when compared with an average of housekeeping genes (*Gapdh* and *Actb*) on 3-6 representative BMDC cultures. Data from one (c) n=1-3 or five (a,b, d-m) independent experiments n=8-14 mice per group. Data shown with median and interquartile range. Each dot represents one mouse but for g and h where dots represent the mean of a group. Kruskal-Wallis with multiple comparisons test (a-f,l,m) and simple linear regression with Pearson analysis (i) were performed in which *, $p < 0.05$; **, $p < 0.01$; and ***, $p < 0.001$.

The proportion of IL-6$^+$ cDC2 cells was similar between all analysed groups *(**Fig 5.22a,b**),* but IL-6 MFI on cDC2 cells was upregulated in LPS adult treated conditions when compared with media or Imiquimod exposed samples at the doses used *(**Fig 5.22c,d**).* IL-6 secretion in the culture supernatant 24h post stimulation was significantly elevated in Poly(I:C)-, LPS- and Imiquimod-stimulated conditions when compared to the unstimulated control group in early life cultures *(**Fig 5.22e**).* In adult cultures however, LPS was the only stimulant that significantly upregulated IL-6 secretion 24h post stimulation when compared with unstimulated controls *(**Fig 5.22f**).* 24h post stimulation, LPS was the strongest inducer of IL-6 secretion at the doses used both in early life and adulthood conditions; being significantly upregulated when compared with CpG cultures at both ages *(**Fig 5.22e,f**).* IL-6 secretion was increased over time by LPS and Imiquimod stimulation; with Imiquimod promoting higher IL-6 secretion, on average, than LPS 48 and 72h post early life BMDC stimulation *(**Fig 5.22g**).* LPS-stimulated conditions secreted the highest amount of IL-6 in adult BM-derived DC cultures, with secretion spiking at 72h post stimulation *(**Fig 5.22h**).* At similar levels of CD86 upregulation by Poly(I:C), LPS and Imiquimod, LPS exposure promoted the highest IL-6 expression *(**Fig 5.22i**).* A positive correlation between IL-6 and iCD25 was observed in Poly(I:C), Imiquimod and CpG conditions *(**Fig 5.22j**).* A positive association between IL-6 and sCD25 was however solely seen in LPS exposed cultures *(**Fig 5.22k**).* Concomitant with the protein data, LPS-stimulation of BM-derived DCs promoted upregulation of *Il6* transcript when compared with unstimulated conditions in both age cultures *(**Fig 5.22l,m**).* This data shows that LPS, and to a lesser extent Poly(I:C) and Imiquimod, can reproduce some of the pro-T_{FH} signatures observed in *A.lwoffii* treated cultures, while CpG stimulation fails to do so.

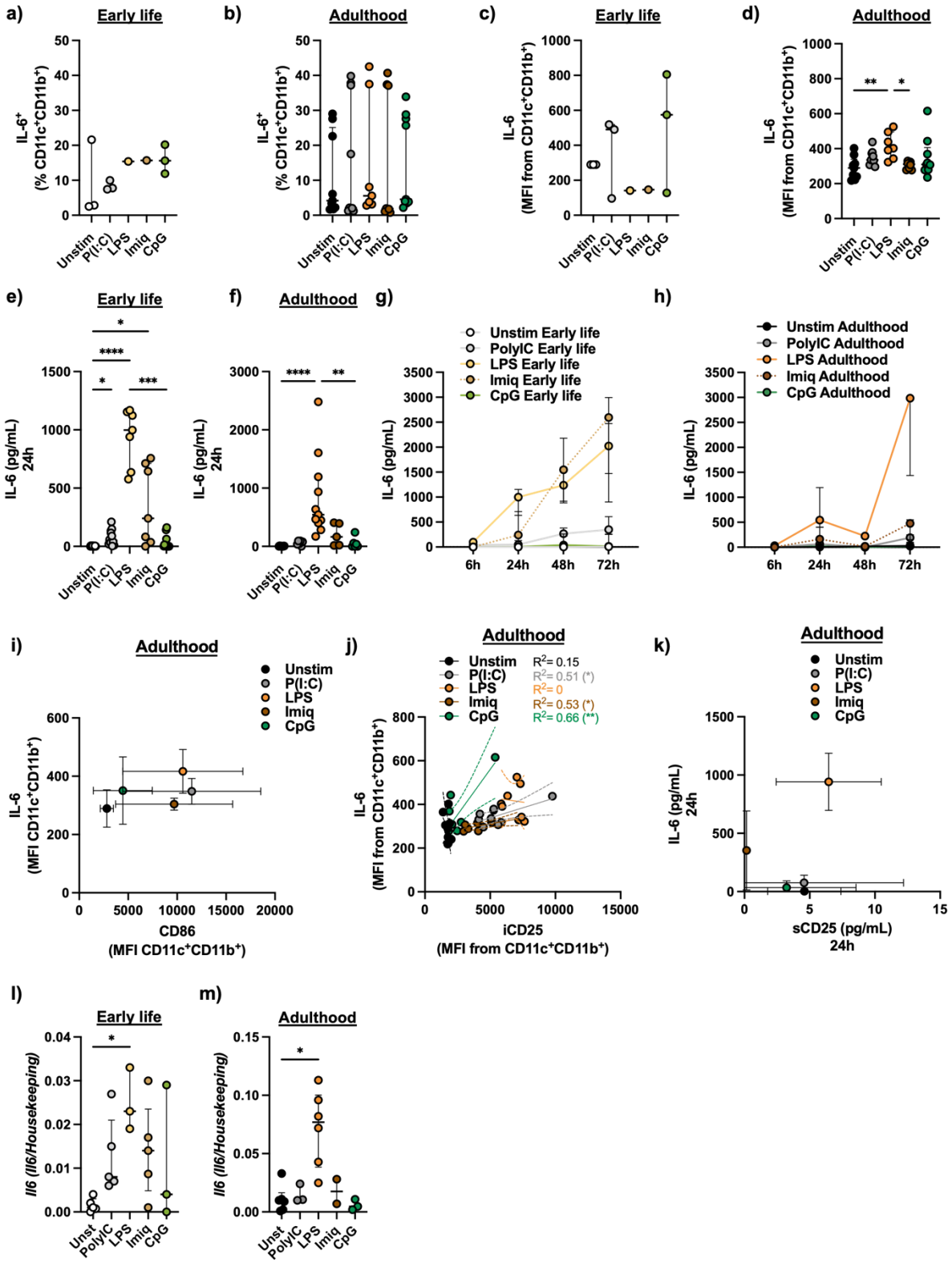


Fig 5.22. LPS-stimulation promotes IL-6 expression by BM-cDC2s

Early life and adult BM progenitors were isolated from Balb/c mice by the centrifugation method and cultured with FLt3-L for 8 to 11 days. Then they were stimulated with Poly(I:C) (100ng/mL), LPS (0.85µg/mL), Imiquimod (1µg/mL), CpG (1µg/mL) or left unstimulated. Flow cytometry analysis and RT-qPCR were performed 24h post-stimulation while supernatants were collected at 6,24, 48 and 72h post stimulation for ELISA. **(a)** Early life and **(b)** adult IL-6 proportion and **(c,d)** MFI of cDC2 cells. **(e)** Early life and **(f)** adult IL-6 production 24h post stimulation. **(g)** Early life and **(h)** adult IL-6 production 6,24,48 and 72h post-stimulation. **(i)** Association between IL-6 and CD86 on adult cDC cells. **(j)** Correlation between IL-6 and iCD25 on adult cDC cells. **(k)** Association

between IL-6 and sCD25. **(l)** Early life and **(m)** adult *Il6* levels on 3-6 representative BMDC cultures. Data from one (a,c) n=1-3 or five (b, d-m) independent experiments n=7 mice per group. Data shown with median and interquartile range. Each dot represents one mouse, but for g and h where dots represent the mean of a group. Kruskal-Wallis with multiple comparisons test (a-f,l,m) and simple linear regression with Pearson analysis (j) were performed in which *, $p < 0.05$; **, $p < 0.01$; and ***, $p < 0.001$.

5.2.6 TLR4 inhibition suppresses LPS, but not *A.lwoffii* or RSV, mediated production of IL-6 and CD25 by BMDCs

TLR4 can effectively recognize *A.lwoffii*, via it's LPS content, and RSV, via its F and G proteins (510,698). LPS, a potent TLR4 agonist (700), has the greatest effect at driving cDC2 CD25 and IL-6 production. Therefore, to determine if TLR4 signaling is responsible for *A.lwoffii* and/or RSV activation of cDC2 *in vitro*, BMDCs were treated with a TLR4 inhibitor (TLR4i) prior to RSV or *A.lwoffii* stimulation. As a control, BMDCs were treated with a concentration of LPS equivalent to that found in *A.lwoffii* extract.

As with previous cultures, BM progenitors preferentially differentiated towards cDC2s when compared with cDC1s or pDCs and no difference in cell populations was observed between conditions treated with TLR4 or different stimulants *(**Fig 5.23a-c**)*. A trend to a decrease cDC2 activation, as marked by CD86 and MHC-II expression, was observed in TLR4i treated LPS exposed cultures when compared with LPS exposed conditions that did not receive the inhibitor *(**Fig 5.23d,e**)*. No difference in CD86 or MHC-II expression was however seen in *A.lwoffii* or RSV stimulated conditions between cultures receiving and not receiving the inhibitor *(**Fig 5.23d,e**)*. Similar SIRPα cDC2 expression was observed among TLR4 inhibited and non-inhibited groups treated with the same stimulant *(**Fig 5.23f**)*. A trend to a reduced mCD25 cDC2 expression was observed in TLR4i LPS and *A.lwoffii* treated conditions when compared with their respective controls, although this did not reach significance, nor was it observed in RSV BMDCs *(**Fig 5.23g**)*. More strikingly, a significant reduction in CD25 secretion was found for TLR4 inhibited LPS treated groups and a trend could also be observed in TLR4 inhibited *A.lwoffii* treated conditions *(**Fig 5.23h**)*. No difference in sCD25 for RSV stimulated groups was however seen *(**Fig 5.23h**)*. While IL-6 secretion was significantly abrogated in TLR4 inhibited LPS treated cultures when compared with non-inhibited groups, this was not the case for *A.lwoffii* or RSV treated conditions *(**Fig 5.23i**)*. A preliminary study using BM progenitors from $Tlr4^{-/-}$ mice showed a failure to secrete CD25, and to a lesser extent IL-6, in LPS and *A.lwoffii* stimulated cultures with little difference seen in RSV treated WT versus $TLR4^{-/-}$ BMDCs *(**Fig 5.23j,k**)*. Taken together this data supports a role for TLR4 signaling in promoting CD25 secretion by DCs upon *A.lwoffii* stimulation.

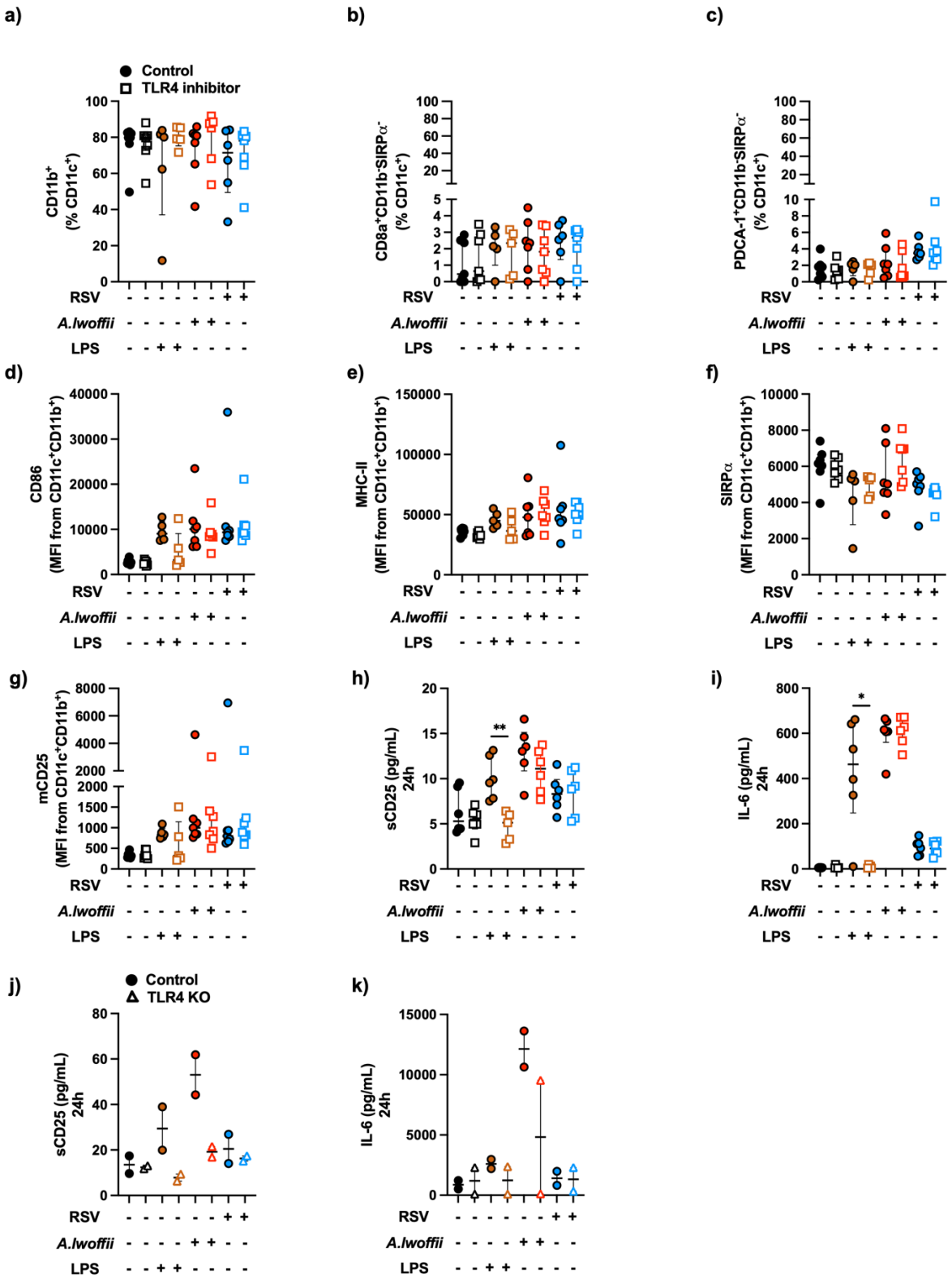


Fig 5.23. sCD25 is affected by TLR4 inhibition in LPS and A.lwoffii-stimulated BMDCs

BM progenitors from Balb/c adult mice were isolated using the centrifugation method and exposed to Flt3-L for 8/11 days. BMDC cultures were exposed to a TLR4 chemical inhibitor for 10 minutes at 37ºC and 5% CO_2 or left unexposed before being stimulated with LPS (8.5 µg/mL), *A.lwoffii* ($2.5x10^8$cfu/mL), RSV (1MOI) or left unstimulated. **(a)** Proportion of cDC2s, **(b)** cDC1s and **(c)** pDCs in control and TLR4 inhibited cultures. **(d)** CD86, **(e)** MHC-II, **(f)** SIRPα and **(g)** mCD25 MFI on cDC2s in control and TLR4 inhibited cultures. **(h)** sCD25 levels on the supernatant of control and TLR4 inhibited cultures 24h post stimulation. **(i)** IL-6 levels on the supernatant of

control and TLR4 inhibited cultures 24h post stimulation. BM progenitors from C57/BL6 WT and Tlr4$^{-/-}$ mice were isolated using the centrifugation method and exposed to FLt3-L for 8/11 days. BM cultures were then exposed to LPS, *A.lwoffii,* RSV or left unstimulated. **(j)** sCD25 and **(k)** IL-6 levels on the supernatant of WT and Tlr4$^{-/-}$ cultures 24h post stimulation. Data from three (a-h, j) n=5-7 or one (i,k) independent experiments n=2 mice per group. Data shown with median and interquartile range. Each symbol represents one mouse. Mann-Whitney test for groups with the same stimulation condition was performed in which *, $p < 0.05$; **, $p < 0.01$; and ***, $p < 0.001$.

5.2.7 Non-proteolytic release of CD25 by BMDCs

One common mechanism by which interleukin receptors are cleaved from the cell surface and secreted into the periphery is by proteolytic cleavage (116,701–703), a process also reported to occur for CD25 on T cells but not explored in the context of DCs (704–707). To test this, BMDC cultures were exposed to protease inhibitors in combination with *A.lwoffii* or RSV stimulation. cDC2 activation, CD25 and IL-6 secretion were analysed 24h post stimulation. All cultures were enriched in cDC2 cells with minimal proportions of cDC1s or pDCs seen *(**Fig 5.24a-c**)*. No difference in cDC2 activation markers, CD86 and MHC-II, nor SIRPα expression was observed between cultures exposed to the protease inhibitor when compared with control groups that received the same stimulation *(**Fig 5.24d-f**)*. mCD25 expression was also similar between protease inhibitor treated and untreated conditions in media, *A.lwoffii* and RSV exposed cultures *(**Fig 5.24g**)*. Most importantly, CD25 secretion was also maintained in all groups analysed with no effect attributed to proteases *(**Fig 5.24h**)*. Likewise, IL-6 was secreted in a protease-independent manner *(**Fig 5.24i**)*. One limitation of the study is the lack of a positive control that confirms the inhibition of proteases by the reagent used, but if the functionality of the inhibitor is accepted, these findings suggest that, unlike other interleukin receptors, CD25 secretion by cDC2s does not depend on proteolytic cleavage.

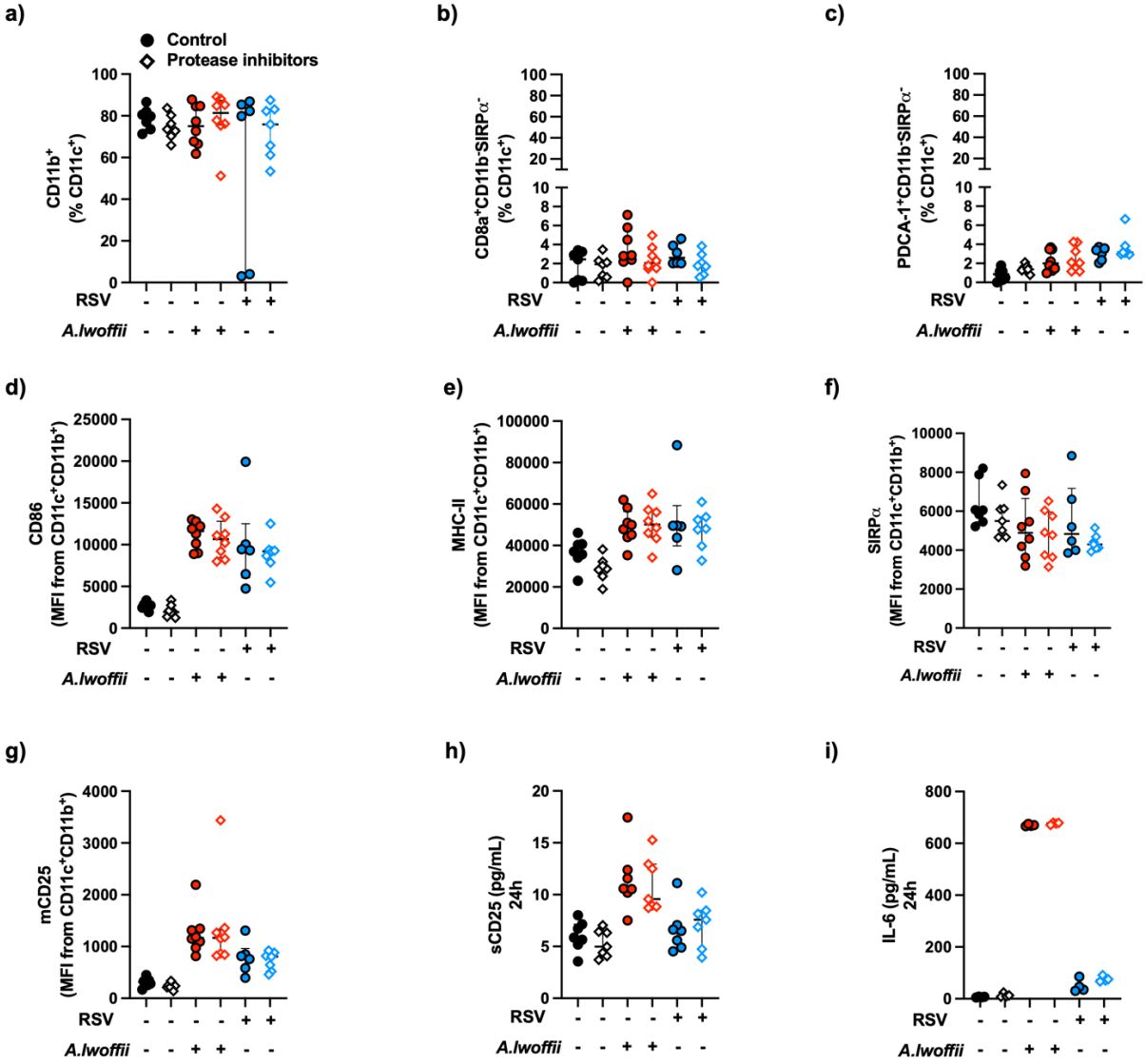


Fig 5.24. Inhibition of proteases does not affect BM-cDC2s CD25 secretion

BM progenitors from Balb/c adult mice were isolated using the centrifugation method and exposed to Flt3-L for 8/11 days. BMDC cultures were exposed to a protease inhibitor at the time of stimulation with *A.lwoffii* ($2.5x10^8$cfu/mL), RSV (1MOI) or left unstimulated. **(a)** Proportion of cDC2s, **(b)** cDC1s and **(c)** pDCs in control and protease inhibited cultures. **(d)** CD86, **(e)** MHC-II, **(f)** SIRPα and **(g)** mCD25 MFI on cDC2s in control and protease inhibited cultures. **(h)** sCD25 and **(i)** IL-6 levels on the supernatant of control and protease inhibited cultures 24h post stimulation. Data from three independent experiments with n=6-8 mice per group. Data shown with median and interquartile range. Each symbol represents one mouse. Mann-Whitney test for groups with the same stimulation condition was performed in which *, $p < 0.05$; **, $p < 0.01$; and ***, $p < 0.001$.

5.2.8 *A.lwoffii* promotes B cell activation and IL-6 secretion

B cells also participate in the T_{FH} differentiation process (38,674). Thus, B cell activation status as well as CD25 and IL-6 expression was analysed after *in vitro A.lwoffii* or RSV stimulation. B cells were isolated from the spleen of 2wk old mice and stimulated with PMA and Ionomycin, *A.lwoffii*, RSV or left unstimulated. Culture supernatants were collected 6,24,48 and 72h post stimulation and B cells were analysed by flow cytometry and RT-qPCR 1 day after stimulant exposure *(**Fig 5.25a**)*. The proportion of $CD19^{+}B220^{+}$ cells was similar between groups *(**Fig 5.25b**)*. B cells were preferentially activated by *A.lwoffii* exposure, as shown by their significantly increased membrane expression of CD86 when compared with unstimulated controls and upregulated MHC-II in comparison to unstimulated- and RSV-treated counterparts *(**Fig 5.25c,d**)*. mCD25 expression was also significantly upregulated in *A.lwoffii*-stimulated B cells *(**Fig 5.25e**)* and a trend to an increase iCD25 when compared with control cells was observed for one representative experiment *(**Fig 5.25f**)*. sCD25 was however similar between both viral and bacterial conditions, with a slight trend to an increase sCD25 observed in RSV-treated cultures at all analysed timepoints when compared with *A.lwoffii* stimulated B cells *(**Fig 5.25g,h**)*. IL-2 receptor transcript levels were similar between all stimulated conditions, but for a significant increase in *Cd122* subunit in PMA/Ionomycin stimulated cultures when compared with control or *A.lwoffii* exposed cells *(**Fig 5.25i**)*.

Similar proportions of $IL\text{-}6^{+}CD19^{+}$ cells were observed among cultures *(**Fig 5.25j**)*. Likewise, no difference was found in IL-6 MFI in B cells *(**Fig 5.25k**)*. IL-6 secretion was however upregulated in *A.lwoffii*-exposed B cells when compared with all other treatment groups, where IL-6 secretion was undetectable at all timepoints *(**Fig 5.25l,m**)*. In accordance with the protein data, *Il6* levels were increased in *A.lwoffii*-treated cultures when compared with all other stimulations, being significant in comparison with PMA/Ionomycin stimulated B cells *(**Fig 5.25n**)*. Taken together, *A.lwoffii* seems to be a potent promoter of B cell activation, membrane CD25 expression and IL-6 secretion when compared with RSV.

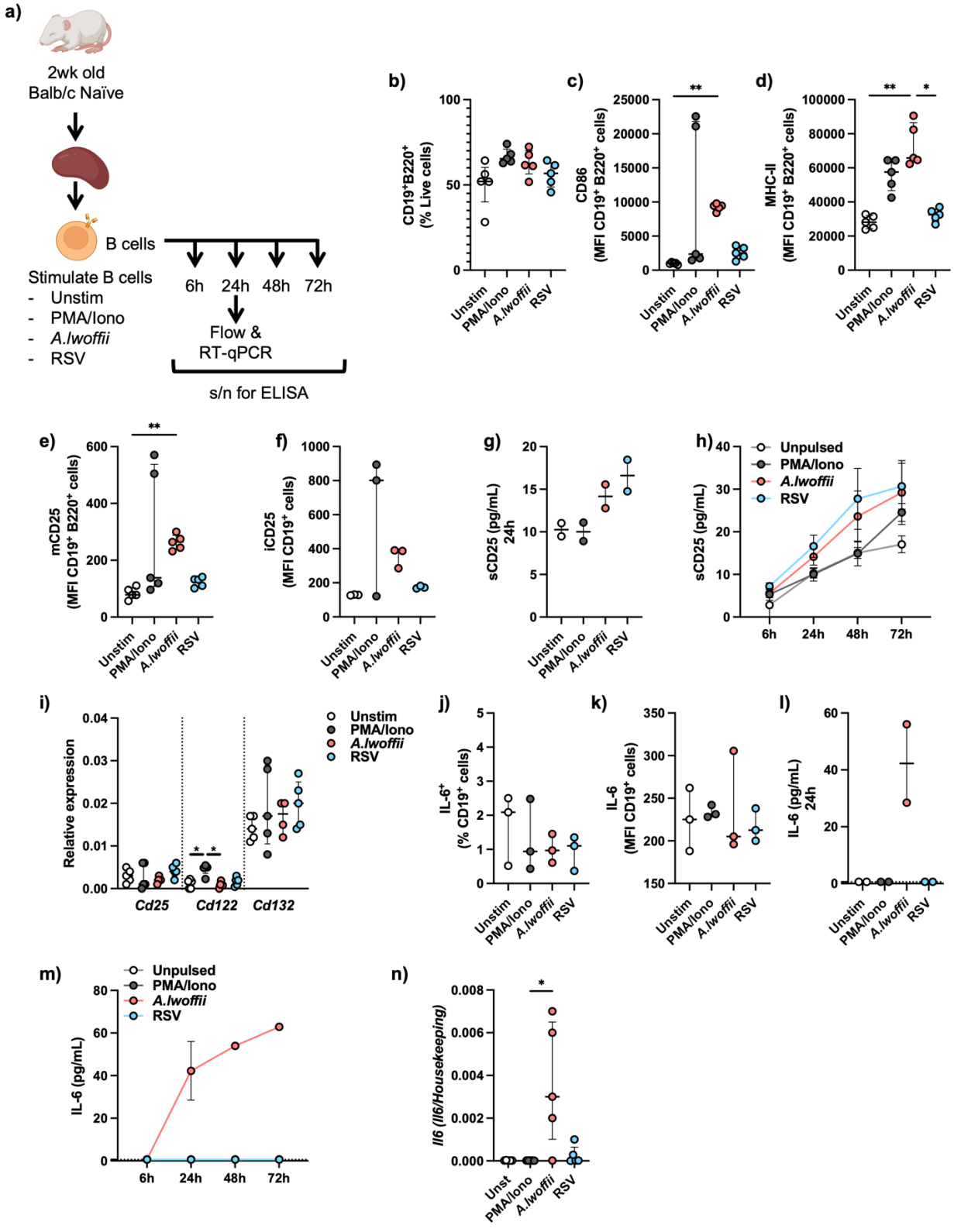


Fig 5.25. A.lwoffii-stimulation promotes early life B cell activation and IL-6 production

(a) Splenic B cells were isolated from 2wk old Balb/c naïve mice and exposed to PMA/Ionomycin (20ng/mL and 1.5µg/mL), *A.lwoffii* ($2.5x10^8$cfu/mL), RSV (1MOI) or left unstimulated. Flow cytometry analysis and RT-qPCR were performed 24h post stimulation while culture supernatants were analysed by ELISA at 6,24,48 and 72h post-stimulation. **(b)** Proportion of B cells. **(c)** CD86, **(d)** MHC-II, **(e)** mCD25 and **(f)** iCD25 MFI on B cells. **(g)** sCD25 levels on the supernatant 24h post stimulation. **(h)** sCD25 levels on the supernatant 6,24,48 and 72h post stimulation. **(i)** Relative expression of *Cd25, Cd122* and *Cd132* when compared with an average of

housekeeping genes *(Gapdh and Actb)* on B cells. **(j)** Proportion of IL-6$^+$ B cells. **(k)** IL-6 MFI on B cells. **(l)** IL-6 levels on the supernatant 24h post stimulation. **(m)** IL-6 levels on the supernatant 6,24,48 and 72h post stimulation. **(n)** *Il6* relative expression when compared with an average of housekeeping genes (*Gapdh* and *Actb*) on B cells. Data are representative of two (b-f, i-k, n) n=5 or one (g,h,l,m) independent experiments with n=2-3 mice per group. Data shown with median and interquartile range. Each dot represents one mouse, but for h and m where dots represent the mean of a group. Kruskal-Wallis with multiple comparisons test was performed in which *, $p < 0.05$; **, $p < 0.01$; and ***, $p < 0.001$.

As with DC cultures, B cells were also stimulated with different TLR agonists to analyse changes in B cell phenotype and molecule secretion when using simpler stimulants that could explain the differences observed between *A.lwoffii* and RSV stimulated conditions. PMA/Ionomycin cultures showed a significant enrichment of CD19$^+$B220$^+$ when compared with Poly(I:C) treated conditions *(**Fig 5.26a**)*. B cell stimulation with TLR agonists had limited effect on B cell activation, CD25 or IL-6 secretion. A significant increase in CD86, MHC-II, mCD25 and a trend to an increase iCD25 was only observed when B cells were stimulated with PMA/Ionomycin, but similar levels of these markers were observed in unstimulated and TLR-stimulated conditions *(**Fig 5.26b-e**)*. CD25 secretion was similar between all groups, including unstimulated control samples, at all timepoints analyzed, but for a minor increase in sCD25 72h post-stimulation in PMA/Ionomycin treated cultures *(**Fig 5.26f,g**)*. As before, no difference in IL-2 receptors transcript was observed, but for a significant increase in *Cd22* by PMA/Ionomycin conditions when compared with unstimulated cells *(**Fig 5.26h**)*. IL-6 expression was very limited or undetectable by flow cytometry, ELISA or RT-qPCR in all stimulation groups *(**Fig 5.26i-m**)*. Overall none of the different TLR agonists at the doses used in these experiments was enough to promote a B cell response similar to the one observed by *A.lwoffii*, suggesting that multiple TLRs, and possible other PRRs, are involved in *A.lwoffii* recognition by B cells.

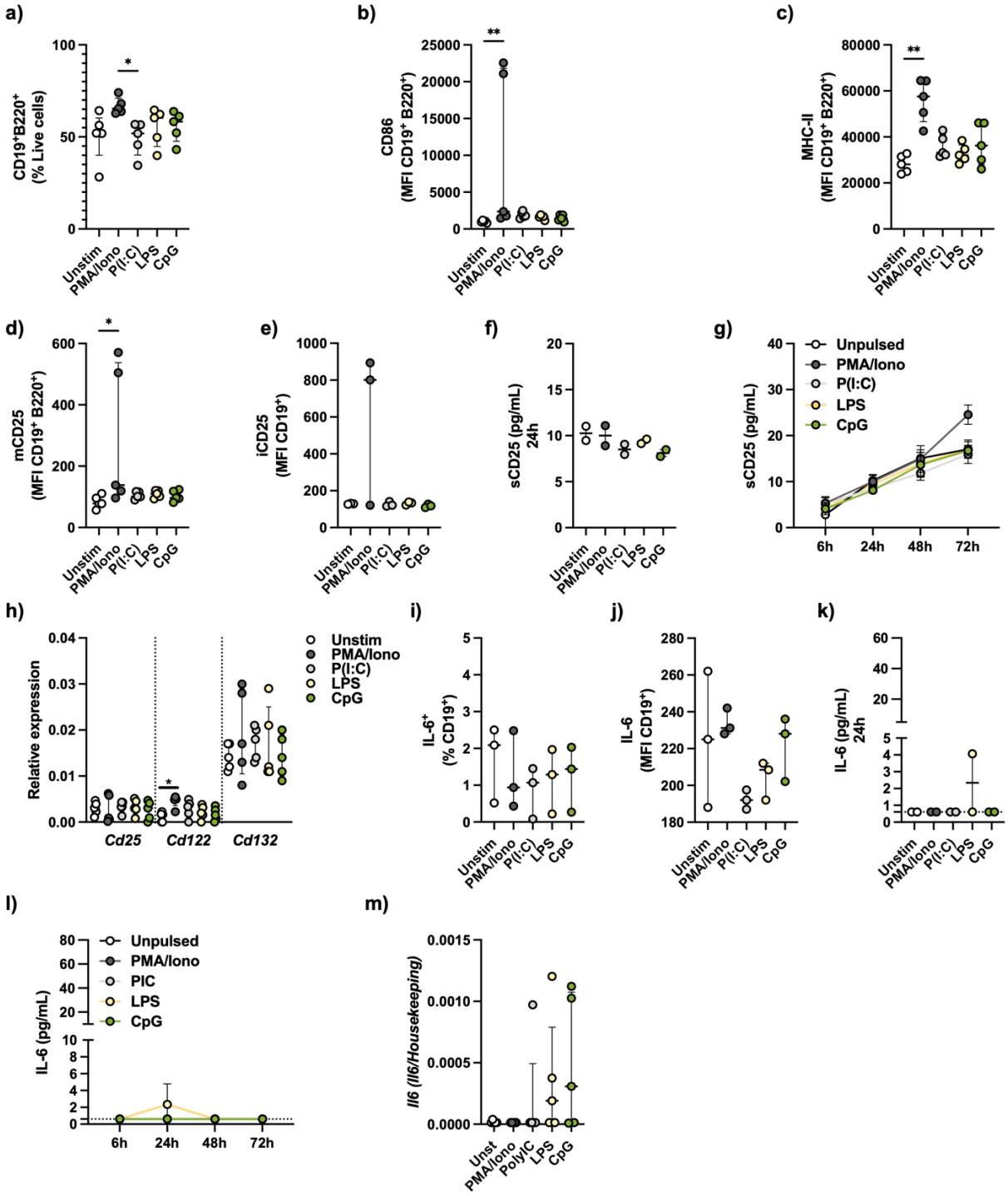


Fig 5.26. Stimulation of early life B cells with TLR-adjuvants has minimal effect on activation, CD25 or IL-6 expression

Splenic B cells were isolated from 2wk old Balb/c naïve mice and exposed to PMA/Ionomycin (20ng/mL and 1.5µg/mL), Poly(I:C) (100ng/mL), LPS (0.3µg/mL), CpG (1µg/mL) or left unstimulated. Flow cytometry analysis and RT-qPCR were performed 24h post stimulation while culture supernatants were analysed by ELISA at 6,24,48 and 72h post-stimulation. **(a)** Proportion of B cells. **(b)** CD86, **(c)** MHC-II, **(d)** mCD25 and **(e)** iCD25 MFI on B cells. **(f)** sCD25 levels on the supernatant 24h post stimulation. **(g)** sCD25 levels on the supernatant 6,24,48 and 72h post stimulation. **(h)** Relative expression of *Cd25, Cd122* and *Cd132* when compared with an average of housekeeping genes *(Gapdh and Actb)* on B cells. **(i)** Proportion of IL-6^{+} B cells. **(j)** IL-6 MFI on B cells. **(k)** IL-6 levels on the supernatant 24h post stimulation. **(l)** IL-6 levels on the supernatant 6,24,48 and 72h post stimulation. **(m)** *Il6* relative expression when compared with an average of housekeeping genes (*Gapdh* and *Actb*) on B cells. Data are representative of two (b-f, i-k, n) n=5 or one (g,h,l,m) independent experiments with

n=2-3. Data shown with median and interquartile range. Each dot represents one mouse, but for h and m where dots represent the mean of a group. Kruskal-Wallis with multiple comparisons test was performed in which *, $p < 0.05$; **, $p < 0.01$; and ***, $p < 0.001$.

5.2.9 *A.lwoffii*-stimulated DCs promote Bcl6 upregulation of co-cultured naïve CD4$^+$ T cells

A.lwoffii-stimulated BMDCs generate a pro-T_{FH} environment by promoting both CD25 and IL-6 secretion. To analyse if the generation of this microenvironment is sufficient to promote naïve CD4$^+$ T cell differentiation towards a T_{FH} phenotype, an *in vitro* co-culture system was stablished. BM-progenitor cells were isolated from 2wk old mice and cultured with Flt3-L to promote their differentiation towards cDC2 as done previously. 8d after Flt3-L exposure DCs were left unstimulated or were stimulated with *A.lwoffii*, RSV or both *A.lwoffii* and RSV. Replication of *in vivo* experiments, where mice were exposed to *A.lwoffii* 6h before RSV infection was used for the combination treatment. 24h after DC-stimulation, naïve CD4$^+$ T cells were isolated from the spleen of age-matched mice and CTV-labelled to be able to track their proliferation. In parallel, supernatants from BMDC cultures were extracted, to prevent direct T cell stimulation of potential stimulant leftover. Finally, BMDCs cell were harvested, counted and co-cultured with naïve CD4$^+$ T cells in a 1:1 ratio. Naïve CD4$^+$ T cells cultured alone and in combination with α-CD3/CD28 activation beads were used as controls. Cells were kept in co-culture for 5d, after which T_{FH} and $T_{effector}$ signatures, mainly by transcription factor expression, were analysed by flow cytometry *(**Fig 5.27a**)*.

CD4$^+$ T cell proliferation index, marked by downregulation of CTV, was significantly upregulated in those cells treated with α-CD3/28 beads or unstimulated BMDCs when compared with T cells cultured alone *(**Fig 5.27b,c**)*. α-CD3/28 beads were the most potent stimulant at promoting CD4$^+$ T cell proliferation being also significant when compared with unstimulated BMDCs *(**Fig 5.27b,c**)*. Co-culture with unstimulated DCs however promoted the highest percentage of Bcl6$^+$CD4$^+$ T cells, with Bcl6 being the major transcription factor for T_{FH} differentiation (57), in two of the three co-cultures analysed *(**Fig 5.27d,e**)*.

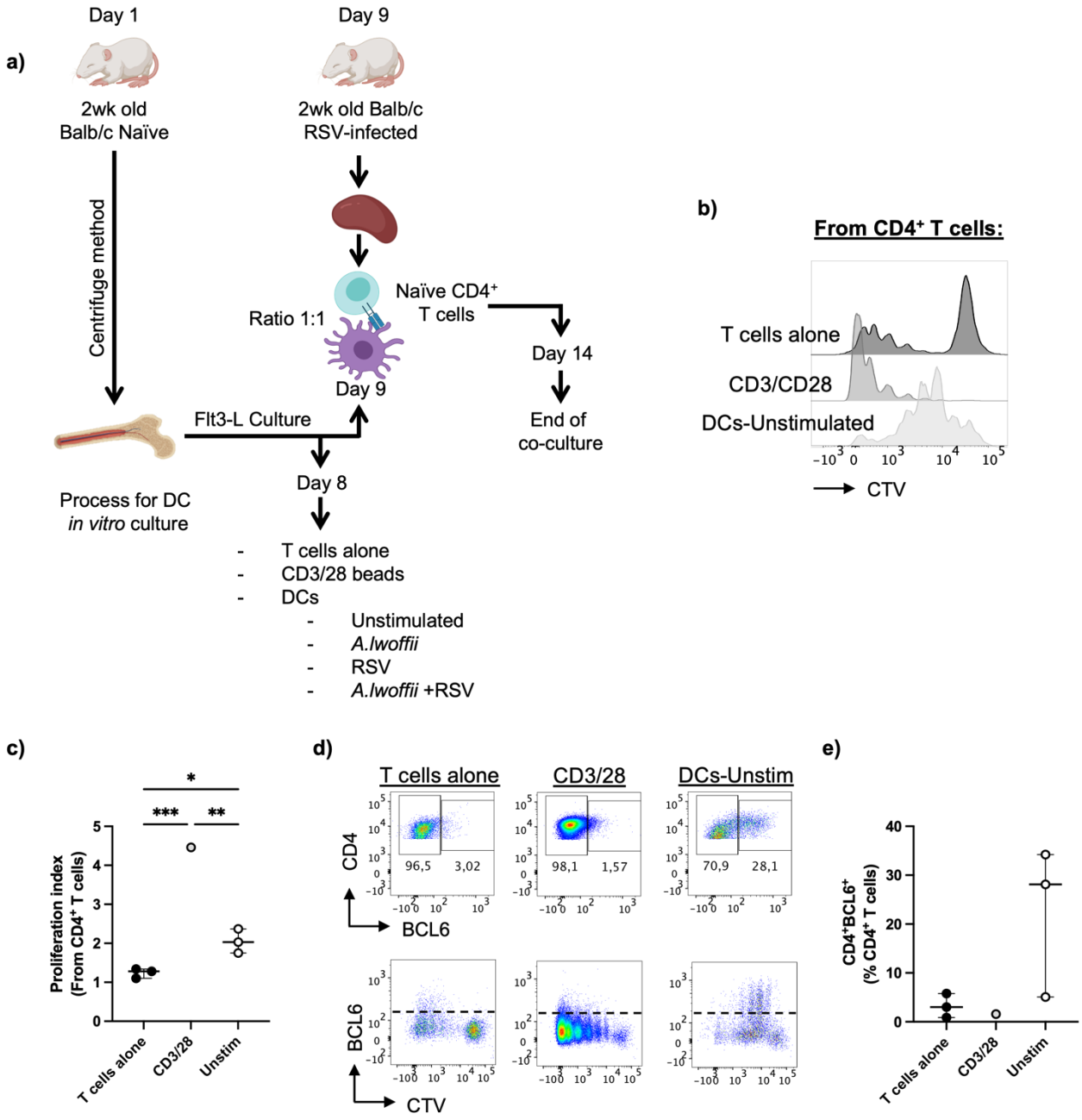


Fig 5.27. Co-culture with BM-derived DCs is needed to promote naïve CD4⁺ T cell proliferation and BCL6 expression in vitro

Bone marrow progenitors from 2wk old Balb/c mice were isolated using the centrifuge method and exposed to Flt3-L for 8 days. On day 8 matured BMDCs were exposed to *A.lwoffii* ($2.5x10^8$cfu/mL), RSV (1MOI), or both. To mimic *in vivo* conditions *A.lwoffii* exposure was performed 6h before RSV stimulation. 24h post RSV stimulation, BMDCs were harvested, pooled, counted and co-cultured with CTV-labelled naïve CD4⁺ T cells isolated from the spleen of age-matched mice in a 1:1 ratio. As controls, naïve T cells were cultured alone or with CD3/28 activation beads. The cultures were maintained at 37ºC and 5% CO_2 for 5 days. **(b)** Representative plots and **(c)** proliferation index of control and unstimulated BMDC conditions. **(d)** Representative plots and **(e)** proportion of CD4⁺BCL6⁺ cells. Data is representative of one independent experiment with n=1-3. Data shown with median and interquartile range. Each dot represents a pool of three mice from which naïve CD4⁺ T cells were isolated. Kruskal-Wallis with multiple comparisons test was performed in which *, $p < 0.05$; **, $p < 0.01$; and ***, $p < 0.001$.

DC-stimulation with *A.lwoffii*, RSV or both showed similar $CD4^+$ T cell proliferation to unstimulated control samples *(**Fig 5.28a,b**)*. The proportion of $Bcl6^+CD4^+$ T cells was increased in T cells co-cultured with *A.lwoffii*-stimulated DCs when compared with RSV-treated ones *(**Fig 5.28c,d**)*. RSV-stimulated DCs instead showed a trend to a decrease ability to promote expression of the T_{FH}-differentiation marker when compared with unstimulated DCs, a feature that *A.lwoffii* treatment in combination with the virus was able to rescue *(**Fig 5.28c,d**)*. Bcl6 MFI was upregulated on those divided $CD4^+$ T cells co-cultured with *A.lwoffii*-stimulated DCs when compared to unstimulated or RSV-exposed conditions *(**Fig 5.28e**)*. Bcl6 upregulation in $CD4^+$ T cells after *A.lwoffii*-DC co-culture was readily detectable after the first 2 cell divisions and maintained in those cells that had undergone 4 rounds of division, but it was not observed at any division in all other groups *(**Fig 5.28f**)*.

The percentage of $CD4^+CTV^{low}Bcl6^+PD\text{-}1^+$ cells was upregulated in cultures with *A.lwoffii*-stimulated DCs, with RSV-treated ones showing a trend to a decrease ability at promoting naïve $CD4^+$ T cell differentiation towards this cell type, but no significant differences between groups were observed *(**Fig 5.29a,b**)*. No difference in $CD4^+CXCR5^+PD\text{-}1^+$ proportions were observed in these cultures, as *A.lwoffii*-stimulation of DCs, equally to all other groups, failed to promote CXCR5 expression on $CD4^+$ T cells *(**Fig 5.29c,d**)*.

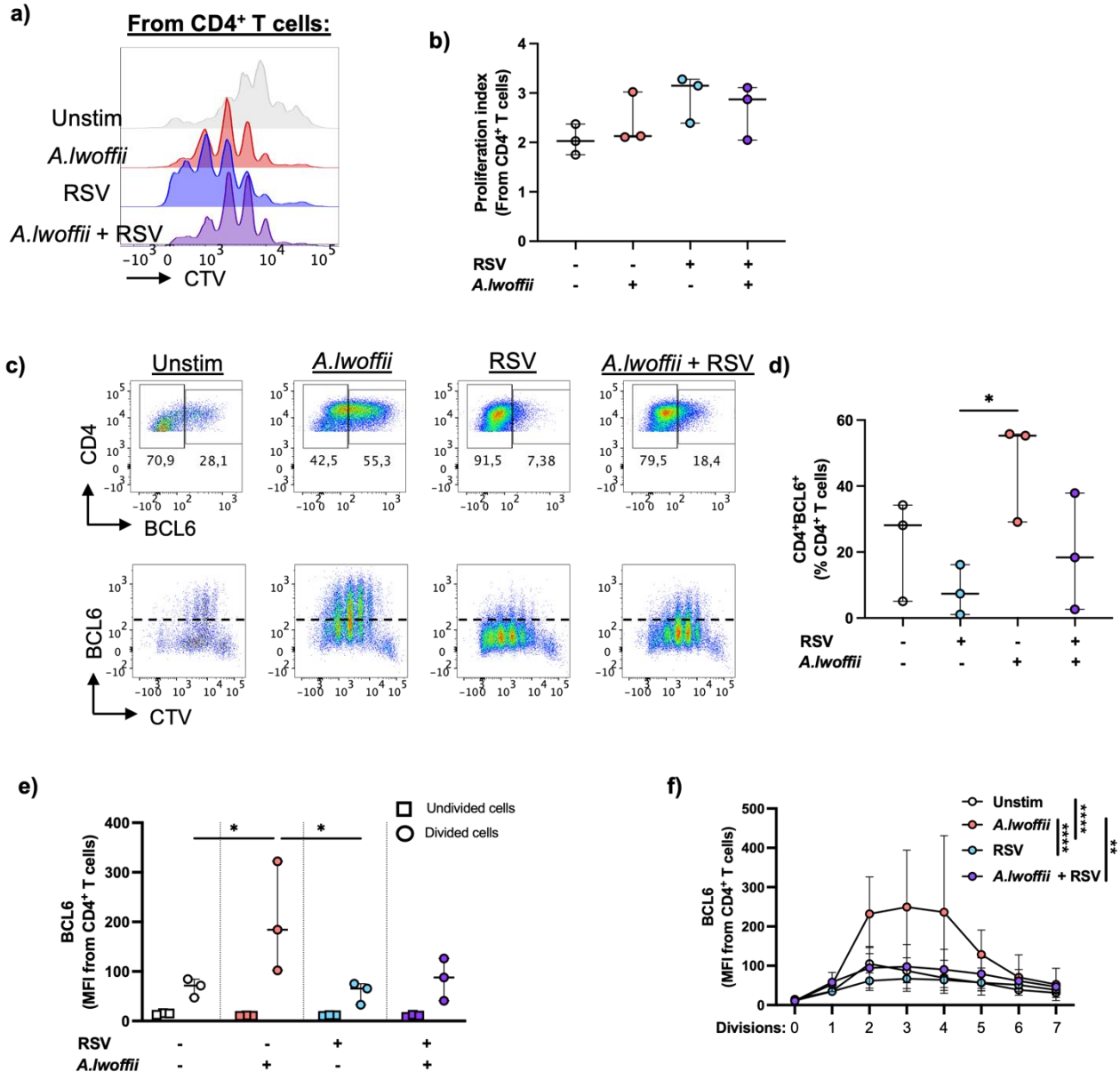


Fig 5.28. A.lwoffii stimulation of BMDCs promotes Bcl6 expression in co-cultured naïve CD4⁺ T cells

Bone marrow progenitors from 2wk old Balb/c mice were isolated using the centrifuge method and exposed to Flt3-L for 8 days. On day 8 matured BMDCs were exposed to *A.lwoffii* ($2.5x10^8$cfu/mL), RSV (1MOI), or both. To mimic *in vivo* conditions *A.lwoffii* exposure was performed 6h before RSV stimulation. 24h post RSV stimulation, BMDCs were harvested, pooled, counted and co-cultured with CTV-labelled naïve CD4⁺ T cells isolated from the spleen of age-matched mice in a 1:1 ratio. The cultures were maintained at 37ºC and 5% CO_2 for 5 days. **(a)** Representative plots and **(b)** proliferation index of different BMDC-stimulated conditions. **(c)** Representative plots and **(d)** proportion of $CD4^+BCL6^+$ cells. **(e)** BCL6 MFI on CD4⁺ T cells. **(f)** BCL6 MFI on CD4⁺ T cells at different divisions. Data is representative of one independent experiment with n=3. Data shown with median and interquartile range. Each dot represents a pool of three mice from which naïve CD4⁺ T cells were isolated. Kruskal-Wallis with multiple comparisons test was performed in which *, $p < 0.05$; **, $p < 0.01$; and ***, $p < 0.001$.

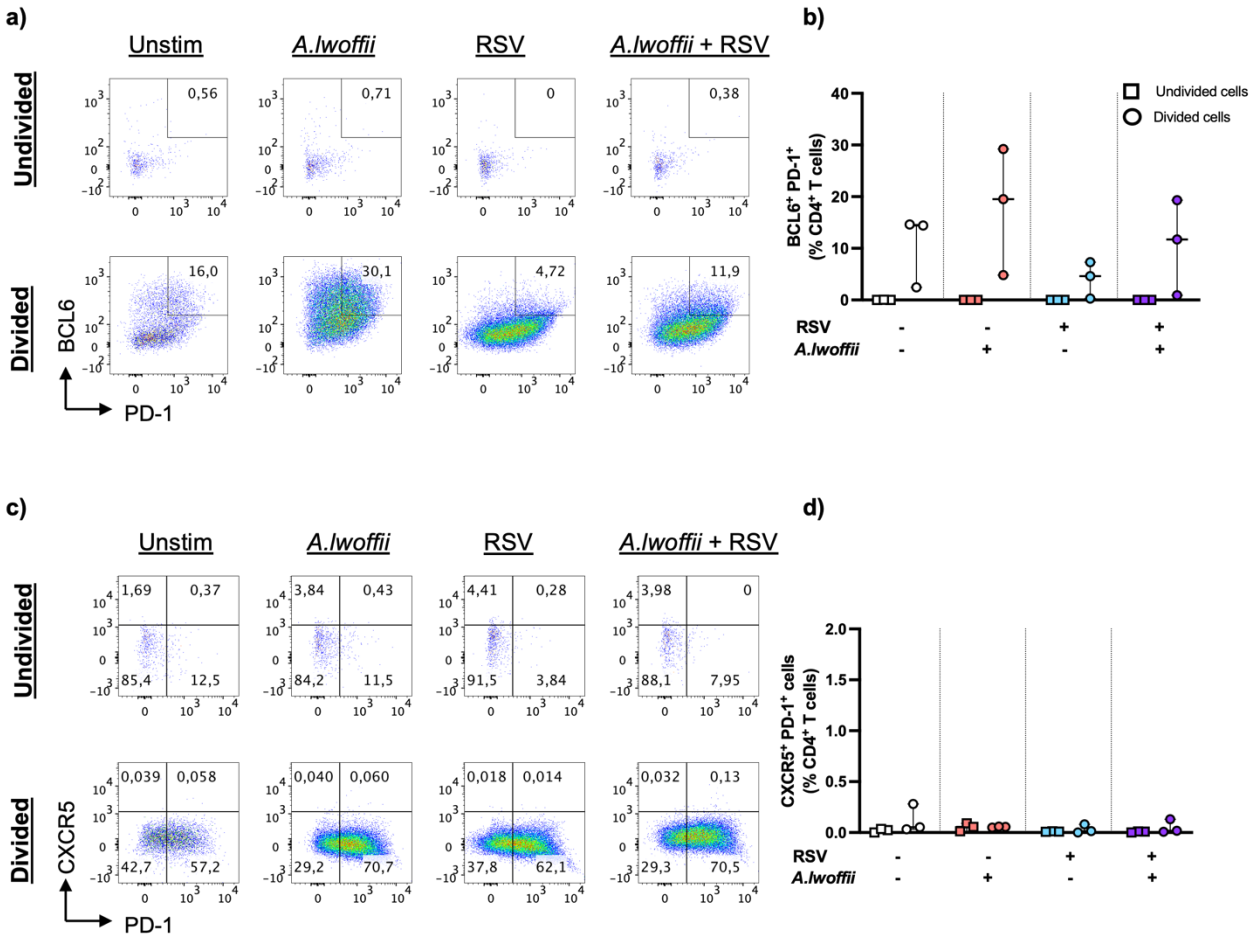


Fig 5.29. After 5 days of co-culture naïve CD4⁺ T cells have not fully differentiated into T_{FH} cells under any stimulating condition

Bone marrow progenitors from 2wk old Balb/c mice were isolated using the centrifuge method and exposed to Flt3-L for 8 days. On day 8 matured BMDCs were exposed to *A.lwoffii* ($2.5x10^8$cfu/mL), RSV (1MOI), or both. To mimic *in vivo* conditions *A.lwoffii* exposure was performed 6h before RSV stimulation. 24h post RSV stimulation, BMDCs were harvested, pooled, counted and co-cultured with CTV-labelled naïve CD4⁺ T cells isolated from the spleen of age-matched mice in a 1:1 ratio. The cultures were maintained at 37ºC and 5% CO_2 for 5 days. **(a)** Representative plots and **(b)** proportion of BCL6⁺PD-1⁺ cells. **(c)** Representative plots and **(d)** proportion of CXCR5⁺PD-1⁺ cells. Data is representative of one independent experiment with n=3. Data shown with median and interquartile range. Each dot represents a pool of three mice from which naïve CD4⁺ T cells were isolated. Kruskal-Wallis with multiple comparisons test was performed in which *, $p < 0.05$; **, $p < 0.01$; and ***, $p < 0.001$.

Tbet is the canonical transcription factor for T_{H1} cells (708). The proportion of Tbet⁺CD4⁺ T cells was similar in all co-cultured conditions when the whole CD4⁺ T cell population was analysed *(**Fig 5.30a,b**)*. Tbet expression was however significantly upregulated in divided CD4⁺ T cells co-cultured with DCs exposed to both *A.lwoffii* and RSV when compared with unstimulated DC cultures *(**Fig 5.30c**)*. Tbet MFI on CD4⁺ T cells was upregulated as early as the 1st division in CD4⁺ T cells co-cultured with *A.lwoffii*+RSV-DCs, but by the 2nd division in those co-cultured with only *A.lwoffii* or only RSV-stimulated DCs *(**Fig 5.30d**)*. Gata3, the canonical T_{H2} transcription factor (709), was preferentially upregulated in CD4⁺ T cells co-cultured with RSV-stimulated DCs as observed by the significant increase in CD4⁺Gata3⁺ proportion in these cultures when compared with the ones exposed to *A.lwoffii*-stimulated DCs *(**Fig 5.30e**)*. Concomitantly, Gata3 MFI on CD4⁺CTV^{low} cells

was significantly upregulated in T cells co-cultured with RSV-DCs when compared with *A.lwoffii* or *A.lwoffii*+RSV-DCs *(Fig 5.30f)*. Gata3 expression was upregulated after the second cell division in $CD4^+$ T cells cultured with RSV-stimulated BMDCs, it was maintained until the 6^{th} cell division and was significantly upregulated in the RSV-stimulated group when compared with all other stimulation conditions *(Fig 5.30g)*. Gata3 upregulation on $CD4^+$ T cells to similar levels to those promoted by RSV-DCs were not observed by *A.lwoffii*-, *A.lwoffii*+RSV- or unstimulated-DCs at any cell division *(Fig 5.30g)*.

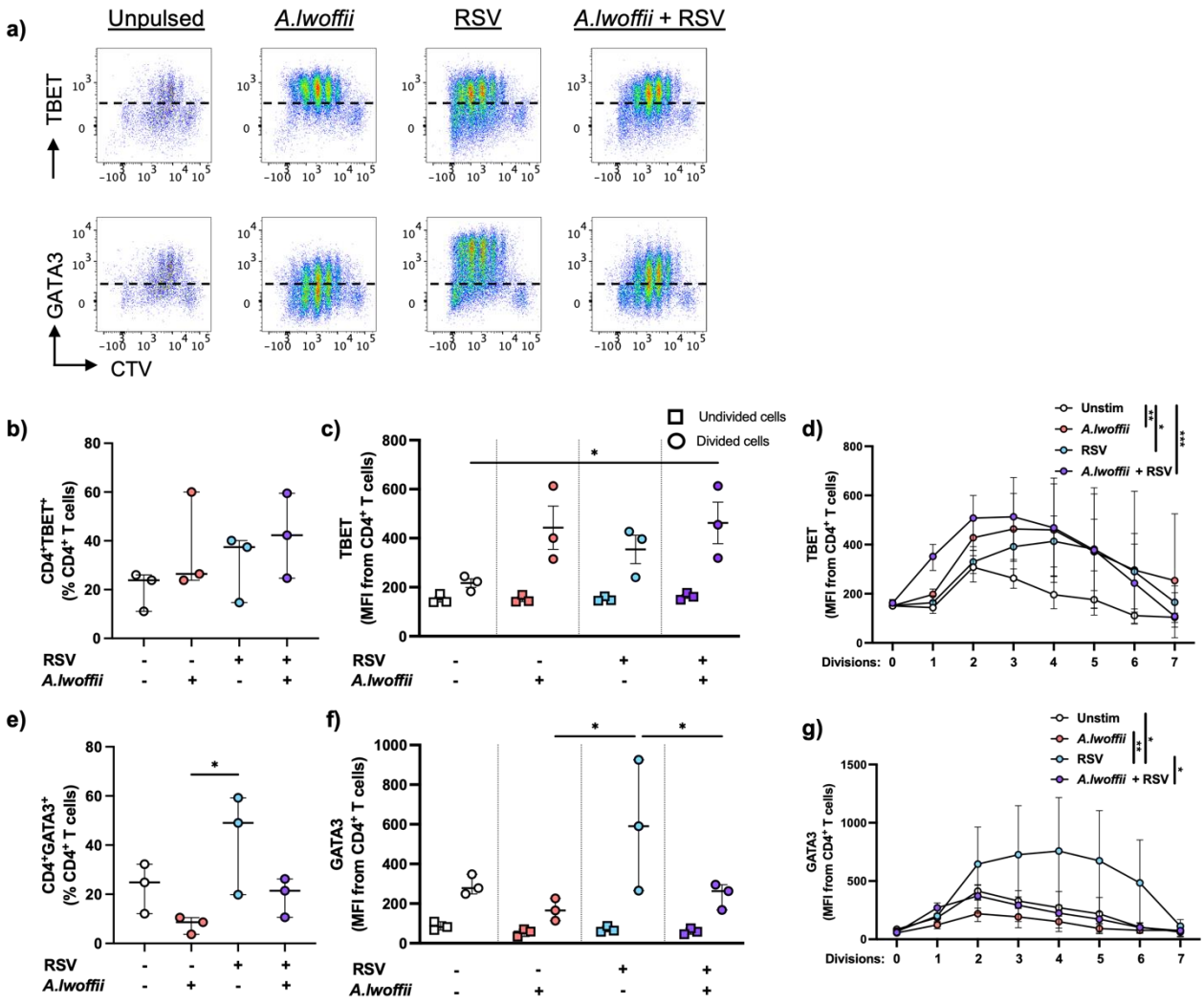


Fig 5.30. RSV-stimulated BMDCs promote Gata3 expression on $CD4^+$ co-cultured T cells

Bone marrow progenitors from 2wk old Balb/c mice were isolated using the centrifuge method and exposed to Flt3-L for 8 days. On day 8 matured BMDCs were exposed to *A.lwoffii* ($2.5x10^8$cfu/mL), RSV (1MOI), or both. To mimic *in vivo* conditions *A.lwoffii* exposure was performed 6h before RSV stimulation. 24h post RSV stimulation, BMDCs were harvested, pooled, counted and co-cultured with CTV-labelled naïve $CD4^+$ T cells isolated from the spleen of age-matched mice in a 1:1 ratio. The cultures were maintained at 37ºC and 5% CO_2 for 5 days. **(a)** Representative plots for TBET and GATA3 expression by $CD4^+$ T cells at different divisions. **(b)** Proportion of $CD4^+TBET^+$ cells. **(c)** TBET MFI on $CD4^+$ T cells. **(d)** TBET MFI on $CD4^+$ T cells at different divisions. **(e)** Proportion of $CD4^+GATA3^+$ cells. **(c)** GATA3 MFI on $CD4^+$ T cells. **(d)** GATA3 MFI on $CD4^+$ T cells at different divisions. Data is representative of one independent experiment with n=3. Data shown with median and interquartile range. Each dot represents a pool of three mice from which naïve $CD4^+$ T cells were isolated. Kruskal-Wallis with multiple comparisons test was performed in which *, $p < 0.05$; **, $p < 0.01$; and ***, $p < 0.001$.

As with other T_{helper} subsets, T_{FH} cells can have plasticity, with some T_{FH} co-expressing Bcl6 and other lineage transcription factors such as Tbet, Gata3 or Rorγt depending on the cytokine environment they are found in (710,711). $CD4^+$ T cell co-cultured with DCs exposed to *A.lwoffii*, RSV or a combination of the two, showed co-expression of several lineage transcription factors *(**Fig 5.31a-d**)*. T cells exposed to unstimulated DCs were predominantly $Bcl6^-$ cells (brighter colours), with approximately 30% of the cells being negative for Tbet, Gata3 or Bcl6 expression (white), 25.57% expressing Gata3 alone (bright red) and another 24.56% expressing Gata3 in combination with Bcl6 (dark blue) *(**Fig 5.31a**)*. Exposure to *A.lwoffii*-stimulated DCs promoted Bcl6 expression (darker colours) with approximately 25% of the cells co-expressing it with Tbet (purple) and ~30% co-expressing it with Tbet and Gata3 (dark blue). $CD4^+Bcl6^-Tbet^+Gata3^-$ cells were the third most represented population in *A.lwoffii*-stimulated conditions, representing approximately 20% of the cells *(**Fig 5.31b**)*. Exposure to RSV-DCs promoted a $Bcl6^-$ signature (brighter colours) which was more pronounced than the ones observed in unstimulated conditions *(**Fig 5.31c**)*. RSV-stimulation predominantly promoted Gata3 expression, with 23.58% of the cells expressing it alone (red) and ~50% of all $CD4^+$ lymphocytes co-expressing it with Tbet (pale blue). Cells negative for all three transcription markers represented 12.24% of the total $CD4^+$ T cell population in RSV exposed conditions *(**Fig 5.31c**)*. $CD4^+$ T cells exposed to *A.lwoffii*+RSV-DCs showed a similar signature to that observed in RSV-treated cultures, but for a slight increase in $Bcl6^+$ cells (darker colours) and a higher representation of Tbet single positive cells (lilac), which represented ~20% of the $CD4^+$ population. $Bcl6^-Gata3^+Tbet^+$ (pale blue) cells however represented the most enriched $CD4^+$ T cell population in these cultures, as was the case with RSV-DC treated conditions *(**Fig 5.31d**)*.

Overall, this data shows that *A.lwoffii*-stimulated DCs are able to generate a pro-T_{FH} environment that is capable of promoting Bcl6 expression in co-cultured $CD4^+$ T cells. RSV-stimulated DCs on the other hand preferentially favour differentiation towards a T_{H2} pathway. Stimulation with *A.lwoffii*-DCs prior to RSV-DCs exposure has an intermediate effect, slightly promoting Bcl6 upregulation but mostly driving Tbet and Gata3 expression.

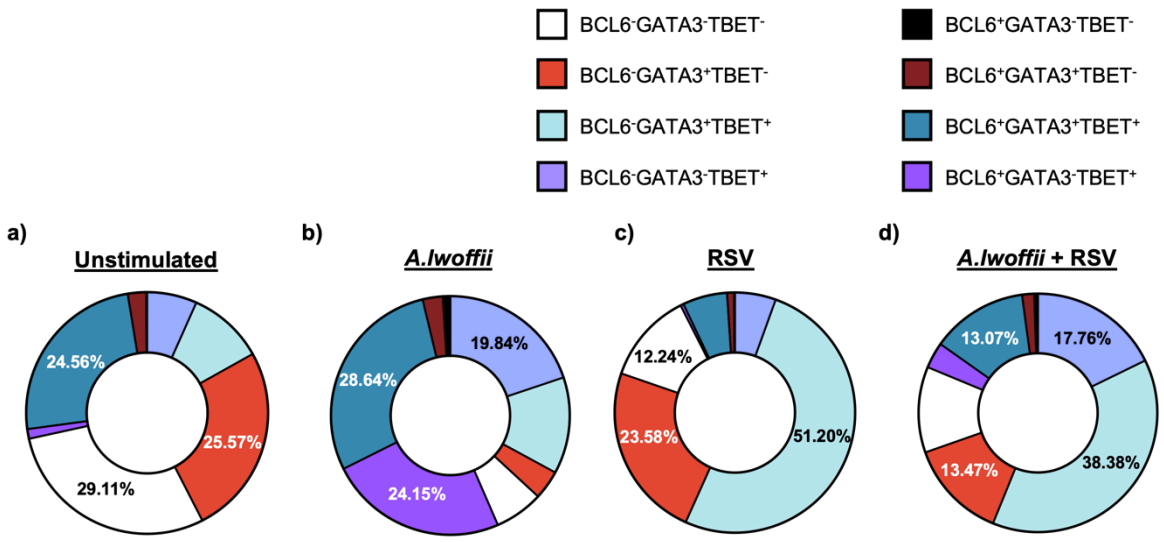


Fig 5.31. Intermediate CD4⁺ T cell phenotype in cells co-cultured with A.lwoffii+RSV-BMDCs

Bone marrow progenitors from 2wk old Balb/c mice were isolated using the centrifuge method and exposed to Flt3-L for 8 days. On day 8 matured BMDCs were exposed to *A.lwoffii* ($2.5x10^8$cfu/mL), RSV (1MOI), or both. To mimic *in vivo* conditions *A.lwoffii* exposure was performed 6h before RSV stimulation. 24h post RSV stimulation, BMDCs were harvested, pooled, counted and co-cultured with CTV-labelled naïve CD4⁺ T cells isolated from the spleen of age-matched mice in a 1:1 ratio. The cultures were maintained at 37ºC and 5% CO_2 for 5 days. **(a)** Pie charts depicting the proportion of BCL6, GATA3 and TBET expressing cells in unstimulated, **(b)** *A.lwoffii*, **(c)** RSV or **(d)** *A.lwoffii*+RSV-stimulated conditions. Data is representative of one independent experiment

5.2.10 RSV-stimulated BMDCs promote mCD25 expression in co-cultured CD4⁺ T cells

Expression of mCD25 by CD4⁺ T cells can be controlled by the IL-6 microenvironment both in early life (534) and adulthood (131). Given the potent role of *A.lwoffii* in promoting IL-6 secretion by BMDCs, its impact on mCD25 CD4⁺ T cell expression was next evaluated. To this end, the BMDC-CD4⁺ T cell co-culture system was used and mCD25 expression on all CD4⁺ T cells and CD4⁺Bcl6⁺ cells was analysed by flow cytometry. The proportion of CD4⁺mCD25⁺ T cells showed a trend to an increase in cultures exposed to RSV- or *A.lwofffii*+RSV-DCs when compared with media or *A.lwoffii*-exposed conditions *(**Fig 5.32a,b**)*. mCD25 MFI on CD4⁺CTV^{low} T cells was significantly increased in T cells co-cultured with DCs exposed to RSV, both alone or in combination with *A.lwoffii* when compared to control or *A.lwoffii* alone treated BMDCs *(**Fig 5.32c**)*. mCD25 MFI on CD4⁺ T cells was increased in those CD4⁺ T cells exposed to RSV-stimulated DCs when compared to RSV-unexposed cells for all divisions analysed *(**Fig 5.32d**)*. Moreover, mCD25 was increased with cell division for RSV- and *A.lwoffii*+RSV-DC exposed T cells but seemed to reach a plateau after the 3rd division for *A.lwoffii* and control-exposed conditions *(**Fig 5.32d**)*. RSV-stimulated DCs failed to promote Bcl6 expression on CD4⁺ T cells to the same extent as *A.lwoffii*-stimulated DCs, but as with all CD4⁺ cells, those cells that expressed Bcl6 showed a significant increase in mCD25 MFI in RSV-DC-T cell cultures when compared with control or *A.lwoffii*-exposed conditions *(**Fig 5.32e**)*. All in all, this experiment shows an increase predisposition of CD4⁺ T cells, and CD4⁺Bcl6⁺

cells, cultured with RSV-DCs to express membrane CD25 when compared with *A.lwoffii* alone treated cultures.

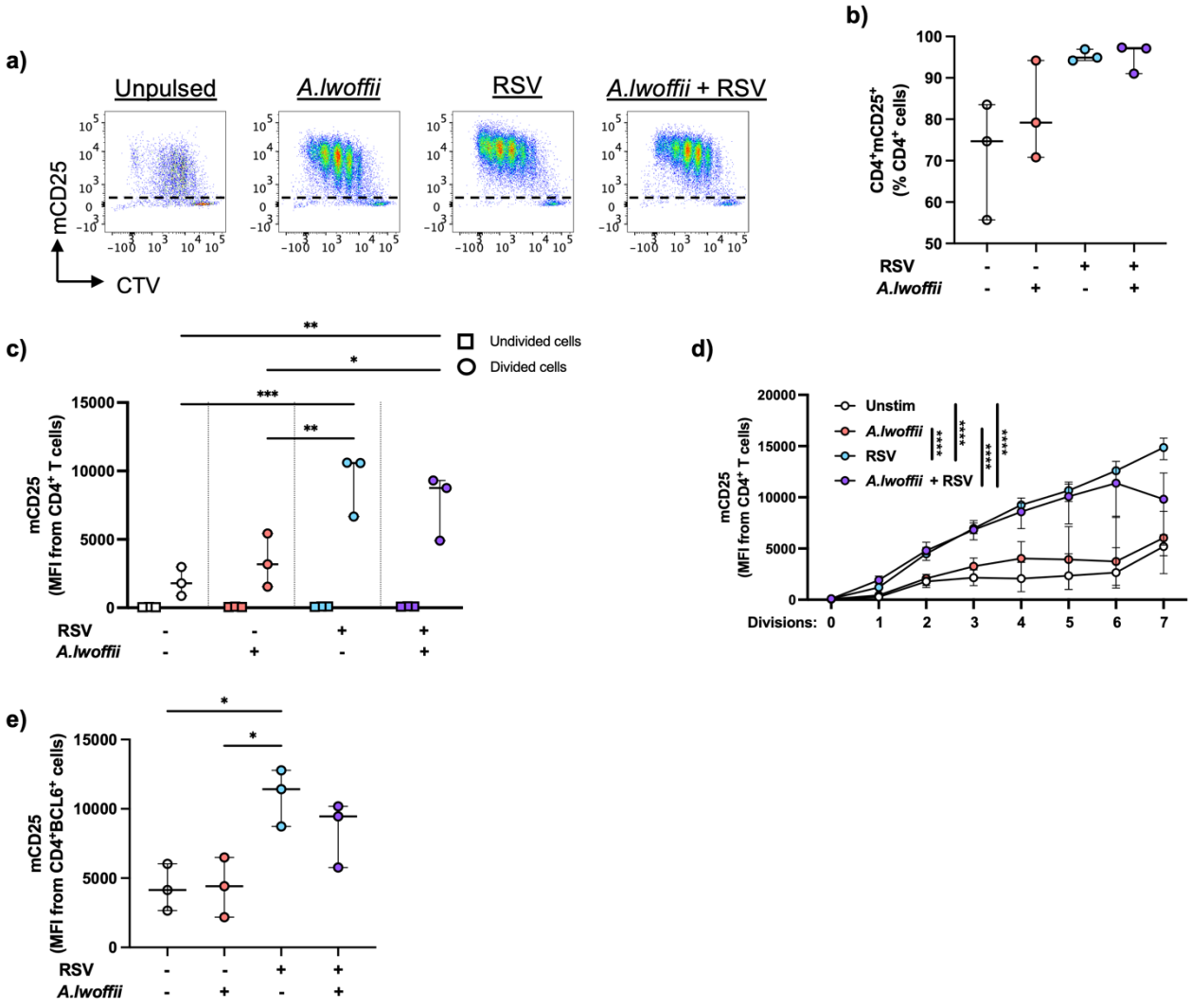


Fig 5.32. Co-culture with RSV-stimulated BM-cDCs promotes mCD25 expression in CD4⁺ T cells

Bone marrow progenitors from 2wk old Balb/c mice were isolated using the centrifuge method and exposed to Flt3-L for 8 days. On day 8 matured BMDCs were exposed to *A.lwoffii* ($2.5x10^8$cfu/mL), RSV (1MOI), or both. To mimic *in vivo* conditions *A.lwoffii* exposure was performed 6h before RSV stimulation. 24h post RSV stimulation, BMDCs were harvested, pooled, counted and co-cultured with CTV-labelled naïve $CD4^+$ T cells isolated from the spleen of age-matched mice in a 1:1 ratio. The cultures were maintained at 37ºC and 5% CO_2 for 5 days. **(a)** Representative plots for mCD25 expression by $CD4^+$ T cells at different divisions. **(b)** Proportion of $CD4^+mCD25^+$ cells. **(c)** mCD25 MFI on $CD4^+$ T cells. **(d)** mCD25 MFI on $CD4^+$ T cells at different divisions. **(e)** mCD25 MFI in $CD4^+BCL6^+$ cells. Data is representative of one independent experiment with n=3. Data shown with median and interquartile range. Each dot represents a pool of three mice from which naïve $CD4^+$ T cells were isolated. Kruskal-Wallis with multiple comparisons test was performed in which *, $p < 0.05$; **, $p < 0.01$; and ***, $p < 0.001$.

5.3 Discussion:

In the previous 2 chapters I have shown that T_{FH} responses are reduced in early life when compared to adulthood (refer to chapter 3), but that early life T_{FH} cells, and the humoral response they generate, can be upregulated when infant mice are intranasally exposed to the farmyard microbe *A.lwoffii* (refer to chapter 4). The precise mechanisms driving this pro-T_{FH} signature by *A.lwoffii* are however unknown. This chapter aimed to analyze the production of pro-T_{FH} factors by cDC2 cells and B cells when exposed to *A.lwoffii* to identify mechanisms that could be driving the observed enhanced T_{FH} response. I found that adult SLOs are enriched in sCD25, a pro-T_{FH} molecule, when compared with neonatal counterparts. Similarly, *A.lwoffii* exposure *in vitro* promotes sCD25 in a DC dependent manner, which together with increased IL-6 production, is sufficient to initiate a T_{FH} response in early life naïve $CD4^+$ T cells. Increased CD25 and IL-6 production by APCs after *A.lwoffii* exposure is also confirmed *in vivo.*

5.3.1 *A.lwoffii* promotes a more potent pro-T_{FH} environment by cDC2s when compared with RSV

Intranasal exposure to *A.lwoffii* in RSV infected infant mice promotes T_{FH} differentiation that is associated with an increased RSV-IgG2a, and possibly RSV-IgA, secretion (refer to chapter 4). The precise mechanisms driving these α-RSV responses by *A.lwoffii* however remain unclear. In this chapter *A.lwoffii,* but not RSV, was found to be able to generate a pro-T_{FH} environment by engaging with cDC2s, potentially via multiple pathways.

In early life, mice are characterised by an increased cDC1/cDC2 ratio in the SLOs (276,277). *A.lwoffii* exposure in infant mice, but not RSV, however increases mediastinal LN cDC2 proportions as well as their SIRPα expression, suggesting increased SLO homing and/or maturation (689,690). This is particularly impeded in RSV alone treated cultures, which show a decrease SIRPα expression even when compared to control conditions. cDC2 MHC-II is elevated in *A.lwoffii* exposed mice and increased CD86 is seen *in vitro*, suggesting activation of DCs with enhanced antigen-presenting abilities, which are known to be beneficial in promoting T_{FH} differentiation (34,89). Findings in line with the increased levels of co-stimulatory molecules seen on murine DCs stimulated with cowshed dust extract (712). Interestingly RSV, while able to activate both human and murine DCs *in vitro*, as shown previously (400,713–715), appears less able to activate DCs *in vivo* in comparison to *A.lwoffii,* which may partially explain the reduced T_{FH} differentiation observed in these mice.

A.lwoffii and RSV also exhibit markedly distinct abilities to promote CD25 and IL-6 production, even *in vitro* where DC activation is similar. *In vivo A.lwoffii* exposure of RSV infected infant mice

enhancing both cDC2 mCD25 and iCD25 production when compared with cDC2s from RSV treated mice alone. *A.lwoffii* also allows for increased release of CD25 from BMDCs *in vitro.* CD25 release from DCs *in vivo* is challenging to directly measure, but *in vitro*, there is strong correlation between sCD25 and CD25 detected by intracellular staining; suggesting this might be a potential surrogate after *A.lwoffii* treatment. Interestingly however, the inverse is true in RSV-treated BMDCs, suggesting RSV exposure may somehow prevent CD25 secretion. *A.lwoffii* but not RSV, also appears to be a potent inducer of DC-derived IL-6 *in vitro* and *in vivo*. In both mice and humans sCD25 can inhibit IL-2 signalling (716–720), with one murine report linking sCD25 quenching function with increased T_{FH} differentiation (166). Likewise, IL-6 is considered the main T_{FH} differentiation cytokine in mice (31,32,127,721). *A.lwoffii* can promote IL-6 production in BMDC cultures (656), and an increase in IL-6-dependent protection after *A.lwoffii* exposure is seen in an adult murine model of asthma, however T_{FH} responses were not analysed (656). In my *in vitro* DC-T cell co-culture system *A.lwoffii*, but not RSV, can induce DCs to promote rapid upregulation of Bcl6, the master transcriptional regulator of T_{FH} (32), in co-cultured $CD4^+$ T cells. While this isn't sufficient to promote the co-expression of CXCR5, alongside PD-1 and Bcl6, in $CD4^+$ T cells, is does suggest *A.lwoffii* can directly act on DCs to induce a pro-T_{FH} environment. Given the roles of IL-6 and CD25 in this process, and their relative abundance upon *A.lwoffii* but not RSV stimulation, these molecules seem likely to be playing a role in driving *A.lwoffii*-dependent T_{FH} differentiation. A recent study in children identified a re-distribution of the T_{FH} cell compartment with age, with T_{FH}-T_{H2} cells predominating in early childhood, while T_{FH}-T_{H1} cells gradually increase to adult levels in the first decade of life coinciding with increased antibody production and protection from infection (572). In the co-culture model, *A.lwoffii* exposure in the absence of RSV stimulation promotes the generation of $Bcl6^+Tbet^+$ T cells when compared with unstimulated conditions, further suggesting a role for *A.lwoffii* in promoting adult like responses associated with increased antibody production.

Overall, this data supports the conclusion that *in vivo A.lwoffii* can overcome the inhibitory micro-environment present in early life to promote T_{FH}-differentiation, and that it does this, at least in part, through modulation of cDC2 proportion and function.

5.3.2 *A.lwoffii* is able to promote IL-6 secretion by early life B cells

While *A.lwoffii* can clearly alter cDC2 proportion and function it may not be the only way in which it can promote T cell dependent antibody responses. Here for instance it clearly had impacts, both *in vivo* and *in vitro*, on B cells in early life SLOs. While less well explored, membrane expression of CD25 by human and mouse B cells has also been reported, although to my knowledge no study has indicated CD25 secretion by B cells except a historic paper showing small amounts of sCD25 by a human B cell line where its function was not analysed (722). *A.lwoffii* exposure on top of RSV infection *in vivo* increases mCD25 expression on B cells and, *in vitro*, *A.lwoffii* stimulation promotes

mCD25, CD86 and MHC-II expression. In both mice and humans mCD25$^+$ B cells have increased proliferation, antigen-presenting capacity and the ability to spontaneously produce IgM and IgG antibodies (169–171). mCD25$^+$ B cells also have high expression of CXCR4, a marker that regulates GC organization and is involved in the migration of plasmablasts to the bone marrow and inflamed tissues (723,724), and CXCR5, a GC-homing protein (725). mCD25$^+$ B cells therefore seem to be particularly poised to enter the GC and interact with T_{FH} cells, suggesting a role for *A.lwoffii* in enhancing B cell antigen-presenting capacity and possible promotion of a GC phenotype. Similar levels of soluble CD25 are however observed after *A.lwoffii* and RSV B cell stimulation *in vitro*, indicating a reduced ability of *A.lwoffii* to promote IL-2Rα secretion by early life B cells when compared with cDC2s.

B cell IL-6 production is however upregulated after *A.lwoffii* exposure both *in vitro* and *in vivo* when compared with RSV. Due to the high overlap in STAT3 activating cytokines in driving T_{FH} differentiation, T_{FH} cell responses can be initiated in the absence of IL-6 signalling (127,135). IL-6 signalling is however crucial for the accumulation of antigen-specific GC-T_{FH} cells (127,131). In adults, a high IL-6 environment is key to maintain T_{FH} IL-2 hyporresponsiveness and allow GC-T_{FH} differentiation (131). Thus, the increased IL-6 production and secretion by B cells observed after *A.lwoffii* exposure both *in vitro* and *in vivo* could further promote the maturation of T_{FH} cells, explaining the increased GC-T_{FH} and antibody response observed in chapter 4. Overall, this data shows that *A.lwoffii* exposure can further enhance the pro-T_{FH} environment generated by cDC2s by promoting the antigen presentation ability and IL-6 secretion of early life B cells, possibly leading to enhanced GC T_{FH} differentiation and function.

5.3.3 RSV-exposed DCs fail to drive T_{FH} differentiation and instead promote a T_{H2} signature

RSV infected neonatal mice fail to generate a strong GC response and secrete limited RSV-specific antibodies (25). The primary focus of this thesis has been to understand how the early life micro-environment enables this, and identify a method to overcome it. In this chapter however I found that not only are RSV-stimulated BMDCs incapable of promoting early T_{FH} differentiation *in vitro,* favouring instead T_{H2} differentiation, but that they can suppress *A.lwoffii*'s capacity to induce T_{FH} differentiation as well.

In accordance with my results, reduced T_{FH} function caused by impaired DC signalling during murine RSV infection has previously been reported (649). The low pro-T_{FH} environment generated by RSV-stimulated DCs is insufficient to drive Bcl6 upregulation in co-cultured CD4$^+$ T cells, instead promoting Gata3 expression and therefore T_{H2} differentiation (709). These two features might be related, as murine BMDC-derived IL-6 can restrict Gata3 and IL-4 expression by T_{FH} cells (151). Indeed, human and murine RSV infection is associated with an increased T_{H2} signature (726,727)

with depletion of T_{H2}-associated cytokine IL-4 prior to acute RSV infection in a murine model leading to increased viral clearance and decreased lung inflammation and mucus production (728–730).

Interestingly, RSV supresses *A.lwoffii*'s capacity to promote T_{FH} differentiation by BMDCs *in vitro*, leading to a reduced Bcl6 signature and increased Gata3 and Tbet expression. *In vivo* however, the ability to promote medLN cDC2 proportion, SIRPα, mCD25, iCD25 and IL-6 expression is not affected by RSV infection in *A.lwoffii* exposed mice. These observations can be explained by differences in the *in vivo* and *in vitro* models, as a more complex tissue response occurs in the first, with cells being able to migrate from the site of infection. Concomitant with my observation, LPS pre-treatment of murine BMDCs *in vitro* doesn't alter their ability to recognise and respond to OVA. Pre-treatment with LPS *in vivo* however reduces DCs ability to interact with OVA, probably by allowing DC migration from the infection site and promoting overall changes in the infection site structure that prevent subsequent encounter with antigen (684). Multiple encounters with antigen, as given here *in vivo* but not *in vitro*, are also linked with enhanced T_{FH} responses (35,85,100,612–614). This suggests that both the *in vivo* environment as well as multiple doses of *A.lwoffii* could affect cDC2 function and modify the cDC2 and T cell phenotype explaining the differences in T_{FH} differentiation observed *in vitro* when compared with the response *in vivo.*

A.lwoffii exposure of BMDCs prior to RSV stimulation in the *in vitro* co-culture model also impairs RSV promotion of T_{H2} signatures, instead driving Tbet upregulation, the canonical transcription marker for T_{H1} cells (708). T_{H1} responses are associated with increased viral clearance and reduced pulmonary pathology (729–731); with depletion of the T_{H1} polarizing cytokine IL-12 prior to viral infection resulting in increased pulmonary inflammation and mucus production (731). Similar to *A.lwoffii*, other T_{H1} polarising adjuvants, such as Advax-SM or CpG, lead to enhanced T_{H1} responses with suppressed RSV viral replication, airway eosinophilia and mucus accumulation in a murine model (730,732). LPS exposure on the other hand promotes T_{H1} responses in a cDC2 dependent manner in adult, but not infant, mice (733); indicating an increased ability for *A.lwoffii* in promoting immune protection in early life when compared to LPS. In conjunction, this data suggest a role for *A.lwoffii* in preventing RSV-dependent T_{H2} poise by promoting T_{H1} and, *in vivo,* T_{FH} responses.

5.3.4 LPS can replicate some, but not all, of *A.lwoffii*'s pro-T_{FH} functions

A.lwoffii promotes the generation of a pro-T_{FH} environment by BMDCs while RSV-stimulation seems to particularly prevent it. Being of bacterial and viral origin *A.lwoffii* and RSV have distinct PAMPs and DAMPs, that can activate different signalling pathways on cDC2s and B cells, probably leading to their distinct immunological responses.

At the doses of TLR agonists used, even when activating the cells to a similar level, the TLR4 agonist LPS is the second highest producer of sCD25 and IL-6, only surpassed by *A.lwoffii.* These findings are in line with LPS having a more potent role than TLR7 ligands at promoting IL-21 secretion by human $CD4^+$ T cells in a DC-dependent manner (144). TLR4 agonists have extensively been linked with increased T_{FH} and antibody responses in both mice and humans when used as vaccine adjuvants (141,734–738), with some reports indicating an increased T_{FH} signature promoted by DC stimulation (15,130,131). As a gram-negative bacteria *A.lwoffii* contains LPS on its extracellular wall, which can be recognized by TLR4 (510,700). Concomitant with LPS ability to bind TLR4, LPS-induced secretion of sCD25 and IL-6 by BMDCs is diminished after TLR4 inhibition. A trend to a reduce sCD25 is also observed in *A.lwoffii*-stimulated BMDCs after TLR4 signalling is impeded, but minimal differences are seen in IL-6 secretion. This suggests that additional PRRs are participating in *A.lwoffii*'s ability to promote a strong pro-T_{FH} response by DCs. As a gram-negative bacteria *A.lwoffii* also has peptidoglycans on its structure, that can bind TLR2 (510). BM-derived macrophages from *TLR2/3/4/7/9*$^{-/-}$ animals are unable to react to *A.lwoffii* exposure in the same way as heterozygous or wild-type mice, suggesting that TLR3, 7 and 9 could also play a role in driving *A.lwoffii*-dependent responses (592). Here *A.lwoffii* was heat inactivated at 70ºC for 15 minutes prior to both *in vivo* and *in vitro* exposure, which maintains bacterial structure, as shown by its ability to promote neutrophil recruitment (604), but impairs *A.lwoffii*'s replication and RNA production. Thus, recognition by TLR3, TLR7 and TLR9 is unlikely. This data combined suggests that TLR4 signalling is important in driving *A.lwoffii* dependent responses but it must act in unison with TLR2 and/or other PRRs, such as NOD1 and NOD2 which are potently activated by *A.lwoffii* (510), to generate a high pro-T_{FH} environment, particularly in regards with IL-6 secretion. Consistent with this idea, LPS supplementation of an RSV-UV vaccine in an adult murine model enhances GC formation and the production of RSV-protective antibody; but simultaneous stimulation of additional PRRs further improves affinity maturation and neutralizing capacity in vaccine recipients (742). Similar to *A.lwoffii,* TLR4 agonists can induce T_{FH} differentiation in neonatal mice, but this is not accompanied by a sustained antibody response after a single dose of the vaccine (573), building up on the idea that stimulation of multiple PRRs and recurrent exposure to PRR agonists is needed to promote enhanced antibody production in the neonatal period.

RSV is also conformed of multiple PAMPs that can be recognised by several TLRs. RSV can activate TLR2/6 through the recognition of RSV G protein (329,330), which together with RSV protein F can also activate TLR4 (338). Due to its viral genome, which possesses distinct structures and requires unique replication and transcription processes when compared with the mammalian DNA, RSV can also activate endosomal TLRs such as TLR3, by recognising RSV dsRNA intermediates during replication (698), and TLR7, by signalling through its ssRNA (699). RSV can directly infect murine and human DCs *in vitro*, albeit this happens at a low frequency (400,401);

particularly when compared with infected epithelial cells (402). RSV virions can however be inactivated to prevent viral infection and replication. Two inactivation mechanisms were used in this study, heat and UV light. Heat inactivation results in the denaturation of viral proteins and the genetic material with the subsequent disassembly of the virions, leading to an impaired attachment to the host cells and viral replication. UV light exposure retains the morphology of virions and only damages the genetic material via induction of reactive oxygen species or creating pyrimidine dimers, therefore preventing viral transcription and replication (697,743).

Recognition of RSV antigen material seems key in promoting cDC2 activation, together with CD25 and IL-6 secretion, as previously described (744,745), indicating that TLR3 and TLR7 signalling are the most important TLRs in driving RSV-dependent responses. TLR2/6 and TLR4 signalling, that are impeded in heat inactivated RSV conditions, appear important at further promoting the TLR3/7 response and key in IL-6 secretion. No difference in cDC2 activation, sCD25 or IL-6 secretion is however observed after TLR4 inhibition or in TLR4$^{-/-}$ RSV-stimulated cells, suggesting a more important role for TLR2/6 in promoting RSV responses. In accordance with this observation a complete inability to secrete IL-6 is reported for murine RSV-exposed TLR2 KO macrophages, while IL-6 secretion is only partially abrogated in TLR4$^{-/-}$ cells (329). Further experiments for instance including TLR2/6 agonists such as FSL-1 or other peptidoglycans (746) are however needed to confirm this observation in cDC2s. Concomitantly, TLR4 signalling by RSV, but not LPS, is redundant for NF-kB activation and infectivity of a human cell line (747). Thus, TLR4 engagement by RSV seems unable to drive a pro-T_{FH} signature despite LPS ability to do so and *A.lwoffii*'s dependence of TLR4 signalling to drive sCD25. TLR3/7 and possibly TLR2 seem instead more important at promoting cDC2 activation and the limited, albeit present, sCD25 and IL-6 secretion observed after live RSV stimulation.

Together this data indicates that LPS stimulation of BMDCs can reproduce some, but not all, of the pro-T_{FH} signatures observed by *A.lwoffii*-stimulated DCs; indicating that other PRRs, such as TLR2, and possibly NOD1 and NOD2, are participating in *A.lwoffi's* ability to promote T_{FH} responses. Despite RSV possessing multiple PAMPs and DAMPs able to bind TLR2/6, TLR3, TLR4 and TLR7 its ability to produce a pro-T_{FH} signature is also reduced when compared with *A.lwoffii*. This is probably due to RSV's low ability to signal through the TLR4 pathway and the lower production of sCD25 and IL-6 by DCs after TLR3 and TLR7 stimulation in our system.

5.4 Concluding remarks:

This chapter sought to investigate the mechanisms driving an increased T_{FH} and RSV-specific antibody response in *A.lwoffii* treated RSV infected infant mice. The results indicate a role for *A.lwoffii* in the generation of a pro-T_{FH} environment by APCs both *in vitro* and *in vivo*, confirming the proposed hypothesis. Early life and adult *A.lwoffii*-exposed cDC2s promote an increased secretion of CD25 and IL-6, when compared with RSV and other TLR agonists, which is probably linked with *A.lwoffii*'s ability to drive Bcl6 upregulation in co-cultured early life $CD4^+$ T cells. *A.lwoffii*-stimulation also increases the IL-6 production by B cells, a feature that is not observed in RSV or TLR-agonist treated conditions. The results shown in this chapter therefore clearly suggest a role for *A.lwoffii* in driving increased T_{FH} responses in early life by altering cDC2 and B cell functions.

6 Discussion

6.1 Rationale of the project and summary of findings:

Immune responses in early life are characterized by a lack of robust long-lasting and protective responses against many common pathogens, or upon vaccination, due to a reduced ability to generate T-cell dependent high affinity antibodies (7). One such pathogen is RSV, which causes mild URTI in adults, but much more severe symptoms in infancy that can culminate in severe bronchiolitis needing hospitalization or even death (9). Little is known about the mechanisms leading to a reduced T_{FH} response in early life, but exposure to adjuvants can enhance the early life antibody response, although not necessarily to the levels seen in adults (21,573,602).

One of the key drivers of immunological development in early life is establishment and diversification of the microbiome, with microbiotal disruption associated with pathology (547). Indeed, in adult mice, administration of microbial products can promote antibody mediated immunity against respiratory viral infections (492,501), but whether this is true in infancy is currently unknown. Exposure to a farmyard environment, and the distinct microbes that are present in this context, during early life is however associated with protection against childhood respiratory illnesses (589,659). This thesis aimed to characterize the mechanisms leading to a reduced T_{FH} response in early life when compared to adulthood during RSV infection and to analyse if and how T_{FH} responses can be boosted by exposure to a farmyard microbe in RSV infected infant mice.

I found that early life is characterised by an enriched IL-2 microenvironment, a known inhibitor for T_{FH} differentiation (42). Moreover, naïve $CD4^+$ T cells, which can give rise to T_{FH} cells upon antigen recognition, are more responsive to IL-2 in early life compared to adults both *in vitro* and *in vivo,* further compromising T_{FH} responses in young mice. Upon RSV infection recurrent exposure to lyophilised *A.lwoffii*, a farmyard microbe, results in a decreased viral load and an increased T_{FH} and $CD138^+$ cell signature. These observations are accompanied by an enhanced RSV-specific antibody response both locally and systemically; confirming the potential for farmyard microbes such as *A.lwoffii* to alter pathogen-specific antibody responses in infants. *A.lwoffii* promotes a pro-T_{FH} environment by enhancing the production of CD25 and IL-6 by cDC2s and B cells *in vivo.* In accordance with the *in vivo* data, direct exposure of BMDCs to *A.lwoffii in vitro* promotes sCD25 and IL-6 secretion*;* allowing *A.lwoffii,* but not RSV exposed, BMDCs to promote Bcl6 upregulation in naïve $CD4^+$ T cells*.* Similarly, consistent with the *in vivo* results, an increased IL-6 transcription and secretion is observed after *A.lwoffii*, but not RSV, exposure of B cells *in vitro.* Overall, these findings suggest that *A.lwoffii* can change the cytokine microenvironment through modulation of APCs, overcoming the IL-2 dependent restriction of T_{FH} differentiation in early life and enhancing the production of pathogen-specific antibodies *(**Fig 6.1**)*.

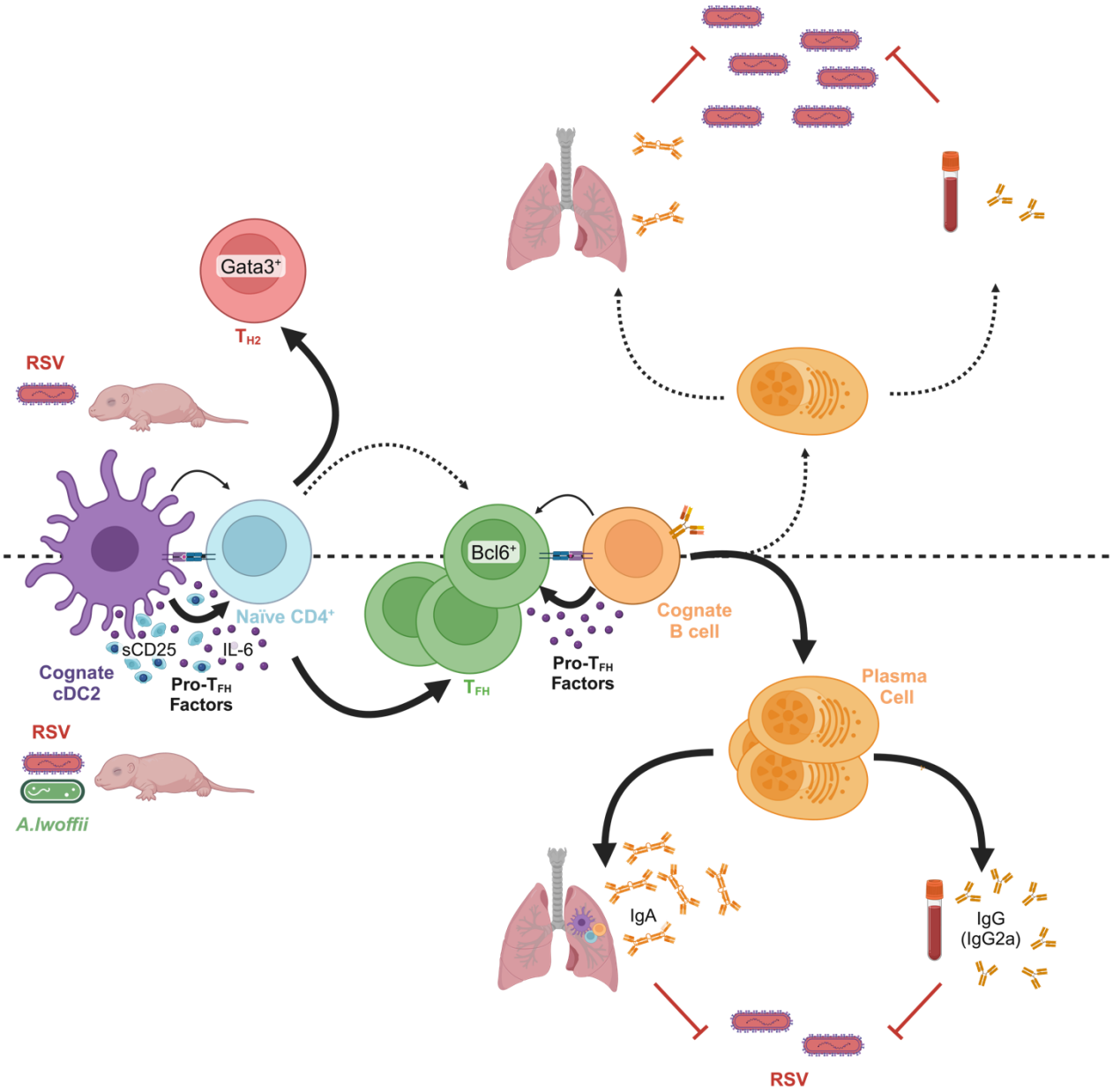


Fig 6.1. Recurrent A.lwoffii exposure promotes T_{FH} and RSV-specific antibody responses in early life

Upon *A.lwoffii* recognition, but not RSV, early life cDC2s are able to secrete CD25 and IL-6, both pro-T_{FH} factors, leading to enhanced T_{FH} differentiation. RSV exposed DCs instead promote the development towards a T_{H2} fate. Recognition of *A.lwoffii* by early life B cells also promotes the secretion of IL-6, which could further contribute to the enhanced differentiation of T_{FH} cells. Concomitantly, recurrent *A.lwoffii* exposure in early life leads to an increased proportion of $CD138^+$ cells, containing both plasma blasts and plasma cells, when compared with RSV alone. As a result, an elevated production of RSV-IgG antibodies is observed systemically, with increased production of IgG2a, a subset linked with viral clearance, in mice exposed to recurrent *A.lwoffii*. Increased BAL expression of RSV-IgA, either by plasma cells migrating to the lung or the enhancement of tertiary lymphoid structures after *A.lwoffii* exposure, is also observed. The upregulation of RSV-specific antibodies probably contributes to the reduced viral load seen in *A.lwoffii* exposed infant mice infected with RSV.

6.2. *A.lwoffii* promotes the generation of a pro-T_{FH} environment

6.2.1 *A.lwoffii* exposure is able to bypass the early life IL-2 dependent restriction and promote T_{FH} responses against RSV infection

IL-2 is a pleiotropic cytokine that promotes T cell proliferation and T_{reg} cell differentiation and maintenance while preventing T_{FH} polarization (42,551,554). As such, IL-2 availability during T cell priming in the SLOs must be tightly controlled. CD25, the high affinity IL-2Rα subunit, can be expressed in the cell membrane of several immune cells, including both APCs and T cells, or be secreted into the supernatant (166). The function of these two forms of CD25 in regards to T cell activation and T_{FH} differentiation, as well as the mechanism by which cells express them, remain elusive.

cDC2s can express both forms of CD25, but both murine and human cDC2s lack expression of CD122 (IL-2Rβ) required for IL-2 signalling; indicating a role for cDC2s in controlling IL-2 signalling on other cells, rather than IL-2 directly shaping DC function itself (166,167). mCD25 expression by human cDC2s is thought to increase IL-2 recognition by T cells (167,748). $mCD25^+$ DCs can cross-present their mCD25 in *trans* to naïve $CD4^+$ T cells expressing low levels of this subunit to facilitate high affinity IL-2 signalling early after activation, thereby promoting rapid T cell proliferation (167), a mechanism not observed with sCD25 (716). The role of mCD25 *trans* signalling on T_{FH} differentiation has not been studied. IL-15 *trans* signalling however, a cytokine that shares both CD122 and the γ chain receptor subunits with IL-2, represses Bcl6 upregulation at least in mice (177), suggesting that mCD25 might have a similar anti-T_{FH} role.

Soluble CD25 is thought to have an opposite effect when compared with mCD25, with a number of studies in mice and humans showing that sCD25 can antagonize IL-2 functions (716–720). One report in adult mice indicates that cDC2-derived sCD25 can quench IL-2 from the microenvironment, promoting T_{FH} differentiation, GC responses and Ag-specific antibodies *in vivo* (166). sCD25 competes with T cell mCD25 for IL-2, with sCD25 inhibitory efficacy being optimal in $mCD25^{low}$ T cell cultures but relatively inefficient against $mCD25^{high}$ expressing T cells (716). CD25 secretion in the SLOs is cDC2-dependent and T cell-independent (166). It is unclear however if sCD25 by cDC2s is generated by shedding mCD25, directly synthetised as a soluble form by alternative splicing from its mCD25 counterpart or released by some other pathway. The latter mechanism might be more plausible as inhibition of proteases, which promote shedding of other interleukin receptors (116,701–703), and indeed CD25 secretion by T cells (707), fails to affect either membrane or sCD25 expression after *A.lwoffii* or RSV stimulation of BMDCs *in vitro*.

In early life, an environment poised towards rapid T cell proliferation and T_{reg} differentiation and thus enhanced IL-2 signalling, T cells, cDC2s and B cells express high levels of mCD25. Low sCD25 is however observed in the SLOs. This signature indicates that the anti-T_{FH} mechanisms of mCD25 *trans*-signalling pathway might be more active. In adults, an age when memory and T_{reg} responses have already been stablished and therefore IL-2 signalling is less prevalent, a pro-T_{FH} quenching mechanism for CD25 could be poised, as observed by elevated sCD25 in the SLOs, and high iCD25 in APCs, but low mCD25 on cDC2s, T cells and B cells. Thus, the high IL-2 recognition by early life naïve $CD4^+$ T cells promotes pSTAT5 signalling which drives their differentiation away from a T_{FH} pathway (42). Conversely, the low IL-2 microenvironment present in adulthood allows the recognition of pSTAT3 cytokines such as IL-6 or IL-21 that promote T_{FH} differentiation (135) *(**Fig 6.2a**)*.

RSV infection in early life may promote the mCD25 *trans*-signalling mechanism since RSV-exposure of BMDCs preferentially promotes mCD25, seemingly at the expense of sCD25. Contrary to RSV, *A.lwoffii* exposure, at least partially through TLR4 signalling, can switch the DC phenotype observed in early life and generate an adult-like environment by promoting CD25 secretion. The expression of the common gamma chain receptor (CD132) is upregulated in BMDC cultures after RSV stimulation, but not *A.lwoffii*, potentially suggesting a mechanism by which the presence of CD132 could complex with, and stabilize, CD25 in the DC plasma membrane, preventing its secretion in RSV stimulated conditions. A distinct signature between RSV and *A.lwoffii* is also observed in mCD25 expression by T cells. Elevated mCD25 is seen on T cells co-cultured with RSV-exposed DCs, suggesting that the low sCD25 present in the environment would be insufficient to compete for IL-2. BMDCs stimulated with *A.lwoffii* however prevents mCD25 upregulation by co-cultured $CD4^+$ T cells, accentuating sCD25 inhibitory efficacy, but whether this is true *in vivo* and the mechanisms leading to this downregulation are currently unknown *(**Fig 6.2b**)*.

This data together suggests that the early life SLOs are characterized by an enriched IL-2 microenvironment at the steady state. During RSV infection IL-2 signalling is enhanced and, when combined with the elevated type-2 signalling classically associated with RSV (749), can drive the $CD4^+$ T cell polarization away from a T_{FH} pathway and into a T_{H2} phenotype. Through inducing the secretion of sCD25, that can quench IL-2, by cDC2s, *A.lwoffii* can promote the generation of a pro-T_{FH} environment similar to that seen in adults upregulating Bcl6 over Blimp-1.

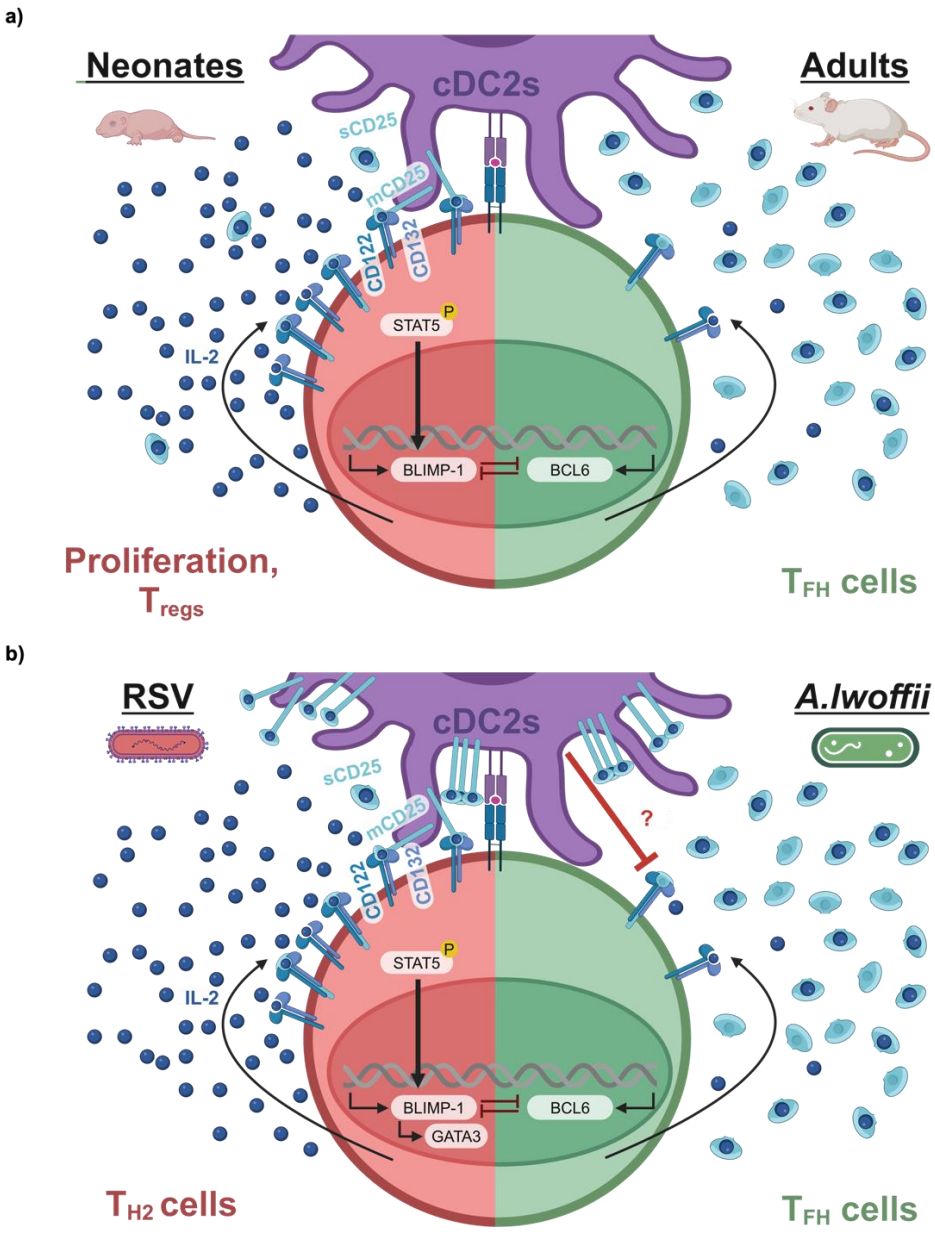


Fig 6.2. The IL-2 microenvironment differs with age and stimulation leading to marked differences in CD4⁺ T cell differentiation

(a) Upon antigen recognition by cognate cDC2s, early life CD4⁺ T cells secrete high quantities of IL-2. The ability of early life cDC2s to secrete CD25, that can quench IL-2, is limited, further promoting a high IL-2 milieu that is readily available to bind the enhanced IL-2R on T cells in early life. Moreover, early life cDC2s express high mCD25 that can act in *trans*, by binding to CD122 and CD132 on CD4⁺ T cells, to promote high affinity IL-2 signalling. IL-2 signals through phosphorylation of STAT5, that can upregulate the transcriptional factor BLIMP-1 preventing T_{FH} differentiation and promoting CD4⁺T cell polarization towards alternative T_{helper} pathways, mostly T_{regs}. Conversely, in adulthood there is reduced IL-2 secretion which is accompanied by increased production of sCD25 by adult cDC2s that can bind IL-2 and quench it from the microenvironment. T cells also express low levels of IL-2R, leading to reduced IL-2 signalling and therefore increased BCL6 expression and enhanced T_{FH} differentiation. **(b)** RSV infection, particularly in young animals, further enhances the IL-2/pSTAT5 signalling observed in early life by increasing membrane CD25 expression on cDC2s, that can act in *trans* with CD122 and CD132 on CD4⁺ T cells to promote IL-2 signalling leading to increased T_{H2} production at the expense of T_{FH} differentiation. *A.lwoffii* exposure also promotes mCD25 on cDC2s, but this is accompanied by an enhanced ability to secrete CD25, that can quench IL-2 from the microenvironment. *A.lwoffii* exposure also prevents mCD25 expression on CD4⁺ T cells, but the mechanisms leading to this observation are currently unknown. Thus, by reducing the IL-2 microenvironment and its recognition by T cells, *A.lwoffii* is able to promote BCL6 upregulation and T_{FH} differentiation on early life naïve CD4⁺ T cells both *in vitro* and *in vivo.*

6.2.2 *A.lwoffii* exposure in early life promotes IL-6 secretion, which contributes to increased T_{FH} differentiation

IL-6 is considered one of the key cytokine signals required for T_{FH} differentiation in adult murine models (58,127,128,131). Its role in controlling T_{FH} polarization in neonatal mice is however controversial. Neonatal immunization with pneumococcal conjugate vaccine (PCV) in combination with IL-6 fails to induce STAT3 phosphorylation in neonatal $CD4^+FOXP3^-$ T cells (237). Instead, promoting phosphorylation of STAT5, and actively limiting T_{FH} differentiation (534). Moreover, contrary to its IL-2Rβ-suppressing effect in adult T_{FH} cells (131), an IL-6 enriched environment is associated with increased IL-2 production and upregulated IL-2 receptors in neonatal T_{FH} cells in the PCV murine model (534). In accordance with this observation, an enhanced pSTAT5 is observed after *in vitro* IL-6 treatment of early life naïve $CD4^+$ T cells when compared to adult cells. No difference is seen in STAT3 phosphorylation between early life and adulthood, pointing to the fact that IL-6 is able to phosphorylate STAT3 on naïve $CD4^+$ T cells to a similar level in both age groups.

The detrimental effect of IL-6 in promoting T_{FH} differentiation in early life may however be context specific. An IL-6 enriched environment associated with the use of C-type lectin as an adjuvant of an influenza hemagglutinin vaccine promotes T_{FH} differentiation in early life mice, generating adult-like levels of IL-21 in the process (750). This is accompanied by reduced expression of CD25 on T_{FH} cells (750). In accordance with the C-type lectin data, recurrent *A.lwoffii* exposure promotes substantial production of IL-6 by both cDC2s and B cells *in vitro* and *in vivo*, and reduces mCD25 on T cells, linked to enhanced early life T_{FH} and pathogen specific antibody responses. When compared with C-type lectin, a TLR4-signalling adjuvant is less capable of generating both an IL-6 enriched environment and a strong GC reaction in neonatal mice (750). Neither intraperitoneal nor subcutaneous administration of IL-6 starting from day 4 post immunization with a TLR4 adjuvant rescues neonatal GC B cell responses (750). This suggests IL-6 alone is not sufficient to enhance humoral responses in early life and a combination of factors, such as the ones generated by C-type lectin or *A.lwoffii*, probably including but not limited to sCD25, are required to create an appropriate pro-T_{FH} environment to generate T_{FH} efficiently in this age group.

While it is evident that IL-6 signalling mediates different signal outcomes in $CD4^+$ T cells depending on age and early life stimuli, the mechanisms leading to these contradictory observations are less clear. One potential explanation could be the production of a different transcriptional signature in $CD4^+$ T cells depending on IL-2 availability. IL-2 prevents T_{FH} differentiation by upregulating pSTAT5/Blimp-1 signalling (161). In both mice and humans early life naïve $CD4^+$ T cells are transcriptionally and functionally distinct from their adult counterparts, probably due to being recent thymic emigrants (239,263,543–546,550,552,553). Early life $CD4^+$ T cells have an increased

Stat5/Stat3 signature and they are more prone to phosphorylate Stat5 upon IL-2 and IL-6 signalling when compared to adult cells. $CD4^+$ T cells from 1wk old mice have increased IL-2R expression and they also produce more IL-2 upon activation than cells from 8wk old mice. This suggests that upon antigen encounter early life naïve $CD4^+$ T cells can rapidly activate the IL-2/pSTAT5/Blimp-1 pathway.

In an *in vitro* OT-II adult murine model, a constitutively active form of STAT5 inhibits T_{FH} differentiation by upregulating Blimp-1 and suppressing T_{FH} related genes such as *Bcl6, Cxcr5, C-maf or Il21* (161). Concomitantly, Blimp-1 overexpression leads to a decrease in T_{FH} differentiation irrespective of IL-6 signalling. Neutralization of IL-2, in combination with IL-6 and IL-21 signalling, is required to fully downregulate Blimp-1 and promote a strong T_{FH} phenotype in adult naïve murine $CD4^+$ T cells (161). Similarly, STAT5 deficiency in murine $CD4^+$ T cells *in vivo* results in enhanced GC B cells and antibody response (161). Adult naïve $CD4^+$ T cells expressing physiological levels of Blimp-1 prior to immunization with murine LCMV fail to differentiate into T_{FH} cells (31). These findings suggest that a strong IL-2/pSTAT5/Blimp-1 signature prevents IL-6 ability to promote Bcl6/pSTAT3 and therefore a pro-T_{FH} differentiation programme. These observations are maintained in other murine $CD4^+$ T cell subsets like T_{regs}. In Blimp-1^+ T_{reg} cells, Blimp-1 can supress IL-6 mediated STAT3 phosphorylation; while IL-6 is only capable of promoting pSTAT3 in Blimp-1 deficient cells (751). In a human cell line, the STAT5 repression of RNA polymerase II at the BCL6 locus is dominant over STAT3-mediated induction (752). Combined, these results indicate that IL-6 cannot promote T_{FH} differentiation in an enhanced IL-2/pSTAT5/Blimp-1 environment.

Similar to the pSTAT5/Blimp-1 overexpression models, an enriched IL-2 microenvironment, such as the one present in the early life steady state, RSV or PVC conditions, together with an increased ability to recognise and respond to this IL-2 by early life naïve $CD4^+$ T cells, could induce a rapid and enhanced STAT5-Blimp-1 signature that could prevent IL-6 dependent Bcl6 upregulation and therefore T_{FH} differentiation. This correlates with the observation that adult $CD25^{hi}$ $CD4^+$ T cells exhibit strong Blimp-1 expression, which directly represses Bcl6 (31,36,37,753). As observed in early life, in this environment IL-6 signalling further promotes STAT5 phosphorylation driving differentiation away from a T_{FH} signature, but the mechanisms leading to this upregulation are currently unknown. It is true that the IL-6 dependent downregulation of IL-2Rβ in adulthood takes place at the stage of B cell signalling, when a T_{FH} fate has already been decided and thus after Blimp-1 downregulation, but it does not occur at the stage of T_{FH} cell priming (cDC2 stage) (131), suggesting that IL-6 dependent downregulation of IL-2R requires a reduced Blimp-1 signature.

In an IL-2 decreased environment however, where STAT5-Blimp-1 signalling is downregulated, IL-6 signalling through STAT3 is sufficient to drive Bcl6 upregulation and therefore T_{FH} differentiation. This is seen in adulthood, or in early life when C-type lectin and *A.lwoffii* are used as adjuvants. In

a Blimp-1 decreased environment, Bcl6 prevents STAT5 association with the *Il2r* locus downregulating IL-2R expression on CD4⁺ T cells and further promoting this response (131). This IL-2R downregulation by a Bcl6 dependent mechanism may be boosted in the context of bacterial exposure and C-type lectin, which together with the increased sCD25 by cDC2 cells could drive the initial IL-2 decreased environment *(**Fig 6.3**)*.

The study of IL-6 responses in the neonatal period is therefore complex and the role of IL-6 in driving T_{FH} differentiation in early life has not been analysed in depth. Additional studies including the use of IL-2 quenching adjuvants, such as *A.lwoffii*, in IL-6 KO mice or IL-6 blocking/supplementation at the time of early life infection would help provide answers about the specific role played by this cytokine in T_{FH} responses in the presence or absence of an enriched IL-2 environment.

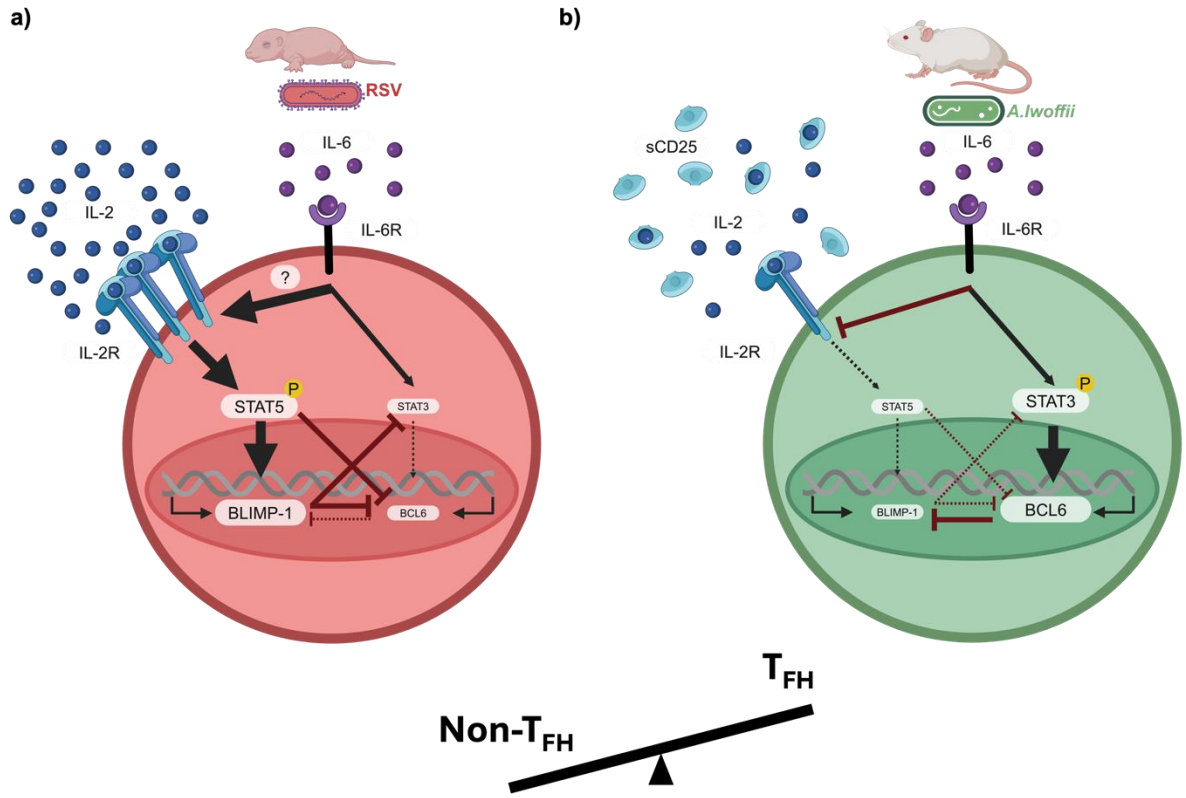


Fig 6.3. The IL-2 microenvironment might dictate IL-6 responses in naïve CD4⁺ T cells

(a) In an enriched IL-2 microenvironment, such as the one observed in early life or RSV infection, STAT5 is upregulated leading to increase Blimp-1 expression and reduced Bcl6. Blimp-1 can prevent both IL-6 dependent STAT3 activation and Bcl6 upregulation. In this scenario, IL-6 can enhance IL-2 signalling by further promoting T cell IL-2R expression, but the mechanisms leading to this observation require further investigation. These cells develop into T_{FH}-alternative pathways. **(b)** In adulthood or *A.lwoffii* stimulated conditions, IL-2 signalling is downregulated, at least partially by increased sCD25 that can quench IL-2, leading to reduced Blimp-1 expression that cannot prevent IL-6 dependent STAT3 phosphorylation or Bcl6 upregulation. When IL-2 signalling is reduced, IL-6 can accentuate the low IL-2 signature by preventing IL-2R upregulation on CD4⁺ T cells. Thus, the IL-6/pSTAT3/Bcl6 pathway is upregulated and cells develop into T_{FH} cells.

6.3 SLOs are specific microanatomical niches where IL-2 responses are tightly regulated

In the SLOs CD25 secretion is a DC-dependent and T cell independent mechanism, as shown by significant reduction of sCD25 in the spleen of Zbtb46$^{-/-}$ mice, but not in TCR KO mice (166). Similarly to previous observations, the serum, lung and thymic response show a different CD25 signature when compared to the SLOs. In these organs *Cd25* transcript and sCD25 levels are increased in early life when compared to adulthood. Developing thymocytes express high amounts of CD25 with their expression associated with clonal deletion (754). Thymic output is accentuated in early life, but adulthood is characterised by thymic atrophy which could explain the difference in thymic sCD25 signature (295–297). T_{reg} differentiation is also enhanced in early life (555), with increased FOXP3^{+} T cell frequency observed in the spleen, lung and circulation of newborn non-human primates (755). T_{regs} derived from human PBMCs can release sCD25 both before and after stimulation *in vitro* (756), potentially explaining the lung and systemic response observed here. High levels of T_{reg} cells correlate with increased sCD25 plasma concentration in patients with B cell malignancies (756), further confirming these results. Human adult naïve CD4^{+} T cells can also secrete CD25 when activated *in vitro,* albeit to a lower extent than T_{reg} cells (756); and mice with a CD4-specific deletion of metalloproteases have lower serum sCD25 levels *in vivo* (707). The lower threshold needed for CD4^{+} T cell activation and the enhanced proliferation observed in early life (239,543,550,552,553), combined with the increased expression of IL-2R in neonatal CD4^{+} T cells, could all be further contributing to the enhanced sCD25 signature observed in the periphery.

A slight increase in sCD25 in all organs analysed is observed after RSV infection, which goes in accordance with previous studies showing increased sCD25 during human infection (757–761) and malignant disease (762,763) in adults and children. This observation is probably a result of either an immunosuppressive mechanism to prevent T cell proliferation or the indication of increased T cell activation upon infection. An increase in serum concentration of sCD25 during the acute phase of RSV infection in hypoxic infants correlates with IL-10 plasma concentration, further pointing towards a T_{reg} origin (764).

Collectively, this data highlights differential regulation of sCD25 responses according to tissue site. Since it is in the SLOs where T cell responses are initiated, and importantly T_{helper} fate is decided, a tight control of the cytokine microenvironment in both lymph nodes and spleen is key.

6.4 Limitations and future directions

This thesis provides compelling evidence that the early life immune system is distinct from that seen in adults in its ability to shape the fate of CD4^{+} T cells, in particular limiting the generation of

T_{FH} cells. It also indicates that this can partially be overcome by exposure to “farmyard” microbiota. There are however key questions that remain to solidify these findings and determine their potential importance and impact.

6.4.1 Investigating the role of sCD25 in driving T_{FH} responses in early life

Both *in vitro* and *in vivo A.lwoffii* has the capacity to modulate APCs responses to promote a pro-T_{FH} environment. This is associated with increased T_{FH} signature and RSV-specific antibodies in *A.lwoffii* exposed RSV infected infant mice. The exact mechanisms driving this response however require further investigation.

A.lwoffii stimulation of BMDCs promotes the secretion of sCD25, a pro-T_{FH} factor (166). To confirm that the production of sCD25 generated by *A.lwoffii* exposure is sufficient to quench IL-2 from the microenvironment, *A.lwoffii* exposed DC supernatants could be pre-mixed with rmIL-2 and then incubated with early life naïve $CD4^+$ T cells, their pSTAT5 signature could then be analysed. In order to increase sensitivity, T_{reg} cells, which have higher expression of mCD25 and therefore are more susceptible to IL-2 signalling, could be used instead of naïve $CD4^+$ T cells (166). To further confirm the role of *A.lwoffii* derived sCD25 in promoting T_{FH} responses, both *in vitro* and *in vivo* experiments could be performed. BMDCs from WT and CD25 KO mice, such as the ones used in (166), could be exposed to *A.lwoffii ex vivo*, co-cultured with naïve $CD4^+$ T cells and their Bcl6 differential expression could be explored. Addition of recombinant sCD25 to RSV-stimulated DC-naïve $CD4^+$ T cell co-cultures will also help confirm if an environment enriched in sCD25 promotes a T_{FH} differentiation programme. *In vivo*, i.n. *A.lwoffii* exposure of RSV infected infant mice with CD25 specifically ablated on cDCs (under the Zbtb46 promoter as used in (166)) could help explore if CD25 expression by *A.lwoffii* exposed DCs is necessary and sufficient to promote T_{FH}, $CD138^+$ and RSV-specific antibody responses. To have control over the timings of CD25 expression, the CD25 KO model could be replaced by $CD25^{fl/fl}$-Cre under the CD11c promoter or by the use of siRNA CD25 in BMDCs (765).

6.4.2 Investigating the role of IL-6 in driving T_{FH} responses in early life

A.lwoffii exposure both *in vitro* and *in vivo* promotes the secretion of IL-6 by cDC2s and B cells. In neonatal mice IL-6 has been shown to have both a favourable and detrimental role in driving T_{FH} differentiation (534,750); and its role might depend on the microenvironment generated by additional cues as previously discussed. The role of IL-6 in driving T_{FH} responses in the context of RSV infection and *A.lwoffii* exposure has not been analysed in detail. As with sCD25 both *in vitro* and *in vivo* experiments could be performed. Again, the murine BMDC-naïve $CD4^+$ T cell co-culture could be used to analyse T_{FH} differentiation in a controlled environment. Supplementation of unstimulated- and RSV-exposed cultures with rmIL-6 or addition of an IL-6 neutralization antibody

such as the one used in (766) in *A.lwoffii*-stimulated cultures could help discern if IL-6 is needed to promote early life T_{FH} differentiation. To further analyse the role of IL-6 in driving RSV-specific antibody responses *in vivo*, recurrent *A.lwoffii* exposure of RSV infected infant mice could be performed in WT and IL-6 KO mice. Both the IL-2/pSTAT5/Blimp-1 and the pSTAT3/Bcl6 pathways and their interrelation could be investigated in this model.

A.lwoffii-exposed BMDCs seem to prevent the upregulation of mCD25 on co-cultured $CD4^+$ T cells. The mechanism leading to this observation is however unknown. First, in order to confirm our observations, it is important to evaluate the expression of mCD25 and CD122 on naïve $CD4^+$ T cells and T_{FH} cells after RSV and *A.lwoffii* exposure *in vivo*. IL-6 has been linked with preventing IL-2R expression in murine adult T_{FH} cells (131). In early life however, the opposite effect is observed (534). It is therefore likely that $mCD25^+$ expression is being regulated in an IL-6 dependent manner. Using the same IL-6 supplemented or decreased BMDC-$CD4^+$ T cell co-culture experiment and IL-6 KO mice exposed to *A.lwoffii* and RSV as above, the mCD25 and mCD122 expression on naïve $CD4^+$ T cells and T_{FH} cells could be studied. To further investigate this mechanism, STAT3 and STAT5 inhibitors as well as $CD4^+$ STAT3 and STAT5 KO models could be used to analyse the interplay between these signals in driving IL-2R expression in early life $CD4^+$ T cells. RNA-seq experiments as well as phosphoproteome experiments could be performed to analyse the transcriptional and protein phosphorylation differences of neonatal and adult $CD4^+$ T cells, as well as cells exposed to adjuvants, that could explain their differential response to IL-2 and IL-6 signalling. Finally, chromatin immunoprecipitation sequencing (ChIP-seq) studies such as the ones used in (131) could be performed to evaluate the interrelationship of STAT5/Blimp-1 and STAT3/Bcl6 pathways and their transcription in early life and adulthood as well as in *A.lwoffii*/RSV conditions. This technique however requires a high number of cells, so $CD4^+$ T cells from several neonatal mice would need to be pooled to obtain meaningful results.

6.4.3 Deciphering the molecular mechanisms of *A.lwoffii*-mediated antibody enhancement

One of the most interesting findings of this thesis is that *A.lwoffii* exposure of RSV infected infant mice leads to enhanced RSV-specific IgG, IgG2a and IgA antibodies. The exact mechanism leading to this upregulation is currently unknown. Unlike OM-85 (501), a mix bacterial lysate compound, *A.lwoffii* exposure does not appear to generate antibodies with broad-specificity that can also bind RSV, as no RSV-specific antibodies are seen in *A.lwoffii* only treated mice. Single-cell RNA sequencing (sc-RNA-seq) of mediastinal LN samples from both the RSV alone and *A.lwoffii*+RSV groups could be used to do an in-depth transcriptomic analysis at a single cell level of the differential pathways expressed between both conditions. This method will also allow investigation of the response to *A.lwoffii* in other cells involved in the GC reaction, such as FRCs and FDCs, that were not analysed in this thesis.

One limitation of the work presented here is the lack of antigen specificity for the T_{FH} and GC B cell responses of the double challenged mice. Thus, with the current data we cannot confirm that *A.lwoffii* exposure promotes the generation of RSV-specific T_{FH}, GC T_{FH}, GC B cells and PC responses. One of the challenges of working with early life models is the limited number of cells that can be isolated from a single animal. While CD4 RSV-specific tetramers are available on a C57BL/6 background, none have been validated on the BALB/c background used here. Pooled peptides could however be utilized to either develop an activation induced marker panel to identify virus-specific $T_{FH,}$ GC T_{FH} and IL-21$^+$ CD4$^+$ T cells, or use cytokine production to identify peptide-specific CD4$^+$ T cells (25,767). Results may however be limited due to the low number of early life recovered cells and the low production of T_{FH} responses in this age group. Improved sensitivity could be achieved by using either an Enzyme-Linked ImmunoSpot Assay (ELISPOT) or Fluorescent ImmunoSpot Assay (FLUOROSPOT), to quantify RSV specific T and B cell responses and analyse if they are upregulated in *A.lwoffii* exposed conditions. The sc-RNA-seq experiment could also be performed in virus specific CD4$^+$ T cells and B cells to analyse the transcriptomic pathways that are upregulated in the presence or absence of *A.lwoffii* exposure in lymphocytes responding to RSV.

6.5 Translating my findings

6.5.1 Effect of *A.lwoffii* exposure on RSV protection in the elderly

RSV is increasingly recognized as an important pathogen in older individuals. Indeed, 78% of RSV-associated deaths occur among people aged above 65 years (768). The underlying causes for the susceptibility to severe RSV disease in the elderly are likely complex and multifactorial. They include the presence of underlying chronic pulmonary diseases, circulatory conditions, changes in lung elasticity, cellular composition, barrier integrity and microbiome in addition to immunological differences when compared with young adults (769,770). Innate immunity in the elderly exhibits both diminished antipathogen responses and chronic, low-level activation (“inflammaging”) which can lead to impairments in innate antiviral immunity (771,772). Adaptive immunity also wanes in the elderly (773). Lower frequency of RSV-specific CD8$^+$ T cells is observed in elderly patients (774–776) and higher viral titres and a diminished cytotoxic lymphocyte response are also observed in aged rodent models (777,778). Owing to a lifetime of exposure to RSV infection, all elderly people have antibodies to RSV (779). Most studies report a higher baseline and vastly higher induction of serum neutralizing antibody after infection in this age group, perhaps resulting from higher viral burden and prolonged and more severe inflammation (779–782). This suggests that the ability to mount an antibody response to RSV is not impaired in the elderly. Low neutralizing antibody titres in old people are however associated with increased risk of RSV infection and severe disease (779,783,784). Concomitantly, elderly people with higher levels of antibody tend to be

resistant to complications of RSV infection, suggesting that induction of a robust antibody response by vaccination might protect this vulnerable age group (779–782). Indeed, recently two new RSV vaccines have been approved for use in people over 65.

Similarly to what is observed in early life, the magnitude and quality of the GC response is reduced in old age mainly due to a dysregulation in both T_{FH} and GC stromal cells (785,786). The recruitment of naïve $CD4^+$ T cells to the SLOs, their priming by DCs and their differentiation into T_{FH} cells in both mice and humans are all impaired (787–789) as is their function (790). At least in mice, TLR4 adjuvants promote a lymphoid stromal cell response to immunization that correlates with an improvement in the aged GC response (791). Use of TLR4 adjuvants however does not fully rescue peak GC, bone marrow plasma cell responses or serum antibody titre (791). Likewise TLR7 agonists are also able to promote murine cDC2s, T_{FH} and GC B cell numbers, but antibody responses are not increased 7d post immunization (788). Pre-treatment of elderly murine DCs *ex vivo* with both Poly(I:C) and CpG TLR agonists however lead to increased APC dependent IL-6 secretion that was sufficient to promote GC T_{FH} and antigen-specific IgG antibody responses in an *in vivo* aged mouse model (792). This suggests that similar to early life exposure, by its multiple PAMPS and DAMPS, *A.lwoffii* might also boost the RSV-specific response in the elderly. The ability of therapeutic microbial treatment to enhance RSV immunity in aged-individuals or murine models has however not been explored and requires further investigation.

6.5.2 Clinical implications

Most of the experiments shown in this thesis have been done in murine models. It is likely however that the majority of the observations are translatable to humans. Cord blood $CD4^+FOXP3^-$ cells are more prone to secrete IL-2 and respond to it than cells isolated from adult peripheral blood (545,793). Human T_{FH} responses are diminished after IL-2 exposure (159) and here I showed that inhibition of pSTAT5 signalling promotes T_{FH} differentiation in a human adult *in vitro* culture system. Likewise, T_{FH} responses and the concomitant antibody response they generate are reduced in infancy (12,13,236). Exposure to a farmyard environment early in life however protects from respiratory diseases in humans (659,661). Combined, these observations highlight that a similar mechanism to the one shown here in mice could take place in infants. Additional experiments however would need to be performed in human samples to validate the observations arising from this thesis.

Recombinant sCD25 antagonises IL-2 mediated responses in human $CD4^+$ T cells, but their T_{FH} differentiation capacity has not yet been analysed (716). The human *in vitro* T_{FH} system could be used to analyse T_{FH} differentiation in the presence of sCD25. Most importantly however, work should address whether *A.lwoffii* exposure is able to generate a pro-T_{FH} environment in infancy

using human samples. Pre-DC precursors could be isolated from cord blood and adult PBMCs and differentiated into matured cDCs as previously described (794). These cells could then be stimulated with *A.lwoffii*, RSV or both to analyse cytokine production. T_{FH} differentiation in humans is mainly driven by DC-derived IL-12 (143,144). Thus, the capacity of human DCs to secrete IL-12 upon RSV and *A.lwoffii*-stimulation should also be analysed. A similar co-culture system to the one used here in mice, with cDCs and naïve $CD4^+$ cells isolated from cord blood or adult PBMCs, could be used to analyse BCL6 upregulation. To build on this observation and use a more *in vivo*-like system, human tonsil organoids could also be utilized to explore the generation of T cell dependent antibody responses against RSV, *A.lwoffii* or both. Tonsil organoids have recently been shown to replicate many of the key cellular interactions that occur in the SLOs *in vitro,* thus being a great model system to translate my findings (795).

6.6 Concluding remarks

T follicular helper cell dependent antibody responses are critical for long term immunity. Antibody responses are however diminished, vaccination less effective and recurrent infections prevalent in early life (7). Collectively, the findings of this thesis contribute to the currently limited understanding of the production of humoral responses in early life. Here it was found that early life is characterised by an increased IL-2/pSTAT5 signalling, which is linked with impaired T_{FH} responses against RSV infection (25). Exposure to *A.lwoffii,* a farmyard microbe, during early life RSV infection can however modulate the APC response and generate a pro-T_{FH} environment that is sufficient to enhance the production of T_{FH}, antibody secreting cells and RSV-specific antibodies, which are associated with a reduced viral load. Together this data highlights the ability of *A.lwoffii* to boost antibody mediated immunity in early life by overcoming the T_{FH} restriction observed in this age group. These observations may ultimately aid in the development of therapeutics and vaccines specifically targeted to children.

7. References

1. UNICEF Data - Neonatal mortality [Internet]. [cited 2023 Aug 9]. Available from: https://data.unicef.org/topic/child-survival/neonatal-mortality/

2. WHO Reports - Children: improving survival and well-being [Internet]. [cited 2023 Aug 9]. Available from: https://www.who.int/news-room/fact-sheets/detail/children-reducing-mortality

3. Prabhudas M, Adkins B, Gans H, King C, Levy O, Ramilo O, et al. Challenges in infant immunity: implications for responses to infection and vaccines. Nat Immunol. 2011;12(3):189–94.

4. Lozano R, Naghavi M, Foreman K, Lim S, Shibuya K, Aboyans V, et al. Global and regional mortality from 235 causes of death for 20 age groups in 1990 and 2010: A systematic analysis for the Global Burden of Disease Study 2010. Lancet. 2012;380(9859):2095–128.

5. Mazur NI, Higgins D, Nunes MC, Melero JA, Langedijk AC, Horsley N, et al. The respiratory syncytial virus vaccine landscape: lessons from the graveyard and promising candidates. Lancet Infect Dis. 2018;18(10):e295–311.

6. Semmes EC, Chen JL, Goswami R, Burt TD, Permar SR, Fouda GG. Understanding Early-Life Adaptive Immunity to Guide Interventions for Pediatric Health. Front Immunol. 2021;21(11).

7. Labeur-Iurman L, Harker JA. Mechanisms of antibody mediated immunity – Distinct in early life. Int J Biochem Cell Biol [Internet]. 2024;172. Available from: https://doi.org/10.1016/j.biocel.2024.106588

8. Kaler J, Hussain A, Patel K, Hernandez T, Ray S. Respiratory Syncytial Virus: A Comprehensive Review of Transmission, Pathophysiology, and Manifestation. Cureus. 2023;15(3).

9. Openshaw PJM, Chiu C, Culley FJ, Johansson C. Protective and harmful immunity to RSV infection. Annu Rev Immunol. 2017;26(35):501–32.

10. Sigurs N, Bjarson R, Sigurbergsson F and Kjellman B. Respiratory Syncytial Virus Bronchiolitis in Infancy Is an Important Risk Factor for Asthma and Allergy at Age 7. Am J Respir Crit Care Med. 2000;161:1501–7.

11. World Health Organization. Malaria [Internet]. 2023. [cited 2023 Aug 9]. Available from: https://www.who.int/news-room/fact-sheets/detail/malaria

12. Karron RA, Buchholz UJ, Collins PL. Live-attenuated respiratory syncytial virus vaccines. Curr Top Microbiol Immunol. 2013;372:259–84.

13. Hill DL, Carr EJ, Rutishauser T, Moncunill G, Campo JJ, Innocentin S, et al. Immune system development varies according to age, location, and anemia in African children. Sci Transl Med. 2020;12(529).

14. Bogaert D, de Groot R, Hermans PWM. Streptococcus pneumoniae colonisation: the key to pneumococcal disease. Lancet Infect Dis [Internet]. 2004;4(March):144–54. Available from: http://infection.thelancet.com

15. Tristram S, Jacobs MR, Appelbaum PC. Antimicrobial resistance in Haemophilus influenzae. Clin Microbiol Rev.

2007;20(2):368–89.

16. Hartzell JD, Blaylock JM. Whooping cough in 2014 and beyond: An update and review. Chest [Internet]. 2014;146(1):205–14. Available from: http://dx.doi.org/10.1378/chest.13-2942

17. Bandyopadhyay AS, Garon J, Seib K, Orenstein WA. Polio vaccination: Past, present and future. Future Microbiol. 2015;10(5):791–808.

18. Thwaites CL, Beeching NJ, Newton CR. Maternal and neonatal tetanus. Lancet [Internet]. 2015;385(9965):362–70. Available from: http://dx.doi.org/10.1016/S0140-6736(14)60236-1

19. UK Health Security Agency. Complete routine immunisation schedule from 1 September 2023 [Internet]. October. 2023 [cited 2024 May 7]. Available from: https://www.gov.uk/government/publications/the-complete-routine-immunisation-schedule/the-complete-routine-immunisation-schedule-from-february-2022

20. Schallert N, Pihlgren M, Kovarik J, Roduit C, Tougne C, Bozzotti P, et al. Generation of adult-like antibody avidity profiles after early-life immunization with protein vaccines. Eur J Immunol. 2002;32(3):752–60.

21. Mastelic B, Kamath AT, Fontannaz P, Tougne C, Rochat A-F, Belnoue E, et al. Environmental and T Cell–Intrinsic Factors Limit the Expansion of Neonatal Follicular T Helper Cells but May Be Circumvented by Specific Adjuvants. J Immunol. 2012;189(12):5764–72.

22. Fouda GG, Cunningham CK, McFarland EJ, Borkowsky W, Muresan P, Pollara J, et al. Infant HIV type 1 gp120 vaccination elicits robust and durable anti-V1V2 immunoglobulin G responses and only rare envelope-specific immunoglobulin a responses. J Infect Dis. 2015;211(4):508–17.

23. Pihlgren M, Tougne C, Bozzotti P, Fulurija A, Duchosal MA, Lambert P-H, et al. Unresponsiveness to Lymphoid-Mediated Signals at the Neonatal Follicular Dendritic Cell Precursor Level Contributes to Delayed Germinal Center Induction and Limitations of Neonatal Antibody Responses to T-Dependent Antigens. J Immunol. 2003;170(6):2824–32.

24. Karron RA, Wright PF, Belshe RB, Thumar B, Casey R, Newman F, et al. Identification of a recombinant live attenuated respiratory syncytial virus vaccine candidate that is highly attenuated in infants. J Infect Dis. 2005;191(7):1093–104.

25. Pyle CJ, Labeur-Iurman L, Groves HT, Puttur F, Lloyd CM, Tregoning JS, et al. Enhanced il-2 in early life limits the development of tfh and protective antiviral immunity. J Exp Med. 2021;218(12).

26. Ranjeva S, Subramanian R, Fang VJ, Leung GM, Ip DKM, Perera RAPM, et al. Age-specific differences in the dynamics of protective immunity to influenza. Nat Commun. 2019;10(1):1–11.

27. Vinuesa CG, Linterman MA, Yu D, MacLennan ICM. Follicular Helper T Cells. Annu Rev Immunol. 2016;34(1):335–68.

28. Crotty S. T Follicular Helper Cell Biology: A Decade of Discovery and Diseases. Immunity [Internet]. 2019;50(5):1132–48. Available from: https://doi.org/10.1016/j.immuni.2019.04.011

29. Fletcher AL, Acton SE, Knoblich K. Lymph node fibroblastic reticular cells in health and disease. Nat Rev Immunol. 2015;15(6):350–61.

30. Schulz O, Hammerschmidt SI, Moschovakis GL, Förster R. Chemokines and Chemokine Receptors in Lymphoid Tissue Dynamics. Annu Rev Immunol. 2016;34:203–42.

31. Johnston RJ, Poholek AC, DiToro D, Yusuf I, Eto D, Barnett B, et al. Bcl6 and Blimp-1 are reciprocal and antagonistic regulators of T follicular helper cell differentiation. Science. 2009;325(5943):1006–10.

32. Nurieva RI, Chung Y, Martínez GJ, Yang XO, Tanaka S, Matskevitch TD, et al. Bcl6 Mediates the Development of T Follicular Helper Cells. Science. 2009;325(5943):1001–5.

33. Yu D, Rao S, Tsai LM, Lee SK, He Y, Sutcliffe EL, et al. The Transcriptional Repressor Bcl-6 Directs T Follicular Helper Cell Lineage Commitment. Immunity [Internet]. 2009;31(3):457–68. Available from: http://dx.doi.org/10.1016/j.immuni.2009.07.002

34. Fazilleau N, McHeyzer-Williams LJ, Rosen H, McHeyzer-Williams MG. The function of follicular helper T cells is regulated by the strength of T cell antigen receptor binding. Nat Immunol. 2009;10(4):375–84.

35. Tubo NJ, Pagán AJ, Taylor JJ, Nelson RW, Linehan JL, Ertelt JM, et al. Single naive CD4+ T cells from a diverse repertoire produce different effector cell types during infection. Cell. 2013;153(4):785–96.

36. DiToro D, Winstead C, Pham D, Witte S, Andargachew R, Singer JR, et al. Differential IL-2 expression defines developmental fates of follicular versus nonfollicular helper T cells. Science. 2018;361(6407).

37. Choi YS, Kageyama R, Eto D, Escobar TC, Johnston RJ, Monticelli L, et al. ICOS Receptor Instructs T Follicular Helper Cell versus Effector Cell Differentiation via Induction of the Transcriptional Repressor Bcl6. Immunity [Internet]. 2011;34(6):932–46. Available from: http://dx.doi.org/10.1016/j.immuni.2011.03.023

38. Liu D, Xu H, Shih C, Wan Z, Ma X, Ma W, et al. T-B-cell entanglement and ICOSL-driven feed-forward regulation of germinal centre reaction. Nature. 2015;517(7533):214–8.

39. Weber JP, Fuhrmann F, Feist RK, Lahmann A, Al Baz MS, Gentz LJ, et al. ICOS maintains the T follicular helper cell phenotype by down-regulating krüppel-like factor 2. J Exp Med. 2015;212(2):217–33.

40. Ray JP, Marshall HD, Laidlaw BJ, Staron MM, Kaech SM, Craft J. Transcription factor STAT3 and type I interferons are corepressive insulators for differentiation of follicular helper and T helper 1 cells. Immunity [Internet]. 2014;40(3):367–77. Available from: http://dx.doi.org/10.1016/j.immuni.2014.02.005

41. Johnston RJ, Choi YS, Diamond JA, Yang JA, Crotty S. STAT5 is a potent negative regulator of T FH cell differentiation. J Exp Med. 2012;209(2):243–50.

42. Ballesteros-Tato A, León B, Graf BA, Moquin A, Adams PS, Lund FE, et al. Interleukin-2 Inhibits Germinal Center Formation by Limiting T Follicular Helper Cell Differentiation. Immunity. 2012;36(5):847–56.

43. Ditoro D, Winstead C, Pham D, Witte S, Andargachew R, Singer JR, et al. Differential IL-2 expression defines developmental fates of follicular versus nonfollicular helper T cells. Science. 2018;361(6407):1–13.

44. Elsner RA, Shlomchik MJ. Germinal Center and Extrafollicular B Cell Responses in Vaccination, Immunity, and Autoimmunity. Immunity [Internet]. 2020;53(6):1136–50. Available from: https://doi.org/10.1016/j.immuni.2020.11.006

45. Roco JA, Mesin L, Binder SC, Nefzger C, Gonzalez-Figueroa P, Canete PF, et al. Class-Switch Recombination Occurs Infrequently in Germinal Centers. Immunity [Internet]. 2019;51(2):337-350.e7. Available from: https://doi.org/10.1016/j.immuni.2019.07.001

46. Zotos D, Coquet JM, Zhang Y, Light A, D'Costa K, Kallies A, et al. IL-21 regulates germinal center B cell differentiation and proliferation through a B cell-intrinsic mechanism. J Exp Med. 2010;207(2):365–78.

47. Reinhardt RL, Liang HE, Locksley RM. Cytokine-secreting follicular T cells shape the antibody repertoire. Nat Immunol. 2009;10(4):385–93.

48. Shehata L, Thouvenel CD, Hondowicz BD, Pew LA, Pritchard GH, Rawlings DJ, et al. Interleukin-4 downregulates transcription factor BCL6 to promote memory B cell selection in germinal centers. Immunity [Internet]. 2024;57(4):843–58. Available from: https://doi.org/10.1016/j.immuni.2024.02.018

49. Kim CH, Lim HW, Kim JR, Rott L, Hillsamer P, Butcher EC. Unique gene expression program of human germinal center T helper cells. Blood. 2004;104(7):1952–60.

50. Crotty S. T Follicular Helper Cell Differentiation, Function, and Roles in Disease. Immunity [Internet]. 2014;41(4):529–42. Available from: http://dx.doi.org/10.1016/j.immuni.2014.10.004

51. Chtanova T, Tangye SG, Newton R, Frank N, Hodge MR, Rolph MS, et al. T Follicular Helper Cells Express a Distinctive Transcriptional Profile, Reflecting Their Role as Non-Th1/Th2 Effector Cells That Provide Help for B Cells. J Immunol. 2004;173(1):68–78.

52. Dorfman DM, Brown JA, Shahsafaei A, Freeman GJ. Programmed Death-1 (PD-1) is a Marker of Germinal Center-associated T Cells and Angioimmunoblastic T-Cell Lymphoma. Am J Surg Pathol. 2006;30(7):802–10.

53. Haynes NM, Allen CDC, Lesley R, Ansel KM, Killeen N, Cyster JG. Role of CXCR5 and CCR7 in Follicular Th Cell Positioning and Appearance of a Programmed Cell Death Gene-1High Germinal Center-Associated Subpopulation. J Immunol. 2007;179(8):5099–108.

54. Kerfoot SM, Yaari G, Patel JR, Johnson KL, Gonzalez DG, Kleinstein SH, et al. Germinal Center B Cell and T Follicular Helper Cell Development Initiates in the Interfollicular Zone. Immunity [Internet]. 2011;34(6):947–60. Available from: http://dx.doi.org/10.1016/j.immuni.2011.03.024

55. Rolf J, Fairfax K, Turner M. Signaling Pathways in T Follicular Helper Cells. J Immunol. 2010;184(12):6563–8.

56. Yu D, Vinuesa CG. The elusive identity of T follicular helper cells. Trends Immunol. 2010;31(10):377–83.

57. Choi YS, Yang JA, Yusuf I, Johnston RJ, Greenbaum J, Peters B, et al. Bcl6 Expressing Follicular Helper CD4 T Cells Are Fate Committed Early and Have the Capacity To Form Memory. J Immunol. 2013;190(8):4014–26.

58. Choi YS, Eto D, Yang JA, Lao C, Crotty S. Cutting Edge: STAT1 Is Required for IL-6–Mediated Bcl6 Induction

for Early Follicular Helper Cell Differentiation. J Immunol. 2013;190(7):3049–53.

59. Xie MM, Koh BH, Hollister K, Wu H, Sun J, Kaplan MH, et al. Bcl6 promotes follicular helper T-cell differentiation and PD-1 expression in a Blimp1-independent manner in mice. Eur J Immunol. 2017;47(7):1136–41.

60. Choi J, Diao H, Faliti CE, Truong J, Rossi M, Bélanger S, et al. Bcl-6 is the nexus transcription factor of T follicular helper cells via repressor-of-repressor circuits. Nat Immunol [Internet]. 2020;21(7):777–89. Available from: http://dx.doi.org/10.1038/s41590-020-0706-5

61. Good-Jacobson KL, Szumilas CG, Chen L, Sharpe AH, Tomayko MM, Shlomchik MJ. PD-1 regulates germinal center B cell survival and the formation and affinity of long-lived plasma cells. Nat Immunol. 2010;11(6):535–42.

62. Onabajo OO, George J, Lewis MG, Mattapallil JJ. Rhesus Macaque Lymph Node PD-1hiCD4+ T Cells Express High Levels of CXCR5 and IL-21 and Display a CCR7loICOS+Bcl6+ T-Follicular Helper (Tfh) Cell Phenotype. PLoS One. 2013;8(3).

63. Shi J, Hou S, Fang Q, Liu X, Liu X, Qi H. PD-1 Controls Follicular T Helper Cell Positioning and Function. Immunity [Internet]. 2018;49(264–274). Available from: https://doi.org/10.1016/j.immuni.2018.06.012

64. Poholek AC, Hansen K, Hernandez SG, Eto D, Chandele A, Weinstein JS, et al. In Vivo Regulation of Bcl6 and T Follicular Helper Cell Development. J Immunol. 2010;185(1):313–26.

65. Marshall HD, Chandele A, Jung YW, Meng H, Poholek AC, Parish IA, et al. Differential Expression of Ly6C and T-bet Distinguish Effector and Memory Th1 CD4+ Cell Properties during Viral Infection. Immunity [Internet]. 2011;35(4):633–46. Available from: http://dx.doi.org/10.1016/j.immuni.2011.08.016

66. Weinstein JS, Laidlaw BJ, Lu Y, Wang JK, Schulz VP, Li N, et al. STAT4 and T-bet control follicular helper T cell development in viral infections. J Exp Med. 2018;215(1):337–55.

67. Liu X, Chen X, Zhong B, Wang A, Wang X, Chu F, et al. Transcription factor achaete-scute homologue 2 initiates follicular T-helper-cell development. Nature [Internet]. 2014;507(7493):513–8. Available from: http://dx.doi.org/10.1038/nature12910

68. Bauquet AT, Jin H, Paterson AM, Mitsdoerffer M, Ho IC, Sharpe AH, et al. The costimulatory molecule ICOS regulates the expression of c-Maf and IL-21 in the development of follicular T helper cells and TH -17 cells. Nat Immunol. 2009;10(2):167–75.

69. Zhu F, McMonigle RJ, Schroeder AR, Xia X, Figge D, Greer BD, et al. Spatiotemporal resolution of germinal center Tfh cell differentiation and divergence from central memory CD4+ T cell fate. Nat Commun. 2023;14(3611):1–15.

70. Chang Y, Bach L, Hasiuk M, Wen L, Elmzzahi T, Tsui C, et al. TGF-β specifies TFH versus TH17 cell fates in murine CD4+ T cells through c-Maf. Sci Immunol. 2024;9(93).

71. Kroenke MA, Eto D, Locci M, Cho M, Davidson T, Haddad EK, et al. Bcl6 and Maf Cooperate To Instruct Human Follicular Helper CD4 T Cell Differentiation. J Immunol. 2012;188(8):3734–44.

72. Betz BC, Jordan-Williams KL, Wang C, Kang SG, Liao J, Logan MR, et al. Batf coordinates multiple aspects of B and T cell function required for normal antibody responses. J Exp Med. 2010;207(5):933–42.

73. Choi YS, Gullicksrud JA, Xing S, Zeng Z, Shan Q, Li F, et al. LEF-1 and TCF-1 orchestrate T follicular helper cell differentiation by regulating differentiation circuits upstream of Bcl6. Nat Immunol. 2015;16(9):980–90.

74. Ogbe A, Miao T, Symonds ALJ, Omodho B, Singh R, Bhullar P, et al. Early growth response genes 2 and 3 regulate the expression of Bcl6 and differentiation of T follicular helper cells. J Biol Chem. 2015;290(33):20455–65.

75. Xu L, Cao Y, Xie Z, Huang Q, Bai Q, Yang X, et al. The transcription factor TCF-1 initiates the differentiation of TFH cells during acute viral infection. Nat Immunol [Internet]. 2015;16(9):991–9. Available from: http://dx.doi.org/10.1038/ni.3229

76. Gong D, Malek TR. Cytokine-Dependent Blimp-1 Expression in Activated T Cells Inhibits IL-2 Production. J Immunol. 2007;178(1):242–52.

77. Hart GT, Hogquist KA, Jameson SC. Krüppel-like Factors in Lymphocyte Biology. J Immunol. 2012;188(2):521–6.

78. Lee JY, Skon CN, Lee YJ, Oh S, Taylor JJ, Malhotra D, et al. The Transcription Factor KLF2 Restrains CD4+ T Follicular Helper Cell Differentiation. Immunity. 2015;42(2):252–64.

79. Feng H, Zhao Z, Zhao X, Bai X, Fu W, Zheng L, et al. A novel memory-like Tfh cell subset is precursor to effector Tfh cells in recall immune responses. J Exp Med. 2024;221(1).

80. Stone EL, Pepper M, Katayama CD, Kerdiles YM, Lai CY, Emslie E, et al. ICOS coreceptor signaling inactivates the transcription factor FOXO1 to promote Tfh cell differentiation. Immunity [Internet]. 2015;42(2):239–51. Available from: http://dx.doi.org/10.1016/j.immuni.2015.01.017

81. Wang H, Geng J, Wen X, Bi E, Kossenkov A V., Wolf AI, et al. The transcription factor Foxp1 is a critical negative regulator of the differentiation of follicular helper T cells. Nat Immunol. 2014;15(7):667–75.

82. Podestà MA, Cavazzoni CB, Hanson BL, Bechu ED, Ralli G, Clement RL, et al. Stepwise differentiation of follicular helper T cells reveals distinct developmental and functional states. Nat Commun. 2023;14(7712).

83. Krishnaswamy JK, Alsén S, Yrlid U, Eisenbarth SC, Williams A. Determination of T Follicular Helper Cell Fate by Dendritic Cells. Front Immunol. 2018;9.

84. Benson RA, Macleod MKL, Hale BG, Patakas A, Garside P, Brewer JM. Antigen presentation kinetics control T cell/dendritic cell interactions and follicular helper T cell generation in vivo. Elife. 2015;4(AUGUST2015):1–16.

85. Baumjohann D, Preite S, Reboldi A, Ronchi F, Ansel KM, Lanzavecchia A, et al. Persistent Antigen and Germinal Center B Cells Sustain T Follicular Helper Cell Responses and Phenotype. Immunity [Internet]. 2013;38(3):596–605. Available from: http://dx.doi.org/10.1016/j.immuni.2012.11.020

86. Tam HH, Melo MB, Kang M, Pelet JM, Ruda VM, Foley MH, et al. Sustained antigen availability during germinal

center initiation enhances antibody responses to vaccination. Proc Natl Acad Sci U S A. 2016;113(43).

87. Shahinian A, Pfefer K, Lee KP, Kündig TM, Kishihara K, Wakeham A, et al. Differential T cell costimulatory requirements in CD28-deficient mice. Science. 1993;261(5121):609–12.

88. Akiba H, Takeda K, Kojima Y, Usui Y, Harada N, Yamazaki T, et al. The Role of ICOS in the CXCR5+ Follicular B Helper T Cell Maintenance In Vivo. J Immunol. 2005;175(4):2340–8.

89. Watanabe M, Fujihara C, Radtke AJ, Chiang YJ, Bhatia S, Germain RN, et al. Co-stimulatory function in primary germinal center responses: CD40 and B7 are required on distinct antigenpresenting cells. J Exp Med. 2017;214(9):2795–810.

90. Linterman MA, Denton AE, Divekar DP, Zvetkova I, Kane L, Ferreira C, et al. CD28 expression is required after T cell priming for helper T cell responses and protective immunity to infection. Elife. 2014;3(October2014):1–21.

91. Sansom DM. CD28, CTLA-4 and their ligands: Who does what and to whom? Immunology. 2000;101:169–77.

92. Lane P, Burdet C, Hubele S, Scheidegger D, Mfiller U, Mcconne F, et al. B cell function in mice transgenic for mCTLA4-H gamma 1: lack of germinal centers correlated with poor affinity maturation and class switching despite normal priming of CD4+ T cells. J Exp Med. 1994;179:819–30.

93. Fillatreau S, Gray D. T cell accumulation in B cell follicles is regulated by dendritic cells and is independent of B cell activation. J Exp Med. 2003;197(2):195–206.

94. Bossaller L, Burger J, Draeger R, Grimbacher B, Knoth R, Plebani A, et al. ICOS Deficiency Is Associated with a Severe Reduction of CXCR5+CD4 Germinal Center Th Cells. J Immunol. 2006;177(7):4927–32.

95. Sage PT, Paterson AM, Lovitch SB, Sharpe AH. The coinhibitory receptor CTLA-4 controls B cell responses by modulating T follicular helper, T follicular regulatory, and T regulatory cells. Immunity [Internet]. 2014;41(6):1026–39. Available from: http://dx.doi.org/10.1016/j.immuni.2014.12.005

96. Tahiliani V, Hutchinson TE, Abboud G, Croft M, Salek-Ardakani S. OX40 Cooperates with ICOS To Amplify Follicular Th Cell Development and Germinal Center Reactions during Infection. J Immunol. 2017;198(1):218–28.

97. Walker LSK, Gulbranson-Judge A, Flynn S, Brocker T, Raykundalia C, Goodall M, et al. Compromised OX40 function in CD28-deficient mice is linked with failure to develop CXC chemokine receptor 5-positive CD4 cells and germinal centers. J Exp Med. 1999;190(8):1115–22.

98. Pattarini L, Trichot C, Bogiatzi S, Grandclaudon M, Meller S, Keuylian Z, et al. TSLP-activated dendritic cells induce human T follicular helper cell differentiation through OX40-ligand. J Exp Med. 2017;214(5):1529–46.

99. Boettler T, Choi YS, Salek-Ardakani S, Cheng Y, Moeckel F, Croft M, et al. Exogenous OX40 Stimulation during Lymphocytic Choriomeningitis Virus Infection Impairs Follicular Th Cell Differentiation and Diverts CD4 T Cells into the Effector Lineage by Upregulating Blimp-1. J Immunol. 2013;191(10):5026–35.

100. Uwadiae FI, Pyle CJ, Walker SA, Lloyd CM, Harker JA. Targeting the ICOS/ICOS-L pathway in a mouse model

of established allergic asthma disrupts T follicular helper cell responses and ameliorates disease. Allergy Eur J Allergy Clin Immunol. 2019;74(4):650–62.

101. Pratama A, Ramiscal RR, Silva DG, Das SK, Athanasopoulos V, Fitch J, et al. Roquin-2 shares functions with its paralog roquin-1 in the repression of mrnas controlling t follicular helper cells and systemic inflammation. Immunity. 2013;38(4):669–80.

102. Vogel KU, Edelmann SL, Jeltsch KM, Bertossi A, Heger K, Heinz GA, et al. Roquin paralogs 1 and 2 redundantly repress the icos and ox40 costimulator mrnas and control follicular helper t cell differentiation. Immunity. 2013;38(4):655–68.

103. Pratama A, Srivastava M, Williams NJ, Papa I, Lee SK, Dinh XT, et al. MicroRNA-146a regulates ICOS-ICOSL signalling to limit accumulation of T follicular helper cells and germinal centres. Nat Commun. 2015;6.

104. Pedros C, Zhang Y, Hu JK, Choi YS, Canonigo-Balancio AJ, Yates JR, et al. A TRAF-like motif of the inducible costimulator ICOS controls development of germinal center TFH cells via the kinase TBK1. Nat Immunol. 2016;17(7):825–33.

105. Auderset F, Schuster S, Fasnacht N, Coutaz M, Charmoy M, Koch U, et al. Notch Signaling Regulates Follicular Helper T Cell Differentiation. J Immunol. 2013;191(5):2344–50.

106. Dell'aringa M, Lee Reinhardt R. Notch signaling represents an important checkpoint between follicular T-helper and canonical T-helper 2 cell fate article. Mucosal Immunol [Internet]. 2018;11(4):1079–91. Available from: http://dx.doi.org/10.1038/s41385-018-0012-9

107. Liu X, Nurieva RI, Dong C. Transcriptional regulation of follicular T-helper (Tfh) cells. Immunol Rev. 2013;252(1):139–45.

108. Eddahri F, Denanglaire S, Bureau F, Spolski R, Leonard WJ, Leo O, et al. Interleukin-6/STAT3 signaling regulates the ability of naive T cells to acquire B-cell help capacities. Blood. 2009;113(11):2426–33.

109. Wilkinson AN, Gartlan KH, Kelly G, Samson LD, Olver SD, Avery J, et al. Granulocytes Are Unresponsive to IL-6 Due to an Absence of gp130. J Immunol. 2018;200(10):3547–55.

110. Korn T, Hiltensperger M. Role of IL-6 in the commitment of T cell subsets. Cytokine [Internet]. 2021;146:155654. Available from: https://doi.org/10.1016/j.cyto.2021.155654

111. Müllberg J, Oberthür W, Lottspeich F, Mehl E, Dittrich E, Graeve L, et al. The soluble human IL-6 receptor. Mutational characterization of the proteolytic cleavage site. J Immunol. 1994;152(10):4958–68.

112. Lust JA, Donovan KA, Kline MP, Greipp PR, Kyle RA, Maihle NJ. Isolation of an mRNA encoding a soluble form of the human interleukin-6 receptor. Cytokine. 1992;4(2):96–100.

113. Horiuchi S, Ampofo W, Koyanagi Y, Yamashita A, Waki M, Matsumoto A, et al. High-level production of alternatively spliced soluble interleukin-6 receptor in serum of patients with adult T-cell leukaemia/HTLV-I-associated myelopathy. Immunology. 1998;95(3):360–9.

114. Sommer J, Garbers C, Wolf J, Trad A, Moll JM, Sack M, et al. Alternative intronic polyadenylation generates the interleukin-6 trans-signaling inhibitor sgp130-E10. J Biol Chem. 2014;289(32):22140–50.

115. Wolf J, Waetzig GH, Reinheimer TM, Scheller J, Rose-John S, Garbers C. A soluble form of the interleukin-6 family signal transducer gp130 is dimerized via a C-terminal disulfide bridge resulting from alternative mRNA splicing. Biochem Biophys Res Commun [Internet]. 2016;470(4):870–6. Available from: http://dx.doi.org/10.1016/j.bbrc.2016.01.127

116. Schumacher N, Meyer D, Mauermann A, Von Der Heyde J, Wolf J, Schwarz J, et al. Shedding of endogenous interleukin-6 receptor (IL-6R) is governed by a disintegrin and metalloproteinase (ADAM) proteases while a full-length IL-6R isoform localizes to circulating microvesicles. J Biol Chem. 2015;290(43):26059–71.

117. Jostock T, Müllberg J, Özbek S, Atreya R, Blinn G, Voltz N, et al. Soluble gp130 is the natural inhibitor of soluble interleukin-6 receptor transsignaling responses. Eur J Biochem. 2001;268(1):160–7.

118. Heink S, Yogev N, Garbers C, Herwerth M, Aly L, Gasperi C, et al. Trans-presentation of IL-6 by dendritic cells is required for the priming of pathogenic TH17 cells. Nat Immunol. 2017;18(1):74–85.

119. Lamertz L, Rummel F, Polz R, Baran P, Hansen S, Waetzig GH, et al. Soluble gp130 prevents interleukin-6 and interleukin-11 cluster signaling but not intracellular autocrine responses. Sci Signal. 2018;11(550):1–13.

120. Oberg HH, Wesch D, Grüssel SS, Rose-John S, Kabelitz D. Differential expression of CD126 and CD130 mediates different STAT-3 phosphorylation in CD4+CD25- and CD25high regulatory T cells. Int Immunol. 2006;18(4):555–63.

121. Jones GW, McLoughlin RM, Hammond VJ, Parker CR, Williams JD, Malhotra R, et al. Loss of CD4+ T Cell IL-6R Expression during Inflammation Underlines a Role for IL-6 Trans Signaling in the Local Maintenance of Th17 Cells. J Immunol. 2010;184(4):2130–9.

122. Mohammed RN, Wehenkel SC, Galkina E V., Yates EK, Preece G, Newman A, et al. ADAM17-dependent proteolysis of L-selectin promotes early clonal expansion of cytotoxic T cells. Sci Rep. 2019;9(1):1–12.

123. Briso EM, Dienz O, Rincon M. Cutting Edge: Soluble IL-6R Is Produced by IL-6R Ectodomain Shedding in Activated CD4 T Cells. J Immunol. 2008;180(11):7102–6.

124. Zohlnhöfer D, Graeve L, Rose-John S, Schooltink H, Dittrich E, Heinrich PC. The hepatic interleukin-6 receptor Down-regulation of the interleukin-6 binding subunit (gp80) by its ligand. FEBS Lett. 1992;306(2–3):219–22.

125. Flynn CM, Kespohl B, Daunke T, Garbers Y, Düsterhöft S, Rose-John S, et al. Interleukin-6 controls recycling and degradation, but not internalization of its receptors. J Biol Chem [Internet]. 2021;296. Available from: https://doi.org/10.1016/j.jbc.2021.100434

126. Kim SJ, Zou YR, Goldstein J, Reizis B, Diamond B. Tolerogenic function of Blimp-1 in dendritic cells. J Exp Med. 2011;208(11):2193–9.

127. Harker JA, Lewis GM, Mack L, Zuniga EI. Late interleukin-6 escalates T follicular helper cell responses and controls a chronic viral infection. Science. 2011;334(6057):825–9.

128. Harker JA, Dolgoter A, Zuniga EI. Cell-intrinsic IL-27 and GP130 cytokine receptor signaling regulates virus-specific CD4+ T cell responses and viral control during chronic infection. Immunity [Internet]. 2013;39(3):548–59. Available from: http://dx.doi.org/10.1016/j.immuni.2013.08.010

129. Noble A, Zhao J. Follicular helper T cells are responsible for IgE responses to Der p 1 following house dust mite sensitization in mice. Clin Exp Allergy. 2016;46(8):1075–82.

130. Wong KA, Harker JA, Dolgoter A, Marooki N, Zuniga EI. T Cell–Intrinsic IL-6R Signaling Is Required for Optimal ICOS Expression and Viral Control during Chronic Infection. J Immunol. 2019;203(6):1509–20.

131. Papillion A, Powell MD, Chisolm DA, Bachus H, Fuller MJ, Weinmann AS, et al. Inhibition of IL-2 responsiveness by IL-6 is required for the generation of GC-TFH cells. Sci Immunol. 2019;4(39).

132. Karnowski A, Chevrier S, Belz GT, Mount A, Emslie D, D'Costa K, et al. B and T cells collaborate in antiviral responses via IL-6, IL-21, and transcriptional activator and coactivator, Oct2 and OBF-1. J Exp Med. 2012;209(11):2049–64.

133. Vogelzang A, McGuire HM, Yu D, Sprent J, Mackay CR, King C. A Fundamental Role for Interleukin-21 in the Generation of T Follicular Helper Cells. Immunity. 2008;29(1):127–37.

134. Hiramatsu Y, Suto A, Kashiwakuma D, Kanari H, Kagami S, Ikeda K, et al. c-Maf activates the promoter and enhancer of the IL-21 gene, and TGF-β inhibits c-Maf-induced IL-21 production in CD4+ T cells. J Leukoc Biol. 2009;87(4):703–12.

135. Eto D, Lao C, DiToro D, Barnett B, Escobar TC, Kageyama R, et al. IL-21 and IL-6 are critical for different aspects of B cell immunity and redundantly induce optimal follicular helper CD4 T cell (Tfh) differentiation. PLoS One. 2011;6(3).

136. Batten M, Ramamoorthi N, Kljavin NM, Ma CS, Cox JH, Dengler HS, et al. IL-27 supports germinal center function by enhancing IL-21 production and the function of T follicular helper cells. J Exp Med. 2010;207(13):2895–906.

137. Gringhuis SI, Kaptein TM, Wevers BA, Van Der Vlist M, Klaver EJ, Van Die I, et al. Fucose-based PAMPs prime dendritic cells for follicular T helper cell polarization via DC-SIGN-dependent IL-27 production. Nat Commun. 2014;5.

138. Harker JA, Greene TT, Barnett BE, Bao P, Dolgoter A, Zuniga EI. IL-6 and IL-27 play both distinct and redundant roles in regulating CD4 T-cell responses during chronic viral infection. Front Immunol. 2023;14:1–11.

139. Barbet G, Sander LE, Geswell M, Leonardi I, Cerutti A, Iliev I, et al. Sensing Microbial Viability through Bacterial RNA Augments T Follicular Helper Cell and Antibody Responses. Immunity [Internet]. 2018;48(3):584–98. Available from: https://doi.org/10.1016/j.immuni.2018.02.015

140. Nakayamada S, Poholek AC, Lu KT, Takahashi H, Kato M, Iwata S, et al. Type I IFN Induces Binding of STAT1 to Bcl6: Divergent Roles of STAT Family Transcription Factors in the T Follicular Helper Cell Genetic Program. J Immunol. 2014;192(5):2156–66.

141. Cucak H, Yrlid U, Reizis B, Kalinke U, Johansson-Lindbom B. Type I Interferon Signaling in Dendritic Cells

Stimulates the Development of Lymph-Node-Resident T Follicular Helper Cells. Immunity [Internet]. 2009;31(3):491–501. Available from: http://dx.doi.org/10.1016/j.immuni.2009.07.005

142. Lee SK, Silva DG, Martin JL, Pratama A, Hu X, Chang PP, et al. Interferon-γ Excess Leads to Pathogenic Accumulation of Follicular Helper T Cells and Germinal Centers. Immunity [Internet]. 2012;37(5):880–92. Available from: http://dx.doi.org/10.1016/j.immuni.2012.10.010

143. Ma CS, Suryani S, Avery DT, Chan A, Nanan R, Santner-Nanan B, et al. Early commitment of naïve human CD4+ T cells to the T follicular helper (TFH) cell lineage is induced by IL-12. Immunol Cell Biol. 2009;87(8):590–600.

144. Schmitt N, Morita R, Bourdery L, Bentebibel SE, Zurawski SM, Banchereau J, et al. Human Dendritic Cells Induce the Differentiation of Interleukin-21-Producing T Follicular Helper-like Cells through Interleukin-12. Immunity [Internet]. 2009;31:158–69. Available from: http://dx.doi.org/10.1016/j.immuni.2009.04.016

145. Powell MD, Read KA, Sreekumar BK, Jones DM, Oestreich KJ. IL-12 signaling drives the differentiation and function of a TH1-derived TFH1-like cell population. Sci Rep. 2019;9(1).

146. Ma CS, Avery DT, Chan A, Batten M, Bustamante J, Boisson-Dupuis S, et al. Functional STAT3 deficiency compromises the generation of human T follicular helper cells. Blood. 2012;119(17):3997–4008.

147. Schmitt N, Liu Y, Bentebibel SE, Munagala I, Bourdery L, Venuprasad K, et al. The cytokine TGF-β 2 co-opts signaling via STAT3-STAT4 to promote the differentiation of human TFH cells. Nat Immunol. 2014;15(9):856–65.

148. Schmitt N, Bustamante J, Bourdery L, Bentebibel SE, Boisson-Dupuis S, Hamlin F, et al. IL-12 receptor b1 deficiency alters in vivo T follicular helper cell response in humans. Blood. 2013;121(17):3375–85.

149. Gao Y, Zeng Y, Xue W, Chen Y, Li Q, Bian Z, et al. Anti−IL-12/23 p40 antibody attenuates chronic graft-versus-host disease with lupus nephritis via inhibiting Tfh cell in mice. Biomed Pharmacother [Internet]. 2020;129. Available from: https://doi.org/10.1016/j.biopha.2020.110396

150. Wu H, Deng Y, Zhao M, Zhang J, Zheng M, Chen G, et al. Molecular control of follicular helper T cell development and differentiation. Front Immunol. 2018;9:1–11.

151. Hercor M, Anciaux M, Denanglaire S, Debuisson D, Leo O, Andris F. Antigen-presenting cell-derived IL-6 restricts the expression of GATA3 and IL-4 by follicular helper T cells. J Leukoc Biol. 2017;101(1):5–14.

152. Elsner RA, Shlomchik MJ. IL-12 Blocks Tfh Cell Differentiation during Salmonella Infection, thereby Contributing to Germinal Center Suppression. Cell Rep [Internet]. 2019;29(9):2796–809. Available from: https://doi.org/10.1016/j.celrep.2019.10.069

153. Chaurio RA, Anadon CM, Lee Costich T, Payne KK, Biswas S, Harro CM, et al. TGF-β-mediated silencing of genomic organizer SATB1 promotes Tfh cell differentiation and formation of intra-tumoral tertiary lymphoid structures. Immunity [Internet]. 2022;55(1):115–28. Available from: https://doi.org/10.1016/j.immuni.2021.12.007

154. Locci M, Wu JE, Arumemi F, Mikulski Z, Dahlberg C, Miller AT, et al. Activin A programs the differentiation of

human T FH cells. Nat Immunol [Internet]. 2016;17(8):976–84. Available from: http://dx.doi.org/10.1038/ni.3494

155. McCarron MJ, Marie JC. TGF-β prevents T follicular helper cell accumulation and B cell autoreactivity. J Clin Invest. 2014;124(10):4375–86.

156. Marshall HD, Ray JP, Laidlaw BJ, Zhang N, Gawande D, Staron MM, et al. The transforming growth factor beta signaling pathway is critical for the formation of CD4 T follicular helper cells and isotype-switched antibody responses in the lung mucosa. Elife. 2015;4.

157. Kenji Ogawa, Masayuki Funaba, Yan Chen and MT. Activin A Functions as a Th2 Cytokine in the Promotion of the Alternative Activation of Macrophages. J Immunol. 2006;177(10):6787–6794.

158. Carnathan DG, Kaushik K, Ellebedy AH, Enemuo CA, Gebru EH, Dhadvai P, et al. Harnessing Activin A Adjuvanticity to Promote Antibody Responses to BG505 HIV Envelope Trimers. Front Immunol. 2020;11.

159. He J, Zhang X, Wei Y, Sun X, Chen Y, Deng J, et al. Low-dose interleukin-2 treatment selectively modulates CD4+ T cell subsets in patients with systemic lupus erythematosus. Nat Med. 2016;22(9):991–3.

160. Wang X, Rickert M, Garcia KC. Structural biology: Structure of the quaternary complex of interleukin-2 with its α, β and γc receptors. Science. 2005;310(5751):1159–63.

161. Nurieva RI, Podd A, Chen Y, Alekseev AM, Yu M, Qi X, et al. STAT5 protein negatively regulates T follicular helper (Tfh) cell generation and function. J Biol Chem. 2012;287(14):11234–9.

162. Oestreich KJ, Mohn SE, Weinmann AS. Molecular mechanisms that control the expression and activity of Bcl-6 in T H1 cells to regulate flexibility with a T FH-like gene profile. Nat Immunol. 2012;13(4):405–11.

163. Sabatos CA, Doh J, Chakravarti S, Friedman RS, Pandurangi PG, Tooley AJ, et al. A Synaptic Basis for Paracrine Interleukin-2 Signaling during Homotypic T Cell Interaction. Immunity. 2008;29(2):238–48.

164. Ray JP, Staron MM, Shyer JA, Ho PC, Marshall HD, Gray SM, et al. The Interleukin-2-mTORc1 Kinase Axis Defines the Signaling, Differentiation, and Metabolism of T Helper 1 and Follicular B Helper T Cells. Immunity [Internet]. 2015;43(4):690–702. Available from: http://dx.doi.org/10.1016/j.immuni.2015.08.017

165. León B, Bradley JE, Lund FE, Randall TD, Ballesteros-Tato A. FoxP3+ regulatory T cells promote influenza-specific Tfh responses by controlling IL-2 availability. Nat Commun. 2014;5(3495).

166. Li J, Lu E, Yi T, Cyster JG. EBI2 augments Tfh cell fate by promoting interaction with IL-2-quenching dendritic cells. Nat Lett [Internet]. 2016;533(7601):110–4. Available from: http://dx.doi.org/10.1038/nature17947

167. Wuest SC, Edwan JH, Martin JF, Han S, Perry JSA, Cartagena CM, et al. A role for interleukin-2 trans-presentation in dendritic cell-mediated T cell activation in humans, as revealed by daclizumab therapy. Nat Med. 2011;17(5):604–9.

168. Waldmann BYTA, Goldman CK, Robb RJ, Depper JM, Leonard WJ, Sharrow SO, et al. Expression of interleukin 2 receptors on activated human B cells. J Exp Med. 1984;160:1450–66.

169. Brisslert M, Bokarewa M, Larsson P, Wing K, Collins LV, Tarkowski A. Phenotypic and functional characterization of human CD25+ B cells. Immunology. 2006;117(4):548–57.

170. Amu S, Gjertsson I, Brisslert M. Functional characterization of murine CD25 expressing B cells. Scand J Immunol. 2010;71(4):275–82.

171. Amu S, Brisslert M. Phenotype and function of CD25-expressing B lymphocytes isolated from human umbilical cord blood. Clin Dev Immunol. 2011;2011:1–10.

172. Liu X, Lu H, Chen T, Nallaparaju KC, Yan X, Tanaka S, et al. Genome-wide Analysis Identifies Bcl6-Controlled Regulatory Networks during T Follicular Helper Cell Differentiation. Cell Rep [Internet]. 2016;14(7):1735–47. Available from: http://dx.doi.org/10.1016/j.celrep.2016.01.038

173. McDonald PW, Read KA, Baker CE, Anderson AE, Powell MD, Ballesteros-Tato A, et al. IL-7 signalling represses Bcl-6 and the T FH gene program. Nat Commun. 2016;7.

174. Seo YB, Im SJ, Namkoong H, Kim SW, Choi YW, Kang MC, et al. Crucial Roles of Interleukin-7 in the Development of T Follicular Helper Cells and in the Induction of Humoral Immunity. J Virol. 2014;88(16):8998–9009.

175. Chen C, Zhou M, Yan X geng, Chen Y xi, Cui M, Chen H chun, et al. A recombinant canine distemper virus expressing interleukin-7 enhances humoral immunity. J Gen Virol. 2019;100:602–15.

176. Pandit H, Valentin A, Angel M, Deleage C, Bergamaschi C, Bear J, et al. Step-dose IL-7 treatment promotes systemic expansion of T cells and alters immune cell landscape in blood and lymph nodes. iScience [Internet]. 2023;26. Available from: https://doi.org/10.1016/j.isci.2023.105929

177. Cooley ID, Read KA, Oestreich KJ. Trans-presentation of IL-15 modulates STAT5 activation and Bcl-6 expression in TH1 cells. Sci Rep. 2015;5.

178. Bravo M, Dileepan T, Dolan M, Hildebrand J, Wolford J, Hamilton SE, et al. IL-15 complex-induced IL-10 enhances Plasmodium-specific CD4+ Tfh differentiation and antibody production. Bioarxive. 2023;

179. Clark SE, Burrack KS, Jameson SC, Hamilton SE, Lenz LL. NK Cell IL-10 Production Requires IL-15 and IL-10 Driven STAT3 Activation. Front Immunol. 2019;10.

180. Mosmann TR, Cherwinski H, Bond MW, Giedlin MA, Coffman RL. Two types of murine helper T cell clone. I. Definition according to profiles of lymphokine activities and secreted proteins. J Immunol [Internet]. 1986;136(7):2348–57. Available from: http://www.ncbi.nlm.nih.gov/pubmed/2419430

181. Kanhere A, Hertweck A, Bhatia U, Gökmen MR, Perucha E, Jackson I, et al. T-bet and GATA3 orchestrate Th1 and Th2 differentiation through lineage-specific targeting of distal regulatory elements. Nat Commun. 2012;3:1268–80.

182. Caucheteux SM, Hu-Li J, Guo L, Bhattacharyya N, Crank M, Collins MT, et al. IL-1β enhances inflammatory TH2 differentiation. J Allergy Clin Immunol. 2016;138(3):898–901.

183. Cote-Sierra J, Foucras G, Guo L, Chiodetti L, Young HA, Hu-Li J, et al. Interleukin 2 plays a central role in Th2 differentiation. Proc Natl Acad Sci U S A. 2004;101(11):3880–5.

184. Mikhalkevich N, Becknell B, Caligiuri MA, Bates MD, Harvey R, Zheng W. Responsiveness of Naive CD4 T Cells to Polarizing Cytokine Determines the Ratio of Th1 and Th2 Cell Differentiation. J Immunol. 2006;176(3):1553–60.

185. Liao W, Spolski R, Li P, Du N, West EE, Ren M, et al. Opposing actions of IL-2 and IL-21 on Th9 differentiation correlate with their differential regulation of BCL6 expression. Proc Natl Acad Sci. 2014;111(9):3508–13.

186. Xue G, Jin G, Fang J, Lu Y. IL-4 together with IL-1β induces antitumor Th9 cell differentiation in the absence of TGF-β signaling. Nat Commun [Internet]. 2019;10(1):1–10. Available from: http://dx.doi.org/10.1038/s41467-019-09401-9

187. Malik S, Awasthi A. Transcriptional control of Th9 cells: Role of Foxo1 in interleukin-9 induction. Front Immunol. 2018;9(MAY):1–11.

188. Carrascosa LC, Klein M, Kitagawa Y, Lückel C, Marini F, König A, et al. Reciprocal regulation of the Il9 locus by counteracting activities of transcription factors IRF1 and IRF4. Nat Commun. 2017;8(May):1–12.

189. Vyas SP, Goswami R. A decade of Th9 cells: Role of Th9 cells in inflammatory bowel disease. Front Immunol. 2018;9:7–10.

190. Korn T, Bettelli E, Gao W, Awasthi A, Jäger A, Strom TB, et al. IL-21 initiates an alternative pathway to induce proinflammatory T H17 cells. Nature. 2007;448(7152):484–7.

191. Muranski P, Restifo NP. Essentials of Th17 cell commitment and plasticity. Blood. 2013;121(13):2402–14.

192. Sandquist I, Kolls J. Update on regulation and effector functions of Th17 cells. F1000Research. 2018;7:205–13.

193. Plitas G, Rudensky AY. Regulatory T Cells: Differentiation and Function. Cancer Immunol Res. 2016;4(9):721–5.

194. Lee W, Lee GR. Transcriptional regulation and development of regulatory T cells. Exp Mol Med [Internet]. 2018;50(3):456–66. Available from: http://dx.doi.org/10.1038/emm.2017.313

195. Mahne AE, Mauze S, Joyce-Shaikh B, Xia J, Bowman EP, Beebe AM, et al. Dual roles for regulatory T-cell depletion and costimulatory signaling in agonistic GITR targeting for tumor immunotherapy. Cancer Res. 2017;77(5):1108–18.

196. Sharabi A, Tsokos MG, Ding Y, Malek TR, Klatzmann D, Tsokos GC. Regulatory T cells in the treatment of disease. Nat Rev [Internet]. 2018;17(11):823–44. Available from: http://dx.doi.org/10.1038/nrd.2018.148

197. Linterman MA, Pierson W, Lee SK, Kallies A, Kawamoto S, Rayner TF, et al. Foxp3+ follicular regulatory T cells control the germinal center response. Nat Med. 2011;17(8):975–82.

198. Chung Y, Tanaka S, Chu F, Nurieva RI, Martinez GJ, Rawal S, et al. Follicular regulatory T cells expressing

Foxp3 and Bcl-6 suppress germinal center reactions. Nat Med. 2011;17(8):983–8.

199. Wollenberg I, Agua-Doce A, Hernández A, Almeida C, Oliveira VG, Faro J, et al. Regulation of the Germinal Center Reaction by Foxp3+ Follicular Regulatory T Cells. J Immunol. 2011;187(9):4553–60.

200. Pape KA, Catron DM, Itano AA, Jenkins MK. The Humoral Immune Response Is Initiated in Lymph Nodes by B Cells that Acquire Soluble Antigen Directly in the Follicles. Immunity. 2007;26(4):491–502.

201. Phan TG, Grigorova I, Okada T, Cyster JG. Subcapsular encounter and complement-dependent transport of immune complexes by lymph node B cells. Nat Immunol. 2007;8(9):992–1000.

202. Carrasco YR, Batista FD. B Cells Acquire Particulate Antigen in a Macrophage-Rich Area at the Boundary between the Follicle and the Subcapsular Sinus of the Lymph Node. Immunity. 2007;27(1):160–71.

203. Qin D, Wu J, Vora KA, Ravetch J V., Szakal AK, Manser T, et al. Fcγ Receptor IIB on Follicular Dendritic Cells Regulates the B Cell Recall Response. J Immunol. 2000;164(12):6268–75.

204. El Shikh MEM, El Sayed RM, Sukumar S, Szakal AK, Tew JG. Activation of B cells by antigens on follicular dendritic cells. Trends Immunol [Internet]. 2010;31(6):205–11. Available from: http://dx.doi.org/10.1016/j.it.2010.03.002

205. Xu Y, Fairfax K, Light A, Huntington ND, Tarlinton DM. CD19 differentially regulates BCR signalling through the recruitment of PI3K. Autoimmunity. 2014;47(7):430–7.

206. Song W, Cho H, Cheng P, Pierce SK. Entry of B cell antigen receptor and antigen into class II peptide-loading compartment is independent of receptor cross-linking. J Immunol. 1995;155(9):4255–63.

207. Reif K, Ekland EH, Ohl L, Nakano H, Lipp M, Cyster JG, et al. Balanced responsiveness to chemoattractants from adjacent zones determines B-cell position. Nat Lett. 2002;416:94–9.

208. Young C, Brink R. The unique biology of germinal center B cells. Immunity [Internet]. 2021;54(8):1652–64. Available from: https://doi.org/10.1016/j.immuni.2021.07.015

209. Ye BH, Cattoretti G, Shen Q, Zhang J, Hawe N, Waard R De, et al. The BCL-6 proto-oncogene controls germinal-centre formation and Th2-type inflammation. Nat Genet. 1997;16:161–70.

210. Dent AL, Shaffer AL, Yu X, Allman D, Louis M, Science S, et al. Control of Inflammation, Cytokine Expression, and Germinal Center Formation by BCL-6. Science. 1997;276(5312):589–92.

211. Victora GD, Schwickert TA, Fooksman DR, Kamphorst AO, Meyer-Hermann M, Dustin ML, et al. Germinal center dynamics revealed by multiphoton microscopy with a photoactivatable fluorescent reporter. Cell [Internet]. 2010;143(4):592–605. Available from: http://dx.doi.org/10.1016/j.cell.2010.10.032

212. De Silva NS, Klein U. Dynamics of B cells in germinal centres. Nat Rev Immunol. 2015;15(3):137–48.

213. Wishnie AJ, Chwat-Edelstein T, Attaway M, Vuong BQ. BCR Affinity Influences T-B Interactions and B Cell Development in Secondary Lymphoid Organs. Front Immunol. 2021;12(July):703918.

214. Nutt SL, Hodgkin PD, Tarlinton DM, Corcoran LM. The generation of antibody-secreting plasma cells. Nat Rev Immunol. 2015;15(3):160–71.

215. Hargreaves DC, Hyman PL, Lu TT, Ngo VN, Bidgol A, Suzuki G, et al. A coordinated change in chemokine responsiveness guides plasma cell movements. J Exp Med. 2001;194(1):45–56.

216. MacLean AJ, Bonifacio JPPL, Oram SL, Mohsen MO, Bachmann MF, Arnon TI. Regulation of pulmonary plasma cell responses during secondary infection with influenza virus. J Exp Med. 2024;221(7).

217. Weisel FJ, Zuccarino-Catania G V., Chikina M, Shlomchik MJ. A Temporal Switch in the Germinal Center Determines Differential Output of Memory B and Plasma Cells. Immunity [Internet]. 2016;44(1):116–30. Available from: http://dx.doi.org/10.1016/j.immuni.2015.12.004

218. Shinnakasu R, Inoue T, Kometani K, Moriyama S, Adachi Y, Nakayama M, et al. Regulated selection of germinal-center cells into the memory B cell compartment. Nat Immunol. 2016;17(7):861–9.

219. Chen C, Laidlaw BJ. Development and function of tissue-resident memory B cells [Internet]. 1st ed. Vol. 155, Advances in Immunology. Elsevier Inc.; 2022. 1–38 p. Available from: http://dx.doi.org/10.1016/bs.ai.2022.08.001

220. Muramatsu M, Sankaranand VS, Anant S, Sugai M, Kinoshita K, Davidson NO, et al. Specific expression of activation-induced cytidine deaminase (AID), a novel member of the RNA-editing deaminase family in germinal center B cells. J Biol Chem [Internet]. 1999;274(26):18470–6. Available from: http://dx.doi.org/10.1074/jbc.274.26.18470

221. Muramatsu M, Kazuo K, Sidonia F, Shuichi Y, Yoichi S, Tasuku H. Class Switch Recombination and Hypermutation Require Activation-Induced Cytidine Deaminase (AID), a Potential RNA Editing Enzyme. Cell. 2000;102(5):553–63.

222. Phuong Pham, Ronda Bransteitter, John Petruska, Myron F. Goodman. Processive AID-catalysed cytosine deamination on single-stranded DNA simulates somatic hypermutation. Nature. 2003;424:103–7.

223. Saha T, Sundaravinayagam D, Di Virgilio M. Charting a DNA Repair Roadmap for Immunoglobulin Class Switch Recombination. Trends Biochem Sci [Internet]. 2021;46(3):184–99. Available from: https://doi.org/10.1016/j.tibs.2020.10.005

224. Suzuki K, Meek B, Doi Y, Muramatsu M, Chiba T, Honjo T, et al. Aberrant expansion of segmented filamentous bacteria in IgA-deficient gut. Proc Natl Acad Sci U S A. 2004;101(7):1981–6.

225. Gutzeit C, Magri G, Cerutti A. Intestinal IgA production and its role in host-microbe interaction. Immunol Rev. 2014;260(1):76–85.

226. Coutelier JP, Van Der Logt JT, Heessen FW, Warnier G, Van Snick J. IgG2a restriction of murine antibodies elicited by viral infections. J Exp Med. 1987;165(January):64–9.

227. Huber VC, McKeon RM, Brackin MN, Miller LA, Keating R, Brown SA, et al. Distinct contributions of vaccine-induced immunoglobulin G1 (IgG1) and IgG2a antibodies to protective immunity against influenza. Clin Vaccine

Immunol. 2006;13(9):981–90.

228. Collins AM. IgG subclass co-expression brings harmony to the quartet model of murine IgG function. Immunol Cell Biol. 2016;94(10):949–54.

229. Vidarsson G, Dekkers G, Rispens T. IgG subclasses and allotypes: From structure to effector functions. Front Immunol. 2014;5(OCT):1–17.

230. Damelang T, Rogerson SJ, Kent SJ, Chung AW. Role of IgG3 in Infectious Diseases. Trends Immunol [Internet]. 2019;40(3):197–211. Available from: https://doi.org/10.1016/j.it.2019.01.005

231. Froidure A, Mouthuy J, Durham SR, Chanez P, Sibille Y, Pilette C. Asthma phenotypes and IgE responses. Eur Respir J [Internet]. 2016;47(1):304–19. Available from: http://dx.doi.org/10.1183/13993003.01824-2014

232. Udoye CC, Manz RA. IgE-Mast cell mediated allergy: a sensor of food quality. Signal Transduct Target Ther. 2023;8(1):1–2.

233. Wilson PC, De Bouteiller O, Liu YJ, Potter K, Banchereau J, Capra JD, et al. Somatic hypermutation introduces insertions and deletions into immunoglobulin V genes. J Exp Med. 1998;187(1):59–70.

234. Pilzecker B, Jacobs H. Mutating for good: DNA damage responses during somatic hypermutation. Front Immunol. 2019;10:1–13.

235. Debock I, Jaworski K, Chadlaoui H, Delbauve S, Passon N, Twyffels L, et al. Neonatal Follicular Th Cell Responses Are Impaired and Modulated by IL-4. J Immunol. 2013;191(3):1231–9.

236. Lakerveld AJ, Gelderloos AT, Schepp RM, Haan CAM de, Binnendijk RS van, Rots NY, et al. Difference in respiratory syncytial virus-specific Fc-mediated antibody effector functions between children and adults. Clin Exp Immunol. 2023;214(1):79–93.

237. Yang J, Sakai J, Siddiqui S, Lee RC, Ireland DDC, Verthelyi D, et al. IL-6 Impairs Vaccine Responses in Neonatal Mice. Front Immunol. 2018;20(9).

238. Mastelic-Gavillet B, Vono M, Gonzalez-Dias P, Ferreira FM, Cardozo L, Lambert PH, et al. Neonatal T follicular helper cells are lodged in a pre-T follicular helper stage favoring innate over adaptive germinal center responses. Front Immunol. 2019;13(10).

239. Zens KD, Chen JK, Guyer RS, Wu FL, Cvetkovski F, Miron M, et al. Reduced generation of lung tissue-resident memory T cells during infancy. J Exp Med. 2017;214(10):2915–32.

240. King IL, Mohrs M. IL-4-producing CD4+ T cells in reactive lymph nodes during helminth infection are T follicular helper cells. J Exp Med. 2009;206(5):1001–7.

241. Yusuf I, Kageyama R, Monticelli L, Johnston RJ, DiToro D, Hansen K, et al. Germinal Center T Follicular Helper Cell IL-4 Production Is Dependent on Signaling Lymphocytic Activation Molecule Receptor (CD150). J Immunol. 2010;185(1):190–202.

242. Sahoo A, Alekseev A, Tanaka K, Obertas L, Lerman B, Haymaker C, et al. Batf is important for IL-4 expression in T follicular helper cells. Nat Commun [Internet]. 2015;6. Available from: http://dx.doi.org/10.1038/ncomms8997

243. Vijayanand P, Seumois G, Simpson LJ, Abdul-Wajid S, Baumjohann D, Panduro M, et al. Interleukin-4 Production by Follicular Helper T Cells Requires the Conserved Il4 Enhancer Hypersensitivity Site V. Immunity. 2012;36(2):175–87.

244. Clement RL, Daccache J, Mohammed MT, Diallo A, Blazar BR, Kuchroo VK, et al. Follicular regulatory T cells control humoral and allergic immunity by restraining early B cell responses. Nat Immunol [Internet]. 2019;20(10):1360–71. Available from: http://dx.doi.org/10.1038/s41590-019-0472-4

245. Gowthaman U, Chen JS, Zhang B, Flynn WF, Lu Y, Song W, et al. Identification of a T follicular helper cell subset that drives anaphylactic IgE. Science. 2019;365(6456):1–14.

246. Montecino-Rodriguez E, Dorshkind K. B-1 B Cell Development in the Fetus and Adult. Immunity [Internet]. 2012;36(1):13–21. Available from: http://dx.doi.org/10.1016/j.immuni.2011.11.017

247. Munguía-Fuentes R, Yam-Puc JC, Silva-Sánchez A, Marcial-Juárez E, Gallegos-Hernández IA, Calderón-Amador J, et al. Immunization of newborn mice accelerates the architectural maturation of lymph nodes, but AID-dependent IgG responses are still delayed compared to the adult. Front Immunol. 2017;8(13).

248. Hayakawa K, Hardy RR, Honda M. Ly-1 B cells: Functionally distinct lymphocytes that secrete IgM autoantibodies. Proc Natl Acad Sci U S A. 1984;81(8 I):2494–8.

249. Rodriguez-Zhurbenko N, Quach TD, Hopkins TJ, Rothstein TL, Hernandez AM. Human B-1 cells and B-1 cell antibodies change with advancing age. Front Immunol. 2019;10(MAR):1–15.

250. Tangye SG. To B1 or not to B1: That really is still the question! Blood. 2013;121(26):5109–10.

251. Schatorjé EJH, Driessen GJ, van Hout RWNM, van der Burg M, de Vries E. Levels of somatic hypermutations in B cell receptors increase during childhood. Clin Exp Immunol. 2014;178(2):394–8.

252. Goodwin E, Gilman MSA, Wrapp D, Chen M, Ngwuta JO, Moin SM, et al. Infants Infected with Respiratory Syncytial Virus Generate Potent Neutralizing Antibodies that Lack Somatic Hypermutation. Immunity [Internet]. 2018;48(2):339–49. Available from: https://doi.org/10.1016/j.immuni.2018.01.005

253. Blanco E, Pérez-Andrés M, Arriba-Méndez S, Contreras-Sanfeliciano T, Criado I, Pelak O, et al. Age-associated distribution of normal B-cell and plasma cell subsets in peripheral blood. J Allergy Clin Immunol. 2018;141(6):2208–19.

254. Tasker L, Marshall-Clarke S. Functional responses of human neonatal B lymphocytes to antigen receptor cross-linking and CpG DNA. Clin Exp Immunol. 2003;134(3):409–19.

255. Glaesener S, Jaenke C, Habener A, Geffers R, Hagendorff P, Witzlau K, et al. Decreased production of class-switched antibodies in neonatal B cells is associated with increased expression of miR-181b. PLoS One. 2018;13(2):1–23.

256. Elliott SR, Roberton DM, Zola H, MacArdle PJ. Expression of the costimulator molecules, CD40 and CD154, on lymphocytes from neonates and young children. Hum Immunol. 2000;61(4):378–88.

257. Nonoyama S, Penix LA, Edwards CP, Lewis DB, Ito S, Aruffo A, et al. Diminished expression of CD40 ligand by activated neonatal T cells. J Clin Invest. 1995;95(1):66–75.

258. Durandy A, De Saint Basile G, Lisowska-Grospierre B, Gauchat JF, Forveille M, Kroczek RA, et al. Undetectable CD40 ligand expression on T cells and low B cell responses to CD40 binding agonists in human newborns. J Immunol. 1995;154(4):1560–8.

259. Ise W, Fujii K, Shiroguchi K, Ito A, Kometani K, Takeda K, et al. T Follicular Helper Cell-Germinal Center B Cell Interaction Strength Regulates Entry into Plasma Cell or Recycling Germinal Center Cell Fate. Immunity [Internet]. 2018;48(4):702–15. Available from: https://doi.org/10.1016/j.immuni.2018.03.027

260. Gatto D, Pfister T, Jegerlehner A, Martin SW, Kopf M, Bachmann MF. Complement receptors regulate differentiation of bone marrow plasma cell precursors expressing transcription factors Blimp-1 and XBP-1. J Exp Med. 2005;201(6):993–1005.

261. Kanswal S, Katsenelson N, Selvapandiyan A, Bram RJ, Akkoyunlu M. Deficient TACI expression on B lymphocytes of newborn mice leads to defective Ig secretion in response to BAFF or APRIL. J Immunol. 2008;181(2):976–90.

262. Holcar M, Goropevšek A, Ihan A, Avčin T. Age-Related Differences in Percentages of Regulatory and Effector T Lymphocytes and Their Subsets in Healthy Individuals and Characteristic STAT1/STAT5 Signalling Response in Helper T Lymphocytes. J Immunol Res. 2015;2015.

263. Thome JJC, Bickham KL, Ohmura Y, Kubota M, Matsuoka N, Gordon C, et al. Early-life compartmentalization of human T cell differentiation and regulatory function in mucosal and lymphoid tissues. Nat Med. 2016;22(1):72–7.

264. Yang S, Fujikado N, Kolodin D, Benoist C, Mathis D. Regulatory T cells generated early in life play a distinct role in maintaining self-tolerance. Science. 2015;348(6234):589–94.

265. Jandl C, Liu SM, Cañete PF, Warren J, Hughes WE, Vogelzang A, et al. IL-21 restricts T follicular regulatory T cell proliferation through Bcl-6 mediated inhibition of responsiveness to IL-2. Nat Commun. 2017;(8).

266. Sarvaria A, Basar R, Mehta RS, Shaim H, Muftuoglu M, Khoder A, et al. IL-10+ regulatory B cells are enriched in cord blood and may protect against cGVHD after cord blood transplantation. Blood. 2016;128(10):1346–61.

267. Sakai J, Yang J, Chou CK, Wu WW, Akkoyunlu M. B cell receptor-induced IL-10 production from neonatal mouse CD19+CD43-cells depends on STAT5-mediated IL-6 secretion. Elife. 2023;12:1–27.

268. Walker WE, Goldstein DR. Neonatal B Cells Suppress Innate Toll-Like Receptor Immune Responses and Modulate Alloimmunity. J Immunol. 2007;179(3):1700–10.

269. Pettengill MA, Van Haren SD, Li N, Dowling DJ, Bergelson I, Jans J, et al. Distinct TLR-mediated cytokine production and immunoglobulin secretion in human newborn naïve B cells. Innate Immun. 2016;22(6):433–43.

270. Papaioannou NE, Pasztoi M, Schraml BU. Understanding the functional properties of neonatal dendritic cells: A doorway to enhance vaccine effectiveness? Front Immunol. 2019;10(9).

271. Calabro S, Gallman A, Gowthaman U, Liu D, Chen P, Liu J, et al. Bridging channel dendritic cells induce immunity to transfused red blood cells. J Exp Med. 2016;213(6):887–96.

272. Krishnaswamy JK, Gowthaman U, Zhang B, Mattsson J, Szeponik L, Liu D, et al. Migratory CD11b+ conventional dendritic cells induce T follicular helper cell–dependent antibody responses. Sci Immunol. 2017;2(18):1–14.

273. Papaioannou NE, Salei N, Rambichler S, Ravi K, Popovic J, Küntzel V, et al. Environmental signals rather than layered ontogeny imprint the function of type 2 conventional dendritic cells in young and adult mice. Nat Commun [Internet]. 2021;12(1):1–20. Available from: http://dx.doi.org/10.1038/s41467-020-20659-2

274. Audiger C, Lesage S. FLT3 Ligand Is Dispensable for the Final Stage of Type 1 Conventional Dendritic Cell Differentiation. J Immunol. 2020;205(8):2117–27.

275. Sikder MAA, Rashid RB, Ahmed T, Sebina I, Howard DR, Ullah MA, et al. Maternal diet modulates the infant microbiome and intestinal Flt3L necessary for dendritic cell development and immunity to respiratory infection. Immunity. 2023;56(5):1098–114.

276. Ruckwardt TJ, Malloy AMW, Morabito KM, Graham BS. Quantitative and Qualitative Deficits in Neonatal Lung-Migratory Dendritic Cells Impact the Generation of the CD8+ T Cell Response. PLoS Pathog. 2014;10(2).

277. Dakic A, Shao Q, D'Amico A, O'Keeffe M, Chen W, Shortman K, et al. Development of the Dendritic Cell System during Mouse Ontogeny. J Immunol. 2004;172(2):1018–27.

278. Granot T, Senda T, Carpenter DJ, Matsuoka N, Weiner J, Gordon CL, et al. Dendritic Cells Display Subset and Tissue-Specific Maturation Dynamics over Human Life. Immunity [Internet]. 2017;46(3):504–15. Available from: http://dx.doi.org/10.1016/j.immuni.2017.02.019

279. McGovern N, Shin A, Low G, Low D, Duan K, Yao LJ, et al. Human fetal dendritic cells promote prenatal T-cell immune suppression through arginase-2. Nature [Internet]. 2017;546(7660):662–6. Available from: http://dx.doi.org/10.1038/nature22795

280. Goriely S, Vincart B, Stordeur P, Vekemans J, Willems F, Goldman M, et al. Deficient IL-12(p35) Gene Expression by Dendritic Cells Derived from Neonatal Monocytes. J Immunol. 2001;166(3):2141–6.

281. Sun CM, Deriaud E, Leclerc C, Lo-Man R. Upon TLR9 signaling, CD5+ B cells control the IL-12-dependent Th1-priming capacity of neonatal DCs. Immunity. 2005;22(4):467–77.

282. Renneson J, Dutta B, Goriely S, Danis B, Lecomte S, Laes JF, et al. IL-12 and type I IFN response of neonatal myeloid DC to human CMV infection. Eur J Immunol. 2009;39(10):2789–99.

283. de Kleer IM, Kool M, de Bruijn MJW, Willart M, van Moorleghem J, Schuijs MJ, et al. Perinatal Activation of the Interleukin-33 Pathway Promotes Type 2 Immunity in the Developing Lung. Immunity. 2016;45(6):1285–98.

284. Li L, Wu J, Abdi R, Jewell CM, Bromberg JS. Lymph node fibroblastic reticular cells steer immune responses.

Trends Immunol [Internet]. 2021;42(8):723–34. Available from: https://doi.org/10.1016/j.it.2021.06.006

285. Li C, Lam E, Perez-Shibayama C, Ward LA, Zhang J, Lee D, et al. Early-life programming of mesenteric lymph node stromal cell identity by the lymphotoxin pathway regulates adult mucosal immunity. Sci Immunol. 2019;4(42):1–18.

286. Bjarnarson SP, Adarna BC, Benonisson H, Del Giudice G, Jonsdottir I. The Adjuvant LT-K63 Can Restore Delayed Maturation of Follicular Dendritic Cells and Poor Persistence of Both Protein- and Polysaccharide-Specific Antibody-Secreting Cells in Neonatal Mice. J Immunol. 2012;189(3):1265–73.

287. Schussek S, Bernasconi V, Mattsson J, Wenzel UA, Strömberg A, Gribonika I, et al. The CTA1-DD adjuvant strongly potentiates follicular dendritic cell function and germinal center formation, which results in improved neonatal immunization. Mucosal Immunol [Internet]. 2020;13(3):545–57. Available from: http://dx.doi.org/10.1038/s41385-020-0253-2

288. Matsumoto R, Gray J, Rybkina K, Oppenheimer H, Levy L, Friedman LM, et al. Induction of bronchus-associated lymphoid tissue is an early life adaptation for promoting human B cell immunity. Nat Immunol. 2023;24:1370–81.

289. Connors TJ, Matsumoto R, Verma S, Szabo PA, Guyer R, Gray J, et al. Site-specific development and progressive maturation of human tissue-resident memory T cells over infancy and childhood. Immunity [Internet]. 2023;56:1–16. Available from: https://doi.org/10.1016/j.immuni.2023.06.008

290. Lund FE, Partida-Sánchez S, Lee BO, Kusser KL, Hartson L, Hogan RJ, et al. Lymphotoxin-α-Deficient Mice Make Delayed, But Effective, T and B Cell Responses to Influenza. J Immunol. 2002;169(9):5236–43.

291. Hwang JY, Silva-Sanchez A, Carragher DM, Garcia-Hernandez M de la L, Rangel–Moreno J, Randall TD. Inducible Bronchus–Associated Lymphoid Tissue (iBALT) Attenuates Pulmonary Pathology in a Mouse Model of Allergic Airway Disease. Front Immunol. 2020;11:1–16.

292. Senda T, Dogra P, Granot T, Furuhashi K, Snyder ME, Carpenter DJ, et al. Microanatomical dissection of human intestinal T-cell immunity reveals site-specific changes in gut-associated lymphoid tissues over life. Mucosal Immunol [Internet]. 2019;12(2):378–89. Available from: http://dx.doi.org/10.1038/s41385-018-0110-8

293. Rangel-Moreno J, Carragher DM, De La Luz Garcia-Hernandez M, Hwang JY, Kusser K, Hartson L, et al. The development of inducible bronchus-associated lymphoid tissue depends on IL-17. Nat Immunol. 2011;12(7):639–46.

294. Hirota K, Turner JE, Villa M, Duarte JH, Demengeot J, Steinmetz OM, et al. Plasticity of TH 17 cells in Peyer's patches is responsible for the induction of T cell-dependent IgA responses. Nat Immunol. 2013;14(4):372–9.

295. Murray JM, Kaufmann GR, Hodgkin PD, Lewin SR, Kelleher AD, Davenport MP, et al. Naive T cells are maintained by thymic output in early ages but by proliferation without phenotypic change after age twenty. Immunol Cell Biol. 2003;81(6):487–95.

296. Sutherland JS, Goldberg GL, Maree V, Uldrich AP, Berzins SP, Tracy S, et al. Activation of Thymic Regeneration in Mice and Humans following Androgen Blockade. J Immunol. 2005;175(4):2741–53.

297. Wu H, Qin X, Dai H, Zhang Y. Time-course transcriptome analysis of medullary thymic epithelial cells in the early phase of thymic involution. Mol Immunol [Internet]. 2018;99(May):87–94. Available from: https://doi.org/10.1016/j.molimm.2018.04.010

298. Dutta S, Sengupta P. Men and mice: Relating their ages. Life Sci [Internet]. 2016;152:244–8. Available from: http://dx.doi.org/10.1016/j.lfs.2015.10.025

299. Aw D, Palmer DB. It's not all equal: A multiphasic theory of thymic involution. Biogerontology. 2012;13(1):77–81.

300. Miller JFAP. Immunological Function of the Thymus. Lancet. 1961;278(7205):748–9.

301. Nagasawa T. Microenvironmental niches in the bone marrow required for B-cell development. Nat Rev Immunol. 2006;6(2):107–16.

302. Piątosa B, Wolska-Kuśnierz B, Pac M, Siewiera K, Gałkowska E, Bernatowska E. B cell subsets in healthy children: Reference values for evaluation of B cell maturation process in peripheral blood. Cytom Part B - Clin Cytom. 2010;78(6):372–81.

303. Jensen K, Schaffer L, Olstad OK, Bechensteen AG, Hellebostad M, Tjønnfjord GE, et al. Striking decrease in the total precursor B-cell compartment during early childhood as evidenced by flow cytometry and gene expression changes. Pediatr Hematol Oncol. 2010;27(1):31–45.

304. Nielsen SCA, Roskin KM, Jackson KJL, Joshi SA, Nejad P, Lee JY, et al. Shaping of infant B cell receptor repertoires by environmental factors and infectious disease. Sci Transl Med. 2019;11(481):1–14.

305. Martins TB, Bandhauer ME, Bunker AM, Roberts WL, Hill HR. New childhood and adult reference intervals for total IgE. J Allergy Clin Immunol [Internet]. 2014;133(2):589–91. Available from: http://dx.doi.org/10.1016/j.jaci.2013.08.037

306. Pihlgren M, Schallert N, Tougne C, Bozzotti P, Kovarik J, Fulurija A, et al. Delayed and deficient establishment of the long-term bone marrow plasma cell pool during early life. Eur J Immunol. 2001;31(3):939–46.

307. Pihlgren M, Friedli M, Tougne C, Rochat A-F, Lambert P-H, Siegrist C-A. Reduced Ability of Neonatal and Early-Life Bone Marrow Stromal Cells to Support Plasmablast Survival. J Immunol. 2006;176(1):165–72.

308. Auner HW, Beham-Schmid C, Dillon N, Sabbattini P. The life span of short-lived plasma cells is partly determined by a block on activation of apoptotic caspases acting in combination with endoplasmic reticulum stress. Blood. 2010;116(18):3445–55.

309. Belnoue E, Pihlgren M, McGaha TL, Tougne C, Rochat AF, Bossen C, et al. APRIL is critical for plasmablast survival in the bone marrow and poorly expressed by early-life bone marrow stromal cells. Blood. 2008;111(5):2755–64.

310. Jackson KJL, Wang Y, Collins AM. Human immunoglobulin classes and subclasses show variability in VDJ gene mutation levels. Immunol Cell Biol. 2014;92(8):729–33.

311. Ridings J, Nicholson IC, Goldsworthy W, Haslam R, Roberton DM, Zola H. Somatic hypermutation of

immunoglobulin genes in human neonates. Clin Exp Immunol. 1997;108(2):366–74.

312. Li Y, Wang X, Blau DM, Caballero MT, Feikin DR, Gill CJ, et al. Global, regional, and national disease burden estimates of acute lower respiratory infections due to respiratory syncytial virus in children younger than 5 years in 2019: a systematic analysis. Lancet. 2022;399(10340):2047–64.

313. Lukacs NW, Moore ML, Rudd BD, Berlin AA, Collins RD, Olson SJ, et al. Differential immune responses and pulmonary pathophysiology are induced by two different strains of respiratory syncytial virus. Am J Pathol [Internet]. 2006;169(3):977–86. Available from: http://dx.doi.org/10.2353/ajpath.2006.051055

314. Agoti CN, Mwihuri AG, Sande CJ, Onyango CO, Medley GF, Cane PA, et al. Genetic relatedness of infecting and reinfecting respiratory syncytial virus strains identified in a birth cohort from rural Kenya. J Infect Dis. 2012;206(10):1532–41.

315. Hall CB, Walsh EE, Long CE, Schnabel KC. Immunity to and frequency of reinfection with respiratory syncytial virus. J Infect Dis. 1991;163(4):693–8.

316. Shishir TA, Saha O, Rajia S, Mondol SM, Masum MHU, Rahaman MM, et al. Genome-wide study of globally distributed respiratory syncytial virus (RSV) strains implicates diversification utilizing phylodynamics and mutational analysis. Sci Rep [Internet]. 2023;13(1):1–11. Available from: https://doi.org/10.1038/s41598-023-40760-y

317. Kim H, Webster RG, Webby RJ. Influenza Virus: Dealing with a Drifting and Shifting Pathogen. Viral Immunol. 2018;31(2):174–83.

318. Bukreyev A, Yang L, Fricke J, Cheng L, Ward JM, Murphy BR, et al. The Secreted Form of Respiratory Syncytial Virus G Glycoprotein Helps the Virus Evade Antibody-Mediated Restriction of Replication by Acting as an Antigen Decoy and through Effects on Fc Receptor-Bearing Leukocytes. J Virol. 2008;82(24):12191–204.

319. Battles MB, McLellan JS. Respiratory syncytial virus entry and how to block it. Nat Rev Microbiol [Internet]. 2019;17(4):233–45. Available from: http://dx.doi.org/10.1038/s41579-019-0149-x

320. Fuentes S, Tran KC, Luthra P, Teng MN, He B. Function of the Respiratory Syncytial Virus Small Hydrophobic Protein. J Virol. 2007;81(15):8361–6.

321. Bian T, Gibbs JD, Örvell C, Imani F. Respiratory syncytial virus matrix protein induces lung epithelial cell cycle arrest through a p53 dependent pathway. PLoS One. 2012;7(5):1–9.

322. Liljeroos L, Krzyzaniak MA, Helenius A, Butcher SJ. Architecture of respiratory syncytial virus revealed by electron cryotomography. Proc Natl Acad Sci U S A. 2013;110(27):11133–8.

323. Lo MS, Brazas RM, Holtzman MJ. Respiratory Syncytial Virus Nonstructural Proteins NS1 and NS2 Mediate Inhibition of Stat2 Expression and Alpha/Beta Interferon Responsiveness. J Virol. 2005;79(14):9315–9.

324. Bitko V, Shulyayeva O, Mazumder B, Musiyenko A, Ramaswamy M, Look DC, et al. Nonstructural Proteins of Respiratory Syncytial Virus Suppress Premature Apoptosis by an NF-κB-Dependent, Interferon-Independent Mechanism and Facilitate Virus Growth. J Virol. 2007;81(4):1786–95.

325. Risso-Ballester J, Rameix-Welti MA. Spatial resolution of virus replication: RSV and cytoplasmic inclusion bodies [Internet]. 1st ed. Vol. 116, Advances in Virus Research. Elsevier Inc.; 2023. 1–43 p. Available from: http://dx.doi.org/10.1016/bs.aivir.2023.06.001

326. Escribano-Romero E, Rawling J, García-Barreno B, Melero JA. The Soluble Form of Human Respiratory Syncytial Virus Attachment Protein Differs from the Membrane-Bound Form in Its Oligomeric State but Is Still Capable of Binding to Cell Surface Proteoglycans. J Virol. 2004;78(7):3524–32.

327. Krusat T, Streckert HJ. Heparin-dependent attachment of respiratory syncytial virus (RSV) to host cells. Arch Virol. 1997;142(6):1247–54.

328. Tripp RA, Jones LP, Haynes LM, Zheng HQ, Murphy PM, Anderson LJ. CX3C chemokine mimicry by respiratory syncytial virus G glycoprotein. Nat Immunol. 2001;2(8):732–8.

329. Murawski MR, Bowen GN, Cerny AM, Anderson LJ, Haynes LM, Tripp RA, et al. Respiratory Syncytial Virus Activates Innate Immunity through Toll-Like Receptor 2. J Virol. 2009;83(3):1492–500.

330. Alshaghdali K, Saeed M, Kamal MA, Saeed A. Interaction of Ectodomain of Respiratory Syncytial Virus G Protein with TLR2/ TLR6 Heterodimer: An In vitro and In silico Approach to Decipher the Role of RSV G Protein in Pro-inflammatory Response against the Virus. Curr Pharm Des. 2021;27(44):4464–76.

331. Anderson CS, Chirkova T, Qiu X, Walsh E, Anderson L, Mariani TJ. CX3CR1 Engagement by Respiratory Syncytial Virus Leads to Induction of Nucleolin and Dysregulation Cilia-Related Genes. 2020;A1171–A1171.

332. Mastrangelo P, Chin AA, Tan S, Jeon AH, Ackerley CA, Siu KK, et al. Identification of rsv fusion protein interaction domains on the virus receptor, nucleolin. Viruses. 2021;13(2):1–13.

333. Yuan X, Hu T, He H, Qiu H, Wu X, Chen J, et al. Respiratory syncytial virus prolifically infects N2a neuronal cells, leading to TLR4 and nucleolin protein modulations and RSV F protein co-localization with TLR4 and nucleolin. J Biomed Sci. 2018;25(1):1–13.

334. Currier MG, Lee S, Stobart CC, Hotard AL, Villenave R, Meng J, et al. EGFR Interacts with the Fusion Protein of Respiratory Syncytial Virus Strain 2-20 and Mediates Infection and Mucin Expression. PLoS Pathog. 2016;12(5):1–22.

335. Griffiths CD, Bilawchuk LM, McDonough JE, Jamieson KC, Elawar F, Cen Y, et al. IGF1R is an entry receptor for respiratory syncytial virus. Nature [Internet]. 2020;583(7817):615–9. Available from: http://dx.doi.org/10.1038/s41586-020-2369-7

336. Hayes RS, Oraby AK, Camargo C, Marchant DJ, Sagan SM. Mapping respiratory syncytial virus fusion protein interactions with the receptor IGF1R and the impact of alanine-scanning mutagenesis on viral infection. J Gen Virol. 2024;105(1).

337. Behera AK, Matsuse H, Kumar M, Kong X, Lockey RF, Mohapatra SS. Blocking intercellular adhesion molecule-1 on human epithelial cells decreases respiratory syncytial virus infection. Biochem Biophys Res Commun. 2001;280(1):188–95.

338. Kinase R, Rna ID, Groskreutz DJ, Monick MM, Powers LS, Yarovinsky TO, et al. Respiratory syncytial virus induces TLR3 protein and protein kinase R, leading to increased double-stranded RNA responsiveness in airway epithelial cells. J Immunol. 2006;176(3):1733–40.

339. Rallabhandi P, Phillips RL, Boukhvalova MS, Pletneva LM, Shirey A, Gioannini TL. Respiratory Syncytial Virus Fusion Protein-Induced Toll-Like Receptor 4 (TLR4) Signaling Is Inhibited by the TLR4 Antagonists Rhodobacter sphaeroides Lipopolysaccharide and Eritoran (E5564) and Requires Direct Interaction with MD-2. MBio. 2012;3(4):1–8.

340. Ghildyal R, Hartley C, Varrasso A, Meanger J, Voelker DR, Anders EM, et al. Surfactant protein A binds to the fusion glycoprotein of respiratory syncytial virus and neutralizes virion infectivity. J Infect Dis. 1999;180(6):2009–13.

341. Bolt G, Pedersen LØ, Birkeslund HH. Cleavage of the respiratory syncytial virus fusion protein is required for its surface expression: Role of furin. Virus Res. 2000;68(1):25–33.

342. Bergeron HC, Tripp RA. Immunopathology of RSV: An updated review. Viruses. 2021;13(12).

343. Ahmad K, Malik HS, Bloom K, Milks KJ, Straight a F, Carroll CW, et al. Structure of RSV Fusion Glycoprotein. Science. 2013;340(May):1113–7.

344. Swanson KA, Settembre EC, Shaw CA, Dey AK, Rappuoli R, Mandl CW, et al. Structural basis for immunization with postfusion respiratory syncytial virus fusion F glycoprotein (RSV F) to elicit high neutralizing antibody titers. Proc Natl Acad Sci U S A. 2011;108(23):9619–24.

345. Wilkins D, Wählby Hamrén U, Chang Y, Clegg LE, Domachowske J, Englund JA, et al. RSV Neutralizing Antibodies Following Nirsevimab and Palivizumab Dosing. Pediatrics [Internet]. 2024;154(5). Available from: http://www.ncbi.nlm.nih.gov/pubmed/39350745

346. Simões EAF, Center KJ, Tita ATN, Swanson KA, Radley D, Houghton J, et al. Prefusion F Protein–Based Respiratory Syncytial Virus Immunization in Pregnancy. N Engl J Med. 2022;386(17):1615–26.

347. Bakker SE, Duquerroy S, Galloux M, Loney C, Conner E, Eléouet JF, et al. The respiratory syncytial virus nucleoprotein-RNA complex forms a left-handed helical nucleocapsid. J Gen Virol. 2013;94:1734–8.

348. Gilman MSA, Liu C, Fung A, Behera I, Jordan P, Rigaux P, et al. Structure of the Respiratory Syncytial Virus Polymerase Complex. Cell. 2019;179(1):193–204.

349. Braun MR, Noton SL, Blanchard EL, Shareef A, Santangelo PJ, Evan Johnson W, et al. Respiratory syncytial virus M2-1 protein associates non-specifically with viral messenger RNA and with specific cellular messenger RNA transcripts. PLoS Pathog [Internet]. 2021;17(5):1–30. Available from: http://dx.doi.org/10.1371/journal.ppat.1009589

350. Noton SL, Tremaglio CZ, Fearns R. Killing two birds with one stone: How the respiratory syncytial virus polymerase initiates transcription and replication. PLoS Pathog. 2019;15(2):1–8.

351. Meshram CD, Baviskar PS, Ognibene CM, Oomens AGP. The Respiratory Syncytial Virus Phosphoprotein,

Matrix Protein, and Fusion Protein Carboxy-Terminal Domain Drive Efficient Filamentous Virus-Like Particle Formation. J Virol. 2016;90(23):10612–28.

352. Ke Z, Dillard RS, Chirkova T, Leon F, Stobart CC, Hampton CM, et al. The morphology and assembly of respiratory syncytial virus revealed by cryo-electron tomography. Viruses. 2018;10(8).

353. Shinoff JJ, O'Brien KL, Thumar B, Shaw JB, Reid R, Hua W, et al. Young infants can develop protective levels of neutralizing antibody after infection with respiratory syncytial virus. J Infect Dis. 2008;198(7):1007–15.

354. Murphy BR, Alling DW, Snyder MH, Walsh EE, Prince GA, Chanock RM, et al. Effect of age and preexisting antibody on serum antibody response of infants and children to the F and G glycoproteins during respiratory syncytial virus infection. J Clin Microbiol. 1986;24(5):894–8.

355. Chu HY, Steinhoff MC, Magaret A, Zaman K, Roy E, Langdon G, et al. Respiratory Syncytial Virus Transplacental Antibody Transfer and Kinetics in Mother-Infant Pairs in Bangladesh. J Infect Dis. 2014;210(10):1582–9.

356. García CG, Bhore R, Soriano-Fallas A, Trost M, Chason R, Ramilo O, et al. Risk factors in children hospitalized with RSV bronchiolitis versus non-RSV bronchiolitis. Pediatrics. 2010;126(6).

357. Hall CB, Weinberg GA, Blumkin AK, Edwards KM, Staat MA, Schultz AF, et al. Respiratory syncytial virus-associated hospitalizations among children less than 24 months of age. Pediatrics. 2013;132(2):341–8.

358. Welliver TP, Garofalo RP, Hosakote Y, Hintz KH, Avendano L, Sanchez K, et al. Severe human lower respiratory tract illness caused by respiratory syncytial virus and influenza virus is characterized by the absence of pulmonary cytotoxic lymphocyte responses. J Infect Dis. 2007;195(8):1126–36.

359. Johnson JE, Gonzales RA, Olson SJ, Wright PF, Graham BS. The histopathology of fatal untreated human respiratory syncytial virus infection. Mod Pathol [Internet]. 2007;20(1):108–19. Available from: http://dx.doi.org/10.1038/modpathol.3800725

360. Johnson SM, McNally BA, Ioannidis I, Flano E, Teng MN, Oomens AG, et al. Respiratory Syncytial Virus Uses CX3CR1 as a Receptor on Primary Human Airway Epithelial Cultures. PLoS Pathog. 2015;11(12):1–16.

361. Nair H, Nokes DJ, Gessner BD, Dherani M, Madhi SA, Singleton RJ, et al. Global burden of acute lower respiratory infections due to respiratory syncytial virus in young children: a systematic review and meta-analysis. Lancet [Internet]. 2010;375(9725):1545–55. Available from: http://dx.doi.org/10.1016/S0140-6736(10)60206-1

362. Lambert L, Sagfors AM, Openshaw PJM, Culley FJ. Immunity to RSV in early-life. Front Immunol. 2014;5:1–14.

363. Cunningham S, Rodriguez A, Adams T, Boyd KA, Butcher I, Enderby B, et al. Oxygen saturation targets in infants with bronchiolitis (BIDS): A double-blind, randomised, equivalence trial. Lancet [Internet]. 2015;386(9998):1041–8. Available from: http://dx.doi.org/10.1016/S0140-6736(15)00163-4

364. DeVincenzo JP, Whitley RJ, Mackman RL, Scaglioni-Weinlich C, Harrison L, Farrell E, et al. Oral GS-5806 Activity in a Respiratory Syncytial Virus Challenge Study. N Engl J Med. 2014;371(8):711–22.

365. DeVincenzo JP, McClure MW, Symons JA, Fathi H, Westland C, Chanda S, et al. Activity of Oral ALS-008176

in a Respiratory Syncytial Virus Challenge Study. N Engl J Med. 2015;373(21):2048–58.

366. DeVincenzo JP, Wilkinson T, Vaishnaw A, Cehelsky J, Meyers R, Nochur S, et al. Viral load drives disease in humans experimentally infected with respiratory syncytial virus. Am J Respir Crit Care Med. 2010;182(10):1305–14.

367. Cunningham S, Piedra PA, Martinon-Torres F, Szymanski H, Brackeva B, Dombrecht E, et al. Nebulised ALX-0171 for respiratory syncytial virus lower respiratory tract infection in hospitalised children: a double-blind, randomised, placebo-controlled, phase 2b trial. Lancet Respir Med. 2021;9(1):21–32.

368. Knowles SR, Phillips EJ, Dresser L, Matukas L. Common Adverse Events Associated with the Use of Ribavirin for Severe Acute Respiratory Syndrome in Canada. Clin Infect Dis. 2003;37(8):1139–42.

369. Wright PF, Ikizler MR, Gonzales RA, Carroll KN, Johnson JE, Werkhaven JA. Growth of Respiratory Syncytial Virus in Primary Epithelial Cells from the Human Respiratory Tract. J Virol. 2005;79(13):8651–4.

370. Pastey MK, Crowe JE, Graham BS. RhoA Interacts with the Fusion Glycoprotein of Respiratory Syncytial Virus and Facilitates Virus-Induced Syncytium Formation. J Virol. 1999;73(9):7262–70.

371. Collins PL, Graham BS. Viral and Host Factors in Human Respiratory Syncytial Virus Pathogenesis. J Virol. 2008;82(5):2040–55.

372. Kolli D, Gupta MR, Sbrana E, Velayutham TS, Chao H, Casola A, et al. Alveolar macrophages contribute to the pathogenesis of human metapneumovirus infection while protecting against respiratory syncytial virus infection. Am J Respir Cell Mol Biol. 2014;51(4):502–15.

373. Makris S, Bajorek M, Culley FJ, Goritzka M, Johansson C. Alveolar macrophages can control respiratory syncytial virus infection in the absence of Type I interferons. J Innate Immun. 2016;8(5):452–63.

374. Empey KM, Orend JG, Peebles RS, Egaña L, Norris KA, Oury TD, et al. Stimulation of immature lung macrophages with intranasal interferon gamma in a novel neonatal mouse model of respiratory syncytial virus infection. PLoS One. 2012;7(7).

375. McNamara PS, Ritson P, Selby A, Hart CA, Smyth RL. Bronchoalveolar lavage cellularity in infants with severe respiratory syncytial virus bronchiolitis. Arch Dis Child. 2003;88(10):922–6.

376. Smith PK, Wang SZ, Dowling KD, Forsyth KD. Leucocyte populations in respiratory syncytial virus-induced bronchiolitis. J Paediatr Child Health. 2001;37(2):146–51.

377. Goritzka M, Makris S, Kausar F, Durant LR, Pereira C, Kumagai Y, et al. Alveolar macrophage-derived type I interferons orchestrate innate immunity to RSV through recruitment of antiviral monocytes. J Exp Med. 2015;212(5):699–714.

378. Hull J, Thomson A, Kwiatkowski D. Association of respiratory syncytial virus bronchiolitis with the interleukin 8 gene region in UK families. Thorax. 2000;55(12):1023–7.

379. Dodd J, Riffault S, Kodituwakku JS, Hayday AC, Openshaw PJM. Pulmonary Vγ4+ γδ T Cells Have

Proinflammatory and Antiviral Effects in Viral Lung Disease. J Immunol. 2009;182(2):1174–81.

380. Huang H, Saravia J, You D, Shaw AJ, Cormier SA. Impaired gamma delta T cell-derived IL-17A and inflammasome activation during early respiratory syncytial virus infection in infants. Immunol Cell Biol. 2015;93(2):126–35.

381. Burgess MO, Janas P, Berry K, Mayr H, Mack M, Jenkins SJ, et al. Helminth induced monocytosis conveys protection from respiratory syncytial virus infection in mice. Allergy Eur J Allergy Clin Immunol. 2024;79(8):2157–72.

382. Kaiko GE, Phipps S, Angkasekwinai P, Dong C, Foster PS. NK Cell Deficiency Predisposes to Viral-Induced Th2-Type Allergic Inflammation via Epithelial-Derived IL-25. J Immunol. 2010;185(8):4681–90.

383. Bem RA, Bos AP, Bots M, Wolbink AM, Van Ham SM, Medema JP, et al. Activation of the granzyme pathway in children with severe respiratory syncytial virus infection. Pediatr Res. 2008;63(6):650–5.

384. Larrañaga CL, Ampuero SL, Luchsinger VF, Carrión FA, Aguilar N V., Morales PR, et al. Impaired immune response in severe human lower tract respiratory infection by respiratory syncytial virus. Pediatr Infect Dis J. 2009;28(10):867–73.

385. Darwich L, Coma G, Peña R, Bellido R, Blanco EJJ, Este JA, et al. Secretion of interferon-γ by human macrophages demonstrated at the single-cell level after costimulation with interleukin (IL)-12 plus IL-18. Immunology. 2009;126(3):386–93.

386. Arase H, Arase N, Saito T. Interferon γ production by natural killer (NK) cells and NK1.1+ T cells upon NKR-P1 cross-linking. J Exp Med. 1996;183(5):2391–6.

387. Eichinger KM, Egaña L, Orend JG, Resetar E, Anderson KB, Patel R, et al. Alveolar macrophages support interferon gamma-mediated viral clearance in RSV infected neonatal mice. Respir Res [Internet]. 2015;16(1):1–13. Available from: http://dx.doi.org/10.1186/s12931-015-0282-7

388. Kumagai Y, Takeuchi O, Kato H, Kumar H, Matsui K, Morii E, et al. Alveolar Macrophages Are the Primary Interferon-α Producer in Pulmonary Infection with RNA Viruses. Immunity. 2007;27(2):240–52.

389. Cella M, Jarrossay D, Facchetti F, Alebardi O, Nakajima H, Lanzavecchia A, et al. Plasmacytoid monocytes migrate to inflamed lymph nodes and produce large amounts of type I interferon. Nat Med. 1999;5(8):919–23.

390. Siegal FP, Kadowaki N, Shodell M, Fitzgerald-Bocarsly PA, Shah K, Ho S, et al. The nature of the principal Type 1 interferon-producing cells in human blood. Science. 1999;284(5421):1835–7.

391. Kato H, Takeuchi O, Sato S, Yoneyama M, Yamamoto M, Matsui K, et al. Differential roles of MDA5 and RIG-I helicases in the recognition of RNA viruses. Nature. 2006;441(1):101–5.

392. Smit JJ, Rudd BD, Lukacs NW. Plasmacytoid dendritic cells inhibit pulmonary immunopathology and promote clearance of respiratory syncytial virus. J Exp Med. 2006;203(5):1153–9.

393. Wang H, Peters N, Schwarze J. Plasmacytoid Dendritic Cells Limit Viral Replication, Pulmonary In?ammation,

and Airway Hyperresponsiveness in Respiratory Syncytial Virus Infection. J Immunol. 2006;177(9):6263–70.

394. Marr N, Wang T-I, Kam SHY, Hu YS, Sharma AA, Lam A, et al. Attenuation of Respiratory Syncytial Virus–Induced and RIG-I–Dependent Type I IFN Responses in Human Neonates and Very Young Children. J Immunol. 2014;192(3):948–57.

395. Cormier SA, Shrestha B, Saravia J, Lee GI, Shen L, DeVincenzo JP, et al. Limited Type I Interferons and Plasmacytoid Dendritic Cells during Neonatal Respiratory Syncytial Virus Infection Permit Immunopathogenesis upon Reinfection. J Virol. 2014;88(16):9350–60.

396. Spann KM, Tran K-C, Chi B, Rabin RL, Collins PL. Suppression of the Induction of Alpha, Beta, and Gamma Interferons by the NS1 and NS2 Proteins of Human Respiratory Syncytial Virus in Human Epithelial Cells and Macrophages. J Virol. 2004;78(8):4363–9.

397. Gill MA, Palucka AK, Barton T, Ghaffar F, Jafri H, Banchereau J, et al. Mobilization of plasmacytoid and myeloid dendritic cells to mucosal sites in children with respiratory syncytial virus and other viral respiratory infections. J Infect Dis. 2005;191(7):1105–15.

398. Owczarczyk AB, Schaller MA, Reed M, Rasky AJ, Lombard DB, Lukacs NW. Sirtuin 1 Regulates Dendritic Cell Activation and Autophagy during Respiratory Syncytial Virus–Induced Immune Responses. J Immunol. 2015;195(4):1637–46.

399. Reed M, Morris SH, Jang S, Mukherjee S, Yue Z, Lukacs NW. Autophagy-Inducing Protein Beclin-1 in Dendritic Cells Regulates CD4 T Cell Responses and Disease Severity during Respiratory Syncytial Virus Infection. J Immunol. 2013;191(5):2526–37.

400. Le Nouën C, Munir S, Losq S, Winter CC, McCarty T, Stephany DA, et al. Infection and maturation of monocyte-derived human dendritic cells by human respiratory syncytial virus, human metapneumovirus, and human parainfluenza virus type 3. Virology [Internet]. 2009;385(1):169–82. Available from: http://dx.doi.org/10.1016/j.virol.2008.11.043

401. Munir S, Le Nouen C, Luongo C, Buchholz UJ, Collins PL, Bukreyev A. Nonstructural Proteins 1 and 2 of Respiratory Syncytial Virus Suppress Maturation of Human Dendritic Cells. J Virol. 2008;82(17):8780–96.

402. Guerrero-Plata A, Casola A, Suarez G, Yu X, Spetch LA, Peeples ME, et al. Differential response of dendritic cells to human metapneumovirus and respiratory syncytial virus. Am J Respir Cell Mol Biol. 2006;34(3):320–9.

403. Beyer M, Bartz H, Hörner K, Doths S, Koerner-Rettberg C, Schwarze J. Sustained increases in numbers of pulmonary dendritic cells after respiratory syncytial virus infection. J Allergy Clin Immunol. 2004;113(1):127–33.

404. Harker JA, Lee DCP, Yamaguchi Y, Wang B, Bukreyev A, Collins PL, et al. Delivery of Cytokines by Recombinant Virus in Early Life Alters the Immune Response to Adult Lung Infection. J Virol. 2010;84(10):5294–302.

405. Culley FJ, Pollott J, Openshaw PJM. Age at first viral infection determines the pattern of T cell-mediated disease during reinfection in adulthood. J Exp Med. 2002;196(10):1381–6.

406. Legg JP, Hussain IR, Warner JA, Johnston SL, Warner JO. Type 1 and type 2 cytokine imbalance in acute

respiratory syncytial virus bronchiolitis. Am J Respir Crit Care Med. 2003;168(6 I):633–9.

407. Caballero MT, Serra ME, Acosta PL, Marzec J, Gibbons L, Salim M, et al. TLR4 genotype and environmental LPS mediate RSV bronchiolitis through Th2 polarization. J Clin Invest. 2015;125(2):571–82.

408. Vu LD, Siefker D, Jones TL, You D, Taylor R, DeVincenzo J, et al. Elevated levels of type 2 respiratory innate lymphoid cells in human infants with severe respiratory syncytial virus bronchiolitis. Am J Respir Crit Care Med. 2019;200(11):1414–23.

409. Heidema J, Lukens M V., van Maren WWC, van Dijk MEA, Otten HG, van Vught AJ, et al. CD8+ T Cell Responses in Bronchoalveolar Lavage Fluid and Peripheral Blood Mononuclear Cells of Infants with Severe Primary Respiratory Syncytial Virus Infections. J Immunol. 2007;179(12):8410–7.

410. Lukens M V., van de Pol AC, Coenjaerts FEJ, Jansen NJG, Kamp VM, Kimpen JLL, et al. A Systemic Neutrophil Response Precedes Robust CD8 + T-Cell Activation during Natural Respiratory Syncytial Virus Infection in Infants. J Virol. 2010;84(5):2374–83.

411. De Weerd W, Twilhaar WN, Kimpen JLL. T cell subset analysis in peripheral blood of children with RSV bronchiolitis. Scand J Infect Dis. 1998;30(1):77–80.

412. Ruckwardt TJ, Malloy AMW, Gostick E, Price DA, Dash P, McClaren JL, et al. Neonatal CD8 T-cell hierarchy is distinct from adults and is influenced by intrinsic T cell properties in respiratory syncytial virus infected mice. PLoS Pathog. 2011;7(12).

413. Eichinger KM, Kosanovich JL, Empey KM. Localization of the T-cell response to RSV infection is altered in infant mice. Pediatr Pulmonol. 2018;53(2):145–53.

414. Hussell T, Baldwin CJ, O'Garra A, Openshaw PJM. CD8+ T cells control Th2-driven pathology during pulmonary respiratory syncytial virus infection. Eur J Immunol. 1997;27(12):3341–9.

415. Aberle JH, Aberle SW, Dworzak MN, Mandl CW, Rebhandl W, Vollnhofer G, et al. Reduced interferon-γ expression in peripheral blood mononuclear cells of infants with severe respiratory syncytial virus disease. Am J Respir Crit Care Med. 1999;160(4):1263–8.

416. Bendelja K, Gagro A, Baće A, Lokar-Kolbas R, Kršulović-Hrešić V, Drazenović V, et al. Predominant type-2 response in infants with respiratory syncytial virus (RSV) infection demonstrated by cytokine flow cytometry. Clin Exp Immunol. 2000;121(2):332–8.

417. Pala P, Bjarnason R, Sigurbergsson F, Metcalfe C, Sigurs N, Openshaw PJM. Enhanced IL-4 responses in children with a history of respiratory syncytial virus bronchiolitis in infancy. Eur Respir J. 2002;20(2):376–82.

418. Kristjansson S, Bjarnarson SP, Wennergren G, Palsdottir AH, Arnadottir T, Haraldsson A, et al. Respiratory syncytial virus and other respiratory viruses during the first 3 months of life promote a local TH2-like response. J Allergy Clin Immunol. 2005;116(4):805–11.

419. Semple MG, Dankert HM, Ebrahimi B, Correia JB, Booth JA, Stewart JP, et al. Severe respiratory syncytial virus bronchiolitis in infants is associated with reduced airway interferon gamma and substance P. PLoS One.

2007;2(10):1–8.

420. Sumino K, Tucker J, Shahab M, Jaffee KF, Visness CM, Gern JE, et al. Antiviral IFN-γ responses of monocytes at birth predict respiratory tract illness in the first year of life. J Allergy Clin Immunol [Internet]. 2012;129(5):1267-1273.e1. Available from: http://dx.doi.org/10.1016/j.jaci.2012.02.033

421. Lee HH, Hoeman CM, Hardaway JC, Guloglu FB, Ellis JS, Jain R, et al. Delayed maturation of an IL-12-producing dendritic cell subset explains the early Th2 bias in neonatal immunity. J Exp Med. 2008;205(10):2269–80.

422. Krishnamoorthy N, Khare A, Oriss TB, Raundhal M, Morse C, Yarlagadda M, et al. Early infection with respiratory syncytial virus impairs regulatory T cell function and increases susceptibility to allergic asthma. Nat Med. 2012;18(10):1525–30.

423. Stoppelenburg AJ, De Roock S, Hennus MP, Bont L, Boes M. Elevated Th17 response in infants undergoing respiratory viral infection. Am J Pathol [Internet]. 2014;184(5):1274–9. Available from: http://dx.doi.org/10.1016/j.ajpath.2014.01.033

424. Stoppelenburg AJ, Salimi V, Hennus M, Plantinga M, Huis in 't Veld R, Walk J, et al. Local IL-17A Potentiates Early Neutrophil Recruitment to the Respiratory Tract during Severe RSV Infection. PLoS One. 2013;8(10):1–10.

425. Mukherjee S, Lindell DM, Berlin AA, Morris SB, Shanley TP, Hershenson MB, et al. IL-17Induced pulmonary pathogenesis during respiratory viral infection and exacerbation of allergic disease. Am J Pathol [Internet]. 2011;179(1):248–58. Available from: http://dx.doi.org/10.1016/j.ajpath.2011.03.003

426. Hashimoto K, Durbin JE, Zhou W, Collins RD, Ho SB, Kolls JK, et al. Respiratory syncytial virus infection in the absence of STAT1 results in airway dysfunction, airway mucus, and augmented IL-17 levels. J Allergy Clin Immunol. 2005;116(3):550–7.

427. Yu X, Tsibane T, McGraw PA, House FS, Keefer CJ, Hicar MD, et al. Neutralizing antibodies derived from the B cells of 1918 influenza pandemic survivors. Nature. 2008;455(7212):532–6.

428. Sanz-Muñoz I, Lajara C, Sánchez-Martínez J, Prada-García C, Rojo-Rello S, Domínguez-Gil M, et al. Long-term influenza antibodies profiles in previously vaccinated and non-vaccinated adults. Vol. 19, Human Vaccines and Immunotherapeutics. 2023.

429. Bochkov YA, Devries M, Tetreault K, Gangnon R, Lee S, Bacharier LB, et al. Rhinoviruses A and C elicit long-lasting antibody responses with limited cross-neutralization. J Med Virol. 2023;95(8):1–11.

430. McIntosh K, McQuillin J, Gardner PS. Cell-free and cell-bound antibody in nasal secretions from infants with respiratory syncytial virus infection. Infect Immun. 1979;23(2):276–81.

431. McIntosh K, Masters HB, Orr I, Kwa Chao R, Barkin RM. The immunologic response to infection with respiratory syncytial virus in infants. J Infect Dis. 1978;138(1):24–32.

432. Sande CJ, Cane PA, Nokes DJ. The association between age and the development of respiratory syncytial virus neutralising antibody responses following natural infection in infants. Vaccine [Internet]. 2014;32(37):4726–9.

Available from: http://dx.doi.org/10.1016/j.vaccine.2014.05.038

433. Domachowske JB. New and Emerging Passive Immunization Strategies for the Prevention of RSV Infection During Infancy. J Pediatric Infect Dis Soc. 2024;13(Suppl 2):S115–24.

434. Suryadevara M. Passive Immunization Strategies to Prevent Severe Respiratory Syncytial Virus Infection Among Newborns and Young Infants. J Pediatric Infect Dis Soc. 2024;13(Suppl 2):S110–4.

435. Spann KM, Tran KC, Collins PL. Effects of Nonstructural Proteins NS1 and NS2 of Human Respiratory Syncytial Virus on Interferon Regulatory Factor 3, NF-κB, and Proinflammatory Cytokines. J Virol. 2005;79(9):5353–62.

436. Ren J, Liu T, Pang L, Li K, Garofalo RP, Casola A, et al. A novel mechanism for the inhibition of interferon regulatory factor-3-dependent gene expression by human respiratory syncytial virus NS1 protein. J Gen Virol. 2011;92(9):2153–9.

437. Swedan S, Andrews J, Majumdar T, Musiyenko A, Barik S. Multiple Functional Domains and Complexes of the Two Nonstructural Proteins of Human Respiratory Syncytial Virus Contribute to Interferon Suppression and Cellular Location. J Virol. 2011;85(19):10090–100.

438. Ban J, Lee NR, Lee NJ, Lee JK, Quan FS, Inn KS. Human respiratory syncytial virus NS 1 targets TRIM25 to suppress RIG-I ubiquitination and subsequent RIG-I-mediated antiviral signaling. Viruses. 2018;10(12).

439. Pei J, Wagner ND, Zou AJ, Chatterjee S, Borek D, Cole AR, et al. Structural basis for IFN antagonism by human respiratory syncytial virus nonstructural protein 2. Proc Natl Acad Sci U S A. 2021;118(10):1–12.

440. Zhang Y, Yang L, Wang H, Zhang G, Sun X. Respiratory syncytial virus non-structural protein 1 facilitates virus replication through miR-29a-mediated inhibition of interferon-α receptor. Biochem Biophys Res Commun [Internet]. 2016;478(3):1436–41. Available from: http://dx.doi.org/10.1016/j.bbrc.2016.08.142

441. Dhar J, Cuevas RA, Goswami R, Zhu J, Sarkar SN, Barik S. 2′-5′-Oligoadenylate Synthetase-Like Protein Inhibits Respiratory Syncytial Virus Replication and Is Targeted by the Viral Nonstructural Protein 1. J Virol. 2015;89(19):10115–9.

442. Munir S, Hillyer P, le Nouën C, Buchholz UJ, Rabin RL, Collins PL, et al. Respiratory syncytial virus interferon antagonist NS1 protein suppresses and skews the human T lymphocyte response. PLoS Pathog. 2011;7(4).

443. Kotelkin A, Belyakov IM, Yang L, Berzofsky JA, Collins PL, Bukreyev A. The NS2 Protein of Human Respiratory Syncytial Virus Suppresses the Cytotoxic T-Cell Response as a Consequence of Suppressing the Type I Interferon Response. J Virol. 2006;80(12):5958–67.

444. Telcian AG, Laza-Stanca V, Edwards MR, Harker JA, Wang H, Bartlett NW, et al. RSV-induced bronchial epithelial cell PD-L1 expression inhibits CD8+ T cell nonspecific antiviral activity. J Infect Dis. 2011;203(1):85–94.

445. Moore EC, Barber J, Tripp RA. Respiratory syncytial virus (RSV) attachment and nonstructural proteins modify the type I interferon response associated with suppressor of cytokine signaling (SOCS) proteins and IFN-stimulated gene-15 (ISG15). Virol J. 2008;5:1–11.

446. Chirkova T, Boyoglu-Barnum S, Gaston KA, Malik FM, Trau SP, Oomens AGP, et al. Respiratory Syncytial Virus G Protein CX3C Motif Impairs Human Airway Epithelial and Immune Cell Responses. J Virol. 2013;87(24):13466–79.

447. Rudd PM, Elliott T, Cresswell P, Wilson IA, Dwek RA. Glycosylation and the immune system. Science. 2001;291(55112):2370–6.

448. Vigerust DJ, Shepherd VL. Virus glycosylation: role in virulence and immune interactions. Trends Microbiol. 2007;15(5):211–8.

449. Melero JA, García-Barreno B, Martínez I, Pringle CR, Cane PA. Antigenic structure, evolution and immunobiology of human respiratory syncytial virus attachment (G) protein. J Gen Virol. 1997;78(10):2411–8.

450. Tabatabai J, Prifert C, Pfeil J, Grulich-Henn J, Schnitzler P. Novel respiratory syncytial virus (RSV) genotype ON1 predominates in germany during winter season 2012-13. PLoS One. 2014;9(10).

451. Roberts SR, Lichtenstein D, Ball LA, Wertz GW. The membrane-associated and secreted forms of the respiratory syncytial virus attachment glycoprotein G are synthesized from alternative initiation codons. J Virol. 1994;68(7):4538–46.

452. Bukreyev A, Yang L, Collins PL. The Secreted G Protein of Human Respiratory Syncytial Virus Antagonizes Antibody-Mediated Restriction of Replication Involving Macrophages and Complement. J Virol. 2012;86(19):10880–4.

453. Arnold R, König B, Werchau H, König W. Respiratory syncytial virus deficient in soluble G protein induced an increased proinflammatory response in human lung epithelial cells. Virology. 2004;330(2):384–97.

454. Zhivaki D, Lemoine S, Lim A, Morva A, Vidalain PO, Schandene L, et al. Respiratory Syncytial Virus Infects Regulatory B Cells in Human Neonates via Chemokine Receptor CX3CR1 and Promotes Lung Disease Severity. Immunity. 2017;46(2):301–14.

455. Gan SW, Tan E, Lin X, Yu D, Wang J, Tan GMY, et al. The small hydrophobic protein of the human respiratory syncytial virus forms pentameric ion channels. J Biol Chem [Internet]. 2012;287(29):24671–89. Available from: http://dx.doi.org/10.1074/jbc.M111.332791

456. Bukreyev A, Whitehead SS, Murphy BR, Collins PL. Recombinant respiratory syncytial virus from which the entire SH gene has been deleted grows efficiently in cell culture and exhibits site-specific attenuation in the respiratory tract of the mouse. J Virol. 1997;71(12):8973–82.

457. Russell RF, McDonald JU, Ivanova M, Zhong Z, Bukreyev A, Tregoning JS. Partial Attenuation of Respiratory Syncytial Virus with a Deletion of a Small Hydrophobic Gene Is Associated with Elevated Interleukin-1β Responses. J Virol. 2015;89(17):8974–81.

458. Céspedes PF, Bueno SM, Ramírez BA, Gomez RS, Riquelme SA, Palavecino CE, et al. Surface expression of the hRSV nucleoprotein impairs immunological synapse formation with T cells. Proc Natl Acad Sci U S A. 2014;111(31).

459. Lifland AW, Jung J, Alonas E, Zurla C, Crowe JE, Santangelo PJ. Human Respiratory Syncytial Virus Nucleoprotein and Inclusion Bodies Antagonize the Innate Immune Response Mediated by MDA5 and MAVS. J Virol. 2012;86(15):8245–58.

460. Stein RT, Sherrill D, Morgan WJ, Holberg CJ, Halonen M, Taussig LM, et al. Respiratory syncytial virus in early life and risk of wheeze and allergy by age 13 years. Lancet. 1999;354:541–5.

461. Sigurs N, Bjarnason R, Sigurbergsson F, Kjellman B. Respiratory syncytial virus bronchiolitis in infancy is an important risk factor for asthma and allergy at age 7. Am J Respir Crit Care Med. 2000;161(5):1501–7.

462. Henderson J, Hilliard TN, Sherriff A, Stalker D, Al Shammari N, Thomas HM. Hospitalization for RSV bronchiolitis before 12 months of age and subsequent asthma, atopy and wheeze: A longitudinal birth cohort study. Pediatr Allergy Immunol. 2005;16(5):386–92.

463. Schauer U, Hoffjan S, Bittscheidt J, Köchling A, Hemmis S, Bongartz S, et al. RSV bronchiolitis and risk of wheeze and allergic sensitisation in the first year of life. Eur Respir J. 2002;20(5):1277–83.

464. Thomsen SF, Van Der Sluis S, Stensballe LG, Posthuma D, Skytthe A, Kyvik KO, et al. Exploring the association between severe respiratory syncytial virus infection and asthma: A registry-based twin study. Am J Respir Crit Care Med. 2009;179(12):1091–7.

465. Bacharier LB, Cohen R, Schweiger T, Yin-Declue H, Christie C, Zheng J, et al. Determinants of asthma after severe respiratory syncytial virus bronchiolitis. J Allergy Clin Immunol [Internet]. 2012;130(1):91–100. Available from: http://dx.doi.org/10.1016/j.jaci.2012.02.010

466. Carroll KN, Wu P, Gebretsadik T, Griffin MR, Dupont WD, Mitchel EF, et al. The severity-dependent relationship of infant bronchiolitis on the risk and morbidity of early childhood asthma. J Allergy Clin Immunol [Internet]. 2009;123(5):1055–61. Available from: http://dx.doi.org/10.1016/j.jaci.2009.02.021

467. Sigurs N, Aljassim F, Kjellman B, Robinson PD, Sigurbergsson F, Bjarnason R, et al. Asthma and allergy patterns over 18 years after severe RSV bronchiolitis in the first year of life. Thorax. 2010;65(12):1045–52.

468. Perkins C, Wills-Karp M, Finkelman FD. IL-4 induces IL-13-independent allergic airway inflammation. J Allergy Clin Immunol. 2006;118(2):410–9.

469. Cohn L, Herrick C, Niu N, Homer RJ, Bottomly K. IL-4 Promotes Airway Eosinophilia by Suppressing IFN-γ Production: Defining a Novel Role for IFN-γ in the Regulation of Allergic Airway Inflammation. J Immunol. 2001;166(4):2760–7.

470. Blanken MO, Rovers MM, Molenaar JM, Winkler-Seinstra PL, Meijer A, Kimpen JLL, et al. Respiratory Syncytial Virus and Recurrent Wheeze in Healthy Preterm Infants. N Engl J Med. 2013;368(19):1791–9.

471. Scheltema NM, Nibbelke EE, Pouw J, Blanken MO, Rovers MM, Naaktgeboren CA, et al. Respiratory syncytial virus prevention and asthma in healthy preterm infants: a randomised controlled trial. Lancet Respir Med. 2018;6(4):257–64.

472. Scheltema NM, Nibbelke EE, Pouw J, Blanken MO, Rovers MM, Naaktgeboren CA, et al. RSV prevention in

infancy and asthma in later life – Authors' reply. Lancet Respir Med. 2018;6(7).

473. Yoshihara S, Kusuda S, Mochizuki H, Okada K, Nishima S, Simões EAF. Effect of palivizumab prophylaxis on subsequent recurrent wheezing in preterm infants. Pediatrics. 2013;132(5):811–8.

474. Simões EAF, Carbonell-Estrany X, Rieger CHL, Mitchell I, Fredrick L, Groothuis JR. The effect of respiratory syncytial virus on subsequent recurrent wheezing in atopic and nonatopic children. J Allergy Clin Immunol. 2010;126(2):256–62.

475. Schwarze J, Hamelmann E, Bradley KL, Takeda K, Gelfand EW. Respiratory syncytial virus infection results in airway hyperresponsiveness and enhanced airway sensitization to allergen. J Clin Invest. 1997;100(1):226–33.

476. Lukacs NW, Tekkanat KK, Berlin A, Hogaboam CM, Miller A, Evanoff H, et al. Respiratory syncytial virus predisposes mice to augmented allergic airway responses via IL-13-mediated mechanisms. J Immunol. 2005;175(12):8442–8442.

477. You D, Becnel D, Wang K, Ripple M, Daly M, Cormier SA. Exposure of neonates to respiratory syncytial virus is critical in determining subsequent airway response in adults. Respir Res. 2006;7:1–10.

478. Siegrist CA, Aspinall R. B-cell responses to vaccination at the extremes of age. Nat Rev Immunol. 2009;9(3):185–94.

479. Pieren DKJ, Boer MC, Wit J de. The adaptive immune system in early life: The shift makes it count. Front Immunol. 2022;13:1–15.

480. Polack FP, Teng MN, Collins PL, Prince GA, Exner M, Regele H, et al. A role for immune complexes in enhanced respiratory syncytial virus disease. J Exp Med. 2002;196(6):859–65.

481. Loebbermann J, Durant L, Thornton H, Johansson C, Openshaw PJ. Defective immunoregulation in RSV vaccineaugmented viral lung disease restored by selective chemoattraction of regulatory T cells. Proc Natl Acad Sci U S A. 2013;110(8):2987–92.

482. Widjaja I, Wicht O, Luytjes W, Leenhouts K, Rottier PJM, van Kuppeveld FJM, et al. Characterization of Epitope-Specific Anti-Respiratory Syncytial Virus (Anti-RSV) Antibody Responses after Natural Infection and after Vaccination with Formalin-Inactivated RSV. J Virol. 2016;90(13):5965–77.

483. Kampmann B, Madhi SA, Munjal I, Simões EAF, Pahud BA, Llapur C, et al. Bivalent Prefusion F Vaccine in Pregnancy to Prevent RSV Illness in Infants. N Engl J Med. 2023;388(16):1451–64.

484. Keam SJ. Nirsevimab: First Approval. Drugs [Internet]. 2023;83(2):181–7. Available from: https://doi.org/10.1007/s40265-022-01829-6

485. Ares-Gómez S, Mallah N, Santiago-Pérez MI, Pardo-Seco J, Pérez-Martínez O, Otero-Barrós MT, et al. Effectiveness and impact of universal prophylaxis with nirsevimab in infants against hospitalisation for respiratory syncytial virus in Galicia, Spain: initial results of a population-based longitudinal study. Lancet Infect Dis. 2024;24:1–12.

486. Drysdale SB, Cathie K, Flamein F, Knuf M, Collins AM, Hill HC, et al. Nirsevimab for Prevention of Hospitalizations Due to RSV in Infants. N Engl J Med. 2023;389(26):2425–35.

487. Arbetter D, Gopalakrishnan V, Aksyuk AA, Ahani B, Chang Y, Dagan R, et al. Lower respiratory tract infections following respiratory syncytial virus monoclonal antibody nirsevimab immunization versus placebo: Analysis from a Phase 3 randomized clinical trial (MELODY). Clin Infect Dis [Internet]. 2024; Available from: http://www.ncbi.nlm.nih.gov/pubmed/39656748

488. Claydon J, Sur A, Callejas A, Ladd M, Kwan E, Taylor R, et al. Respiratory syncytial virus-neutralizing serum antibody titers in infants following palivizumab prophylaxis with an abbreviated dosing regimen. PLoS One. 2017;12(4):1–9.

489. Mazur NI, Terstappen J, Baral R, Bardají A, Beutels P, Buchholz UJ, et al. Respiratory syncytial virus prevention within reach: the vaccine and monoclonal antibody landscape. Lancet Infect Dis. 2023;23(1).

490. Walsh EE, Pérez Marc G, Zareba AM, Falsey AR, Jiang Q, Patton M, et al. Efficacy and Safety of a Bivalent RSV Prefusion F Vaccine in Older Adults. N Engl J Med. 2023;388(16):1465–77.

491. FDA. MRESVIA [Internet]. 2024 [cited 2024 Jul 17]. Available from: https://www.fda.gov/vaccines-blood-biologics/vaccines/mresvia

492. Ichinohe T, Pang IK, Kumamoto Y, Peaper DR, Ho JH, Murray TS, et al. Microbiota regulates immune defense against respiratory tract influenza A virus infection. Proc Natl Acad Sci U S A. 2011;108(13):5354–9.

493. Lamousé-Smith ES, Tzeng A, Starnbach MN. The intestinal flora is required to support antibody responses to systemic immunization in infant and germ free mice. PLoS One. 2011;6(11):1–8.

494. Oh JZ, Ravindran R, Chassaing B, Carvalho FA, Maddur MS, Bower M, et al. TLR5-Mediated Sensing of Gut Microbiota Is Necessary for Antibody Responses to Seasonal Influenza Vaccination. Immunity. 2014;41(3):478–92.

495. Kim M, Qie Y, Park J, Kim CH. Gut Microbial Metabolites Fuel Host Antibody Responses. Cell Host Microbe [Internet]. 2016;20(2):202–14. Available from: http://dx.doi.org/10.1016/j.chom.2016.07.001

496. Robak OH, Heimesaat MM, Kruglov AA, Prepens S, Ninnemann J, Gutbier B, et al. Antibiotic treatment-induced secondary IgA deficiency enhances susceptibility to Pseudomonas aeruginosa pneumonia. J Clin Invest. 2018;128(8):3535–45.

497. Sanchez HN, Moroney JB, Gan H, Shen T, Im JL, Li T, et al. B cell-intrinsic epigenetic modulation of antibody responses by dietary fiber-derived short-chain fatty acids. Nat Commun [Internet]. 2020;11(1):1–19. Available from: http://dx.doi.org/10.1038/s41467-019-13603-6

498. Harris VC, Armah G, Fuentes S, Korpela KE, Parashar U, Victor JC, et al. Significant Correlation Between the Infant Gut Microbiome and Rotavirus Vaccine Response in Rural Ghana. J Infect Dis. 2017;215(1):34–41.

499. Huda MN, Ahmad SM, Alam MJ, Khanam A, Kalanetra KM, Taft DH, et al. Bifidobacterium Abundance in Early Infancy and Vaccine Response at 2 Years of Age. Pediatrics. 2019;143(2):1–10.

500. Zhao T, Li J, Fu Y, Ye H, Liu X, Li G, et al. Influence of gut microbiota on mucosal IgA antibody response to the polio vaccine. npj Vaccines [Internet]. 2020;5(1). Available from: http://dx.doi.org/10.1038/s41541-020-0194-5

501. Pasquali C, Salami O, Taneja M, Gollwitzer ES, Trompette A, Pattaroni C, et al. Enhanced mucosal antibody production and protection against respiratory infections following an orally administered bacterial extract. Front Med. 2014;1(41):1–9.

502. Kim D, Kim YG, Seo SU, Kim DJ, Kamada N, Prescott D, et al. Nod2-mediated recognition of the microbiota is critical for mucosal adjuvant activity of cholera toxin. Nat Med. 2016;22(5):524–30.

503. Saglani S, Gregory LG, Manghera AK, Branchett WJ, Uwadiae F, Entwistle LJ, et al. Inception of early-life allergen – induced airway hyperresponsiveness is reliant on IL-13+CD4+ T cells. Sci Immunol. 2018;3(27).

504. Di Luccia B, Ahern PP, Griffin NW, Cheng J, Guruge JL, Byrne AE, et al. Combined Prebiotic and Microbial Intervention Improves Oral Cholera Vaccination Responses in a Mouse Model of Childhood Undernutrition. Cell Host Microbe [Internet]. 2020;27(6):899–908. Available from: https://doi.org/10.1016/j.chom.2020.04.008

505. New JS, Dizon BLP, Fucile CF, Rosenberg AF, Kearney JF, King RG. Neonatal Exposure to Commensal-Bacteria-Derived Antigens Directs Polysaccharide-Specific B-1 B Cell Repertoire Development. Immunity [Internet]. 2020;53(1):172–86. Available from: https://doi.org/10.1016/j.immuni.2020.06.006

506. Tiffany Ludka-Gaulke, MD,1,# Princy Ghera, MD,1 Stephen C. Waring, DVM, PhD,2 Matthew Keifer, MD, MPH,3,* Christine Seroogy, MD,4 James E. Gern, MD,4 and Steven Kirkhorn, MD, MPH3,5 §. Farm Exposure in Early Childhood is Associated with a Lower Risk of Severe Respiratory Illnesses. J Allergy Clin Immunol. 2018;141(1):454–456.e4.

507. Pechlivanis S, von Mutius E. Effect of Farming on Asthma. Acta Med Acad. 2020;49(2):144–55.

508. Wells AD, Poole JA, Romberger DJ. Influence of farming exposure on the development of asthma and asthma-like symptoms. Int Immunopharmacol [Internet]. 2014;23(1):356–63. Available from: http://dx.doi.org/10.1016/j.intimp.2014.07.014

509. Fuchs O, Genuneit J, Latzin P, Büchele G, Horak E, Loss G, et al. Farming environments and childhood atopy, wheeze, lung function, and exhaled nitric oxide. J Allergy Clin Immunol. 2012;130(2):382–8.

510. Debarry J, Garn H, Hanuszkiewicz A, Dickgreber N, Blümer N, von Mutius E, et al. Acinetobacter lwoffii and Lactococcus lactis strains isolated from farm cowsheds possess strong allergy-protective properties. J Allergy Clin Immunol. 2007;119(6):1514–21.

511. Hagner S, Harb H, Zhao M, Stein K, Holst O, Ege MJ, et al. Farm-derived Gram-positive bacterium Staphylococcus sciuri W620 prevents asthma phenotype in HDM- and OVA-exposed mice. Allergy Eur J Allergy Clin Immunol. 2013;68(3):322–9.

512. Pribul PK, Harker J, Wang B, Wang H, Tregoning JS, Schwarze J, et al. Alveolar Macrophages Are a Major Determinant of Early Responses to Viral Lung Infection but Do Not Influence Subsequent Disease Development. J Virol. 2008;82(9):4441–8.

513. Saglani S, Mathie SA, Gregory LG, Bell MJ, Bush A, Lloyd CM. Pathophysiological features of asthma develop in parallel in house dust mite-exposed neonatal mice. Am J Respir Cell Mol Biol. 2009;41(3):281–9.

514. Naik SH, Proietto AI, Wilson NS, Dakic A, Schnorrer P, Fuchsberger M, et al. Cutting Edge: Generation of Splenic CD8+ and CD8− Dendritic Cell Equivalents in Fms-Like Tyrosine Kinase 3 Ligand Bone Marrow Cultures. J Immunol. 2005;174(11):6592–7.

515. Pyle CJ, Uwadiae FI, Swieboda DP, Harker JA. Early IL-6 signalling promotes IL-27 dependent maturation of regulatory T cells in the lungs and resolution of viral immunopathology. PLoS Pathog. 2017;13(9):1–27.

516. Foster WS. Investigating the role of cytokine signalling in human T follicular helper cell differentiation and function. 2020.

517. Foster WS, Grime CJ, Tan HL, Williams GS, Robinson MJ, Carlesso G, et al. Enhanced frequency and function of follicular T cells in the tonsils of house dust mite-sensitized children. Allergy Eur J Allergy Clin Immunol. 2020;75(5):1240–3.

518. Abbas, Abul K, Andrew H Lichtman and SP. Cellular and Molecular Immunology. Tenth edition. 2022.

519. Korn T, Kallies A. T cell responses in the central nervous system. Nat Rev Immunol. 2017;17(3):179–94.

520. Ganusov V V., De Boer RJ. Do most lymphocytes in humans really reside in the gut? Trends Immunol. 2007;28(12):514–8.

521. Clark RA. Skin-resident T cells: The ups and downs of on site immunity. J Invest Dermatol [Internet]. 2010;130(2):362–70. Available from: http://dx.doi.org/10.1038/jid.2009.247

522. Tavian M, Péault B. Embryonic development of the human hematopoietic system. Int J Dev Biol. 2005;49:243–50.

523. Belyavsky A, Petinati N, Drize N. Hematopoiesis during ontogenesis, adult life and aging. Int J Mol Sci. 2021;22(17):1–27.

524. Steier Z, Aylard DA, McIntyre LL, Baldwin I, Kim EJY, Lutes LK, et al. Single-cell multiomic analysis of thymocyte development reveals drivers of CD4+ T cell and CD8+ T cell lineage commitment. Nat Immunol. 2023;24(9):1579–90.

525. Kumar B V., Connors TJ, Farber DL. Human T Cell Development, Localization, and Function throughout Life. Immunity [Internet]. 2018;48(2):202–13. Available from: https://doi.org/10.1016/j.immuni.2018.01.007

526. Choi J, Crotty S. Bcl6-Mediated Transcriptional Regulation of Follicular Helper T cells (TFH). Trends Immunol [Internet]. 2021;42(4):336–49. Available from: https://doi.org/10.1016/j.it.2021.02.002

527. Fairfax KC, Everts B, Amiel E, Smith AM, Schramm G, Haas H, et al. IL-4–Secreting Secondary T Follicular Helper (Tfh) Cells Arise from Memory T Cells, Not Persisting Tfh Cells, through a B Cell–Dependent Mechanism. J Immunol. 2015;194(7):2999–3010.

528. He J, Tsai LM, Leong YA, Hu X, Ma CS, Chevalier N, et al. Circulating precursor CCR7loPD-1hi CXCR5+ CD4+ T cells indicate tfh cell activity and promote antibody responses upon antigen reexposure. Immunity. 2013;39(4):770–81.

529. Vella LA, Buggert M, Manne S, Herati RS, Sayin I, Kuri-Cervantes L, et al. T follicular helper cells in human efferent lymph retain lymphoid characteristics. J Clin Invest. 2019;129(8):3185–200.

530. de Winde CM, Munday C, Acton SE. Molecular mechanisms of dendritic cell migration in immunity and cancer. Med Microbiol Immunol [Internet]. 2020;209(4):515–29. Available from: https://doi.org/10.1007/s00430-020-00680-4

531. Eisenbarth SC. Dendritic cell subsets in T cell programming: location dictates function. Nat Rev Immunol [Internet]. 2019;19(2):89–103. Available from: http://dx.doi.org/10.1038/s41577-018-0088-1

532. Mastelic Gavillet B, Eberhardt CS, Auderset F, Castellino F, Seubert A, Tregoning JS, et al. MF59 Mediates Its B Cell Adjuvanticity by Promoting T Follicular Helper Cells and Thus Germinal Center Responses in Adult and Early Life. J Immunol. 2015;194(10):4836–45.

533. Tregoning JS, Wang BL, McDonald JU, Yamaguchi Y, Harker JA, Goritzka M, et al. Neonatal antibody responses are attenuated by interferon-γ produced by NK and T cells during RSV infection. Proc Natl Acad Sci U S A. 2013;110(14):5576–81.

534. Parvathaneni S, Yang J, Lotspeich-Cole L, Sakai J, Lee RC, Akkoyunlu M. IL-6 suppresses vaccine responses in neonatal mice by enhancing IL-2 activity on T follicular helper cells. npj Vaccines. 2023;8(173).

535. Setoguchi R, Hori S, Takahashi T, Sakaguchi S. Homeostatic maintenance of natural Foxp3+ CD25+ CD4+ regulatory T cells by interleukin (IL)-2 and induction of autoimmune disease by IL-2 neutralization. J Exp Med. 2005;201(5):723–35.

536. James A. Harker, 1 Gavin M. Lewis, 1 Lauren Mack 1 Elina I. Zuniga1*. Late Interleukin-6 Escalates T Follicular Helper Cell Responses and Controls a Chronic Viral Infection. Science. 2011;334(6057):825–9.

537. Starr TK, Jameson SC, Hogquist KA. Positive and negative selection of T cells. Annu Rev Immunol. 2003;21:139–76.

538. Owen DL, Mahmud SA, Vang KB, Kelly RM, Blazar BR, Smith KA, et al. Identification of Cellular Sources of IL-2 Needed for Regulatory T Cell Development and Homeostasis. J Immunol. 2018;200(12):3926–33.

539. Argyris BF, DeStefano M ZK. Interleukin-2 production in the neonatal mouse. Transplantation. 1985;40(3):284–7.

540. Adkins B, Du R-Q. Newborn Mice Develop Balanced Th1/Th2 Primary Effector Responses In Vivo But Are Biased to Th2 Secondary Responses. J Immunol. 1998;160(9):4217–24.

541. Yamamoto M, Seki Y, Iwai K, Ko I, Martin A, Tsuji N, et al. Ontogeny and localization of the cells produce IL-2 in healthy animals. Cytokine [Internet]. 2013;61(3):831–41. Available from: http://dx.doi.org/10.1016/j.cyto.2012.11.026

542. Hemmers S, Schizas M, Azizi E, Dikiy S, Zhong Y, Feng Y, et al. IL-2 production by self-reactive CD4 thymocytes scales regulatory T cell generation in the thymus. J Exp Med. 2019;216(11):2466–78.

543. Palin AC, Ramachandran V, Acharya S, Lewis DB. Human Neonatal Naive CD4+ T Cells Have Enhanced Activation-Dependent Signaling Regulated by the MicroRNA miR-181a. J Immunol. 2013;190(6):2682–91.

544. Sinnott BD, Park B, Boer MC, Lewinsohn DA, Lancioni CL. Direct TLR-2 Costimulation Unmasks the Proinflammatory Potential of Neonatal CD4+ T Cells. J Immunol. 2016;197(1):68–77.

545. Bunis DG, Bronevetsky Y, Krow-Lucal E, Bhakta NR, Kim CC, Nerella S, et al. Single-Cell Mapping of Progressive Fetal-to-Adult Transition in Human Naive T Cells. Cell Rep [Internet]. 2021;34(1):108573. Available from: https://doi.org/10.1016/j.celrep.2020.108573

546. Lei L, Zhang X, Yang X, Su Y, Liu H, Yang H, et al. A Genetic Model Reveals Biological Features of Neonatal CD4 Helper Cells Undergone Homeostasis in Mice. Front Cell Dev Biol. 2021;9(March):1–9.

547. Olin A, Henckel E, Chen Y, Lakshmikanth T, Pou C, Mikes J, et al. Stereotypic Immune System Development in Newborn Children. Cell [Internet]. 2018;174(5):1277-1292.e14. Available from: https://doi.org/10.1016/j.cell.2018.06.045

548. Rudd BD. Neonatal T Cells: A Reinterpretation. Annu Rev Immunol. 2020;38:229–47.

549. Saule P, Trauet J, Dutriez V, Lekeux V, Dessaint JP, Labalette M. Accumulation of memory T cells from childhood to old age: Central and effector memory cells in CD4+ versus effector memory and terminally differentiated memory cells in CD8+ compartment. Mech Ageing Dev. 2006;127(3):274–81.

550. Schönland SO, Zimmer JK, Lopez-Benitez CM, Widmann T, Ramin KD, Goronzy JJ, et al. Homeostatic control of T-cell generation in neonates. Blood. 2003;102(4):1428–34.

551. Bendickova K, Fric J. Roles of IL-2 in bridging adaptive and innate immunity, and as a tool for cellular immunotherapy. J Leukoc Biol. 2020;108(1):427–37.

552. Kempis-Calanis LA, Rodríguez-Jorge O, Gutiérrez-Reyna DY, Ventura-Martínez CJ, Spicuglia S, Medina-Rivera A, et al. Neonatal CD4+ T cells have a characteristic transcriptome and epigenome and respond to TCR stimulation with proliferation and yet a limited immune response. J Leukoc Biol. 2023;(December 2023):1–13.

553. Li G, Yu M, Lee WW, Tsang M, Krishnan E, Weyand CM, et al. Decline in miR-181a expression with age impairs T cell receptor sensitivity by increasing DUSP6 activity. Nat Med. 2012;18(10):1518–24.

554. Bayer AL, Yu A, Adeegbe D, Malek TR. Essential role for interleukin-2 for CD4+CD25+ T regulatory cell development during the neonatal period. J Exp Med. 2005;201(5):769–77.

555. Ng MSF, Roth TL, Mendoza VF, Marson A, Burt TD. Helios enhances the preferential differentiation of human fetal CD4+ naïve T cells into regulatory T cells. Sci Immunol. 2019;4(41):1–19.

556. Bronevetsky Y, Burt TD, McCune JM. Lin28b Regulates Fetal Regulatory T Cell Differentiation through Modulation of TGF-β Signaling. J Immunol. 2016;197(11):4344–50.

557. Amado IF, Berges J, Luther RJ, Mailhé MP, Garcia S, Bandeira A, et al. IL-2 coordinates IL-2-producing and regulatory T cell interplay. J Exp Med. 2013;210(12):2707–20.

558. Almeidal ARM, Amado IF, Reynolds J, Berges J, Lythe G, Molina-París C, et al. Quorum-sensing in CD4+ T cell homeostasis: A hypothesis and a model. Front Immunol. 2012;3:1–15.

559. Aguilera-Sandoval CR, Yang OO, Jojic N, Lovato P, Chen DY, Boechat MI, et al. Supranormal thymic output up to 2 decades after HIV-1 infection. Aids. 2016;30(5):701–11.

560. Luo M, Xu L, Qian Z, Sun X. Infection-Associated Thymic Atrophy. Front Immunol. 2021;12:1–21.

561. Rosichini M, Bordoni V, Silvestris DA, Mariotti D, Matusali G, Cardinale A, et al. SARS-CoV-2 infection of thymus induces loss of function that correlates with disease severity. J Allergy Clin Immunol. 2023;151(4):911–21.

562. Gul KA, Sonerud T, Fjærli HO, Nakstad B, Abrahamsen TG, Inchley CS. Thymus activity measured by T-cell receptor excision circles in patients with different severities of respiratory syncytial virus infection. BMC Infect Dis [Internet]. 2017;17(1):1–8. Available from: http://dx.doi.org/10.1186/s12879-016-2148-0

563. Sananez I, Raiden S, Erra-Díaz F, De Lillo L, Holgado MP, Geffner J, et al. Dampening of IL-2 Function in Infants with Severe Respiratory Syncytial Virus Disease. J Infect Dis. 2018;218(1):75–83.

564. Sage PT, Sharpe AH. T follicular regulatory cells. Immunol Rev. 2016;271(1):246–59.

565. Wing JB, Kitagawa Y, Locci M, Hume H, Tay C, Morita T, et al. A distinct subpopulation of CD25− T-follicular regulatory cells localizes in the germinal centers. Proc Natl Acad Sci U S A. 2017;114(31):E6400–9.

566. Botta D, Fuller MJ, Marquez-Lago TT, Bachus H, Bradley JE, Weinmann AS, et al. Dynamic regulation of T follicular regulatory cell responses by interleukin 2 during influenza infection. Nat Immunol. 2017;18(11):1249–60.

567. Wu H, Xu L-L, Teuscher P, Liu H, Kaplan MH, Dent AL. An Inhibitory Role for the Transcription Factor Stat3 in Controlling IL-4 and Bcl6 Expression in Follicular Helper T Cells. J Immunol. 2015;195(5):2080–9.

568. Habibi MS, Jozwik A, Makris S, Dunning J, Paras A, DeVincenzo JP, et al. Impaired antibody-mediated protection and defective iga b-cell memory in experimental infection of adults with respiratory syncytial virus. Am J Respir Crit Care Med. 2015;191(9):1040–9.

569. Duong TE, Wu Y, Sos BC, Dong W, Limaye S, Rivier LH, et al. A single-cell regulatory map of postnatal lung alveologenesis in humans and mice. Cell Genomics [Internet]. 2022;2(3):100108. Available from: https://doi.org/10.1016/j.xgen.2022.100108

570. Adkins B, Leclerc C, Marshall-Clarke S. Neonatal adaptive immunity comes of age. Nat Rev Immunol. 2004;4(7):553–64.

571. Simon AK, Hollander GA, McMichael A. Evolution of the immune system in humans from infancy to old age. Proc R Soc B Biol Sci. 2015;282(1821).

572. Chan JA, Loughland JR, de la Parte L, Okano S, Ssewanyana I, Nalubega M, et al. Age-dependent changes in circulating Tfh cells influence development of functional malaria antibodies in children. Nat Commun. 2022;13(1):1–15.

573. Vono M, Eberhardt CS, Mohr E, Auderset F, Christensen D, Schmolke M, et al. Overcoming the neonatal limitations of inducing germinal centers through liposome-based adjuvants including C-type lectin agonists trehalose dibehenate or Curdlan. Front Immunol. 2018;9(FEB):1–12.

574. Natalini JG, Singh S, Segal LN. The dynamic lung microbiome in health and disease. Nat Rev Microbiol. 2023;21(4):222–35.

575. Yagi K, Asai N, Huffnagle GB, Lukacs NW, Fonseca W. Early-Life Lung and Gut Microbiota Development and Respiratory Syncytial Virus Infection. Front Immunol. 2022;13.

576. Pattaroni C, Watzenboeck ML, Schneidegger S, Kieser S, Wong NC, Bernasconi E, et al. Early-Life Formation of the Microbial and Immunological Environment of the Human Airways. Cell Host Microbe. 2018;24(6):857-865.e4.

577. Enaud R, Prevel R, Ciarlo E, Beaufils F, Wieërs G, Guery B, et al. The Gut-Lung Axis in Health and Respiratory Diseases: A Place for Inter-Organ and Inter-Kingdom Crosstalks. Front Cell Infect Microbiol. 2020;10(February):1–11.

578. Bisgaard H, Hermansen MN, Buchvald F, Loland L, Halkjaer LB, Bonnelykke K, et al. Childhood asthma after bacterial colonization of the airway in neonates. N Engl J Med. 2007;357:1487–95.

579. Tang HHF, Lang A, Teo SM, Judd LM, Gangnon R, Evans MD, et al. Developmental patterns in the nasopharyngeal microbiome during infancy are associated with asthma risk. J Allergy Clin Immunol [Internet]. 2021;147(5):1683–91. Available from: https://doi.org/10.1016/j.jaci.2020.10.009

580. Razi CH, Harmanc K, Abac A, Özdemir O, Hizli S, Renda R, et al. The immunostimulant OM-85 BV prevents wheezing attacks in preschool children. J Allergy Clin Immunol. 2010;126(4):763–9.

581. Esposito S, Cassano M, Cutrera R, Menzella F, Varricchio A, Uberti M. Expert consensus on the role of OM-85 in the management of recurrent respiratory infections: A Delphi study. Hum Vaccines Immunother [Internet]. 2022;18(6). Available from: https://doi.org/10.1080/21645515.2022.2106720

582. Cao C, Wang J, Li Y, Li Y, Ma L, Abdelrahim MEA, et al. Efficacy and safety of OM-85 in paediatric recurrent respiratory tract infections which could have a possible protective effect on COVID-19 pandemic: A meta-analysis. Int J Clin Pract. 2021;75(5):1–8.

583. Troy NM, Strickland D, Serralha M, de Jong E, Jones AC, Read J, et al. Protection against severe infant lower respiratory tract infections by immune training: Mechanistic studies. J Allergy Clin Immunol [Internet]. 2022;150(1):93–103. Available from: https://doi.org/10.1016/j.jaci.2022.01.001

584. Sly PD, Galbraith S, Islam Z, Holt B, Troy N, Holt PG. Primary prevention of severe lower respiratory illnesses in at-risk infants using the immunomodulator OM-85. J Allergy Clin Immunol. 2019;144(3):870-872.e11.

585. Esposito S, Ballarini S, Argentiero A, Ruggiero L, Rossi GA, Principi N. Microbiota profiles in pre-school children with respiratory infections: Modifications induced by the oral bacterial lysate OM-85. Front Cell Infect Microbiol. 2022;12(August):1–17.

586. Stein MM, Hrusch CL, Gozdz J, Igartua C, Pivniouk V, Murray SE, et al. Innate immunity and asthma risk in amish and hutterite farm children. N Engl J Med. 2016;375(5):411–21.

587. Ege, M. J., Mayer, M., Normand, A. C., Genuneit, J., Cookson, W. O., Braun- Fahrländer, C., Heederik, D., Piarroux, R., & von Mutius E. Exposure to Environmental Microorganisms and Childhood Asthma. N Engl J Med. 2011;364(8):701–9.

588. Müller-Rompa SEK, Markevych I, Hose AJ, Loss G, Wouters IM, Genuneit J, et al. An approach to the asthma-protective farm effect by geocoding: Good farms and better farms. Pediatr Allergy Immunol. 2018;29(3):275–82.

589. Kirjavainen P V., Karvonen AM, Adams RI, Täubel M, Roponen M, Tuoresmäki P, et al. Farm-like indoor microbiota in non-farm homes protects children from asthma development. Nat Med. 2019;25(7):1089–95.

590. Rathinavelu S, Zavros Y, Merchant JL. Acinetobacter lwoffii infection and gastritis. Microbes Infect. 2003;5(7):651–7.

591. Ruokolainen L, Paalanen L, Karkman A, Laatikainen T, von Hertzen L, Vlasoff T, et al. Significant disparities in allergy prevalence and microbiota between the young people in Finnish and Russian Karelia. Clin Exp Allergy. 2017;47(5):665–74.

592. Conrad ML, Ferstl R, Teich R, Brand S, Blümer N, Yildirim AÖ, et al. Maternal TLR signaling is required for prenatal asthma protection by the nonpathogenic microbe Acinetobacter lwoffii F78. J Exp Med. 2009;206(13):2869–77.

593. Debarry J, Hanuszkiewicz A, Stein K, Holst O, Heine H. The allergy-protective properties of Acinetobacter lwoffii F78 are imparted by its lipopolysaccharide. Allergy Eur J Allergy Clin Immunol. 2010;65(6):690–7.

594. Alashkar Alhamwe B, Gao Z, Alhamdan F, Harb H, Pichene M, Garnier A, et al. Intranasal administration of Acinetobacter lwoffii in a murine model of asthma induces IL-6-mediated protection associated with cecal microbiota changes. Vol. 78, Allergy: European Journal of Allergy and Clinical Immunology. 2023. p. 1245–57.

595. Tian K, Dangarh P, Zhang H, Hines CL, Bush A, Pybus HJ, et al. Role of epithelial barrier function in inducing type 2 immunity following early-life viral infection. Clin Exp Allergy. 2024;54(2):109–19.

596. Hara S, Sasaki T, Satoh-Takayama N, Kanaya T, Kato T, Takikawa Y, et al. Dietary Antigens Induce Germinal Center Responses in Peyer's Patches and Antigen-Specific IgA Production. Front Immunol. 2019;10.

597. Bossie A, Vitetta ES. IFN-γ enhances secretion of IgG2a from IgG2a-committed LPS-stimulated murine B cells: Implications for the role of IFN-γ in class switching. Cell Immunol. 1991;135(1):95–104.

598. Metzger DW, McNutt RM, Collins JT, Buchanan JM, Van Cleave VH, Dunnick WA. Interleukin-12 acts as an adjuvant for humoral immunity through interferon-γ-dependent and -independent mechanisms. Eur J Immunol. 1997;27(8):1958–65.

599. Schopf LR, Filutowicz H, Bi XJ, Mansfield JM. Interleukin-4-dependent immunoglobulin G1 isotype switch in the presence of a polarized antigen-specific Th1-cell response to the trypanosome variant surface glycoprotein. Infect Immun. 1998;66(2):451–61.

600. Klasse PJ. How to assess the binding strength of antibodies elicited by vaccination against HIV and other viruses. Expert Rev Vaccines [Internet]. 2016;15(3):295–311. Available from: http://dx.doi.org/10.1586/14760584.2016.1128831

601. Renz H, Adkins BD, Bartfeld S, Blumberg RS, Farber DL, Garssen J, et al. The neonatal window of opportunity—early priming for life. J Allergy Clin Immunol [Internet]. 2018;141(4):1212–4. Available from: https://doi.org/10.1016/j.jaci.2017.11.019

602. Clemens EA, Holbrook BC, McNeilly B, Kanekiyo M, Graham BS, Alexander-Miller MA. TLR agonists induce sustained IgG to hemagglutinin stem and modulate T cells following newborn vaccination. npj Vaccines. 2022;7(1):1–13.

603. Holbrook BC, Kim JR, Blevins LK, Jorgensen MJ, Kock ND, D'Agostino RB, et al. A Novel R848-Conjugated Inactivated Influenza Virus Vaccine Is Efficacious and Safe in a Neonate Nonhuman Primate Model. J Immunol. 2016;197(2):555–64.

604. Tian K. Viral-induced type 2 immunity and immune regulation by farmyard microbes in early life. 2023.

605. Fahey LM, Wilson EB, Elsaesser H, Fistonich CD, McGavern DB, Brooks DG. Viral persistence redirects CD4 T cell differentiation toward T follicular helper cells. J Exp Med. 2011;208(5):987–99.

606. Ma X, Sun Z, Zhai P, Yu W, Wang T, Li F, et al. Effect of follicular helper T cells on the pathogenesis of asthma. Exp Ther Med. 2017;14(2):967–72.

607. Zhang YN, Song J, Wang H, Wang H, Zeng M, Zhai GT, et al. Nasal IL-4+CXCR5+CD4+ T follicular helper cell counts correlate with local IgE production in eosinophilic nasal polyps. J Allergy Clin Immunol [Internet]. 2016;137(2):462–73. Available from: http://dx.doi.org/10.1016/j.jaci.2015.07.025

608. Chu Y, Wang F, Zhou M, Chen L, Lu Y. A preliminary study on the characterization of follicular helper T (Tfh) cells in rheumatoid arthritis synovium. Acta Histochem [Internet]. 2014;116(3):539–43. Available from: http://dx.doi.org/10.1016/j.acthis.2013.10.009

609. Jia Y, Zeng Z, Li Y, Li Z, Jin L, Zhang Z, et al. Impaired function of CD4+ T follicular helper (Tfh) cells associated with hepatocellular carcinoma progression. PLoS One. 2015;10(2):1–15.

610. Tripodo C, Petta S, Guarnotta C, Pipitone R, Cabibi D, Colombo MP, et al. Liver follicular helper T-cells predict the achievement of virological response following interferon-based treatment in HCV-infected patients. Antivir Ther. 2012;17(1):111–8.

611. Lindqvist M, Van Lunzen J, Soghoian DZ, Kuhl BD, Ranasinghe S, Kranias G, et al. Expansion of HIV-specific T follicular helper cells in chronic HIV infection. J Clin Invest. 2012;122(9):3271–80.

612. Naessens T, Morias Y, Hamrud E, Gehrmann U, Budida R, Mattsson J, et al. Human lung conventional dendritic

cells orchestrate lymphoid Neogenesis during chronic obstructive pulmonary disease. Am J Respir Crit Care Med. 2020;202(4):535–48.

613. Gong, Fang; Qian, Chunyan; Zhu, HuaYan; Zhu, Jie; Pan, Yuhong; Dong, QiaoJing; Jiang D. Circulating follicular T-helper cell subset distribution in patients with asthma. Allergy Asthma Proc. 2016;37(6).

614. Yao Y, Chen CL, Wang N, Wang ZC, Ma J, Zhu RF, et al. Correlation of allergen-specific T follicular helper cell counts with specific IgE levels and efficacy of allergen immunotherapy. J Allergy Clin Immunol. 2018;142(1):321–4.

615. Lüthje K, Kallies A, Shimohakamada Y, Belz GT, Light A, Tarlinton DM, et al. The development and fate of follicular helper T cells defined by an IL-21 reporter mouse. Nat Immunol. 2012;13(5):491–8.

616. Ise W, Inoue T, McLachlan JB, Kometani K, Kubo M, Okada T, et al. Memory B cells contribute to rapid Bcl6 expression by memory follicular helper T cells. Proc Natl Acad Sci U S A. 2014;111(32):11792–7.

617. Ochola R, Sande C, Fegan G, Scott PD, Medley GF, Cane PA, et al. The level and duration of RSV-specific maternal IgG in infants in kilifi Kenya. PLoS One. 2009;4(12):4–9.

618. Piedra PA, Jewell AM, Cron SG, Atmar RL, Paul Glezen W. Correlates of immunity to respiratory syncytial virus (RSV) associated-hospitalization: Establishment of minimum protective threshold levels of serum neutralizing antibodies. Vaccine. 2003;21(24):3479–82.

619. Boyoglu-Barnum S, Chirkova T, Todd SO, Barnum TR, Gaston KA, Jorquera P, et al. Prophylaxis with a Respiratory Syncytial Virus (RSV) Anti-G Protein Monoclonal Antibody Shifts the Adaptive Immune Response to RSV rA2-line19F Infection from Th2 to Th1 in BALB/c Mice. J Virol. 2014;88(18):10569–83.

620. Lee SK, Rigby RJ, Zotos D, Tsai LM, Kawamoto S, Marshall JL, et al. B cell priming for extrafollicular antibody responses requires Bcl-6 expression by T cells. J Exp Med. 2011;208(7):1377–88.

621. Toyama H, Okada S, Hatano M, Takahashi Y, Takeda N, Ichii H, et al. Memory B cells without somatic hypermutation are generated from Bcl6-deficient B cells. Immunity. 2002;17(3):329–39.

622. Elsner RA, Hastey CJ, Olsen KJ, Baumgarth N. Suppression of Long-Lived Humoral Immunity Following Borrelia burgdorferi Infection. PLoS Pathog. 2015;11(7).

623. Männe C, Takaya A, Yamasaki Y, Mursell M, Hojyo S, Wu TY, et al. Salmonella SiiE prevents an efficient humoral immune memory by interfering with IgG+ plasma cell persistence in the bone marrow. Proc Natl Acad Sci U S A. 2019;116(15):7425–30.

624. Racine R, Jones DD, Chatterjee M, McLaughlin M, MacNamara KC, Winslow GM. Impaired Germinal Center Responses and Suppression of Local IgG Production during Intracellular Bacterial Infection. J Immunol. 2010;184(9):5085–93.

625. Faro J, von Haeften B, Gardner R, Faro E. A sensitivity analysis comparison of three models for the dynamics of germinal centers. Front Immunol. 2019;10(AUG):1–17.

626. Allen CDC, Okada T, Tang HL, Cyster JG. Imaging of germinal center selection events during affinity maturation. Science. 2007;315(5811):528–31.

627. Anderson SM, Khalil A, Uduman M, Hershberg U, Louzoun Y, Haberman AM, et al. Taking Advantage: High-Affinity B Cells in the Germinal Center Have Lower Death Rates, but Similar Rates of Division, Compared to Low-Affinity Cells. J Immunol. 2009;183(11):7314–25.

628. Mayer CT, Gazumyan A, Kara EE, Gitlin AD, Golijanin J, Viant C, et al. The microanatomic segregation of selection by apoptosis in the germinal center. Science. 2017;358(6360).

629. Di Niro R, Lee SJ, Vander Heiden JA, Elsner RA, Trivedi N, Bannock JM, et al. Salmonella Infection Drives Promiscuous B Cell Activation Followed By Extrafollicular Affinity Maturation. Immunity [Internet]. 2015;43(1):120–31. Available from: http://dx.doi.org/10.1016/j.immuni.2015.06.013

630. Cunningham AF, Gaspal F, Serre K, Mohr E, Henderson IR, Scott-Tucker A, et al. Salmonella Induces a Switched Antibody Response without Germinal Centers That Impedes the Extracellular Spread of Infection. J Immunol. 2007;178(10):6200–7.

631. Trivedi N, Weisel F, Smita S, Joachim S, Kader M, Radhakrishnan A, et al. Liver Is a Generative Site for the B Cell Response to Ehrlichia muris. Immunity [Internet]. 2019;51(6):1088-1101.e5. Available from: https://doi.org/10.1016/j.immuni.2019.10.004

632. Ersching J, Efeyan A, Mesin L, Jacobsen JT, Pasqual G, Grabiner BC, et al. Germinal Center Selection and Affinity Maturation Require Dynamic Regulation of mTORC1 Kinase. Immunity [Internet]. 2017;46(6):1045-1058.e6. Available from: http://dx.doi.org/10.1016/j.immuni.2017.06.005

633. Thomas P, Rees-Spear C, Griffith S, Muir L, Touizer E, Andrabi R, et al. High affinity mAb infusion can enhance maximum affinity maturation during HIV Env immunization. iScience [Internet]. 2024;27(4):109495. Available from: https://doi.org/10.1016/j.isci.2024.109495

634. Moriyama S, Adachi Y, Sato T, Tonouchi K, Sun L, Fukushi S, et al. Temporal maturation of neutralizing antibodies in COVID-19 convalescent individuals improves potency and breadth to circulating SARS-CoV-2 variants. Immunity [Internet]. 2021;54(8):1841–52. Available from: https://doi.org/10.1016/j.immuni.2021.06.015

635. Weltzin R, Hsu SA, Mittler ES, Georgakopoulos K, Monath TP. Intranasal monoclonal immunoglobulin A against respiratory syncytial virus protects against upper and lower respiratory tract infections in mice. Antimicrob Agents Chemother. 1994;38(12):2785–91.

636. Weltzin R, Traina-Dorge V, Soike K, Zhang JY, Mack P, Soman G, et al. Intranasal monoclonal IgA antibody to respiratory syncytial virus protects rhesus monkeys against upper and lower respiratory tract infection. J Infect Dis. 1996;174(2):256–61.

637. Kunkel EJ, Butcher EC. Plasma-cell homing. Nat Rev Immunol. 2003;3(10):822–9.

638. Polosukhin V V., Richmond BW, Du RH, Cates JM, Wu P, Nian H, et al. Secretory IgA deficiency in individual small airways is associated with persistent inflammation and remodeling. Am J Respir Crit Care Med. 2017;195(8):1010–21.

639. Stavnezer J, Kang J. The Surprising Discovery That TGFβ Specifically Induces the IgA Class Switch. J Immunol. 2009;182(1):5–7.

640. Borsutzky; S, Cazac; BB, Roes; J, Guzmán CA. Receptor Signaling Is Critical for Mucosal IgA Responses. J Immunol. 2004;173(5):3305–9.

641. Allie SR, Bradley JE, Mudunuru U, Schultz MD, Graf BA, Lund FE, et al. The establishment of resident memory B cells in the lung requires local antigen encounter. Nat Immunol [Internet]. 2019;20(1):97–108. Available from: http://dx.doi.org/10.1038/s41590-018-0260-6

642. Oh JE, Song E, Moriyama M, Wong P, Zhang S, Jiang R, et al. Intranasal priming induces local lung-resident B cell populations that secrete protective mucosal antiviral IgA. Sci Immunol. 2021;6(66):1–11.

643. Bertrand Y, Sánchez-Montalvo A, Hox V, Froidure A, Pilette C. IgA-producing B cells in lung homeostasis and disease. Front Immunol. 2023;14.

644. Moyron-Quiroz JE, Rangel-Moreno J, Kusser K, Hartson L, Sprague F, Goodrich S, et al. Role of inducible bronchus associated lymphoid tissue (iBALT) in respiratory immunity. Nat Med. 2004;10(9):927–34.

645. Geurtsvankessel CH, Willart MAM, Bergen IM, Van Rijt LS, Muskens F, Elewaut D, et al. Dendritic cells are crucial for maintenance of tertiary lymphoid structures in the lung of influenza virus-infected mice. J Exp Med. 2009;206(11):2339–49.

646. Neyt K, GeurtsvanKessel CH, Deswarte K, Hammad H, Lambrecht BN. Early IL-1 signaling promotes iBALT induction after influenza virus infection. Front Immunol. 2016;7.

647. Van Pottelberge GR, Bracke KR, Van Den Broeck S, Reinartz SM, Van Drunen CM, Wouters EF, et al. Plasmacytoid dendritic cells in pulmonary lymphoid follicles of patients with COPD. Eur Respir J. 2010;36(4):781–91.

648. Elliot JG, Jensen CM, Mutavdzic S, Lamb JP, Carroll NG, James AL. Aggregations of Lymphoid Cells in the Airways of Nonsmokers, Smokers, and Subjects with Asthma. Am J Respir Crit Care Med. 2004;169(6):712–8.

649. Gassen RB, Fazolo T, Nascimento de Freitas D, Borges TJ, Lima K, Antunes GL, et al. IL-21 treatment recovers follicular helper T cells and neutralizing antibody production in respiratory syncytial virus infection. Immunol Cell Biol. 2021;99(3):309–22.

650. Dieu-Nosjean MC, Goc J, Giraldo NA, Sautès-Fridman C, Fridman WH. Tertiary lymphoid structures in cancer and beyond. Trends Immunol. 2014;35(11):571–80.

651. Silva-Cayetano A, Linterman MA. Stromal cell control of conventional and ectopic germinal centre reactions. Curr Opin Immunol [Internet]. 2020;64:26–33. Available from: https://doi.org/10.1016/j.coi.2020.03.007

652. Fagundes CT, Amaral FA, Vieira AT, Soares AC, Pinho V, Nicoli JR, et al. Transient TLR Activation Restores Inflammatory Response and Ability To Control Pulmonary Bacterial Infection in Germfree Mice. J Immunol. 2012;188(3):1411–20.

653. Reikvam DH, Erofeev A, Sandvik A, Grcic V, Jahnsen FL, Gaustad P, et al. Depletion of murine intestinal microbiota: Effects on gut mucosa and epithelial gene expression. PLoS One. 2011;6(3).

654. Grasa L, Abecia L, Forcén R, Castro M, de Jalón JAG, Latorre E, et al. Antibiotic-Induced Depletion of Murine Microbiota Induces Mild Inflammation and Changes in Toll-Like Receptor Patterns and Intestinal Motility. Microb Ecol. 2015;70(3):835–48.

655. Hashiguchi M, Kashiwakura Y, Kojima H, Kobayashi A, Kanno Y, Kobata T. Peyer's patch innate lymphoid cells regulate commensal bacteria expansion. Immunol Lett [Internet]. 2015;165(1). Available from: http://dx.doi.org/10.1016/j.imlet.2015.03.002

656. Alashkar Alhamwe B, Gao Z, Alhamdan F, Harb H, Pichene M, Garnier A, et al. Intranasal administration of Acinetobacter lwoffii in a murine model of asthma induces IL-6-mediated protection associated with cecal microbiota changes. Allergy Eur J Allergy Clin Immunol. 2023;78(5):1245–57.

657. Johansson EL, Bergquist C, Edebo A, Johansson C, Svennerholm AM. Comparison of different routes of vaccination for eliciting antibody responses in the human stomach. Vaccine. 2004;22(8):984–90.

658. Holmgren J, Czerkinsky C. Mucosal immunity and vaccines. Nat Med. 2005;11(4).

659. Riedler J, Braun-Fahrländer C, Eder W, Schreuer M, Waser M, Maisch S, et al. Exposure to farming in early life and development of asthma and allergy: A cross-sectional survey. Lancet. 2001;358(9288):1129–33.

660. Von Ehrenstein OS, Von Mutius E, Illi S, Baumann L, Böhm O, Von Kries R. Reduced risk of hay fever and asthma among children of farmers. Clin Exp Allergy. 2000;30(2):187–93.

661. Douwes J, Travier N, Huang K, Cheng S, McKenzie J, Le Gros G, et al. Lifelong farm exposure may strongly reduce the risk of asthma in adults. Allergy Eur J Allergy Clin Immunol. 2007;62(10):1158–65.

662. Hilligan KL, Ronchese F. Antigen presentation by dendritic cells and their instruction of CD4+ T helper cell responses. Cell Mol Immunol [Internet]. 2020;17(6):587–99. Available from: http://dx.doi.org/10.1038/s41423-020-0465-0

663. Cabeza-Cabrerizo M, Cardoso A, Minutti CM, Pereira Da Costa M, Reis E Sousa C. Dendritic Cells Revisited. Annu Rev Immunol. 2021;39:131–66.

664. Dudziak D, Kampfhorst A, Heidkamp G, Buhcholz V, Trumpfheller C, Yamazaki S, et al. Dendritic Cell Subsets in Vivo. Science. 2007;315:107–12.

665. Ingulli E, Ulman DR, Lucido MM, Jenkins MK. In Situ Analysis Reveals Physical Interactions Between CD11b+ Dendritic Cells and Antigen-Specific CD4 T Cells After Subcutaneous Injection of Antigen. J Immunol. 2002;169(5):2247–52.

666. Schlitzer A, McGovern N, Teo P, Zelante T, Atarashi K, Low D, et al. IRF4 Transcription Factor-Dependent CD11b+ Dendritic Cells in Human and Mouse Control Mucosal IL-17 Cytokine Responses. Immunity [Internet]. 2013;38(5):970–83. Available from: http://dx.doi.org/10.1016/j.immuni.2013.04.011

667. León B, Ballesteros-Tato A, Browning JL, Dunn R, Randall TD, Lund FE. Regulation of T H2 development by CXCR5 + dendritic cells and lymphotoxin-expressing B cells. Nat Immunol. 2012;13(7):681–90.

668. Ferrer IR, Liu D, Pinelli DF, Koehn BH, Stempora LL, Ford ML. CD40/CD154 Blockade Inhibits Dendritic Cell Expression of Inflammatory Cytokines but Not Costimulatory Molecules. J Immunol. 2012;189(9):4387–95.

669. Sato A, Hashiguchi M, Toda E, Iwasaki A, Hachimura S, Kaminogawa S. CD11b+ Peyer's Patch Dendritic Cells Secrete IL-6 and Induce IgA Secretion from Naive B Cells. J Immunol. 2003;171(7):3684–90.

670. Ghosh D, Jiang W, Mukhopadhyay D, Mellins ED. New insights into B cells as antigen presenting cells. Curr Opin Immunol [Internet]. 2021;70:129–37. Available from: https://doi.org/10.1016/j.coi.2021.06.003

671. Gao J, Ma X, Gu W, Fu M, An J, Xing Y, et al. Novel functions of murine B1 cells: Active phagocytic and microbicidal abilities. Eur J Immunol. 2012;42(4):982–92.

672. Garraud O, Borhis G, Badr G, Degrelle S, Pozzetto B, Cognasse F, et al. Revisiting the B-cell compartment in mouse and humans: More than one B-cell subset exists in the marginal zone and beyond. BMC Immunol. 2012;13(63).

673. Hong S, Zhang Z, Liu H, Tian M, Zhu X, Zhang Z, et al. B Cells Are the Dominant Antigen-Presenting Cells that Activate Naive CD4+ T Cells upon Immunization with a Virus-Derived Nanoparticle Antigen. Immunity [Internet]. 2018;49(4):695–708. Available from: https://doi.org/10.1016/j.immuni.2018.08.012

674. Zaretsky I, Atrakchi O, Mazor RD, Stoler-Barak L, Biram A, Feigelson SW, et al. ICAMs support B cell interactions with T follicular helper cells and promote clonal selection. J Exp Med. 2017;214(11):3435–48.

675. Barnett LG, Simkins HMA, Barnett BE, Korn LL, Johnson AL, Wherry EJ, et al. B Cell Antigen Presentation in the Initiation of Follicular Helper T Cell and Germinal Center Differentiation. J Immunol. 2014;192(8):3607–17.

676. Turner JS, Marthi M, Benet ZL, Grigorova I. Transiently antigen-primed B cells return to naive-like state in absence of T-cell help. Nat Commun. 2017;8:1–11.

677. Schwickert TA, Victora GD, Fooksman DR, Kamphorst AO, Mugnier MR, Gitlin AD, et al. A dynamic T cell-limited checkpoint regulates affinity-dependent B cell entry into the germinal center. J Exp Med. 2011;208(6):1243–52.

678. Jiang W, Adler LN, Macmillan H, Mellins ED. Synergy between B cell receptor/antigen uptake and MHCII peptide editing relies on HLA-DO tuning. Sci Rep [Internet]. 2019;9(1):1–17. Available from: http://dx.doi.org/10.1038/s41598-019-50455-y

679. Arkatkar T, Du SW, Jacobs HM, Dam EM, Hou B, Buckner JH, et al. B cell-derived IL-6 initiates spontaneous germinal center formation during systemic autoimmunity. J Exp Med. 2017;214(11):3207–17.

680. Duan T, Du Y, Xing C, Wang HY, Wang RF. Toll-Like Receptor Signaling and Its Role in Cell-Mediated Immunity. Front Immunol. 2022;13.

681. Li D, Wu M. Pattern recognition receptors in health and diseases. Signal Transduct Target Ther [Internet]. 2021;6(1). Available from: http://dx.doi.org/10.1038/s41392-021-00687-0

682. Buchta CM, Bishop GA. Toll-like receptors and B cells: Functions and mechanisms. Immunol Res. 2014;59(1–3):12–22.

683. Mantegazza AR, Zajac AL, Twelvetrees A, Holzbaur ELF, Amigorena S, Marks MS. TLR-dependent phagosome tubulation in dendritic cells promotes phagosome cross-talk to optimize MHC-II antigen presentation. Proc Natl Acad Sci U S A. 2014;111(43):15508–13.

684. Platt CD, Ma JK, Chalouni C, Ebersold M, Bou-Reslan H, Carano RAD, et al. Mature dendritic cells use endocytic receptors to capture and present antigens. Proc Natl Acad Sci U S A. 2010;107(9):4287–92.

685. Kugelberg E. Making mice more human the TLR8 way. Nat Rev Immunol. 2014;14(1).

686. Kayesh MEH, Kohara M, Tsukiyama-Kohara K. TLR agonists as vaccine adjuvants in the prevention of viral infections: an overview. Front Microbiol. 2023;14.

687. Wilson KR, Gressier E, McConville MJ, Bedoui S. Microbial Metabolites in the Maturation and Activation of Dendritic Cells and Their Relevance for Respiratory Immunity. Front Immunol. 2022;13.

688. Nishimura T, Saito Y, Washio K, Komori S, Respatika D, Kotani T, et al. SIRPα on CD11c+ cells induces Th17 cell differentiation and subsequent inflammation in the CNS in experimental autoimmune encephalomyelitis. Eur J Immunol. 2020;50(10):1560–70.

689. Van VQ, Lesage S, Bouguermouh S, Gautier P, Rubio M, Levesque M, et al. Expression of the self-marker CD47 on dendritic cells governs their trafficking to secondary lymphoid organs. EMBO J. 2006;25(23):5560–8.

690. Hagnerud S, Manna PP, Cella M, Frazier WA, Colonna M, Stenberg Å, et al. Deficit of CD47 Results in a Defect of Marginal Zone Dendritic Cells, Blunted Immune Response to Particulate Antigen and Impairment of Skin Dendritic Cell Migration. J Immunol. 2006;176(10):5772–8.

691. Li H, Limenitakis JP, Greiff V, Yilmaz B, Schären O, Urbaniak C, et al. Mucosal or systemic microbiota exposures shape the B cell repertoire. Nature [Internet]. 2020;584(7820):274–8. Available from: http://dx.doi.org/10.1038/s41586-020-2564-6

692. Liu X, Quan N. Immune Cell Isolation from Mouse Femur Bone Marrow. bio-protocol. 2015;5(20).

693. Amend SR, Valkenburg KC, Pienta KJ. Murine hind limb long bone dissection and bone marrow isolation. J Vis Exp. 2016;(110).

694. Naik SH, O'Keeffe M, Proietto A, Hochrein Ken Shortman H, Wu L. CD8+, CD8−, and plasmacytoid dendritic cell generation in vitro using flt3 ligand. Methods Mol Biol [Internet]. 2010;595:167–76. Available from: www.springer.com/series/7651

695. Puttur F, Francozo M, Solmaz G, Bueno C, Lindenberg M, Gohmert M, et al. Conventional Dendritic Cells Confer Protection against Mouse Cytomegalovirus Infection via TLR9 and MyD88 Signaling. Cell Rep. 2016;17(4):1113–27.

696. Estripeaut D, Torres JP, Somers CS, Tagliabue C, Khokhar S, Bhoj VG, et al. Respiratory syncytial virus

persistence in the lungs correlates with airway hyperreactivity in the mouse model. J Infect Dis. 2008;198(10):1435–43.

697. Loveday EK, Hain KS, Kochetkova I, Hedges JF, Robison A, Snyder DT, et al. Effect of inactivation methods on sars-cov-2 virion protein and structure. Viruses. 2021;13(562).

698. Haynes LM, Moore DD, Kurt-Jones EA, Finberg RW, Anderson LJ, Tripp RA. Involvement of Toll-Like Receptor 4 in Innate Immunity to Respiratory Syncytial Virus. J Virol. 2001;75(22):10730–7.

699. Lukacs NW, Smit JJ, Mukherjee S, Morris SB, Nunez G, Lindell DM. Respiratory Virus-Induced TLR7 Activation Controls IL-17–Associated Increased Mucus via IL-23 Regulation. J Immunol. 2010;185(4):2231–9.

700. Ciesielska A, Matyjek M, Kwiatkowska K. TLR4 and CD14 trafficking and its influence on LPS-induced pro-inflammatory signaling. Cell Mol Life Sci [Internet]. 2021;78(4):1233–61. Available from: https://doi.org/10.1007/s00018-020-03656-y

701. Arnold P, Boll I, Rothaug M, Schumacher N, Schmidt F, Wichert R, et al. Meprin metalloproteases generate biologically active soluble interleukin-6 receptor to induce trans-signaling. Sci Rep. 2017;7(March):1–11.

702. Sammel M, Peters F, Lokau J, Scharfenberg F, Werny L, Linder S, et al. Differences in shedding of the interleukin-11 receptor by the proteases ADAM9, ADAM10, ADAM17, meprin α, meprin β and MT1-MMP. Int J Mol Sci. 2019;20(15).

703. Mansurov A, Hosseinchi P, Chang K, Lauterbach AL, Gray LT, Alpar AT, et al. Masking the immunotoxicity of interleukin-12 by fusing it with a domain of its receptor via a tumour-protease-cleavable linker. Nat Biomed Eng. 2022;6(7):819–29.

704. Schulz O, Sewell HF, Shakib F. Proteolytic cleavage of CD25, the alpha subunit of the human T cell interleukin 2 receptor, by Der p 1, a major mite allergen with cysteine protease activity. J Exp Med. 1998;187(2):271–5.

705. Bank U, Reinhold D, Schneemilch C, Kunz D, Synowitz HJ, Ansorge S. Selective proteolytic cleavage of IL-2 receptor and IL-6 receptor ligand binding chains by neutrophil-derived serine proteases at foci of inflammation. J Interf Cytokine Res. 1999;19(11):1277–87.

706. Sheu BC, Hsu SM, Ho HN, Lien HC, Huang SC, Lin RH. A novel role of metalloproteinase in cancer-mediated immunosuppression. Cancer Res. 2001;61(1):237–42.

707. Kirschke S, Ogunsulire I, Selvakumar B, Schumacher N, Sezin T, Rose-John S, et al. The metalloprotease ADAM10 generates soluble interleukin-2 receptor alpha (sCD25) in vivo. J Biol Chem [Internet]. 2022;298(6):101910. Available from: https://doi.org/10.1016/j.jbc.2022.101910

708. Szabo SJ, Kim ST, Costa GL, Zhang X, Fathman CG, Glimcher LH. A novel transcription factor, T-bet, directs Th1 lineage commitment. Cell. 2000;100(6):655–69.

709. Zhu J, Yamane H, Cote-Sierra J, Guo L, Paul WE. GATA-3 promotes Th2 responses through three different mechanisms: Induction of Th2 cytokine production, selective growth of Th2 cells and inhibition of Th1 cell-specific factors. Cell Res. 2006;16(1):3–10.

710. Cannons JL, Lu KT, Schwartzberg PL. T follicular helper cell diversity and plasticity. Trends Immunol [Internet]. 2013;34(5):200–7. Available from: http://dx.doi.org/10.1016/j.it.2013.01.001

711. Ma X, Nakayamada S, Wang J. Multi-Source Pathways of T Follicular Helper Cell Differentiation. Front Immunol. 2021;12.

712. Gorelik L, Kauth M, Gehlhar K, Bufe A, Holst O, Peters M. Modulation of dendritic cell function by cowshed dust extract. Innate Immun. 2008;14(6):345–55.

713. Bartz H, Türkel Ö, Hoffjan S, Rothoeft T, Gonschorek A, Schauer U. Respiratory syncytial virus decreases the capacity of myeloid dendritic cells to induce interferon-γ in naïve T cells. Immunology. 2003;109(1):49–57.

714. Jones A, Morton I, Hobson L, Evans GS, Everard ML. Differentiation and immune function of human dendritic cells following infection by respiratory syncytial virus. Clin Exp Immunol. 2006;143(3):513–22.

715. Rothoeft T, Fischer K, Zawatzki S, Schulz V, Schauer U, Körner Rettberg C. Differential response of human naive and memory/effector T cells to dendritic cells infected by respiratory syncytial virus. Clin Exp Immunol. 2007;150(2):263–73.

716. Nickle RA, DeOca KB, Garcia BL, Mannie MD. Soluble CD25 imposes a low-zone IL-2 signaling environment that favors competitive outgrowth of antigen-experienced CD25high regulatory and memory T cells. Cell Immunol [Internet]. 2023;384. Available from: https://doi.org/10.1016/j.cellimm.2023.104664

717. Maier LM, Anderson DE, Severson CA, Baecher-allan C, Healy B, Liu D V, et al. Soluble IL-2RA Levels in Multiple Sclerosis Subjects and the Effect of Soluble IL-2RA on Immune Responses. J Immunol. 2009;182(3):1542–7.

718. Russell SE, Moore AC, Fallon PG, Walsh PT. Soluble IL-2Rα (sCD25) Exacerbates Autoimmunity and Enhances the Development of Th17 Responses in Mice. PLoS One. 2012;7(10).

719. Popov A, Driesen J, Abdullah Z, Wickenhauser C, Beyer M, Debey-Pascher S, et al. Infection of Myeloid Dendritic Cells with Listeria monocytogenes Leads to the Suppression of T Cell Function by Multiple Inhibitory Mechanisms . J Immunol. 2008;181(7):4976–88.

720. Rubinstein MP, Kovar M, Purton JF, Cho JH, Boyman O, Surh CD, et al. Converting IL-15 to a superagonist by binding to soluble IL-15Rα. Proc Natl Acad Sci U S A. 2006;103(24):9166–71.

721. Harker JA, Wong KA, Dolgoter A, Zuniga EI. Cell-Intrinsic gp130 Signaling on CD4 + T Cells Shapes Long-Lasting Antiviral Immunity. J Immunol. 2015;195(3):1071–81.

722. Rubin LA, Kurman CC, Fritz ME, Biddison WE, Boutin B, Yarchoan R, et al. Soluble interleukin 2 receptors are released from activated human lymphoid cells in vitro. J Immunol [Internet]. 1985 Nov 1;135(5):3172–7. Available from: https://doi.org/10.4049/jimmunol.135.5.3172

723. Allen CDC, Ansel KM, Low C, Lesley R, Tamamura H, Fujii N, et al. Germinal center dark and light zone organization is mediated by CXCR4 and CXCR5. Nat Immunol. 2004;5(9):943–52.

724. Hauser AE, Debes GF, Arce S, Cassese G, Hamann A, Radbruch A, et al. Chemotactic Responsiveness Toward

Ligands for CXCR3 and CXCR4 Is Regulated on Plasma Blasts During the Time Course of a Memory Immune Response. J Immunol. 2002;169(3):1277–82.

725. Ansel KM, VuN.Ngo, Hyman PL, Luther SA, FoÈrster R, Sedgwick JD, et al. A chemokine-driven positive feedback loop organizes lymphoid follicles. Nature [Internet]. 2000;406(6793):309–14. Available from: http://ovidsp.ovid.com/ovidweb.cgi?T=JS&PAGE=reference&D=emed5&NEWS=N&AN=2000274660

726. Qin L, Qiu KZ, Hu CP, Wu GJ, Wang LL, Tan YR. Bronchial Epithelial Cells Promote the Differentiation of Th2 Lymphocytes in Airway Microenvironment through Jagged/Notch-1 Signaling after RSV Infection. Int Arch Allergy Immunol. 2019;179(1):43–52.

727. Lee HC, Headley MB, Loo YM, Berlin A, Gale M, Debley JS, et al. Thymic stromal lymphopoietin is induced by respiratory syncytial virus-infected airway epithelial cells and promotes a type 2 response to infection. J Allergy Clin Immunol [Internet]. 2012;130(5):1187–96. Available from: http://dx.doi.org/10.1016/j.jaci.2012.07.031

728. Fischer JE, Johnson JE, Kuli-Zade RK, Johnson TR, Aung S, Parker RA, et al. Overexpression of interleukin-4 delays virus clearance in mice infected with respiratory syncytial virus. J Virol. 1997;71(11):8672–7.

729. Moore ML, Newcomb DC, Parekh V V., Van Kaer L, Collins RD, Zhou W, et al. STAT1 Negatively Regulates Lung Basophil IL-4 Expression Induced by Respiratory Syncytial Virus Infection. J Immunol. 2009;183(3):2016–26.

730. Eichinger KM, Kosanovich JL, Gidwani S V., Zomback A, Lipp MA, Perkins TN, et al. Prefusion RSV F Immunization Elicits Th2-Mediated Lung Pathology in Mice When Formulated With a Th2 (but Not a Th1/Th2-Balanced) Adjuvant Despite Complete Viral Protection. Front Immunol. 2020;11(July):1–16.

731. Tekkanat KK, Maassab H, Berlin AA, Lincoln PM, Evanoff HL, Kaplan MH, et al. Role of interleukin-12 and Stat-4 in the regulation of airway inflammation and hyperreactivity in respiratory syncytial virus infection. Am J Pathol [Internet]. 2001;159(2):631–8. Available from: http://dx.doi.org/10.1016/S0002-9440(10)61734-8

732. Yamaguchi Y, Harker JA, Wang B, Openshaw PJ, Tregoning JS, Culley FJ. Preexposure to CpG Protects against the Delayed Effects of Neonatal Respiratory Syncytial Virus Infection. J Virol. 2012;86(19):10456–61.

733. Bachus H, Kaur K, Papillion AM, Marquez-Lago TT, Yu Z, Ballesteros-Tato A, et al. Impaired Tumor-Necrosis-Factor-α-driven Dendritic Cell Activation Limits Lipopolysaccharide-Induced Protection from Allergic Inflammation in Infants. Immunity. 2019;50(1):225–40.

734. Hill DL, Pierson W, Bolland DJ, Mkindi C, Carr EJ, Wang J, et al. The adjuvant GLA-SE promotes human Tfh cell expansion and emergence of public TCRβ clonotypes. J Exp Med. 2019;216(8):1857–73.

735. Desbien AL, Dubois Cauwelaert N, Reed SJ, Bailor HR, Liang H, Carter D, et al. IL-18 and Subcapsular Lymph Node Macrophages are Essential for Enhanced B Cell Responses with TLR4 Agonist Adjuvants. J Immunol. 2016;197(11):4351–9.

736. Radtke AJ, Anderson CF, Riteau N, Rausch K, Scaria P, Kelnhofer ER, et al. Adjuvant and carrier protein-dependent T-cell priming promotes a robust antibody response against the Plasmodium falciparum Pfs25 vaccine candidate. Sci Rep [Internet]. 2017;7:1–12. Available from: http://dx.doi.org/10.1038/srep40312

737. Chen C, Zhang C, Li R, Wang Z, Yuan Y, Li H, et al. Monophosphoryl-Lipid A (MPLA) is an efficacious adjuvant for inactivated rabies vaccines. Viruses. 2019;11(12).

738. Lu L, Fong CHY, Zhang AJ, Wu WL, Li IC, Lee ACY, et al. Repurposing of miltefosine as an adjuvant for influenza vaccine. Vaccines. 2020;8(4).

739. Krishnaswamy JK, Gowthaman U, Zhang B, Mattsson J, Szeponik L, Liu D, et al. Migratory CD11b+ conventional dendritic cells induce T follicular helper cell–dependent antibody responses. Sci Immunol. 2017;2(18):1–13.

740. Shin C, Han JA, Koh H, Choi B, Cho Y, Jeong H, et al. CD8α- Dendritic Cells Induce Antigen-Specific T Follicular Helper Cells Generating Efficient Humoral Immune Responses. Cell Rep [Internet]. 2015;11(12):1929–40. Available from: http://dx.doi.org/10.1016/j.celrep.2015.05.042

741. Yin Q, Luo W, Mallajosyula V, Bo Y, Guo J, Xie J, et al. A TLR7-nanoparticle adjuvant promotes a broad immune response against heterologous strains of influenza and SARS-CoV-2. Nat Mater. 2023;22(3):380–90.

742. Delgado MF, Coviello S, Monsalvo AC, Melendi GA, Hernandez JZ, Batalle JP, et al. Lack of antibody affinity maturation due to poor Toll-like receptor stimulation leads to enhanced respiratory syncytial virus disease. Nat Med. 2009;15(1):34–41.

743. Patterson EI, Prince T, Anderson ER, Casas-Sanchez A, Smith SL, Cansado-Utrilla C, et al. Methods of Inactivation of SARS-CoV-2 for Downstream Biological Assays. J Infect Dis. 2020;222(9):1462–7.

744. Graaff PMA De, Jong EC De, Capel TM Van, Dijk MEA Van, Roholl PJM, Boes J, et al. Respiratory Syncytial Virus Infection of Monocyte-Derived Dendritic Cells Decreases their Capacity to Activate CD4 T cells. J Immunol. 2005;175(9):5904–11.

745. González PA, Prado CE, Leiva ED, Carreño LJ, Bueno SM, Riedel CA, et al. Respiratory syncytial virus impairs T cell activation by preventing synapse assembly with dendritic cells. Proc Natl Acad Sci U S A. 2008;105(39):14999–5004.

746. Kurkjian CJ, Guo H, Montgomery ND, Cheng N, Yuan H, Merrill JR, et al. The Toll–Like Receptor 2/6 Agonist, FSL–1 Lipopeptide, Therapeutically Mitigates Acute Radiation Syndrome. Sci Rep. 2017;7(1).

747. Marr N, Turvey SE. Role of human TLR4 in respiratory syncytial virus-induced NF-κB activation, viral entry and replication. Innate Immun. 2012;18(6):856–65.

748. Velten FW, Rambow F, Metharom P, Goerdt S. Enhanced T-cell activation and T-cell-dependent IL-2 production by CD83+, CD25high, CD43high human monocyte-derived dendritic cells. Mol Immunol. 2007;44(7):1544–50.

749. Pinto RA, Arredondo SM, Bono MR, Gaggero AA, Díaz P V. T helper 1/T helper 2 cytokine imbalance in respiratory syncytial virus infection is associated with increased endogenous plasma cortisol. Pediatrics. 2006;117(5).

750. Vono M, Mastelic-Gavillet B, Mohr E, Östensson M, Persson J, Olafsdottir TA, et al. C-type lectin receptor agonists elicit functional IL21-expressing Tfh cells and induce primary B cell responses in neonates. Front Immunol. 2023;31(14).

751. Garg G, Muschaweckh A, Moreno H, Vasanthakumar A, Floess S, Lepennetier G, et al. Blimp1 Prevents Methylation of Foxp3 and Loss of Regulatory T Cell Identity at Sites of Inflammation. Cell Rep [Internet]. 2019;26(7):1854-1868.e5. Available from: https://doi.org/10.1016/j.celrep.2019.01.070

752. Walker SR, Nelson EA, Yeh JE, Pinello L, Yuan G-C, Frank DA. STAT5 Outcompetes STAT3 To Regulate the Expression of the Oncogenic Transcriptional Modulator BCL6. Mol Cell Biol. 2013;33(15):2879–90.

753. Cimmino L, Martins GA, Liao J, Grunig G, Perez RK, Calame L, et al. Blimp-1 Attenuates Th1 Differentiation by Repression of ifng, tbx21, and bcl6 Gene Expression. J Immunol. 2008;181(4):2338–47.

754. Mellery J, Nicholls PJ. Possible mechanism for the alpha subunit of the interleukin-2 receptor (CD25) to influence interleukin-2 receptor signal transduction. Immunol Cell Biol. 2002;80(4):351–7.

755. Holbrook BC, Alexander-Miller MA. Higher Frequency and Increased Expression of Molecules Associated with Suppression on T Regulatory Cells from Newborn Compared with Adult Nonhuman Primates. J Immunol. 2020;205(8):2128–36.

756. Lindqvist CA, Christiansson LH, Simonsson B, Enblad G, Olsson-Strömberg U, Loskog ASI. T regulatory cells control T-cell proliferation partly by the release of soluble CD25 in patients with B-cell malignancies. Immunology. 2010;131(3):371–6.

757. Toossi Z, Sedor JR, Lapurga JP, Ondash RJ, Ellner JJ. Expression of functional interleukin 2 receptors by peripheral blood monocytes from patients with active pulmonary tuberculosis. J Clin Invest. 1990;85(6):1777–84.

758. Barral-Netto M, Barral A, Santos SB, Carvalho EM, Badaro R, Rocha H, Reed SG JWJ. Soluble IL-2 receptor as an agent of serum-mediated suppression in human visceral leishmaniasis. J Immunol. 1991;147(1):281–4.

759. Makis AC, Galanakis E, Hatzimichael EC, Papadopoulou ZL, Siamopoulou A, Bourantas KL. Serum levels of soluble interleukin-2 receptor alpha (sIL-2Rα) as a predictor of outcome in brucellosis. J Infect. 2005;51(3):206–10.

760. Zhang Y, Wang X, Li X, Xi D, Mao R, Wu X, et al. Potential contribution of increased soluble IL-2R to lymphopenia in COVID-19 patients. Cell Mol Immunol. 2020;17(8):878–80.

761. Ma A, Zhang L, Ye X, Chen J, Yu J, Zhuang L, et al. High Levels of Circulating IL-8 and Soluble IL-2R Are Associated With Prolonged Illness in Patients With Severe COVID-19. Front Immunol. 2021;12.

762. Sheibani K, Winberg CD, van De Velde S, Blayney DW, Rappaport H. Distribution of lymphocytes with interleukin-2 receptors (TAC antigens) in reactive lymphoproliferative processes, Hodgkin's disease, and non-Hodgkin's lymphomas: An immunohistologic study of 300 cases. Am J Pathol. 1987;127(1):27–37.

763. Janik JE, Morris JC, Pittaluga S, McDonald K, Raffeld M, Jaffe ES, et al. Elevated serum-soluble interleukin-2 receptor levels in patients with anaplastic large cell lymphoma. Blood. 2004;104(10):3355–7.

764. Fernández J, Roine I, Vasquez A, Cáneo M. Soluble interleukin-2 receptor (sCD25) and interleukin-10 plasma concentrations are associated with severity of primary respiratory syncytial virus (RSV) infection. Eur Cytokine

Netw. 2005;16(1).

765. Qin Q, Luo D, Shi Y, Zhao Q, Chen Y, Wu J, et al. CD25 siRNA induces Treg/Th1 cytokine expression in rat corneal transplantation models. Exp Eye Res [Internet]. 2016;151:134–41. Available from: http://dx.doi.org/10.1016/j.exer.2016.08.010

766. Long F, Bhatti MR, Kellenberger A, Sun W, Modica S, Höring M, et al. A low-carbohydrate diet induces hepatic insulin resistance and metabolic associated fatty liver disease in mice. Mol Metab [Internet]. 2023;69(January):101675. Available from: https://doi.org/10.1016/j.molmet.2023.101675

767. Schmidt ME, Varga SM. Identification of Novel Respiratory Syncytial Virus CD4+ and CD8+ T Cell Epitopes in C57BL/6 Mice. ImmunoHorizons. 2019;3(1):1–12.

768. Thompson WW, Shay DK, Weintraub E, Cox N, Anderson LJ, Fukuda K. Mortality associated with influenza and respiratory syncytial virus in the United States. J Am Med Assoc. 2003;289(2):179–86.

769. Duncan CB, Walsh EE, Peterson DR, Lee FEH, Falsey AR. Risk factors for respiratory failure associated with respiratory syncytial virus infection in adults. J Infect Dis. 2009;200(8):1242–6.

770. Lee N, Chan MCW, Lui GCY, Li R, Wong RYK, Yung IMH, et al. High viral load and respiratory failure in adults hospitalized for respiratory syncytial virus infections. J Infect Dis. 2015;212(8):1237–40.

771. Shaw AC, Goldstein DR, Montgomery RR. Age-dependent dysregulation of innate immunity. Nat Rev Immunol. 2013;13(12):875–87.

772. Pillai PS, Molony RD, Martinod K, Dong H, Pang IK, Tal MC, et al. Mx1 reveals innate pathways to antiviral resistance and lethal influenza disease. Am Assoc Adv Sci. 2016;352(6284).

773. Kasler H, Verdin E. How inflammaging diminishes adaptive immunity. Nat aging [Internet]. 2021;1:24–5. Available from: http://dx.doi.org/10.1038/s43587-020-00021-3

774. De Bree GJ, Heidema J, Van Leeuwen EMM, Van Bleek GM, Jonkers RE, Jansen HM, et al. Respiratory syncytial virus-specific CD8+ memory T cell responses in elderly persons. J Infect Dis. 2005;191(10):1710–8.

775. Cusi MG, Martorelli B, Di Genova G, Terrosi C, Campoccia G, Correale P. Age related changes in T cell mediated immune response and effector memory to Respiratory Syncytial Virus (RSV) in healthy subjects. Immun Ageing. 2010;7:1–8.

776. Cherukuri A, Patton K, Gasser RA, Zuo F, Woo J, Esser MT, et al. Adults 65 years old and older have reduced numbers of functional memory T cells to respiratory syncytial virus fusion protein. Clin Vaccine Immunol. 2013;20(2):239–47.

777. Wong TM, Boyapalle S, Sampayo V, Nguyen HD, Bedi R, Kamath SG, et al. Respiratory Syncytial Virus (RSV) infection in elderly mice results in altered antiviral gene expression and enhanced pathology. PLoS One. 2014;9(2).

778. Fulton RB, Weiss KA, Pewe LL, Harty JT, Varga SM. Aged Mice Exhibit a Severely Diminished CD8 T Cell

Response following Respiratory Syncytial Virus Infection. J Virol. 2013;87(23):12694–700.

779. Falsey AR, Walsh EE. Relationship of serum antibody to risk of respiratory syncytial virus infection in elderly adults. J Infect Dis. 1998;177(2):463–6.

780. Walsh EE, Falsey AR. Age Related Differences in Humoral Immune Response to Respiratory Syncytial Virus Infection in Adults. J Med Virol. 2004;73(2):295–9.

781. Agius G, Dindinaud G, Biggar RJ, Peyre R, Vaillant V, Ranger S, et al. An epidemic of respiratory syncytial virus in elderly people: Clinical and serological findings. J Med Virol. 1990;30(2):117–27.

782. Murata Y, Lightfoote PM, Biear JN, Falsey AR, Walsh EE. Humoral response to the central unglycosylated region of the respiratory syncytial virus attachment protein. Vaccine [Internet]. 2010;28(38):6242–6. Available from: http://dx.doi.org/10.1016/j.vaccine.2010.07.011

783. EE W, DR P, AR F. Risk Factors for Severe Respiratory Syncytial Virus Infection in Hospitalized Children. J Infect Dis. 2004;189(2):233–8.

784. Luchsinger V, Piedra PA, Ruiz M, Zunino E, Martínez MA, MacHado C, et al. Role of neutralizing antibodies in adults with community-acquired pneumonia by respiratory syncytial virus. Clin Infect Dis. 2012;54(7):905–12.

785. Lee J Le, Linterman MA. Mechanisms underpinning poor antibody responses to vaccines in ageing. Immunol Lett [Internet]. 2022;241:1–14. Available from: https://doi.org/10.1016/j.imlet.2021.11.001

786. Silva-Cayetano A, Fra-Bido S, Robert PA, Innocentin S, Burton AR, Watson EM, et al. Spatial dysregulation of T follicular helper cells impairs vaccine responses in aging. Vol. 24, Nature Immunology. Springer US; 2023. 1124–1137 p.

787. Lefebvre JS, Maue AC, Eaton SM, Lanthier PA, Tighe M, Haynes L. The aged microenvironment contributes to the age-related functional defects of CD4 T cells in mice. Aging Cell. 2012;11(5):732–40.

788. Stebegg M, Bignon A, Hill DL, Silva-Cayetano A, Krueger C, Vanderleyden I, et al. Rejuvenating conventional dendritic cells and T follicular helper cell formation after vaccination. Elife. 2020;9.

789. Hill DL, Whyte CE, Innocentin S, Le Lee J, Dooley J, Wang J, et al. Impaired HA-specific T follicular helper cell and antibody responses to influenza vaccination are linked to inflammation in humans. Elife. 2021;10:1–30.

790. Lefebvre JS, Masters AR, Hopkins JW, Haynes L. Age-related impairment of humoral response to influenza is associated with changes in antigen specific T follicular helper cell responses. Sci Rep [Internet]. 2016;6(25051):1–14. Available from: http://dx.doi.org/10.1038/srep25051

791. Denton AE, Dooley J, Cinti I, Silva-Cayetano A, Fra-Bido S, Innocentin S, et al. Targeting TLR4 during vaccination boosts MAdCAM-1+ lymphoid stromal cell activation and promotes the aged germinal center response. Sci Immunol. 2022;7(71):1–17.

792. Brahmakshatriya V, Kuang Y, Devarajan P, Xia J, Zhang W, Vong AM, et al. IL-6 Production by TLR-Activated APC Broadly Enhances Aged Cognate CD4 Helper and B Cell Antibody Responses In Vivo. J Immunol.

2017;198(7):2819–33.

793. Hsu PS, Lai CL, Hu M, Santner-Nanan B, Dahlstrom JE, Lee CH, et al. IL-2 Enhances Gut Homing Potential of Human Naive Regulatory T Cells Early in Life. J Immunol. 2018;200(12):3970–80.

794. Breton G, Zheng S, Valieris R, da Silva IT, Satija R, Nussenzweig MC. Human dendritic cells (DCs) are derived from distinct circulating precursors that are precommitted to become CD1c+ or CD141+ DCs. J Exp Med. 2016;213(13):2861–70.

795. Wagar LE, Salahudeen A, Constantz CM, Wendel BS, Lyons MM, Mallajosyula V, et al. Modeling human adaptive immune responses with tonsil organoids. Nat Med [Internet]. 2021;27(1):125–35. Available from: http://dx.doi.org/10.1038/s41591-020-01145-0

Appendix I: Publications arising from this thesis

1. Pyle CJ, **Labeur-Iurman L**, Groves HT, Puttur F, Lloyd CM, Tregoning JS, Harker JA. Enhanced IL-2 in early life limits the development of T_{FH} and protective antiviral immunity. *Journal of Experimental Medicine* 2021. https://doi.org/10.1084/jem.20201555

Abstract

T follicular helper cell (T_{FH})–dependent antibody responses are critical for long-term immunity. Antibody responses are diminished in early life, limiting long-term protective immunity and allowing prolonged or recurrent infection, which may be important for viral lung infections that are highly prevalent in infancy. In a murine model using respiratory syncytial virus (RSV), we show that T_{FH} and the high-affinity antibody production they promote are vital for preventing disease on RSV reinfection. Following a secondary RSV infection, T_{FH}-deficient mice had significantly exacerbated disease characterized by delayed viral clearance, increased weight loss, and immunopathology. T_{FH} generation in early life was compromised by heightened IL-2 and STAT5 signaling in differentiating naive T cells. Neutralization of IL-2 during early-life RSV infection resulted in a T_{FH}-dependent increase in antibody-mediated immunity and was sufficient to limit disease severity upon reinfection. These data demonstrate the importance of T_{FH} in protection against recurrent RSV infection and highlight a mechanism by which this is suppressed in early life.

2. **Labeur-Iurman L**, Harker JA. Mechanisms of antibody mediated immunity – Distinct in early life. *The International Journal of Biochemistry & Cell Biology* 2024. https://doi.org/10.1016/j.biocel.2024.106588

Abstract

Immune responses in early life are characterized by a failure to robustly generate long-lasting protective responses against many common pathogens or upon vaccination. This is associated with a reduced ability to generate T-cell dependent high affinity antibodies. This review highlights the differences in T-cell dependent antibody responses observed between infants and adults, in particular focussing on the alterations in immune cell function that lead to reduced T follicular helper cell-B cell crosstalk within germinal centres in early life. Understanding the distinct functional characteristics of early life humoral immunity, and how these are regulated, will be critical in guiding age-appropriate immunological interventions in the very young.

Appendix II: Conference presentations arising from this thesis

1. ***Two oral presentations at British Society for Immunology Congress, December 2021, Edimburgh, UK. Winner of PhD Bright Sparks***

An enriched IL-2 Environment in early life limits T follicular helper cell development and protective immunity after respiratory virus infection

Lucia Labeur Iurman[1], Chloe J. Pyle[1], Helen T. Groves[2], Franz Puttur[1], Sejal Saglani[1], Clare M. Lloyd[1], John S. Tregoning[2], James A. Harker[1]

[1]Imperial College London, South Kensington Campus, London, United Kingdom
[2]Imperial College London, St. Mary's Campus, London, United Kingdom

T follicular helper cell (T_{FH}) dependent antibody responses are critical for long term immunity. Antibody responses are however diminished, vaccination less effective and recurrent infections prevalent in early life. Respiratory syncytial virus (RSV) is the most common cause of viral bronchiolitis in infancy, and regularly causes recurrent infections. Using a murine model of RSV, we found that T_{FH} differentiation and antibody responses were reduced in early life compared to adulthood. This was associated with decreased STAT3 phosphorylation, a pro-T_{FH} factor, and increased STAT5 phosphorylation, a T_{FH} antagonist, in CD4 T cells early after infection in neonates compared to adults. This change in STAT3/5 balance was associated with changes in key components regulating the signalling of IL-2 within the secondary lymphoid tissue. This included differential expression of CD25 (IL-2Ra), the secreted form of which is associated with quenching IL-2 from the microenvironment, by both DCs and B cells. Foxp3$^-$ CD4 T cells from neonates also expressed elevated CD25, CD122 (IL2Rb) and IL-2 compared to adults. Fitting with this, naïve CD4 T cells isolated from neonatal mice were more responsive to IL-2 *in vitro* than those from adult mice. Neutralization of IL-2 during early RSV infection promoted increased T_{FH} differentiation and antibody production in neonatal mice; this dampening IL-2 in early life also limited disease on RSV re-infection 8 weeks later in wildtype, but not T_{FH} deficient, mice. Taken together this data highlights the role of altered IL-2 signalling in limiting T dependent antibody responses in early life, and that manipulating this pathway can improve protective immunity.

2. ***Oral presentation at European Academy of Allergy and Clinical Immunology 20th Immunology Winter School on Basic Immunology Research in Allergy and Clinical Immunology, January 2022, virtual***

Exposure to *Acinetobacter lwoffii F78* overcomes IL-2 dependent restriction of T dependent antibody responses against respiratory viral infection in infancy

Lucia Labeur Iurman[1], Chloe J. Pyle[1], Kunyuan Tian[1], Helen T. Groves[2], Franz Puttur[1], Minerva Garcia Martin[2], Clare M. Lloyd[1], John S. Tregoning[2], Sejal Saglani[1], James A. Harker[1]

[1]Imperial College London, South Kensington Campus, London, United Kingdom
[2]Imperial College London, St. Mary's Campus, London, United Kingdom

Introduction: T follicular helper cell (TFH) dependent antibody responses are critical for long term immunity. They are however diminished in early life limiting protective immunity against vaccination and infection. For example after infection with Respiratory Syncytial virus (RSV), the leading cause of viral bronchiolitis in infants, and a risk factor for wheeze and asthma in later life, TFH numbers are reduced. Early life is also a period of dynamic microbiotal colonization, and administration of microbial products can modulate antibody responses in adult mice, but whether this is effective in infancy is unknown.

Methods: Neonatal and adult BALB/c and C57/BL6 mice were infected intranasally with RSV. In some experiments Acinetobacter lwoffii F78, a microbiotal bacteria, was co- administered. Antibody and TFH responses were evaluated by ELISA and flow cytometry. In vitro, the capacity of A.lwoffii and RSV to modulate TFH-regulating factors was evaluated using Flt3L-derived bone-marrow dendritic cells (BMDCs).

Results: Using a murine model of RSV, we found that TFH differentiation and antibody responses were reduced in early life compared to adulthood. This was associated with decreased STAT3 phosphorylation, a pro-TFH factor, and increased STAT5 phosphorylation, a TFH antagonist, in CD4+ T cells early after infection in neonates compared to adults. This was associated with increased levels of IL-2- STAT5 signalling in neonates compared to adults in the lung draining lymph nodes (dLNs), blockade of which enhanced TFH formation. Intranasal exposure of neonatal mice to A.lwoffii during recurrent RSV infections was sufficient to overcome IL-2 mediated suppression and augment TFH and B cell responses. A.lwoffii boosted both dLN DCs, and their expression of CD25, the secreted form of which is associated with quenching IL-2. Likewise, in vitro stimulation of BMDCs with A.lwoffii potently induced both soluble CD25 and IL-6 secretion, a potent STAT3 inducer, when compared with RSV.

Conclusions: Taken together this data highlights the role of IL-2 signalling in limiting T dependent antibody responses in early life. In addition, manipulating this pathway either by neutralising IL-2 or exposure to microbiota may be sufficient to boost antibody mediated immunity.

3. ***Oral presentation at British Society for Immunology Congress B cell meeting, April 2022, London UK***

Exposure to *Acinetobacter lwoffii F78* overcomes germinal centre restriction of T dependent antibody responses against respiratory viral infection in infancy

Lucia Labeur Iurman[1], Kunyuan Tian[1], Minerva Garcia Martin[1], Chloe J. Pyle[1], Sejal Saglani[1], James A. Harker[1]

[1]Imperial College London, South Kensington Campus, London, United Kingdom

Antibody-mediated responses are vital for long term immunity, but can be compromised early in life. Respiratory syncytial virus (RSV) infection, the most common cause of bronchiolitis in infancy, for instance promotes limited antibody responses and frequent recurrent infections. Using a murine model, we recently showed that RSV limited T-cell dependent antibody responses in early life via an IL-2 dependent pathway. Microbiota, and microbiotal products, however have been reported to be capable of promoting antibody-mediated immunity, but whether this is effective in infancy is unknown.

We therefore examined the capacity of the common farmyard microbe, *Acinetobacter lwoffi F78*, to promote antibody-mediated immunity in early life. *In vitro* neither TLR3, 4 or 9 agonists nor RSV, was sufficient to activate neonatal B cells, or cause the release of pro-T follicular helper cell (T_{FH}) factors IL-6 and CD25, however *A.lwoffii* potently stimulated both. A similar effect was observed when *A.lwoffii* was used to stimulate *in vitro* differentiated bone marrow DCs. *In vivo,* intranasal exposure to *A.lwoffii* led to increased numbers of GC B cells, memory B cells and plasma cells alongside T_{FH}, in RSV-infected neonatal mice. Together this data highlights the ability of microbiota to boost antibody mediated immunity in early life by overcoming the GC restriction observed in neonatal RSV infection.

4. ***Poster presentation at La Jolla Immunology Conference, October 2022, San Diego, USA***

Exposure to farmyard microbes in early life overcomes the IL-2-dependent germinal centre restriction during respiratory viral infection

Lucia Labeur Iurman[1], Kunyuan Tian[1], Minerva Garcia Martin[1], Lorena Mejias Martinez, Sejal Saglani[1], James A. Harker[1]

[1]Imperial College London, South Kensington Campus, London, United Kingdom

T follicular helper cell (T_{FH}) dependent antibody responses are critical for long term immunity, but can be compromised early in life. Respiratory syncytial virus (RSV), the most common cause of bronchiolitis in infancy, promotes limited antibody responses in early life when compared to adults leading to increase susceptibility to reinfection. Using a murine model, we recently showed that RSV limits T-cell dependent antibody responses in early life via an IL-2 dependent pathway. Microbiota, and microbiotal products, however have been reported to be capable of promoting antibody-mediated immunity, but whether this is effective in infancy is unknown.

Stimulation of bone marrow derived dendritic cells (BMDC) revealed that the common farmyard microbe *Acinetobacter Iwoffii F78*, and to a lesser extent LPS, but not RSV nor TLR3, 7 or 9 agonists could promote DC-derived secretion of the pro-T_{FH} factors IL-6 and CD25. Co-culture of *A. Iwoffii* stimulated BMDCs with naïve $CD4^+$ T cells promoted T_{FH} like differentiation, a process RSV stimulation of BMDCs inhibited. Critically, neonatal exposure to *A. Iwoffii* enhanced cDC2 frequency, and their expression of CD25, which was accompanied by an increase in T_{FH}, GC B and plasma cell responses to RSV infection *in vivo*. Together this data highlights the ability of microbiota to boost antibody mediated immunity in early life by overcoming the IL-2-dependent restriction GCs undergo after neonatal viral infection.

5. ***Poster presentation at Kings, UCL and Imperial Conference, November 2023, London, UK***

Exposure to farmyard microbes in early life overcomes the IL-2 germinal centre restriction against respiratory viral infections

Lucia Labeur Iurman[1], Kunyuan Tian[1], Minerva Garcia Martin[1], Lorena Mejias Martinez, Sejal Saglani[1], James A. Harker[1]

[1]Imperial College London, South Kensington Campus, London, United Kingdom

T follicular helper cell (T_{FH}) dependent antibody responses are critical for long term immunity, but can be compromised early in life. Respiratory syncytial virus (RSV), the most common cause of bronchiolitis in infancy, promotes limited antibody responses in early life when compared to adults leading to increase susceptibility to reinfection; a process dependent on heightened IL-2 signalling in early life. Microbiota, and microbial products, have been shown to be capable of promoting antibody-mediated immunity, but whether this is effective in infancy is unknown. We sought to examine the capacity of the common farmyard microbe, *Acinetobacter lwoffi F78*, to promote a pro-T_{FH} phenotype in DCs and antibody-mediated immunity *in vivo*.

In vitro neither TLR3, 7 or 9 agonists nor RSV, promoted secretion of the pro-T_{FH} factors IL-6 and CD25 by bone-marrow DCs. LPS-stimulation of TLR4 promoted IL-6 secretion, while *A.lwoffii* potently stimulated both. Further, co-culture of *A.lwoffii* pulsed DCs with naïve $CD4^+$ T cells promoted upregulation of Bcl6, the defining T_{FH} transcriptional factor, while RSV-stimulated DCs inhibited it; which was partially overcome by addition of *A.lwoffi*. Concomitant with this, intranasal exposure to *A.lwoffii*, alongside RSV infection, of mice *in vivo* led to increased cDC2 frequency and their expression of CD25 in mediastinal lymph node. This was associated with increased numbers of T_{FH} cells alongside germinal centre (GC) B cells and plasma cells in RSV-infected neonatal mice treated with *A.lwoffi*. Together, this data highlights the ability of microbiota to overcome IL-2-dependent GC restriction in early life, and promote antibody mediated immunity.

6. ***Poster Presentation at British Society for Immunology Congress, December 2023, Belfast, UK***

Exposure to farmyard microbes in early life overcomes the IL-2 germinal centre restriction against respiratory viral infections

Lucia Labeur Iurman[1], Kunyuan Tian[1], Minerva Garcia Martin[1], Lorena Mejias Martinez, Sejal Saglani[1], James A. Harker[1]

[1]Imperial College London, South Kensington Campus, London, United Kingdom

T follicular helper cell (T_{FH}) dependent antibody responses are critical for long term immunity, but can be compromised early in life. Respiratory syncytial virus (RSV), the most common cause of bronchiolitis in infancy, promotes limited antibody responses in early life when compared to adults leading to increase susceptibility to reinfection; a process dependent on heightened IL-2 signalling in early life. Microbiota, and microbial products, have been shown to be capable of promoting antibody-mediated immunity, but whether this is effective in infancy is unknown. We sought to examine the capacity of the common farmyard microbe, *Acinetobacter lwoffi F78*, to promote a pro-T_{FH} phenotype in DCs and antibody-mediated immunity *in vivo*.

In vitro neither TLR3, 7 or 9 agonists nor RSV, promoted secretion of the pro-T_{FH} factors IL-6 and CD25 by bone-marrow DCs. LPS-stimulation of TLR4 promoted IL-6 secretion, while *A.lwoffii* potently stimulated both. Further, co-culture of *A.lwoffii* pulsed DCs with naïve $CD4^+$ T cells promoted upregulation of Bcl6, the defining T_{FH} transcriptional factor, while RSV-stimulated DCs inhibited it; which was partially overcome by addition of *A.lwoffi*. Concomitant with this, intranasal exposure to *A.lwoffii*, alongside RSV infection, of mice *in vivo* led to increased cDC2 frequency and their expression of CD25 in mediastinal lymph node. This was associated with increased numbers of T_{FH} cells alongside germinal centre (GC) B cells and plasma cells in RSV-infected neonatal mice treated with *A.lwoffi*. Together, this data highlights the ability of microbiota to overcome IL-2-dependent GC restriction in early life, and promote antibody mediated immunity.